# ABSTRACT


| | |
|---|---|
| Title of Document: | TIMING OF OROGENESIS IN THE SOUTHERN BRASÍLIA BELT |
| | Barry L. Reno, Ph.D., 2009 |
| Directed By: | Professor Michael Brown and Associate Research Scientist Philip Piccoli, Department of Geology |



The Neoproterozoic–Cambrian Brasília Orogeny records suturing of the passive margin on the western side of the São Francisco Craton with magmatic arcs and the Paranapanema Block in the south or the Amazon Craton in the north during the assembly of West Gondwana. In the southern sector of the Southern Brasília Belt, the Andrelândia Nappe Complex comprises a stack of passive margin-derived nappes metamorphosed to high-pressure granulite facies during subduction-to-collision orogenesis and overlain by an arc-derived high-pressure granulite facies nappe. I present the results of an integrated petrologic and chronologic study on the metamorphic conditions and the timing and duration of orogenesis in the Andrelândia Nappe Complex. I also report on my implementation of the (U-Th)-Pb monazite EPMA dating technique at the University of Maryland, and propose a protocol for statistical analysis and interpretation of monazite ages.

Using the U-Pb zircon chronometer in conjunction with Ti-in-zircon thermometry, REE distribution data and petrologic observations, a minimum age for timing of initial nappe detachment is constrained to 678±29 Ma, whereas just-post-peak-*T* metamorphism of the uppermost passive margin-derived Três Pontas–Varginha Nappe is interpreted to have occurred at *ca.* 648 Ma. (U-Th)-Pb monazite ages in the Três Pontas–Varginha and underlying Carmo da Cachoeira Nappes indicate that they were accreted to the hanging wall of the subduction zone at depths corresponding to near-peak-*P* by 635–624 Ma. High-*P* granulite facies metamorphism of the arc-derived nappe is dated by a U-Pb zircon age of 622±28 Ma. Two Rb-Sr multimineral–whole rock isochrons record cooling of the Três Pontas–Varginha Nappe below ~700˚C at *ca.* 590 Ma, suggesting slow cooling from peak-*T*. $^{40}Ar/^{39}Ar$ biotite ages between 591.4±6.6 and 568.9±6.1 for the Três Pontas–Varginha Nappe indicate an increased cooling rate interpreted to be due to tectonically-driven exhumation. $^{40}Ar/^{39}Ar$ biotite ages of *ca.* 540 Ma in the Carmo da Cachoeira Nappe indicate that this nappe was exhumed after the Três Pontas–Varginha Nappe had cooled below ~300˚C. In the southeast part of the Nappe Complex, the Andrelândia Nappe yields $^{40}Ar/^{39}Ar$ biotite ages consistent with emplacement directly on the São Francisco Craton and cooling from the bottom up.

# TIMING OF OROGENESIS IN THE SOUTHERN BRASÍLIA BELT

By

Barry L. Reno

Dissertation submitted to the Faculty of the Graduate School of the
University of Maryland, College Park, in partial fulfillment
of the requirements for the degree of
Doctor of Philosophy
2009

Advisory Committee:
Professor Michael Brown, Chair
Associate Research Scientist Philip Piccoli, Co-Chair
Professor Bruce James
Assistant Professor Aaron Martin
Professor Roberta Rudnick

# Acknowledgements

I thank Michael Brown and Philip Piccoli for providing advice and support throughout the course of this project. Rudolph A.J. Trouw and Renato Moraes provided invaluable help by introducing me to the intricacies of the Southern Brasília Belt, and helping me while I was in Brazil.

I thank Andrew Masterson, Andrew Shansby and Camilo Trouw for assistance in the field, Chie Sakaguchi for assistance with Rb-Sr and Sm-Nd analyses, Katsura Kobayashi and Tomohiro Usui for assistance with SIMS zircon analyses, Richard Ash and Ricardo Arévalo Jr. for assistance with LA-ICP-MS analyses, Richard White and Fawna Korhonen for assistance with THERMOCALC, Laura Webb, Suzanne Baldwin and the Syracuse University Noble Gas Isotopic Research Laboratory (SUNGIRL) for assistance with argon analyses, Marty Grove and the ion microprobe facility at UCLA, which is partly supported by a grant from the Instrumentation and Facilities Program, National Science Foundation, for assistance with monazite SIMS chronology, Chris Clark and the John de Laeter Centre for Mass Spectrometry at Curtin University for assistance with U-Pb SHRIMP analyses, Roger Powell and Aaron Martin for helpful discussions, Julie Baldwin, James Crowley, Nigel Kelly and two anonymous reviewers for comments on earlier versions of Chapter 2 and Roberta Rudnick, Aaron Martin and Bruce James for serving on my committee.

I appreciate the support of the Maryland NanoCenter and the NispLab. The NispLab is supported in part by the NSF as a MRSEC Shared Experimental Facility. This project was funded by the National Science Foundation (grant EAR-0227553 to

Brown and Piccoli), the COE-21 program from the Ministry of Education, Culture, Sports, Science and Technology of Japan at ISEI, the Brazilian Research Council (CNPq to Trouw), the Geological Society of America and the University of Maryland.

# Table of Contents

# List of Tables

# List of Figures

# Chapter 1: Introduction

*Motivation*

The Gondwana continent was characterized by a network of metamorphic belts that sutured the cratons and tectonic blocks now located in the southern hemisphere continents during the late Neoproterozoic and early Cambrian. The Brasiliano Event, which led to the suturing of West Gondwna, is recorded in present day South America by the Tocantins and Mantiqueira Provinces (Fig. 1-1)(*e.g.*, Fuck *et al.* 1994; Campos Neto 2000; Valeriano *et al*. 2008). The Tocantins Province comprises three metamorphic belts (Fig. 1-1): the Brasília Belt lies to the west and southwest of the São Francisco Craton; the Araguaia Belt lies to the northwest of the São Francisco Craton and east of the Amazon Craton; and, the Paraguai Belt lies to the south of the Amazon Craton. The Mantiqueira Province comprises the Ribeira and Arçuaí Belts to the east and southeast of the São Francisco Craton (Fig. 1-1).

The Brasília Belt was formed from a sequence of sedimentary rocks that were deposited in the Brazilide Ocean on the passive margin along the western side (present day coordinates) of the São Francisco Craton as well as volcanic rocks related to a series of magmatic arcs. These rocks were metamorphosed during closure of the Brazilide Ocean basin between the Amazon Craton (north), Paranapanema Block (south) and a series of intervening magmatic arcs to the west and the São Francisco Craton to the east (Fig. 1-1).

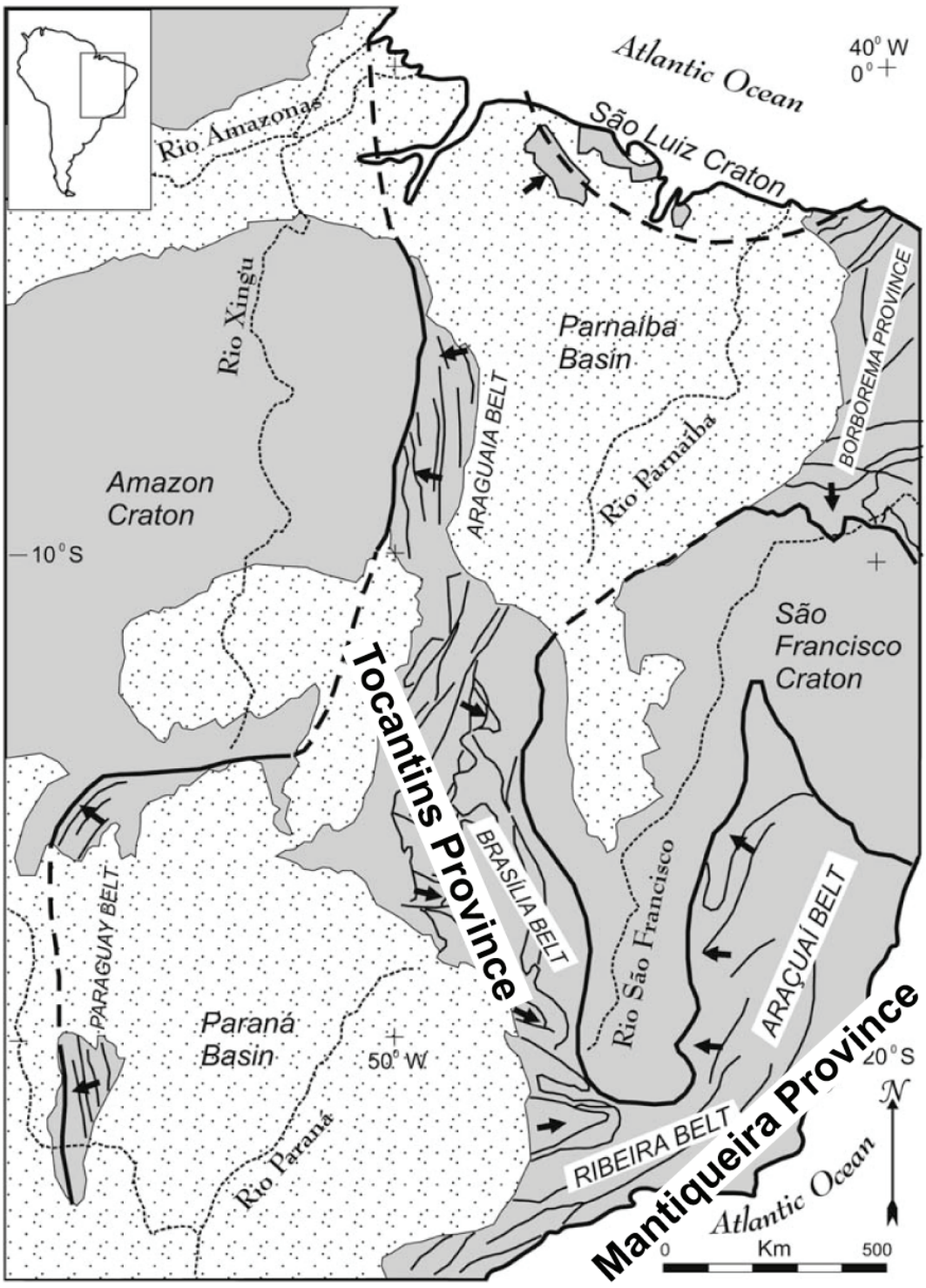


**Figure 1-1.** Map of eastern Brazil indicating the location of the Tocantins and Mantiqueira Provinces. Modified from Valeriano *et al*. (2008).

Over the past two decades high-grade granulite facies rocks have been found to occur in the Brasília Belt, with ultrahigh temperature granulites in the Anápolis–Itauçu Complex in the northern sector of the Southern Brasília Belt, and high pressure granulites in the Andrelândia Nappe Complex in the southern sector of the Southern Brasília Belt (*e.g.,* Fuck et al. 1994; Ribeiro *et al*. 1995; Moraes & Fuck 2000; Campos Neto & Caby 2000; Moraes *et al*. 2002; Baldwin *et al*. 2005). Advances in modern petrologic techniques such as thermodynamic modeling of equilibrium phase assemblages using THERMOCALC has allowed for more detailed constraints on the *P-T* evolution of the Anápolis–Itauçu Complex (Baldwin *et al.* 2005), and recent advances in linking zircon growth to metamorphic conditions allowed Baldwin & Brown (2008) to constrain the duration of ultrahigh temperature conditions in the Anápolis–Itauçu Complex to the interval 649 to 634 Ma.

In the southern sector of the Southern Brasília Belt, the Andrelândia Nappe Complex has been the subject of detailed structural and sedimentological studies (*e.g.,* Trouw *et al*. 1983; Paciullo *et al*. 1993; Ribeiro *et al*. 1995; Campos Neto & Caby 1999; Trouw *et al*. 2000). However, constraints on the *P-T* evolution are limited to traditional thermobarometric techniques, such as Fe-Mg exchange thermometry in combination with net-transfer reaction barometry. Fe-Mg exchange thermometry is subject to returning erroneously low temperatures in high and ultrahigh temperature rocks due to the effects of retrograde Fe-Mg diffusive exchange. Consequently, the temperature dependence of net-transfer reactions will lead to erroneously low calculated pressures if close-to-peak temperatures are not retrieved. Many of the published *P-T* paths calculated for the individual nappes in the Andrelândia Nappe

Complex using traditional thermobarometry (*e.g.,* Garcia & Campos Neto 2003) coincidently follow a trajectory that would be expected for retrograde exchange of Fe and Mg above the closure temperature of this system for minerals such as biotite, essentially tracking a net-transfer reaction down-temperature. Metamorphism in the Andrelândia Nappe Complex has been suggested to have occurred at *ca.* 630 Ma based on limited chronologic data (*e.g.,* Campos Neto *et al.* 2004). However, there has been no detailed chronologic study that constrains the timing and duration of metamorphism in each of the nappes. In order to understand the tectonic processes that led to the emplacement and exhumation of the nappes, it is necessary to constrain not only the *P-T* evolution of the nappes, but also the timing and duration of metamorphism in each nappe.

One of the biggest challenges in interpreting chronologic data is correctly linking ages to metamorphic *P-T* conditions. The assumption that a chronometer records the timing of peak metamorphism is a simplistic view that has been shown to not always hold true. Recent advances in linking ages obtained by chronometers such as zircon to temperatures potentially allow ages to be linked to precise points along the *P-T* evolution. Chronometers such as the U-Pb system in zircon and the (U-Th)-Pb system in monazite have high closure temperatures > 900˚C but may record growth at lower temperatures due to processes such as crystallization from a melt (*e.g.,* Roberts & Finger 1997), liberation of Zr during retrograde ilmenite breakdown (Bingen *et al.* 2001) or dissolution-reprecipitation due to interaction with fluids (*e.g.,* Martin *et al.* 2007). Advances in the application of geochemical tools such as the Ti-in-zircon thermometer (Watson *et al*. 2006; Ferry & Watson 2007) and elemental

distributions such as the rare earth elements between zircon and garnet (*e.g.,* Rubatto & Hermann 2007; Harley & Kelly 2007) allow zircon ages to be linked directly to *P-T* conditions. Conversely, chronometers such as the Rb-Sr system in biotite, which generally is assigned a low closure temperature of ~300˚C, may record closure at much higher temperatures than this due to modally controlled closed-system behavior or shielding, in which case the effective closure temperature for biotite is controlled by the surrounding phases (Glodny *et al*. 2003).

The proper interpretation of age information also requires a detailed statistical evaluation of the data. However, most statistical techniques commonly used in the interpretation of age information are based on the assumption that data are taken from a normally distributed population. Ages calculated from skewed or non-normal data will be erroneous, and uncertainties calculated from such data may underestimate the true uncertainty. The interpretation of rates of geologic process requires accurate ages and a realistic understanding of their uncertainties. In order to assign accurate ages and realistic uncertainties to chronologic data, a robust statistical protocol is required that is able to account for non-normal behavior.

The focus of my Ph.D. research has been to address the challenge of understanding the timing and duration of orogenesis in the Andrelândia Nappe Complex using an integrated petrologic and chronologic study of the upper-most high-pressure granulite nappes. The purpose of this study is to constrain a model for nappe formation, emplacement and exhumation and to contribute to understanding the amalgamation of West Gondwana. Here I present the results of my study in which I constrain both the high-grade metamorphic history and the retrograde

exhumation history of several of the nappes. Partly to address this challenge, I implemented the electron probe microanalyzer (EPMA) (U-Th)-Pb monazite dating technique here at the University of Maryland and developed a robust statistical protocol for calculating ages and uncertainties. I provide details of the (U-Th)-Pb monazite microprobe method and a description of the statistical protocol in the context of monazite from the Andrelândia Nappe Complex. I present U-Pb zircon ages that have been interpreted in the context of *P-T* conditions using recently developed geochemical and modern petrologic tools. I constrain the cooling history of the nappes using the U-Pb zircon, EPMA monazite, Rb-Sr multimineral–whole rock isochron and $^{40}Ar/^{39}Ar$ hornblende and biotite ages. I briefly discuss a tectonic model for the evolution of the Andrelândia Nappe Complex in the Southern Brasília Belt.

*Dissertation Structure and Content*

This dissertation is divided into five chapters. This first chapter is intended to provide an introduction to the motivation behind this study and to outline the questions addressed in the dissertation. Chapters 2 through 4 comprise the core of the dissertation, with each of the chapters addressing a subset of these questions. The final chapter is a synopsis that provides a summary of the results of my research.

Each of the core chapters is written in a manner that allows it to be read and understood on its own. The questions addressed in each chapter are introduced and addressed and the results are discussed independently of the other chapters. Where necessary, data from an earlier chapter is summarized in order to facilitate interpretation and discussion of data in a later chapter.

***Chapter 2***

Chapter 2 presents an integrated petrologic, chronologic and geochemical study of the two uppermost high-pressure granulite nappes in the Andrelândia Nappe Complex. Zircon $^{206}Pb/^{238}U$ SIMS ages are presented in conjunction with Ti-in-zircon temperatures, REE distribution data and petrologic observations to constrain the timing of initial nappe formation, and just-post-peak-*T* zircon growth during crystallization of residual melt in the high-pressure granulites. Equilibrium phase diagrams for particular rock compositions (pseudosections) are used to constrain the retrograde *P-T* evolution of the uppermost passive-margin-derived nappe (Três Pontas–Varginha Nappe) in the Andrelândia Nappe Complex. A Rb-Sr multimineral-whole rock isochron age obtained from the uppermost passive-margin-derived nappe is used to constrain the duration of high-*T* (>700˚C) conditions experienced by the granulites.

I provide the first ages from the Andrelândia Nappe Complex that are linked to specific metamorphic conditions. A U-Pb zircon age from eclogite demonstrates for the first time that high-pressure metamorphism in the Southern Brasília Belt was occurring *ca.* 50 Ma earlier than previously inferred. In addition, the range of ages from U-Pb zircons to Rb-Sr multimineral–whole rock isochrons provides the first constraints on the duration of orogenesis in the Andrelândia Nappe Complex. In conjunction with recently published data from elsewhere in the Southern Brasília Belt, implications for the early assembly of West Gondwana are discussed.

***Chapter 3***

Chapter 3 focuses on the EPMA (U-Th)-Pb monazite dating technique that I implemented at the University of Maryland during the course of this project, the contributions I have made to advancing the technique and the statistical protocol that I have developed for analyzing monazite dates and other geochemical data. The statistical protocol that I propose accounts for non-normal behavior in datasets that otherwise may lead to erroneous calculated ages and the underestimation of uncertainties if traditional statistical techniques are used.

These techniques are demonstrated using monazite chronologic data from the Andrelândia Nappe Complex. Monazite from the Andrelândia Nappe Complex is shown to record younger ages than zircon, which is interpreted to record the timing of post-peak-*P* monazite growth and dissolution-reprecipitation.

***Chapter 4***

In Chapter 4 I present $^{40}Ar/^{39}Ar$ cooling ages collected for hornblende and biotite from the Andrelândia Nappe Complex to constrain the exhumation history of the nappes. The $^{40}Ar/^{39}Ar$ ages are compared with the $^{206}Pb/^{238}U$ zircon, Rb-Sr multimineral–whole rock isochron and (U-Th)-Pb monazite ages from Chapters 2 and 3 in order to constrain *T-t* histories for the uppermost nappes in the Andrelândia Nappe Complex. The retrograde *P-T* evolution of another of the high-pressure granulite facies passive margin-derived nappes (Carmo da Cachoeira Nappe) is constrained using equilibrium phase diagrams for particular rock compositions (pseudosections). Data presented in this chapter constrain the duration of nappe residence at depth, the switch to an extensional regime that likely led to nappe

exhumation, and the timing of nappe exhumation. A tectonic model for nappe exhumation is suggested, and far-field tectonic activity is proposed as the likely driving force behind nappe exhumation.

***Chapter 5***

Chapter 5 summarizes the findings of the earlier chapters and briefly discusses the tectonic evolution of the Andrelândia Nappe Complex. The new results from this study that contribute to understanding the evolution of the Southern Brasília Belt are discussed, together with the new contributions to analyzing and interpreting monazite (U-Th)-Pb chronologic data.

*Peer-Reviewed Publications Resulting from This Study*

Chapters 2, 3 and 4 either have been submitted or are close to submission to scientific journals for publication, and are in various stages of the peer-review process. A version of Chapter 2, "Eclogite–High-Pressure Granulite Metamorphism Records Early Collision in West Gondwana: New Data From the Southern Brasília Belt, Brazil" with co-authors Michael Brown, Katsura Kobayashi, Eizo Nakamura, Philip Piccoli and Rudolph Trouw, has been accepted for publication in the Journal of the Geological Society, London. A version of chapter 3, "Robust Statistical Methods for Assessment and Analysis of Monazite Microprobe Geochronologic Data Applied to the Neoproterozoic Brasília Belt, Brazil" with co-authors Philip Piccoli, Michael Brown and Rudolph Trouw, has been submitted to Chemical Geology and is currently in review. Chapter 4, "$^{40}Ar/^{39}Ar$ chronology of high-pressure granulite nappes in the Southern Brasília Belt, Brazil: implications for nappe exhumation" with co-authors

Michael Brown and Philip Piccoli, will be submitted to the Journal of Metamorphic Geology soon.

# Chapter 2: Eclogite–High-Pressure Granulite Metamorphism Records Early Collision in West Gondwana: New Data From the Southern Brasília Belt, Brazil

*Abstract*

Nappes in the southern sector of the Southern Brasília Belt record suturing of the Socorro–Guaxupé Arc–Paranapanema Block with a subducted passive margin on the western side of the São Francisco Craton. I report SIMS U–Pb zircon ages that for the first time constrain the age of metamorphism in: (1) retrograded eclogite from a tectonic block along the contact beneath the uppermost nappe in a stack of passive margin-derived nappes; (2) high-pressure granulite from the uppermost passive margin-derived nappe; and, (3) high-pressure granulite from the overlying arc-derived nappe. Rare zircons from a retrograded eclogite yield a U–Pb concordia age of 678 ± 29 Ma, which I interpret to most likely date close-to-peak-*P* metamorphism and to provide a minimum age for detachment of the overlying passive margin-derived nappe from the subducting plate. Zircon associated with ilmenite in samples from two different structural levels through the passive margin-derived high-pressure granulite nappe yields $^{206}Pb/^{238}U$ ages of *ca.* 648 and 647 Ma, and Ti-in-zircon crystallization temperatures from ~860˚C down to ~785˚C, but skewed toward the lower part of the range. These data indicate zircon formation during cooling from high-*T* down to the solidus. Rb-Sr multimineral–whole rock isochrons from two samples from this nappe date the initial stage of decompression at ~700˚C at *ca.* 590

Ma. Rare zircons from leucosome in high-pressure granulite from the overlying arc-derived nappe yield a $^{206}Pb/^{238}U$ age of 622±28 Ma and Ti-in-zircon crystallization temperatures from ~970˚C down to ~820˚C, which I interpret to record formation of zircon at immediately post-peak high-pressure granulite facies conditions. These ages indicate that the first stage of craton amalgamation in West Gondwana occurred earlier than previously inferred.

*Introduction*

In tectonic studies, linking age (*t*) information to a well-constrained set of metamorphic pressure–temperature (*P–T*) conditions is currently one of the great challenges. Ideally a sequence of *P–T* conditions from a sample provides a context for the interpretation of ages obtained from this sample using chronometers with decreasing closure temperatures. These data may be used in concert to construct a *P–T–t* path or to calculate rates of cooling, both of which may provide constraints useful in developing tectonic interpretations for the evolution of orogenic belts. The age data alone provide an estimate of the minimum duration of the metamorphic event.

In granulites, zircon ages commonly have been interpreted in rather simplistic terms in relation to the *P–T* evolution, usually following an assumption that the ages retrieved date the peak of metamorphism. These inferred peak metamorphic ages have then been used to constrain tectonic models. However, recent advances have enabled links to be made between the age retrieved and the *P–T* point or segment along the prograde or retrograde evolution where zircon crystallization occurred.

These advances include the use of trace element partitioning between coeval zircon and garnet (*e.g.*, Rubatto 2002; Rubatto & Hermann 2003; Harley & Kelly

2007; Rubatto *et al.* 2007) and Ti-in-zircon thermometry (Watson *et al.* 2006; Baldwin *et al.* 2007; Ferry & Watson 2007). In addition, thermodynamic modelling of accessory phase stability by Kelsey *et al.* (2008) has provided a framework to understand crystallization of zircon from anatectic melt.

The utility of zircon dating in granulites and ultrahigh temperature metamorphic rocks has significantly improved as a result of these advances (*e.g.,* Hermann & Rubatto 2003; Whitehouse & Platt 2003; Kelly & Harley 2005; Rubatto et al. 2006; Harley & Kelly 2007; Baldwin & Brown 2008), and the simplistic interpretation of zircon ages as dating the peak of metamorphism is no longer acceptable. Furthermore, it has been shown that zircon ages commonly record an event along the high-temperature segment of the retrograde *P–T–t* path (*e.g.,* Hokada & Harley 2004; Kelly & Harley 2005; Harley & Kelly 2007; Baldwin & Brown 2008), particularly for zircon located in leucosome where the age and temperature of crystallization are likely to provide well-constrained data along the retrograde *P–T-t* path. However, careful documentation and interpretation is required since it has also been shown that relict zircon can survive ultrahigh temperature metamorphism even when temperatures of ~950˚C have been maintained for at least 1 Ma (Möller *et al.* 2002).

In this chapter I address the timing of high-grade metamorphism in the southern sector of the Southern Brasília Belt, which has implications for the beginning of the amalgamation of West Gondwanan elements in South America and for the timescale of this process, since amalgamation was not finally completed until the Middle Cambrian Epoch (Schmitt *et al.* 2004). The southern sector of the

Southern Brasília Belt comprises a stack of nappes metamorphosed to high-pressure granulite facies conditions during the Neoproterozoic Brasília Orogeny. Although the timing of metamorphism is suggested to be *ca.* 630 Ma in the literature (*e.g.,* Campos Neto *et al.* 2004), no detailed study of the timing of nappe formation and emplacement or of the age of the high-pressure granulite metamorphism has been undertaken previously.

I present the first results from an integrated microstructural, chemical and chronological study of zircon for samples from the high-pressure granulite nappes in the southern sector of the Southern Brasília Belt. I use the petrographic setting of zircon, the rare earth element chemistry of zircon and garnet, and temperatures from Ti-in-zircon thermometry to interpret the environment of zircon growth and provide a context for the interpretation of U–Pb crystallization ages. The results provide the first well-constrained ages dating the early amalgamation of cratons in West Gondwana.

Recently, Baldwin & Brown (2008) reported ages from the northern sector of the Southern Brasília Belt that indicate that ultra-high temperature metamorphism occurred during the interval *ca.* 649–634 Ma. The data I present here include the first evidence that eclogite facies metamorphism in the southern sector of the Southern Brasília Belt may have begun up to *ca.* 30 Ma before this time. In addition, I show that the age of zircon formation along the high-temperature retrograde segment of the *P–T* evolution for the high-pressure granulites in the southern sector of the Southern Brasília Belt is similar to the age of the ultrahigh temperature metamorphism in the northern sector of the Belt.

*Geologic Setting*

The Neoproterozoic assembly of Gondwanan elements in southeastern Brazil (Fig. 2-1) began with the closure of the Brazilide Ocean and suturing of the Paranapanema Block and several intervening arcs (*e.g.,* Goiás Magmatic Arc, Socorro–Guaxupé Arc) in the south (older) and the Amazon Craton and Mara Rosa Arc in the north (younger) to the western margin (present co-ordinates) of the São Francisco Craton, creating the Brasília Belt. Subsequent closure of the Adamastor Ocean, a restricted southward-opening ocean, between the eastern margin of the São Francisco craton and the Congo craton, involving several intervening arcs (*e.g.,* Rio Negro Magmatic Arc), produced the Araçuaí–Ribeira and Buzios Belts along the South American coast and the West Congo and Kaoko Belts along the African coast (*e.g.*, Machado *et al.* 1996; Campos Neto & Caby 1999; Junges *et al.* 2002; Pimentel *et al.* 2004; Schmitt *et al.* 2004, 2008; Alkmim *et al.* 2006; Heilbron *et al.* 2008).

The southern sector of the Southern Brasília Belt comprises a stack of flat-lying nappes that were transported to the ENE during the Brasília Orogeny (Campos Neto & Caby 1999). The lower-grade nappes (Fig. 2-1c) record the lowest pressures but are structurally deeper in the nappe stack, whereas the higher-grade Carmo da Cachoeira, Lambari/Liberdade and Três Pontas–Varginha Nappes (Fig. 2-1c) record higher pressures and occur structurally higher in the nappe stack (*e.g.*, Campos Neto & Caby 1999, 2000; Garcia & Campos Neto 2003). The Socorro–Guaxupé Nappe, at the top of the nappe stack, comprises part of the magmatic arc from the hanging-wall

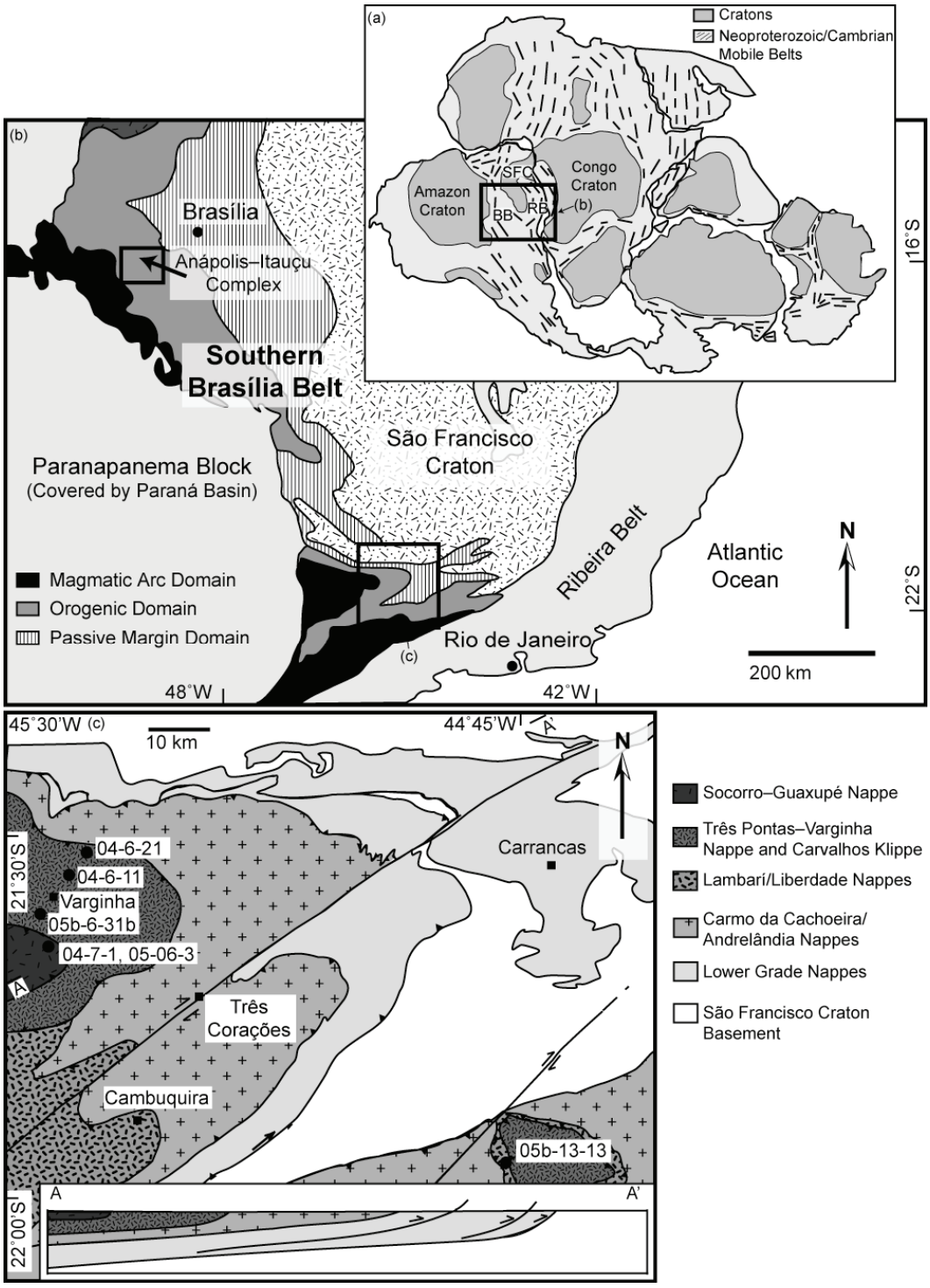


**Figure 2-1.** (a) Simplified map of Gondwana with cratons indicated by gray, and Neoproterozoic mobile belts indicated by hash marks. The box indicates the location of the Southern Brasília Belt. (b) Geological map of the Southern Brasília Belt, with box indicating the location of the Anápolis-Itauçu Complex in the northern sector and the study area in the southern sector of the Southern Brasília Belt. (c) Tectonic map of the Andrelândia Nappe Complex in the southern sector of the Southern Brasília Belt.

(Campos Neto & Caby 1999). The nappes beneath the Socorro–Guaxupé Nappe are composed of metasedimentary rocks originally deposited along the western (present co-ordinates) passive margin of the São Francisco Craton prior to subduction and terminal collision (*e.g.*, Ribeiro *et al.* 1995).

My focus in this study concerns two of the higher-grade nappes, the arc-derived Socorro–Guaxupé Nappe and the underlying passive margin-derived Três Pontas–Varginha Nappe. Using a variety of conventional exchange thermometers and net-transfer barometers, Campos Neto & Caby (2000) estimated *P-T* conditions of ~1.4 GPa and ~850˚C for the lower portion of the Socorro–Guaxupé Nappe. Using the same methods, these authors estimated *P-T* conditions of ~1.5 GPa and ~700˚C from lower structural levels and ~1.4 GPa and ~870˚C from higher structural levels of the Três Pontas–Varginha Nappe, although there is variation in the results from sample to sample. Based on these results, Campos Neto & Caby (2000) proposed that the apparent upward increase in temperature was related to the syn-emplacement intrusion of charnockitic-mangeritic magmas into the lower part of the overlying Socorro–Guaxupé Nappe.

Retrograded eclogites (locally referred to as retroeclogites) are located along the tectonic contact between the Liberdade Nappe and the underlying Andrelândia Nappe, inferred to be lateral equivalents to the Três Pontas–Varginha and Carmo da Cachoeira Nappes, respectively (Fig. 2-1c). These eclogites are interpreted to represent slivers of ocean crust (Trouw *et al.* 2000) forming the basement of the Liberdade Nappe (Três Pontas–Varginha Nappe) transported along the lower contact of this nappe after it was detached from the downgoing plate while it was being

underthrust by the passive margin prior to detachment of the next nappe to be accreted in the subduction system. Pressures of up to ~1.75 GPa have been reported from retrograded eclogites located between the Liberdade and Andrelândia Nappes (Campos Neto & Caby 1999).

The timing of metamorphism in the Anápolis-Itauçu Complex in the northern sector of the Southern Brasília Belt is constrained to *ca.* 649–634 Ma, based on high-precision TIMS U–Pb zircon ages (Baldwin & Brown 2008). In contrast, the timing of metamorphism in the southern part of the Southern Brasília Belt has been inferred to be *ca.* 630 Ma based on limited data (*e.g.*, Trouw & Pankhurst 1993; Campos Neto & Caby 1999; Vlach & Gualda 2000; Campos Neto *et al.* 2004).

*Methods*

Zircon was located in thin section using a HITACHI S-3100 scanning electron microscope at the Pheasant Memorial Laboratory (PML), at the Institute for the Study of the Earth's Interior in Misasa, Okayama University, Japan. Backscattered electron (BSE) and cathodoluminescence (CL) images were taken at PML using the HITACHI S-3100 and at the University of Maryland (UMD) using a JEOL 8900 Superprobe with an accelerating voltage of 15 kV and a cup current of ~50 nA.

Uranium and Pb isotopes were measured using a Cameca ims-1270 high resolution secondary ion mass spectrometer (HR-SIMS) at PML, following the protocol of Usui *et al.* (2002). Zircons were analyzed *in situ* in one-inch rounds cut from conventional polished thin sections in order to preserve petrographic context. To reduce common Pb contamination on the sample surface, rounds were rinsed with 0.1M HF and placed in a 0.1M $HNO_3$ ultrasonic bath for 3 minutes. The clean

sample was coated with gold. A focused $O^-$ primary beam of 5-15 nA was used, resulting in a primary beam diameter of ~10 μm and a ~25 μm sampling diameter. Signals from $^{204}Pb^+$, $^{206}Pb^+$, $^{207}Pb^+$ and $^{208}Pb^+$ were simultaneously collected using individual electron multipliers, and $UO^+$ was collected by adjusting magnet power. Raw data were corrected for instrumental mass discrimination and mass fractionation of the U/Pb atomic ratio and Pb isotopic ratios using calibration curves obtained for the 91500 zircon standard at the beginning of each analytical session using an in-house Microsoft Excel macro.

Trace element compositions in zircon were measured using a Cameca 5f secondary ion mass spectrometer at PML using the protocol of Nakamura & Kushiro (1998). Zircon grains were sputtered with a primary $O^-$ beam of ~6 nA, resulting in a primary beam diameter of ~10 μm and a ~20 μm sampling diameter. Fifteen trace elements were analyzed at each spot, with atomic masses of interest being normalized to $^{30}Si$. High Yb values in some analyses are attributed to an interference of $^{174}Hf$ on $^{174}Yb$ during analysis. Analytical uncertainty is on the order of 5–10 % ($2\sigma$).

Trace element compositions in garnet were measured using a Finnigan Element 2 ICP-MS coupled to a 213-nm quintuple-coupled Nd-YAG laser at UMD. Individual analysis spot sizes were 40-55 μm, and analysis was carried out at a photon fluence of ~2.4-2.9 J $cm^{-2}$ and a flash repetition of 7 Hz. All analyses were conducted *in situ* on garnets contained in the same one inch rounds prepared for zircon analysis. A single analysis comprised collection of approximately 20 s of background with the laser off followed by approximately 70 s of ablation. Concentration data for elements of interest were obtained by ratioing a 30-70s plateau

of counts during the ablation to the Ca concentration as measured using an electron probe microanalyzer for the same spots. Calibration was carried out relative to the NIST 610 glass standard, which was analyzed twice at the beginning and twice at the end of each twenty-analysis block. The standard deviation on the calibration was between 0.5% and 3.4%. Chemical data for the NIST 610 reference material are listed in Table A-2 in Appendix A.

Electron microprobe analysis of titanium in zircon was carried out on zircons from the same thin sections used for U-Pb zircon dating using the JEOL 8900 Superprobe at UMD. An accelerating voltage of 20 kV, a beam current of 150 nA and a spot size of 3 μm was used for all analyses. The titanium Kα peak was measured simultaneously on three channels with PETH/PETJ crystals for 300 s, and for 150 s on each background position. Zirconium Lα was measured with a PETJ crystal for 10 s on the peak and 5 s on each background, silicon Kα was measured with a TAP crystal for 100 s on the peak and 50 s on each background and hafnium Mα was measured on a TAP crystal for 60 s on the peak and 30 s on each background. Synthetic zircon ($ZrSiO_4$), hafnon ($HfSiO_4$) and the NIST 610 glass were used as standards. Data were reduced using ZAF correction procedures. The uncertainties on individual temperatures are calculated by propagating counting statistics together with uncertainties on the calibration through the temperature equation.

Watson *et al*. (2006) observed problems with secondary fluorescence of Ti in Ti-rich minerals such as rutile and ilmenite when using the EPMA to analyze small zircons (<5–10μm) closely associated with rutile. In most instances, zircon in this

study is significantly larger (100–250μm) than those analyzed by Watson *et al*. (2006). In this study, I did not observe any noticeable difference between Ti concentrations measured in zircons adjacent to ilmenite and those from zircons not touching ilmenite in the same domains in single thin sections.

Rb-Sr and Sm-Nd compositions were analyzed on whole rock powders and separates of biotite, garnet and a white mineral fraction of quartz, plagioclase and kyanite/sillimanite following the protocol of Nakamura *et al.* (2003) at PML. A 20-80 mg aliquot of each sample was weighed in a Teflon beaker, and Rb (87 enriched), Sr (84 enriched), Sm (149 enriched) and Nd (150 enriched) spikes were added to each sample.

Sample digestion followed the protocol of Yokoyama *et al.* (1999). 30M HF, 7M $HClO_4$ and 6M HCl was added to the samples before placing them in a heated ultrasonic bath overnight. The digested samples were dried by step-wise heating in a cleaned evaporator. A combination of $HClO_4$ addition and step-wise drying was used to ensure complete decomposition of insoluble fluoride. Separation of Rb, Sr, Sm and Nd followed the procedures of Yoshikawa & Nakamura (1993) and Nakamura *et al.* (2003) using Bio-Rad AG-50W "X10" cation exchange resin.

Sr and Nd isotope ratios and Sr, Rb, Sm and Nd concentrations were determined on a Finnigan-MAT 262 thermal ionization mass spectrometer at PML. The Sr and Nd data were corrected to $^{86}Sr/^{88}Sr = 0.1194$ and $^{146}Nd/^{144}Nd = 0.7291$ for internal fractionation. Repeat analyses of a Sr reference material (NIST SRM 987) gave a mean $^{87}Sr/^{86}Sr = 0.710191 \pm 20$ ($2\sigma$, n=7). Repeat analyses of a Nd internal laboratory standard (PML Nd) gave a mean $^{143}Nd/^{144}Nd = 0.511721 \pm 17$ ($2\sigma$, n=10).

This value corresponds with $^{143}Nd/^{144}Nd = 0.511856 \pm 17 (2\ \sigma)$ for the La Jolla Nd standard. The total procedural blank for Rb, Sr, Sm and Nd was 2pg, 9pg, 0.8pg and 3pg, respectively. This blank is negligible for the purposes of this study.

For this study, three samples of high-pressure granulite from the Três Pontas–Varginha Nappe were analyzed by X-ray fluorescence (XRF) for major elements to determine the bulk rock compositions. The XRF analyses were carried out using a Phillips 2404 XRF spectrometer at Franklin & Marshall College. FeO contents were analyzed by $Fe^{2+}$ titration; $Fe_2O_3$ contents were calculated by difference. Whole rock chemical analyses are listed in Table A-3 in Appendix A.

*Sample Description*

Zircons were analyzed from two samples from the Socorro–Guaxupé Nappe, one sample from a tectonic block of retrograded eclogite and three samples from different structural levels in the Três Pontas–Varginha Nappe. Sm-Nd and Rb-Sr data were collected for two separates from one of the samples from the Três Pontas–Varginha Nappe. Mineral abbreviations are after Kretz (1983). The petrographic context of zircons in thin section provides first order information to link *P-T* conditions derived from the major phases or using Ti-in-zircon thermometry with U-Pb age information derived from the zircon. Sample locations are listed in Table A-4 in Appendix A.

***Socorro–Guaxupé Nappe***

Two samples were taken from 1-2 m diameter blocks interpreted to be *in situ* from close to the base of the arc-derived Socorro–Guaxupé Nappe from south of the city of Varginha. These samples are interpreted to represent igneous protoliths that formed

in a magmatic arc environment before being metamorphosed at high-pressure granulite facies conditions. Sample 05-06-3 comprises an unfoliated, medium grained (1-3 mm grain size) K-feldspar-bearing two pyroxene granulite. Rare rounded zircon grains 30-50 μm in diameter occur as inclusions in orthopyroxene; in cathodoluminescence images they are unzoned. Sample 04-7-1 comprises a foliated, migmatitic Grt–Opx–Qtz–Pl–Hbl rock with garnet up to 1 cm in diameter and accessory ilmenite. Leucosomes contain euhedral to subhedral garnet together with quartz and plagioclase. Rare rounded zircons (50-100 μm diameter) occur as inclusions in plagioclase in leucosomes (Fig. 2-2a); in cathodoluminescence images they exhibit concentric zoning (Fig 3a).

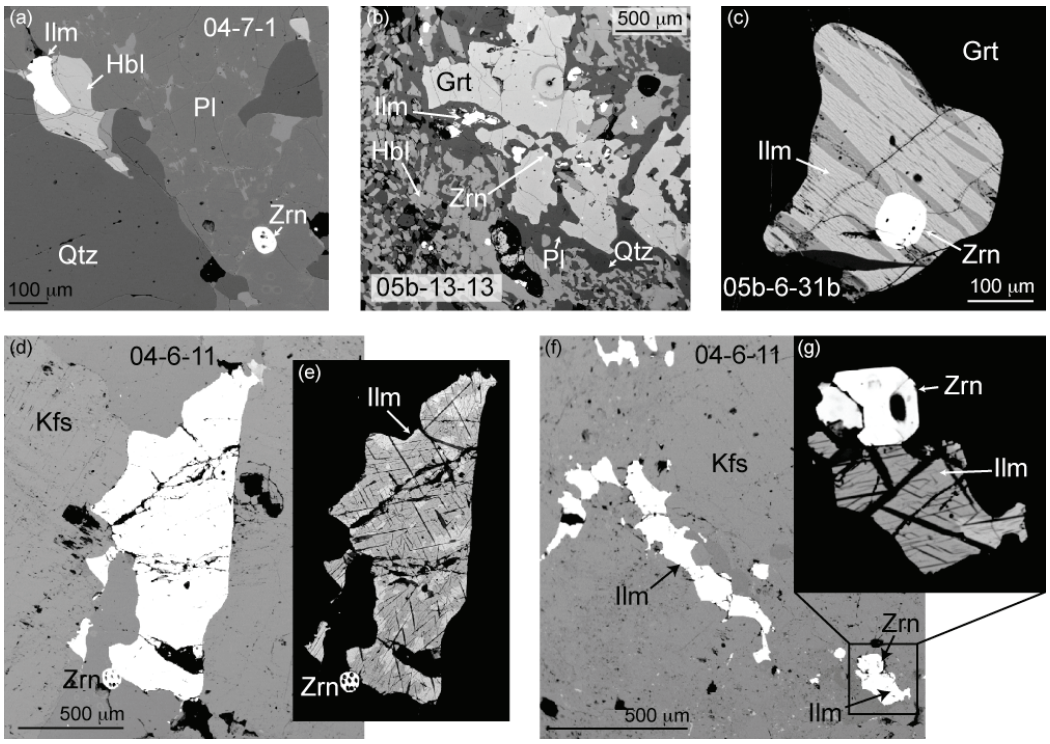


**Figure 2-2.** Backscattered electron images of (a) sample 04-7-1, (b) sample 05-13-13, (c) sample 05-6-31b and (d-g) sample 04-6-11.

***Retrograded Eclogite***

A retrograded eclogite sample was collected from a tectonic block located between the Liberdade and Andrelândia Nappes, inferred to be lateral equivalents to the Três

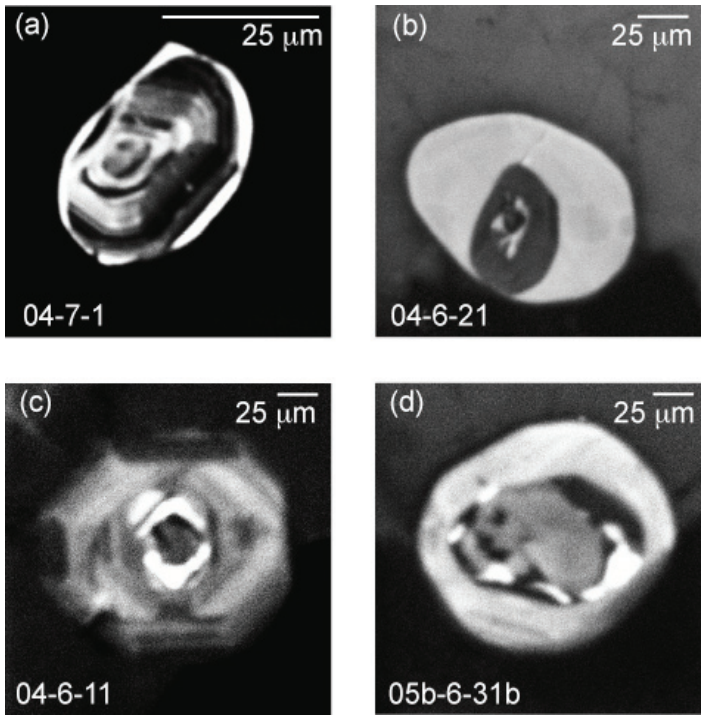


**Figure 2-3.** Cathodoluminescence images of exemplar zircons. (a) Zircon from the Socorro–Guaxupé Nappe. (b) Zircon associated with leucosome close to the bottom of the TPV nappe. (c) Zircon associated with ilmenite in the middle of the Três Pontas–Varginha (TPV) Nappe. (d) Zircon from close to the top of the TPV Nappe.

Pontas–Varginha and Carmo da Cachoeira Nappes. Sample 05-13-13 comprises millimeter size garnets that are separated by an irregular rim of granoblastic plagioclase from symplectic aggregates of plagioclase and clinopyroxene that I infer to have replaced a more jaditic pyroxene. The aggregates of plagioclase and clinopyroxene are in a microstructural relationship with millimeter size prismatic hornblende that I interpret to record replacement by hornblende. Rare rounded unzoned zircons (~20 μm diameter) occur as inclusions in garnet and in the symplectic aggregates of plagioclase and clinopyroxene associated with ilmenite (Fig.

2-2b). I interpret the rare zircons most likely to have grown as zirconium was liberated by the breakdown of igneous pyroxene on the prograde *P–T* path. However, I cannot rule out some or all of the zircon being relict from the igneous precursor, and it is possible that some of the zircon could have grown in repsponse to the breakdown of a jaditic pyroxene to symplectic plagioclase and clinopyroxene during post-peak pressure high-temperature decompression.

***Três Pontas–Varginha Nappe***

Samples were taken from three locations in the passive margin-derived high-pressure granulite facies Três Pontas–Varginha Nappe. Samples 04-6-21 and 04-6-108/110 are from the Santo Antonio Quarry near the base of the nappe, samples 04-6-11 and 04-6-2 are from the Três Pontas Quarry near the structural middle of the nappe and sample 05b-6-31b is from the Lixão (quarry used as a garbage dump) in the city of Varginha near the top of the nappe.

Sample 04-6-21 comprises a Grt–Sil/Ky–Kfs gneiss with coarse garnet (1–1.5 cm across) and millimetric K-feldspar and sillimanite/kyanite grains, fine-grained biotite as inclusions in garnet, forming thin rims around some garnets and in aggregates with sillimanite/kyanite as layers defining the foliation, and quartz. Sporadic bulbous myrmekite occurs along some K-feldpsar grain boundaries. Zircon (40-80 μm diameter) occurs as inclusions in garnet and in the leucocratic matrix. Cathodoluminescence imaging reveals distinct dark cores surrounded by bright rims (Fig. 2-3b).

Sample 04-6-11 is leucosome-dominated and comprises primarily quartz, plagioclase and K-feldspar, with clusters of 3-5 mm euhedral garnets and minor

retrograde muscovite. Stringers of ilmenite up to 2 mm long occur along K-feldspar–K-feldspar grain boundaries. Euhedral zircon up to 250 μm in diameter (Fig. 2-2d-g) occurs in association with ilmenite, typically with a common grain boundary. Cathodoluminescence imaging reveals the zircons are concentrically zoned (Fig. 2-3c).

Sample 04-6-2 is a Grt–Kfs–Ky– Qtz–Bt–Ms–Rt–Ilm gneiss. Biotite occurs as inclusions in garnet (generally ~5mm in diameter), as retrograde fringes sporadically around garnet or as intersertal grains molded on K-feldspar, and sometimes as fine grains associated with kyanite (~1mm long) in the discontinuous foliation. Rare coarse-grained muscovite is intersertal between K-feldspar grains, and between K-feldpsar and quartz grains and is interpreted to have formed close to the solidus. Modally minor intersertal plagioclase occurs between euhedral K-feldspar grains, and along grain boundaries between euhedral K-feldspar and garnet or quartz grains and is interpreted to have formed during final crystallization of residual melt. Accessory rutile occurs as inclusions in garnet, and both rutile and ilmenite occur in the matrix. Zircon was not analyzed in this sample, which was used to constrain *P–T* conditions.

Sample 05b-6-31b is a Grt–Bt–Qtz–Pl–Sil/Ky-Ilm gneiss that is strongly foliated. Large sillimanite and kyanite grains up to 5mm in length occur defining the foliation. Sillimanite also occurs as aggregates of small (<0.5 mm) grains formed along cracks that separate fragments of large (2-5 mm) garnets. Biotite occurs as sporadic fine grains in the foliation and as millimetric grains interpreted to replace garnet. Kyanite and accessory ilmenite occur as inclusions in the mantle regions of

garnet, and ilmenite occurs in the matrix. Rounded to euhedral zircons (Fig. 2-2c) up to 100 μm in diameter are associated with the ilmenite grains, both in the mantle regions of garnet and in the matrix. Cathodoluminescence imaging reveals that zircons have patchy cores surrounded by bright rims (Fig. 2-3d).

*Metamorphic conditions*

For orthogranulite samples from the arc-derived Socorro–Guaxupé Nappe at the top of the nappe stack (Fig. 2-1), average thermobarometry based on the chemical composition of peak mineral phases calculated using THERMOCALC and an internally consistent thermodynamic dataset (Holland & Powell,1998; Powell *et al*. 1998) yields *P-T* conditions of 1.5 ± 0.2 GPa and >900°C that are inferred to be close to the peak metamorphic conditions.

For the underlying passive margin-derived metasedimentary rocks of the Três Pontas–Varginha Nappe I have constructed isochemical phase diagrams (pseudosections) for three samples from two different structural levels within the nappe. Mineral equilibria modelling was undertaken using THERMOCALC 3.26 (Powell & Holland 1988; updated August 2007) and the internally consistent dataset of Holland & Powell (1998: dataset tcds55, created in November 2003). The calculations were done in the chemical system $Na_2O$–CaO–$K_2O$–FeO–MgO–$Al_2O_3$–$SiO_2$–$H_2O$–$TiO_2$–$Fe_2O_3$ (NCKFMASHTO) using the most recently available activity–composition (*a–x)* models: biotite and melt (White *et al*. 2007), orthopyroxene and spinel–magnetite (White *et al*. 2002), garnet (Diener *et al*. 2008), cordierite (Holland & Powell 1998), K-feldspar and plagioclase (Holland & Powell 2003), white mica (Coggon & Holland 2002), and ilmenite–hematite (White *et al*. 2000). The

aluminosilicates, quartz, and aqueous fluid ($H_2O$) are taken to be pure end-member phases. The modelling does not include Mn, for which the *a–x* models currently are being revised (R. Powell, pers. comm. 2008), or minor components such as F or Cl in biotite or $Cr_2O_3$ in magnetite, which may affect the stability of these phases. However, the NCKFMASHTO system is currently the most realistic approximation of rock compositions within which modelling of high-grade metamorphic assemblages can be undertaken (White *et al.* 2003, 2007).

The preservation of peak metamorphic assemblages without significant retrogression in the Três Pontas–Varginha Nappe samples is consistent with melt loss from these rocks (*e.g.,* Powell & Downes 1990; Brown 2002; Moraes *et al*. 2002; White & Powell 2002). The analyzed bulk compositions are residual with respect to an average amphibolite facies pelite (*e.g.,* Brown & Korhonen 2009) and are considered to be appropriate for investigating the *P-T* evolution after the last melt loss event (White & Powell 2002; White *et al.* 2004; Diener *et al.* 2008), which corresponds to the close-to-peak and retrograde evolution of these samples. The $H_2O$ contents in the compositions used for modelling were based on loss on ignition (LOI) values from the whole-rock chemical analyses. The low $H_2O$ contents estimated from LOI reflect the dehydrated nature of these rocks and modification of the protolith bulk composition by melt loss.

**Figure 2-4.** Equilibrium phase diagrams constructed using the bulk compositions of sample 04-6-2 (a) and 05-6-31b (b). Compositions are given in mol. %. The peak phase assemblage field for sample 04-6-11 (Fig. A1), taken from the same outcrop as sample 04-6-2, has been overlaid on the pseudosection for sample 04-6-2. The peak assemblage for sample 04-6-2 is garnet, biotite, K-feldspar, plagioclase feldspar, quartz, ilmenite and silicate melt. The peak assemblage for sample 05-6-31b is garnet, K-feldspar, kyanite, ilmenite, plagioclase, quartz and silicate melt. Isopleths (c) of garnet and biotite calculated mole percent are presented for sample 04-6-2.

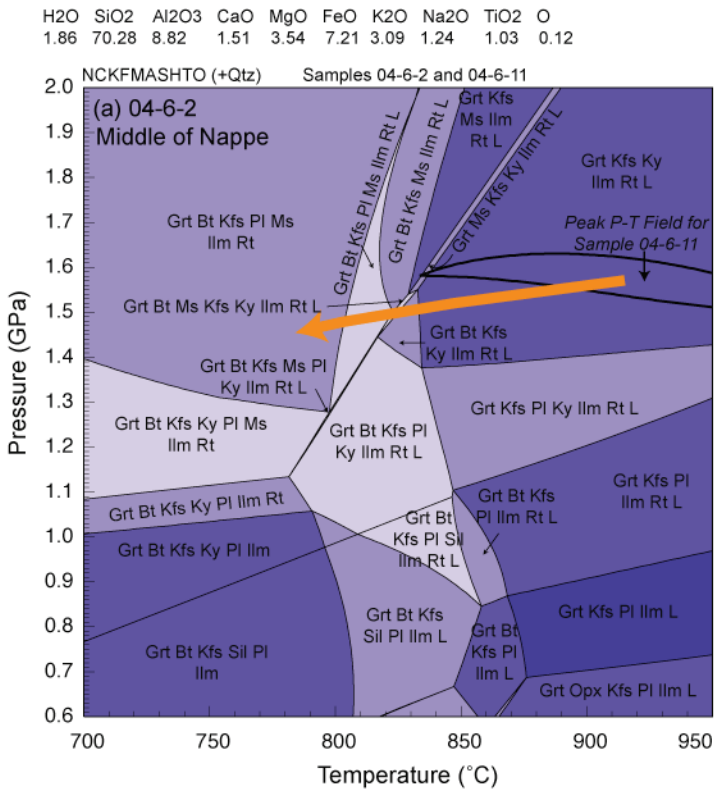
H2O SiO2 Al2O3 CaO MgO FeO K2O Na2O TiO2 O
1.86 70.28 8.82 1.51 3.54 7.21 3.09 1.24 1.03 0.12
NCKFMASHTO (+Qtz) Samples 04-6-2 and 04-6-11
(a) 04-6-2
Middle of Nappe
Grt Bt Kfs Pl Ms Ilm Rt
Grt Bt Ms Kfs Ky Ilm Rt L
Grt Bt Kfs Ms Pl Ky Ilm Rt L
Grt Bt Kfs Ky Pl Ms Ilm Rt
Grt Bt Kfs Ky Pl Ilm Rt
Grt Bt Kfs Ky Pl Ilm
Grt Bt Kfs Sil Pl Ilm
Grt Bt Kfs Pl Ky Ilm Rt L
Grt Bt Kfs Pl Sil Ilm Rt L
Grt Bt Kfs Sil Pl Ilm L
Grt Bt Kfs Pl Ilm Rt L
Grt Bt Kfs Pl Ilm L
Grt Kfs Pl Ky Ilm Rt L
Grt Kfs Pl Ilm Rt L
Grt Kfs Pl Ilm L
Grt Opx Kfs Pl Ilm L
Grt Kfs Ky Ilm Rt L
Grt Kfs Ms Ilm Rt L
Grt Bt Kfs Ky Ilm Rt L
Grt Bt Kfs Pl Ms Ilm Rt L
Grt Bt Kfs Ms Ilm Rt L
Grt Ms Kfs Ky Ilm Rt L
Peak P-T Field for Sample 04-6-11
Pressure (GPa)
Temperature (˚C)
2.0
1.9
1.8
1.7
1.6
1.5
1.4
1.3
1.2
1.1
1.0
0.9
0.8
0.7
0.6
700
750
800
850
900
950

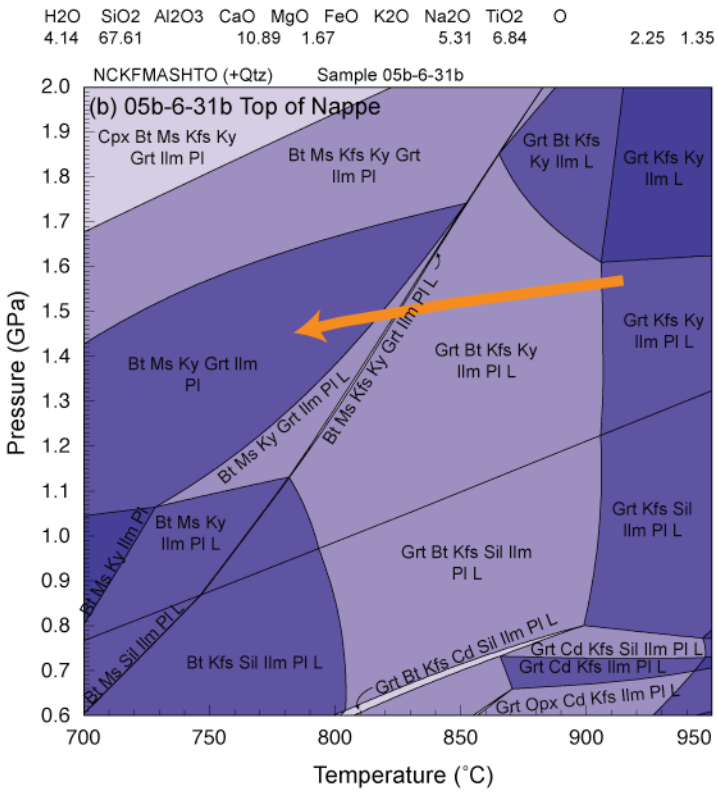
H2O SiO2 Al2O3 CaO MgO FeO K2O Na2O TiO2 O
4.14 67.61 10.89 1.67 5.31 6.84 2.25 1.35
NCKFMASHTO (+Qtz) Sample 05b-6-31b
(b) 05b-6-31b Top of Nappe
Cpx Bt Ms Kfs Ky Grt Ilm Pl
Bt Ms Kfs Ky Grt Ilm Pl
Bt Ms Ky Grt Ilm Pl
Bt Ms Ky Ilm Pl
Bt Ms Sil Ilm Pl L
Bt Kfs Sil Ilm Pl L
Bt Ms Ky Grt Ilm Pl L
Bt Ms Kfs Ky Grt Ilm Pl L
Bt Ms Ky Ilm Pl L
Grt Bt Kfs Sil Ilm Pl L
Grt Bt Kfs Cd Sil Ilm Pl L
Grt Bt Kfs Ky Ilm Pl L
Grt Bt Kfs Ky Ilm L
Grt Kfs Ky Ilm L
Grt Kfs Ky Ilm Pl L
Grt Kfs Sil Ilm Pl L
Grt Cd Kfs Sil Ilm Pl L
Grt Cd Kfs Ilm Pl L
Grt Opx Cd Kfs Ilm Pl L
Pressure (GPa)
Temperature (˚C)
2.0
1.9
1.8
1.7
1.6
1.5
1.4
1.3
1.2
1.1
1.0
0.9
0.8
0.7
0.6
700
750
800
850
900
950

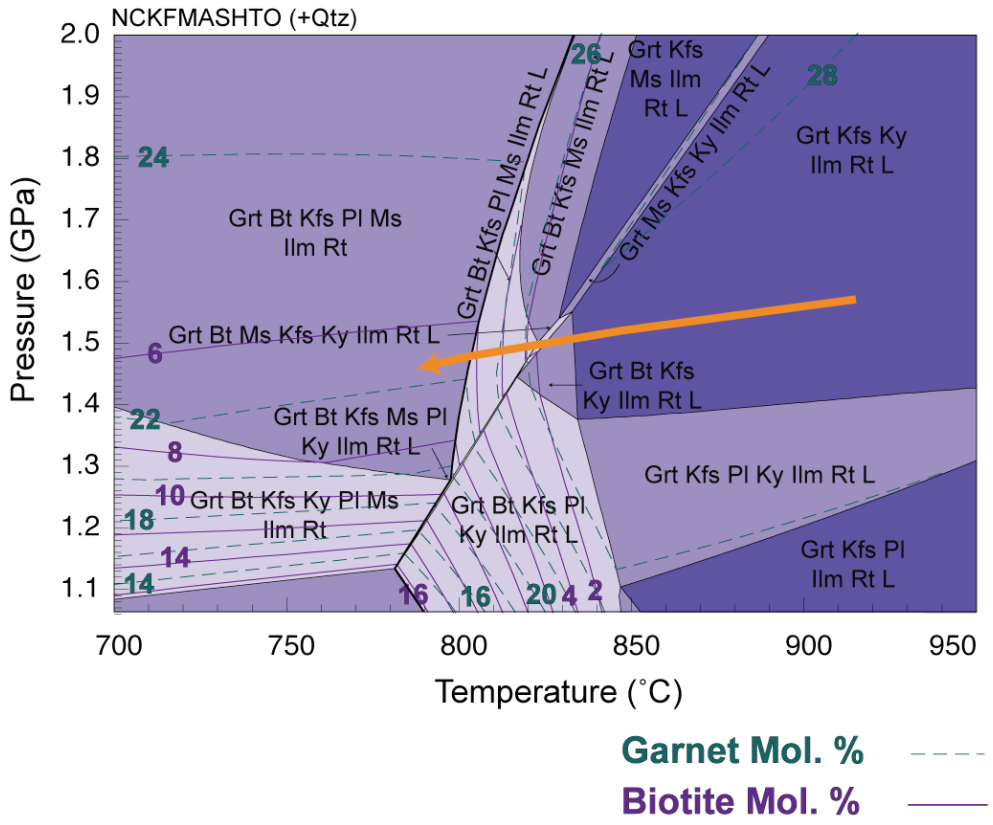


A detailed discussion of the uncertainties associated with the calculation of equilibrium phase relations is beyond the scope of this paper. Powell & Holland (2008) discuss the effects of factors such as bias, analytical uncertainty and *a-x* relations on the uncertainties of the field apices, boundaries and contours in equilibrium phase diagrams, and White *et al*. (2001; 2007) discuss the effect of adding components to or subtracting them from the chemical system. I estimate uncertainties on the position of isopleths in the equilibrium phase diagrams to be on the order of 20–30˚C and 0.3–0.6 GPa.

Equilibrium phase diagrams were constructed for the two samples from the Três Pontas–Varginha Nappe for which I present U-Pb zircon age data, 04-6-11 from the structural middle of the Três Pontas–Varginha Nappe (Fig. A-1) and 05b-6-31b from close to the top of the Três Pontas–Varginha Nappe (Fig. 2-4a), and an

additional sample, 04-6-2 (Fig. 2-4b), taken from the same outcrop as sample 04-6-11. For sample 04-6-2 the calculated phase assemblages may include both rutile and ilmenite (Fig. 2-4a). For phase assemblage fields that border the rutile-out line on the high pressure side phase, the phase assemblages contain less than 0.7 mol % ilmenite, and for phase assemblage fields at higher pressures, the phase assemblages contain less than 0.3 mol % ilmenite.

Samples 04-6-2 and 04-6-11 were collected from the same outcrop, and in the absence of any tectonic breaks must have experienced the same metamorphic history. As such, information from pseudosections from both samples may be considered together to interpret the metamorphic evolution of the middle part of the Três Pontas–Varginha Nappe. The peak *P–T* conditions for sample 04-6-11 are defined by the phase assemblage field involving quartz, garnet, biotite, K-feldspar, plagioclase, ilmenite and silicate melt, which occurs at pressures of ~1.5–1.6 GPa at temperatures greater than ~830˚C (overlay on Fig. 2-4a; Fig. A-1). Peak *P–T* conditions for sample 04-6-2 are defined by the phase assemblage field involving quartz, garnet, K-feldspar, kyanite, ilmenite, rutile and silicate melt, which occurs at pressures greater than ~1.4 GPa at temperatures greater than ~840˚C (Fig. 2-4a). Combining information from both samples, I interpret the peak metamorphic conditions to have been *P* of ~1.5 GPa and *T* >840˚C based on the overlap of the peak phase assemblage fields.

Microstructural observations in sample 04-6-2 are consistent with close-to-isobaric cooling. Biotite replacing garnet, intersertal to K-feldpsar or aligned in the foliation is interpreted to be retrograde, consistent with cooling through the quartz, garnet, biotite, K-feldspar, kyanite, ilmenite, rutile and silicate melt field in Figs. 2-4a

and 2-4c. Then sporadic coarse-grained intersertal muscovite is interpreted to have formed by cooling through the quartz, garnet, biotite, muscovite, K-feldspar, kyanite, ilmenite, rutile and silicate melt field in Figs. 2-4a and 2-4c. Finally, intersertal plagioclase is interpreted to have formed during final crystallization of residual melt as the rock cooled through the quartz, garnet, biotite, K-feldspar, plagioclase, muscovite, ilmenite, rutile and silicate melt field to the solidus in Fig. 2-4a. At temperatures below ~820˚C kyanite is inferred to persist as a metastable phase in the field of quartz, garnet, biotite, K-feldspar, plagioclase, muscovite, ilmenite, rutile and silicate melt (Figs. 2-4a and 2-4c).

The peak assemblage in sample 05-6-31b, from the top of the Três Pontas–Varginha nappe, is best represented by the phase assemblage field involving quartz, garnet, K-feldspar, kyanite, ilmenite, plagioclase and silicate melt in Fig. 2-4b, which constrains peak pressures to ~1.2–1.6 GPa, and peak temperatures to >900˚C. Biotite is present only in the foliation and is not interpreted to be part of the peak assemblage. The natural biotite composition is similar to that calculated for biotite in the phase stability field quartz, biotite, muscovite, kyanite, garnet, ilmenite, plagioclase and silicate melt, which occurs at temperatures of ~830 to ~810˚C on the retrograde *P-T* path, supporting growth during final crystallization of residual melt close to the solidus.

This range of peak *P–T* conditions determined from sample 05-6-31b is broadly consistent with the range determined from lower in the nappe. Only a minimum temperature was determined from the appropriate phase assemblage fields for samples 04-6-2 and 04-6-11 from lower in the nappe. The peak phase assemblages

for all three samples from both lower and higher in the nappe are consistent with temperatures >850–900˚C (Fig. 2-4), and there is no evidence that temperature increased significantly upward as postulated by Campos Neto & Caby (2000).

*Rare Earth Element Data*

Rare earth element (REE) data were collected from zircons for five of the samples, including three from the Três Pontas–Varginha Nappe (04-6-11, 05b-6-31b and 04-6-21) and two from the Socorro–Guaxupé Nappe (05-06-3 and 04-7-1)(Table 2-1). REE data were not collected for zircon from the retrograded eclogite sample because the limited number of zircons in the thin section large enough to analyze with a single SIMS spot was used for dating. REE data were collected from garnet for all three Três Pontas–Varginha Nappe samples and sample 04-7-1 from the Socorro–Guaxupé Nappe (Table 2-2).

Establishing the relative timing of zircon growth, garnet growth and melt crystallization is invaluable to the interpretation of the *P-T-t* history of high-grade rocks. Recent work has indicated that the distribution of the heavy REE (HREE: Tb-Lu) between garnet and zircon, minerals which both preferentially incorporate HREE into their crystal structure during growth, provides insight into these relationships (*e.g.*, Hoskin & Schaltegger 2003; Whitehouse & Platt 2003; Kelly & Harley 2005; Buick *et al.* 2006; Rubatto *et al.* 2006; Harley & Kelly 2007; Rubatto & Hermann 2007; Baldwin & Brown 2008). The environment of formation of garnet and zircon controls the relative abundance of the REE in these minerals based on the availability

**Table 2-1.** Zircon REE chemistry determined by Cameca 5f secondary ion mass spectrometer.

| Sample | Location | Sr | Y | Nb | Ba | La | Ce | Pr | Nd | Sm | Eu | Gd | Dy | Er | Yb | Lu | Eu/Eu* |
|---|---|---|---|---|---|---|---|---|---|---|---|---|---|---|---|---|---|
| 04-7-1_Zrn23REE@1 | core | 2.4 | 348 | 1.2 | 0.25 | 0.019 | 4.258 | 0.126 | 2.13 | 1.7 | 0.7 | 4.2 | 18 | 41.6 | 115.4 | 27.63 | 0.77 |
| 04-7-1_Zrn2REE@1 | core | 2.1 | 736 | 0.7 | 0.25 | 0.020 | 8.768 | 0.056 | 1.60 | 1.9 | 0.7 | 7.8 | 45 | 94.5 | 176.1 | 37.31 | 0.58 |
| 04-7-1_Zrn30REE@1 | core | 2.0 | 610 | 0.6 | 0.23 | 0.016 | 6.053 | 0.062 | 1.71 | 1.7 | 0.7 | 6.9 | 38 | 79.5 | 159.0 | 35.87 | 0.60 |
| 04-7-1_Zrn30REE@2 | core | 13.8 | 1030 | 1.7 | 0.39 | 0.023 | 8.047 | 0.061 | 1.50 | 2.0 | 0.9 | 10.6 | 64 | 127.8 | 204.2 | 47.45 | 0.57 |
| 04-7-1_Zrn5REE@1 | rim | 1.8 | 98 | 1.5 | 0.24 | 0.018 | 7.333 | 0.081 | 1.98 | 1.9 | 0.7 | 3.1 | 5 | 6.3 | 20.3 | 2.42 | 0.86 |
| 04-7-1_Zrn23REE@2 | core | 3.5 | 411 | 0.6 | 0.23 | 0.053 | 8.382 | 0.577 | 5.24 | 3.3 | 1.2 | 6.7 | 22 | 50.8 | 131.6 | 32.59 | 0.79 |
| 04-7-1_Zrn23REE@3 | core | 2.1 | 435 | 1.0 | 0.16 | 0.019 | 4.605 | 0.094 | 1.90 | 1.5 | 0.5 | 5.2 | 26 | 55.2 | 118.1 | 26.95 | 0.59 |
| 04-7-1_Zrn28REE@1 | core | 2.1 | 937 | 0.3 | 0.73 | 0.024 | 9.102 | 0.178 | 3.25 | 3.7 | 1.2 | 16.0 | 75 | 124.5 | 187.1 | 39.60 | 0.46 |
| | | | | | | | | | | | | | | | | | |
| 04-6-11_Zrn8REE@1 | rim | 1.9 | 191 | 0.5 | 0.24 | 0.019 | 8.892 | 0.051 | 1.59 | 2.0 | 1.2 | 6.8 | 21 | 14.2 | 24.9 | 2.64 | 0.98 |
| 04-6-11_Zrn8REE@2 | rim | 2.3 | 171 | 0.3 | 0.24 | 0.021 | 9.257 | 0.125 | 2.18 | 2.5 | 1.4 | 7.5 | 19 | 12.3 | 22.4 | 2.09 | 0.96 |
| 04-6-11_Zrn8REE@3 | rim | 1.9 | 180 | 0.3 | 0.26 | 0.017 | 9.058 | 0.050 | 1.71 | 2.0 | 1.2 | 6.7 | 20 | 13.4 | 22.8 | 2.35 | 0.99 |
| 04-6-11_Zrn3REE@1 | rim | 2.0 | 230 | 0.2 | 0.28 | 0.020 | 7.777 | 0.045 | 1.64 | 1.8 | 1.2 | 6.0 | 20 | 20.3 | 33.8 | 4.59 | 1.08 |
| 04-6-11_Zrn3REE@2 | rim | 1.8 | 241 | 0.3 | 0.28 | 0.020 | 7.712 | 0.048 | 1.65 | 1.5 | 1.0 | 4.6 | 19 | 27.2 | 54.8 | 8.60 | 1.12 |
| 04-6-11_Zrn4REE@1 | rim | 2.0 | 195 | 0.2 | 0.29 | 0.020 | 7.431 | 0.047 | 1.61 | 1.5 | 1.0 | 4.6 | 17 | 22.0 | 46.9 | 8.13 | 1.13 |
| 04-6-11_Zrn15REE@1 | rim | 1.9 | 236 | 0.2 | 0.25 | 0.020 | 8.518 | 0.045 | 1.71 | 1.7 | 1.1 | 5.2 | 21 | 21.7 | 35.4 | 4.38 | 1.09 |
| 04-6-11_Zrn1REE@1 | rim | 18.9 | 376 | 0.3 | 0.39 | 0.304 | 35.330 | 4.729 | 33.73 | 8.0 | 3.6 | 26.4 | 32 | 41.8 | 78.3 | 13.26 | 0.75 |
| | | | | | | | | | | | | | | | | | |
| 05b-6-31b_Zrn1REE@1 | core | 3.1 | 1033 | 1.4 | 0.24 | 0.097 | 33.605 | 1.439 | 13.31 | 11.7 | 4.3 | 30.4 | 83 | 124.2 | 206.0 | 43.18 | 0.70 |
| 05b-6-31b_Zrn2REE@1 | rim | 0.2 | 52 | 0.1 | 0.02 | 0.001 | 0.074 | 0.018 | 0.85 | 2.0 | 0.2 | 4.9 | 7 | 4.4 | 5.3 | 0.87 | 0.20 |
| 05b-6-31b_Zrn7REE@1 | rim | 5.6 | 388 | 0.7 | 0.33 | 0.194 | 14.595 | 2.964 | 25.02 | 18.1 | 4.6 | 31.4 | 45 | 37.0 | 56.7 | 9.18 | 0.59 |
| | | | | | | | | | | | | | | | | | |
| 05-06-3_Zrn15REE@1 | core | 1.8 | 669 | 1.3 | 0.34 | 0.018 | 3.173 | 0.084 | 2.15 | 2.7 | 1.0 | 9.5 | 45 | 93.4 | 161.9 | 36.15 | 0.58 |
| 05-06-3_Zrn15REE@2 | core | 2.0 | 280 | 0.9 | 0.24 | 0.014 | 2.281 | 0.030 | 1.20 | 1.0 | 0.4 | 3.1 | 18 | 40.1 | 80.2 | 17.28 | 0.65 |
| 05-06-3_Zrn15REE@3 | core | 2.0 | 223 | 0.7 | 0.19 | 0.012 | 1.805 | 0.029 | 1.05 | 0.9 | 0.3 | 2.5 | 14 | 30.6 | 64.2 | 13.10 | 0.65 |

| Sample | Location | Sr | Y | Nb | Ba | La | Ce | Pr | Nd | Sm | Eu | Gd | Dy | Er | Yb | Lu | Eu/Eu* |
|---|---|---|---|---|---|---|---|---|---|---|---|---|---|---|---|---|---|
| 04-6-21aZir51a | core | 2.7 | 342 | 1.8 | 0.23 | 0.012 | 1.752 | 0.050 | 1.13 | 1.8 | 0.8 | 9.5 | 35 | 38.5 | 79.5 | 17.13 | 0.60 |
| 04-6-21aZir71a | core | 3.0 | 261 | 0.8 | 0.24 | 0.029 | 2.291 | 0.188 | 1.89 | 2.6 | 1.2 | 12.0 | 25 | 27.0 | 82.6 | 19.54 | 0.67 |
| 04-6-21aZir90 | core | 4.6 | 603 | 1.1 | 0.33 | 0.038 | 3.846 | 0.647 | 3.75 | 5.3 | 2.2 | 32.3 | 247 | 161.6 | 216.9 | 47.79 | 0.51 |
| 04-6-21aZir93 | core | 2.7 | 229 | 0.2 | 0.19 | 0.013 | 1.594 | 0.046 | 2.00 | 2.3 | 0.7 | 10.0 | 25 | 27.2 | 70.9 | 14.82 | 0.45 |
| 04-6-21aZir78 | core | 2.6 | 364 | 0.2 | 0.27 | 0.020 | 1.438 | 0.097 | 2.41 | 2.6 | 1.2 | 10.6 | 32 | 54.6 | 142.8 | 34.13 | 0.70 |
| 04-6-21aZir60a | rim | 2.6 | 130 | 1.5 | 0.25 | 0.022 | 3.110 | 0.192 | 2.17 | 5.2 | 1.4 | 15.1 | 22 | 13.1 | 31.7 | 4.82 | 0.49 |
| 04-6-21aZir60b | rim | 2.5 | 104 | 0.5 | 0.18 | 0.009 | 2.681 | 0.062 | 1.56 | 3.2 | 0.8 | 9.2 | 13 | 9.6 | 26.2 | 2.28 | 0.43 |
| 04-6-21aZir83 | rim | 2.4 | 112 | 0.9 | 0.21 | 0.012 | 2.154 | 0.049 | 2.38 | 3.0 | 1.2 | 12.7 | 20 | 7.3 | 24.6 | 2.92 | 0.59 |
| 04-6-21aZir71b | rim | 2.8 | 133 | 0.4 | 0.19 | 0.012 | 1.680 | 0.062 | 4.31 | 3.6 | 0.8 | 9.0 | 18 | 9.1 | 22.4 | 2.50 | 0.45 |
| 04-6-21aZir95a | rim | 1.9 | 111 | 0.5 | 0.15 | 0.011 | 2.217 | 0.058 | 1.33 | 2.6 | 0.6 | 8.2 | 13 | 9.0 | 22.7 | 2.52 | 0.41 |
| 04-6-21aZir95b | rim | 2.1 | 102 | 0.4 | 0.24 | 0.012 | 2.830 | 0.073 | 1.46 | 2.8 | 0.7 | 8.0 | 13 | 8.2 | 23.5 | 2.35 | 0.43 |
| 04-6-21aZir95c | rim | 1.9 | 80 | 0.5 | 0.12 | 0.008 | 1.737 | 0.039 | 1.04 | 1.9 | 0.4 | 6.2 | 10 | 6.4 | 19.0 | 1.84 | 0.35 |

**Table 2-2.** Garnet REE chemistry determined by LA-ICP-MS.

| Comments | CaO | Sr | Y | Nb | Ba | La | Ce | Pr | Nd | Sm | Eu | Gd | Tb | Dy | Ho | Er | Tm | Yb | Lu | Hf | Yb/Gd |
|---|---|---|---|---|---|---|---|---|---|---|---|---|---|---|---|---|---|---|---|---|---|
| 04-7-1 | 7.16 | <0.76 | 78.7 | <0.08 | <1.03 | 0.05 | 0.84 | 0.48 | 6.92 | 8.35 | 2.28 | 14.1 | 2.63 | 14.5 | 2.67 | 6.32 | 0.85 | 6.26 | 0.75 | 0.36 | 0.55 |
| 04-7-1 | 7.16 | <0.33 | 33.2 | <0.09 | <0.79 | <0.04 | 0.86 | 0.53 | 7.87 | 9.21 | 2.32 | 13.0 | 1.89 | 8.57 | 1.13 | 2.17 | 0.26 | 1.73 | 0.26 | 0.36 | 0.16 |
| 04-7-1 | 7.73 | <0.44 | 78.0 | <0.09 | <1.01 | 0.04 | 0.43 | 0.30 | 5.33 | 8.11 | 2.37 | 17.1 | 3.17 | 17.4 | 2.78 | 6.00 | 0.79 | 5.42 | 0.66 | 0.32 | 0.39 |
| 04-7-1 | 6.87 | <0.32 | 30.2 | <0.06 | <0.79 | 0.08 | 1.27 | 0.50 | 6.61 | 7.42 | 2.31 | 11.0 | 1.55 | 6.95 | 0.94 | 1.63 | 0.23 | 1.38 | 0.16 | 0.29 | 0.16 |
| 04-7-1 | 7.16 | <0.35 | 65.7 | <0.07 | <0.62 | 0.06 | 1.07 | 0.55 | 6.51 | 7.45 | 2.38 | 12.3 | 2.18 | 11.8 | 2.09 | 4.48 | 0.58 | 3.61 | 0.43 | 0.31 | 0.36 |
| 04-7-1 | 7.04 | <0.25 | 80.3 | <0.05 | <0.54 | 0.07 | 1.14 | 0.56 | 6.87 | 7.43 | 2.42 | 13.0 | 2.54 | 14.7 | 2.48 | 5.23 | <0.76 | 4.44 | 0.51 | 0.19 | 0.42 |
| 04-7-1 | 6.84 | <0.31 | 75.7 | <0.06 | <0.42 | <0.07 | 0.58 | 0.37 | 4.98 | 5.85 | 2.06 | 11.2 | 2.19 | 13.5 | 2.51 | 6.11 | 0.79 | 5.63 | 0.70 | 0.34 | 0.62 |
| | | | | | | | | | | | | | | | | | | | | | |
| 05b-6-31b | 2.28 | <0.43 | 80.4 | <0.13 | <1.21 | <0.10 | <0.10 | 0.06 | 1.62 | 5.38 | 1.44 | 17.0 | 3.43 | 17.3 | 2.51 | 5.40 | 0.74 | 5.09 | 0.78 | 0.33 | 0.37 |
| 05b-6-31b | 3.03 | <0.47 | 499 | <0.06 | <0.88 | <0.07 | 0.07 | 0.07 | 2.07 | 7.19 | 1.93 | 23.9 | 9.12 | 81.2 | 16.7 | 37.4 | 4.33 | 24.3 | 2.78 | 0.35 | 1.26 |
| 05b-6-31b | 2.8 | <0.38 | 866 | <0.10 | <0.86 | <0.08 | <0.06 | <7.25 | 1.52 | 5.56 | 1.65 | 19.6 | 7.15 | 83.8 | 29.6 | 120 | 20.2 | 147 | 21.0 | 0.30 | 9.26 |
| 05b-6-31b | 3.42 | <0.49 | 867 | <0.13 | <0.68 | <0.07 | 0.05 | 0.05 | 1.95 | 6.08 | 1.84 | 24.3 | 9.18 | 94.7 | 28.9 | 103 | 16.2 | 113 | 14.7 | 0.43 | 5.74 |
| 05b-6-31b | 3.66 | <0.35 | 498 | <0.18 | <1.25 | <0.13 | 0.10 | 0.09 | 2.54 | 6.68 | 2.45 | 27.9 | 9.50 | 82.2 | 17.1 | 40.7 | 5.02 | 29.5 | 3.62 | 2.16 | 1.31 |
| 05b-6-31b | 3.07 | <0.34 | 351 | <0.10 | <0.37 | <0.04 | 0.08 | 0.13 | 3.10 | 7.37 | 2.13 | 22.1 | 7.43 | 59.0 | 12.4 | 32.0 | 4.61 | 32.3 | 4.82 | 0.41 | 1.81 |
| 05b-6-31b | 2.75 | <0.33 | 230 | <0.09 | <0.52 | <0.04 | 0.16 | 0.15 | 2.62 | 3.85 | 1.48 | 17.1 | 5.80 | 43.3 | 8.29 | 18.6 | 2.22 | 14.7 | 2.06 | 0.52 | 1.06 |
| 05b-6-31b | 2.01 | <0.38 | 121 | <0.09 | <0.62 | <0.05 | <0.07 | 0.03 | 0.61 | 3.40 | 1.00 | 16.8 | 4.02 | 23.9 | 4.02 | 9.18 | 1.24 | 8.55 | 1.33 | 0.30 | 0.63 |
| | | | | | | | | | | | | | | | | | | | | | |
| 04-6-11 | 3.65 | <0.32 | 377 | <0.08 | <1.22 | <0.05 | 0.13 | 0.11 | 1.70 | 4.39 | 2.65 | 18.1 | 5.59 | 51.6 | 14.6 | 46.9 | 7.52 | 53.8 | 7.55 | 0.46 | 3.68 |
| 04-6-11 | 3.57 | <0.34 | 377 | <0.04 | <0.92 | <0.10 | 0.14 | <0.07 | 1.53 | 3.93 | 2.44 | 17.0 | 5.33 | 50.7 | 14.1 | 43.6 | 6.73 | 49.2 | 6.93 | 0.47 | 3.58 |
| 04-6-11 | 3.57 | <0.33 | 373 | <0.08 | <0.76 | <0.04 | 0.13 | 0.08 | 1.75 | 4.33 | 2.41 | 16.6 | 5.26 | 50.2 | 13.6 | 42.4 | 6.25 | 44.8 | 5.79 | 0.47 | 3.34 |
| 04-6-11 | 3.58 | <0.32 | 416 | <0.10 | <1.19 | <0.05 | 0.10 | 0.08 | 1.58 | 4.27 | 2.40 | 17.5 | 5.79 | 55.4 | 15.3 | 50.2 | 7.87 | 56.1 | 8.27 | 0.55 | 3.97 |
| 04-6-11 | 3.58 | <0.30 | 473 | <0.06 | <0.34 | <0.04 | 0.12 | 0.09 | 1.98 | 5.30 | 2.83 | 20.3 | 6.70 | 65.1 | 17.9 | 57.8 | 8.97 | 65.8 | 9.19 | 0.59 | 4.02 |
| 04-6-11 | 3.59 | <0.41 | 387 | <0.08 | <0.64 | <0.05 | 0.14 | 0.09 | 1.92 | 4.50 | 2.28 | 18.1 | 5.66 | 54.5 | 15.2 | 48.6 | 7.51 | 54.3 | 7.87 | 0.53 | 3.70 |
| 04-6-11 | 3.58 | <0.37 | 300 | <0.08 | <0.65 | <0.08 | 0.11 | 0.06 | 1.64 | 3.81 | 2.07 | 14.0 | 4.34 | 40.8 | 10.4 | 31.8 | 4.84 | 34.8 | 4.47 | 0.17 | 3.08 |
| 04-6-11 | 3.62 | <0.38 | 390 | <0.05 | <0.65 | <0.08 | <0.07 | 0.06 | 1.31 | 4.21 | 2.19 | 15.8 | 5.18 | 51.9 | 15.0 | 50.7 | 7.87 | 59.5 | 8.77 | 0.48 | 4.65 |
| 04-6-11 | 3.69 | <0.31 | 678 | <0.06 | <0.38 | <0.10 | 0.16 | 0.15 | 2.97 | 7.56 | 4.33 | 30.4 | 9.47 | 87.5 | 24.4 | 77.0 | 12.0 | 86.3 | 11.7 | 0.53 | 3.51 |
| | | | | | | | | | | | | | | | | | | | | | |
| 04-6-21 | 1.73 | <0.33 | 66.7 | <0.06 | <0.44 | <0.04 | 0.07 | 0.06 | 1.37 | 3.35 | 0.88 | 8.93 | 1.85 | 11.4 | 2.36 | 6.24 | 0.92 | 6.89 | 0.87 | 0.47 | 0.95 |
| 04-6-21 | 2.4 | <0.33 | 341 | <0.07 | 1.03 | <0.03 | 0.06 | 0.04 | 0.97 | 4.69 | 1.28 | 16.3 | 6.07 | 56.2 | 13.5 | 37.5 | 5.29 | 35.4 | 4.97 | 3.54 | 2.69 |
| 04-6-21 | 1.89 | <0.33 | 132 | <0.10 | <0.40 | <0.06 | <0.06 | <0.03 | 0.31 | 4.20 | 0.95 | 14.5 | 3.08 | 20.0 | 4.74 | 15.5 | 2.58 | 19.7 | 2.86 | 0.35 | 1.69 |
| 04-6-21 | 1.83 | <0.24 | 139 | <0.03 | <0.36 | <0.03 | <0.03 | <0.02 | 0.50 | 4.16 | 1.09 | 14.8 | 3.14 | 21.5 | 5.00 | 16.1 | 2.74 | 21.8 | 3.31 | 3.85 | 1.83 |
| 04-6-21 | 1.83 | <0.25 | 138 | <0.04 | <0.30 | <0.02 | 0.03 | <0.02 | 0.74 | 4.46 | 0.98 | 13.7 | 2.95 | 20.5 | 5.09 | 15.6 | 2.64 | 21.0 | 2.92 | 0.27 | 1.89 |
| 04-6-21 | 1.82 | <0.30 | 153 | <0.09 | <0.35 | <0.04 | <0.03 | <0.02 | 0.54 | 4.11 | 1.01 | 14.2 | 3.13 | 22.4 | 5.71 | 16.9 | 2.65 | 17.9 | 2.31 | 0.36 | 1.55 |
| 04-6-21 | 1.84 | <0.33 | 148 | <0.09 | <0.41 | <0.05 | 0.06 | 0.04 | 0.89 | 4.45 | 0.98 | 12.7 | 2.64 | 20.4 | 5.39 | 17.6 | 2.79 | 20.8 | 3.10 | 0.31 | 2.01 |
| 04-6-21 | 1.96 | <0.28 | 152 | <0.08 | <0.69 | <0.09 | <0.04 | <0.05 | 0.51 | 3.88 | 0.95 | 17.2 | 4.40 | 27.0 | 5.81 | 16.3 | 2.42 | 18.4 | 2.62 | 0.47 | 1.32 |

of REE to the crystallising phase, and the partitioning of REE between these two phases (*e.g.*, Hoskin & Schaltegger 2003; Harley & Kelly 2007; Rubatto & Hermann 2007).

There are currently two contrasting schools of thought regarding the degree to which the REE, in particular the HREE, are partitioned between garnet and zircon. Using distribution coefficients empirically determined for zircon and garnet from ultrahigh temperature granulites, one group advocates for a flat $D_{REE(Zrn/Grt)}$ pattern at values near unity for the HREE when zircon and garnet are formed in equilibrium (*e.g.*, Hokada & Harley 2004; Kelly & Harley 2005; Harley & Kelly 2007). In contrast, using distribution coefficients empirically determined for zircon that crystallized from granulite facies rocks at ~800˚C, the other group advocates for positively sloping $D_{REE(Zrn/Grt)}$ patterns with values ranging between 0.7–2.3 for Gd and 6.3–24 for Lu when zircon and garnet are formed in equilibrium (*e.g.*, Rubatto 2002; Hermann & Rubatto 2003; Rubatto & Hermann 2003; Buick *et al*. 2006; Rubatto *et al*. 2006). Rubatto & Hermann (2007) present experimental data that suggest a temperature dependence for the partitioning of the HREE between garnet and zircon that could reconcile the difference between the two schools of thought. As the nappes in the Southern Brasília Belt were subjected to high-pressure granulite facies conditions at temperatures similar to the samples used in the empirical determinations of the second group, and the REE partitioning between garnet and zircon could be temperature dependent, in this study I compare REE data for Southern Brasília Belt zircon and garnet to the $D_{REE(Zrn/Grt)}$ patterns presented by the second group of authors and by Rubatto & Hermann (2007).

Zircon formed in an igneous environment lacking a competing phase that strongly sequesters REE will exhibit enrichment in the HREE and depletion in the light REE (LREE: La-Pr) relative to chondritic abundances. If unaltered, these igneous zircons will typically show a steeply rising slope between the LREE and HREE, and will typically have positive Ce and negative Eu anomalies. Zircon formed in the presence of a melt that has not crystallized a phase that strongly sequesters REE will display similar REE patterns to igneous zircon (*e.g.,* Schaltegger *et al.* 1999; Rubatto *et al.* 2001). The crystallization of phases with strong affinities for the REE, such as garnet, will lead to REE depletion in the melt; zircon crystallized from REE-depleted melt may exhibit similarly depleted REE patterns.

Metamorphic or altered zircons deviate from these patterns (Rubatto 2002; Whitehouse & Platt 2003; Kelly & Harley 2005; Harley & Kelly 2007). The REE patterns of zircon formed concurrently with garnet will be relatively depleted in HREE due to the preference of the HREE for garnet over zircon (Rubatto 2002; Whitehouse & Platt 2003; Kelly & Harley 2005), and competition with monazite may lead to depletion in the LREE (Bea & Montero 1999). Metamorphic zircon that grew in equilibrium with garnet typically displays a flat to depleted HREE pattern. Sub-solidus metamorphic zircon grown in the absence of a competing phase such as garnet will exhibit an enriched HREE pattern.

Zircon from sample 04-7-1 from the Socorro–Guaxupé Nappe typically has steep positively sloping normalized REE patterns (Fig. 2-5a), with most $Yb_N/Gd_N$ ratios between 14.4 and 34.1. Small negative Eu anomalies are present (Eu/Eu* = 0.46–0.86), Th/U ratios range from 0.41 to 4.47 and Y concentrations range from 98

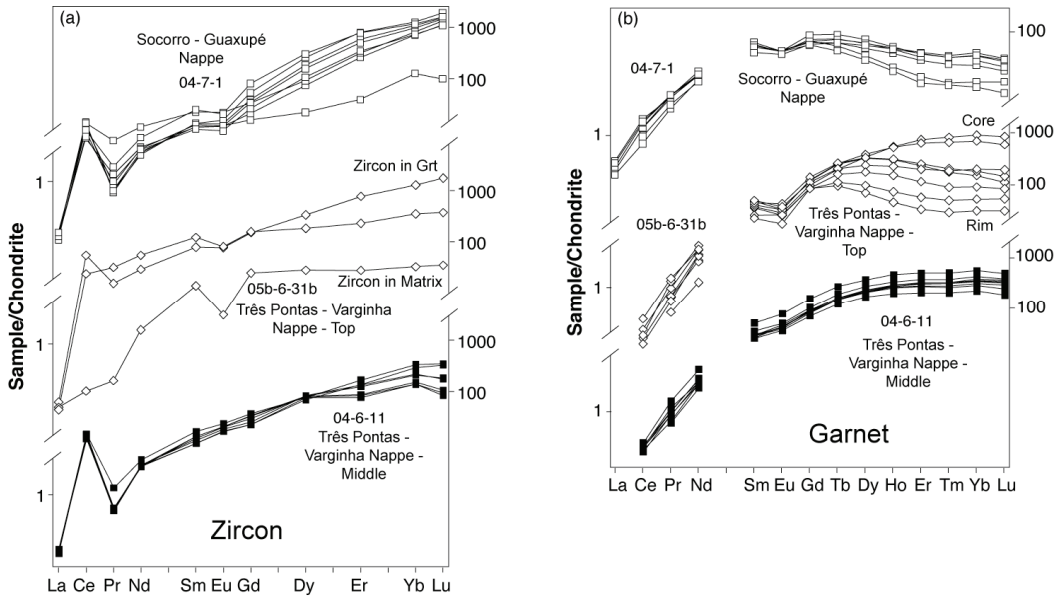


**Figure 2-5.** Chondrite normalized rare earth element patterns (normalization after McDonough & Sun 1995). (a) REE patterns for zircon from the Socorro–Guaxupé Nappe and zircon from the top, middle and bottom of the Três Pontas–Varginha (TPV) Nappe. (b) REE patterns for garnet for the same samples shown in (a).

to 1030 ppm. One analysis yields a flatter normalized REE patterns (Yb/Gd = 8.1). Garnet from this sample has upwardly convex normalized REE patterns with negatively sloping normalized HREE patterns ($Yb_N/Gd_N$ = 0.16-0.62; Fig. 2-5b) and Y concentrations between 30 and 80 ppm. $D_{REE(Zrn/Grt)}$ values increase from ~0.2 for the MREE to ~50 for the HREE (Fig. 2-6).

Zircon from sample 05-06-3 from the Socorro–Guaxupé Nappe has steep positively sloping normalized REE patterns, with $Yb_N/Gd_N$ ratios between 21.0 and 32.2, negative Eu anomalies (Eu/Eu* = 0.58-0.65) and Y concentrations between 223 and 669 ppm.

Zircon from sample 04-6-11, from near the structural middle of the Três Pontas–Varginha Nappe, is contained in leucosome and occurs in close petrographic association with ilmenite. These zircons have steep positively sloping normalized

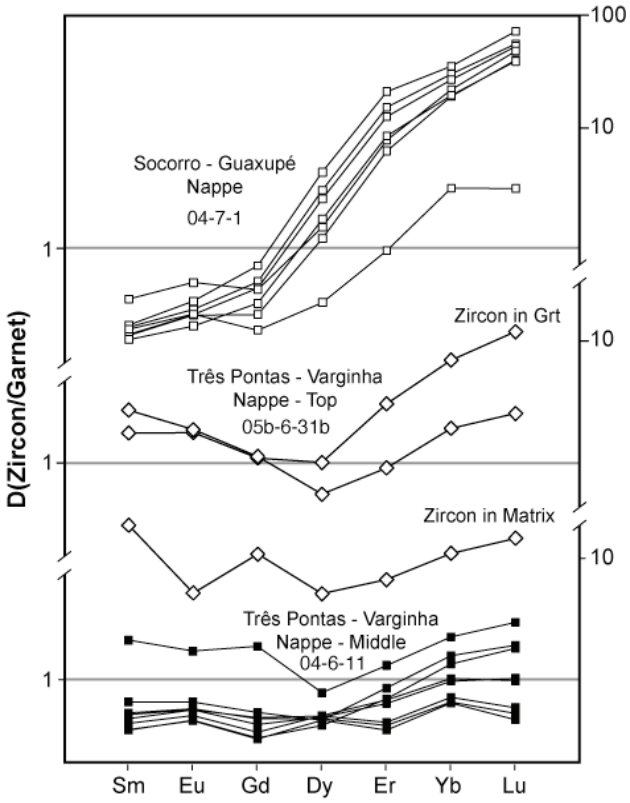


**Figure 2-6.** HREE distribution coefficients between zircon and garnet. Zircon and garnet exhibit $D_{REE(Zrn/Grt)}$ values consistent with zircon growth in equilibrium with garnet in sample 04-7-1, and for a zircon in the garnet mantle in sample 05b-6-31b. $D_{REE(Zrn/Grt)}$ values for zircon in sample 04-6-11 are inconsistent with growth of zircon in equilibrium with garnet.

REE patterns ($Yb_N/Gd_N$ = 3.7-14.8; Fig. 2-5a) with small Eu anomalies (Eu/Eu* = 0.75-1.13), Th/U ratios between 0.06 and 0.21 and Y concentrations between 171 and 376 ppm. Garnet in this sample is 5-10 mm in diameter and located in the leucosome; garnet has upwardly convex normalized REE patterns with flat to slightly positively sloping HREE patterns ($Yb_N/Gd_N$ = 3.08-4.65; Fig. 2-5b) and Y concentrations between 67 and 341 ppm. Zircon and garnet rim compositions yield $D_{REE(Zrn/Grt)}$ values close to unity (Fig. 2-6).

Zircon from sample 05b-6-31b from near the structural top of the Três Pontas–Varginha Nappe occurs in close petrographic association with ilmenite. Only

three zircons were large enough to allow for REE analysis in addition to U–Pb analysis. The normalized REE patterns (Fig. 2-5a) range from flat ($Yb_N/Gd_N$ = 1.1) with a large Eu anomaly (Eu/Eu* = 0.70) and an Y concentration of 1033 ppm to steeply sloping ($Yb_N/Gd_N$ = 6.8) with a smaller Eu anomaly (Eu/Eu* = 0.20) and an Y concentration of 52 ppm. Garnet in this sample has upwardly convex normalized REE patterns (Fig. 2-5b) that range from steeply positively sloping ($Yb_N/Gd_N$ = 9.26) in garnet cores to moderately negatively sloping ($Yb_N/Gd_N$ = 0.37) in garnet rims. Y concentrations range from 80 to 867 ppm. Zircon and rims of garnet yield $D_{REE(Zrn/Grt)}$ values close to unity for the MREE increasing to ~10 for the HREE (Fig. 2-6).

*Trace Element Thermometry*

Titanium was measured in zircon (Table 2-3) for one sample from the Socorro–Guaxupé Nappe (04-7-1), and three samples from the Três Pontas–Varginha Nappe (05b-6-31b, 04-6-11 and 04-6-21). The assemblage zircon–rutile–quartz buffers the titanium partitioning in sample 05b-6-31b. Samples 04-6-11, 04-6-21 and 04-7-1 contain quartz and ilmenite, but not rutile, which leaves the $a_{TiO2}$ unconstrained. Although Watson *et al.* (2006) have argued that $a_{TiO2}$ is likely to be high, possibly close to 1, this is an upper limit and the $a_{TiO2}$ could be much lower. In this case, the Ti-in-zircon temperatures will provide a minimum estimate for these samples (E.J. Essene, pers. comm. 2009). Temperatures were calculated using the Ferry & Watson (2007) Ti-in-zircon thermometer calibration for zircon crystallized at 1 GPa. I did not incorporate a pressure correction into the temperature calculation;

**Figure 2-3.** Ti-in-zircon thermometry data determined by EPMA.

| Comment | TiO2 | SiO2 | ZrO2 | HfO2 | Total | T(˚C) | 2σ unc[(a)] |
|---|---|---|---|---|---|---|---|
| 04-7-1_CORE_20 | 0.0031 | 31.8 | 66.2 | 1.19 | 99.1 | 808 | 64 |
| 04-7-1_CORE_21 | 0.0033 | 31.8 | 66.1 | 1.19 | 99.1 | 814 | 59 |
| 04-7-1_CORE_22 | 0.0035 | 31.9 | 66.5 | 1.31 | 99.6 | 821 | 55 |
| 04-7-1_CORE_23 | 0.0039 | 31.8 | 66.2 | 1.23 | 99.2 | 832 | 57 |
| 04-7-1_CORE_1 | 0.0065 | 31.1 | 65.9 | 1.17 | 98.2 | 892 | 47 |
| 04-7-1_CORE_2 | 0.0075 | 31.1 | 66.4 | 1.16 | 98.7 | 910 | 50 |
| 04-7-1_CORE_3 | 0.0082 | 31.0 | 66.5 | 1.15 | 98.7 | 921 | 44 |
| 04-7-1_CORE_4 | 0.0086 | 31.0 | 66.8 | 1.04 | 98.9 | 927 | 45 |
| 04-7-1_CORE_6 | 0.0095 | 30.9 | 66.5 | 1.13 | 98.5 | 941 | 43 |
| 04-7-1_CORE_5 | 0.0100 | 30.9 | 66.5 | 1.02 | 98.5 | 947 | 43 |
| 04-7-1_RIM_18 | 0.0023 | 30.9 | 65.9 | 1.20 | 98.1 | 777 | 54 |
| 04-7-1_RIM_16 | 0.0027 | 30.9 | 65.8 | 1.20 | 98.0 | 793 | 60 |
| 04-7-1_RIM_27 | 0.0030 | 31.8 | 66.5 | 1.19 | 99.5 | 804 | 52 |
| 04-7-1_RIM_19 | 0.0034 | 31.0 | 66.3 | 1.14 | 98.4 | 817 | 58 |
| 04-7-1_RIM_25 | 0.0034 | 31.8 | 65.3 | 1.24 | 98.3 | 817 | 47 |
| 04-7-1_RIM_26 | 0.0035 | 31.9 | 65.8 | 1.31 | 99.0 | 821 | 56 |
| 04-7-1_RIM_28 | 0.0035 | 31.8 | 65.7 | 1.26 | 98.7 | 821 | 64 |
| 04-7-1_RIM_17 | 0.0037 | 30.9 | 66.1 | 1.22 | 98.2 | 827 | 63 |
| 04-7-1_RIM_24 | 0.0051 | 31.7 | 64.7 | 2.41 | 98.8 | 863 | 44 |
| 04-7-1_RIM_10 | 0.0089 | 31.0 | 66.5 | 1.07 | 98.6 | 932 | 46 |
| 04-7-1_RIM_11 | 0.0108 | 31.0 | 66.7 | 1.12 | 98.8 | 958 | 47 |
| 04-7-1_RIM_13 | 0.0119 | 31.1 | 66.5 | 1.11 | 98.7 | 971 | 44 |
| 04-7-1_RIM_12 | 0.0120 | 31.1 | 66.4 | 1.10 | 98.6 | 972 | 43 |
| 04-7-1_RIM_9 | 0.0139 | 31.0 | 66.9 | 1.12 | 99.0 | 993 | 44 |
| 04-7-1_RIM_14 | 0.0140 | 31.2 | 65.6 | 2.00 | 98.9 | 994 | 41 |
| 04-7-1_RIM_8 | 0.0141 | 31.0 | 67.1 | 1.19 | 99.3 | 996 | 42 |
| 04-7-1_RIM_7 | 0.0170 | 31.0 | 66.2 | 1.18 | 98.4 | 1023 | 41 |
| 05b-6-31b_CORE_26 | 0.0019 | 31.7 | 66.2 | 0.93 | 98.8 | 758 | 58 |
| 05b-6-31b_CORE_1 | 0.0024 | 32.0 | 66.4 | 1.43 | 99.8 | 781 | 51 |
| 05b-6-31_Zrn1 | 0.0025 | 31.5 | 65.9 | 1.44 | 98.8 | 785 | 58 |
| 05b-6-31b_CORE_2 | 0.0029 | 32.0 | 66.0 | 1.49 | 99.5 | 801 | 52 |
| 05b-6-31b_CORE_22 | 0.0030 | 31.7 | 66.5 | 0.98 | 99.2 | 804 | 52 |
| 05b-6-31b_CORE_23 | 0.0030 | 31.7 | 66.0 | 1.38 | 99.2 | 804 | 51 |
| 05b-6-31b_CORE_27 | 0.0030 | 31.7 | 65.6 | 1.02 | 98.3 | 804 | 51 |
| 05b-6-31b_CORE_3 | 0.0030 | 32.0 | 65.9 | 1.49 | 99.4 | 804 | 50 |
| 05b-6-31b_CORE_24 | 0.0031 | 31.7 | 66.4 | 1.21 | 99.3 | 808 | 60 |
| 05b-6-31b_CORE_28 | 0.0031 | 31.7 | 66.9 | 1.42 | 100.0 | 808 | 51 |
| 05b-6-31b_CORE_25 | 0.0040 | 31.7 | 66.2 | 1.13 | 99.0 | 835 | 57 |
| 05b-6-31b_CORE_12 | 0.0214 | 30.9 | 66.6 | 1.46 | 99.0 | 1059 | 41 |
| 05b-6-31b_RIM_17 | 0.0023 | 31.8 | 66.2 | 1.44 | 99.4 | 777 | 52 |
| 05b-6-31b_RIM_19 | 0.0023 | 31.6 | 66.3 | 1.40 | 99.2 | 777 | 52 |
| 05b-6-31b_RIM_5 | 0.0024 | 31.9 | 65.6 | 1.46 | 99.0 | 781 | 55 |
| 05b-6-31b_RIM_4 | 0.0029 | 32.0 | 66.3 | 1.45 | 99.8 | 801 | 58 |
| 05b-6-31b_RIM_18 | 0.0030 | 31.6 | 66.3 | 1.40 | 99.3 | 804 | 55 |
| 05b-6-31b_RIM_6 | 0.0039 | 32.0 | 66.1 | 1.42 | 99.6 | 832 | 60 |
| 05b-6-31b_RIM_21 | 0.0045 | 31.8 | 66.7 | 1.43 | 99.9 | 848 | 50 |

| Comment | TiO2 | SiO2 | ZrO2 | HfO2 | Total | T(˚C) | 2σ unc[a] |
|---|---|---|---|---|---|---|---|
| 05b-6-31b_RIM_20 | 0.0051 | 31.7 | 66.2 | 1.44 | 99.3 | 863 | 49 |
| 05b-6-31b_RIM_8 | 0.0134 | 30.8 | 66.5 | 1.47 | 98.8 | 988 | 42 |
| 05b-6-31b_RIM_7 | 0.0199 | 30.6 | 66.3 | 1.45 | 98.4 | 1048 | 41 |
| 04-6-11_CORE_11 | 0.0022 | 32.8 | 66.6 | 1.15 | 100.5 | 773 | 63 |
| 04-6-11_CORE_12 | 0.0023 | 32.8 | 67.0 | 1.26 | 101.1 | 777 | 52 |
| 04-6-11_CORE_5 | 0.0026 | 32.0 | 66.4 | 1.26 | 99.7 | 789 | 68 |
| 04-6-11_CORE_8 | 0.0026 | 32.7 | 66.1 | 1.31 | 100.1 | 789 | 49 |
| 04-6-11_CORE_6 | 0.0031 | 31.9 | 67.0 | 1.23 | 100.2 | 808 | 60 |
| 04-6-11_CORE_13 | 0.0035 | 32.5 | 66.5 | 1.26 | 100.2 | 821 | 58 |
| 04-6-11_CORE_7 | 0.0035 | 31.7 | 65.8 | 1.03 | 98.5 | 821 | 61 |
| 04-6-11_CORE_10 | 0.0038 | 34.3 | 58.6 | 0.88 | 93.8 | 830 | 68 |
| 04-6-11_CORE_9 | 0.0048 | 32.5 | 65.9 | 1.05 | 99.5 | 856 | 48 |
| 04-6-11_RIM_3 | 0.0020 | 48.9 | 0.0 | 0.00 | 48.9 | 763 | 90 |
| 04-6-11_RIM_22 | 0.0021 | 32.9 | 66.9 | 1.25 | 101.0 | 768 | 59 |
| 04-6-11_RIM_4 | 0.0021 | 32.0 | 66.8 | 1.21 | 100.0 | 768 | 62 |
| 04-6-11_RIM_21 | 0.0023 | 32.8 | 66.5 | 1.27 | 100.6 | 777 | 53 |
| 04-6-11_RIM_2 | 0.0025 | 32.1 | 67.1 | 1.23 | 100.4 | 785 | 54 |
| 04-6-11_RIM_16 | 0.0027 | 32.8 | 66.7 | 1.23 | 100.7 | 793 | 57 |
| 04-6-11_RIM_15 | 0.0028 | 32.9 | 66.5 | 1.24 | 100.7 | 797 | 60 |
| 04-6-11_Zrn1 | 0.0028 | 31.7 | 66.4 | 1.20 | 99.3 | 797 | 57 |
| 04-6-11_RIM_1 | 0.0029 | 31.9 | 66.7 | 1.23 | 99.8 | 801 | 70 |
| 04-6-11_RIM_14 | 0.0030 | 33.0 | 67.0 | 1.27 | 101.3 | 804 | 60 |
| 04-6-11_RIM_20 | 0.0035 | 32.8 | 66.4 | 1.25 | 100.4 | 821 | 52 |
| 04-6-11_RIM_17 | 0.0037 | 32.8 | 66.1 | 1.24 | 100.1 | 827 | 50 |
| 04-6-11_RIM_18 | 0.0043 | 32.8 | 67.1 | 1.24 | 101.1 | 843 | 52 |
| 04-6-11_RIM_19 | 0.0046 | 32.7 | 66.2 | 1.24 | 100.1 | 851 | 50 |
| 04-6-11_RIM_27 | 0.0062 | 31.3 | 65.6 | 1.26 | 98.2 | 886 | 47 |
| 04-6-11_RIM_26 | 0.0113 | 31.7 | 65.7 | 1.31 | 98.7 | 964 | 44 |
| 04-6-11_RIM_25 | 0.0148 | 31.6 | 64.9 | 1.30 | 97.9 | 1003 | 45 |
| 04-6-21_CORE_18 | 0.0022 | 31.0 | 66.1 | 1.45 | 98.6 | 773 | 76 |
| 04-6-21_CORE_1 | 0.0028 | 31.1 | 65.8 | 1.26 | 98.1 | 797 | 57 |
| 04-6-21_CORE_15 | 0.0028 | 31.2 | 66.3 | 1.43 | 98.9 | 797 | 56 |
| 04-6-21_CORE_16 | 0.0028 | 31.1 | 66.6 | 1.49 | 99.2 | 797 | 61 |
| 04-6-21_CORE_17 | 0.0031 | 31.0 | 66.4 | 1.46 | 98.9 | 808 | 68 |
| 04-6-21_CORE_2 | 0.0031 | 31.6 | 66.8 | 1.33 | 99.8 | 808 | 58 |
| 04-6-21_CORE_3 | 0.0031 | 31.3 | 65.7 | 1.30 | 98.3 | 808 | 55 |
| 04-6-21_CORE_4 | 0.0034 | 31.3 | 66.0 | 1.29 | 98.5 | 817 | 55 |
| 04-6-21_CORE_21 | 0.0108 | 32.0 | 66.5 | 1.34 | 99.8 | 958 | 43 |
| 04-6-21_CORE_22 | 0.0111 | 32.0 | 66.5 | 1.32 | 99.8 | 962 | 43 |
| 04-6-21_CORE_19 | 0.0116 | 32.0 | 66.6 | 1.34 | 100.0 | 968 | 43 |
| 04-6-21_CORE_20 | 0.0118 | 32.1 | 66.1 | 1.31 | 99.5 | 970 | 44 |
| 04-6-21_CORE_23 | 0.0147 | 32.0 | 66.4 | 1.34 | 99.7 | 1002 | 42 |
| 04-6-21_RIM_5 | 0.0019 | 31.3 | 65.7 | 1.33 | 98.4 | 758 | 59 |
| 04-6-21_RIM_12 | 0.0021 | 31.1 | 66.4 | 1.36 | 98.8 | 768 | 56 |
| 04-6-21_RIM_6 | 0.0024 | 31.4 | 66.1 | 1.34 | 98.9 | 781 | 52 |
| 04-6-21_RIM_11 | 0.0027 | 31.3 | 66.5 | 1.31 | 99.1 | 793 | 55 |
| 04-6-21_RIM_14 | 0.0027 | 31.4 | 66.2 | 1.33 | 98.9 | 793 | 54 |
| 04-6-21_RIM_9 | 0.0028 | 31.3 | 65.8 | 1.33 | 98.5 | 797 | 58 |

| Comment | TiO2 | SiO2 | ZrO2 | HfO2 | Total | T(˚C) | 2σ unc[(a)] |
|---|---|---|---|---|---|---|---|
| 04-6-21_RIM_10 | 0.0031 | 31.2 | 66.6 | 1.31 | 99.1 | 808 | 64 |
| 04-6-21_RIM_7 | 0.0032 | 31.5 | 66.0 | 1.31 | 98.8 | 811 | 54 |
| 04-6-21_RIM_13 | 0.0035 | 31.2 | 66.7 | 1.28 | 99.2 | 821 | 57 |
| 04-6-21_RIM_8 | 0.0038 | 31.4 | 66.3 | 1.33 | 99.0 | 830 | 54 |
| 04-6-21_RIM_28 | 0.0134 | 32.0 | 66.4 | 1.34 | 99.7 | 988 | 43 |
| 04-6-21_RIM_27 | 0.0135 | 32.2 | 66.6 | 1.36 | 100.1 | 989 | 43 |
| 04-6-21_RIM_25 | 0.0152 | 32.1 | 66.9 | 1.34 | 100.4 | 1007 | 41 |

(a) uncertainty based on propogation of counting statistics through the temperature equation.

however, if the pressure correction of Ferriss *et al*. (2008) is used, the temperatures presented here could be ~50˚C higher for a pressure of 1.5 GPa.

Temperature measurements for each zircon population are plotted as box and whisker plots, where the box represents the middle 50% of the data, the line through the box represents the median of the data, the whiskers extend to 95% of the data and dots represent outliers. This method provides a first pass way of analyzing the distribution of the data. A non-normal distribution of data has implications for the crystallization history of zircon. The sample mean and standard deviation of a skewed dataset would be shifted away from the peak of the distribution, potentially yielding a geologically meaningless temperature. Here I report the interquartile range, which represents the middle 50% of the data between the 25$^{th}$ and 75$^{th}$ percentiles.

***Socorro–Guaxupé Nappe***

In sample 04-7-1 (Fig. 2-7), zircon cores records temperatures ranging from 947˚C to 808˚C, with an interquartile range of 925˚C to 823˚C. Zircon rims record temperatures ranging from 1023˚C to 777˚C, with an interquartile range of 972˚C to 817˚C. Although these two populations show a broad distribution with the middle

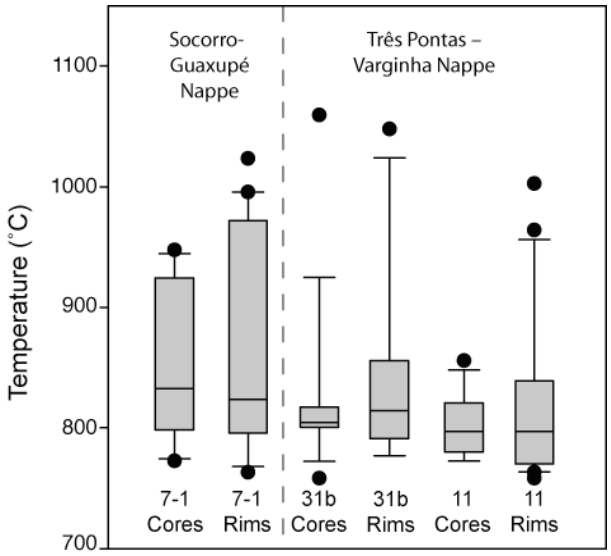


**Figure 2-7.** Ti-in-zircon temperatures for zircon from samples 04-7-1 (7-1), 05b-6-31b (31b) and 04-6-11 (11) presented as box-and-whisker plots.

50% of data occurring over a temperature range of ~100˚C to ~150˚C, in both cases the data are strongly skewed to the lower end of this range.

***Três Pontas–Varginha Nappe***

Zircon cores from sample 05b-6-31b (Fig. 2-7) record temperatures ranging from 1059˚C to 758˚C, with an interquartile range of 807˚C to 797˚C. Zircon rims record temperatures of 1048˚C to 777˚C, with an interquartile range of 859˚C to 786˚C. In both cases, the middle 50% of the data occur over a narrow range, and these data are strongly skewed to the lower end of the temperature scale, with the bottom 75% of the data occurring over a range of ~50˚C for cores and ~80˚C for rims, respectively.

Zircon cores from sample 04-6-11 (Fig. 2-7) record temperatures ranging from 856˚C to 773˚C, with an interquartile range of 821˚C to 789˚C. These data are close to normally distributed. Zircon rims record temperatures ranging from 1003˚C to 763˚C, with an interquartile range of 843˚C to 785˚C. These data are skewed

towards the lower end of the temperature scale, with the bottom 75% of the data occurring over a range of ~80˚C.

*Uranium-Lead Zircon Chronology*

Zircon from two samples from the Socorro–Guaxupé Nappe (04-7-1 and 05-06-3), one sample from the retrograded eclogite (05b-13-13) and three samples from the Três Pontas–Varginha Nappe (05b-6-31b, 04-6-11 and 05b-6-110/108) was dated *in situ* by HR-SIMS to preserve the petrographic context (Table 2-4). The zircons for dating were chosen only after examination of petrographic context via backscattered electron and cathodoluminescence imaging. Preference was given to inclusion and crack free zircons with cathodoluminescence zones large enough to contain a SIMS spot. In all samples except 05b-6-110/108, zircon was chosen that is either adjacent to ilmenite grains or within close (<1 mm) proximity to ilmenite grains.

A combined total of 49 analyses were obtained from the 6 samples (The unreduced dataset is given in Table A-1). Dates were calculated from $^{206}Pb/^{238}U$, $^{207}Pb/^{235}U$ and $^{207}Pb/^{206}U$ isotopic data using Isoplot (Ludwig 1999). Data were reduced to consider only analyses that were less than 10% discordant. Ages were calculated by regressing single populations of dates using Isoplot, and uncertainties are presented as 95% confidence on the mean. The $^{206}Pb/^{238}U$ ages are presented here to avoid problems associated with measuring small amounts of $^{207}Pb$ in relatively young (Neoproterozoic) zircons (Table 2-5).

The reduced dataset for sample 04-7-1 from the Socorro–Guaxupé Nappe yields seven $^{206}Pb/^{238}U$ zircon dates ranging from 666±45 Ma to 590±47 Ma (Fig. 2-8), leading to an age of 622±28 Ma (MSWD = 1.4, pfit = 0.22). The second sample

**Table 2-4.** U-Pb zircon geochronologic data. Samples 04-7-1 and 05-06-3 from the Socorro-Guaxupé Nappe; Sample 05b-13-13 from the retrograded eclogite; Samples 05b-6-31b and 04-6-11 from the Tres Pontas - Varginha Nappe.

| | | | | | Isotope Ratio | | | | | | Age (Ma) | | | | | |
|---|---|---|---|---|---|---|---|---|---|---|---|---|---|---|---|---|
| Sample Name | U (ppm) | Th (ppm) | Th/U | $^{206}Pb/^{204}Pb$ | $^{206}Pb/^{238}U$ | err (2σ) | $^{207}Pb/^{235}U$ | err (2σ) | $^{207}Pb/^{206}Pb$ | err (2σ) | $^{206}Pb/^{238}U$ | 2σ | $^{207}Pb/^{235}U$ | 2σ | $^{207}Pb/^{206}Pb$ | 2σ | Discordance | Rho |
| *Socorro-Guaxupé Nappe* | | | | | | | | | | | | | | | | | | |
| 04-7-1_Zrn2@3 | 15 | 54 | 3.62 | 1026 | 0.0959 | 0.0076 | 0.80 | 0.18 | 0.0599 | 0.0014 | 590 | ±47 | 597 | ±133 | 601 | ±52 | 2% | 0.6944 |
| 04-7-1_Zrn5@1 | 30 | 132 | 4.47 | 2166 | 0.1000 | 0.0098 | 0.85 | 0.14 | 0.0607 | 0.0010 | 614 | ±60 | 624 | ±103 | 628 | ±34 | 2% | 0.8929 |
| 04-7-1_Zrn5@2 | 175 | 96 | 0.55 | 15710 | 0.1089 | 0.0074 | 0.94 | 0.09 | 0.0628 | 0.0004 | 666 | ±45 | 675 | ±63 | 700 | ±14 | 5% | 0.9617 |
| 04-7-1_Zrn23@1 | 112 | 46 | 0.41 | 8452 | 0.1048 | 0.0088 | 0.91 | 0.09 | 0.0626 | 0.0005 | 643 | ±54 | 655 | ±65 | 694 | ±18 | 7% | 0.9628 |
| 04-7-1_Zrn4@1 | 210 | 135 | 0.65 | 19436 | 0.1046 | 0.0105 | 0.91 | 0.10 | 0.0627 | 0.0003 | 641 | ±64 | 655 | ±72 | 697 | ±11 | 8% | 0.9865 |
| 04-7-1_Zrn2@1 | 36 | 44 | 1.23 | 2494 | 0.0969 | 0.0066 | 0.83 | 0.12 | 0.0615 | 0.0009 | 596 | ±40 | 612 | ±88 | 657 | ±30 | 9% | 0.8473 |
| 04-7-1_Zrn28@1 | 444 | 199 | 0.45 | 34177 | 0.1015 | 0.0109 | 0.88 | 0.10 | 0.0625 | 0.0003 | 623 | ±67 | 640 | ±74 | 691 | ±9 | 10% | 0.9904 |
| 05-06-3_Zrn15@2 | 55 | 22 | 0.40 | 61927 | 0.1320 | 0.0098 | 1.20 | 0.14 | 0.06598 | 0.00084 | 799 | ±59 | 800 | ±96 | 806 | ±27 | 1% | 0.9226 |
| 05-06-3_Zrn15@1 | 108 | 88 | 0.81 | 457930 | 0.1319 | 0.0064 | 1.21 | 0.12 | 0.06616 | 0.00062 | 799 | ±39 | 805 | ±78 | 812 | ±20 | 2% | 0.9607 |
| *Retrograded Eclogite* | | | | | | | | | | | | | | | | | | |
| 05b-13-13b_Zrn15@1 | 101 | 2 | 0.02 | 2245 | 0.1115 | 0.0078 | 0.95 | 0.14 | 0.0606 | 0.0011 | 681 | ±48 | 677 | ±100 | 626 | ±39 | -9% | 0.8276 |
| 05b-13-13b_Zrn20@1 | 312 | 22 | 0.07 | 5707 | 0.1103 | 0.0098 | 0.92 | 0.11 | 0.0606 | 0.0006 | 675 | ±60 | 664 | ±80 | 626 | ±21 | -8% | 0.9511 |
| 05b-13-13b_Zrn16@1 | 96 | 6 | 0.06 | 1767 | 0.1116 | 0.0158 | 0.96 | 0.32 | 0.0612 | 0.0018 | 682 | ±96 | 683 | ±226 | 647 | ±63 | -5% | 0.7613 |
| 05b-13-13b_Zrn18@1 | 67 | 2 | 0.03 | 1689 | 0.1102 | 0.0092 | 0.96 | 0.17 | 0.0636 | 0.0010 | 674 | ±56 | 683 | ±122 | 729 | ±34 | 8% | 0.8589 |
| *Três Pontas–Varginha Nappe* | | | | | | | | | | | | | | | | | | |
| 05b-6-31b_Zrn12@1 | 813 | 12 | 0.02 | 25313 | 0.1070 | 0.0064 | 0.91 | 0.06 | 0.06125 | 0.00026 | 655 | ±39 | 655 | ±43 | 648 | ±9 | -1% | 0.9892 |
| 05b-6-31b_Zrn6@1 | 233 | 10 | 0.04 | 10072 | 0.1083 | 0.0060 | 0.92 | 0.08 | 0.06160 | 0.00042 | 663 | ±36 | 664 | ±55 | 660 | ±15 | 0% | 0.9678 |
| 05b-6-31b_Zrn16@1 | 309 | 16 | 0.05 | 13211 | 0.1072 | 0.0056 | 0.90 | 0.07 | 0.06116 | 0.00045 | 656 | ±34 | 654 | ±49 | 645 | ±16 | -2% | 0.9498 |
| 05b-6-31b_Zrn1@1 | 107 | 17 | 0.16 | 5125 | 0.1080 | 0.0054 | 0.90 | 0.08 | 0.06057 | 0.00064 | 661 | ±33 | 654 | ±57 | 624 | ±23 | -6% | 0.8656 |
| 05b-6-31b_Zrn7@1 | 112 | 20 | 0.18 | 5408 | 0.1066 | 0.0064 | 0.89 | 0.09 | 0.06094 | 0.00071 | 653 | ±39 | 648 | ±68 | 637 | ±50 | -2% | 0.9195 |
| 05b-6-31b_Zrn24@4 | 166 | 10 | 0.06 | 5696 | 0.1045 | 0.0035 | 0.88 | 0.06 | 0.06093 | 0.00042 | 641 | ±21 | 639 | ±47 | 637 | ±15 | -1% | 0.9575 |
| 05b-6-31b_Zrn24@5 | 132 | 14 | 0.11 | 6606 | 0.1037 | 0.0031 | 0.88 | 0.07 | 0.06130 | 0.00052 | 636 | ±19 | 640 | ±52 | 650 | ±18 | 2% | 0.9405 |
| 04-6-11_Zrn8@3 | 322 | 32 | 0.10 | 13673 | 0.1081 | 0.0037 | 0.92 | 0.05 | 0.06137 | 0.00031 | 662 | ±23 | 662 | ±36 | 652 | ±11 | -2% | 0.9796 |
| 04-6-11_Zrn3@1 | 284 | 31 | 0.11 | 10316 | 0.1068 | 0.0044 | 0.91 | 0.06 | 0.06159 | 0.00034 | 654 | ±27 | 657 | ±42 | 660 | ±12 | 1% | 0.9735 |
| 04-6-11_Zrn2@1 | 369 | 50 | 0.14 | 11862 | 0.1060 | 0.0052 | 0.91 | 0.06 | 0.06181 | 0.00029 | 649 | ±32 | 656 | ±45 | 668 | ±10 | 3% | 0.9835 |
| 04-6-11_Zrn8@1 | 345 | 31 | 0.09 | 12603 | 0.1045 | 0.0063 | 0.89 | 0.06 | 0.06176 | 0.00030 | 641 | ±39 | 647 | ±42 | 666 | ±10 | 4% | 0.9831 |
| 04-6-11_Zrn4@1 | 342 | 21 | 0.06 | 11694 | 0.1044 | 0.0063 | 0.89 | 0.06 | 0.06201 | 0.00030 | 640 | ±39 | 648 | ±43 | 674 | ±10 | 5% | 0.9860 |
| 04-6-11_Zrn8@4 | 338 | 37 | 0.11 | 20073 | 0.1016 | 0.0046 | 0.87 | 0.07 | 0.06174 | 0.00037 | 624 | ±28 | 635 | ±49 | 665 | ±13 | 6% | 0.9759 |

| | | $^{206}Pb/^{238}U$ | | | $^{207}Pb/^{235}U$ | | | $^{207}Pb/^{206}Pb$ | | |
|---|---|---|---|---|---|---|---|---|---|---|
| Sample Name | n | Age[(a)] | MSWD | pfit | Age[(a)] | MSWD | pfit | Age[(a)] | MSWD | pfit |
| 04-7-1 | 7 | 622 ±28 | 1.4 | 0.22 | 647 ±29 | 0.39 | 0.89 | 690 ±16 | 5.6 | 0 |
| 05-13-13 | 4 | 678 ±29 | 0.02 | 0.996 | 673 ±54 | 0.32 | 0.992 | 649 ±77 | 9.4 | 0 |
| 05-6-31b | 7 | 647 ±11 | 0.6 | 0.73 | 650 ±19 | 0.1 | 0.99 | 646 ±9 | 1.5 | 0.17 |
| 04-6-11 | 6 | 648 ±12 | 0.98 | 0.43 | 652 ±17 | 0.19 | 0.97 | 665 ±8 | 2 | 0.078 |

**Table 2-5.** U-Pb zircon ages. (a) error expressed as 95% uncertainty on the mean

from the Socorro–Guaxupé Nappe, 05-06-3, yields two $^{206}Pb/^{238}U$ dates of 799±59 and 799±39 Ma; an age is not reported for this sample due to the limited dataset.

Zircons from sample 05b-13-13, the retrograded eclogite, yield four $^{206}Pb/^{238}U$ zircon dates ranging from 682±96 Ma to 674±56 Ma (Fig. 2-8), leading to an age of 678±29 Ma (MSWD = 0.02, pfit = 0.996). The large uncertainties on these dates

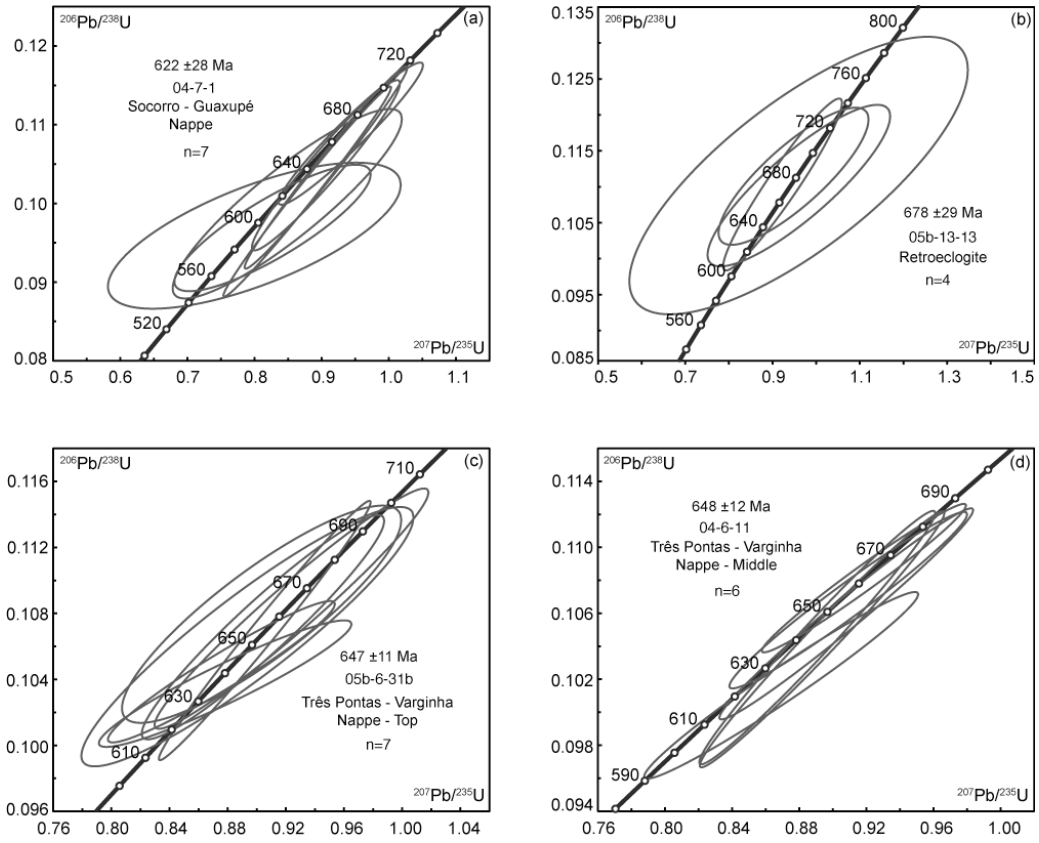


**Figure 2-8.** U–Pb concordia diagrams for zircon from samples 04-7-1 (a), 05b-13-13 (b), 05b-6-31b (c) and 04-6-11 (d). Sample 04-7-1 yields an average age of 622±28 Ma, sample 05-b-13-13 yields an average age of 678±29 Ma, sample 05b-6-31b yields an average age of 647±11 Ma and sample 04-6-11 yields an average age of 648±12 Ma. The average age is based on the $^{206}Pb/^{238}U$ ages.

are due to the small (≤20 μm) grain size of these zircons, requiring a smaller sampling volume. The age of 678±29 Ma is consistent with the $^{207}Pb/^{235}U$ and $^{207}Pb/^{206}U$ ages of 673±54 Ma and 649±79 Ma, respectively.

Seven $^{206}Pb/^{238}U$ zircon dates from sample 05b-6-31b, from the top of the Três Pontas–Varginha Nappe, range from 663±36 Ma to 636±19 Ma (Fig. 2-8), leading to an age of 647±11 Ma (MSWD = 0.6, pfit = 0.73). This age is consistent with the $^{207}Pb/^{235}U$ and $^{207}Pb/^{206}U$ ages of 650±19 Ma and 646±9 Ma, respectively.

Six $^{206}Pb/^{238}U$ zircon dates from sample 04-6-11, from the structural middle of the Três Pontas–Varginha Nappe, range from 662±23 Ma to 624±28 (Fig. 2-8), leading to an age of 648±12 Ma (MSWD = 0.98, pfit = 0.43). This age is consistent with the $^{207}Pb/^{235}U$ and $^{207}Pb/^{206}U$ ages of 652±17 and 665±8 Ma, respectively.

Sample 05-6-110/108, from the bottom of the Três Pontas–Varginha Nappe, yields eight $^{206}Pb/^{238}U$ zircon dates ranging from 722±36 Ma to 618±61 Ma. The age calculated for this sample has a very low pfit of 0.008, and so no age is reported for this sample.

*Rb-Sr and Sm-Nd Isochrons*

A whole rock powder and three mineral fractions (biotite, garnet and a white mineral fraction of quartz, feldspar and sillimanite/kyanite) from two separates of sample 04-6-21 were prepared for Rb-Sr and Sm-Nd analysis (Table 2-6). The first separate (04-6-21A) of this sample yields a Rb-Sr multimineral–whole rock isochron age of 590.0 ± 3.7 Ma (MSWD = 171) and an initial $^{87}Sr/^{86}Sr$ of 0.71394±0.00061 (Fig. 2-9a), and a Sm-Nd multimineral–whole rock isochron with an age of 563±140 Ma (MSWD =

| | concentration blank corr(g/g) | | | | | | | |
|---|---|---|---|---|---|---|---|---|
| Sample No. | Rb | err (1σ) | Sr | err (1σ) | Sm | err (1σ) | Nd | err (1σ) |
| 04-6-21A WR | 1.4698E-04 | 9.5E-08 | 1.45611E-04 | 1.8E-09 | 6.410E-06 | 7.2E-09 | 3.1832E-05 | 5.2E-10 |
| 04-6-21A Bt | 5.2366E-04 | 2.7E-07 | 6.22465E-05 | 6.9E-10 | 1.142E-05 | 1.2E-08 | 7.2204E-05 | 1.3E-09 |
| 04-6-21A Gt | 3.8196E-06 | 3.0E-09 | 4.27191E-06 | 4.2E-11 | 7.422E-06 | 5.3E-09 | 2.5010E-05 | 5.3E-10 |
| 04-6-21A Wt | 2.0696E-04 | 1.3E-07 | 3.82009E-04 | 7.0E-09 | 7.964E-07 | 5.1E-10 | 5.0639E-06 | 9.4E-11 |
| 04-6-21B WR | 1.1052E-04 | 7.2E-08 | 1.04302E-04 | 1.3E-09 | 9.078E-06 | 3.9E-09 | 4.9143E-05 | 9.2E-10 |
| 04-6-21B Bt | 5.3193E-04 | 4.5E-07 | 7.24854E-05 | 7.2E-10 | 8.128E-06 | 3.2E-09 | 4.9689E-05 | 1.2E-09 |
| 04-6-21B Gt | 1.6244E-06 | 1.6E-09 | 1.97176E-06 | 1.9E-11 | 8.363E-06 | 7.0E-09 | 2.7863E-05 | 4.6E-10 |
| 04-6-21B Wt | 1.5747E-04 | 8.9E-08 | 2.91877E-04 | 3.7E-09 | 1.586E-06 | 1.1E-09 | 9.8324E-06 | 1.7E-10 |

| | | | Isotope Ratio | | | | | |
|---|---|---|---|---|---|---|---|---|
| Sample No. | 87Rb | 86Sr | 87Rb/86Sr | err (2σ) | err (2σ%) | 87Sr/86Sr | err (2σ) | err (2σ%) |
| 04-6-21A WR | 4.78E-07 | 1.63E-07 | 2.931 | 0.004 | 0.13 | 0.737462 | 7.9E-06 | 1.07E-03 |
| 04-6-21A Bt | 1.70E-06 | 6.86E-08 | 24.865 | 0.025 | 0.10 | 0.922255 | 9.1E-06 | 9.87E-04 |
| 04-6-21A Gt | 1.24E-08 | 4.79E-09 | 2.595 | 0.004 | 0.16 | 0.735079 | 7.6E-06 | 1.03E-03 |
| 04-6-21A Wt | 6.74E-07 | 4.29E-07 | 1.571 | 0.002 | 0.12 | 0.726281 | 7.2E-06 | 9.91E-04 |
| 04-6-21B WR | 3.60E-07 | 1.17E-07 | 3.077 | 0.004 | 0.13 | 0.738871 | 7.8E-06 | 1.06E-03 |
| 04-6-21B Bt | 1.73E-06 | 8.00E-08 | 21.635 | 0.036 | 0.17 | 0.895772 | 9.4E-06 | 1.05E-03 |
| 04-6-21B Gt | 5.29E-09 | 2.21E-09 | 2.391 | 0.005 | 0.20 | 0.734373 | 7.7E-06 | 1.05E-03 |
| 04-6-21B Wt | 5.13E-07 | 3.28E-07 | 1.565 | 0.002 | 0.11 | 0.726234 | 8.1E-06 | 1.11E-03 |

| | | | Isotope Ratio | | | | | |
|---|---|---|---|---|---|---|---|---|
| Sample No. | 147Sm | 144Nd | 147Sm/144Nd | err (2σ) | err (2σ%) | 143Nd/144Nd | err (2σ) | err (2σ%) |
| 04-6-21A WR | 6.39E-09 | 5.25E-08 | 0.1217 | 0.0003 | 0.22 | 0.512114 | 6.1E-06 | 0.001198953 |
| 04-6-21A Bt | 1.14E-08 | 1.19E-07 | 0.0956 | 0.0002 | 0.21 | 0.512021 | 5.6E-06 | 0.001097611 |
| 04-6-21A Gt | 7.40E-09 | 4.12E-08 | 0.1794 | 0.0003 | 0.14 | 0.512317 | 8.0E-06 | 0.001553726 |
| 04-6-21A Wt | 7.94E-10 | 8.35E-09 | 0.0951 | 0.0001 | 0.13 | 0.511993 | 6.0E-06 | 0.001171892 |
| 04-6-21B WR | 9.05E-09 | 8.10E-08 | 0.1117 | 0.0001 | 0.09 | 0.512113 | 8.0E-06 | 0.001562155 |
| 04-6-21B Bt | 8.10E-09 | 8.19E-08 | 0.0989 | 0.0001 | 0.08 | 0.512061 | 8.0E-06 | 0.001562314 |
| 04-6-21B Gt | 8.34E-09 | 4.59E-08 | 0.1815 | 0.0003 | 0.17 | 0.512401 | 6.3E-06 | 0.001221699 |
| 04-6-21B Wt | 1.58E-09 | 1.62E-08 | 0.0975 | 0.0001 | 0.13 | 0.512038 | 5.8E-06 | 0.001132729 |

**Table 2-6.** Rb-Sr and Sm-Nd isotope data determined for whole rock and mineral separates using thermal ionzation mass spectrometry.

23) and an initial $^{143}Nd/^{144}Nd$ of 0.51166±0.00012 (Fig. 2-9b). The second separate (04-6-21B) from this sample defines a Rb-Sr multimineral–whole rock isochron with a model age of 591±13 Ma (MSWD = 1444) and an initial $^{87}Sr/^{86}Sr$ of 0.7134±0.0020 (Fig. 2-9c), and a Sm-Nd multimineral–whole rock isochron with a model age of 643±90 (MSWD=8.0) and an initial $^{143}Nd/^{144}Nd$ of 0.511637±0.000076 (Fig. 2-9d).

*Discussion*

The southern sector of the Southern Brasília Belt preserves remnants of a passive margin sedimentary sequence in the east which becomes progressively metamorphosed in a subduction-to-collision orogen towards the west. The São

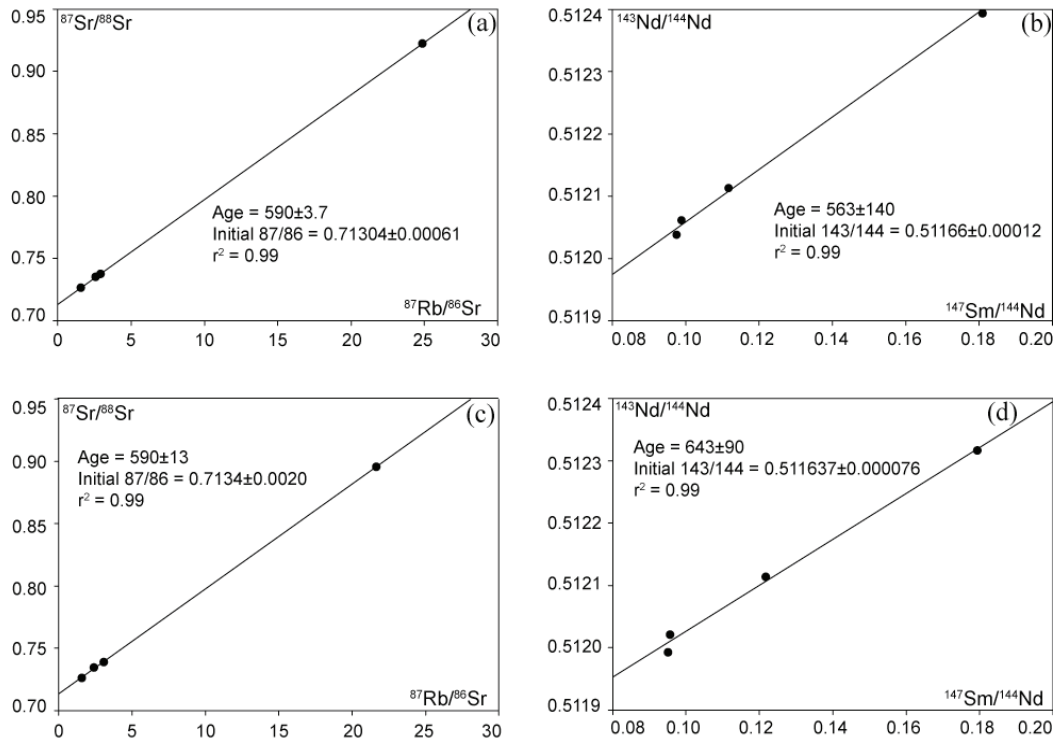


**Figure 2-9.** Rb-Sr and Sm-Nd isochrons for two separates of sample 04-6-21.

Francisco Craton was progressively subducted beneath an accretionary magmatic arc at a convergent plate margin leading to the emplacement of an arc-derived and several passive margin-derived nappes onto the craton during terminal collision.

***Statistical evaluation of ages***

Two-sample t tests were performed to calculate the probability that ages are statistically identical. Table 2-7 lists the p-values associated with each possible scenario. A p-value less than 0.05 indicates with 95% confidence that two ages are unique.

The age of zircon growth in the retrograded eclogite (05-13-13, 678±29 Ma) has a high statistical probability of being older than the age of zircon growth in the Três Pontas–Varginha Nappe (05-6-31b, 647±11Ma; 04-6-11, 648±12 Ma), with p-

| Age 1 | | Age 2 | | t test p-value | Monte Carlo probability |
|---|---|---|---|---|---|
| 678 | ±29 | 622 | ±28 | <0.001 | 0.001 |
| 678 | ±29 | 647 | ±11 | 0.013 | 0.009 |
| 678 | ±29 | 648 | ±12 | 0.015 | 0.044 |
| 678 | ±29 | 648.9 | ±0.3 | 0.014 | 0.006 |
| 622 | ±28 | 647 | ±11 | 0.002 | 0.111 |
| 622 | ±28 | 648 | ±12 | 0.001 | 0.099 |
| 622 | ±28 | 648.9 | ±0.3 | <0.001 | 0.029 |
| 648.9 | ±0.3 | 647 | ±11 | 0.198 | 0.386 |
| 648.9 | ±0.3 | 648 | ±12 | 0.364 | 0.459 |
| 647 | ±11 | 648 | ±12 | 0.381 | 0.933 |

**Table 2-7.** p-values for testing statistical independence of the ages. A p-value less than 0.05 indicates a low probability that the two ages are statistically identical.

values of <0.015, and is also older than the age of zircon growth in the Socorro–Guaxupé Nappe (04-7-1, 622±28 Ma), with a p-value of <0.001. The zircon age for the retrograded eclogite is also statistically older, with a p-value of ~0.014, than the oldest zircon age of 648.9±0.3 Ma reported by Baldwin & Brown (2008) for the ultrahigh temperature metamorphism in the Anapolis–Itauçu Complex in the northern sector of the Southern Brasília Belt. The age of zircon growth in the Socorro–Guaxupé Nappe has a high statistical probability of being younger than that in the Três Pontas–Varginha Nappe, with p-values <0.002, and is also younger than that in the Anapolis-Itauçu Complex, with a p-value <0.001. The age of zircon growth in the Três Pontas–Varginha Nappe is statistically indistinguishable from the age of zircon growth in the Anapolis–Itauçu Complex.

A Monte Carlo simulation was run as an additional test of uniqueness for these ages. Each age was simulated 10,000 times in Microsoft Excel using a normal random number generator. The probability of overlap of two ages was determined by calculating the intersection of the probability that one age falls within the 95%

confidence interval of the second age with the probability that the second age falls within the 95% confidence interval of the first age.

The Monte Carlo simulation indicates a ~0.1% probability that zircon growth in the retrograded eclogite and the Socorro–Guaxupé Nappe are the same age, a ~0.6% probability that zircon growth in the retrograded eclogite and the Anapolis–Itauçu Complex are the same age, a <5% probability that zircon growth in the retrograded eclogite and the Três Pontas–Varginha Nappe are the same age, a ~10% probability that zircon growth in the Socorro–Guaxupé Nappe and the Três Pontas–Varginha Nappe are the same age and a ~3% probability that zircon growth in the Socorro–Guaxupé Nappe and the Anapolis–Itauçu Complex are the same age. The Monte Carlo simulation indicates that the ages of zircon growth in the Três Pontas–Varginha Nappe and the Anapolis-Itauçu Complex are statistically indistinguishable.

***Socorro–Guaxupé Nappe***

The accretionary magmatic arc is partly represented by the Socorro–Guaxupé Nappe at the top of the nappe stack. The timing of arc magmatism is unknown, but single dates from sample 05-06-3 of *ca.* 800 Ma suggest that the arc may have been active at this time. Zircon inclusions in plagioclase in the leucosome of sample 04-7-1 are interpreted to have formed during crystallization of an anatectic melt at granulite facies conditions. Rare earth element patterns for these zircons show enrichment in the HREE consistent with formation in the presence of a HREE-rich melt, and a negative Eu anomaly, suggesting crystallization in equilibrium with plagioclase. Distribution coefficients for the REE between garnet and zircon indicate enrichment in the HREE in zircon by an order of magnitude more than would be observed for

zircon in equilibrium with garnet, with $D_{Lu(Zrn/Grt)}$ approaching 100 (*cf.* Rubatto & Hermann 2007). These data suggest that zircon crystallized in equilibrium with plagioclase in a HREE-enriched melt, and the age is interpreted to date crystallization of anatectic melt in the leucosome.

The range of Ti-in-zircon temperatures for zircon rims from sample 04-7-1, from 972˚C to 817˚C, indicates that crystallization occurred over a broad interval of ~150˚C. However, the distribution is strongly skewed towards the lower part of the temperature range. These data are consistent with crystallization beginning near the peak of granulite metamorphism at *P* of 1.5±0.2 GPa and *T* >900˚C, as retrieved using average thermobarometry from rocks close to the base of this nappe, and continuing during cooling to the solidus.

In summary, I interpret the $^{206}Pb/^{238}U$ zircon age of 622±28 Ma in this nappe to record the timing of immediately post-peak-temperature zircon crystallization from anatectic melt as it cooled down to the solidus. Crystallization probably began early during exhumation as the Socorro–Guaxupé Nappe was being emplaced over the stack of passive margin-derived nappes during the late stage of the collision.

***Retrograded Eclogite***

The very small size (<20 μm) of the six grains in the thin section of retrograded eclogite sample 05-13-13 resulted in all zircon being exhausted during ablation for SIMS U–Pb analysis. As such, no REE or titanium elemental compositions were collected for zircon in this sample. The zircons are included in garnet or associated with ilmenite in symplectic aggregates of plagioclase and clinopyroxene that are inferred to replace a more jaditic pyroxene. The zircons are interpreted most likely to

have grown as zirconium was liberated either by the breakdown of igneous pyroxene on the prograde *P–T* path. However, some of the zircons could have grown during the breakdown of a jaditic pyroxene to plagioclase and clinopyroxene during post-peak pressure high-temperature decompression. It is also possible that zircon is residual from crystallization of mid-ocean ridge basalt or gabbro. However, this last possibility is considered to be less likely due to the short time span available between ocean crust formation and the peak of high-*P* granulite facies metamorphism. Thus, I interpret the zircon $^{206}Pb/^{238}U$ age of 678±29 Ma from this sample to record either close to peak eclogite facies metamorphism or initial decompression at high temperatures.

As the Três Pontas–Varginha/Liberdade Nappe became detached from the distal part of the subducting passive margin and accreted to the hanging wall of the subduction zone, I propose that slivers of eclogite (formerly ocean floor basalt) were detached from the underlying ocean lithosphere basement with the metasedimentary rocks. These slivers were preserved as tectonic blocks along the tectonic contact with the next package of metasedimentary rocks that underthrust the accreted Três Pontas–Varginha/Liberdade Nappe. This second package of underthrust metasedimentary rocks subsequently became detached from the subducting passive margin and accreted to the hanging wall of the subduction zone to form the Carmo da Cachoeira/Andrelândia Nappe (Fig. 2-10). Thus, the age of 678±29 Ma also provides a minimum age for the initial detachment of the Três Pontas–Varginha/Liberdade Nappe from the subducting passive margin.

***Três Pontas–Varginha Nappe***

The Três Pontas–Varginha Nappe lies immediately beneath the Socorro–Guaxupé Nappe. This high-pressure granulite facies nappe is the uppermost of the metapelitic nappes formed by subduction of passive margin sediments during the Brasília Orogeny, and it records the highest pressures of metamorphism. Granulite facies rocks from this nappe achieved peak pressure of ~1.5 GPa and temperatures of >850–900˚C.

Sample 05-6-31b is from near the structural top of this nappe. Zircon occurs in the outer mantles of garnet and in the matrix. It is closely associated with ilmenite, either sharing grain boundaries or occurring as inclusions in ilmenite, suggesting zircon formation from ilmenite during the retrograde *P–T* evolution (*e.g.*, Bingen *et al*., 2001). The Ti-in-zircon temperatures from this sample have an interquartile range of 807–797˚C, which is consistent with zircon formation during final crystallization of residual melt (Fig. 2-4).

Two of the rare earth element patterns for these zircons show enrichment in the HREE, consistent with crystallization in the presence of a melt, and a slight negative Eu anomaly, consistent with crystallization in equilibrium with plagioclase.

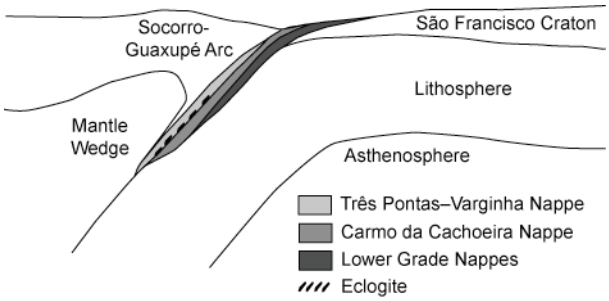


**Figure 2-10.** Schematic tectonic setting for nappe stacking by detachment from the downgoing plate and accretion to the hanging wall of the subduction zone.

The third pattern has a flatter HREE pattern, is depleted in all REE except La compared with the other two zircons and exhibits a more pronounced negative Eu anomaly.

Garnet in this sample is zoned with respect to major elements, with cores enriched in Fe and depleted in Ca as compared to the mantles and rims, and REE, with the cores enriched in HREE compared with the mantles and rims. The REE composition of the outer mantle of garnet is used in the calculation of $D_{REE(Zrn/Grt)}$ values for this sample because a majority of the zircon occurs as inclusions in ilmenite in the outer mantles of garnet. For the two zircons with HREE enriched REE patterns, $D_{REE(Zrn/Grt)}$ values are near unity for the MREE, whereas the HREE are partitioned preferentially into the zircon. One of these patterns is for zircon in ilmenite included in garnet, and the $D_{REE(Zrn/Grt)}$ increasing from 1 to >10 is consistent with zircon growth in equilibrium with the outer mantle composition of garnet, but not with the core or rim compositions of garnet, whereas the pattern for the second zircon, which is for a matrix zircon associated with ilmenite, suggests it did not equilibrate fully with garnet.

These REE features suggest that zircon forming from ilmenite included in garnet was able to maintain equilibrium with the surrounding garnet. The zircon $^{206}Pb/^{238}U$ age of 647±11 Ma is interpreted to record the growth of zircon at ~800˚C during final crystallization of residual melt along the high temperature part of the retrograde *P–T* evolution.

Sample 04-6-11 is close to the structural middle of the Três Pontas–Varginha Nappe. Zircons from this sample are associated with ilmenite in the matrix of garnet-

bearing leucosomes. The interquartile range of the Ti-in-zircon temperatures for the cores of these zircons is 821–789˚C, consistent with formation close to the solidus (Fig. 2-4).

Rare earth element patterns for these zircons show enrichment in the MREE and HREE, with no Eu anomalies, indicating crystallization in the presence of a melt but not synchronous with crystallization of plagioclase or garnet. Garnet REE patterns were measured from core to rim, and show enrichment in MREE and HREE, but do not show significant zoning. The $D_{REE(Zrn/Grt)}$ values are near unity for both the MREE and the HREE, suggesting that zircon did not form in equilibrium with garnet, but likely following growth of garnet and depletion of the REE reservoir.

The zircon $^{206}Pb/^{238}U$ age of 648±12 Ma is interpreted to record the formation of zircon from ilmenite at a temperature near 800˚C during the high temperature part of the retrograde evolution, likely prior to final melt crystallization. This is consistent with the temperature–time conditions seen for the top of this nappe in sample 05b-6-31b.

Sample 04-6-21 is from the base of the Três Pontas–Varginha Nappe. Zircons from this sample occur in both the matrix and as inclusions in garnet, and are not associated with a specific metamorphic reaction. All U–Pb ages for this sample were highly discordant, and no age could be interpreted. Two Rb-Sr Bt-Grt-Pl/Sil±Ky/Qtz-WR isochrons for this sample yield ages of 590.0±3.7 Ma and 591±13 Ma. The presence of coarse prismatic sillimanite in the fabric requires high-temperatures decompression to the sillimanite stability field. Since biottie associated with sillmanite defines the foliation, I interpret the age of *ca.* 590 Ma to date the initial

stage of decompression and exhumation of the high-pressure granulites at temperatures of ~700˚C (*cf.* Glodny *et al.* 2008). Two Sm-Nd Bt-Grt-Pl/Sil±Ky/Qtz-WR isochrons for sample 04-6-21 yield ages of 563±140 Ma and 643±90 Ma. The large uncertainties make it difficult to assign any geologic significance to these ages.

As there are no major faults, folds or other structural features mapped between sample 04-6-21 and samples 05b-6-31b and 04-6-11, it is likely that these samples experienced similar *P–T–t* paths. Given that the Três Pontas–Varginha Nappe was at temperatures of ~800˚C at 648±12 Ma, and ~700˚C at 590.0±3.7 Ma, an average cooling rate of 3.5 ˚ C $Ma^{-1}$ is implied as the nappe is exhumed.

*Conclusions*

In this paper I reported the results of the first integrated petrological, chronological and geochemical study of multiple samples from the uppermost high-pressure granulite nappes in the southern sector of the Southern Brasília Belt.

Zircons in retrograded eclogite that occur as blocks along the tectonic contact between the upper two passive margin-derived high-pressure granulite nappes are interpreted most likely to have grown as zirconium was liberated either by the breakdown of igneous pyroxene on the prograde *P–T* path. These zircons yield an age of 678±29 Ma, which is a minimum for detachment of the overlying nappe from the subducting passive margin and the beginning of the Brasília Orogeny in the Southern Brasília Belt. This result demonstrates for the first time that high-pressure metamorphism occurred up to *ca.* 50 Ma before 630 Ma, the age previously inferred for the peak of metamorphism in the southern sector of the Southern Brasília Belt.

I obtained two ages of *ca.* 648 and *ca.* 647 Ma for high-temperature, post-peak zircon growth in high-pressure granulites in the Três Pontas–Varginha Nappe, the uppermost of the passive margin-derived nappes. This age overlaps ages retrieved by Baldwin & Brown (2008) from ultrahigh temperature metamorphic rocks in the Anapolis-Itauçu Complex further north in the Southern Brasília Belt. The proposal by Campos Neto & Caby (2000) that there is an upward increase in temperature in the Três Pontas–Varginha Nappe is not supported by my data, which indicates peak temperatures of >850-900˚C throughout the nappe.

I determined a zircon crystallization age of *ca.* 622 Ma from leucosome in granulites close to the base of the overlying Socorro–Guaxupé Nappe, which represents part of the upper plate magmatic arc. I interpret this age as dating the time of high pressure granulite facies metamorphism in the Socorro–Guaxupé Nappe.

I determined Rb-Sr multimineral–whole rock isochron ages of *ca.* 590 Ma from the Três Pontas–Varginha Nappe that I interpret to record cooling through high-temperature decompression at ~700˚C by that time. When this age is combined with the U-Pb age of *ca.* 648 Ma, inferred to date close-to-solidus temperatures of ~800˚C, an average cooling rate of 3.5 ˚C $Ma^{-1}$ is implied during the initial stage of exhumation of the Três Pontas–Varginha Nappe.

Based on these new age constraints, I propose that the early stage of amalgamation of West Gondwana began in the Cryogenian with suturing of the Socorro–Guaxupé Arc–Paranapanema Block to the São Francisco Craton along the southern sector of the Southern Brasília Belt. Data from retrograde eclogite indicate that the earliest impingement and beginning of the suturing process occurred before

*ca.* 678 Ma in the southern sector of the Southern Brasília Belt. This age is statistically distinguishable from the two *ca.* 648 and *ca.* 647 Ma ages in both the Três Pontas–Varginha Nappe and the oldest ages for metamorphism in the Anapolis-Itauçu Complex.

# Chapter 3: Robust Statistical Methods for Assessment and Analysis of Monazite Microprobe Geochronologic Data Applied to the Neoproterozoic Brasília Belt, Brazil

*Abstract*

Many statistical techniques commonly used to evaluate ages and their uncertainties rely on an assumption that the analytical data used in calculating ages and uncertainties are representative of a normally distributed population. This is not always a valid assumption, and using traditional statistical techniques on non-normally distributed data may result in erroneous ages and underestimation of an uncertainty. To avoid these issues, I therefore propose that the robust statistical tanh estimator should be used to calculate ages, and the bootstrap method should be used to calculate uncertainties. The statistical methods used should be able to account for outliers and skewed datasets. Here I describe and exemplify the application of these robust statistical methods to multiple (U-Th)-Pb monazite electron probe microanalytical datasets collected from granulite facies rocks from the southern sector of the Southern Brasília Belt. Based on SIMS $^{206}Pb/^{238}U$ zircon ages, the southern sector of the Southern Brasília Belt comprises a stack of nappes metamorphosed to granulite facies conditions immediately prior to zircon growth at 648±12 and 647±11 Ma. Monazite microprobe ages of 635–624 Ma in the highest-pressure nappe record post-peak-*T* growth of monazite in this nappe. An age of 631±12 Ma dates formation of foliation in a structurally lower nappe. Ages of 607–595 Ma recorded throughout the nappe stack are interpreted to date emplacement of a magmatic arc on top of the

nappe stack during terminal arc collision. Monazite ages of 588–561 Ma throughout the southernmost portion of the southern sector of the Southern Brasília Belt record overprinting related to the Ribeira Orogeny.

*Introduction*

Monazite is a light rare earth element phosphate that incorporates U and Th into its structure during growth, but tends to exclude Pb (Parrish *et al.* 1990). Assuming that all Pb contained in monazite is radiogenic, and that all isotopes of U were incorporated in their naturally occurring abundances, monazite dates can be calculated by measuring the concentrations of U, Pb and Th using an electron probe microanalyzer (EPMA) (*e.g.*, Montel *et al.* 1996; Williams *et al.* 1999).

Significant advances have been made in the monazite EPMA dating technique over the past two decades (*e.g.*, Suzuki *et al.* 1991; Scherrer *et al.* 2000; Williams & Jercinovic 2002; Foster *et al.* 2004; Cocherie *et al.* 2005; Dahl *et al.* 2005; Goncalves *et al.* 2005; Jercinovic & Williams 2005; Pyle *et al.* 2005; Williams *et al.* 2006; Corrie *et al.* 2008; Jercinovic *et al.* 2008; Kelsey *et al.* 2008). The EPMA technique is a relatively inexpensive and efficient non-destructive method for obtaining chronologic data. The ability to date monazite in situ allows preservation of the petrographic context, which is especially useful for dating metamorphic rocks as petrographic context is essential to link an age to calculated *P-T* conditions.

Several protocols have been proposed for presenting data, calculating ages and estimating uncertainties in dating monazite by EPMA (*e.g.*, Suzuki *et al.* 1991; Montel *et al.* 1996, 2000; Cocherie & Albarede 2001; Williams *et al.* 2006). These protocols have been developed to provide a foundation for statistical evaluation of the

analytical data. However, many of the statistical techniques used to calculate ages and uncertainties are based on an assumption that analytical data are representative of a normally distributed population, which is an assumption that can be difficult to verify in small datasets.

One source of uncertainty in the EPMA monazite dating technique (or any in situ technique) is associated with the binning of data. Compositional zoning is widely used as a proxy for age zoning, as different compositional domains within single monazite grains commonly can be linked to different metamorphic reactions or microstructures (*e.g.*, Terry *et al.* 2000; Simpson *et al.* 2000; Foster *et al.* 2000; Williams & Jercinovic 2002; Pyle & Spear 2003; Foster *et al.* 2004; Dahl *et al.* 2005). Uncertainty arises due to factors such as: 1) lack of precision in locating analytical points on a compositional map, and therefore correctly assigning a single analysis point to the correct population; 2) the possibility that a single analysis point samples multiple age domains in a single grain, and therefore the single analysis should not be included in any population; or, 3) the possibility that compositional zoning is unrelated to age zoning in a particular grain, in which case data would be incorrectly binned.

In this work I found that monazite dates that were collected from a single age domain did tend to follow a normal distribution. In this case it would be reasonable to use these traditional statistical methods on such datasets, and the ages and uncertainties based on mean and standard deviation for a given population of monazite dates should be statistically acceptable. However, I found also that monazite dates collected from analytical volumes that sample multiple age domains

tended to follow non-normal, skewed distributions. Non-normal, skewed distributions were also retrieved from monazite that records a resetting event. Using traditional statistical techniques on such mixed datasets would result in erroneous ages and uncertainties.

For these reasons, I propose that EPMA data for monazite be evaluated using robust statistical techniques that can take into account outliers in the dataset, and accommodate skewed or non-normally distributed datasets likely caused by mixing age populations. Such techniques require a similar amount of effort as traditional statistical techniques, and yield similar results as traditional statistical techniques for normally distributed data.

To illustrate the recommended protocol, I present an example where I have applied these statistical techniques to high-grade metamorphic rocks of the southern sector of the Neoproterozoic–Cambrian Southern Brasília Belt, Brazil. The southern sector of the Southern Brasília Belt comprises a stack of mostly passive-margin-derived nappes metamorphosed to high-pressure granulite facies conditions during the Brasília Orogeny (*e.g.*, Campos Neto & Caby 2000; Chapter 2). Recent studies have shown that high-temperature metamorphism began as early as *ca.* 678 Ma, and that just-post-peak granulite facies metamorphism occurred at *ca.* 648 Ma (648±12 Ma, 647±11 Ma; Chapter 2). Final emplacement of the arc-related nappe over the passive-margin derived nappes occurred at *ca.* 622 Ma (Chapter 2). Based on a Rb-Sr multimineral–whole rock isochron, the Southern Brasília Belt had cooled to ~700˚C by *ca.* 590 Ma (Chapter 2). The subsequent Ribeira Orogeny at 590–550 Ma imparted a thermal overprint on the southernmost portion of the southern sector of the

Southern Brasília Belt (Trouw *et al.* 2006). The macroscopic petrologic expression of this event is an overprinting of sillimanite in this part of the Brasília Belt. Here I present new geochronologic data that further constrains the tectonometamorphic history, and shows that the thermal overprint is recorded by monazite ages in areas north of the macroscopic petrologic overprint.

## *Analytical Methods*

In the following sections I will describe the analytical and statistical methods I use at the University of Maryland in more detail, and I will report the analytical protocol (Fig. 3-1) established for routine EPMA dating of monazite at the University of Maryland.

### *X-Ray Mapping*

Most monazite grains are compositionally zoned, and also exhibit age zoning. These types of zoning are sometimes, but not necessarily linked. Consequently, it is critical to fully characterize any zoning present in individual monazite grains prior to analysis for dating. Zoning may be characterized by various methods, including backscattered electron imaging, X-ray element composition mapping and age mapping. In this work, I used a combination of backscattered electron imaging and X-ray element composition mapping, and yttrium X-ray element composition maps are the primary method I use for interpreting individual growth zones in monazite crystals. However, yttrium zoning is not always related to age zoning. In monazite grains that exhibit yttrium zoning, data were initially binned by yttrium compositional domains. If t tests indicated that the ages of two zones are statistically identical, then the data were

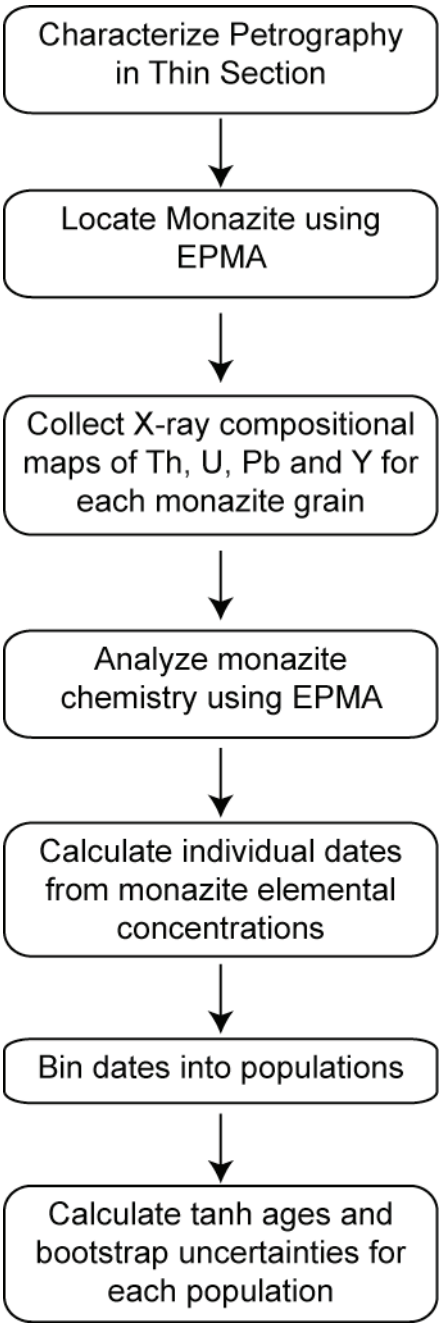


**Figure 3-1.** Flow chart summarizing the protocol for (U-Th)-Pb EPMA dating of monazite at the University of Maryland.

combined prior to further statistical analysis.

Backscattered electron images may reveal zoning in monazite. In this case, the zoning is primarily a function of Th concentration, a major element in most monazite, which can overwhelm any compositional zoning by Pb and U, elements

that are present in much lower concentrations (<1000 ppm level). In order to avoid dating multiple zones within a monazite grain, which would lead to a geologically meaningless age, I used wavelength dispersive X-ray element composition maps to identify compositional zoning within a monazite crystal (*e.g.*, Williams & Jercinovic 2002; Pyle & Spear 2003; Goncalves *et al.* 2005).

In this work, wavelength dispersive X-ray element composition maps were collected using a JEOL JXA-8900 electron probe microanalyzer at the University of Maryland. Petrographic thin sections were coated with a standard carbon coat, and a single, small (~2 mm diameter) drop of carbon paint was applied to the interface between the edge of the thin section and the stage mount in order to prevent charging. An accelerating voltage of 15 kV and a cup current of 250 nA were utilized to collect X-ray maps of U, Th, Pb and Y. The crystals, X-ray lines and detectors used during map collection are listed in Table 3-1. A peak search using the relevant crystal and X-ray line was conducted for each element, and single channel analyzer (SCA) settings were optimized prior to mapping. The distance between adjacent points on a map

| Channel | Element | X-Ray Line | Detector | Crystal |
|---|---|---|---|---|
| 2 | U | Mβ | Xenon | PETH |
| 3 | Th | Mα | GFPC | PETJ |
| 4 | Pb | Mα | Xenon | PETJ |
| 5 | Y | Lα | GFPC | TAP |

**Table 3-1.** Summary of analytical conditions employed for X-ray elemental composition mapping.

varied from 0.5 to 1 μm, and I used a count time for each point of between 200 and 500 ms. These two parameters were adjusted based on the size of each individual monazite grain, primarily to adjust collection time for an individual map. A larger

distance between points was used for larger grains. Fig. 3-2 shows examples of X-ray element composition maps for U, Th, Pb and Y together with a backscattered electron map of a typical monazite from the Southern Brasília Belt.

### *Monazite Chemical Dating*

In this work, monazite EPMA chemical data were collected following a protocol modified from that suggested by Pyle *et al.* (2005; Pers. Comm., 2006). Modifications were made to ensure greater efficiency in collection of X-ray data while maintaining the highest possible accuracy in analysis using a JEOL JXA-8900 electron microprobe microanalyzer.

High-resolution qualitative scans on both reference and unknown monazite grains were routinely performed on the regions of the WD spectra containing Y on the TAP crystal and Pb, Th and U peaks on the PET crystals prior to each analytical session. These spectra were used to identify potential peak and background interferences, and to verify background collection positions. Generally I did not find it necessary to change the background collection positions appreciably between analytical sessions.

An accelerating voltage of 15 kV, a cup current of 200 nA and a beam diameter of 3 to 5 μm were used for both standardization and analysis. Standardization for Th, Si, U and Pb was done on synthetic $ThSiO_4$ and $UO_2$ and natural $PbCO_3$ respectively, standardization for Y, P and Ce was done on synthetic $YPO_4$ and $CePO_4$ respectively, and standardization for Ca was done on a garnet (12442/USGS GTAL) standard. Some authors (*e.g.,* Pyle *et al.* 2005) utilize a smaller cup current during standardization in order obtain comparable count rates on the

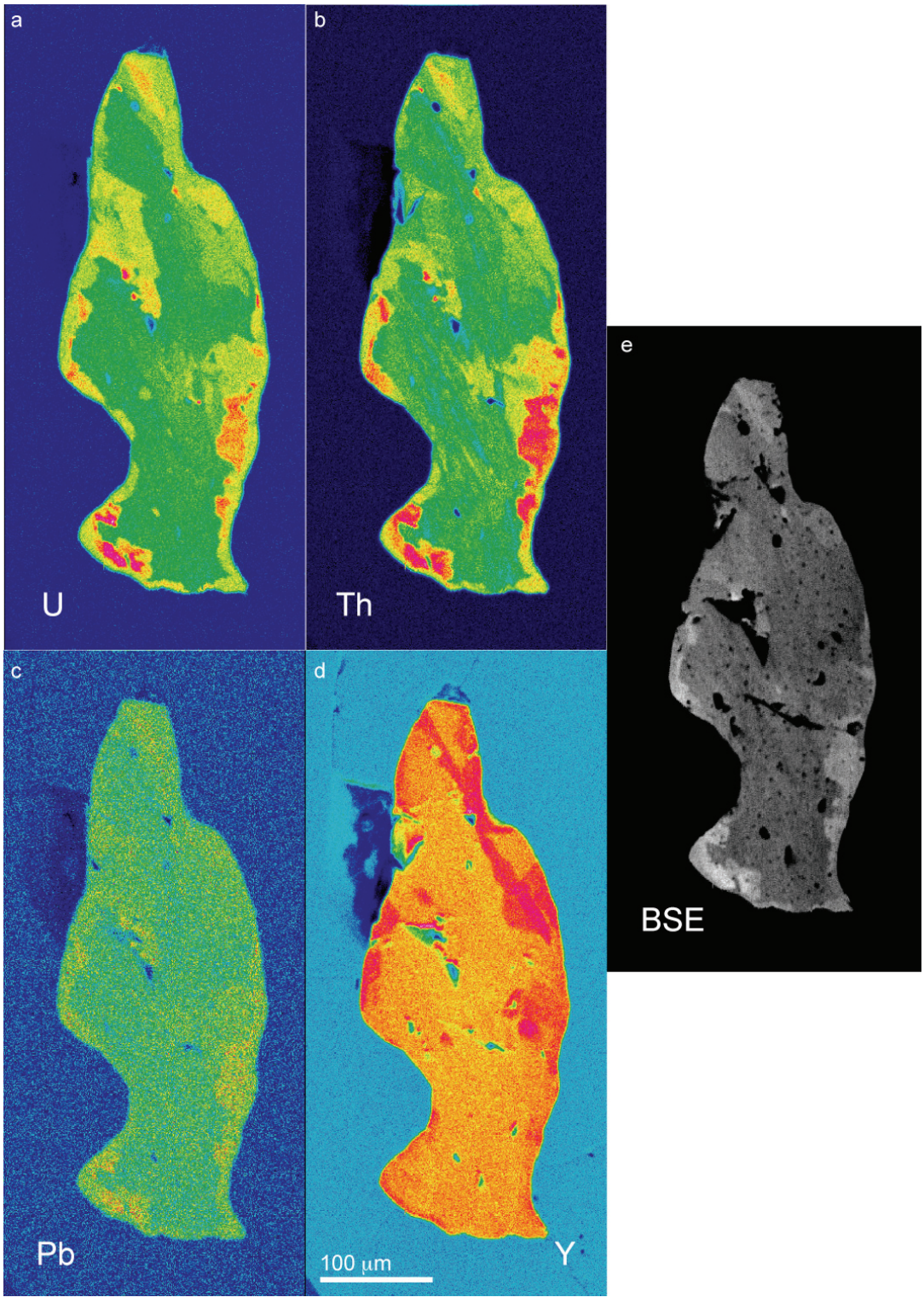


**Figure 3-2.** Exemplar X-ray element composition maps of (a) uranium, (b) thorium, (c) lead and (d) yttrium and (e) a backscattered electron map of monazite from the Southern Brasília Belt.

standards and unknowns. I explicitly looked at count rates as a function of current and found that minimal clipping occurred at different count rates. These observations were substantiated by analyzing Corning standards using the protocol described here, from which accurate U, Pb (Corning X) and Th (Corning W) concentrations were retrieved.

A peak search using the relevant crystal and X-ray line was conducted for each element on the appropriate standard. An SCA scan was run for each element on the appropriate channel immediately following the peak search for that element. The SCA settings were adjusted to eliminate peak clipping while maximizing counts, by ensuring that the peak was entirely enclosed within the scan window, with the minimum base level value not falling below a minimum value of 0.5. The SCA scan is a critical step for U and Pb measurement, as these elements occur in low concentrations in monazite, and I found that miscalibration of the SCA settings can lead to errors on the order of ±10 m.y., or greater, on an individual date. The pulse discriminators were set to the differential mode (DIFF) in order to filter out escape peaks that would interfere with element analysis and to filter out higher order reflections from other elements. Absorbed current and x-ray count degradation were monitored on standards and unknowns and were generally found to remain constant, with the exception of Pb on the $PbCO_3$ standard at extremely small beam diameters, smaller than those used during analysis.

After collecting X-ray element composition maps for monazite grains of interest, and determining background positions, a quantitative analysis was performed to allow calculation of dates for individual points in the monazite grain. During

quantitative analysis I measured P, Ce, Si, Ca and Y in addition to the Th, U and Pb necessary for calculating an age. It was generally sufficient to use an average monazite composition in the ZAF correction, and estimating, or not including, major element (La, Nd, etc.) concentrations did not have a significant effect on the calculated date.

Monazite analysis took *ca.* 9 minutes, with the measurement time primarily a function of the count time for Pb. For a typical analysis, lead was counted for 240 seconds plus 120 seconds on each background position; when analyzing young monazite (*e.g.*, Cretaceous), longer count times were used. Analytical conditions are summarized in Table 3-2.

***Reference Monazites***

In this study, I analyzed the Trebilcock monazite and the GSC-8153 monazite during each analytical session as a quality control check. The Trebilcock monazite has a $^{207}Pb/^{235}U$ age of 272±2 Ma, and a $^{206}Pb/^{238}U$ age of *ca.* 279 (Tomascak *et al.* 1996). There is no available $^{208}Pb/^{232}Th$ age. Tomascak *et al.* (1996) interpret the $^{207}Pb/^{235}U$ age of *ca.* 272 Ma to represent to age of monazite formation, and suggest that the $^{206}Pb/^{238}U$ age is slightly older due to incorporation of excess $^{206}Pb$ during monazite growth.

The GSC-8153 monazite has a $^{208}Pb/^{232}Th$ age of 501±11 Ma, a $^{206}Pb/^{238}U$ age of 505±2 Ma and a $^{207}Pb/^{235}U$ age of 494±9 Ma. The (U-Th)-Pb chemical age, calculated based on relative contribution of each isotopic age, is *ca.* 501 Ma. Williams *et al.* (2005) measured the chemical age to be 498±8.

**Table 3-2.** Summary of analytical conditions employed for EPMA dating of monazite in this work.

| Standard | Element | X-ray | Peak | Crystal | Bkg (+mm) | Bkg (–mm) | Peak (s) | Back (s) | Gain | High V | Base L | Window |
|---|---|---|---|---|---|---|---|---|---|---|---|---|
| UO2 | U | Mb | 119.0208 | PETH | 2.5 | 3 | 80 | 40 | 16 | 1750 | 0.5 | 3.5 |
| ThSiO4 | Th | Ma | 132.5404 | PETJ | 2.5 | 3.5 | 80 | 40 | 8 | 1700 | 0.5 | 3 |
| ThSiO4 | Si | Ka | 77.459 | TAP | 5 | 1.5 | 100 | 50 | 32 | 1680 | 0.5 | 5 |
| PbCO3 | Pb | Ma | 169.3068 | PETH | 4.7 | 2.8 | 480 | 240 | 32 | 1700 | 0.5 | 3.1 |
| PbCO3 | Pb | Ma | 169.3068 | PETJ | 4.7 | 2.8 | 240 | 120 | 32 | 1750 | 0.5 | 1.7 |
| YPO4 | Y | La | 70.1234 | TAP | 1 | 1 | 30 | 15 | 32 | 1680 | 0.5 | 6 |
| YPO4 | P | Ka | 66.9534 | TAP | 4 | 3 | 10 | 5 | 32 | 1680 | 0.5 | 6 |
| CePO4 | Ce | La | 82.0622 | PETJ | 1.5 | 1.5 | 10 | 5 | 32 | 1700 | 0.5 | 3 |
| Grt-12442 | Ca | Ka | 107.5864 | PETJ | 2.5 | 2.5 | 60 | 30 | 8 | 1680 | 0.8 | 2.3 |

***Background Modeling***

WD spectra exhibit some degree of curvature that is significant on the large scale, but may not be significant on the small scale. Using a Cameca SX-Ultrachron and SX50, Williams *et al.* (2007) have observed that the curvature of the background is significant enough to warrant using a non-linear background fit during the analysis of trace elements, and Jercinovic *et al*. (2008) observed considerable background curvature when using PET crystals on a JEOL 8200. Pyle *et al.* (2005) observed that an exponential background fit leads to an older age when using a JEOL 733 Superprobe. I explored this issue for analysis using the JEOL JXA-8900 at the University of Maryland, and found the curvature to occasionally have a small effect on trace element concentrations. This effect is less extreme than those reported by Williams *et al.* (2007), Jercinovic *et al*. (2008) and Pyle *et al.* (2005). To evaluate this for the JEOL JXA-8900 I utilized qualitative scans covering 30 mm of the X-ray spectrum centered around the peaks for each of Pb, Th and U using the GSC-8153 reference monazite, the Trebilcock reference monazite, and an unknown monazite from the Brasília Belt. The background for each spectrum was modeled using both a linear and an exponential fit for each spectrum.

I calculated the difference between peak-to-background ratios for Pb, Th and U using both exponential and linear fits for each of the spectra (Fig. 3-3). An exponential fit yields a 3.2±0.8 % difference in the Pb peak-to-background ratio, a 0.3±0.2 % difference in the Th peak-to-background ratio and a 1.3±0.5 % difference in the U peak-to-background ratio. When applied to the U, Th and Pb chemical data

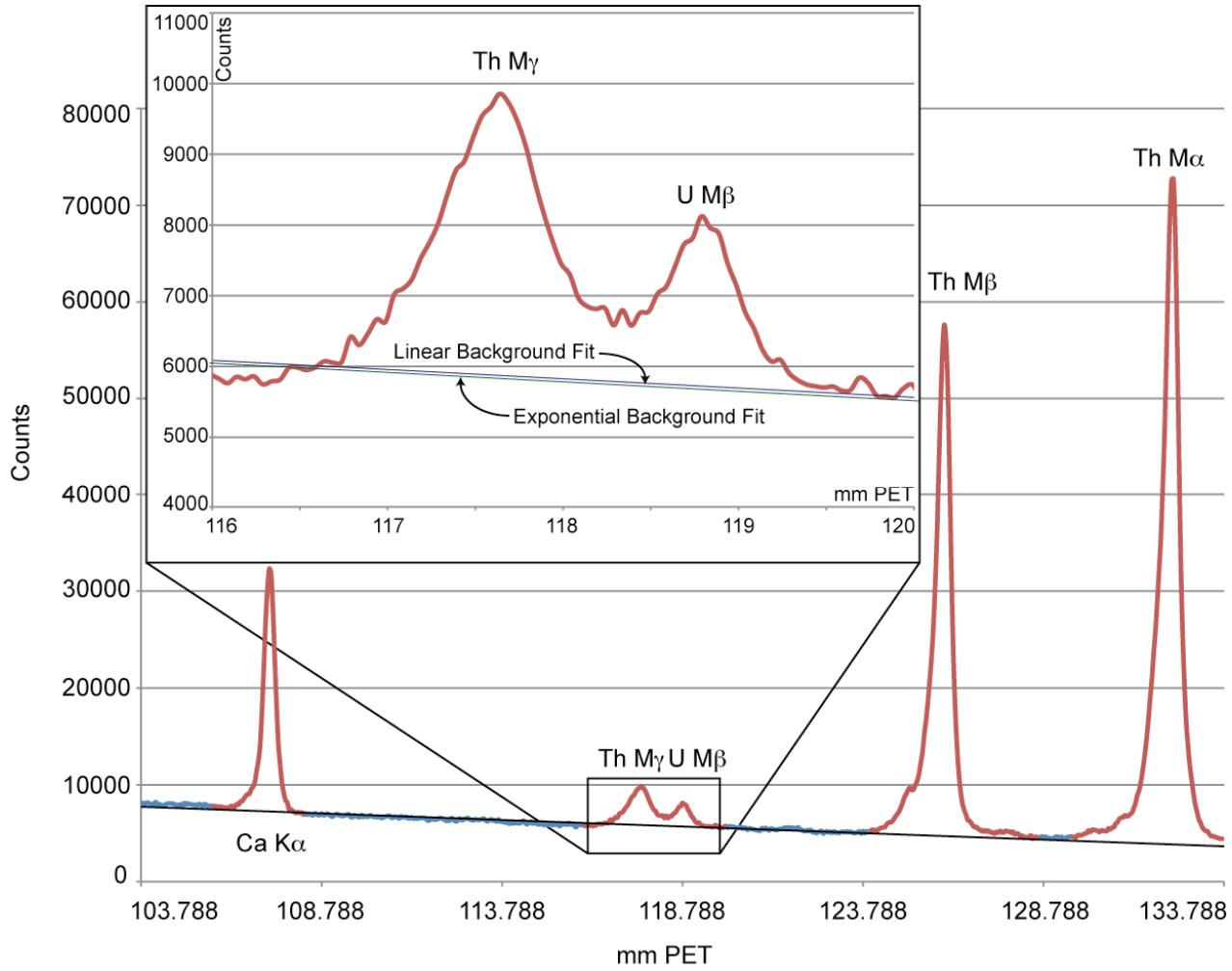


**Figure 3-3.** WD intensity scan of the GSC-8153 reference monazite in the region of U Mβ with peaks labeled. A linear and exponential background is fit through the blue region of the spectra.

and propagated through the age equation, these differences yield a difference in age of 2.7±1.0 %.

I calculated tanh ages and bootstrap uncertainties for the GSC-8153 and Trebilcock reference standards using both linear and exponential fits for data collected during a single analytical session. For the GSC-8153 reference monazite, with a chemical age of *ca.* 501 Ma, I obtained a (U-Th)-Pb tanh age of 504±5 Ma when I utilized a linear background fit and a (U-Th)-Pb tanh age of 518±5 Ma when I utilized the exponential background fit. For the Trebilcock monazite, with a $^{207}Pb/^{235}U$ age of 272±2 Ma, I obtained a (U-Th)-Pb tanh age of 274±2 Ma when I utilized a linear background fit and a (U-Th)-Pb tanh age of 281±2 Ma when I utilized an exponential background fit. In both instances, the linear background fit yields (U-Th)-Pb ages statistically identical to isotopically determined ages, whereas the exponential fit yields ages ~2.7% older than the isotopic ages. Therefore, I utilized a linear background model in this work.

***Age, Error and Pb Isotope Calculations***

The equation used to calculate the age is

$$Pb = \frac{Th \cdot Ma_{Pb\,208}}{Ma_{Th\,232}}\left(e^{\lambda_{Th232}t} - 1\right) + \frac{U \cdot Ma_{Pb\,206}}{Ma_{U}} \cdot \frac{137.88}{138.88}\left(e^{\lambda_{U238}t} - 1\right) + \frac{U \cdot Ma_{Pb\,207}}{Ma_{U}}\left(1 - \frac{137.88}{138.88}\right)\left(e^{\lambda_{U235}t} - 1\right)$$

where Pb, Th and U are total element concentrations, Ma is the atomic mass of an isotope or element, λ is the decay constant for an isotope and t is time (*e.g.,* Montel *et al.* 1996). The monazite microprobe dating technique does not distinguish between individual isotopes of Pb and U, but instead uses total Pb and U measurements. Thorium is considered to be mononuclidic since $^{232}Th$ is the only isotope of Th stable

on a timescale relevant to this technique. The date calculated based on EPMA data is a mixture of the $^{207}Pb/^{235}U$, $^{206}Pb/^{238}U$ and $^{208}Pb/^{232}Th$ ages, with the percent each contributes to the chemical age based on the relative concentrations of Th and U and the age of the monazite grain. As $^{235}U$ comprises ~0.7200% of the U system, the $^{207}Pb/^{235}U$ age is a minor component of the overall chemical age.

A program was written in C to calculate the monazite chemical dates based on the monazite age equation of Montel *et al.* (1996) and errors based on standard error propagation techniques (Appendix D). The program reads a standard tab delimited text file containing the following fields: comment, $ThO_2$, $UO_2$, PbO, percent error on $ThO_2$, percent error on $UO_2$, percent error on PbO, $Y_2O_3$ k-ratio and $ThO_2$ k-ratio. The oxides are first converted to element concentrations. Corrections for Y and Th interference on Pb, and Th interference on U are applied according to the method of Pyle *et al.* (2005).

The error on an individual date is obtained by calculating the absolute error on each element, and propogating these values through the error equation, together with the calculated date and concentration of each element, as follows

$$\sigma_t = \sqrt{\frac{\sigma_{Pb}^2 - \left(\frac{Ma_{Pb208}}{Ma_{Th232}} \cdot e^{\lambda_{Th232} t} - \frac{Ma_{Pb208}}{Ma_{Th232}}\right)^2 \cdot \left(\sigma_{Th}^2\right) - \left[\left(\frac{Ma_{Pb206}}{Ma_U} \cdot \frac{137.88}{138.88} \cdot e^{\lambda_{U/238} t} - \frac{Ma_{Pb206}}{Ma_U} \cdot \frac{137.88}{138.88}\right) + \left(\frac{Ma_{Pb207}}{Ma_U} \cdot \left(1 - \frac{137.88}{138.88}\right) \cdot e^{\lambda_{U/235} t} - \frac{Ma_{Pb207}}{Ma_U} \cdot \left(1 - \frac{137.88}{138.88}\right)\right)\right]^2 \cdot \left(\sigma_U^2\right)}{\left(\frac{Ma_{Pb208}}{Ma_{Th232}} \cdot e^{\lambda_{Th232} t} \cdot Th \cdot \lambda_{Th232} + \frac{Ma_{Pb206}}{Ma_U} \cdot \frac{137.88}{138.88} \cdot e^{\lambda_{U/238} t} \cdot U \cdot \lambda_{U/238} + \frac{Ma_{Pb207}}{Ma_U} \cdot \left(1 - \frac{137.88}{138.88}\right) \cdot e^{\lambda_{U/235} t} \cdot U \cdot \lambda_{U/235}\right)^2}}$$

where Ma is atomic mass for an isotope or element, $\lambda$ is the decay constant for an isotope, $\sigma$ is the error on a quantity and t is time. Th, U and Pb are element concentrations.

### *Protocol for Monazite EPMA Dating*

In this work the following protocol was used for EPMA dating of monazite (Fig. 3-1). 1) The petrography of the sample was characterized in hand sample and petrographic thin section in order to understand the metamorphic history of the rock prior to any mineral chemical study. 2) Monazite was located in petrographic thin sections using backscattered electron imaging on the JEOL JXA 8900. 3) X-ray elemental composition maps were collected for Th, U, Pb and Y for each monazite grain of interest. 4) Monazite chemistry was analyzed at select points using the JEOL JXA 8900. 5) U, Th and Pb concentrations, and Y and Th k-ratios were input into a software package used to calculate individual dates from the elemental concentrations. 6) Individual dates were binned into populations. 7) The tanh ages and bootstrap uncertanties were calculated for each population.

## *Recommended Statistical Methods*

I employed a rigorous statistical approach to the analysis of chronologic data that comprises descriptive, traditional and robust statistical methods. This combination allows for a complete statistical evaluation of each dataset to be compiled.

### *Descriptive Statistical Techniques*

Descriptive statistical tools are a simple technique for visualizing data, and comparing datasets. The simplest method for visually examining a dataset is a box-and-whisker plot (Tukey 1977). Box-and-whisker plots show the middle 50% of a dataset plotted as a box, with the lower bound of the box at the first quartile ($25^{th}$ percentile) of the dataset, the upper bound of the box at the third quartile ($75^{th}$ percentile) of the dataset

and a line drawn to represent the median ($50^{th}$ percentile) of the dataset within the box. Whiskers are drawn at the top and bottom of the box extending to 1.5 times the interquartile range past the limit of the box, where the interquartile range is the range between the first and third quartiles. Data that lie more than 1.5 times the interquartile range from the box are treated as outliers and plotted as individual points.

Box-and-whisker plots reveal features in the dataset that are necessary to know prior to continuing the statistical analysis of a dataset. Most importantly, they provide a first pass method to determine the distribution of a dataset. Many of the statistical techniques that are traditionally used in interpreting geochronologic datasets, including some of the techniques that I present here, are based on the assumption of a normally distributed population. As discussed earlier, this assumption is not always valid and performing traditional statistical analysis of non-normally distributed data can result in erroneous interpretations. A symmetric box-and-whisker plot, where the median plots approximately equidistant from the $25^{th}$ and $75^{th}$ percentiles, likely indicates an approximately normally distributed dataset. An asymmetric box-and-whisker plot, where the median is not equidistant from the $25^{th}$ and $75^{th}$ percentiles, is a first warning sign that a dataset has a non-normal distribution, and that additional statistics such as the kurtosis and skewness should be carefully considered prior to any interpretations being made about the dataset.

Box-and-whisker plots also provide a first-pass method of distinguishing between statistically distinct populations of data. Datasets that are represented by overlapping boxes in box-and-whisker plots may be treated as having been derived

from the same population. If the boxes do not overlap, then the two datasets initially may be considered to be statistically distinct from one another (Powell, Pers. Comm.).

***Analyzing the Distribution***

Prior to performing any additional statistical analysis, a quantitative assessment of the normality of the data should be performed by analyzing the skewness and kurtosis of the data and by constructing a probability plot.

The skewness is a measure of asymmetry of a distribution defined by

$$S = \frac{n}{(n-1)(n-2)} \sum_{i=1}^{n} \left( \frac{x_i - \bar{x}}{s} \right)^3$$

where n is the sample size, the $x_i$ is the individual data, $\bar{x}$ is the sample mean and s is the sample standard deviation. Datasets skewed to the right (towards an older age in conventionally plotted geochronologic datasets) have positive skewness values, and datasets skewed to the left (towards a younger age in geochronologic datasets) have negative skewness values. A skewness of 0 indicates a symmetric dataset, consistent with a normally distributed dataset. In practice, it is highly improbable to have a sample dataset with a skewness of 0 because of random errors that cannot be accounted for. I consider datasets to be asymmetric if the skewness departs from 0 by more than 2 standard errors of skewness, which is defined as

$$SE_S = \sqrt{\frac{6}{n}}$$

by Tabachnick and Fidell (1996).

Kurtosis, the measure of peakedness, or flatness in a dataset when compared to a normal distribution, is defined by

$$K = \left\lfloor \frac{n(n-1)}{(n-1)(n-2)(n-3)} \sum_{i=1}^{n} \left( \frac{x_i - \bar{x}}{s} \right)^4 \right\rfloor - \frac{3(n-1)^2}{(n-2)(n-3)}$$

where n is the sample size, $x_i$ is the individual data, $\bar{x}$ is the sample mean and s is the sample standard deviation. A positive kurtosis value indicates a taller-than-normal distribution whereas a negative kurtosis value indicates a flatter-than-normal distribution. A normally distributed dataset will have a kurtosis of 0. I consider the dataset to have a kurtosis near 0 if the kurtosis does not depart from 0 by more than 2 standard errors of kurtosis, defined as

$$SE_K = \sqrt{\frac{24}{n}}$$

by Tabachnick and Fidell (1996).

Probability plots are a graphical method for comparing the probability distribution of a random sample taken from a given population to a reference distribution (Devore, 2008). Probability plots are constructed by ordered observed data on the y-axis versus the normal order statistic medians on the x-axis. More simply, the observed data are plotted against a theoretical normal distribution. If the observed data are normally distributed, they will plot on a straight line in a normal probability plot and the data will be evenly distributed between 0 and 100% probability. The data are taken to plot in a straight line if they fall within the 95% prediction interval of a linear fit to the data.

Data that fail the tests for normality likely do not represent a single population of monazite ages. Non-normal age distributions could indicate a mixed dataset taken from more than one age population or the accidental measurement of inclusions or neighboring phases. The sample mean and standard deviation for these datasets will

not represent a geologically significant age. These datasets should be carefully re-evaluated in the context of chemical zoning and petrographic setting of individual grains to ensure that only data taken from a single age population are included prior to interpreting an age.

In the ideal case of large monazite grains with clearly defined zones it is simple to bin data into groups that represent single age populations. Many populations of monazite are far from ideal, and grouping data into individual populations can be tricky in situations where there is little or no geological, petrographic, structural or chemical evidence for individual age populations. Analyses unknowingly taken from multiple age zones could be common in situations where monazite grains are small. These unknowns can lead to asymmetric, non-normally distributed datasets with many outliers.

***Robust Statistical Age and Uncertainty Calculation***

Kelsey *et al.* (2003) suggest using the robust tanh estimator in the interpretation of monazite ages. The tanh estimator, a robust statistic that is able to accommodate non-normally distributed data and outliers, is defined by

$$t_{\text{tanh}} = \frac{\sum_{i=1}^{n} \frac{d_i}{\sigma_{d_i}^2}}{\sum_{i=1}^{n} \sigma_{d_i}^{-2}}$$

where $t_{tanh}$ is the tanh age, $d_i$ is an individual date, $\sigma_{di}$ is the analytical uncertainty on $d_i$ and n is the number of data. The tanh estimator will return an age identical to the sample mean for normally distributed data. Therefore, I recommend reporting the tanh age for all populations of monazite dates.

Powell *et al.* (2002) suggest using the boostrap method for calculating uncertainties for isochron ages. This is an appropriate statistical method for expressing uncertainty on ages in general, and I recommend this method for calculation of uncertainty on EPMA ages. A bootstrap uncertainty is calculated by choosing n samples at random, with replacement from a given dataset, in this case a single population of dates taken to represent a single age. For these n samples, a simple average is calculated. This procedure is repeated m times, each time for n samples. The bootstrap uncertainty is the standard deviation of the m averages (Devore, 2008). Uncertainty reported at the 95% confidence interval is taken to be twice the bootstrap uncertainty. In this work I have used n values of 20 and m values of 200 samples, which I recommend as minimum values.

If the individual chemical data are taken randomly from a single normally distributed population, it is acceptable to calculate these statistics from a relatively small number of data ($n>10$). However, in the event that the data are taken from a non-normally distributed population, it becomes necessary to collect larger random samples ($n>30$) in order to satisfy the central limit theorem, which states that the sample mean and standard deviation of large datasets approximate a normal distribution. It is not always possible to collect datasets this large. I have observed that most chemical data taken from single age zones in monazite follow normal distributions. As such, small datasets are acceptable as long as other evidence exists that the data are derived from a single age population.

A two-sample t test is a statistical method for evaluating the uniqueness of two datasets. This test is useful for determining whether two ages are statistically

distinct from one another. The t test is based on the assumption that the data are taken from normally distributed populations, and should only be used when it can be reasonably assumed that the data follow normal distributions.

### *Application with Reference Monazite*

In this work I have analyzed both the GSC-8153 and the Trebilcock reference monazites during each analytical session as a quality control check. Table 3-3 summarizes data collected for GSC-8153 during 14 analytical sessions over a 1.5 year

| Sample | n | tanh Age | 95% Bootstrap Uncertainty | Kurtosis | SEk | KURT? | Skewness | SEs | SKEWED? |
|---|---|---|---|---|---|---|---|---|---|
| 8153-1 | 48 | 500 | ±6 | 0.40 | 0.71 | NO | 0.34 | 0.35 | NO |
| 8153-2 | 20 | 510 | ±3 | -1.10 | 1.10 | NO | -0.27 | 0.55 | NO |
| 8153-3 | 20 | 517 | ±3 | 0.12 | 1.10 | NO | 0.16 | 0.55 | NO |
| 8153-4 | 15 | 512 | ±2 | -1.03 | 1.26 | NO | 0.10 | 0.63 | NO |
| 8153-5 | 32 | 504 | ±4 | -0.22 | 0.87 | NO | 0.10 | 0.43 | NO |
| 8153-6 | 87 | 506 | ±4 | -0.18 | 0.53 | NO | -0.07 | 0.26 | NO |
| 8153-7 | 15 | 508 | ±4 | -0.52 | 1.26 | NO | -0.08 | 0.63 | NO |
| 8153-8 | 17 | 507 | ±3 | -0.97 | 1.19 | NO | -0.06 | 0.59 | NO |
| 8153-9 | 44 | 499 | ±4 | 0.05 | 0.74 | NO | 0.33 | 0.37 | NO |
| 8153-10 | 40 | 505 | ±5 | -0.70 | 0.77 | NO | -0.03 | 0.39 | NO |
| 8153-11 | 32 | 504 | ±5 | -0.22 | 0.87 | NO | 0.10 | 0.43 | NO |
| 8153-12 | 113 | 505 | ±4 | -0.48 | 0.46 | NO | 0.19 | 0.23 | NO |
| 8153-13 | 88 | 507 | ±4 | -0.17 | 0.52 | NO | -0.02 | 0.26 | NO |
| 8153-14 | 42 | 504 | ±6 | -0.82 | 0.76 | NO | 0.32 | 0.38 | NO |

**Table 3-3.** Summary of monazite microprobe data for the GSC-8153 reference monazite collected at the University of Maryland. SEk is the standard error on the kurtosis; KURT? asks if the data lie within 2 SEk of 0; SEs is the standard error on the skewness; SKEWED? asks if the data lie within 2 SEs of 0.

period. In all instances, the skewness and kurtosis values are within 2 standard errors of zero, which suggests that each dataset represents a normally distributed sample population. Probability plots, which show that the data follow a normal distribution in each case for two exemplar sessions (12 & 13) are given in Fig. 3-4. The boxes in the box-and-whisker plots for each session (Fig. 3-5) overlap, providing an indication that the data represent the same age population.

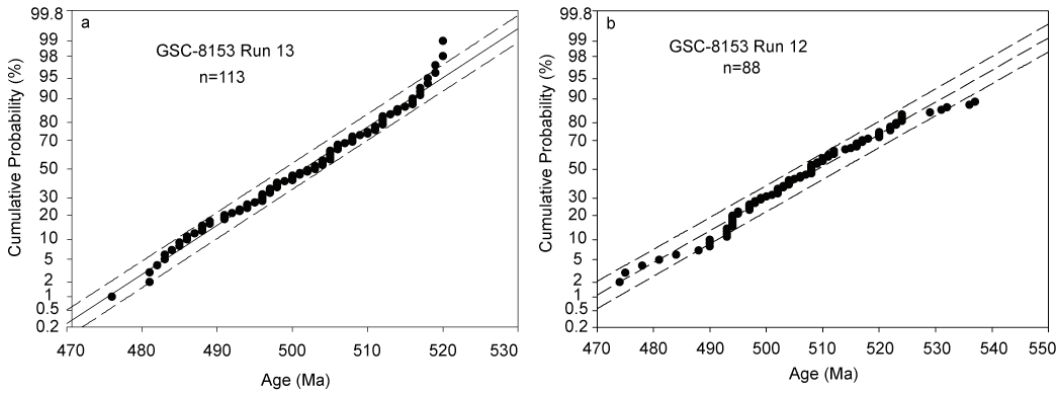


**Figure 3-4.** Exemplar probability plots for data from two of the GSC-8153 analytical sessions. The linear fit, along with the uniform spread of the data suggest a normally distributed dataset.

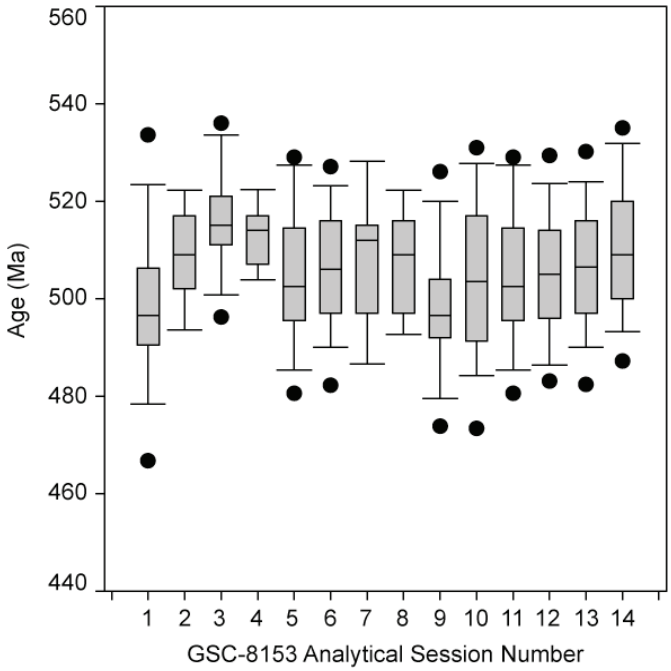


**Figure 3-5.** Box-and-whisker Plot for GSC-8153 Analyses. The box in the box-and-whisker plot represents the middle 50% of the data. The whiskers extend to 1.5 times the interquartile range and solid circles are used to represent outliers. The box-and-whisker plot indicates that the GSC-8153 reference monazite has been consistently reproduced in the analyses obtained using the JEOL/JXA-8900 at the University of Maryland.

I used the tanh estimator to calculate ages for each session. Because the data are normally distributed, the tanh ages are similar to the mean ages for each sample. The bootstrap uncertainty calculated for each age ranges between ±4 and ±12 Ma. In most instances, the 95% bootstrap confidence interval includes the SIMS (U-Th)-Pb

age of the GSC-8153 monazite of *ca.* 505 Ma. The two exceptions to this are sessions 8153-3 and 8153-4 for which I suggest that the small number of data collected during these sessions may be the reason for the SIMS age not falling within the 95% confidence intervals.

### *Comparison of EPMA Monazite Ages with SIMS Monazite Ages*

Monazite dated using the EPMA dating technique at the University of Maryland was analyzed for U, Th and Pb using a Cameca ims 1270 secondary ion mass spectrometer at the University of California at Los Angeles following the protocols of Harrison *et al*. (1995). Data were collected for monazite from sample 05b-5-23 from the Southern Brasília Belt, and reference monazite GSC-8153. Table 3-4 lists the (U-Th)-Pb chemical ages and the $^{206}Pb/^{238}U$ and $^{207}Pb/^{235}U$ isotopic ages for these monazites. In all cases, the (U-Th)-Pb ages are statistically identical with a p-value >0.05 to the $^{206}Pb/^{238}U$ age, and are similar to the $^{207}Pb/^{235}U$ age. The correspondence between the EPMA ages presented in this work, and the SIMS ages for the same samples provides evidence that I am able to accurately collect (U-Th)-Pb data in monazite using the protocol presented in this work.

| | ***UMD EPMA*** | | ***UCLA SIMS*** | | ***UCLA SIMS*** | |
|---|---|---|---|---|---|---|
| | (U-Th)-Pb Age | 95% Bootstrap Unc. | 206/238 Age | 2σ error | 207/235 Age | 2σ error |
| 05b-5-23 Cores | 631 | ±12 | 630 | ±13 | 623 | ±10 |
| 05b-5-23 Rims | 605 | ±6 | 605 | ±8 | 602 | ±6 |
| GSC-8153 | 504 | ±5 | 506 | ±5 | 494 | ±7 |

**Table 3-4.** Comparison of isotopic ages and (U-Th)-Pb chemical ages for an exemplar sample of monazite from the Southern Brasília Belt and from the GSC-8153 reference. Isotopic ages were obtained using a Cameca ims 1270 SIMS at UCLA, and (U-Th)-Pb chemical ages were obtained using a JEOL/JXA-8900 EPMA at the University of Maryland.

*Brasília Belt Metamorphism*

I illustrate these protocols using data from the southern sector of the Southern Brasília Belt.

### *Geologic Background*

The Neoproterozoic assembly of Gondwanan elements in southeastern Brazil (Fig. 3-6) began with the closure of the Brazilide Ocean and suturing of the Paranapanema Block in the south (older) and the Amazon Craton in the north (younger), together with intervening magmatic arcs, to the São Francisco Craton creating the Brasília Belt. Subsequent closure of a restricted southward-opening ocean between the São Francisco and Congo cratons produced the Ribeira and Araçuaí Belts along the South American coast and the West Congo and Kaoko Belts along the African coast (*e.g.*, Machado *et al.* 1996; Campos Neto & Caby 1999; Junges *et al.* 2002; Pimentel *et al.* 2004; Schmitt *et al.* 2004, 2008; Alkmim *et al.* 2006; Heilbron *et al.* 2008).

The southern sector of the Southern Brasília Belt comprises a stack of flat-lying nappes that were transported to the ENE during the Brasília Orogeny (Campos Neto & Caby 1999). The lower-grade nappes (Fig. 3-6c) record the lowest pressures but are structurally deeper in the nappe stack, whereas the higher-grade Carmo da Cachoeira, Lambari/Liberdade and Três Pontas–Varginha Nappes (Fig. 3-6c) record higher pressures and occur structurally higher in the nappe stack (*e.g.*, Campos Neto & Caby 1999, 2000; Garcia & Campos Neto 2003). Klippen of high-grade granulite facies rocks found in the southernmost portion of the Brasília Belt are inferred to be associated with the Três Pontas–Varginha Nappe. The Socorro–Guaxupé Nappe, at the top of the nappe stack, comprises part of the magmatic arc from the hanging-wall

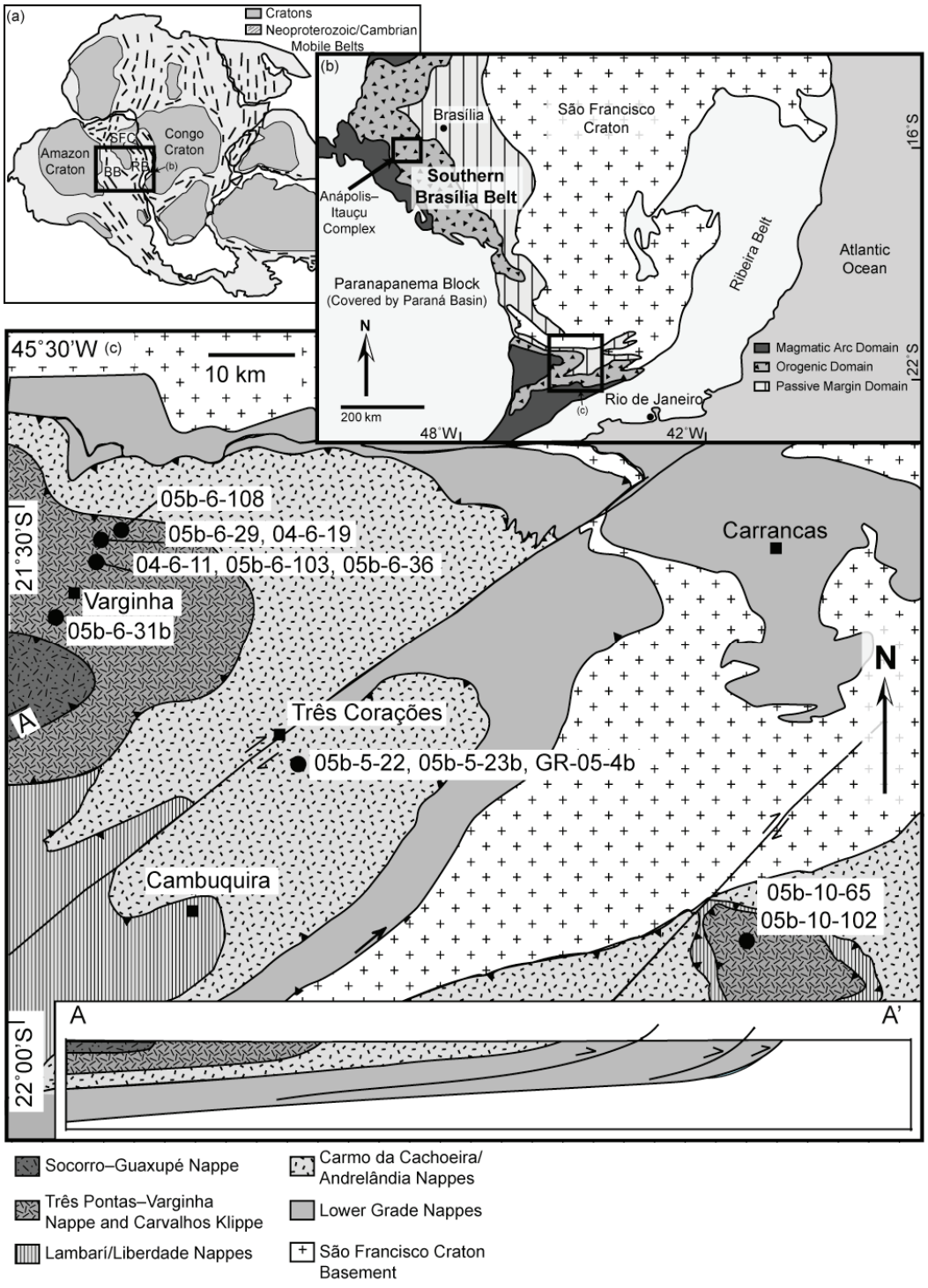


**Figure 3-6.** (a) Simplified map of Gondwana with cratons indicated by grey, and Neoproterozoic mobile belts indicated by hash marks. The box indicates the location of the Southern Brasília Belt. (b) Geological map of the Southern Brasília Belt, with box indicating the location of the Anápolis-Itauçu Complex in the northern sector and the study area in the southern sector of the Southern Brasília Belt. (c) Tectonic map of the Andrelândia Nappe Complex in the southern sector of the Southern Brasília Belt.

(Campos Neto & Caby 1999). The nappes beneath the Socorro–Guaxupé Nappe are composed of metasedimentary rocks originally deposited along the passive margin of the São Francisco Craton prior to subduction and terminal collision (*e.g.*, Ribeiro *et al.* 1995).

A second orogenic event affected eastern Brazil during the Ediacaran to Cambrian Periods when the eastern edge of the São Francisco plate subducted beneath the Serra do Mar microplate, forming the Rio Negro magmatic arc between *ca.* 635 Ma and 600 Ma. This magmatic arc collided with the São Francisco Craton at 590–550 Ma (*e.g.*, Machado *et al.* 1996; Heilbron *et al.* 2000; Schmitt *et al.* 2004), leading to the formation of the Ribeira belt, as the arc accreted to the southeastern margin of the São Francisco Craton. The Ribeira Belt comprises a thrust and fold belt extending 1500 km from Bahia in the north to Paraná in the south (Machado *et al.* 1996). The central portion of this belt, which, in part, underlies the states of Rio de Janeiro and southeastern Minas Gerais consists of a series of thrust slices emplaced at amphibolite facies conditions (Machado *et al.* 1996). A younger event, the Búzios Orogeny, occurred between 525 and 505 Ma on the eastern edge of the Ribeira Belt (Schmitt *et al.* 2004).

In the southern Brasília Belt, nappes of the Andrelândia Nappe Complex lie in the interference zone between these two orogenic belts, where the effects of the Ribeira Orogeny are superimposed on rocks deformed and metamorphosed in the Brasília Orogeny (Trouw *et al.* 2006). In the southern portion of the nappe complex, sillimanite pseudomorphs after kyanite occur together with matrix sillimanite. Trouw *et al.* (2006) suggest that the Ribeira orogenic event led to an overprinting of

sillimanite in the southern portion of the Andrelândia Nappe Complex. A metamorphic map indicates a sillimanite-in isograd trending E-W that crosscuts the NE-SW trending isograds produced by Brasília Belt metamorphism; this is the macroscopic petrographic evidence for the overprint. The klippen associated with the Três Pontas–Varginha Nappe occur within this overprinting zone, whereas the Três Pontas–Varginha and Carmo da Cachoeira Nappes both lie north of the overprinting zone.

My focus in this study concerns two of the higher-grade nappes and their associated klippen. In Chapter 2 I interpret peak *P-T* conditions of ~1.5 GPa and 840–900˚C for the Três Pontas–Varginha Nappe based on isochemical *P-T* phase diagrams (pseudosections). A U-Pb zircon age of *ca.* 648 Ma (648±12 Ma, 647±11 Ma; Table 3-5) is interpreted in Chapter 2 to record the timing of just post-peak metamorphism in the this nappe, whereas a U-Pb zircon age of *ca.* 622 Ma (Table 3-5) from the uppermost Socorro–Guaxupé Nappe is interpreted to record crystallization at close-to-peak granulite facies conditions. A (U-Th)-Pb monazite age of 609±7 Ma is interpreted by Martins *et al*. (2008) to record crystallization of granitic leucosomes further to the west in the Socorro–Guaxupé Nappe and outside the study area.

| Sample | Nappe | $^{206}Pb/^{238}U$ Age |
|---|---|---|
| 04-7-1 | Socorro–Guaxupé | 622 ±28 |
| 05-13-13 | Retrograded Eclogite | 678 ±29 |
| 05-6-31b | Três Pontas–Varginha | 647 ±11 |
| 04-6-11 | Três Pontas–Varginha | 648 ±12 |

**Table 3-5.** Summary of previous zircon chronology from the Southern Brasília Belt from Chapter 2.

Retrograded eclogites located along the tectonic contact between the Três Pontas–Varginha and Carmo da Cachoeira Nappes are interpreted to represent slivers of ocean crust (Trouw *et al.* 2006) transported along the contact between an upper nappe already detached from the downgoing plate and a lower nappe continuing to underthrust prior to detachment from the downgoing plate in the subduction system. Pressures of up to ~1.75 GPa have been reported from retrograded eclogites located between the Liberdade and Andrelândia Nappes (Campos Neto & Caby 1999). In Chapter 2 I interpret a U-Pb zircon age of 678±29 Ma (Table 3-5) to represent the minimum age for detachment of the nappes from the subducting slab.

Further north, the timing of metamorphism in the Anápolis-Itauçu Complex in the northern sector of the Southern Brasília Belt is constrained to *ca.* 649–634 Ma, based on high-precision TIMS U–Pb zircon ages (Baldwin & Brown 2008).

### *Sample Description*

Monazite was analyzed in seven samples from the Três Pontas–Varginha Nappe, three samples from the Carmo da Cachoeira Nappe and two samples from the Carvalhos Klippe, a klippe inferred to be associated with the Três Pontas–Varginha Nappe. All data are listed in Table B-1 in appendix B.

#### Três Pontas–Varginha Nappe Samples

Monazite was analyzed in seven samples from the Três Pontas–Varginha Nappe. Sample 05b-6-108 was taken from the Santo Antonio Quarry near the base of the nappe. Samples 04-6-11, 05b-6-103 and 05b-6-36 were taken from the Três Pontas Quarry near the middle of the nappe. Samples 04-6-19 and 05b-6-29 were taken from the Four Level Quarry between the Três Pontas and Santo Antonio Quarries.

Sample 05b-6-31b was taken from the Lixão (garbage dump) of the city of Varginha, at the top of the nappe.

Sample 04-6-11 is leucosome-dominated and comprises primarily medium grained (2–4 mm) quartz, plagioclase, K-feldspar, with clusters of 3–5 mm euhedral garnets and minor retrograde muscovite. Stringers of ilmenite up to 2 mm long occur along K-feldspar–K-feldspar grain boundaries. Monazite up to 350 μm in diameter occurs in the leucosome.

Sample 04-6-19 is a medium grained quartz-rich garnet granulite. Subhedral garnets up to 5 mm in diameter have inclusions of kyanite, biotite, quartz and plagioclase and show microstructural evidence of partial replacement by biotite. The matrix is comprised of 50% quartz, with plagioclase and K-feldspar and rare biotite and kyanite/sillimanite. Accessory monazite, ilmenite and rutile also occur in the matrix.

Sample 05b-6-29 comprises a garnet–biotite–K-feldspar gneiss. Subhedral garnet up to 6 mm in diameter contain inclusions of quartz, kyanite and plagioclase. Garnet is rimmed by biotite, kyanite/sillimanite and K-feldspar. Biotite is aligned within the foliation. Quartz, K-feldspar and plagioclase comprise the matrix, together with accessory monazite, rutile and ilmenite.

Sample 05b-6-103 is a garnet–kyanite–K-feldspar gneiss. Garnet up to 5 mm in diameter contains inclusions of biotite, plagioclase, quartz, monazite and rutile. Kyanite up to 5 mm long is aligned with foliation. A matrix of quartz, K-feldspar and plagioclase contains accessory ilmenite. Millimeter bands of biotite occur aligned with foliation.

Sample 05b-6-108 is a garnet–kyanite/sillimanite–biotite gneiss. Euhedral garnet up to 1 cm in diameter has inclusions of quartz and muscovite. Sillimanite ± kyanite and biotite up to 3 mm long are both aligned with foliation. Quartz and K-feldspar, together with accessory ilmenite and monazite occur in the matrix.

Sample 05b-6-31b is a garnet–biotite–quartz–plagioclase–kyanite/sillimanite gneiss that is strongly foliated. Large sillimanite grains up to 5mm in length occur in the foliation whereas smaller sillimanite grains (<0.5 mm) occur primarily between large (2–5 mm) garnet grains. Accessory ilmenite occurs as inclusions in the mantle regions of garnet, and in the matrix. Monazite up to 250 μm in diameter occurs as inclusions in garnet, and along garnet grain boundaries.

Sample 05b-6-36 is a garnet–kyanite/sillimanite–K-feldspar gneiss. Subhedral garnet up to 5 mm in diameter has inclusions of ilmenite and rutile. The matrix of quartz, plagioclase and sillimanite up to 5 mm in length is strongly foliated. Rare K-feldspar and accessory rutile occur in the matrix. Monazite up to 500 μm in length occurs as inclusions in garnet.

**Carmo da Cachoeira Nappe Samples**

Monazite was analyzed in samples collected from different sections of the INCOPE working quarry south of Tres Coraçoes in the Carmo da Cachoeira Nappe.

Sample 05b-5-23 is a strongly foliated biotite–garnet gneiss. Euhedral garnet up to 5 mm in diameter has inclusions of biotite, plagioclase, quartz and rutile. The matrix comprises 3–5 mm long biotite grains foliated with kyanite, quartz and plagioclase. Accessory ilmenite occurs in the matrix. Monazite up to 250 μm in diameter occurs as inclusions in biotite.

Sample 05b-5-22 is a strongly foliated biotite–garnet gneiss. Subhedral to euhedral garnet up to 2 mm in diameter has inclusions of quartz, plagioclase and rutile. Biotite and kyanite up to 1 mm in length are aligned within the foliation with plagioclase and quartz. Rare muscovite and accessory ilmenite, rutile and tourmaline are present in the matrix. Monazite up to 100 μm in diameter occurs as inclusions in biotite.

Sample GR-05-4B is a strongly foliated biotite–garnet gneiss. Euhedral garnet up to 7 mm in diameter has inclusions of biotite, quartz, plagioclase and rutile. Biotite 2–4 mm long is aligned within the foliation with plagioclase and quartz. Accessory ilmenite, rutile and tourmaline are present in the matrix. Monazite up to 200 μm in diameter occurs in the matrix.

**Carvalhos Klippe Samples**

Monazite was analyzed in two samples from the Carvalhos Klippe. Samples 05b-10-102 and 05b-10-65 were both taken from a waterfall just north of the city of Carvalhos.

Sample 05b-10-102 has large (1 cm) euhedral garnets that are rimmed by small (<0.1 mm) biotite grains. The garnet includes rutile and ilmenite. The rock is weakly foliated with biotite and kyanite grains (1–2 mm). Quartz, plagioclase, rare muscovite and accessory ilmenite and rutile occur in the matrix. Monazite up to 150 μm in diameter is associated with biotite and kyanite in the matrix. One larger grain (250 μm) was found as an inclusion in garnet.

Sample 05b-10-65 is a coarse-grained garnet–kyanite–K-feldspar gneiss. Garnets up to 1 cm in diameter contain inclusions of ilmenite, biotite and monazite up

to 400 μm long. Kyanite grains 5-8 mm long are aligned within the foliation and contain inclusions of biotite and monazite (75 μm diameter). Biotite (1–5 mm) grains are aligned with foliation. Quartz, plagioclase and K-feldspar are contained in the matrix. Accessory ilmenite is associated with biotite and kyanite in the foliation.

### *Monazite Geochronology*

#### Três Pontas–Varginha Nappe

Monazite in sample 05b-6-108 shows distinct cores and rims in yttrium X-ray element composition maps (Fig. 3-7q, r). Culling the data by core and rim for this sample did not yield statistically significant ages. As such, the data were combined and a single tanh age of 588±10 Ma (Fig. 3-8; Fig. 3-9) was calculated for the 35 dates from this sample. A low kurtosis of -0.17 and skewness of -0.01 suggest these data represent a single age population. A probability plot for this sample confirms a normal distribution and is shown as an example of a normally distributed dataset (Fig. 3-10a).

Monazite in sample 04-6-11 shows distinct cores and rims in yttrium X-ray element composition maps (Fig. 3-7m, n). High-Y cores yield a tanh age of 611±6 Ma (Fig. 3-8; Fig. 3-9) based on 31 dates. A low kurtosis of -0.68 and skewness of 0.09 suggest these data represent a single age population. Low-Y cores yield a tanh age of 582±6 Ma (Fig. 3-8; Fig. 3-9) based on 36 dates. A low kurtosis of -0.49 and skewness of -0.31 suggest these data represent a single age population.

Sample 05b-6-103 contains monazite with distinct high-Y cores and low-Y rims (Fig. 3-7k, l). The high-Y cores yield a tanh age of 630±10 Ma (Fig. 3-8;

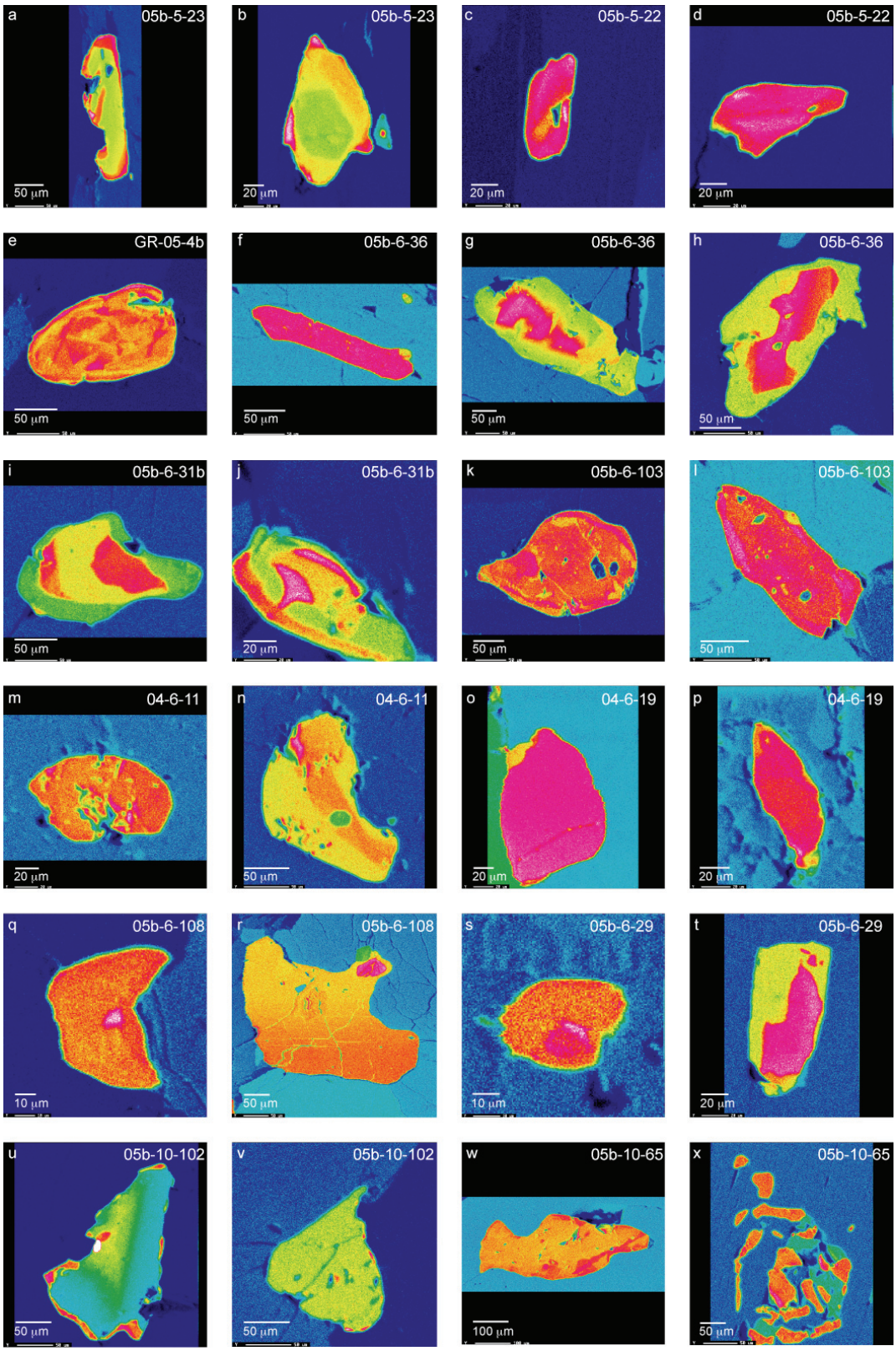


**Figure 3-7.** Yttrium X-ray element composition maps of monazite. The color scale represents relative count intensity, with warmer colors representing higher count rates.

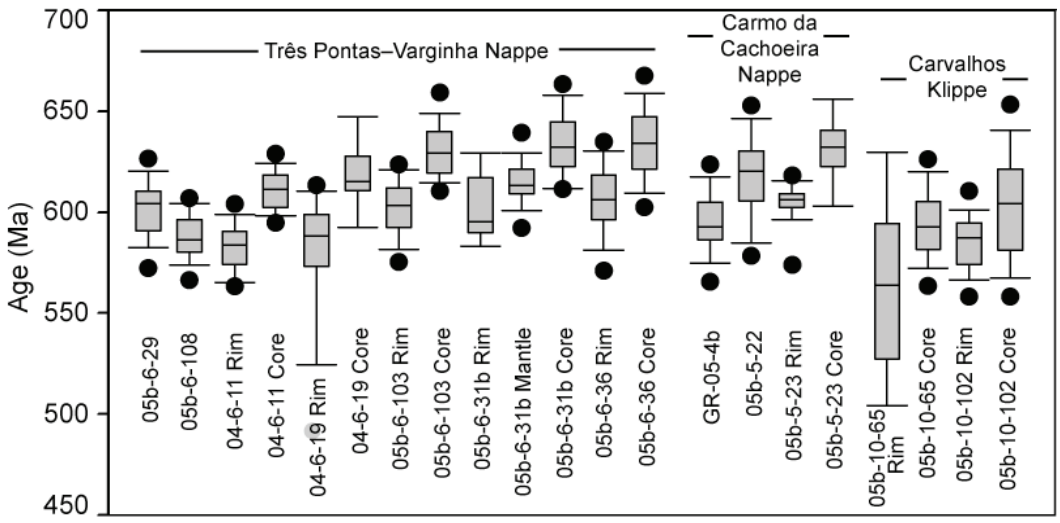


**Figure 3-8.** Box-and-whisker plot of monazite from the Andrelândia Nappe Complex.

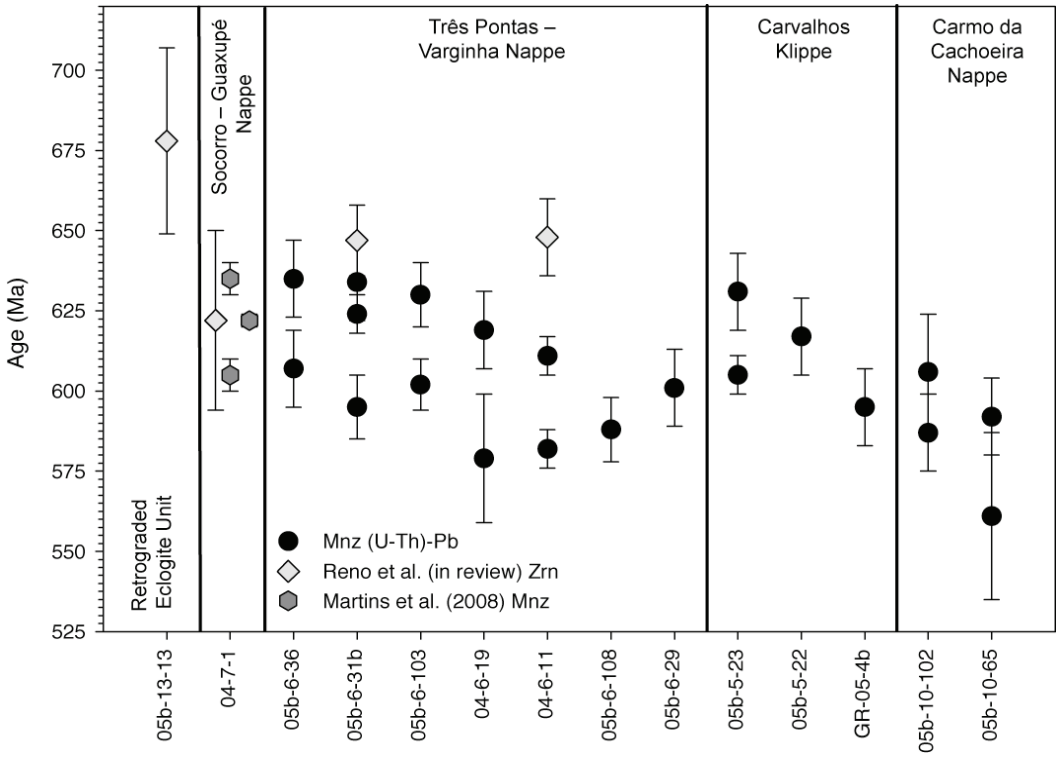


**Figure 3-9.** Summary of chronologic data from the Andrelândia Nappe Complex. Uncertainties on (U-Th)-Pb monazite data are expressed at 95% bootstrap confidence intervals; uncertainties on other data are 2σ.

**Table 3-6.** Summary of monazite microprobe ages from the Southern Brasília Belt. TPV – Três Pontas–Varginha Nappe; CK – Carvalhos Klippe; CdC – Carmo da Cachoeira Nappe.

| Sample | Population | Nappe | n | tanh Age | 95% Bootstrap Uncertainty | Kurtosis | SEk | KURT? | Skewness | SEs | SKEWED? |
|---|---|---|---|---|---|---|---|---|---|---|---|
| 04-6-19 | rim | TPV | 29 | 579 | ±20 | 2.33 | 0.91 | YES | -1.63 | 0.45 | YES |
| 04-6-11 | rim | TPV | 36 | 582 | ±6 | -0.49 | 0.82 | NO | -0.01 | 0.41 | NO |
| 05b-6-108 | | TPV | 35 | 588 | ±5 | -0.17 | 0.83 | NO | -0.01 | 0.41 | NO |
| 05b-6-31b | rim | TPV | 13 | 595 | ±10 | -0.96 | 1.36 | NO | 0.23 | 0.68 | NO |
| 05b-6-29 | | TPV | 58 | 601 | ±6 | -0.02 | 0.64 | NO | -0.24 | 0.32 | NO |
| 05b-6-103 | rim | TPV | 72 | 602 | ±8 | -0.36 | 0.58 | NO | -0.33 | 0.29 | NO |
| 05b-6-36 | rim | TPV | 169 | 607 | ±12 | 0.92 | 0.38 | YES | -0.20 | 0.19 | NO |
| 04-6-11 | core | TPV | 31 | 611 | ±6 | -0.68 | 0.88 | NO | 0.09 | 0.44 | NO |
| 04-6-19 | core | TPV | 17 | 619 | ±12 | 3.00 | 1.19 | YES | 1.09 | 0.59 | NO |
| 05b-6-31b | mantle | TPV | 21 | 624 | ±6 | 1.14 | 1.07 | NO | 0.34 | 0.53 | NO |
| 05b-6-103 | core | TPV | 82 | 630 | ±10 | 2.35 | 0.54 | YES | -0.14 | 0.27 | NO |
| 05b-6-31b | core | TPV | 24 | 634 | ±12 | -0.49 | 1.00 | NO | 0.37 | 0.50 | NO |
| 05b-6-36 | core | TPV | 131 | 635 | ±12 | 0.18 | 0.43 | NO | 0.22 | 0.21 | NO |
| 05b-10-65 | rim | CK | 16 | 561 | ±26 | -0.76 | 1.22 | NO | 0.10 | 0.61 | NO |
| 05b-10-65 | core | CK | 80 | 592 | ±12 | 0.33 | 0.55 | NO | 0.05 | 0.27 | NO |
| 05b-10-102 | core | CK | 111 | 606 | ±18 | 0.53 | 0.46 | NO | -0.36 | 0.23 | NO |
| 05b-10-102 | rim | CK | 97 | 587 | ±12 | 0.25 | 0.50 | NO | -0.46 | 0.25 | NO |
| GR-05-4b | | CdC | 42 | 595 | ±12 | -0.26 | 0.76 | NO | 0.07 | 0.38 | NO |
| 05b-5-22 | | CdC | 48 | 617 | ±12 | -0.29 | 0.71 | NO | -0.31 | 0.35 | NO |
| 05b-5-23 | core | CdC | 18 | 631 | ±12 | 2.45 | 1.15 | YES | -0.11 | 0.58 | NO |
| 05b-5-23 | rim | CdC | 23 | 605 | ±6 | 9.06 | 1.02 | YES | -2.43 | 0.51 | YES |

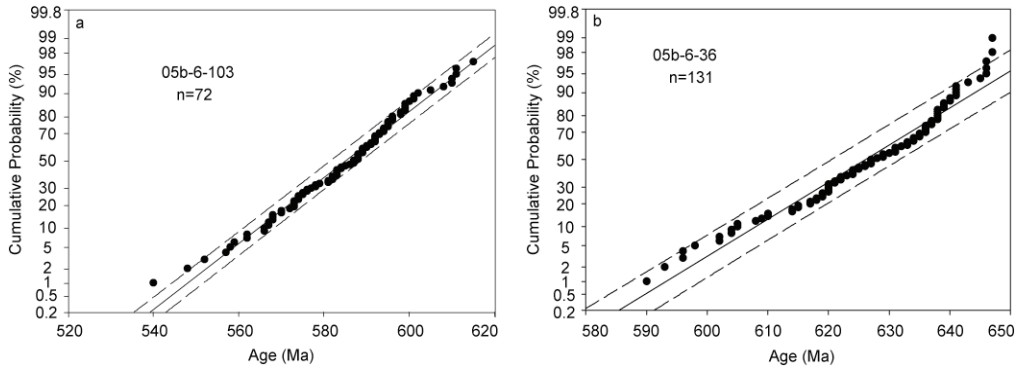


**Figure 3-10.** Probability plot of two exemplar monazite age populations from the Southern Brasília Belt monazite. (a) Sample 05b-6-103 represents an approximately normally distributed dataset. (b) Sample 05b-6-36 is also approximately normally distributed.

Fig. 3-9) based on 82 dates. A high kurtosis of 2.35 indicates the distribution is more peaked than normal, however it is unskewed, with a skewness of -0.14. The low-Y rims yield a tanh age of 602±8 Ma (Fig. 3-8) based on 72 dates. A low kurtosis of -0.36 and skewness of -0.33 suggest these data represent a single population.

Monazite from sample 05b-6-36 shows distinct high-Y cores and low-Y rims (Fig. 3-7f, g, h). The high-Y cores yield a tanh age of 635±12 Ma (Fig. 3-8; Fig. 3-9) based on 131 dates. The low kurtosis of 0.18 and skewness of 0.22 suggest this age represents a single population; a probability plot is shown for this sample as an example of a normally distributed datatset (Fig. 3-10b). The low-Y rims yield a tanh age of 607±12 Ma (Fig. 3-8; Fig. 3-9) based on 169 dates. A high kurtosis of 0.92 suggests the dataset is peaked, but the low skewness of -0.20 indicates that it is not skewed.

Sample 04-6-19 contains monazite with high-Y cores and low-Y rims (Fig. 3-7o, p). The high-Y cores yield an age of 619±12 Ma (Fig. 3-8; Fig. 3-9) based on 17 dates. The high kurtosis of 3.00 suggests the data are peaked, but the skewness of

1.09 indicate that they are not skewed. The low-Y rims yield an age of 579±20 Ma (Fig. 3-8; Fig. 3-9) based on 29 dates. The high kurtosis of 2.33 and skewness of -1.63 indicate that the data do not represent a single age population.

Sample 05b-6-29 contains monazite with at least two distinct Y zones (Fig. 3-7s, t). Culling the data by zone for this sample did not yield statistically different ages. As such, the data were combined and yield a single tanh age of 601±12 Ma (Fig. 3-8; Fig. 3-9) based on 26 dates. The low kurtosis of -0.02 and skewness of -0.24 suggest that these data represent a single population.

Monazite from sample 05b-6-31b show three distinct zones in yttrium X-ray element composition maps maps (Fig. 3-7i, j). High-Y cores yield an age of 634±12 Ma (Fig. 3-8; Fig. 3-9) based on 24 dates. A low kurtosis of -0.49 and skewness of 0.37 suggest that these data represent a single population. Dates from the medium-Y mantle yield an age of 624±6 Ma (Fig. 3-8; Fig. 3-9) based on 21 dates. A low kurtosis of 1.14 and skewness of 0.34 suggest that these data represent a single population. Dates from the low-Y rim yield an age of 595±10 Ma (Fig. 3-8; Fig. 3-9) based on 13 dates. A low kurtosis of -0.96 and skewness of 0.23 suggest that these data represent a single population.

**Carmo da Cachoeira Nappe**

Yttrium X-ray maps of monazite from sample 05b-5-23 show distinct low-Y cores and high-Y rims (Fig. 3-7a, b). Dates were culled based on Y-zoning in this sample. Eighteen dates from the low-Y cores yield a tanh age of 631±12 Ma. The kurtosis of 2.45 indicates that the data are peaked, however the skewness of -0.11 indicates an unskewed population. Twenty-three dates from the high-Y rims yield a tanh age of

605±6 Ma (Fig. 3-8; Fig. 3-9). The high kurtosis of 9.06 and skewness of -2.43 indicate that the data are both peaked and skewed, and likely represent a mixed population.

In sample 05b-6-22, a gradational zoning pattern ranging from high-Y in the cores and low-Y in the rims (Fig. 3-7c, d) means there is no rational basis to group data in this sample. The gradational zoning is interpreted to represent one monazite growth event. A tanh age of 617±12 Ma (Fig. 3-8; Fig. 3-9) is retrieved based on 48 dates. A low kurtosis of -0.29 and skewness of -0.31 suggest a close-to-normal distribution for the data that supports the interpretation that the data represent a single event.

In sample GR-05-4b, a complex patchwork-zoning pattern in monazite (Fig. 3-7e) means there is no rational basis to group the data in this sample, and all data are taken to represent a single event. A tanh age of 595±12 Ma (Fig. 3-8; Fig. 3-9) was calculated from 42 dates. A low kurtosis of -0.26 and skewness of 0.07 suggest a close-to-normal distribution for the data that supports the interpretation that the data represent a single event.

**Carvalhos Klippe**

Sample 05b-10-102 contains monazite with high-Y cores and low-Y rims (Fig. 3-7u, v). In some monazites, an additional thin high-Y rim encompasses the grain. The high-Y cores yield a tanh age of 606±18 Ma (Fig. 3-8; Fig. 3-9) based on 111 dates. A low kurtosis of 0.53 and skewness of -0.36 suggests that these data represent a single age population. Data from the high-Y rims are statistically indistinguishable from the low-Y rims, and data from the two zones were combined. These rims yield

a tanh age of 587±12 Ma (Fig. 3-8; Fig. 3-9) based on 97 dates. The low kurtosis of 0.25 and skewness of -0.46 suggest that these data represent a single population.

Monazite from sample 05b-10-65 contains high-Y cores and low-Y rims (Fig. 3-1d; Fig. 3-7w, x). The high-Y cores yield a tanh age of 592±12 Ma (Fig. 3-8; Fig. 3-9) based on 80 dates. The low kurtosis of 0.33 and skewness of 0.05 suggest that these data represent a single population. The low-Y rims yield a tanh age of 561±26 Ma (Fig. 3-8; Fig. 3-9) based on 16 dates. The low kurtosis of -0.76 and skewness of 0.10 suggest that these data represent a single population.

**Test for Uniqueness**

Two-sample t tests were performed to calculate the probability that ages are statistically identical. A p-value less than 0.05 indicates with 95% confidence that two ages are unique, whereas a p-value greater than or equal to 0.05 indicates that two ages cannot be statistically distinguished. Tests were conducted for all possible combinations, and p-values are listed in Table B-3.

Table 3-7 lists the probability that ages are unique between the different core and rim populations seen within a single sample. In every instance where multiple ages are presented for the same sample, the ages are unique with p-values <0.0005.

Table 3-8 lists the probability that ages are unique between populations defined as rims. Generally, these ages show a degree of overlap, suggesting that the

| Sample | Pop 1 | Pop 2 | p-value |
|---|---|---|---|
| 04-6-11 | rim | core | 0.000 |
| 04-6-19 | core | rim | 0.000 |
| 05-10-102 | pop A | pop B | 0.000 |
| 05-10-65 | pop A | pop B | 0.000 |
| 05-6-103 | rim | core | 0.000 |
| 05-6-31 | mantle | core | 0.000 |
| | mantle | rim | 0.000 |
| | core | rim | 0.000 |
| 05-6-36 | core | rim | 0.000 |
| 05b-5-23 | core | rim | 0.000 |

**Table 3-7.** Summary of t-test values for monazite grains that had both core and rim populations.

ages are not all statistically unique. However, all rim ages are not statistically identical, indicating that it is not possible to interpret one event based solely on rim ages.

| | 05-10-65 | 05-6-31 | 05-6-103 | 05b-5-23 | 05-10-102 | 05-6-36 |
|---|---|---|---|---|---|---|
| 05-10-65 | — | 0.248 | 0.000 | 0.000 | 0.000 | 0.000 |
| 05-6-31 | 0.248 | — | 0.085 | 0.036 | 0.038 | 0.017 |
| 05-6-103 | 0.000 | 0.085 | — | 0.156 | 0.172 | 0.022 |
| 05b-5-23 | 0.000 | 0.036 | 0.156 | — | 0.453 | 0.246 |
| 05-10-102 | 0.000 | 0.038 | 0.172 | 0.453 | — | 0.338 |
| 05-6-36 | 0.000 | 0.017 | 0.022 | 0.246 | 0.338 | — |

**Table 3-8.** Summary of t-test values of all monazite rim populations.

Table 3-9 lists the probability that ages are unique between populations defined as cores. Again, these ages show a degree of overlap, suggesting that the ages are not all statistically unique. However, all core ages are not statistically identical, indicating that it is not possible to interpret one event based solely on core ages.

| | 04-6-11 | 04-6-19 | 05-6-31 | 05-6-103 | 05b-5-23 | 05-6-31 | 05-6-36 |
|---|---|---|---|---|---|---|---|
| 04-6-11 | — | 0.073 | 0.000 | 0.000 | 0.000 | 0.000 | 0.000 |
| 04-6-19 | 0.073 | — | 0.149 | 0.014 | 0.037 | 0.006 | 0.002 |
| 05-6-31 | 0.000 | 0.149 | — | 0.018 | 0.106 | 0.008 | 0.000 |
| 05-6-103 | 0.000 | 0.014 | 0.018 | — | 0.457 | 0.176 | 0.025 |
| 05b-5-23 | 0.000 | 0.037 | 0.106 | 0.457 | — | 0.317 | 0.213 |
| 05-6-31 | 0.000 | 0.006 | 0.008 | 0.176 | 0.317 | — | 0.347 |
| 05-6-36 | 0.000 | 0.002 | 0.000 | 0.025 | 0.213 | 0.347 | — |

**Table 3-9.** Summary of t-test values of all monazite core populations.

Table 3-10 lists the probability that all Ribeira-aged monazites in the Brasília Belt have unique ages. These ages show a degree of overlap, suggesting that the ages are not all statistically unique. However, the ages are not statistically identical, indicating that it is not possible to interpret one event for these data.

| | 05-5-29 | 05-6-108 | 05-10-65 | 04-6-19 | 04-6-11 | 05-10-102 |
|---|---|---|---|---|---|---|
| 05-6-29 | — | 0.466 | 0.080 | 0.000 | 0.000 | 0.000 |
| 05-6-108 | 0.466 | — | 0.080 | 0.000 | 0.000 | 0.000 |
| 05-10-65 | 0.080 | 0.080 | — | 0.072 | 0.031 | 0.014 |
| 04-6-19 | 0.000 | 0.000 | 0.072 | — | 0.313 | 0.124 |
| 04-6-11 | 0.000 | 0.000 | 0.031 | 0.313 | — | 0.049 |
| 05-10-102 | 0.000 | 0.000 | 0.014 | 0.124 | 0.049 | — |

**Table 3-10.** Summary of t-test values of populations possibly affected by the Ribeira Overprint.

***Brasília Belt Metamorphism and Ribeira Overprint***

Prior to interpreting the monazite (U-Th)-Pb ages, it is important to discuss some of the limitations of monazite microprobe dating. One of the fundamental assumptions in this technique is that all Pb contained in a monazite grain is radiogenic. The amount of common lead, or lead incorporated into a grain during initial formation, is typically assumed to be negligible (*e.g.*, Parrish, 1990). However, this may not always be the case as the amount of common lead present in monazite has been shown to be variable (*e.g.*, Williams *et al.* 1983; Copeland *et al.* 1988; Corfu 1988; DeWolf *et al.*

1993; Kingsbury *et al.* 1993; Zhu *et al.* 1997; Bingen & Van Breemen 1998; Zhu & O'Nions 1999).

The non-radiogenic isotope $^{204}Pb$ is an indicator of the amount of common lead in a system, and can be used to correct for excess non-radiogenic lead in an isotopic measurement. The EPMA is incapable of distinguishing isotopes of Pb, and as such it is not possible to provide this quantitative constraint on, or to correct for, common lead in an EPMA (U-Th)-Pb analysis. Excess non-radiogenic lead has the effect of producing an artificially old monazite microprobe age. In the absence of supplementary isotopic data, it is necessary to interpret microprobe ages as maximums. The statistical methods I recommend here are not capable of correcting for excess common lead; the bootstrap uncertainty is the uncertainty on the data as measured, and does not account for common lead.

The closure temperature for Pb diffusion in monazite is determined by the grain size, composition, cooling rate, presence of fluids and melts, effective bulk composition, and degree of recrystallization (*e.g.*, Parrish 1990; DeWolf *et al.* 1993; Dahl, 1997; Smith & Giletti 1997; Bingen & van Breemen 1998; Ayers *et al.* 1999; Zhu & O'Nions 1999; Cherniak *et al.* 2000; Rubatto *et al.* 2001). It is likely that the temperature of peak metamorphism in the southern Brasília Belt of 840–900˚C is less than the closure temperature of Pb in monazite, which is greater than 900˚C (*e.g.*, Cherniak *et al.* 2004). There have been numerous studies suggesting that Pb diffusion is negligible in monazite, even at high temperatures (*e.g.*, Parrish 1990; Spear & Parrish 1996; Braun *et al.* 1998; Crowley & Ghent 1999; Cocherie & Albarede 2001; Rubatto *et al.* 2001; Foster *et al.* 2002; Schmitz & Bowring 2003).

However, a study by Smith and Giletti (1997) suggests that Pb may diffuse in monazite at moderate temperatures over geologic timescales.

**Três Pontas–Varginha Nappe**

The Três Pontas–Varginha Nappe lies immediately beneath the Socorro–Guaxupé Nappe. This high-pressure granulite facies nappe is the uppermost of the metapelitic nappes formed by subduction of passive margin sediments at the edge of the São Francisco Craton during the Brasília Orogeny, and it records the highest pressures of metamorphism. Granulite facies rocks from this nappe achieved peak pressure of ~1.5 GPa and temperatures of 840˚–900˚C. Previous U-Pb zircon geochronology indicates that this nappe achieved just post-peak metamorphic conditions at *ca.* 648 Ma (648±12 Ma, 647±11 Ma; Chapter 2). This nappe does not record a macroscopic sillimanite overprint related to the 590–550 Ma Ribeira Orogeny.

Monazite ages from this nappe fall predominantly into three statistically distinct groups, where ages within a single group are largely statistically identical based on t-tests with p-values greater than or equal to 0.05, and ages between different groups are statistically unique with t-test p-values less than 0.05. The oldest is a group of ages taken from high-Y cores of garnet hosted monazite. These core ages are 635±12 Ma for sample 05b-6-36, 634±12 Ma and 624±6 Ma for sample 05b-6-31b and 630±10 Ma for sample 05b-6-103, all from the upper and middle portion of the nappe. A second group of ages is associated with the low-Y rims on monazite grains of the first group, together with matrix-hosted monazite in sample 05b-6-29. These ages are 607±12 Ma for sample 05b-6-36, 602±8 Ma for sample 05b-6-103, 601±12 Ma for sample 05b-6-29 and 595±13 Ma for sample 05b-6-31b. The core-age

of matrix-hosted monazite from sample 04-6-11, with an age of 611±6 Ma, may fall into this second group. The core age of matrix-hosted monazite from sample 04-6-19, with an age of 619±12, does not fall into either the first or second group. The youngest group of ages is associated with matrix-hosted monazite. Monazite from sample 05b-6-108 records an age of 588±10 Ma, monazite rims from sample 04-6-19 record an age of 579±20 Ma and monazite rims from sample 04-6-11 record an age of 582±6 Ma.

In Chapter 2 I interpret zircon to have grown during just-post-peak-T ilmenite breakdown at 648±12 Ma and 647±11 in samples 05b-6-31b and 04-6-11. I interpret the oldest group of ages of 635–624 Ma from garnet-hosted monazite to represent post-peak, high-T growth of monazite. These monazite grains occur adjacent to microcracks in garnet, which could allow communication between the interior and exterior of the garnet crystal. Assuming a grain boundary fluid, this would permit mass exchange between monazite inclusions and the matrix, allowing for dissolution–reprecipitation of old monazite grains or intergrowth of monazite (*e.g.*, Seydoux-Guillaume *et al.* 2004; Martin *et al.* 2007). T-tests indicate that the monazite ages of 635–630 Ma are statistically identical to one another with p-values >0.05, and that they are all statistically younger than the U-Pb zircon ages of 648±12 Ma and 647±11 Ma, with p-values <0.01.

Matrix-hosted monazite in samples 04-6-19, with an age of 619±12 Ma, and 04-6-11, with an age of 611±6 Ma, may have been exposed to fluid that could accelerate Pb diffusion. The high skewness of sample 04-6-19 suggests the sample

does not represent a single age population, which could be due to incomplete resetting during dissolution–reprecipitation.

The second group of ages of 607–595 Ma in the rims of the garnet-hosted monazite correspond with the (U-Th)-Pb monazite ages of 609±7 Ma from Martins *et al*. (2008) for crystallization of granitic leucosome in the overlying Socorro–Guaxupé Nappe. Seyboux-Guillaume *et al*. (2002) suggest that fluid mobilization of the Ca in Ca-bearing host-minerals such as garnet can promote the partial resetting of monazite inclusions in that host-mineral. I interpret this second group of monazite ages to record partial dissolution/reprecipitation of these garnet-hosted monazite grains due to interaction with fluids.

The third group of monazite ages of 588–579 Ma from matrix hosted monazite records late monazite growth in the Andrelândia Nappe Complex. These ages correspond with the beginning of the Ribeira Orogeny, and may be related to an otherwise cryptic metamorphic overprint on the Southern Brasília Belt caused by the Ribeira Orogeny. The ages are statistically identical to $^{40}Ar/^{39}Ar$ Bt ages from this nappe (Chapter 4), so the ages could alternatively be related to low-T monazite growth or resetting during exhumation and cooling due to fluid flow caused by orogenic loading (*e.g.*, Appold & Garven 1999; Garven 1995; Ge & Garven 1992) due to the developing Ribiera Orogen to the southeast of the Andrelândia Nappe Complex.

**Carmo da Cachoeira Nappe**

The Carmo da Cachoeira Nappe lies beneath the Três Pontas–Varginha Nappe, and comprises upper amphibolite to granulite facies rocks that achieved peak pressures of

1.0–1.5 GPa and peak temperatures of 820–870˚C. This nappe is interpreted to have been formed by subduction of passive margin sediments similar to those found in the Três Pontas–Varginha Nappe during the Brasília Orogeny. This nappe does not record a macroscopic sillimanite overprint related to the 590–550 Ma Ribeira Orogeny.

Sample 05b-5-23 contains monazite that records statistically distinct core and rim populations. Small monazite grains (~10μm or smaller) are present throughout the petrographic thin section only as inclusions in biotite. Biotite in this sample is primarily aligned within the foliation, with only a few larger grains not aligned with foliation. A (U-Th)-Pb age of 631±12 Ma from monazite cores in this sample likely dates (or pre-dates) the timing of biotite formation and is likely an age associated with the growth of foliation-parallel biotite after peak metamorphism. The rims of these monazite grains yield an age of 605±6 Ma. This age is significantly skewed, suggesting that the age comprises a mixed population. However, the tanh estimator takes this skew into account when calculating an age. The age of *ca.* 605 is similar to the age of 607–595 Ma seen in monazite rims in the Três Pontas–Varginha Nappe.

Sample 05b-5-22 contains monazite that occurs primarily as inclusions in biotite, but monazite also occurs in association with plagioclase and quartz. An age of 617±12 Ma is interpreted to record post-peak monazite growth in this sample. The low kurtosis of -0.29 and skewness of -0.31, together with the lack of distinct chemical zoning suggest that this age represents a single monazite growth event.

Sample GR-05-4b contains monazite grains in the quartz–plagioclase matrix of the rock, and not as inclusions in biotite. The age of 595±12 Ma for this sample is

statistically similar with p values ≥ 0.05 to the ages of *ca.* 605 Ma in sample 05b-5-23 and of 607–595 Ma in the overlying Três Pontas–Varginha Nappe.

**Carvalhos Klippe**

The Carvalhos Klippe is infered to be part of the Três Pontas–Varginha Nappe now isolated in the southernmost portion of the Southern Brasília Belt. It is interpreted to have experienced similar peak metamorphic conditions as the Três Pontas–Varginha Nappe. The Ribeira Orogeny (590–550 Ma) led to a tectonothermal overprinting recorded by sillimanite in the Carvalhos Klippe. There is no macroscopic sillimanite overprint related to the Ribeira Orogeny in the Três Pontas–Varginha or Carmo da Cachoeira Nappes.

Kyanite grains in sample 05b-10-65 contain inclusions of monazite that record statistically distinct cores and rims. The age of 592±12 Ma provides a minimum age for the formation of kyanite in this rock. This age is statistically similar with p values ≥ 0.05 to the youngest group of ages of 588–579 Ma recorded in the Três Pontas–Varginha Nappe, and may be associated with the same late monazite growth event, possibly related to the overprinting caused by the Ribeira Orogeny. However, this age is also statistically similar with p values ≥ 0.05 to the age of 595±12 Ma recorded in the group of monazite ages ranging from 607–595 Ma. A younger rim age of 561±26 Ma is difficult to interpret due to the large uncertainty and the small sample size; it is likely that this age relates to overprinting by the Ribeira Orogeny on the Southern Brasília Belt.

Monazite in sample 05b-10-102 has statistically distinct cores and rims. The core age of 606±18 Ma is statistically similar with p values ≥ 0.05 to the 607-595 Ma

group of ages. The rim age of 587±12 Ma is statistically similar with p values ≥ 0.05 to the youngest group of ages of 588–579 Ma recorded in the Três Pontas–Varginha Nappe. This age may be related to the Ribiera Orogeny, perhaps dating the beginning of the overprinting event.

*Conclusions*

Traditional statistical techniques for calculating ages and uncertainties are based on an assumption of a normally distributed dataset. This assumption is valid for datasets that represent a single age population. A dataset obtained exclusively from one normally-distributed age population is an ideal situation, but this may not always be achieved. In the event that data are taken from non-normally distributed populations, it is necessary to use robust statistical techniques to calculate reliable ages and complete uncertainties. A simple way of testing for normality is to calculate the skewness and kurtosis of a dataset. I propose that these statistics should be routinely utilized in the analysis of chronologic datasets.

I propose that the tanh estimator should be used to calculate ages and the bootstrap to calculate uncertainties. These robust statistics enable the calculation of ages while minimizing the effect of outliers in a dataset and these methods are appropriate to use on non-normally distributed data.

In the southern sector of the Southern Brasília Belt, (U-Th)-Pb monazite ages of 635–624 Ma in the Três Pontas–Varginha Nappe are interpreted to date post-peak monazite growth. In the Carmo da Cachoeira Nappe, an age of 631±12 Ma is interpreted to date the post-peak formation of foliation in this nappe. A group of ages ranging between 607 and 595 Ma for monazite throughout the nappe stack is

interpreted to record fluid related dissolution–reprecipitation. A third group of ages between 588 and 561 Ma is interpreted to record the beginning of the metamorphic overprinting caused by the Ribiera Orogeny.

# Chapter 4: $^{40}Ar/^{39}Ar$ chronology of high-pressure granulite nappes in the Southern Brasília Belt, Brazil: implications for nappe exhumation

*Abstract*

In the southern sector of the Southern Brasília Belt the Neoproterozoic Brasília Orogeny a subduction-to-collision event occurred between the Socorro–Guaxupé Arc–Paranapanema Block to the west (present coordinates) and the passive margin on the west side of the São Francisco Craton to the east. The Andrelândia Nappe Complex comprises a stack of passive margin-derived nappes metamorphosed up to high-pressure granulite facies conditions that have been overthrust by an arc-derived high-pressure granulite facies nappe during terminal collision. I report $^{40}Ar/^{39}Ar$ ages from the upper-most passive margin-derived nappes in the Complex to constrain the timing of exhumation, and I use zircon and monazite ages from Chapters 2 and 3 to derive average cooling rates for these nappes. Biotite from high-pressure granulites from the Três Pontas–Varginha Nappe yields $^{40}Ar/^{39}Ar$ ages between 591.4±6.6 and 568.9±6.1 Ma. In combination with U-Pb zircon, (U-Th)-Pb monazite and Rb-Sr isochron ages, an initial slow average rate of cooling from high-*T* conditions to ~700˚C was followed by an increased average rate of cooling of >14˚C $Ma^{-1}$ from ~700˚C to ~300˚C. I suggest the change in cooling rate was due to tectonically driven exhumation, perhaps related to far-field stresses associated with the Ribeira Orogeny to the east (present coordinates) of the São Francisco Craton. Biotite from high-

pressure granulites of the underlying Carmo da Cachoeira Nappe yields $^{40}Ar/^{39}Ar$ ages of 543±12 and 539.7±4.0 Ma. In combination with (U-Th)-Pb monazite ages, I derive an average rate of cooling of 3–7 ˚C $Ma^{-1}$ for this nappe, but I cannot determine whether the cooling rate increased in the same manner as the Três Pontas–Varginha Nappe. If these $^{40}Ar/^{39}Ar$ ages record cooling due to exhumation, then the the Três Pontas–Varginha Nappe was the first of the passive-margin derived nappes to be exhumed, followed by the underlying Carmo da Cachoeira Nappe. Hornblende from the overlying Socorro–Guaxupé arc-derived nappe yields $^{40}Ar/^{39}Ar$ ages of 576±30 Ma. In combination with U-Pb zircon ages, I derive an average rate of cooling of 3–7 ˚C $Ma^{-1}$ for this nappe. In the southeastern part of the Andrelândia Nappe Complex, biotite from the Andrelândia Nappe yields $^{40}Ar/^{39}Ar$ ages of 490.6±4.1 Ma. Using additional $^{40}Ar/^{39}Ar$ ages from the literature reveals that the biotite ages in this nappe young upwards from *ca.* 540 to *ca.* 490 Ma, which may be explained by emplacement of the São Francisco Craton directly beneath the Andrelândia Nappe, resulting in bottom up cooling. Further southeast, high-pressure granulites of the Carvalhos Klippe show a sillimanite-grade metamorphic overprint due to the earliest phase of the Ribeira Orogeny in which the Rio Negro Arc was emplaced onto the passive margin on the east side of the São Francisco Craton. Biotite from this nappe yields a $^{40}Ar/^{39}Ar$ age of 560.7±3.9 Ma that may relate to exhumation after this early phase of the Ribera Orogeny. Biotite from the high-grade migmatite from the core of the Ribera Belt yields a $^{40}Ar/^{39}Ar$ age of 455.5±3.6 Ma. When combined with a U-Pb zircon age of *ca.* 553 Ma this suggests a slow average cooling rate of ~5-6 ˚C $Ma^{-1}$.

*Introduction*

The study of ancient orogenic belts exposed at the surface provides insight into tectonic processes that are active during orogenesis. Petrographic and geochemical information preserved in metamorphic rocks can yield information about the depth to which crustal material was buried during orogenesis, the magnitude of the thermal anomaly involved, the timing of close-to-peak metamorphism and rates of burial and exhumation. When this pressure-temperature-time (*P–T–t*) information is combined with structural setting it allows for an evaluation of the process by which crustal materials were transported from the surface to depth and back to the surface during orogenesis.

Recent advances in the interpretation of ages retrieved from high-temperature chronometers using microstructural and chemical information (*e.g.*, Rubatto & Hermann 2003; Kelley & Harley 2005; Harley & Kelley 2007; Rubatto *et al.* 2007), and in the calibration and application of accessory phase thermometers (*e.g.*, Ferry & Watson 2007; Baldwin *et al*. 2007) have enabled us to link U-Pb zircon ages or (U-Th)-Pb monazite ages to specific points on the metamorphic *P–T* path to better understand the evolution of the Southern Brasília Belt (*e.g.*, Baldwin & Brown 2008; Chapter 2). These high-temperatures chronometers are commonly linked to a high-*T* portion of the *P–T* path, generally constraining the timing of peak or near-peak metamorphism, or the immediately post-peak segment of the *P–T* path. However, in order to reconstruct the full post-peak exhumation history of an orogen, it is essential to combine these data with ages for lower-*T* chronometers such as from $^{40}Ar/^{39}Ar$ dating of hornblende and biotite.

The assembly of Gondwanan elements in South America is recorded in southeast Brazil by a series of orogenic belts (Fig. 4-1b), with the Brasília, Ribeira and Buzios orogenic events in successive periods as follows, *ca.* 680–595 Ma (*e.g.*, Campos Neto & Caby 1999; 2000; Campos Neto *et al.* 2004; Chapter 3), *ca.* 580–550 Ma (*e.g.*, Heilbron & Machado 2003) and *ca.* 525–505 Ma (Schmitt *et al.* 2004), respectively. The Southern Brasília Belt records the suturing of the Paranapanema block and several magmatic arcs in the west (present coordinates) to the subducted passive margin along the western side of the São Francisco Craton in the east. It preserves a record of extreme metamorphism, with UHT-granulites exposed in the northern sector (*e.g.*, Ferreira Filho *et al.* 1992; 1998; Moraes & Fuck 2000; Moraes *et al.* 2002; Baldwin *et al.* 2005; Baldwin & Brown 2008) and high-pressure granulites exposed in the Andrelândia Nappe Complex (Fig. 4-1a) in the southern sector (*e.g.*, Campos Neto & Caby 1999; 2000; Garcia & Campos Neto 2003; Chapter 2).

Understanding the tectonic processes that led to the exhumation of nappes in the Andrelândia Nappe Complex requires establishing a detailed thermochronologic history of each nappe. In the southern sector of the Southern Brasília Belt, I have recently reported U-Pb zircon ages (Chapter 2), (U-Th)-Pb monazite ages (Chapter 3) and Rb-Sr multimineral–whole rock isochron ages (Chapter 2) for the uppermost three high-pressure granulite

**Figure 4-1.** (a) Map of the São Francisco Craton showing the relative position of the Brasília and Ribeira Belts. The Andrelândia Nappe complex is marked by a box south of the São Francisco Craton, and a more detailed (b) tectonic map of the Andrelândia Nappe Complex indicates location of samples analyzed in this study.

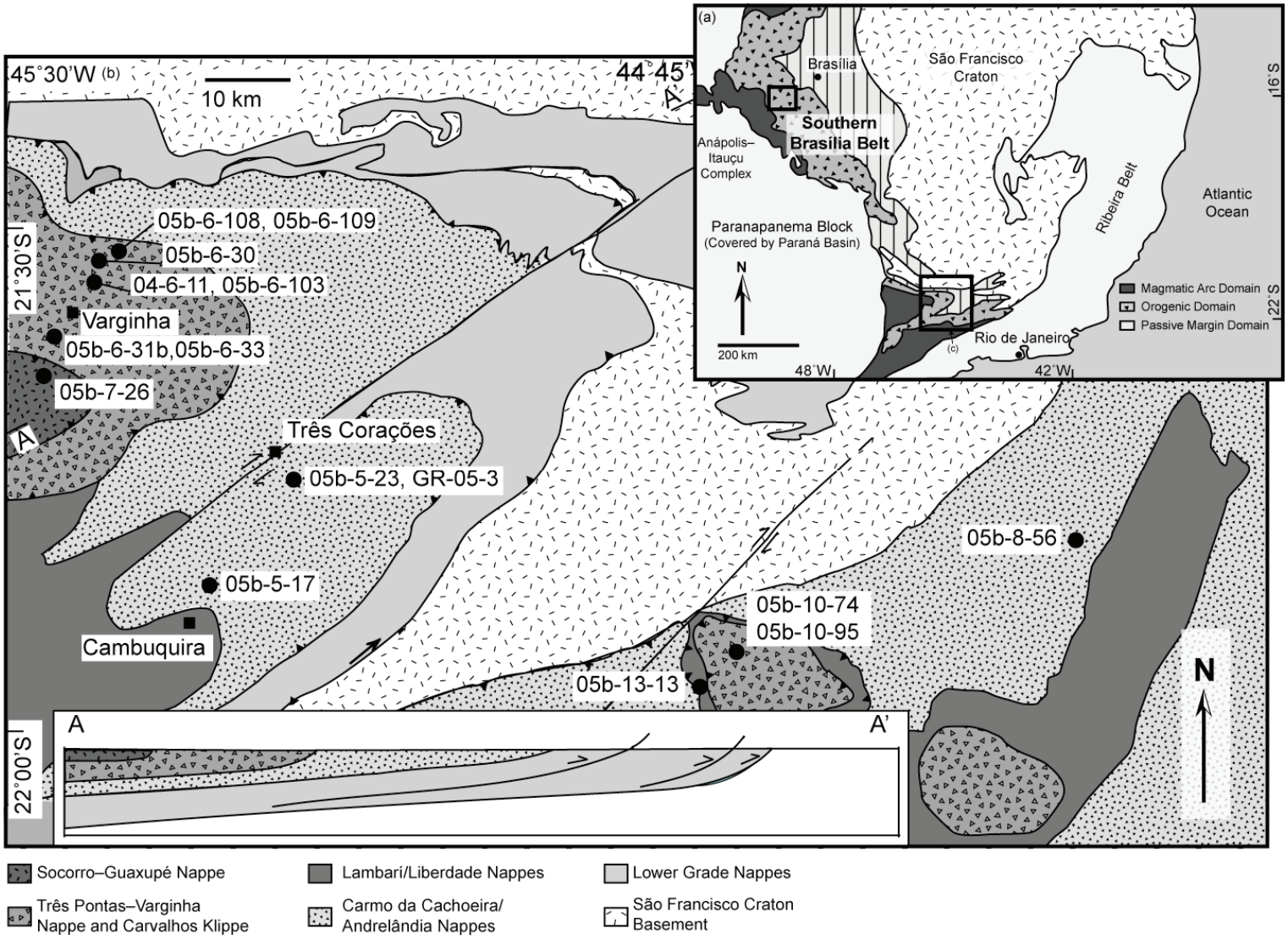
45°30'W (b)
10 km
44°45'
A'
21°30'S
22°00'S
A
A'
05b-6-108, 05b-6-109
05b-6-30
04-6-11, 05b-6-103
Varginha
05b-6-31b,05b-6-33
05b-7-26
Três Corações
05b-5-23, GR-05-3
05b-5-17
Cambuquira
05b-10-74
05b-10-95
05b-13-13
05b-8-56
N
(a)
Brasília
São Francisco Craton
Southern Brasília Belt
Anápolis–Itauçu Complex
Paranapanema Block (Covered by Paraná Basin)
Ribeira Belt
Atlantic Ocean
Rio de Janeiro
(c)
200 km
48°W
42°W
16°S
22°S
Magmatic Arc Domain
Orogenic Domain
Passive Margin Domain
Socorro–Guaxupé Nappe
Três Pontas–Varginha Nappe and Carvalhos Klippe
Lambarí/Liberdade Nappes
Carmo da Cachoeira/ Andrelândia Nappes
Lower Grade Nappes
São Francisco Craton Basement

facies nappes and associated tectonic blocks of eclogite in the Andrelândia Nappe Complex. In conjunction with petrographic and geochemical information, these data have been used to determine the timing of initial nappe detachment from the downgoing slab at *ca.* 678 Ma, the timing of near-peak metamorphism in the nappes at *ca.* 648 Ma, and the high-temperature part of the retrograde evolution down to ~700˚C at *ca.* 590 Ma.

In this article I present the results of a $^{40}Ar/^{39}Ar$ thermochronologic study from the Andrelândia Nappe Complex in the southern sector of the Southern Brasília Belt. I combine previously published zircon U-Pb and monazite (U-Th)-Pb ages and Rb-Sr multimineral–whole rock isochron ages with $^{40}Ar/^{39}Ar$ ages for biotite and hornblende from individual tectonic units within the Andrelândia Nappe Complex to constrain the retrograde *P-T* path for several of these units. As a result, I am able to provide a more complete *P-T-t* history of the nappes, calculate average cooling rates during exhumation for three nappes and suggest a tectonic model for nappe exhumation.

## *Geologic Background*

The Andrelândia Nappe Complex in the southern sector of the Southern Brasília Belt, located in southern Minas Gerais, Brazil, comprises a system of flat-lying nappes composed of passive margin-derived metasedimentary units that were displaced to the ENE (present coordinates) onto the São Francisco craton during the subduction-to-collision phase of the Brasília Orogeny (Fig. 4-1a; Ribeiro *et al.* 1995; Campos Neto & Caby 1999). The lowest grade greenschist facies nappes are structurally at the base

of the system, whereas the high-pressure granulite facies Três Pontas–Varginha, Carmo da Cachoeira, Andrelândia and Lambari/Liberdade Nappes overlie the low-grade nappes in the nappe stack (Figs 1a & 2; *e.g.*, Campos Neto & Caby 1999, 2000; Garcia & Campos Neto 2003). Several klippe associated with the Três Pontas–Varginha Nappe are isolated in the southeastern part of the Complex (Fig. 4-1a; Trouw *et al.* 2006). The Socorro–Guaxupé nappe, at the top of the nappe stack, comprises part of the magmatic arc from the hanging wall plate (Campos Neto & Caby 1999). The main focus of this study is the uppermost three high-pressure granulite facies nappes, the Socorro–Guaxupé, Três Pontas–Varginha and Carmo da Cachoeira Nappes, and their lateral equivalents and outlying klippe.

The Três Pontas–Varginha Nappe (Fig. 4-1a) was detached from the subducting passive margin at 678±29 Ma (Table 4-1), based on a U-Pb zircon age from a retrograded eclogite interpreted to represent one of a number of slivers of oceanic crust forming basement to the metasedimentary rocks that were transported along the contact with the underlying nappe. The Três Pontas–Varginha Nappe was subjected to peak temperatures >850–900˚C at pressures of 1.5–1.6 GPa; this nappe had cooled to ~800˚C by *ca.* 648–647 Ma (Chapter 2). Monazite (U-Th)-Pb ages of 635–624 Ma (Table 4-1) for the same samples are interpreted in Chapter 3 to record timing of post-peak-*T* monazite growth in the Três Pontas–Varginha Nappe. Rb-Sr multimineral–whole rock isochron ages of *ca.* 590 Ma from samples close to the

**Figure 4-2.** Metamorphic map of the Andrelândia Nappe Complex illustrating the metamorphic grade of individual tectonic units. In the south of the Complex, the appearance of sillimanite relates to a tectono-thermal overprint on the Southern Brasília Belt imparted by the Ribeira Orogeny. Modified from Trouw (pers. comm.).

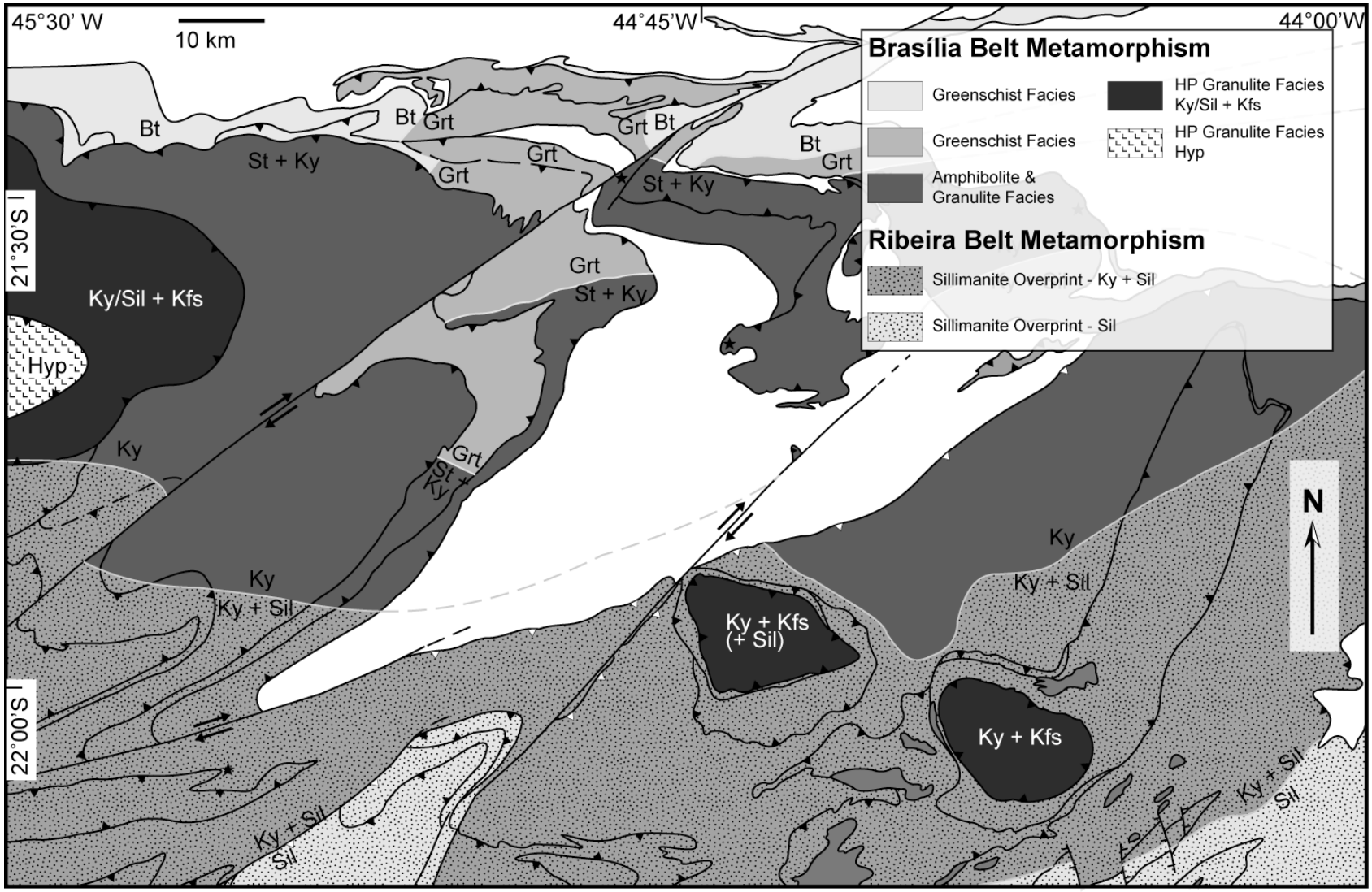
45°30' W
10 km
44°45'W
44°00'W
21°30'S
22°00'S
Brasília Belt Metamorphism
Greenschist Facies
Greenschist Facies
Amphibolite & Granulite Facies
HP Granulite Facies Ky/Sil + Kfs
HP Granulite Facies Hyp
Ribeira Belt Metamorphism
Sillimanite Overprint - Ky + Sil
Sillimanite Overprint - Sil
Bt
Grt
St + Ky
Ky/Sil + Kfs
Hyp
Ky
Ky + Sil
Ky + Kfs (+ Sil)
Ky + Kfs
Sil
N

**Zircon Isotope Ages**

| Sample | Nappe | $^{206}Pb/^{238}U$ Age | |
|---|---|---|---|
| 04-7-1 | Socorro–Guaxupé | 622 | ±28 |
| 05-13-13 | Retrograded Eclogite | 678 | ±29 |
| 05-6-31b | Três Pontas–Varginha | 647 | ±11 |
| 04-6-11 | Três Pontas–Varginha | 648 | ±12 |

**Monazite (U-Th)-Pb Ages**

| Sample | Population | Nappe | tanh age | |
|---|---|---|---|---|
| 04-6-19 | rim | Três Pontas–Varginha | 579 | ±20 |
| 04-6-11 | rim | Três Pontas–Varginha | 582 | ±6 |
| 05b-6-108 | | Três Pontas–Varginha | 588 | ±5 |
| 05b-6-31b | rim | Três Pontas–Varginha | 595 | ±10 |
| 05b-6-29 | | Três Pontas–Varginha | 601 | ±6 |
| 05b-6-103 | rim | Três Pontas–Varginha | 602 | ±8 |
| 05b-6-36 | rim | Três Pontas–Varginha | 607 | ±12 |
| 04-6-11 | core | Três Pontas–Varginha | 611 | ±6 |
| 04-6-19 | core | Três Pontas–Varginha | 619 | ±12 |
| 05b-6-31b | mantle | Três Pontas–Varginha | 624 | ±6 |
| 05b-6-103 | core | Três Pontas–Varginha | 630 | ±10 |
| 05b-6-31b | core | Três Pontas–Varginha | 634 | ±12 |
| 05b-6-36 | core | Três Pontas–Varginha | 635 | ±12 |
| 05b-10-65 | rim | Carvalhos Klippe | 561 | ±26 |
| 05b-10-65 | core | Carvalhos Klippe | 592 | ±12 |
| 05b-10-102 | core | Carvalhos Klippe | 606 | ±18 |
| 05b-10-102 | rim | Carvalhos Klippe | 587 | ±12 |
| GR-05-4b | | Carmo da Cachoeira | 595 | ±12 |
| 05b-5-22 | | Carmo da Cachoeira | 617 | ±12 |
| 05b-5-23 | core | Carmo da Cachoeira | 631 | ±12 |
| 05b-5-23 | rim | Carmo da Cachoeira | 605 | ±6 |

**Table 4-1.** U-Pb zircon and (U-Th)-Pb monazite chronologic data from Chapters 2 and 3.

structural base of the Três Pontas–Varginha Nappe are interpreted in Chapter 2 to record high temperature decompression of this nappe at around ~700˚C, suggesting an initial slow average cooling rate between just-post-peak-temperature to ~700˚C. In the Carmo da Cachoeira Nappe (Fig. 4-1a), a monazite (U-Th)-Pb age of 631±12 Ma (Table 4-1) is interpreted to record timing of retrograde biotite formation (Chapter 3). Monazite (U-Th)-Pb ages of 588–561 Ma (Table 4-1) found throughout the nappe

stack are interpreted in Chapter 3 to record metamorphic overprinting on the Andrelândia Nappe Complex caused by the Ribeira orogenic event to the south-southeast (present coordinates). Campos Neto *et al.* (2004) present $^{40}Ar/^{39}Ar$ biotite cooling ages from the Andrelândia Nappe, laterally equivalent to the Carmo da Cachoeira Nappe, that range from 541.0±1.3 Ma at the base to 492.0±1.0 Ma at the top of the nappe.

In Chapter 2, I interpret the Socorro–Guaxupé Nappe to have been at close-to-peak high-pressure granulite facies conditions at *ca.* 622 Ma (Table 4-1) based on U-Pb zircon ages. (U-Th)-Pb monazite ages from the Três Pontas–Varginha and Carmo da Cachoeira Nappes of 607–595 Ma (Table 4-1; Chapter 3) are interpreted to record fluid-related dissolution–reprecipitation.

Further north in the Southern Brasília Belt, Baldwin & Brown (2008) constrain the timing of metamorphism in the Anápolis-Itauçu Complex to *ca.* 649–634 Ma, based on high-precision TIMS U–Pb zircon ages.

*Analytical Methods*

In this study, one sample of metapelitic rock from the Carmo da Cachoeira Nappe was analyzed by X-ray fluorescence (XRF) for major oxides to determine the bulk rock compositions for phase equilibrium modelling to establish the *P–T* conditions for this nappe. The XRF analysis was carried out using a Phillips 2404 XRF spectrometer at Franklin & Marshall College. The FeO content was analyzed by $Fe^{2+}$ titration, and the $Fe_2O_3$ content was calculated by difference. The $H_2O$ content in the composition used for modelling was based on the loss on ignition (LOI) value from the whole-rock chemical analysis. The low $H_2O$ content estimated from LOI reflects

the dehydrated nature of the high-pressure granulite and modification of the protolith bulk composition by melt loss.

$^{40}Ar/^{39}Ar$ analyses of samples from the Southern Brasília Belt were undertaken at the Syracuse University Noble Gas Isotopic Research Laboratory (SUNGIRL). Following petrographic characterization, samples for Ar chronology were selected to give wide geographic spread approximating a N-S transect across the Andrelândia Nappe Complex. High-purity mineral separates (> 99%) were prepared by standard rock-crushing and mineral-separation techniques, and biotite >200 μm in diameter and hornblende >80 μm in diameter were handpicked to avoid aggregate and altered grains. Mineral separates were washed in acetone and individually wrapped in Cu foil and stacked with the 77-600 hornblende standard to monitor the neutron dose. Samples were vacuum-sealed in a Suprasil quartz tube and irradiated for 30 hours in the CLICIT facility at the Oregon State University Radiation Center.

$^{40}Ar/^{39}Ar$ analysis of unknowns was undertaken by double-vacuum resistance-furnace heating experiments. Gas was extracted during standard furnace dwell times of twelve minutes and was then exposed for ten minutes to hot and cold SAES ST-707 getters for purification. The purified gas was analyzed on a Micromass 5400 mass spectrometer equipped with an ion-counting electron multiplier.

Sample data were corrected for blanks, mass discrimination, decay of $^{37}Ar$ and $^{39}Ar$, neutron-induced interfering isotopes, and atmospheric argon. Correction factors used to account for interfering nuclear reactions were determined by analyzing argon extracted from irradiated optical grade, fused $CaF_2$ and K-glass. Correction factors used to account for interfering nuclear reactions for the irradiated samples are:

$(^{40}Ar/^{39}Ar)_K = 3.12563 \times 10^{-03} \pm 1.54563 \times 10^{-03}$; $(^{36}Ar/^{37}Ar)_{Ca} = 3.04878 \times 10^{-04} \pm 7.83537 \times 10^{-06}$; and, $(^{39}Ar/^{37}Ar)_{Ca} = 7.98549 \times 10^{-04} \pm 5.82941 \times 10^{-06}$. All ages were calculated using the decay constants recommended by Steiger & Jäger (1977). Two-sigma analytical errors are reported in this manuscript, and include an error associated with flux monitor age and the irradiation parameter, J, typically < 1.0 % (2σ).

Inverse isochron ages and apparent age data were calculated utilizing the program Isoplot 3.0 (Ludwig 1994). On plots of age versus cumulative $^{39}Ar$ fraction, an age plateau is defined if ages for a minimum of 3 consecutive heating steps, representing 60% of the $^{39}Ar$, lie within 95% confidence of each other.

*Sample Description*

Hornblende was analyzed from one sample from a retrograded eclogite unit, one sample from the Carvalhos Klippe, and one sample from the Socorro–Guaxupé Nappe. Biotite was analyzed from seven samples from a range of structural levels within the Três Pontas–Varginha Nappe, one sample from the Carvalhos Klippe, three samples from the Carmo da Cachoeira Nappe, one sample from the Andrelândia Nappe, and one sample from the Ribeira Belt as exposed in Botafogo, Rio de Janeiro.

***Retrograded Eclogite***

The retrograded eclogite sample was collected from a tectonic block located between the Liberdade and Andrelândia Nappes, inferred to be lateral equivalents to the Três Pontas–Varginha and Carmo da Cachoeira Nappes, respectively. Sample 05-13-13 (Fig. 4-3a) comprises millimeter size garnets that are separated by an irregular rim of granoblastic plagioclase from symplectic aggregates of plagioclase and clinopyroxene

that I infer to have replaced a more jaditic pyroxene. Millimeter size prismatic hornblende is in a microstructural relationship with the symplectic aggregates of plagioclase and clinopyroxene that I interpret to record their replacement by the hornblende. The age of zircon growth in this sample is 678±29 Ma (Chapter 2).

***Três Pontas–Varginha Nappe***

Samples were analyzed from four locations within the high-pressure granulite facies Três Pontas–Varginha Nappe. Samples 05b-6-109 and 05b-6-108 were taken from the Santo Antonio Quarry, near the structural base of the nappe. Sample 05b-6-30 was taken from a working quarry that lies towards the structural base of the nappe, but structurally above the Santo Antonio Quarry. Samples 04-6-11 and 05b-6-103 were taken from the Três Pontas Quarry, in the structural middle of the nappe. Samples 05b-6-31b and 05b-6-33 were taken from the Lixão (quarry used as a garbage dump) in the city of Varginha near the top of the nappe.

Sample 05b-6-109 (Fig. 4-3c) is a strongly foliated garnet–sillimanite/kyanite–K-feldspar gneiss. Large 1–1.5 cm garnets have rare kyanite inclusions in the outer mantle and are rimmed by fine-grained biotite less than 1 mm long. Coarser tabular biotite up to 3 mm long occurs together with 4–5 mm long sillimanite and kyanite grains associated with low strain areas adjacent to and between large garnets. Overall, microstructural relationships in these areas are interpreted to record partial replacement of garnet and alumino-silicate by biotite. Matrix-hosted biotite, sillimanite and kyanite up to 3 mm in length are aligned with compositional layering defining the foliation; sillimanite and kyanite are folded in the foliation, which wraps around garnet. Leucocratic layers away from the large

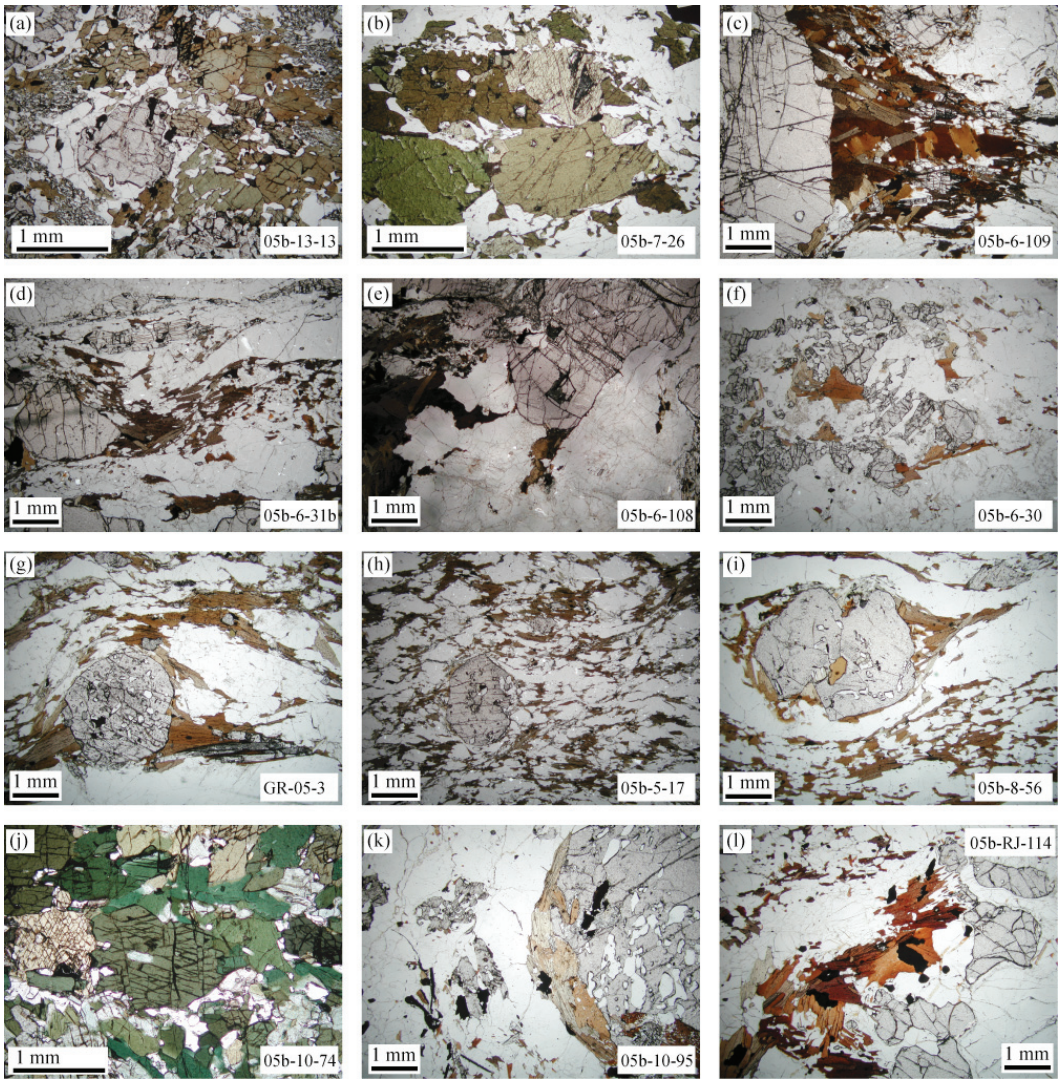


**Figure 4-3.** Photomicrographs of samples analyzed for $^{40}Ar/^{39}Ar$ ages.

garnets comprise fine-grained (~1 mm) quartz, K-feldspar and plagioclase, with rare subhedral ternary feldspar.

Sample 05b-6-108 (Fig. 4-3e) is a garnet–sillimanite/kyanite–K-feldspar gneiss. Euhedral garnets up to 1 cm in diameter include quartz, muscovite and kyanite. In the biotite-bearing layers, quartz and feldspar occur with sillimanite, kyanite and biotite up to 1 mm long that are aligned with compositional layering defining the foliation, which wraps around the garnets. Coarser grained biotite

several millimeters across occurs in garnet pressure shadows and is interpreted to partially replace garnet. Leucocratic layers are dominantly quartz and K-feldspar. Accessory ilmenite and monazite occur in the matrix. Monazite in this sample records a single age of growth of 588±5 Ma (Chapter 3).

Sample 05b-6-30 (Fig. 4-3f) is a garnet granulite. Anhedral garnet up to 1 cm in diameter contains inclusions of biotite, plagioclase, quartz and rutile. The matrix is composed of dominantly quartz and plagioclase grains 1–4 mm in diameter. Biotite up to 3 mm long occurs adjacent to garnet, and is interpreted to replace it, and finer grained biotite less than 1 mm long occurs in the matrix. There are sporadic flakes of retrograde muscovite up to 5 mm in length.

Sample 04-6-11 is leucosome-dominated and comprises primarily medium grained (2–4 mm) quartz, plagioclase and K-feldspar, with clusters of euhedral garnets 3–5 mm in diameter, sporadic sub-millimeter grains of biotite interpreted to partially replace garnet, and rare intersertal or patchy retrograde muscovite. Stringers of ilmenite up to 2 mm long occur along K-feldspar–K-feldspar grain boundaries. Biotite 2–3 mm in length occurs as melanosomes defining the foliation. The age of zircon growth in this sample is 648±12 Ma (Chapter 2). Monazite in this sample records an age of 611±6 Ma in cores and an age of 582±6 Ma in rims (Chapter 3).

Sample 05b-6-103 is a garnet–kyanite–K-feldspar gneiss. Garnet up to 5 mm in diameter contains inclusions of biotite, plagioclase, quartz, monazite and rutile. Kyanite up to 5 mm long and biotite occur aligned with compositional layering defining the foliation. A matrix of quartz, K-feldspar and plagioclase contains accessory ilmenite. Monazite in this sample records an age of growth of 630±10 Ma

in cores and an age of 602±8 Ma in rims (Chapter 3). A Rb-Sr multimineral–whole rock isochron calculated for a similar sample taken from the same outcrop yielded a cooling age of 590.0±3.7 Ma (Chapter 2).

Sample 05b-6-31b (Fig. 4-3d) is a garnet–biotite–quartz–plagioclase–sillimanite/ kyanite gneiss that is strongly foliated. Large sillimanite and kyanite grains up to 5mm in length occur defining the foliation; sillimanite also occurs as aggregates of small (<0.5 mm) grains formed along cracks that separate fragments of large (2-5 mm) garnets. Biotite occurs as sporadic fine grains in the foliation and as millimetric grains interpreted to replace garnet. Kyanite and accessory ilmenite occur as inclusions in the mantle regions of garnet, and ilmenite occurs in the matrix. The age of zircon growth in this sample is 647±11 Ma (Chapter 2). Monazite in this sample records an age of 634±12 Ma in cores, an age of 624±6 Ma in mantles and an age of 595±10 Ma in rims (Chapter 3).

Sample 05b-6-33 is a garnet–kyanite–K-feldspar gneiss. Garnet up to 5 mm in diameter contains inclusions of biotite, plagioclase and quartz. Kyanite up to 5 mm long and biotite 1-3 mm long occurs in the matrix aligned with compositional layering defining the foliation, which wraps garnet; biotite may occur in garnet pressure shadows. A matrix of quartz, K-feldspar and plagioclase contains accessory ilmenite.

***Carvalhos Klippe***

Samples were analyzed from two locations within the Carvalhos Klippe. Sample 05b-10-74 was taken from a railroad cut near the city of Carvalhos. Sample 05b-10-95 was taken from an outcrop at a waterfall just north of the city of Carvalhos.

Sample 05b-10-74 (Fig. 4-3j) is a foliated clinopyroxene-bearing amphibolite. Hornblende is the dominant phase in the rock and occurs as subhedral grains up to 5 mm in diameter. Subhedral pale green clinopyroxene up to 7 mm in length exhibits microstructural relationships interpreted to record breakdown to green hornblende. Quartz and plagioclase up to 2 mm across comprise ~25-30% of the sample and occur in layers 2–4 mm thick. Minor epidote, rare biotite and accessory apatite occur throughout the rock.

Sample 05b-10-95 (Fig. 4-3k) is a garnet–kyanite–biotite gneiss. Subhedral rounded garnet up to 5 mm in diameter contains inclusions of predominantly quartz but plagioclase, ilmenite and biotite may also occur. Symplectic tabular biotite with quartz up to 3 mm long occurs around and replacing garnet; later sillimanite aggregates cut across the symplectic biotite. Matrix-hosted biotite up to 2 mm long and subhedral kyanite up to 4 mm long are aligned with compositional layering defining the foliation. Rare unoriented muscovite is up to 0.5 mm in length. Monazite ages for similar samples collected at the same outcrop are 606±18 Ma for cores and 587±12 Ma for rims for one sample and 592±12 Ma for cores and 561±26 Ma for rims for a second sample (Chapter 3).

***Carmo da Cachoeira Nappe***

Biotite was analyzed from three samples taken from two locations within the Carmo da Cachoeira Nappe. Samples 05b-5-23 and GR-05-3 were taken from the INCOPE working quarry south of the city of Três Coraçoes near the structural top of the nappe. Sample 05b-5-17 was taken from an abandoned quarry in the structural middle of the

nappe. An equilibrium phase diagram to quantify the retrograde *P-T* evolution was constructed for a third sample, 04-5-8, from the INCOPE working quarry.

Sample 05b-5-23 is a strongly foliated garnet–kyanite–biotite gneiss. Euhedral garnet up to 5 mm in diameter has inclusions of biotite, plagioclase, quartz, rutile and irregular polymineralic quartzo-feldspathic aggregates (+/- biotite) interpreted to represent former melt. The matrix comprises 3–5 mm long biotite grains defining a strong mylonitic foliation together with kyanite, centimetric plagioclase, strongly internally-strained quartz and rare muscovite. Accessory ilmenite and tourmaline occur in the matrix. Monazite occurs as inclusions in biotite. Monazite in this sample records an age of 631±12 Ma in cores and an age of 605±6 Ma in rims (Chapter 3).

Sample GR-05-3 (Fig. 4-3g) is a strongly foliated garnet–kyanite–biotite–muscovite gneiss. Euhedral garnet up to 7 mm in diameter has inclusions of biotite, quartz, euhedral plagioclase, irregular polymineralic quartzo-feldspathic aggregates interpreted to represent former melt and rutile. Biotite and muscovite 2–4 mm long are aligned within the strong mylonitic foliation wrapping centimetric plagioclase grains. Accessory ilmenite, rutile and tourmaline are present in the matrix. Monazite occurs as inclusions in biotite.

Sample 05b-5-17 (Fig. 4-3h) is a strongly foliated garnet–kyanite–biotite schist. Rounded garnets ~2 mm in diameter contain inclusions of ilmenite, rutile, quartz, plagioclase and irregular polymineralic quartzo-feldspathic aggregates interpreted to represent former melt. The matrix consists of biotite (~1 mm long) that has partially replaced kyanite grains, both of which are aligned with compositional

layering defining the foliation, and strongly internally-strained quartz and plagioclase grains 1–2 mm in diameter. The foliation wraps around the garnet, which is partly replaced by biotite.

Sample 04-5-8 is a strongly foliated biotite-garnet gneiss. Tabular biotite and muscovite 2–4 mm long and rare kyanite all record internal strain and are aligned with compositional layering defining the foliation. Rounded subhedral garnets up to 5 mm in diameter contain inclusions of biotite, rutile, quartz, both euhedral and irregular plagioclase, irregular polymineralic quartzo-feldspathic aggregates interpreted to represent former melt, chlorite and muscovite. Biotite rims garnet and larger biotite grains 2–3 mm across occur in the interiors of some C-shaped garnets due to replacement. Quartz and plagioclase 1–2 mm in diameter occurs in the matrix, and lenses of internally-strained quartz and plagioclase up to 1 cm across occur wrapped by the micaceous foliation. Accessory ilmenite and rutile are present in the matrix.

***Andrelândia Nappe***

The Andrelândia Nappe is interpreted by Trouw *et al.* (2006) to be laterally equivalent to the Carmo da Cachoeira Nappe, and the two nappes are separated by a series of NE-SW oriented shear zones. Sample 05b-8-56 (Fig. 4-3i) was taken from near the Cristo Redentor statue overlooking the city of Andrelândia, approximately 100 km east of the Carmo da Cachoeira samples. This sample is a strongly foliated biotite–garnet schist. Subhedral rounded garnets up to 8 mm in diameter contain irregular inclusions of quartz and plagioclase, and irregular polymineralic quartzo-feldspathic aggregates interpreted to represent former melt. Biotite up to 8 mm long

and kyanite up to 5 mm long are aligned within the foliation. The matrix contains quartz and plagioclase up to 3 mm in diameter, together with accessory ilmenite and apatite.

***Socorro–Guaxupé Nappe***

Hornblende was analyzed from sample 05b-7-26 (Fig. 4-3b) collected from a 1–2 m diameter block interpreted to be *in situ* from close to the base of the Socorro–Guaxupé Nappe to the south of the city of Varginha. This sample is interpreted to have an igneous protolith that formed in a magmatic arc environment before being metamorphosed at high-pressure granulite facies conditions. The sample comprises a migmatitic garnet–orthopyroxene–hornblende granulite with minor clinopyroxene and accessory ilmenite; garnet is up to 1 cm in diameter. Leucosomes contain euhedral to subhedral garnet, which themselves contain small inclusions of brown biotite, together with quartz and plagioclase. There is a strong mylonitic foliation. The age of zircon growth in this sample is 622±28 Ma (Chapter 2).

***Ribeira Belt***

Biotite was analyzed in sample 05b-RJ-114 (Fig. 4-3l) collected from within the Ribeira Belt near the Rio Sul shopping mall in the Botafogo neighborhood of Rio de Janeiro. This sample is a garnet–cordierite–biotite migmatite in which anhedral garnet up to 1 cm in diameter and millimetric cordierite occur within a matrix of finer-grained quartz, plagioclase, ternary feldspar and biotite. Cordierite may occur adjacent to and partly replacing garnet.

*Metamorphic History*

For the Três Pontas–Varginha nappe, I interpret peak *P–T* conditions of 1.5–1.6 GPa and >850–900˚C to have been followed by close-to-isobaric cooling until final crystallization of residual melt in leucosomes at ~800˚C (Chapter 2). In this chapter, most of the biotite in samples from this nappe is interpreted to have grown along the high-temperature retrograde *P-T* path during crystallization of the residual melt, which is consistent with the mole proportions of biotite predicted from an equilibrium phase diagram calculated for sample 05b-6-31b (Chapter 2). For sample 04-6-11, I interpret biotite to have been part of the peak assemblage at temperatures >850–900˚C (Chapter 2). These data are summarized in Fig. 4-4(a).

An equilibrium phase diagram constructed for sample 04-5-8 from the Carmo da Cachoeira Nappe is shown in Fig. 4-4(b). The mineral equilibria modelling was undertaken using THERMOCALC 3.26 (Powell & Holland 1988; updated August 2007) and the internally consistent dataset of Holland & Powell (1998: dataset tcds55, created in November 2003). The calculations were done in the chemical system $Na_2O$–CaO–$K_2O$–FeO–MgO–$Al_2O_3$–$SiO_2$–$H_2O$–$TiO_2$–$Fe_2O_3$ (NCKFMASHTO) using the most recently available *a–x* models: biotite and melt (White *et al.* 2007), orthopyroxene and spinel–magnetite (White *et al.* 2002), garnet (Diener *et al.* 2008), cordierite (Holland & Powell 1998), K-feldspar and plagioclase (Holland & Powell 2003), white mica (Coggon & Holland 2002), and ilmenite–hematite (White *et al.* 2000). The aluminosilicates, quartz, and aqueous fluid ($H_2O$) are taken to be pure end-member phases. The modelling does not include minor components, such as F or Cl in biotite or $Cr_2O_3$ in magnetite, which can affect the stability of these phases.

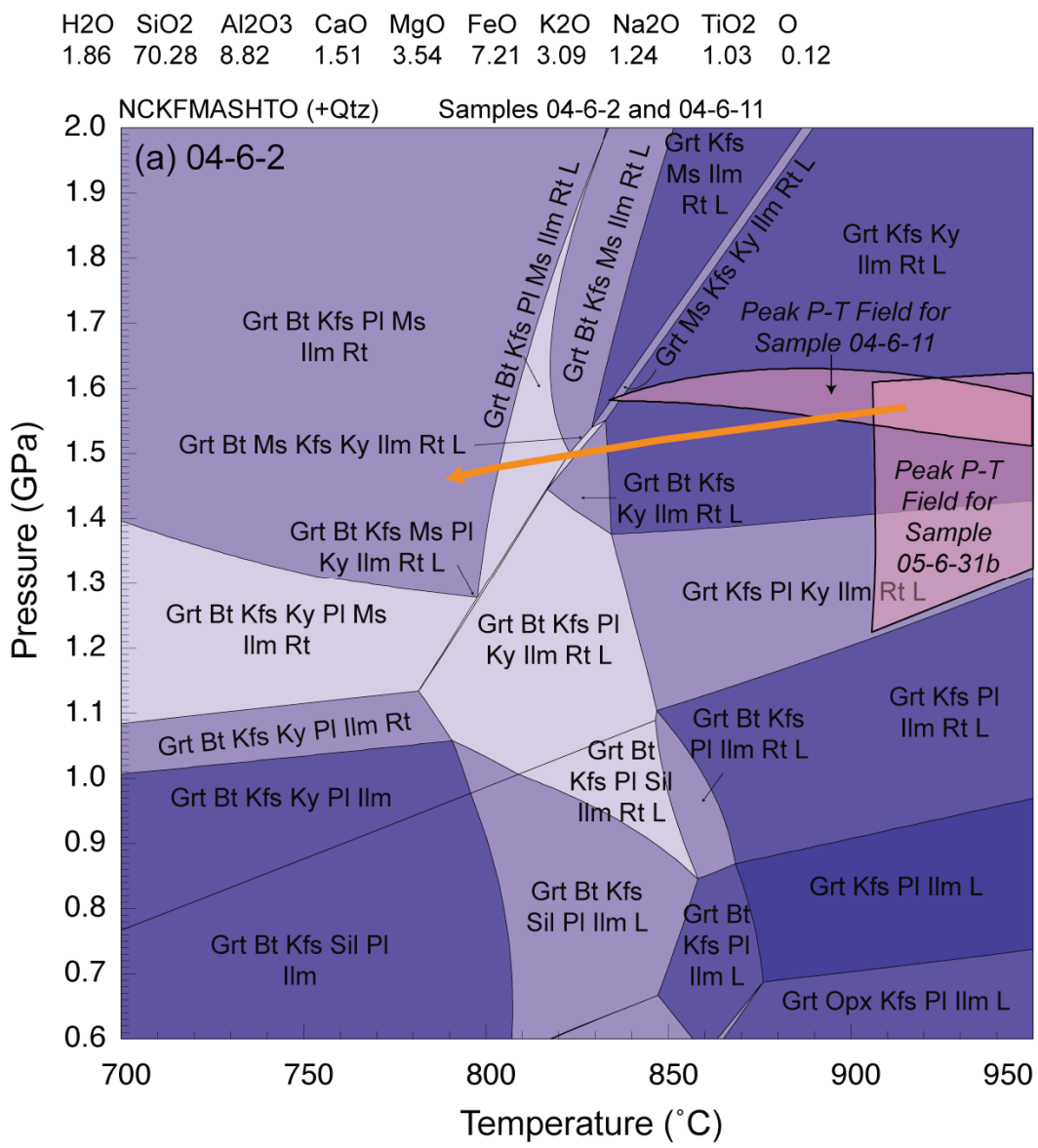


**Figure 4-4.** (a) summary of *P-T* isochemical phase diagrams (pseudosections) constructed for the Três Pontas–Varginha Nappe. The main diagram is constructed for sample 04-6-2 from Chapter 2. Overlain in pink are the phase stability fields corresponding to the peak assemblages for samples 05b-6-31b and 04-6-11. The high-*T* portion of the retrograde *P-T* path is indicated by the orange arrow. Composition is given in mol. %. (b; on following page) *P-T* isochemical phase diagram (pseudosection) constructed for sample 04-5-8 from the Carmo da Cachoeira Nappe. The bulk composition used to construct this pseudosection is interpreted to be residual and is only appropriate for interpreting the retrograde *P-T* evolution. The high-*T* portion of the retrograde *P-T* path is indicated by the orange arrow. Biotite modal abundance isopleths are plotted throughout the entire diagram, and garnet modal abundance isopleths are plotted in the fields intersecting the retrograde *P-T* path. Composition is given in mol. %.

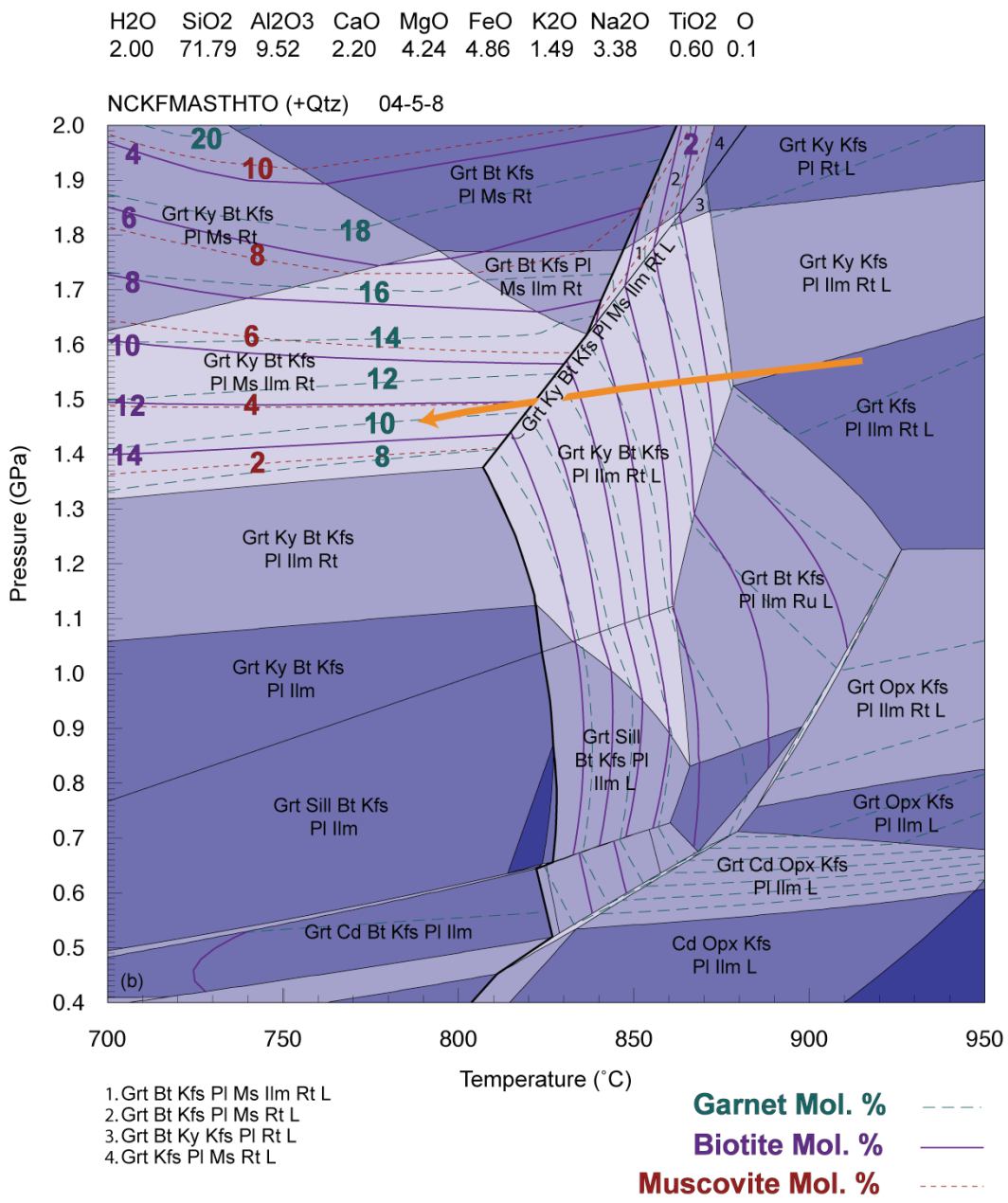


However, the NCKFMASHTO system is currently the most realistic approximation of rock compositions within which modelling can be undertaken (White *et al.* 2003, 2007).

The equilibrium phase diagram in Fig. 4-4(b) is contoured for mole proportion of biotite. In thin section, the strong foliation in all samples from the Carmo da

Cachoeira Nappe means that any microstructures consistent with the presence of a silicate melt likely have been overprinted by the strong sub-solidus strain. However, irregular polymineralic quartzo-feldspathic aggregates included in garnets are interpreted to represent former melt, and the bulk composition of sample 04-5-8 is strongly depleted in a silicate melt component in comparison with an average amphibolite facies metapelite (*cf.* Brown & Korhonen 2009). Therefore we infer that the peak mineral assemblage likely was in equilibrium with silicate melt. Thus, the peak assemblage for this sample is represented by the phase assemblage field containing quartz, garnet, kyanite, biotite, K-feldspar, plagioclase, ilmenite, rutile and silicate melt. This assemblage constrains the peak metamorphic conditions to pressures between 1.35 and 1.8 GPa and temperatures > 810˚C. Calculated mole proportions of biotite increase from < 2 mol. % to > 14 mol. % as a function of decreasing temperature, whereas calculated mole proportions of garnet decrease from ~20 mol. % to < 8 mol. % as a function of decreasing temperature in this phase stability field (Fig. 4-4b). The occurrence of muscovite constrains the high-temperature retrograde path to be close to isobaric, crossing the solidus in the subsolidus muscovite-bearing mineral assemblage fields (Fig. 4-4b). Calculated mole proportions of K-feldspar are less than 0.5 mol. % at sub-solidus temperatures. The replacement of garnet by biotite is interpreted to have occurred during close-to-isobaric cooling, and most of the biotite in this sample is interpreted to have grown at pressures > 1.35 GPa.

Trouw *et al.* (2006) interpret the Andrelândia Nappe to be the tectonic equivalent of the Carmo da Cachoeira Nappe. Campos Neto & Caby (1999) calculate

peak *P-T* conditions of 1.3 GPa and ~665˚C for the Andrelândia Nappe based on traditional thermobarometric techniques. These conditions are lower temperature han the *P-T* conditions estimated above for the Carmo da Cachoeira Nappe, which may be related to the use of traditional thermobarometric techniques and the reliance on Fe-Mg exchange thermometry.

The Carvalhos Klippe is inferred to be part of the Três Pontas–Varginha Nappe now isolated in the southernmost portion of the Southern Brasília Belt. Based on the mineral assemblages, the granulites in the Klippe are inferred to have experienced peak metamorphic conditions similar to the Três Pontas–Varginha Nappe. The Ribeira Orogeny (590–550 Ma) led to a tectonothermal overprinting recorded by sillimanite in the Carvalhos Klippe (Fig. 4-2). There is no macroscopic sillimanite overprint related to the Ribeira Orogeny in the Três Pontas–Varginha or Carmo da Cachoeira Nappes.

Kühn *et al.* (2004) interpret peak *P-T* conditions of ~0.7 GPa and 750–800˚C for the migmatites of the Ribeira Belt based on an equilibrium phase diagram constructed for a sample taken from the same outcrop as 05b-RJ-114 (Kühn *et al.* 2004 sample Rio-A3). Biotite in melanosomes is interpreted by Kühn *et al*. (2004) to be part of the pre-melt assemblage, and they interpret biotite to have also grown during the retrograde evolution at temperatures > 750˚C.

*Argon Chronology*

The Ar-Ar system in biotite, with closure temperatures between 345˚C for a cooling rate of 100 ˚C $Ma^{-1}$ and 280˚C for a cooling rate of 1 ˚C $Ma^{-1}$ (Harrison *et al.* 1985), and the Ar-Ar system in hornblende, with closure temperatures between 580˚C for a

cooling rate of 500 ˚C $Ma^{-1}$and 490˚C for a cooling rate of 5 ˚C $Ma^{-1}$ (Harrison *et al.* 1981), are suitable for constraining the intermediate part of the cooling history and dating overprinting tectonothermal events. The lower closure temperature estimates are more relevant to slowly cooled metamorphic terranes, and if the initial average cooling rate throughout the Andrelândia Nappe Complex is slow similar to the high-temperature retrograde evolution of the Três Pontas–Varginha Nappe, then the lower estimates of closure temperature are probably more relevant to this study.

Here I report both plateau ages obtained from age spectra, and inverse isochron ages. Except where noted, these ages are statistically identical. The calculation of a plateau age requires an assumption of the initial $^{40}Ar/^{36}Ar$ ratio, which in most cases is not significantly different from that of present day atmospheric argon of $^{40}Ar/^{36}Ar = 295.5$. The presence of an initial $^{40}Ar/^{36}Ar$ ratio >295.5 indicates the presence of an excess reservoir of argon in the sample. In this case, the interpretation of an age using the plateau method is not reliable. However, the calculation of an isochron age is independent of this ratio, and therefore it may be possible to interpret a geologically meaningful age from samples with non-atmospheric initial $^{40}Ar/^{36}Ar$ based on the isochron age (McDougall & Harrison 1999). For this reason, I refer only to the isochron ages when discussing the data. All argon step heating data are reported in Table 4-2, and isochron and plateau ages are reported in Table 4-3.

***Retrograded Eclogite***

The hornblende $^{40}Ar/^{39}Ar$ age spectrum for sample 05b-13-13 (Fig. 4-5) from the retrograded eclogite exhibits a saddle-shaped pattern typical of hornblende with

excess argon (McDougall & Harrison 1999), possibly due to multiple argon reservoirs within the hornblende crystals. The inverse isochron indicates a high degree of scatter, and yields an age of 705±140 Ma, with initial $^{40}Ar/^{36}Ar$ of 702±360. The youngest date obtained of 651±5.5 Ma was for the 1080˚C heating step. 27% of the $^{39}Ar$ was released at this step, which could have hidden any younger dates present in this portion of the spectrum. The high initial $^{40}Ar/^{36}Ar$ indicates the presence of a non-atmospheric excess argon reservoir in this sample that makes the age spectrum unreliable, and the large uncertainty and MSWD on the isochron age limits the utility of this age.

***Três Pontas–Varginha Nappe***

The biotite $^{40}Ar/^{39}Ar$ age spectrum for sample 05b-6-109 (Fig. 4-5) yields a plateau age of 591.4±6.6 Ma (MSWD=1.6; p=0.10) that comprises 98.6% of the $^{39}Ar$. The inverse isochron yields an age of 591.4±6.6 Ma, with initial $^{40}Ar/^{36}Ar$ of 300±18. The near-atmospheric initial $^{40}Ar/^{36}Ar$ ratio suggests that there is no significant excess argon reservoir in this sample. I consider this age to be geologically meaningful and to date cooling of this sample through ~300˚C.

The biotite $^{40}Ar/^{39}Ar$ age spectrum for sample 05b-6-108 (Fig. 4-5) yields a plateau age of 569.4±7.4 Ma (MSWD=1.7; p=0.13) that comprises 74.9% of the $^{39}Ar$. The inverse isochron yields an age of 573.1±8.3 Ma, with initial $^{40}Ar/^{36}Ar$ of 300±18. The near-atmospheric initial $^{40}Ar/^{36}Ar$ ratio suggests that there is no significant excess argon reservoir in this sample. I consider this age to be geologically meaningful and to date cooling of this sample through ~300˚C.

**Table 4-2.** $^{40}Ar/^{39}Ar$ analytical data for incremental heating experiments on biotite and hornblende from the Andrelândia Nappe Complex.

| Temperature (˚C) | $^{38}Ar/^{39}Ar$ | $^{37}Ar/^{39}Ar$ | $^{36}Ar/^{39}Ar$ | Cumulative Percent $^{39}Ar$ Released | % $^{40}Ar$* | $^{40}Ar*/^{39}Ar$ | Age (Ma) | ±2σ |
|---|---|---|---|---|---|---|---|---|
| **Sample 05b-13-13, Hornblende, 0.0086 g, J=0.00793395** | | | | | | | | |
| 500 | 0.066017 | 2.714587 | 0.25987584 | 0.2 | 36.77 | 45.105068 | 552 | ±36 |
| 600 | 0.039179 | 3.339561 | 0.12782122 | 0.3 | 81.98 | 172.831265 | 1558 | ±82 |
| 700 | 0.025112 | 4.085416 | 0.09471353 | 0.4 | 74.35 | 81.834746 | 903 | ±44 |
| 800 | 0.027080 | 7.313630 | 0.04498915 | 0.7 | 87.87 | 97.586704 | 1034 | ±26 |
| 900 | 0.025190 | 8.010128 | 0.02433667 | 1.4 | 92.18 | 86.073324 | 939 | ±18 |
| 950 | 0.034158 | 7.081792 | 0.00753149 | 3.4 | 97.33 | 82.323233 | 907 | ±12 |
| 990 | 0.035736 | 7.191011 | 0.00438822 | 11.0 | 98.05 | 66.396671 | 763.4 | ±6.4 |
| 1015 | 0.035148 | 7.651201 | 0.00400416 | 19.0 | 98.21 | 66.012449 | 759.8 | ±6.6 |
| 1040 | 0.036118 | 6.854068 | 0.00017931 | 47.2 | 99.91 | 56.920647 | 672.3 | ±5.9 |
| 1080 | 0.035751 | 6.547746 | 0.00439772 | 74.4 | 97.64 | 54.724865 | 650.5 | ±5.5 |
| 1130 | 0.035373 | 7.169635 | 0.00373135 | 97.7 | 98.05 | 56.358283 | 666.8 | ±5.5 |
| 1250 | 0.035895 | 6.726719 | 0.00917335 | 99.8 | 95.44 | 57.718486 | 680.2 | ±7.2 |
| 1350 | 0.041288 | 6.019553 | 0.05083625 | 100.0 | 79.77 | 60.131807 | 704 | ±19 |
| **Sample 05b-6-109, Biotite, 0.0015 g, J=0.0080184** | | | | | | | | |
| 500 | 0.024102 | 0.225273 | 0.05413671 | 0.1 | 47.33 | 14.423552 | 197 | ±13 |
| 575 | 0.019652 | 0.166805 | 0.02618081 | 0.3 | 75.68 | 24.116678 | 318.9 | ±7.0 |
| 650 | 0.015671 | 0.016010 | 0.01245753 | 1.4 | 93.06 | 49.381951 | 601.8 | ±7.6 |
| 710 | 0.012812 | 0.003644 | 0.00200866 | 7.9 | 98.79 | 48.648720 | 594.2 | ±7.1 |
| 770 | 0.012756 | 0.001061 | 0.00045270 | 21.0 | 99.72 | 47.953988 | 587.0 | ±6.9 |
| 830 | 0.012296 | 0.000904 | 0.00036989 | 35.5 | 99.77 | 48.222008 | 589.8 | ±7.0 |
| 890 | 0.012616 | 0.000010 | 0.00003433 | 44.2 | 99.98 | 48.597890 | 593.7 | ±6.9 |
| 950 | 0.012575 | 0.000307 | 0.00013082 | 49.6 | 99.92 | 48.437941 | 592.0 | ±7.0 |
| 1010 | 0.011729 | 0.000861 | 0.00004145 | 55.3 | 99.97 | 48.529782 | 593.0 | ±7.0 |
| 1080 | 0.013225 | 0.003265 | 0.00019802 | 82.0 | 99.88 | 48.507724 | 592.7 | ±7.7 |

| | | | | | | | | |
|---|---|---|---|---|---|---|---|---|
| 1150 | 0.012346 | 0.001954 | 0.00010181 | 98.8 | 99.94 | 47.739442 | 584.7 | ±6.8 |
| 1250 | 0.019624 | 0.002265 | 0.03500012 | 100.0 | 82.55 | 48.974461 | 597.6 | ±8.7 |
| 1350 | 0.414779 | 0.060759 | 2.33939891 | 100.0 | 5.88 | 43.909978 | 544 | ±593 |
| | | | | | | | | |
| **Sample 05b-6-108, Biotite, 0.0013 g, J=0.00800404** | | | | | | | | |
| 500 | 0.034543 | 0.282648 | 0.07238746 | 0.1 | 45.18 | 17.694881 | 239 | ±13 |
| 575 | 0.017972 | 0.156459 | 0.02758337 | 0.3 | 78.42 | 29.662501 | 384.3 | ±8.7 |
| 650 | 0.013592 | 0.009041 | 0.00758832 | 3.0 | 95.51 | 47.766156 | 584.1 | ±8.0 |
| 710 | 0.012628 | 0.002513 | 0.00122366 | 12.0 | 99.24 | 47.182928 | 578.0 | ±7.6 |
| 770 | 0.012292 | 0.000685 | 0.00062368 | 28.5 | 99.60 | 46.361198 | 569.4 | ±7.5 |
| 830 | 0.012667 | 0.000885 | 0.00027084 | 41.8 | 99.83 | 46.663995 | 572.5 | ±7.4 |
| 890 | 0.012236 | 0.002446 | 0.00032211 | 49.3 | 99.80 | 46.900670 | 575.0 | ±7.9 |
| 950 | 0.012439 | 0.002524 | 0.00014014 | 56.1 | 99.91 | 46.168118 | 567.3 | ±7.5 |
| 1010 | 0.012153 | 0.001074 | 0.00021533 | 64.0 | 99.86 | 46.140318 | 567.0 | ±7.5 |
| 1080 | 0.012319 | 0.000333 | 0.00016331 | 86.9 | 99.90 | 46.068775 | 566.3 | ±7.4 |
| 1150 | 0.012175 | 0.000588 | 0.00051328 | 98.1 | 99.68 | 47.149481 | 577.6 | ±7.6 |
| 1250 | 0.025937 | 0.000871 | 0.06912140 | 99.9 | 70.23 | 48.240012 | 589 | ±10 |
| 1350 | 0.066172 | 0.061208 | 0.29868286 | 100.0 | 33.15 | 43.900219 | 543 | ±65 |
| | | | | | | | | |
| **Sample 05b-6-30, Biotite, 0.002 g, J=00798044** | | | | | | | | |
| 500 | 0.031733 | 0.246665 | 0.09120788 | 0.1 | 41.00 | 18.794838 | 252.1 | ±8.8 |
| 600 | 0.015873 | 0.519156 | 0.01668935 | 0.7 | 88.94 | 39.745240 | 497.0 | ±7.0 |
| 680 | 0.012901 | 0.061244 | 0.00325785 | 5.6 | 97.97 | 46.621786 | 570.7 | ±6.9 |
| 740 | 0.012284 | 0.002101 | 0.00049767 | 18.7 | 99.68 | 45.845833 | 562.5 | ±6.7 |
| 800 | 0.012222 | 0.002571 | 0.00034025 | 32.0 | 99.78 | 45.994648 | 564.1 | ±6.6 |
| 860 | 0.012369 | 0.004645 | 0.00020806 | 41.7 | 99.87 | 46.455915 | 568.9 | ±6.7 |
| 920 | 0.012453 | 0.003743 | 0.00001564 | 48.7 | 99.99 | 46.670994 | 571.2 | ±6.7 |
| 955 | 0.012580 | 0.002938 | 0.00000138 | 54.6 | 100.00 | 46.316503 | 567.5 | ±7.0 |
| 990 | 0.012276 | 0.003533 | 0.00004205 | 63.2 | 99.97 | 45.929048 | 563.4 | ±6.8 |
| 1025 | 0.012175 | 0.004939 | 0.00014374 | 72.1 | 99.91 | 46.157118 | 565.8 | ±6.9 |
| 1060 | 0.012498 | 0.001763 | 0.00013404 | 82.7 | 99.91 | 46.336390 | 567.7 | ±6.7 |
| 1100 | 0.012480 | 0.000904 | 0.00001048 | 95.4 | 99.99 | 46.601097 | 570.4 | ±6.7 |
| 1160 | 0.012348 | 0.003451 | 0.00071297 | 98.5 | 99.56 | 47.791742 | 582.9 | ±7.0 |
| 1250 | 0.013775 | 0.006442 | 0.00214443 | 100.0 | 98.69 | 47.806503 | 583.0 | ±7.2 |

| | | | | | | | | |
|---|---|---|---|---|---|---|---|---|
| 1350 | 0.216817 | 1.051452 | 1.25841429 | 100.0 | 24.40 | 120.697171 | 1217 | ±305 |

**Sample 04-6-11, Biotite, 0.0011 g, J=0.00786243**

| | | | | | | | | |
|---|---|---|---|---|---|---|---|---|
| 500 | 0.038118 | 0.437501 | 0.13710522 | 0.2 | 24.34 | 13.119391 | 177 | ±18 |
| 575 | 0.016967 | 0.175500 | 0.02823250 | 0.8 | 72.99 | 22.584808 | 295 | ±11 |
| 650 | 0.017195 | 0.331819 | 0.01369974 | 2.9 | 91.95 | 46.331094 | 560.4 | ±6.9 |
| 710 | 0.013940 | 0.041926 | 0.00327364 | 11.4 | 98.06 | 49.014079 | 588.1 | ±5.8 |
| 770 | 0.012314 | 0.002406 | 0.00099407 | 26.2 | 99.40 | 49.102380 | 589.0 | ±5.0 |
| 830 | 0.012670 | 0.002090 | 0.00057460 | 46.6 | 99.65 | 48.668575 | 584.5 | ±4.7 |
| 890 | 0.012835 | 0.002292 | 0.00047014 | 62.5 | 99.72 | 48.769139 | 585.6 | ±4.8 |
| 950 | 0.012345 | 0.000032 | 0.00032293 | 74.9 | 99.81 | 49.488371 | 592.9 | ±5.1 |
| 1010 | 0.014708 | 0.007213 | 0.00340018 | 76.0 | 97.97 | 48.539610 | 583 | ±15 |
| 1080 | 0.012378 | 0.000118 | 0.00001684 | 93.9 | 99.99 | 49.707298 | 595.2 | ±5.3 |
| 1250 | 0.013038 | 0.012864 | 0.00004970 | 99.5 | 99.97 | 49.483375 | 592.9 | ±9.8 |
| 1350 | 0.028049 | 0.013137 | 0.05243376 | 100.0 | 76.47 | 50.419989 | 602 | ±12 |

**Sample 05b-6-103, Biotite, 0.0014 g, J=0.00801456**

| | | | | | | | | |
|---|---|---|---|---|---|---|---|---|
| 500 | 0.038132 | 0.178534 | 0.07240500 | 0.1 | 54.36 | 25.547162 | 336.0 | ±14 |
| 600 | 0.017851 | 0.085957 | 0.01791855 | 0.8 | 86.51 | 34.003563 | 434.8 | ±7.0 |
| 680 | 0.013673 | 0.004516 | 0.00601529 | 4.1 | 96.36 | 47.073466 | 577.5 | ±7.9 |
| 740 | 0.012505 | 0.001451 | 0.00039144 | 14.0 | 99.76 | 47.821740 | 585.3 | ±7.7 |
| 800 | 0.012441 | 0.001333 | 0.00040813 | 23.3 | 99.75 | 47.855054 | 585.7 | ±7.8 |
| 860 | 0.012497 | 0.003242 | 0.00102242 | 30.1 | 99.37 | 47.747982 | 584.6 | ±8.0 |
| 920 | 0.012744 | 0.000476 | 0.00010945 | 36.9 | 99.93 | 47.541806 | 582.4 | ±7.6 |
| 980 | 0.012516 | 0.000780 | 0.00047219 | 42.7 | 99.71 | 48.029753 | 587.5 | ±7.7 |
| 1020 | 0.012339 | 0.002914 | 0.00032359 | 51.9 | 99.80 | 47.657710 | 583.6 | ±7.7 |
| 1050 | 0.012264 | 0.002084 | 0.00003995 | 66.3 | 99.97 | 47.094691 | 577.7 | ±7.6 |
| 1080 | 0.012093 | 0.000447 | 0.00010561 | 83.4 | 99.93 | 47.164089 | 578.4 | ±7.6 |
| 1110 | 0.012486 | 0.000618 | 0.00017986 | 94.4 | 99.89 | 47.852320 | 585.7 | ±7.6 |
| 1150 | 0.012815 | 0.000950 | 0.00262085 | 98.4 | 98.41 | 47.833533 | 585.5 | ±7.8 |
| 1250 | 0.015615 | 0.014907 | 0.01843535 | 100.0 | 90.03 | 49.269705 | 600.4 | ±8.8 |
| 1350 | 0.313775 | 0.168253 | 1.51880817 | 100.0 | 16.55 | 89.540939 | 976 | ±150 |

**Sample 05b-6-31b, Biotite, 0.0015 g, J=0.00799868**

| | | | | | | | | |
|---|---|---|---|---|---|---|---|---|
| 500 | 0.025695 | 0.134025 | 0.04460406 | 0.4 | 62.61 | 22.117805 | 294 | ±11 |
| 575 | 0.015259 | 0.093825 | 0.01692264 | 1.6 | 88.75 | 39.499436 | 495.3 | ±8.0 |
| 650 | 0.013102 | 0.006817 | 0.00408415 | 10.0 | 97.48 | 46.814002 | 573.8 | ±6.8 |
| 710 | 0.012693 | 0.000947 | 0.00060265 | 31.3 | 99.62 | 46.437910 | 569.8 | ±6.7 |
| 770 | 0.012294 | 0.000542 | 0.00034937 | 52.2 | 99.78 | 46.591136 | 571.5 | ±6.7 |
| 830 | 0.012605 | 0.001059 | 0.00032983 | 65.9 | 99.79 | 46.904637 | 574.7 | ±6.8 |
| 890 | 0.012729 | 0.002643 | 0.00007546 | 74.6 | 99.95 | 46.921365 | 574.9 | ±7.1 |
| 950 | 0.012488 | 0.002366 | 0.00021396 | 84.3 | 99.86 | 46.793002 | 573.6 | ±6.8 |
| 1010 | 0.011874 | 0.000496 | 0.00020788 | 88.8 | 99.87 | 45.933668 | 564.5 | ±7.3 |
| 1080 | 0.012226 | 0.000068 | 0.00115556 | 99.1 | 99.27 | 46.435603 | 569.8 | ±7.2 |
| 1150 | 0.023116 | 0.010331 | 0.04828522 | 99.8 | 77.44 | 49.033606 | 597 | ±11 |
| 1250 | 0.153298 | 0.029962 | 0.73939244 | 100.0 | 18.42 | 49.593236 | 603 | ±41 |
| 1350 | 1.208354 | 1.491542 | 6.59755091 | 100.0 | 2.57 | 53.582303 | 643 | ±1225 |

**Sample 05b-6-33, Biotite, 0.0010 g, J=0.00801487**

| | | | | | | | | |
|---|---|---|---|---|---|---|---|---|
| 500 | 0.027536 | 0.388591 | 0.05449870 | 0.2 | 66.94 | 32.691786 | 419.8 | ±14 |
| 600 | 0.014586 | 0.015131 | 0.00767550 | 1.5 | 95.16 | 44.667473 | 552.1 | ±8.7 |
| 680 | 0.012714 | 0.001792 | 0.00111722 | 13.9 | 99.26 | 44.193698 | 547.0 | ±7.3 |
| 740 | 0.011846 | 0.000052 | 0.00029063 | 31.5 | 99.80 | 43.930729 | 544.2 | ±7.2 |
| 800 | 0.012434 | 0.001412 | 0.00026162 | 44.2 | 99.82 | 43.924295 | 544.1 | ±7.2 |
| 860 | 0.011966 | 0.003505 | 0.00068867 | 48.9 | 99.54 | 44.255677 | 547.7 | ±7.4 |
| 920 | 0.012422 | 0.006509 | 0.00004300 | 53.0 | 99.97 | 43.933275 | 544.2 | ±7.6 |
| 980 | 0.012505 | 0.002234 | 0.00022865 | 81.4 | 99.84 | 42.924694 | 533.4 | ±7.1 |
| 1020 | 0.012425 | 0.004313 | 0.00013111 | 92.3 | 99.91 | 44.049590 | 545.5 | ±7.2 |
| 1050 | 1.241248 | 0.009048 | 0.00030240 | 97.5 | 99.80 | 44.457920 | 549.8 | ±7.4 |
| 1080 | 0.012629 | 0.014208 | 0.00045062 | 99.2 | 99.70 | 44.742394 | 552.9 | ±7.6 |
| 1140 | 0.013758 | 0.026244 | 0.01698585 | 99.9 | 89.83 | 44.404609 | 549.3 | ±12 |
| 1250 | 0.200027 | 0.014431 | 0.88880857 | 100.0 | 16.64 | 52.714134 | 636 | ±119 |
| 1350 | 1.904219 | 0.434109 | 8.71852030 | 100.0 | 4.76 | 131.397328 | 1298 | ±3748 |

**Sample 05b-10-74, Hornblende, 0.0059 g, J=0.00790982**

| | | | | | | | | |
|---|---|---|---|---|---|---|---|---|
| 600 | 0.042689 | 2.426395 | 0.12731989 | 0.1 | 37.34 | 22.732869 | 298 | ±22 |
| 700 | 0.019218 | 1.895797 | 0.05084476 | 0.2 | 80.17 | 61.063286 | 711 | ±15 |
| 800 | 0.016576 | 1.100961 | 0.01754594 | 0.5 | 92.01 | 59.893717 | 700 | ±16 |

| | | | | | | | | |
|---|---|---|---|---|---|---|---|---|
| 975 | 0.015211 | 1.357428 | 0.01343359 | 0.8 | 93.82 | 60.530552 | 706 | ±11 |
| 1000 | 0.012409 | 2.196684 | 0.00160130 | 2.5 | 98.95 | 44.832472 | 547.6 | ±4.7 |
| 1025 | 0.012842 | 2.211152 | 0.00109545 | 17.5 | 99.28 | 44.778024 | 547.0 | ±4.7 |
| 1050 | 0.012521 | 2.222358 | 0.00085343 | 44.5 | 99.42 | 43.873046 | 537.4 | ±4.5 |
| 1075 | 0.011883 | 2.073426 | 0.00065461 | 86.8 | 99.55 | 43.101622 | 529.2 | ±4.9 |
| 1100 | 0.012169 | 2.418575 | 0.00159404 | 91.6 | 98.95 | 44.931633 | 548.6 | ±5.0 |
| 1150 | 0.013152 | 2.781696 | 0.00129564 | 99.9 | 99.15 | 45.012602 | 549.5 | ±4.8 |
| 1350 | 0.022665 | 2.606724 | 0.07073530 | 100.0 | 66.57 | 41.988674 | 517 | ±19 |
| **Sample 05b-10-95, Biotite, 0.0014 g, J=0.00785641** | | | | | | | | |
| 500 | 0.045286 | 0.156296 | 0.06792572 | 0.2 | 52.45 | 22.191762 | 289.9 | ±9.6 |
| 575 | 0.019546 | 0.058616 | 0.02123347 | 0.7 | 77.22 | 21.300697 | 279.2 | ±5.4 |
| 650 | 0.014152 | 0.029388 | 0.00826031 | 2.7 | 94.90 | 45.430403 | 550.6 | ±7.3 |
| 710 | 0.013042 | 0.005174 | 0.00238821 | 9.6 | 98.51 | 46.677761 | 563.6 | ±4.8 |
| 770 | 0.012415 | 0.001286 | 0.00058642 | 23.7 | 99.63 | 46.388450 | 560.6 | ±4.5 |
| 830 | 0.012762 | 0.001546 | 0.00035028 | 35.9 | 99.78 | 46.789484 | 564.8 | ±4.4 |
| 890 | 0.012557 | 0.001910 | 0.00044225 | 43.8 | 99.72 | 46.812885 | 565.0 | ±4.7 |
| 950 | 0.012516 | 0.003052 | 0.00029264 | 49.6 | 99.81 | 46.569918 | 562.5 | ±4.9 |
| 1010 | 0.012696 | 0.002283 | 0.00003756 | 56.6 | 99.98 | 46.519099 | 562.0 | ±4.6 |
| 1080 | 0.012160 | 0.001883 | 0.00021704 | 74.6 | 99.86 | 45.596877 | 552.4 | ±4.4 |
| 1150 | 0.012079 | 0.000911 | 0.00004996 | 96.4 | 99.97 | 45.739075 | 553.9 | ±4.3 |
| 1250 | 0.012051 | 0.001453 | 0.00076926 | 99.8 | 99.52 | 47.482785 | 571.9 | ±5.7 |
| 1080 | 0.031806 | 0.006973 | 0.10484510 | 100.0 | 59.86 | 46.256994 | 559 | ±16 |
| **Sample 05b-5-23, Biotite, 0.0017 g, J=0.00788200** | | | | | | | | |
| 650 | 0.012890 | 0.008670 | 0.00307967 | 4.6 | 97.97 | 44.012941 | 537.3 | ±4.6 |
| 710 | 0.012181 | 0.003420 | 0.00087170 | 15.6 | 99.42 | 44.151676 | 538.7 | ±4.3 |
| 770 | 0.011961 | 0.002255 | 0.00046274 | 34.5 | 99.69 | 43.642788 | 533.4 | ±4.4 |
| 830 | 0.012101 | 0.005037 | 0.00064216 | 45.2 | 99.57 | 44.307077 | 540.4 | ±4.3 |
| 890 | 0.012069 | 0.006272 | 0.00060014 | 55.7 | 99.60 | 44.660030 | 544.1 | ±4.9 |
| 950 | 0.012362 | 0.003666 | 0.00046312 | 68.5 | 99.69 | 44.402768 | 541.4 | ±4.6 |
| 1010 | 0.012210 | 0.000525 | 0.00027671 | 93.6 | 99.81 | 43.687541 | 533.8 | ±4.2 |
| 1150 | 0.013199 | 0.002995 | 0.00026188 | 99.6 | 99.83 | 44.766149 | 545.2 | ±5.0 |
| 1250 | 0.018702 | 0.186782 | 0.01531722 | 100.0 | 91.22 | 47.061449 | 569 | ±16 |

| | | | | | | | | |
|---|---|---|---|---|---|---|---|---|
| 1350 | 1.577655 | 1.107713 | 7.17344185 | 100.0 | 2.54 | 57.325360 | 673 | ±5697 |

**Sample GR-05-3, Biotite, 0.0021 g, J=00797022**

| | | | | | | | | |
|---|---|---|---|---|---|---|---|---|
| 500 | 0.031599 | 0.160750 | 0.06661289 | 0.0 | 54.63 | 23.754139 | 312.8 | ±6.4 |
| 600 | 0.014936 | 0.055268 | 0.01306410 | 0.0 | 89.29 | 32.213353 | 412.3 | ±2.9 |
| 680 | 0.013767 | 0.005250 | 0.00424766 | 0.1 | 97.21 | 43.726460 | 539.4 | ±2.5 |
| 740 | 0.000102 | 0.002447 | 0.00111392 | 0.2 | 99.24 | 43.206488 | 533.9 | ±2.4 |
| 800 | 0.000108 | 0.001014 | 0.00041120 | 0.3 | 99.72 | 42.722595 | 528.7 | ±2.4 |
| 860 | 0.012570 | 0.004582 | 0.00064697 | 0.4 | 99.56 | 43.732666 | 539.5 | ±2.5 |
| 920 | 0.012157 | 0.004913 | 0.00028456 | 0.4 | 99.81 | 44.094456 | 543.3 | ±2.5 |
| 980 | 0.012579 | 0.002927 | 0.00001081 | 0.7 | 99.99 | 44.420193 | 546.8 | ±2.8 |
| 1020 | 0.013063 | 0.001619 | 0.00051575 | 0.8 | 99.66 | 44.249297 | 545.0 | ±2.5 |
| 1050 | 0.012344 | 0.000664 | 0.00010056 | 1.0 | 99.93 | 43.472775 | 536.7 | ±2.4 |
| 1080 | 0.012123 | 0.000743 | 0.00039664 | 1.0 | 99.73 | 44.102739 | 543.4 | ±2.7 |
| 1110 | 0.008475 | 0.020368 | 0.00072951 | 1.0 | 99.52 | 44.607815 | 548.8 | ±5.2 |
| 1150 | 0.020819 | 0.014345 | 0.04906222 | 1.0 | 77.71 | 50.603957 | 611 | ±10 |
| 1250 | 0.039016 | 0.068690 | 0.16599942 | 1.0 | 56.79 | 64.595402 | 749 | ±13 |
| 1350 | 0.768759 | 2.297100 | 3.55178638 | 1.0 | 16.23 | 205.065883 | 1748 | ±213 |

**Sample 05b-5-17, Biotite, 0.0016 g, J=0.00787537**

| | | | | | | | | |
|---|---|---|---|---|---|---|---|---|
| 500 | 0.027344 | 0.147511 | 0.04758692 | 0.2 | 61.51 | 22.515480 | 294 | ±11 |
| 575 | 0.016450 | 0.055802 | 0.01160494 | 0.8 | 89.99 | 30.873403 | 392.6 | ±6.2 |
| 650 | 0.012873 | 0.004230 | 0.00279929 | 5.4 | 98.04 | 41.490011 | 510.1 | ±4.3 |
| 710 | 0.012607 | 0.003947 | 0.00063965 | 15.5 | 99.55 | 41.576112 | 511.0 | ±4.2 |
| 770 | 0.012318 | 0.007641 | 0.00056647 | 24.7 | 99.60 | 41.273561 | 507.8 | ±4.2 |
| 830 | 0.012232 | 0.012773 | 0.00052307 | 31.0 | 99.63 | 41.607680 | 511.3 | ±4.1 |
| 890 | 0.012646 | 0.014013 | -0.00013696 | 37.7 | 100.10 | 41.811532 | 513.5 | ±4.1 |
| 950 | 0.012170 | 0.006509 | -0.00020765 | 48.4 | 100.15 | 41.882390 | 514.3 | ±4.1 |
| 1010 | 0.012161 | 0.001682 | 0.00009621 | 67.7 | 99.93 | 41.076016 | 505.6 | ±3.8 |
| 1080 | 0.012186 | 0.002377 | 0.00000901 | 90.8 | 99.99 | 40.710697 | 501.7 | ±4.1 |
| 1150 | 0.011994 | 0.003979 | 0.00018729 | 98.5 | 99.87 | 41.847464 | 513.9 | ±4.1 |
| 1250 | 0.011472 | 0.006652 | 0.00012104 | 99.7 | 99.92 | 42.349094 | 519.2 | ±6.0 |
| 1350 | 0.019299 | 0.008935 | 0.02339205 | 100.0 | 86.32 | 43.641946 | 533.0 | ±9.7 |

**Sample 05b-8-56, Biotite, 0.0014 g, J=0.00795760**

| | | | | | | | | |
|---|---|---|---|---|---|---|---|---|
| 500 | 0.036497 | 0.322341 | 0.07024922 | 0.1 | 53.64 | 24.094002 | 317 | ±21 |
| 575 | 0.014982 | 0.067188 | 0.01192579 | 0.6 | 90.33 | 32.949029 | 420.7 | ±6.5 |
| 650 | 0.012870 | 0.004609 | 0.00223271 | 5.3 | 98.37 | 39.738450 | 496.4 | ±4.9 |
| 710 | 0.012682 | 0.002549 | 0.00065198 | 14.2 | 99.51 | 39.372228 | 492.4 | ±4.6 |
| 770 | 0.012611 | 0.001701 | 0.00041750 | 27.7 | 99.68 | 39.049892 | 488.9 | ±4.5 |
| 830 | 0.012727 | 0.003578 | 0.00078147 | 33.7 | 99.42 | 39.464814 | 493.4 | ±4.7 |
| 890 | 0.012184 | 0.002915 | 0.00002874 | 44.3 | 99.98 | 39.465154 | 493.4 | ±4.4 |
| 950 | 0.011941 | 0.001375 | 0.00005062 | 63.1 | 99.96 | 38.909999 | 487.3 | ±4.4 |
| 1010 | 0.012209 | 0.001075 | 0.00022815 | 80.3 | 99.83 | 38.869929 | 486.9 | ±4.4 |
| 1080 | 0.012186 | 0.001139 | 0.00016698 | 92.6 | 99.87 | 39.264345 | 491.2 | ±4.4 |
| 1150 | 0.015947 | 0.003442 | 0.02147663 | 99.6 | 86.25 | 39.864787 | 497.8 | ±5.7 |
| 1250 | 0.235014 | 0.014624 | 1.16592757 | 100.0 | 11.80 | 46.431267 | 568 | ±58 |
| 1350 | 1.169238 | 0.428157 | 5.85064985 | 100.0 | 6.79 | 127.672739 | 1266 | ±1418 |

**Sample 05b-7-26, Hornblende, 0.005 g, J=0.00788133**

| | | | | | | | | |
|---|---|---|---|---|---|---|---|---|
| 600 | 0.085968 | 2.677277 | 0.35291658 | 0.2 | 31.39 | 48.194419 | 581 | ±37 |
| 700 | 0.040331 | 0.963831 | 0.14855689 | 0.7 | 49.84 | 43.823230 | 535.2 | ±15 |
| 800 | 0.017686 | 0.690520 | 0.02592669 | 3.0 | 84.77 | 42.766081 | 524.0 | ±5.3 |
| 900 | 0.012550 | 0.816212 | 0.00094786 | 6.7 | 99.38 | 44.885498 | 546.4 | ±4.9 |
| 980 | 0.019590 | 1.852284 | 0.00111823 | 18.0 | 99.33 | 49.569165 | 595.0 | ±4.9 |
| 1010 | 0.020471 | 2.039542 | 0.00083928 | 44.9 | 99.49 | 48.609308 | 585.1 | ±4.5 |
| 1030 | 0.020239 | 2.008179 | 0.00048764 | 56.1 | 99.71 | 49.725314 | 596.6 | ±4.6 |
| 1050 | 0.020066 | 2.067447 | 0.00056541 | 77.7 | 99.66 | 49.024833 | 589.4 | ±4.6 |
| 1070 | 0.020451 | 2.167125 | 0.00080338 | 94.0 | 99.52 | 49.677817 | 596.1 | ±4.6 |
| 1090 | 0.018776 | 4.762701 | 0.00177615 | 99.6 | 98.98 | 51.358279 | 613.2 | ±5.3 |
| 1120 | 0.031629 | 58.418456 | 0.05830061 | 99.9 | 77.09 | 66.416727 | 759.5 | ±18 |
| 1250 | 0.143412 | 9.136438 | 0.69993864 | 100.0 | 28.71 | 85.013530 | 925 | ±116 |
| 1350 | 0.766313 | 4.101667 | 6.14140862 | 100.0 | 20.82 | 481.331498 | 2827 | ±3148 |

**Sample 05b-RJ-114, Biotite, 0.0010 g, J=0.00786152**

| | | | | | | | | |
|---|---|---|---|---|---|---|---|---|
| 550 | 0.028712 | 0.287619 | 0.05754414 | 0.2 | 52.31 | 18.705097 | 248 | ±14 |
| 630 | 0.017983 | 0.030946 | 0.02067359 | 1.1 | 85.50 | 36.069355 | 450.4 | ±6.4 |
| 700 | 0.012523 | 0.003412 | 0.00372764 | 8.1 | 97.08 | 36.661781 | 456.9 | ±3.9 |

| | | | | | | | | |
|---|---|---|---|---|---|---|---|---|
| 760 | 0.012741 | 0.001521 | 0.00056363 | 24.2 | 99.54 | 36.356138 | 453.5 | ±3.5 |
| 820 | 0.012306 | 0.004621 | 0.00046967 | 33.6 | 99.62 | 36.441344 | 454.5 | ±3.6 |
| 880 | 0.012625 | 0.011089 | 0.00078036 | 39.2 | 99.37 | 36.568894 | 455.9 | ±4.3 |
| 940 | 0.012155 | 0.008213 | -0.00014150 | 43.7 | 100.11 | 36.683476 | 457.1 | ±5.1 |
| 1000 | 0.012353 | 0.007176 | 0.00037331 | 48.0 | 99.70 | 36.931946 | 459.9 | ±4.0 |
| 1100 | 0.012655 | 0.003774 | 0.00039421 | 63.0 | 99.68 | 36.292736 | 452.8 | ±3.6 |
| 1200 | 0.012204 | 0.000940 | -0.00002744 | 100.0 | 100.02 | 36.601800 | 456.2 | ±4.4 |

**Table 4-3.** Summary of $^{40}Ar/^{39}Ar$ plateau and isochron ages for the Andrelândia Nappe Complex.

| | | Plateau Age | | | | | Inverse Isochron Age | | | | |
|---|---|---|---|---|---|---|---|---|---|---|---|
| Sample | Mineral | Age (Ma) | ±2s | MSWD | Probability | % 39Ar | Age (Ma) | ±2s | MSWD | Iniital $^{40}Ar/^{39}Ar$ | ±2s |
| *Retrograded Eclogite* | | | | | | | | | | | |
| 05b-13-13 | Hornblende | 651 | ±5.5 | – | – | – | 705 | ±140 | 56 | 705 | ±140 |
| *Três Pontas–Varginha Nappe* | | | | | | | | | | | |
| 05b-6-109 | Biotite | 591.1 | ±6.5 | 1.6 | 0.1 | 98.6 | 591.4 | ±6.6 | 0.6 | 300 | ±18 |
| 05b-6-108 | Biotite | 569.4 | ±7.4 | 1.7 | 0.13 | 74.9 | 573.1 | ±8.3 | 1.5 | 292 | ±14 |
| 05b-6-30 | Biotite | 567.2 | ±6.2 | 1.5 | 0.13 | 94.7 | 568.9 | ±6.1 | 1.19 | 360 | ±53 |
| 04-6-11 | Biotite | 587.8 | ±2.9 | 1.4 | 0.24 | 66.1 | 589 | ±11 | 3.2 | 310 | ±76 |
| 05b-6-103 | Biotite | 583.5 | ±7.4 | 1.5 | 0.13 | 94.3 | 583.2 | ±7.1 | 0.65 | 325 | ±14 |
| 05b-6-31b | Biotite | 571.8 | ±6.3 | 1.5 | 0.18 | 97.5 | 572.5 | ±6.6 | 1 | 300.5 | ±7.0 |
| 05b-6-33 | Biotite | 546 | ±11 | – | – | – | 545.5 | ±6.8 | 0.71 | 305.1 | ±6.9 |
| *Carvalhos Klippe* | | | | | | | | | | | |
| 05b-10-74 | Hornblende | 529 | ±5.0 | – | – | – | 564 | ±92 | 17 | 386 | ±250 |
| 05b-10-95 | Biotite | 559 | ±11 | – | – | – | 560.7 | ±3.9 | 1.18 | 292 | ±22 |
| *Carmo da Cachoeira Nappe* | | | | | | | | | | | |
| 05b-5-23 | Biotite | 539 | ±2.4 | 2.1 | 0.064 | 68.5 | 539.7 | ±4.0 | 1.4 | 304 | ±26 |
| GR-05-3 | Biotite | 542.9 | ±3.7 | 2.1 | 0.064 | 61.7 | 543 | ±12 | 3 | 362 | ±25 |
| 05b-5-17 | Biotite | 509.5 | ±2.0 | 1.5 | 0.19 | 62.3 | 509.2 | ±3.5 | 0.79 | 385 | ±75 |
| *Andrelândia Nappe* | | | | | | | | | | | |
| 05b-8-56 | Biotite | 490.4 | ±3.2 | 1.6 | 0.13 | 87.3 | 490.6 | ±4.1 | 0.54 | 302.1 | ±3.9 |
| *Socorro–Guaxupé Nappe* | | | | | | | | | | | |
| 05b-7-26 | Hornblende | 592 | ±10 | – | – | – | 576 | ±30 | 20 | 335 | ±37 |
| *Ribeira Belt* | | | | | | | | | | | |
| 05b-RJ-114 | Biotite | 455.2 | ±1.6 | 1.15 | 0.32 | 99.8 | 455.5 | ±3.6 | 0.22 | 273 | ±51 |

**Figure 4-5.** Age spectra for $^{40}Ar/^{39}Ar$ step heating experiments and inverse isochrons.

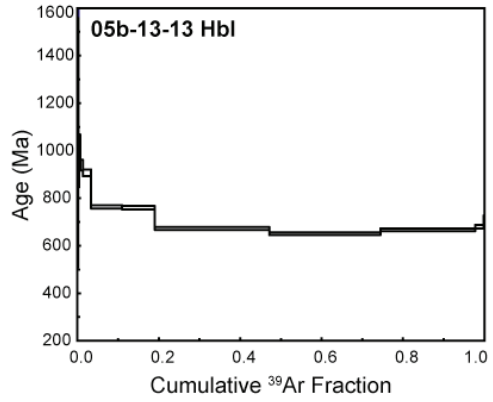
05b-13-13 Hbl
Age (Ma)
Cumulative $^{39}$Ar Fraction

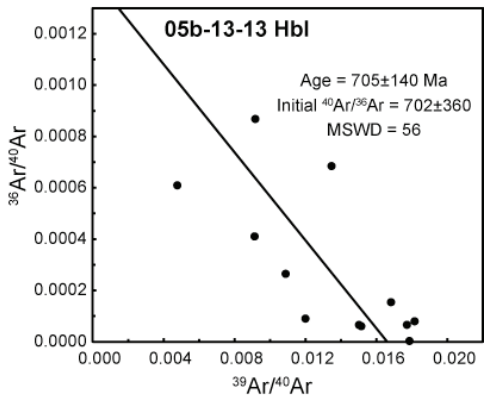
05b-13-13 Hbl
Age = 705±140 Ma
Initial $^{40}$Ar/$^{36}$Ar = 702±360
MSWD = 56
$^{36}$Ar/$^{40}$Ar
$^{39}$Ar/$^{40}$Ar

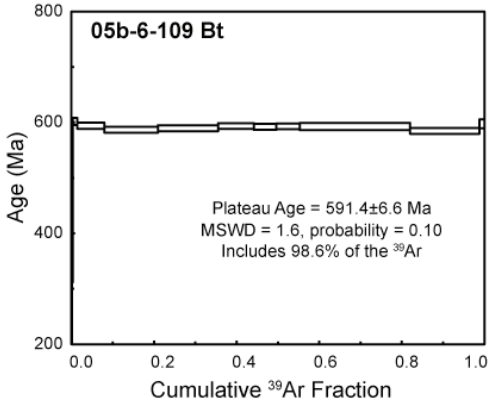
05b-6-109 Bt
Plateau Age = 591.4±6.6 Ma
MSWD = 1.6, probability = 0.10
Includes 98.6% of the $^{39}$Ar
Age (Ma)
Cumulative $^{39}$Ar Fraction

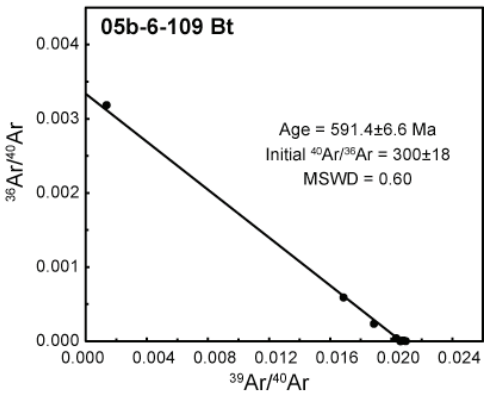
05b-6-109 Bt
Age = 591.4±6.6 Ma
Initial $^{40}$Ar/$^{36}$Ar = 300±18
MSWD = 0.60
$^{36}$Ar/$^{40}$Ar
$^{39}$Ar/$^{40}$Ar

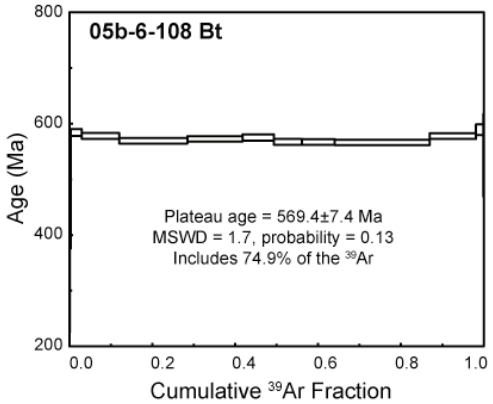
05b-6-108 Bt
Plateau age = 569.4±7.4 Ma
MSWD = 1.7, probability = 0.13
Includes 74.9% of the $^{39}$Ar
Age (Ma)
Cumulative $^{39}$Ar Fraction

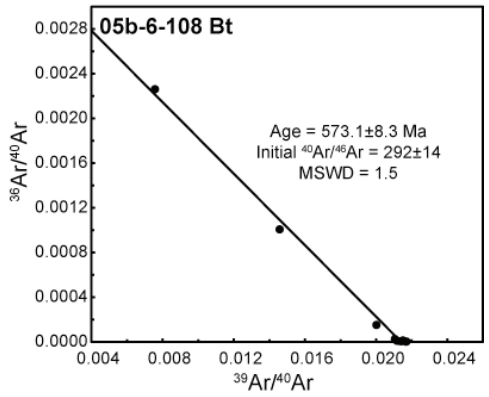
05b-6-108 Bt
Age = 573.1±8.3 Ma
Initial $^{40}$Ar/$^{46}$Ar = 292±14
MSWD = 1.5
$^{36}$Ar/$^{40}$Ar
$^{39}$Ar/$^{40}$Ar

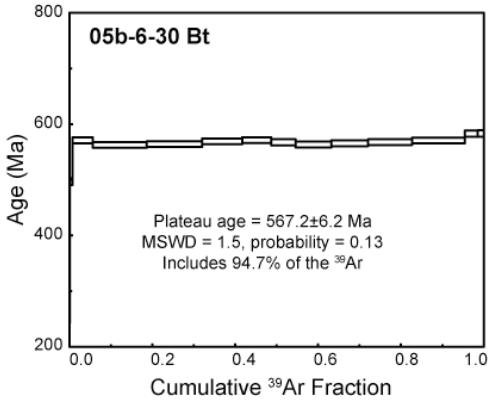
05b-6-30 Bt
Plateau age = 567.2±6.2 Ma
MSWD = 1.5, probability = 0.13
Includes 94.7% of the $^{39}$Ar
Age (Ma)
Cumulative $^{39}$Ar Fraction

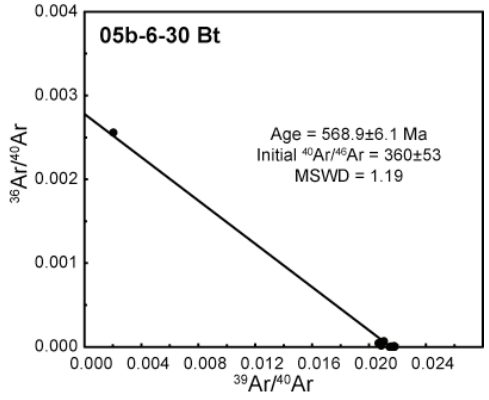
05b-6-30 Bt
Age = 568.9±6.1 Ma
Initial $^{40}$Ar/$^{46}$Ar = 360±53
MSWD = 1.19
$^{36}$Ar/$^{40}$Ar
$^{39}$Ar/$^{40}$Ar

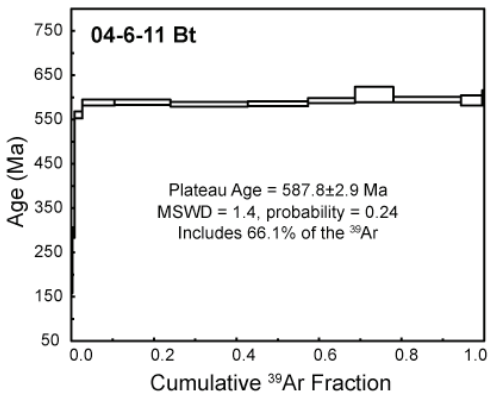
04-6-11 Bt
Plateau Age = 587.8±2.9 Ma
MSWD = 1.4, probability = 0.24
Includes 66.1% of the 39Ar
Age (Ma)
Cumulative 39Ar Fraction

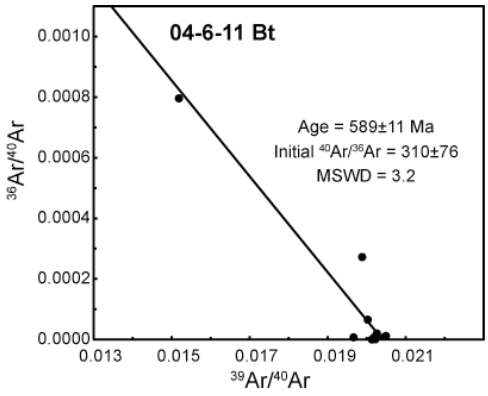
04-6-11 Bt
Age = 589±11 Ma
Initial 40Ar/36Ar = 310±76
MSWD = 3.2
36Ar/40Ar
39Ar/40Ar

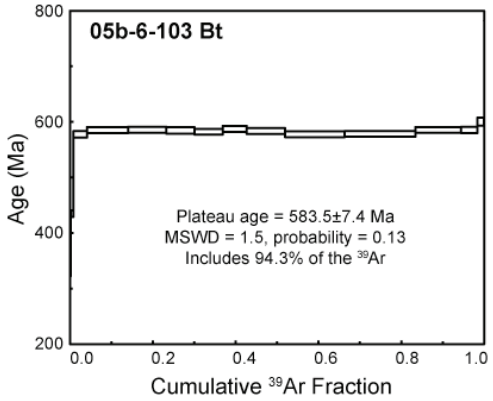
05b-6-103 Bt
Plateau age = 583.5±7.4 Ma
MSWD = 1.5, probability = 0.13
Includes 94.3% of the 39Ar
Age (Ma)
Cumulative 39Ar Fraction

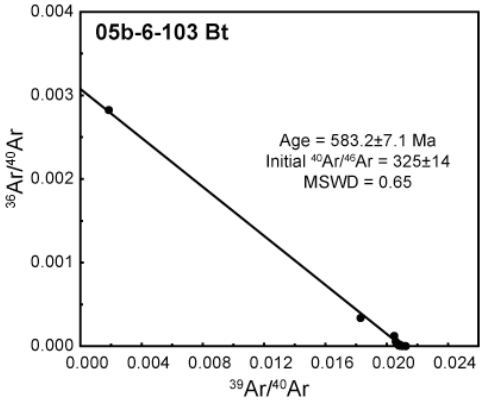
05b-6-103 Bt
Age = 583.2±7.1 Ma
Initial 40Ar/46Ar = 325±14
MSWD = 0.65
36Ar/40Ar
39Ar/40Ar

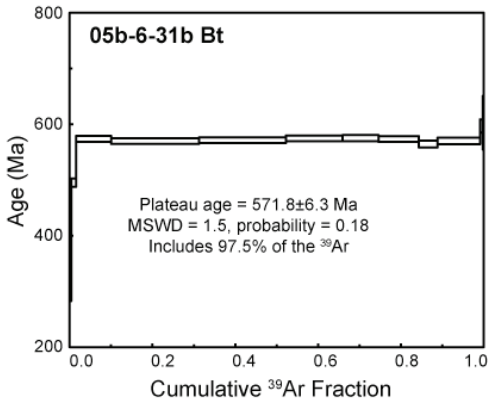
05b-6-31b Bt
Plateau age = 571.8±6.3 Ma
MSWD = 1.5, probability = 0.18
Includes 97.5% of the 39Ar
Age (Ma)
Cumulative 39Ar Fraction

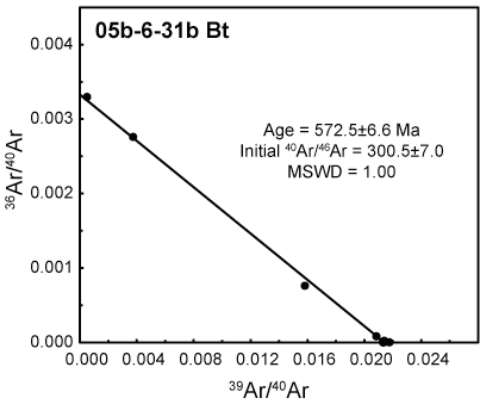
05b-6-31b Bt
Age = 572.5±6.6 Ma
Initial 40Ar/46Ar = 300.5±7.0
MSWD = 1.00
36Ar/40Ar
39Ar/40Ar

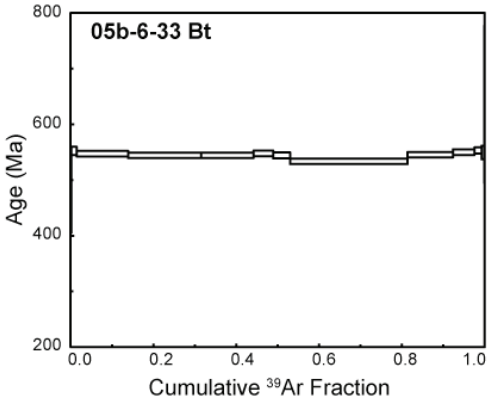
05b-6-33 Bt
Age (Ma)
Cumulative 39Ar Fraction

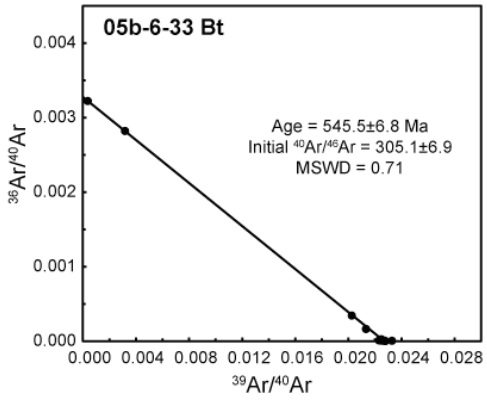
05b-6-33 Bt
Age = 545.5±6.8 Ma
Initial 40Ar/46Ar = 305.1±6.9
MSWD = 0.71
36Ar/40Ar
39Ar/40Ar

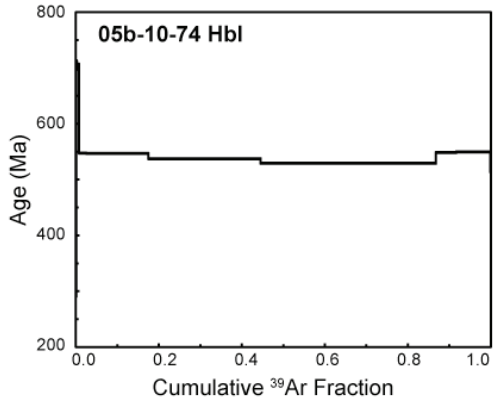
05b-10-74 Hbl
Age (Ma)
Cumulative $^{39}$Ar Fraction

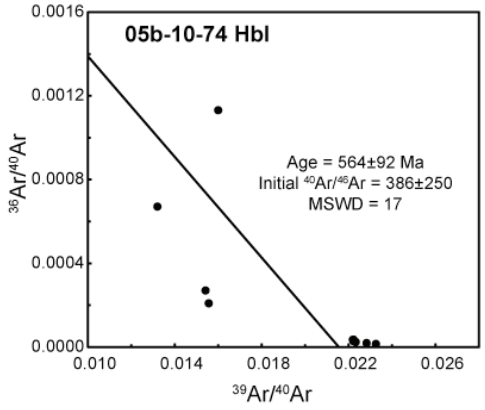
05b-10-74 Hbl
Age = 564±92 Ma
Initial $^{40}$Ar/$^{46}$Ar = 386±250
MSWD = 17
$^{36}$Ar/$^{40}$Ar
$^{39}$Ar/$^{40}$Ar

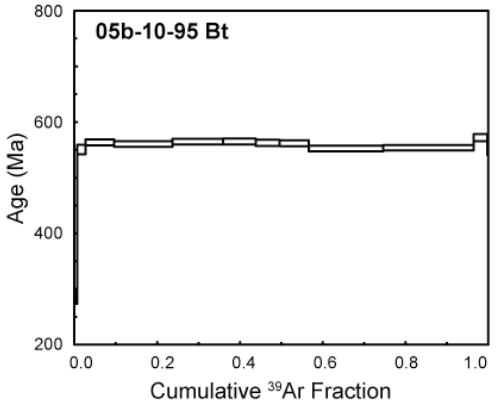
05b-10-95 Bt
Age (Ma)
Cumulative $^{39}$Ar Fraction

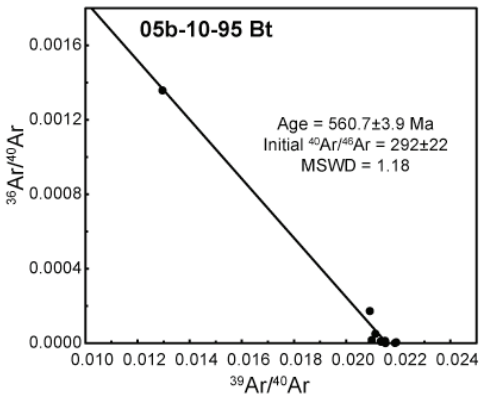
05b-10-95 Bt
Age = 560.7±3.9 Ma
Initial $^{40}$Ar/$^{46}$Ar = 292±22
MSWD = 1.18
$^{36}$Ar/$^{40}$Ar
$^{39}$Ar/$^{40}$Ar

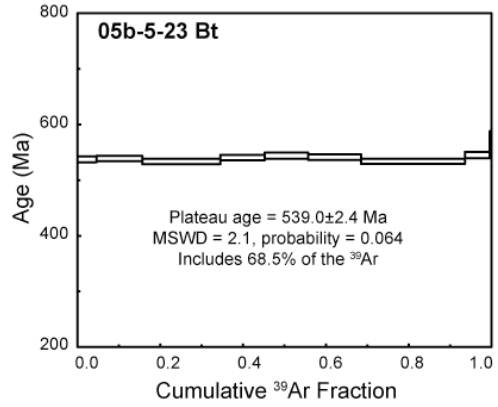
05b-5-23 Bt
Plateau age = 539.0±2.4 Ma
MSWD = 2.1, probability = 0.064
Includes 68.5% of the $^{39}$Ar
Age (Ma)
Cumulative $^{39}$Ar Fraction

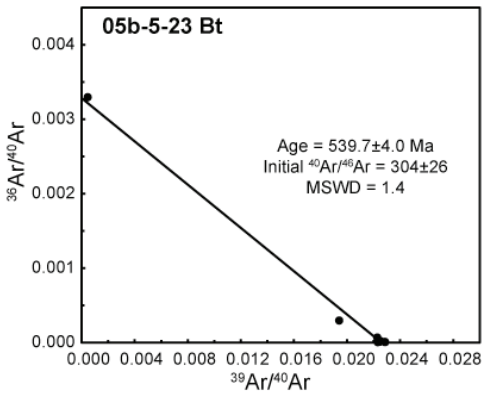
05b-5-23 Bt
Age = 539.7±4.0 Ma
Initial $^{40}$Ar/$^{46}$Ar = 304±26
MSWD = 1.4
$^{36}$Ar/$^{40}$Ar
$^{39}$Ar/$^{40}$Ar

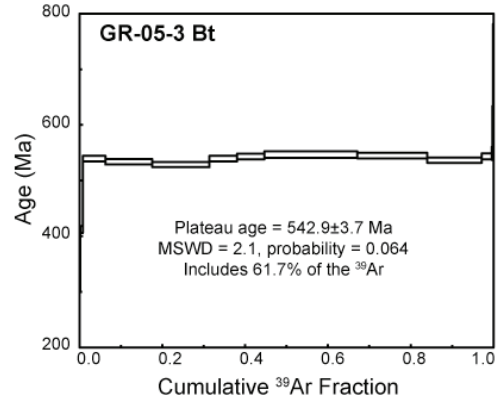
GR-05-3 Bt
Plateau age = 542.9±3.7 Ma
MSWD = 2.1, probability = 0.064
Includes 61.7% of the $^{39}$Ar
Age (Ma)
Cumulative $^{39}$Ar Fraction

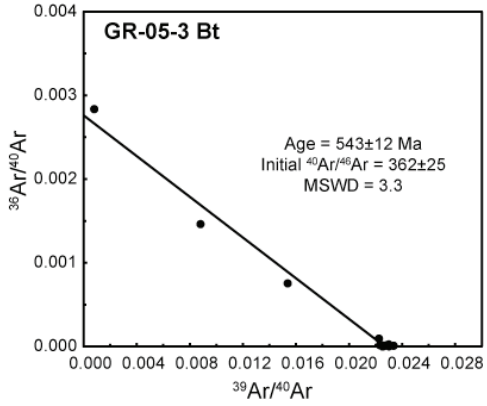
GR-05-3 Bt
Age = 543±12 Ma
Initial $^{40}$Ar/$^{46}$Ar = 362±25
MSWD = 3.3
$^{36}$Ar/$^{40}$Ar
$^{39}$Ar/$^{40}$Ar

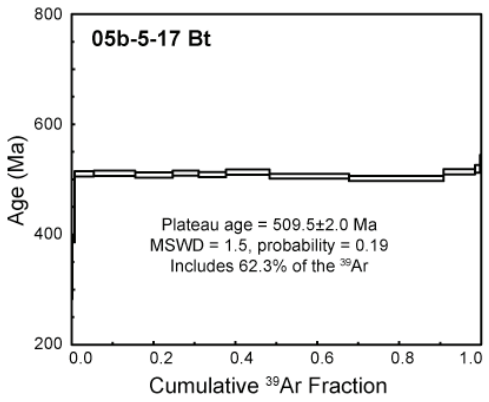
05b-5-17 Bt
Plateau age = 509.5±2.0 Ma
MSWD = 1.5, probability = 0.19
Includes 62.3% of the 39Ar
Age (Ma)
Cumulative 39Ar Fraction

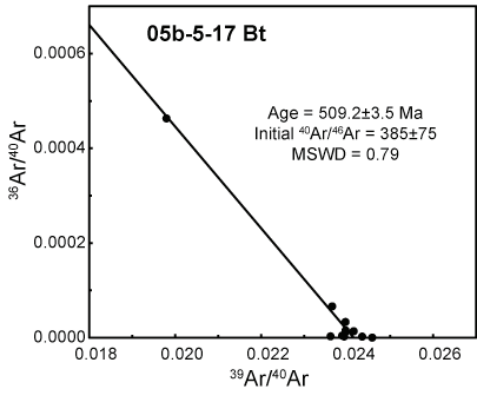
05b-5-17 Bt
Age = 509.2±3.5 Ma
Initial 40Ar/36Ar = 385±75
MSWD = 0.79
36Ar/40Ar
39Ar/40Ar

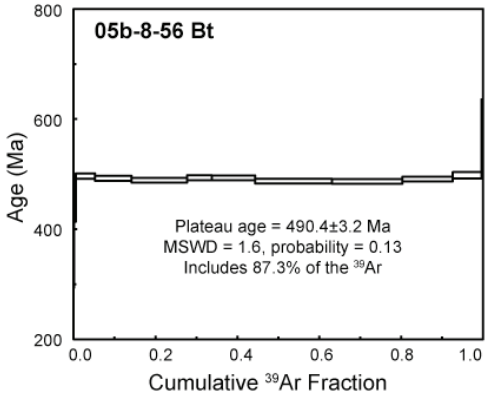
05b-8-56 Bt
Plateau age = 490.4±3.2 Ma
MSWD = 1.6, probability = 0.13
Includes 87.3% of the 39Ar
Age (Ma)
Cumulative 39Ar Fraction

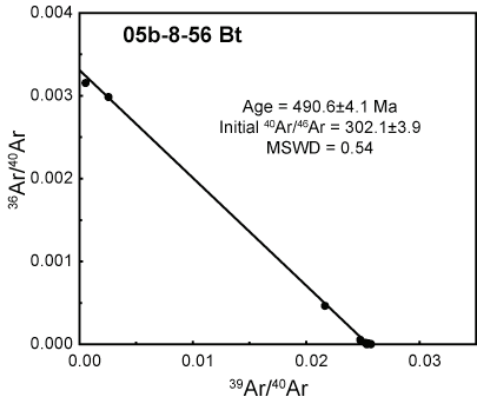
05b-8-56 Bt
Age = 490.6±4.1 Ma
Initial 40Ar/36Ar = 302.1±3.9
MSWD = 0.54
36Ar/40Ar
39Ar/40Ar

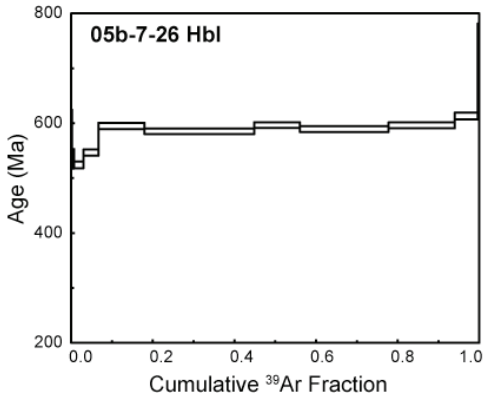
05b-7-26 Hbl
Age (Ma)
Cumulative 39Ar Fraction

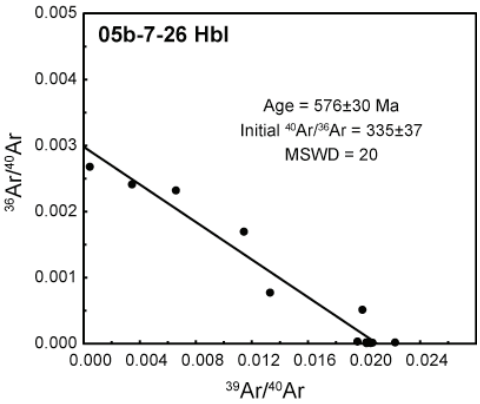
05b-7-26 Hbl
Age = 576±30 Ma
Initial 40Ar/36Ar = 335±37
MSWD = 20
36Ar/40Ar
39Ar/40Ar

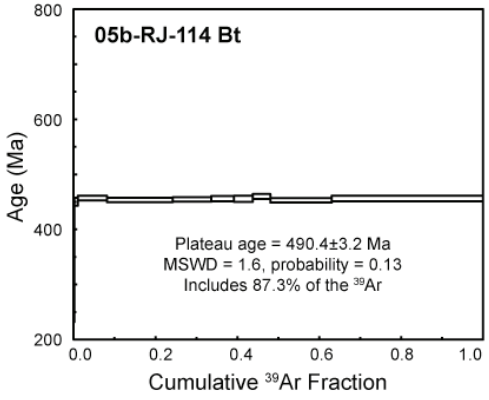
05b-RJ-114 Bt
Plateau age = 490.4±3.2 Ma
MSWD = 1.6, probability = 0.13
Includes 87.3% of the 39Ar
Age (Ma)
Cumulative 39Ar Fraction

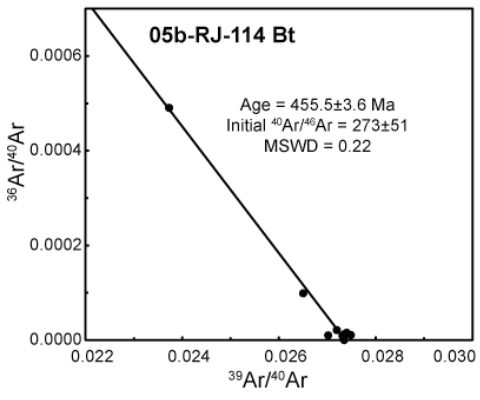
05b-RJ-114 Bt
Age = 455.5±3.6 Ma
Initial 40Ar/36Ar = 273±51
MSWD = 0.22
36Ar/40Ar
39Ar/40Ar

The biotite $^{40}Ar/^{39}Ar$ age spectrum for sample 05b-6-30 (Fig. 4-5) yields a plateau age of 567.2±6.2 Ma (MSWD=1.5; p=0.13) that comprises 94.7% of the $^{39}Ar$. The inverse isochron yields an age of 568.9±6.1 Ma, with initial $^{40}Ar/^{36}Ar$ of 360±53. The initial $^{40}Ar/^{36}Ar$ ratio indicates that there may be an excess argon component in this sample, however the plateau ages and isochron ages are statistically identical. I consider this age to be geologically meaningful and to date cooling of this sample through ~300˚C.

The biotite $^{40}Ar/^{39}Ar$ age spectrum for sample 04-6-11 (Fig. 4-5) yields a plateau age of 587.8±2.9 Ma (MSWD=1.4; p=0.24) that comprises 66.1% of the $^{39}Ar$. The inverse isochron yields an age of 589±11 Ma, with initial $^{40}Ar/^{36}Ar$ of 310±76. The near-atmospheric initial $^{40}Ar/^{36}Ar$ ratio suggests that there is no significant excess argon reservoir in this sample. I consider this age to be geologically meaningful and to date cooling of this sample through ~300˚C.

The biotite $^{40}Ar/^{39}Ar$ age spectrum for sample 05b-6-103 (Fig. 4-5) yields a plateau age of 583.5±7.4 Ma (MSWD=1.5; p=0.13) that comprises 94.3% of the $^{39}Ar$. The inverse isochron yields an age of 583.2±7.1 Ma, with initial $^{40}Ar/^{36}Ar$ of 325±14. The near-atmospheric initial $^{40}Ar/^{36}Ar$ ratio suggests that there is no significant excess argon reservoir in this sample. I consider this age to be geologically meaningful and to date cooling of this sample through ~300˚C.

The biotite $^{40}Ar/^{39}Ar$ age spectrum for sample 05b-6-31b (Fig. 4-5) yields a plateau age of 571.8±6.3 Ma (MSWD=1.5; p=0.18) that comprises 97.5% of the $^{39}Ar$. The inverse isochron yields an age of 572.5±6.6 Ma, with initial $^{40}Ar/^{36}Ar$ of 300.5±7.0. The near-atmospheric initial $^{40}Ar/^{36}Ar$ ratio suggests that there is no

significant excess argon reservoir in this sample. I consider this age to be geologically meaningful and to date cooling of this sample through ~300˚C.

The biotite $^{40}Ar/^{39}Ar$ age spectrum for sample 05b-6-33 (Fig. 4-5) does not yield a plateau age because there are not 3 continuous steps containing at least 60% of the $^{39}Ar$ that are within 95% confidence of each other. An average of steps containing 98.4% of the $^{39}Ar$ yields an age of 546±11 Ma. The inverse isochron yields an age of 545.5±6.8 Ma, with initial $^{40}Ar/^{36}Ar$ of 305.1±6.9. The near-atmospheric initial $^{40}Ar/^{36}Ar$ ratio suggests that there is no significant excess argon reservoir in this sample. I consider this age to be geologically meaningful and to date cooling of this sample through ~300˚C.

***Carvalhos Klippe***

The hornblende $^{40}Ar/^{39}Ar$ age spectrum for sample 05b-10-74 (Fig. 4-5) exhibits a saddle-shaped pattern typical of hornblende with excess argon. The youngest date obtained of 529.0±5.0 Ma was for the 1075˚C heating step. 42.2% of the $^{39}Ar$ was released at this step, which could have hidden any younger dates present in this portion of the spectrum. The inverse isochron yields an age of 564±92 Ma, with initial $^{40}Ar/^{36}Ar$ of 386±250. The large uncertainty on the initial $^{40}Ar/^{36}Ar$ ratio makes it difficult to interpret the excess argon component in this sample. As such, it is not possible to interpret the meaning of the youngest age in the spectrum. The large uncertainty on the isochron age limits the utility of this age.

The biotite $^{40}Ar/^{39}Ar$ age spectrum for sample 05b-10-95 (Fig. 4-5) does not yield a plateau age because there are not 3 continuous steps containing at least 60% of the $^{39}Ar$ that are within 95% confidence of each other. An average of steps

containing 95.8% of the $^{39}$Ar yields an age of 559±11 Ma. The inverse isochron yields an age of 560.7±3.9 Ma, with initial $^{40}$Ar/$^{36}$Ar of 292±22. The near-atmospheric initial $^{40}$Ar/$^{36}$Ar ratio suggests that there is no significant excess argon reservoir in this sample. I consider this age to be geologically meaningful and to date cooling of this sample through ~300˚C.

***Carmo da Cachoeira Nappe***

The biotite $^{40}$Ar/$^{39}$Ar age spectrum for sample 05b-5-23 (Fig. 4-5) yields a plateau age of 539.0±2.4 Ma (MSWD=2.1; p=0.064) that comprises 68.5% of the $^{39}$Ar. The inverse isochron yields an age of 539.7±4.0 Ma, with initial $^{40}$Ar/$^{36}$Ar of 304±26. The near-atmospheric initial $^{40}$Ar/$^{36}$Ar ratio suggests that there is no significant excess argon reservoir in this sample. I consider this age to be geologically meaningful and to date cooling of this sample through ~300˚C.

The biotite $^{40}$Ar/$^{39}$Ar age spectrum for sample GR-05-3 (Fig. 4-5) yields a plateau age of 542.9±3.7 Ma (MSWD=2.1; p=0.064) that comprises 61.7% of the $^{39}$Ar. The inverse isochron yields an age of 543±12 Ma, with initial $^{40}$Ar/$^{36}$Ar of 362±25. The initial $^{40}$Ar/$^{36}$Ar ratio indicates that there may be an excess argon component in this sample, however the plateau ages and isochron ages are statistically identical. I consider this age to be geologically meaningful and to date cooling of this sample through ~300˚C.

The biotite $^{40}$Ar/$^{39}$Ar age spectrum for sample 05b-5-17 (Fig. 4-5) yields a plateau age of 509.5±2.0 Ma (MSWD=1.5; p=0.19) that comprises 62.3% of the $^{39}$Ar. The inverse isochron yields an age of 509.2±3.5 Ma, with initial $^{40}$Ar/$^{36}$Ar of 385±75. The initial $^{40}$Ar/$^{36}$Ar ratio indicates that there may be an excess argon component in

this sample, however the plateau ages and isochron ages are statistically identical. I consider this age to be geologically meaningful and to date cooling of this sample through ~300˚C.

***Andrelândia Nappe***

The biotite $^{40}Ar/^{39}Ar$ age spectrum for sample 05b-8-56 (Fig. 4-5) yields a plateau age of 490.4±3.2 Ma (MSWD=1.6; p=0.13) that comprises 87.3% of the $^{39}Ar$. The inverse isochron yields an age of 490.6±4.1 Ma, with initial $^{40}Ar/^{36}Ar$ of 302.1±3.9. The near-atmospheric initial $^{40}Ar/^{36}Ar$ ratio suggests that there is no significant excess argon reservoir in this sample. I consider this age to be geologically meaningful and to date cooling of this sample through ~300˚C.

***Socorro–Guaxupé Nappe***

The hornblende $^{40}Ar/^{39}Ar$ age spectrum for sample 05b-7-26 (Fig. 4-5) from the Socorro–Guaxupé Nappe does not yield a plateau age because there are not 3 continuous steps containing at least 60% of the $^{39}Ar$ that are within 95% confidence of each other. An average of steps containing 87.3% of the $^{39}Ar$ yields an age of 592±10 Ma. The inverse isochron yields an age of 576±30 Ma, with initial $^{40}Ar/^{36}Ar$ of 335±37. The near-atmospheric initial $^{40}Ar/^{36}Ar$ ratio suggests that there is no significant excess argon reservoir in this sample. I consider this age to be geologically meaningful and to date cooling of this sample through ~500˚C. However, the large uncertainty on this age limits its usefulness.

### *Ribeira Belt*

The biotite $^{40}Ar/^{39}Ar$ age spectrum for sample 05b-RJ-114 (Fig. 4-5) yields a plateau age of 455.2±1.6 Ma (MSWD=1.15; p=0.32) that comprises 99.8% of the $^{39}Ar$. The inverse isochron yields an age of 455.5±3.6 Ma, with initial $^{40}Ar/^{36}Ar$ of 273±51. The near-atmospheric initial $^{40}Ar/^{36}Ar$ ratio suggests that there is no significant excess argon reservoir in this sample. I consider this age to be geologically meaningful and to date cooling of this sample through ~300˚C.

## *Discussion*

### *Interpretation of the $^{40}Ar/^{39}Ar$ ages and average cooling rates*

The Andrelândia Nappe Complex in the southern sector of the Southern Brasília Belt comprises a passive margin sedimentary sequence metamorphosed during subduction-to-collision orogenesis. The stack of passive margin-derived nappes exhibits a range of metamorphic grades, with the highest-pressure, highest-grade nappes at the top of the stack. I suggest that individual nappes were taken to progressively shallower depths in the subduction system prior to detachment from the downgoing slab and accretion to the hanging-wall accretionary complex, with the early nappes being subjected to higher *P-T* conditions than the later nappes. All chronologic data are summarized in Fig. 4-6.

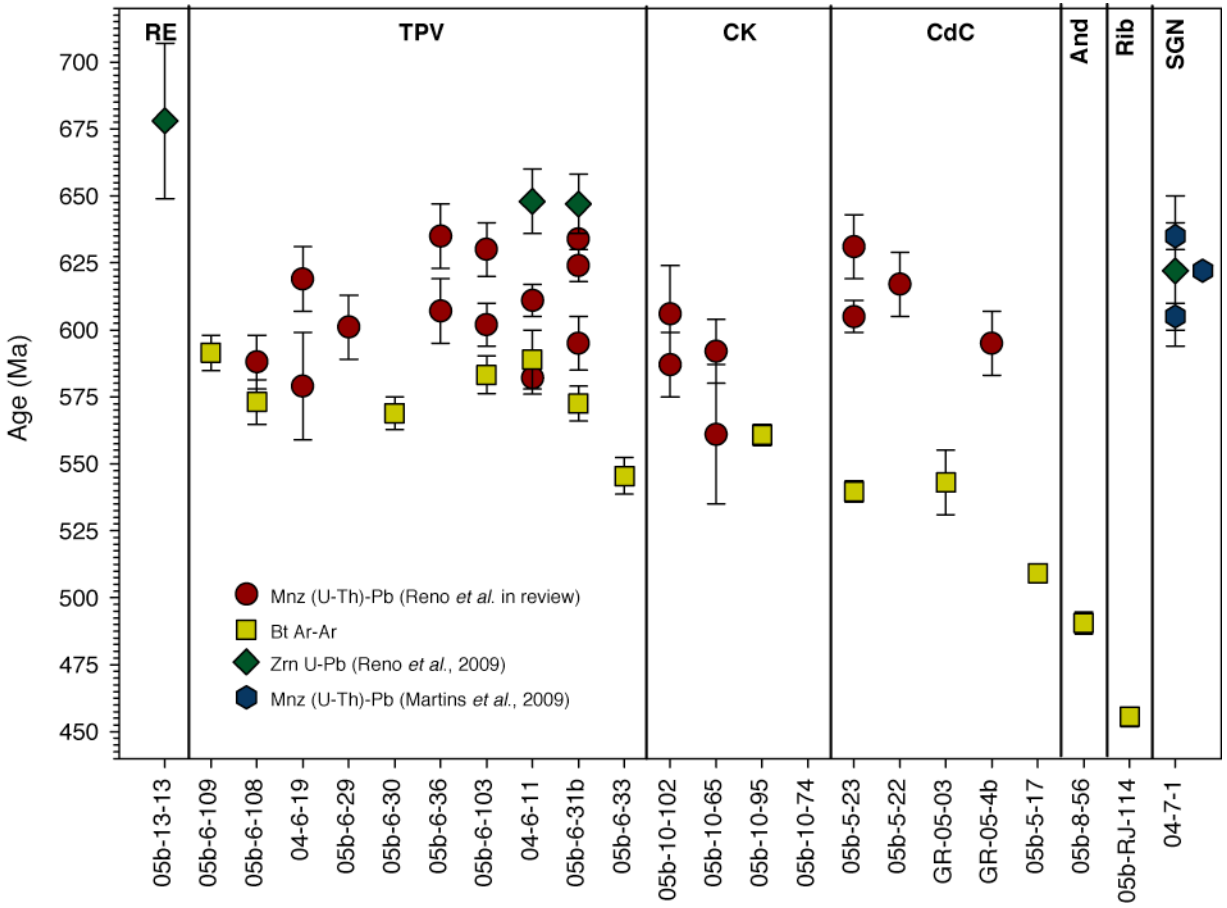


**Figure 4-6.** Summary of all geochronologic data from this study from Chapters 2 and 3. RE – retrograded eclogite unit; TPV – Três Pontas–Varginha Nappe; CK – Carvalhos Klippe; CdC – Carmo da Cachoeira Nappe; And – Andrelândia Nappe; Rib – Ribeira Belt sample; SGN – Socorro–Guaxupé Nappe. Diamonds are $^{206}Pb/^{238}U$ zircon ages from Chapter 2, circles are (U-Th)-Pb monazite ages from Chapter 3, hexagons are (U-Th)-Pb monazite ages from Martins *et al*. (2009) and squares are $^{40}Ar/^{39}Ar$ data from this study.

The high-pressure granulite facies Três Pontas–Varginha Nappe close to the top of the nappe stack lies underneath the Socorro–Guaxupé Nappe, which represents part of the former Socorro–Guaxupé Arc. The Três Pontas–Varginha Nappe yields the oldest age for growth of metamorphic zircon among the passive margin-derived nappes in the Andrelândia Nappe Complex. The Três Pontas–Varginha Nappe is interpreted to have cooled to ~800˚C at a pressure of ~1.5 GPa by *ca.* 648–647 Ma (Chapter 2). Biotite in sample 05b-6-31b from near the top of this nappe grew during this initial cooling phase, at temperatures greater than 800˚C. The U-Pb zircon age of 648±12 Ma (Chapter 2) provides a minimum constraint on the timing of biotite growth in this sample. Biotite in sample 04-6-11 from the middle of the Três Pontas–Varginha Nappe was stable at peak metamorphic temperatures, and the U-Pb zircon age of 647±11 (Chapter 2) Ma provides a minimum constraint on the timing of biotite growth in this sample. Given the association of biotite in the foliation with sillimanite, I infer that biotite likely recrystallized during high temperature decompression due to the initial state of exhumation.

$^{40}Ar/^{39}Ar$ biotite inverse isochron ages from the Três Pontas–Varginha Nappe are dominantly between 591.4±6.6 and 568.9±6.1 Ma. One sample is an outlier with an age of 545.5±6.8 Ma, but the spectrum does not meet the criteria for defining a plateau age. The ages do not exhibit any geographic trends, nor do they exhibit a trend with structural level within the nappe. I interpret the Três Pontas–Varginha Nappe to have cooled below ~300˚C between *ca.* 591 and 569 Ma. This spread has implications for the average cooling rate of the Três Pontas–Varginha Nappe. Considering the Rb-Sr multimineral–whole rock isochron age of 590.0±3.7 Ma

(Chapter 2), which is interpreted to record cooling through ~700˚C, calculated cooling rates vary from near instantaneous to ~20 ˚C $Ma^{-1}$. In either case, final cooling of the Três Pontas–Varginha Nappe occurred at a faster rate than initial cooling (Fig. 4-7).

The biotite $^{40}Ar/^{39}Ar$ inverse isochron age from the Carvalhos Klippe is 560.7±3.9 Ma. The isochron age is the same within uncertainty as a monazite (U-Th)-Pb age of 561±26 Ma reported in Chapter 3. The monazite age was interpreted to record a fluid flow event inferred to have been related to the Ribeira Orogeny, and I suggest the biotite $^{40}Ar/^{39}Ar$ isochron age records the same event. The hornblende $^{40}Ar/^{39}Ar$ data for sample 05b-10-74 from the Carvalhos Klippe yielded a saddle-shaped spectrum and an inverse isochron age of 564±92 Ma that is geologically meaningless.

The Carmo da Cachoeira Nappe is structurally beneath the Três Pontas–Varginha Nappe in the nappe stack. This nappe is interpreted to represent the second package of metasedimentary rocks to be detached from the downgoing slab during subduction related metamorphism, following detachment of the Três Pontas–Varginha Nappe. In the Carmo da Cachoeira Nappe, biotite is interpreted to have been present in the peak assemblage at pressures between 1.3 GPa and 1.75 GPa and temperatures between 630˚C and 840˚C. The monazite (U-Th)-Pb age of 631±12 Ma reported in Chapter 3 for sample 05b-5-23 is interpreted to record timing of biotite formation. The $^{40}Ar/^{39}Ar$ biotite inverse isochron age from the same sample is 539.7±4.0 Ma, and the isochron age is 543±12 Ma for sample GR-05-3 from the same

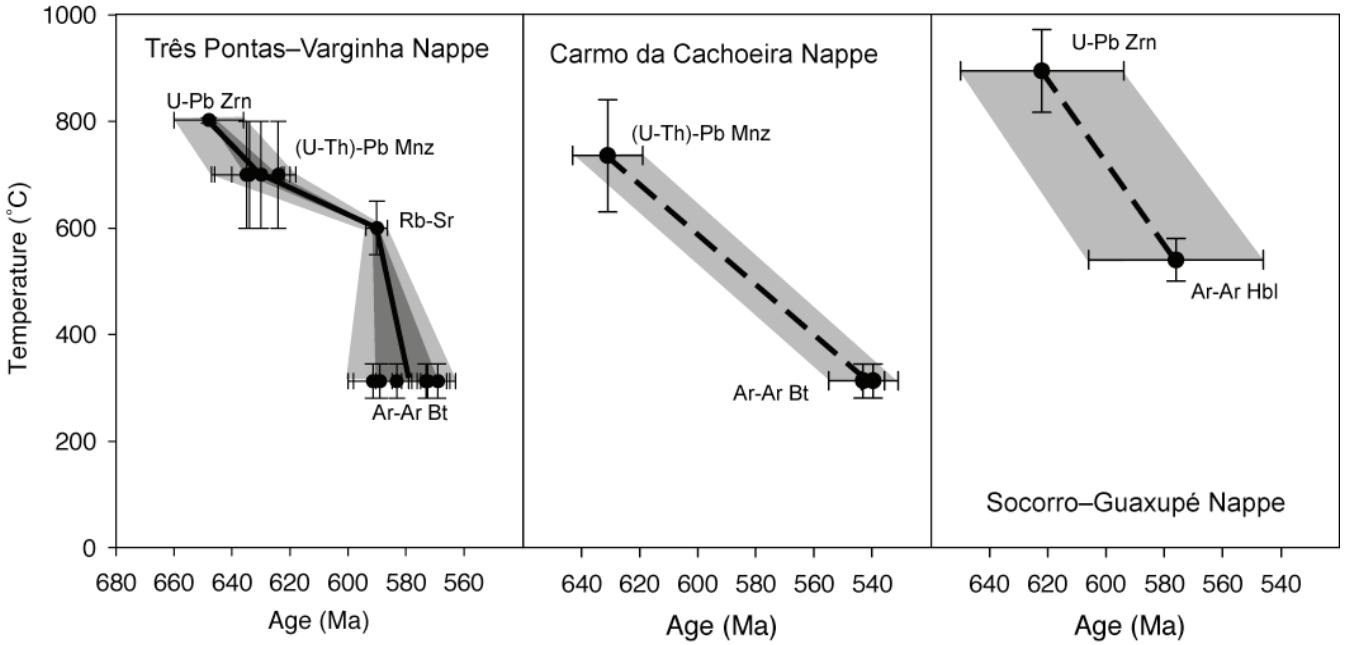


**Figure 4-7.** Temperature-time paths for the Três Pontas–Varginha, Carmo da Cachoeira and Socorro–Guaxupé Nappes based on U-Pb zircon, (U-Th)-Pb monazite, Rb-Sr isochron and $^{40}Ar/^{39}Ar$ biotite and hornblende data. The solid line reflects the T-t path, and the shaded region takes into account the uncertainty on the age.

outcrop. These data yield an average cooling rate of 3–7 ˚C $Ma^{-1}$ for the Carmo da Cachoeira Nappe (Fig. 4-7). Without additional data I cannot determine whether a change in cooling rate at *ca.* 590 Ma occurred during exhumation of this nappe, similar to that observed in the overlying Três Pontas–Varginha Nappe.

The accretionary magmatic arc is partly represented by the Socorro–Guaxupé Nappe at the top of the nappe stack. The hornblende $^{40}Ar/^{39}Ar$ data for sample 05b-7-26 from the Socorro–Guaxupé Nappe has an age spectrum that does not meet the criteria for a plateau age, and the inverse isochron indicates a high degree of scatter in the data resulting in an imprecise age of 576±30 Ma.

***Tectonic Interpretation***

The Brasília Orogeny involved subduction of the passive margin on the western side (present coordinates) of the São Francisco Craton under the Soccoro–Guaxupe Arc to the west closing the Brazilide Ocean. Passive margin-derived sediment was being subducted at this margin as early as 678±29 Ma, when the Três Pontas–Varginha nappe is inferred to have been detached from the downgoing slab (Chapter 2), based on zircon ages in eclogite blocks from along the tectonic contact with the underlying nappe. The Carmo da Cachoeira Nappe was thrust under the Três Pontas–Varginha Nappe during continued subduction.

The Três Pontas–Varginha nappe reached high-*T* conditions >900˚C due to radiogenic heating, and is interpreted to have cooled through ~800˚C by *ca.* 648 Ma, based on zircon crytallization ages in leucosomes. Peak-*T* conditions recorded in the Carmo da Cachoeira Nappe were close to those recorded in the Três Pontas–Varginha nappe, and the maximum recorded pressures are similar, consistent with a period of

incubation as temperatures rose prior to the main phase of exhumation. The oldest monazite ages in the Três Pontas–Varginha Nappe of 635–624 Ma relate to monazite growth at temperatures > 600˚C but < 800˚C and pressure of ~1.5 GPa, and in the Carmo da Cachoeira Nappe, a monazite age of 631±12 Ma relates to monazite growth at temperatures < 800˚C and pressure >1.3 GPa. These data suggest that the two nappes were together by 635–624 Ma at depths close to peak-*P*. The Rb-Sr multimineral–whole rock isochron age of 590.0±3.7 Ma from the Três Pontas–Varginha Nappe records initial high temperature decompression at ~700˚C, which suggests an initial slow average cooling rate, and both nappes likely cooled slowly at depth.

The Socorro–Guaxupé Arc on the hanging-wall plate above the subduction system may have been active as early as *ca.* 799 Ma (Chapter 2). The lower part of this arc was emplaced over the top of the nappe stack during terminal arc collision near the end of the orogenic cycle. A U-Pb zircon age is interpreted to record the age of close-to-peak metamorphism around 622±28 Ma (Chapter 2), and a (U-Th)-Pb monazite age of 609±7 Ma (Martins *et al.* 2009) in interpreted to record growth of monazite after emplacement.

A second orogenic event affected the passive margin on the eastern side (present coordinates) of the São Francisco Craton during Neoproterozoic to Cambrian time when the São Francisco plate subducted beneath the Serra do Mar microplate, forming the Rio Negro magmatic arc between *ca.* 635 Ma and 600 Ma (Fig. 4-8).

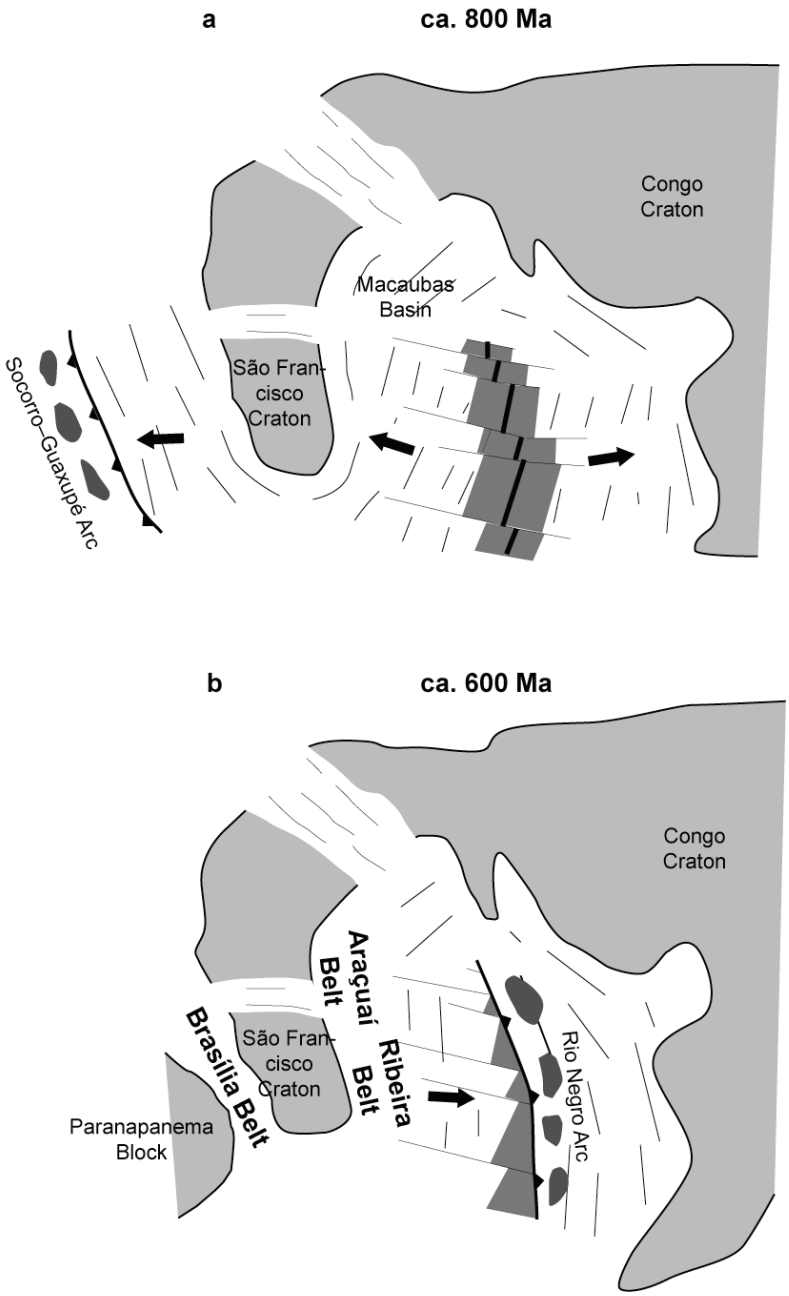


**Figure 4-8.** Generalized map of tectonic activity during the Cryogenian–Ediacaran (a) opening and (b) closing of the Macaubas basin that led to final suturing of West Godnwana along the Arçuaí and Ribeira Belts in Brazil. Subduction of the São Francisco Plate to the east may have generated extension in the Brasília Belt to the west of the São Francisco Craton. After Alkmim *et al*. (2006).

This magmatic arc collided with the São Francisco Craton at *ca.* 595–550 Ma (Machado *et al.* 1996; Valeriano *et al.* 2004), leading to the formation of the Ribeira Belt as the arc accreted to the eastern margin of the craton. As the São Francisco plate was subducted towards the east (present coordinates), it is likely that a component of regional extension was imposed on the Brasília Belt on the western side of the craton.

In the western portion of the Andrelândia Nappe Complex, the Socorro–Guaxupé Nappe cooled to ~500˚C by 576±30 Ma. The Três Pontas–Varginha Nappe immediately underneath the Socorro–Guaxupé Nappe cooled through ~300˚C in the interval 591–569 Ma. The increased rate of cooling observed in this nappe is interpreted to record tectonically driven exhumation due to the switch to regional extension caused by eastward subduction of the São Francisco Plate during the Ribeira Orogeny. The younger $^{40}Ar/^{39}Ar$ biotite age of 545.5±6.8 seen at the structural top of the Três Pontas–Varginha Nappe may record the effect of the hotter Socorro–Guaxupé Nappe above. Alternatively, this young age may be due to fluid flow along the contact with the Socorro–Guaxupé Nappe. The Carmo da Cachoeira Nappe, which underlies the Três Pontas–Varginha Nappe, cooled through ~300˚C at *ca.* 540 Ma. Fluid flow along the contact with the Três Pontas–Varginha Nappe may have led to late resetting of the $^{40}Ar/^{39}Ar$ age (509.2±3.5 Ma) for sample 05b-5-17 taken from near the top of the nappe.

The Andrelândia Nappe, in the southeastern portion of the Nappe Complex, was thrust directly on top of the São Francisco Craton during exhumation. A south-southeast plunging lineation is present in this nappe that is interpreted to relate to tectonothermal overprinting by the Ribeira Orogeny; this lineation is not present in

the western portion of the Nappe Complex. The thermal overprint related to the Ribeira Orogeny in the southernmost portion of the Andrelândia Nappe Complex was at high enough temperatures to grow sillimanite. The $^{40}Ar/^{39}Ar$ age of 490.6±4.1 Ma reported in this study for the Andrelândia Nappe is from a sample from close to the structural top of the nappe. The $^{40}Ar/^{39}Ar$ biotite ages from Campos Neto *et al.* (2004) show a increase from *ca.* 490 Ma close to the structural top of the nappe to *ca.* 540 Ma close to the base of the nappe. These data suggest that the Andrelândia Nappe was cooled from the bottom up, perhaps due to the emplacement of the cold São Francisco Craton underneath it. Alternatively, the younger ages may be due to fluid flow along the contact with the overlying Carvalhos Klippe as a far-field effect of the Ribeira Orogeny. The age of 490.6±4.1 Ma from close to the top of the Andrelândia Nappe suggests that this nappe was buried far longer than the equivalent Carmo da Cachoeira Nappe further to the west, possibly due to the overprinting Ribeira Orogeny.

Further southeast, high-pressure granulites of the Carvalhos Klippe show a sillimanite-grade metamorphic overprint due to the earliest phase of the Ribeira Orogeny in which the Rio Negro Arc was emplaced onto the passive margin on the eastern side of the São Francisco Craton. Biotite from this nappe yields a $^{40}Ar/^{39}Ar$ age of 560.7±3.9 Ma that may relate to exhumation after this early phase of the Ribera Orogeny. Biotite from the high-grade migmatite from the core of the Ribera Belt yields a $^{40}Ar/^{39}Ar$ age of 455.5±3.6 Ma. When combined with a U-Pb zircon age of *ca.* 553 Ma from Schmitt *et al*. (2004) this suggests a slow average cooling rate of ~5–6 ˚C $Ma^{-1}$.

*Conclusion*

I reported the results of an integrated petrologic and thermochronologic study of the Andrelândia Nappe Complex in the southern sector of the Southern Brasília Belt. The high-pressure granulite facies Três Pontas–Varginha Nappe was the first of the passive margin-derived nappes to be exhumed through ~300˚C at 591–569 Ma, followed by the Carmo da Cachoeira Nappe at *ca.* 540 Ma. Initially, the Três Pontas–Varginha Nappe cooled slowly from ~800˚C at *ca.* 648 Ma to ~700˚C at *ca.* 590 Ma. The cooling rate increased dramatically to greater than ~20 ˚C $Ma^{-1}$ after cooling below ~700˚C due to tectonically driven exhumation caused by regional extension as a far-field effect of the Ribeira Orogeny. The Carmo da Cachoeira Nappe cooled at an average rate of 3–7 ˚C $Ma^{-1}$, however it is unclear if this nappe experienced a change in cooling rate similar to the Três Pontas–Varginha Nappe. The Andrelândia Nappe was separated from the Carmo da Cachoeira Nappe during orogenic loading caused by the Ribeira Orogeny. This nappe was exhumed after the Carmo da Cachoeira Nappe, but records cooling from the bottom up due to emplacement on top of the cold São Francisco Craton.

# Chapter 5: Synthesis

I began my study of the Southern Brasília Belt shortly after my arrival in Maryland in 2003. At the time, the structural context of the nappes in the Southern Brasília Belt had already been well established due to the efforts of groups at the Federal University of Rio de Janeiro led by Rudolph Trouw, and at the University of São Paulo led by Mario Campos Neto. These two groups, though not agreeing on every detail, had established that the Andrelândia Nappe Complex comprises a stack of passive margin-derived nappes that had been subjected to metamorphic conditions ranging from greenschist facies in the nappes at the base of the nappe stack to high-pressure granulite facies in the Três Pontas–Varginha and Carmo da Cachoeira Nappes, and their lateral equivalents, at the top of the stack (Fig. 2-1). The lower part of the magmatic arc from the hanging wall, the Socorro–Guaxupé Nappe, formed the uppermost nappe lying above the passive margin-derived nappes. The biggest hindrance to understanding the emplacement and exhumation of the nappes was the lack of reliable age information and the limited knowledge of the *P-T* evolution of the nappes.

The focus of my Ph.D. dissertation research has been to address these important gaps in knowledge about the Andrelândia Nappe Complex by examining the timing, duration and degree of metamorphism in the uppermost high-pressure granulite facies nappes. In addressing these topics, I engaged in an integrated

petrologic and chronologic study of the uppermost high-pressure granulite nappes in the Nappe Complex.

*Contributions to Understanding the Geologic History of the Southern Brasília Belt*

The Neoproterozoic–Cambrian Brasília Orogeny records closure of the Brazilide Ocean and suturing of the western margin of the São Francisco Craton with several magmatic arcs and the Paranapanema Block in the south and the Amazon Craton in the north (Fig. 2-1; Fig. 3-6; Fig. 4-1). The timing of the beginning of subduction of the São Francisco Plate to the west, which led to the formation of magmatic arcs including the Socorro–Guaxupé Arc, is unknown. However, two individual $^{206}Pb/^{238}U$ zircon dates of *ca.* 799 Ma from the Socorro–Guaxupé Nappe (Table 2-4), representing the lower part of the Socorro–Guaxupé Arc, indicate that it may have been active at this time.

Zircon from blocks of retrograded eclogite that occur along the contact beneath the uppermost passive margin-derived high-pressure granulite nappe records a $^{206}Pb/^{238}U$ age of 678±29 Ma (Fig. 2-8). This age is a minimum for the detachment of the overlying nappe from the subducting passive margin, and provides the earliest record of high-pressure metamorphism during the Brasília Orogeny. This indicates that the Brasília Orogeny began up to *ca.* 50 Ma earlier than the previously inferred estimate of 630 Ma (Campos Neto & Caby 1999). This age is statistically older than U-Pb zircon ages of 649–634 Ma (Table 2-7) retrieved from the Anápolis–Itauçu Complex (Baldwin & Brown 2008), indicating that suturing of the Southern Brasília Belt probably began in the south and progressed northward.

Microstructural observations in conjunction with equilibrium phase diagrams constructed for samples from the Três Pontas–Varginha Nappe indicate that it achieved peak-*T* conditions >850–900˚C at pressures of ~1.5–1.6 GPa and experienced close-to-isobaric cooling to temperatures below the solidus at ~800˚C (Fig. 2-4). Zircon ages of *ca.* 648–647 (Fig. 2-8) Ma from this nappe record zircon growth at ~800˚C (Fig. 2-7) during liberation of Zr due to the breakdown of ilmenite.

In the Três Pontas–Varginha Nappe, garnet-hosted monazite yields (U-Th)-Pb ages of 634–624 (Fig. 3-9) that are interpreted to record the timing of a fluid related dissolution–reprecipitation event in the nappe at high-*T,* but post-peak-*T*. Monazite in the Carmo da Cachoeira Nappe yields ages of 631±12 Ma (Fig. 3-9) interpreted to record just-post-peak-*P* biotite growth at temperatures > 810˚C at pressures > 1.3 GPa (Fig. 4-4). This indicates that the Carmo da Cachoeira Nappe had been subducted to approximately the same depth as the Três Pontas–Varginha Nappe by this time. A Rb-Sr age of 590.0±3.7 (Fig. 2-9) Ma from the Três Pontas–Varginha Nappe indicates initial slow average cooling (Fig. 4-7), interpreted to record cooling at depth in the accretionary complex.

A $^{206}Pb/^{238}U$ zircon age of 622±28 Ma (Fig. 2-8) from the Socorro–Guaxupé Nappe is interpreted to record the age of close-to-peak metamorphism. $D_{REE}$ and Ti-in-zircon data are consistent with crystallization of zircon from anatectic melt cooling from high-*T* conditions down to the solidus (Fig. 2-6; Fig. 2-7; Fig. 2-4). Martins *et al*. (2009) show that post-emplacement monazite growth in the Scorro–Guaxupé Nappe occurred at *ca.* 609 Ma. Monazite (U-Th)-Pb ages of 607–595 Ma in the Três

Pontas–Varginha Nappe, are interpreted to record the effects of fluid related dissolution–reprecipitation (Fig. 3-9).

A second orogeny, the Ribiera Orogeny, affected the eastern margin of São Francisco Craton during the late Neoproterozoic and early Cambrian (Fig. 4-2; Fig. 4-8). The eastern margin of the São Francisco Craton is inferred to have been subducted beneath the Serra do Mar microplate during the interval 635–600 Ma, which led to the formation of the Rio Negro magmatic arc. This arc collided with the São Francisco Craton at *ca.* 595–550 Ma (Heilbron & Machado 2003; Schmitt *et al.* 2008). The eastward subduction of the eastern margin of the São Francisco Craton before collision with the Rio Negro Arc is inferred to have imposed a component of regional extension on the Brasília Belt along the western margin of the São Francisco craton.

Tectonically driven exhumation of the nappes of the Andrelândia Nappe Complex was caused by the regional extension due to the Ribiera Orogeny. $^{40}Ar/^{39}Ar$ biotite ages record cooling of the Três Pontas Varginha Nappe below ~300 ˚C between 591–569 Ma (Fig. 4-5). A switch from initially slow cooling between *ca.* 648 Ma and *ca.* 590 Ma to more rapid cooling rates > 20 ˚C $Ma^{-1}$ (Fig. 4-7) after *ca.* 590 Ma is interpreted to record the initiation of exhumation.

The Ribiera Orogeny imposed a thermal overprint on the southern part of the Andrelândia Nappe Complex; the macroscopic petrologic expression of this event is an overprinting of sillimanite on this part of the Complex (Fig. 4-2). A group of (U-Th)-Pb monazite ages between 588 and 579 Ma in the Três Pontas–Varginha Nappe (Fig. 3-9) may record a cryptic metamorphic overprint related to the Ribeira Orogeny.

This group of ages is statistically identical to $^{40}Ar/^{39}Ar$ biotite cooling ages from the same nappe and likely records low-*T* monazite growth during exhumation or cooling, possibly due to fluid flow caused by orogenic loading brought on by the Ribiera Orogen to the southeast.

$^{40}Ar/^{39}Ar$ ages from the Andrelândia Nappe Complex indicate different cooling and exhumation histories for the western and southeastern parts of the Complex. A $^{40}Ar/^{39}Ar$ age hornblende from the Socorro–Guaxupé Nappe in the western part of the Complex records cooling below ~500˚C by 576±30 Ma (Fig. 4-5). The underlying Três Pontas–Varginha Nappe was the first of the passive margin derived nappes to be exhumed, cooling below ~300˚C at 591–569 Ma (Fig. 4-5). A younger age of 545.5±6.8 Ma at the structural top of the Três Pontas–Varginha Nappe may indicate slower cooling at the top of the nappe due to the effects of the overlying hotter Socorro–Guaxupé Nappe. $^{40}Ar/^{39}Ar$ biotite ages from the Carmo da Cachoeira Nappe, immediately beneath the Três Pontas–Varginha Nappe, indicate that it cooled below ~300˚C at *ca.* 540 Ma (Fig. 4-5).

The southeastern portion of the Andrelândia Nappe Complex records a south-southeast plunging lineation related to the tectonothermal overprint caused by the Ribeira Orogeny. This lineation is not present in the western portion of the Andrelândia Nappe Complex. This thermal overprint was hot enough to cause sillimanite growth in this portion of the Complex. Biotite from the high-pressure granulites of the Carvalhos Klippe, the lateral equivalent of the Três Pontas–Varginha Nappe, yields a $^{40}Ar/^{39}Ar$ age of 560.7±3.9 (Fig. 4-5), which may relate to exhumation after the early phase of the Ribeira Orogeny. A $^{40}Ar/^{39}Ar$ biotite age of

490.6±4.1 Ma is recorded near the structural top of the Andrelândia Nappe (Fig. 4-5), which is the lateral equivalent of the Carmo da Cachoeira Nappe further to the west. A suite of $^{40}Ar/^{39}Ar$ biotite ages for this nappe reported by Campos Neto *et al*. (2004) show a decreasing trend from *ca.* 540 Ma at the structural base of the nappe to *ca.* 490 at the structural top of the nappe. I interpret these ages to record cooling from the bottom up due to emplacement of the Andrelândia Nappe directly over the São Francisco Craton. The younger ages of *ca.* 490 Ma at the top of the nappe indicate that the southeastern portion of the Nappe Complex was buried far longer than the western portion, likely due to the Ribeira Orogeny.

Biotite from a high-grade migmatite taken from the Ribiera Belt yields a $^{40}Ar/^{39}Ar$ age of 455.5±3.6 Ma (Fig. 4-5). When combined with a U-Pb zircon age of *ca.* 533 Ma from Schmitt *et al*. (2004), this yields an average cooling rate of ~5–6 ˚C $Ma^{-1}$ for the Ribiera Belt.

*Contributions to the Monazite Microprobe Chronologic Technique*

In addressing the challenges presented by the Southern Brasília Belt, I quickly realized that it would be necessary to collect a variety of chronologic data. I was able to obtain U-Pb zircon data using a SIMS at the Institute for the Study of the Earth's Interior in Misasa, Japan and $^{40}Ar/^{39}Ar$ biotite and hornblende data at the Syracuse University Noble Gas Isotope Research Laboratory. One of the more important chronometers in the study of high-grade metapelitic rocks is the (U-Th)-Pb system in monazite, which can be dated relatively efficiently and inexpensively using an electron probe microanalyzer (EPMA). One of my early tasks was to implement the EPMA (U-Th)-Pb monazite dating technique using the JEOL JXA-8900 in the

Nanoscale Imaging Spectroscopy and Properties Laboratory at the University of Maryland.

Implementation of the monazite microprobe dating technique introduced a new and important tool for chronologic studies at the University of Maryland. Aside from being used in this study of the Southern Brasília Belt, researchers at the University of Maryland have used this tool to study a Barrovian sequence in Dutchess County, New York and high-grade polyphase metamorphism and anatexis in the Fosdick Mountains, Antarctica.

I addressed several important challenges related to the collection and analysis of EPMA (U-Th)-Pb monazite data during this project. I present a formula for calculating uncertainty on individual dates, which is something that had not been specifically addressed in the literature, and so uncertainties had not been consistently calculated between various working groups. I also wrote a program in the C programming language to calculate dates and the associated uncertainties from monazite chemical data (Appendix C).

The most important contribution of this dissertation to the monazite microprobe dating technique, however, is my proposal of a robust statistical protocol for analyzing monazite (U-Th)-Pb dates and other geochemical data. Traditional statistical techniques have routinely relied on the assumption that the data follow a normal distribution. I show that although dates taken from single age zones do typically follow a normal distribution, this is not always the case, and outliers and skewed data are common. Using traditional statistical techniques on such data results in erroneous age calculations and underestimation of uncertainties. I propose using

the robust tanh estimator for calculating monazite ages, and the bootstrap for calculating uncertainties. These robust statistics allow for the calculation of ages while minimizing the effect of outliers in the data, and skewed datasets

# Appendices

## *Appendix A: Supplementary Data and Figure for Chapter 2*

***Figure A-1 – Pseudosection for Sample 04-6-11***

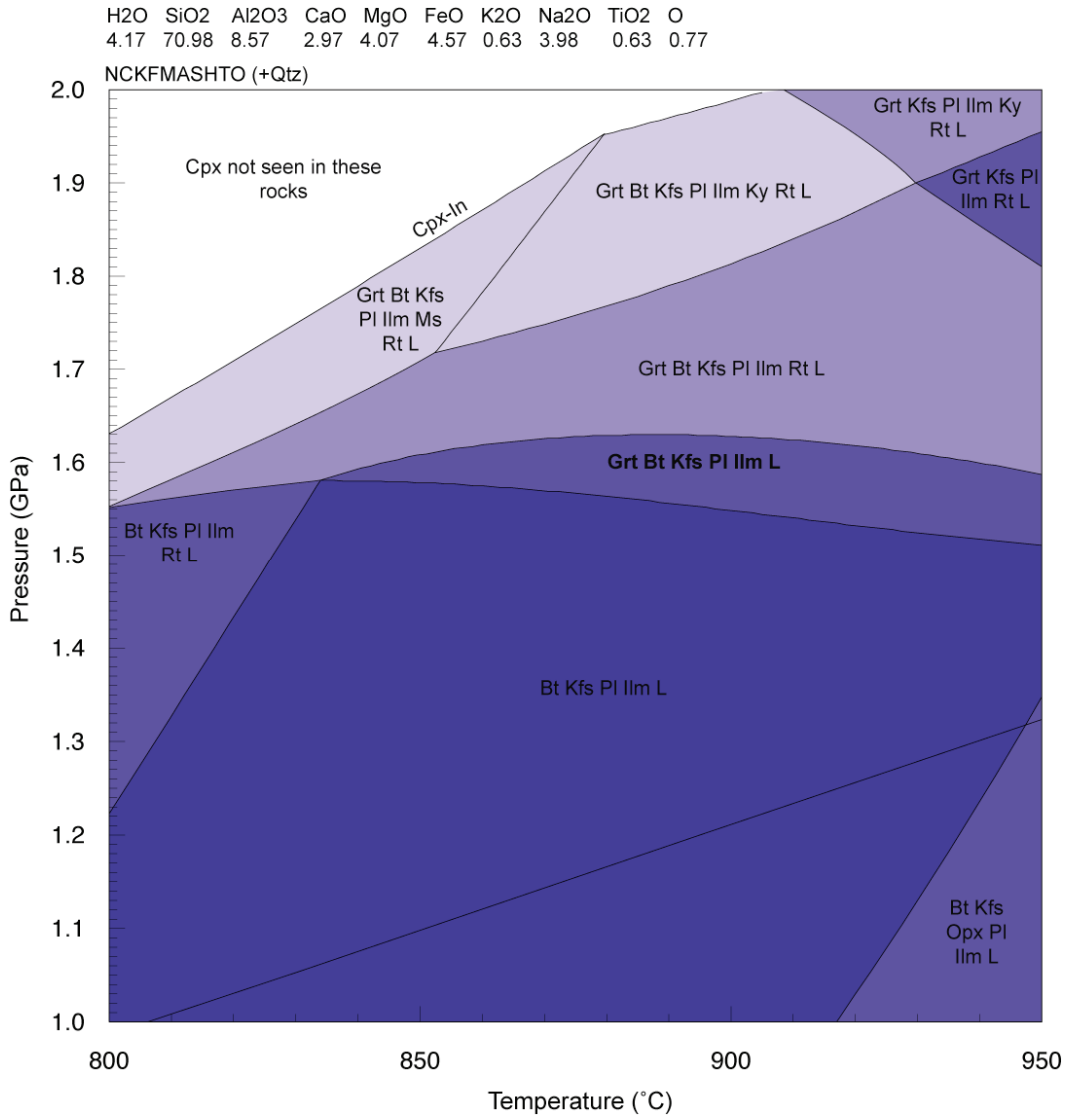


**Figure A-1.** Equilibrium phase diagram constructed using the bulk composition of sample 04-6-11. The peak assemblage for this sample is garnet, biotite, quartz, K-feldspar, plagioclase, ilmenite and silicate melt.

## *Table A-1 – Unreduced Zircon U-Pb Data*

**Table A-1.** Unreduced U-Pb zircon SIMS dataset used in Chapter 2.

**Table A-1.** U-Pb zircon SIMS data.

Sample 05-06-3 from the Socorro - Guaxupé Nappe

| Sample | Core/Rim | 207Pb/206Pb | 2σ | 7/6 Date | 2σ | 207/235U | 2σ | 206Pb/238U | 2σ | Rho | 206Pb/204Pb | Concordia Age | 2σ | U (ppm) | Th (ppm) | Th/U |
|---|---|---|---|---|---|---|---|---|---|---|---|---|---|---|---|---|
| 05-06-3_Zrn15@1 | core | 0.06616 | 0.00062 | **812** | **±20** | 1.21 | 0.12 | 0.1319 | 0.0064 | 0.9607 | 457930 | 791 | ±25 | 108 | 88 | 0.81 |
| 05-06-3_Zrn15@2 | rim | 0.06598 | 0.00084 | **806** | **±27** | 1.20 | 0.14 | 0.1320 | 0.0098 | 0.9226 | 61927 | 798 | ±54 | 55 | 22 | 0.40 |
| 05-06-3_Zrn15@3 | rim | 0.06590 | 0.00050 | **803** | **±16** | 0.95 | 0.07 | 0.1051 | 0.0057 | 0.9434 | 266000 | DISC | - | 222 | 58 | 0.26 |
| 05-06-3_Zrn2@1 | core | 0.06619 | 0.00019 | **813** | **±6** | 1.06 | 0.06 | 0.1156 | 0.0071 | 0.9941 | 14810250 | DISC | - | 1,259 | 625 | 0.50 |

Sample 04-7-1 from the Socorro - Guaxupé Nappe

| Sample | Core/Rim | 207Pb/206Pb | 2σ | 7/6 Date | 2σ | 207/235U | 2σ | 206Pb/238U | 2σ | Rho | 206Pb/204Pb | Concordia Age | 2σ | U (ppm) | Th (ppm) | Th/U |
|---|---|---|---|---|---|---|---|---|---|---|---|---|---|---|---|---|
| 04-7-1_Zrn30@1 | 1 zone | 0.0641 | 0.0005 | **744** | **±18** | 0.96 | 0.10 | 0.1078 | 0.0102 | 0.9770 | 10797 | 718 | ±46 | 158 | 37 | 0.24 |
| 04-7-1_Zrn5@1 | 1 zone | 0.0607 | 0.0010 | **628** | **±34** | 0.85 | 0.14 | 0.1000 | 0.0098 | 0.8929 | 2166 | 609 | ±55 | 30 | 132 | 4.47 |
| 04-7-1_Zrn5@2 | 1 zone | 0.0628 | 0.0004 | **700** | **±14** | 0.94 | 0.09 | 0.1089 | 0.0074 | 0.9617 | 15710 | 662 | ±43 | 175 | 96 | 0.55 |
| 04-7-1_Zrn2@1 | rim | 0.0615 | 0.0009 | **657** | **±30** | 0.83 | 0.12 | 0.0969 | 0.0066 | 0.8473 | 2494 | 589 | ±34 | 36 | 44 | 1.23 |
| 04-7-1_Zrn23@1 | rim | 0.0626 | 0.0005 | **694** | **±18** | 0.91 | 0.09 | 0.1048 | 0.0088 | 0.9628 | 8452 | 660 | ±47 | 112 | 46 | 0.41 |
| 04-7-1_Zrn28@1 | rim | 0.0625 | 0.0003 | **691** | **±9** | 0.88 | 0.10 | 0.1015 | 0.0109 | 0.9904 | 34177 | 695 | ±34 | 444 | 199 | 0.45 |
| 04-7-1_Zrn4@1 | 1 zone | 0.0627 | 0.0003 | **697** | **±11** | 0.91 | 0.10 | 0.1046 | 0.0105 | 0.9865 | 19436 | 693 | ±38 | 210 | 135 | 0.65 |
| 04-7-1_Zrn2@3 | rim | 0.0599 | 0.0014 | **601** | **±52** | 0.80 | 0.18 | 0.0959 | 0.0076 | 0.6944 | 1026 | 589 | ±42 | 15 | 54 | 3.62 |

Sample 05b-13-13b - retrograded eclogite

| Sample | Core/Rim | 207Pb/206Pb | 2σ | 7/6 Date | 2σ | 207/235U | 2σ | 206Pb/238U | 2σ | Rho | 206Pb/204Pb | Concordia Age | 2σ | U (ppm) | Th (ppm) | Th/U |
|---|---|---|---|---|---|---|---|---|---|---|---|---|---|---|---|---|
| 05b-13-13b~Zrn18@1 | 1 zone | 0.0636 | 0.0010 | **729** | **±34** | 0.96 | 0.17 | 0.1102 | 0.0092 | 0.8589 | 1689 | 669 | ±47 | 67 | 2 | 0.03 |
| 05b-13-13b~Zrn16@1 | 1 zone | 0.0612 | 0.0018 | **647** | **±63** | 0.96 | 0.32 | 0.1116 | 0.0158 | 0.7613 | 1767 | 681 | ±87 | 96 | 6 | 0.06 |
| 05b-13-13b~Zrn15@1 | 1 zone | 0.0606 | 0.0011 | **626** | **±39** | 0.95 | 0.14 | 0.1115 | 0.0078 | 0.8276 | 2245 | 683 | ±42 | 101 | 2 | 0.02 |
| 05b-13-13b~Zrn20@1 | 1 zone | 0.0606 | 0.0006 | **626** | **±21** | 0.92 | 0.11 | 0.1103 | 0.0098 | 0.9511 | 5707 | 672 | ±57 | 312 | 22 | 0.07 |
| 05b-13-13b~Zrn14@1 | 1 zone | 0.0587 | 0.0006 | **556** | **±23** | 0.85 | 0.10 | 0.1042 | 0.0070 | 0.9087 | 5409 | 647 | ±38 | 241 | 12 | 0.05 |
| 05b-13-13b~Zrn9@1 | 1 zone | 0.0714 | 0.0014 | **969** | **±40** | 1.14 | 0.27 | 0.1161 | 0.0181 | 0.6785 | 1103 | 716 | ±100 | 138 | 11 | 0.08 |

Sample 05b-6-31b from the top of the Três Pontas - Varginha Nappe

| Sample | Core/Rim | 207Pb/206Pb | 2σ | 7/6 Date | 2σ | 207/235U | 2σ | 206Pb/238U | 2σ | Rho | 206Pb/204Pb | Concordia Age | 2σ | U (ppm) | Th (ppm) | Th/U |
|---|---|---|---|---|---|---|---|---|---|---|---|---|---|---|---|---|
| 05b-6-31b_Zrn12@1 | 1 zone | 0.06125 | 0.00026 | **648** | **±9** | 0.91 | 0.06 | 0.1070 | 0.0064 | 0.9892 | 25313 | 654 | ±23 | 813 | 12 | 0.02 |
| 05b-6-31b_Zrn16@1 | 1 zone | 0.06116 | 0.00045 | **645** | **±16** | 0.90 | 0.07 | 0.1072 | 0.0056 | 0.9498 | 13211 | 657 | ±32 | 309 | 16 | 0.05 |
| 05b-6-31b_Zrn1@1 | 1 zone | 0.06057 | 0.00064 | **624** | **±23** | 0.90 | 0.08 | 0.1080 | 0.0054 | 0.8656 | 5125 | 663 | ±31 | 107 | 17 | 0.16 |
| 05b-6-31b_Zrn24@3 | 1 zone | 0.06079 | 0.00071 | **632** | **±50** | 0.80 | 0.09 | 0.0956 | 0.0051 | 0.9175 | 4509 | 583 | ±23 | 112 | 15 | 0.13 |
| 05b-6-31b_Zrn7@1 | 1 zone | 0.06094 | 0.00071 | **637** | **±50** | 0.89 | 0.09 | 0.1066 | 0.0064 | 0.9195 | 5408 | 656 | ±34 | 112 | 20 | 0.18 |
| 05b-6-31b_Zrn24@4 | core | 0.06093 | 0.00042 | **637** | **±15** | 0.88 | 0.06 | 0.1045 | 0.0035 | 0.9575 | 5696 | 642 | ±13 | 166 | 10 | 0.06 |
| 05b-6-31b_Zrn24@5 | core | 0.06130 | 0.00052 | **650** | **±18** | 0.88 | 0.07 | 0.1037 | 0.0031 | 0.9405 | 6606 | 634 | ±11 | 132 | 14 | 0.11 |
| 05b-6-31b_Zrn6@1 | 1 zone | 0.06160 | 0.00042 | **660** | **±15** | 0.92 | 0.08 | 0.1083 | 0.0060 | 0.9678 | 10072 | 661 | ±31 | 233 | 10 | 0.04 |
| 05b-6-31b_Zrn24@1 | rim | 0.05979 | 0.00072 | **596** | **±26** | 0.90 | 0.09 | 0.1081 | 0.0047 | 0.9121 | 5019 | 670 | ±21 | 114 | 14 | 0.12 |
| 05b-6-31b_Zrn24@6 | rim | 0.06018 | 0.00066 | **610** | **±24** | 0.81 | 0.08 | 0.0973 | 0.0029 | 0.8551 | 4396 | 596 | ±13 | 120 | 15 | 0.13 |

Sample 05b-6-33 from the top of the Três Pontas - Varginha Nappe

| Sample | Core/Rim | 207Pb/206Pb | 2σ | 7/6 Date | 2σ | 207/235U | 2σ | 206Pb/238U | 2σ | Rho | 206Pb/204Pb | Concordia Age | 2σ | U (ppm) | Th (ppm) | Th/U |
|---|---|---|---|---|---|---|---|---|---|---|---|---|---|---|---|---|
| 05b-6-33_Zrn4@1 | rim | 0.0686 | 0.0011 | **887** | **±34** | 1.08 | 0.21 | 0.1117 | 0.0059 | 0.9609 | 4716 | 656 | ±13 | 494 | 29 | 0.06 |
| 05b-6-33_Zrn1@2 | rim | 0.0755 | 0.0012 | **1081** | **±33** | 1.23 | 0.22 | 0.1179 | 0.0070 | 0.7695 | 4414 | 692 | ±34 | 454 | 418 | 0.92 |
| 05b-6-33_Zrn2@1 | rim | 0.0620 | 0.0004 | **675** | **±14** | 1.00 | 0.08 | 0.1162 | 0.0056 | 0.7442 | 7982 | 708 | ±32 | 527 | 28 | 0.05 |
| 05b-6-33_Zrn2@2 | core | 0.0895 | 0.0029 | **1416** | **±62** | 1.39 | 1.02 | 0.1019 | 0.0175 | 0.6567 | 1492 | 593 | ±43 | 888 | 114 | 0.13 |
| 05b-6-33_Zrn7@1 | core | 0.0616 | 0.0003 | **661** | **±11** | 0.98 | 0.08 | 0.1139 | 0.0073 | 0.9852 | 11936 | 692 | ±42 | 394 | 12 | 0.03 |
| 05b-6-33_Zrn7@2 | core | 0.0610 | 0.0003 | **640** | **±10** | 0.87 | 0.06 | 0.1027 | 0.0057 | 0.9889 | 20230 | 644 | ±28 | 571 | 15 | 0.03 |
| 05b-6-33_Zrn7@3 | rim | 0.0639 | 0.0012 | **738** | **±38** | 0.85 | 0.13 | 0.0954 | 0.0052 | 0.6817 | 13093 | 581 | ±29 | 512 | 12 | 0.02 |
| 05b-6-33_Zrn8@2 | core | 0.0621 | 0.0002 | **679** | **±8** | 0.95 | 0.07 | 0.1101 | 0.0058 | 0.9933 | 51583 | 665 | ±30 | 1353 | 5 | 0.00 |

Sample 04-6-11 from the middle of the Três Pontas - Varginha Nappe

| Sample | Core/Rim | 207Pb/206Pb | 2σ | 7/6 Date | 2σ | 207/235U | 2σ | 206Pb/238U | 2σ | Rho | 206Pb/204Pb | Concordia Age | 2σ | U (ppm) | Th (ppm) | Th/U |
|---|---|---|---|---|---|---|---|---|---|---|---|---|---|---|---|---|
| 04-6-11_Zrn8@1 | rim | 0.06176 | 0.00030 | **666** | **±10** | 0.89 | 0.06 | 0.1045 | 0.0063 | 0.9831 | 12603 | 664 | ±24 | 345 | 31 | 0.09 |
| 04-6-11_Zrn8@3 | rim | 0.06137 | 0.00031 | **652** | **±11** | 0.92 | 0.05 | 0.1081 | 0.0037 | 0.9796 | 13673 | 662 | ±17 | 322 | 32 | 0.10 |
| 04-6-11_Zrn9@1 | rim | 0.06187 | 0.00041 | **670** | **±14** | 0.73 | 0.04 | 0.0853 | 0.0033 | 0.9846 | 7297 | - | - | 315 | 24 | 0.08 |
| 04-6-11_Zrn3@1 | rim | 0.06159 | 0.00034 | **660** | **±12** | 0.91 | 0.06 | 0.1068 | 0.0044 | 0.9735 | 10316 | 650 | ±21 | 284 | 31 | 0.11 |
| 04-6-11_Zrn3@2 | rim | 0.06222 | 0.00045 | **682** | **±15** | 0.82 | 0.12 | 0.0949 | 0.0126 | 0.9176 | 6900 | 610 | ±65 | 331 | 28 | 0.08 |
| 04-6-11_Zrn4@1 | rim | 0.06201 | 0.00030 | **674** | **±10** | 0.89 | 0.06 | 0.1044 | 0.0063 | 0.9860 | 11694 | 669 | ±24 | 342 | 21 | 0.06 |
| 04-6-11_Zrn4@3 | rim | 0.06193 | 0.00040 | **672** | **±14** | 0.77 | 0.06 | 0.0899 | 0.0047 | 0.9142 | 13013 | 540 | ±25 | 401 | 85 | 0.21 |
| 04-6-11_Zrn2@1 | rim | 0.06181 | 0.00029 | **668** | **±10** | 0.91 | 0.06 | 0.1060 | 0.0052 | 0.9835 | 11862 | 638 | ±28 | 369 | 50 | 0.14 |
| 04-6-11_Zrn2@2 | rim | 0.06173 | 0.00041 | **665** | **±14** | 0.80 | 0.05 | 0.0937 | 0.0029 | 0.9390 | 9291 | 563 | ±12 | 238 | 42 | 0.18 |
| 04-6-11_Zrn8@4 | rim | 0.06174 | 0.00037 | **665** | **±13** | 0.87 | 0.07 | 0.1016 | 0.0046 | 0.9759 | 20073 | 605 | ±18 | 338 | 37 | 0.11 |

Sample 05b-6-110 from the base of the Três Pontas - Varginha Nappe

| Sample | Core/Rim | 207Pb/206Pb | 2σ | 7/6 Date | 2σ | 207/235U | 2σ | 206Pb/238U | 2σ | Rho | 206Pb/204Pb | Concordia Age | 2σ | U (ppm) | Th (ppm) | Th/U |
|---|---|---|---|---|---|---|---|---|---|---|---|---|---|---|---|---|
| 05b-6-110_Zrn6@1 | core | 0.06212 | 0.00029 | **678** | **±10** | 0.86 | 0.08 | 0.1007 | 0.0099 | 0.9824 | 17988 | 657 | ±30 | 667 | 40 | 0.06 |
| 05b-6-110_Zrn7@1 | core | 0.06163 | 0.00026 | **661** | **±9** | 0.81 | 0.07 | 0.0955 | 0.0082 | 0.9930 | 17749 | DISC | - | 618 | 12 | 0.02 |
| 05b-6-110_Zrn8@1 | core | 0.06190 | 0.00026 | **671** | **±9** | 0.91 | 0.06 | 0.1070 | 0.0067 | 0.9867 | 16301 | 670 | ±21 | 485 | 72 | 0.15 |
| 05b-6-108_Zrn15@1 | core | 0.06113 | 0.00025 | **644** | **±9** | 1.01 | 0.06 | 0.1195 | 0.0071 | 0.9883 | 13648 | - | - | 581 | 25 | 0.04 |
| 05b-6-108_Zrn10@1 | core | 0.06184 | 0.00071 | **669** | **±25** | 0.99 | 0.10 | 0.1168 | 0.0057 | 0.9449 | 1714 | 723 | ±26 | 83 | 15 | 0.18 |
| 05b-6-108_Zrn10@2 | core | 0.06142 | 0.00059 | **654** | **±21** | 0.98 | 0.09 | 0.1156 | 0.0036 | 0.8948 | 3208 | 711 | ±14 | 106 | 13 | 0.12 |
| 05b-6-108_Zrn8@1 | core | 0.06234 | 0.00044 | **686** | **±15** | 1.01 | 0.07 | 0.1174 | 0.0074 | 0.9614 | 3927 | 706 | ±37 | 221 | 13 | 0.06 |
| 05b-6-108_Zrn11@1 | rim | 0.05974 | 0.00163 | **594** | **±59** | 0.81 | 0.26 | 0.0965 | 0.0145 | 0.6362 | 2650 | 594 | ±85 | 182 | 39 | 0.21 |
| 05b-6-108_Zrn17@1 | core | 0.06159 | 0.00034 | **660** | **±12** | 1.01 | 0.07 | 0.1186 | 0.0059 | 0.9847 | 10446 | DISC | - | 407 | 13 | 0.03 |
| 05b-6-108_Zrn18@1 | core | 0.06164 | 0.00048 | **662** | **±17** | 0.99 | 0.08 | 0.1162 | 0.0056 | 0.9559 | 5476 | 717 | ±30 | 151 | 9 | 0.06 |
| 05b-6-108_Zrn25@1 | core | 0.06103 | 0.00047 | **640** | **±16** | 1.00 | 0.08 | 0.1185 | 0.0058 | 0.9604 | 3172 | 744 | ±30 | 173 | 56 | 0.32 |
| 05b-6-110_Zrn5@1 | core | 0.06118 | 0.00053 | **646** | **±19** | 0.91 | 0.08 | 0.1079 | 0.0061 | 0.9459 | 6075 | 662 | ±33 | 205 | 28 | 0.14 |

Samples from leucosomes in the base of the Três Pontas - Varginha Nappe

| Sample | Core/Rim | 207Pb/206Pb | 2σ | 7/6 Date | 2σ | 207/235U | 2σ | 206Pb/238U | 2σ | Rho | 206Pb/204Pb | Concordia Age | 2σ | U (ppm) | Th (ppm) | Th/U |
|---|---|---|---|---|---|---|---|---|---|---|---|---|---|---|---|---|
| 4_6_19_@Zr1 | core | 0.06119 | 0.00037 | **646** | **±13** | 0.87 | 0.07 | 0.1024 | 0.0075 | 0.9933 | 37719 | 661 | ±32 | 752 | 8 | 0.01 |
| 4_6_19_@Zr6b | core | 0.06061 | 0.00032 | **625** | **±11** | 0.82 | 0.06 | 0.0975 | 0.0048 | 0.9590 | 43116 | 596 | ±14 | 761 | 13 | 0.02 |
| 04-6-21a2 Zir60b | core | 0.06148 | 0.00067 | **656** | **±23** | 0.84 | 0.10 | 0.0985 | 0.0066 | 0.9422 | 8850 | 593 | ±30 | - | - | - |

| | | | | | | | | | | | | | | | | |
|---|---|---|---|---|---|---|---|---|---|---|---|---|---|---|---|---|
| 04-6-21a2 Zir95b | core | 0.06147 | 0.00071 | **656** | **±25** | 0.91 | 0.11 | 0.1072 | 0.0060 | 0.9428 | 5593 | 656 | ±24 | - | - | - |
| 04-6-18 Zir34C | core | 0.06070 | 0.00041 | **629** | **±14** | 0.90 | 0.06 | 0.1069 | 0.0043 | 0.9737 | 23480 | 661 | ±19 | - | - | - |
| 04-6-18 Zir34R1 | core | 0.06116 | 0.00074 | **645** | **±26** | 0.75 | 0.09 | 0.0888 | 0.0034 | 0.8748 | 6641 | 541 | ±14 | - | - | - |
| 04-6-18 Zir2c1 | core | 0.06135 | 0.00036 | **652** | **±13** | 0.85 | 0.06 | 0.1011 | 0.0064 | 0.9769 | 13988 | 636 | ±32 | - | - | - |
| 04-6-21a2 Zir51 | rim | 0.05972 | 0.00102 | **593** | **±37** | 0.84 | 0.15 | 0.1018 | 0.0073 | 0.8936 | 2836 | 627 | ±33 | - | - | - |
| 04-6-21a2 Zir60 | rim | 0.05997 | 0.00082 | **602** | **±29** | 0.91 | 0.11 | 0.1082 | 0.0037 | 0.8778 | 6048 | 665 | ±15 | - | - | - |
| 04-6-21a2 Zi90b | rim | 0.06013 | 0.00037 | **608** | **±13** | 0.92 | 0.11 | 0.1104 | 0.0061 | 0.9423 | 47240 | 685 | ±13 | - | - | - |
| 04-6-21a2 Zi88 | rim | 0.05982 | 0.00037 | **597** | **±13** | 0.93 | 0.10 | 0.1136 | 0.0107 | 0.9804 | 29094 | 625 | ±45 | - | - | - |
| 04-6-21a2 Zi71 | rim | 0.06019 | 0.00064 | **610** | **±23** | 0.92 | 0.15 | 0.1104 | 0.0123 | 0.9238 | 6367 | 675 | ±72 | - | - | - |
| 4_6_19_@Zr3b | rim | 0.06022 | 0.00040 | **612** | **±15** | 0.93 | 0.06 | 0.1119 | 0.0038 | 0.9594 | 15752 | 702 | ±17 | 257 | 21 | 0.08 |
| 04-6-21a2 Zir95 | rim | 0.05985 | 0.00077 | **598** | **±28** | 0.92 | 0.11 | 0.1109 | 0.0070 | 0.9241 | 6565 | 690 | ±36 | - | - | - |

**Table A-2.** Chondrite normalized REE analyses of NIST-610 reference material using the LA-ICP-MS.

| Sample | CaO | Sr | Y | Nb | Ba | La | Ce | Pr | Nd | Sm | Eu | Gd | Tb | Dy | Ho | Er | Tm | Yb | Lu | Hf |
|---|---|---|---|---|---|---|---|---|---|---|---|---|---|---|---|---|---|---|---|---|
| NIST610 | 11.5 | 504 | 455 | 422 | 432 | 464 | 455 | 437 | 440 | 445 | 467 | 430 | 453 | 435 | 461 | 436 | 430 | 470 | 443 | 427 |
| NIST610 | 11.5 | 500 | 453 | 424 | 424 | 459 | 449 | 430 | 429 | 451 | 463 | 418 | 440 | 426 | 445 | 423 | 418 | 461 | 435 | 415 |
| NIST610 | 11.5 | 509 | 456 | 426 | 421 | 455 | 442 | 427 | 427 | 440 | 452 | 410 | 429 | 415 | 436 | 418 | 414 | 454 | 430 | 416 |
| NIST610 | 11.5 | 495 | 451 | 420 | 434 | 468 | 462 | 440 | 442 | 469 | 478 | 437 | 464 | 446 | 471 | 442 | 434 | 477 | 447 | 427 |
| NIST610 | 11.5 | 504 | 459 | 425 | 423 | 452 | 438 | 424 | 427 | 437 | 463 | 425 | 450 | 433 | 455 | 431 | 424 | 460 | 428 | 419 |
| NIST610 | 11.5 | 499 | 449 | 421 | 433 | 471 | 465 | 443 | 442 | 461 | 468 | 422 | 444 | 428 | 452 | 429 | 424 | 471 | 449 | 424 |
| NIST610 | 11.5 | 516 | 469 | 437 | 435 | 468 | 455 | 432 | 430 | 451 | 459 | 418 | 441 | 423 | 443 | 416 | 411 | 453 | 427 | 418 |
| NIST610 | 11.5 | 502 | 458 | 429 | 428 | 463 | 455 | 435 | 436 | 442 | 466 | 426 | 446 | 434 | 460 | 439 | 439 | 486 | 462 | 434 |
| NIST610 | 11.5 | 501 | 450 | 417 | 428 | 460 | 449 | 432 | 433 | 454 | 464 | 421 | 448 | 427 | 447 | 420 | 408 | 445 | 415 | 409 |

**Table A-3.** Whole rock chemistry for samples used to construct pseudosections. Values are wt. % oxide.

| | 04-5-8 | 04-6-11 | 05b-6-31b | 04-6-2 |
|---|---|---|---|---|
| SiO2 | 66.71 | 68.13 | 63.24 | 67.62 |
| TiO2 | 0.74 | 0.81 | 0.94 | 0.75 |
| Al2O3 | 15.01 | 13.96 | 17.28 | 15.22 |
| Fe2O3 | 6.01 | 1.95 | 2.38 | 0.50 |
| FeO | - | 3.49 | 5.51 | 5.25 |
| MnO | 0.12 | 0.21 | 0.21 | 0.00 |
| Mg0 | 2.64 | 2.62 | 3.33 | 2.68 |
| CaO | 1.91 | 2.66 | 1.42 | 1.93 |
| Na2O | 3.24 | 3.94 | 1.30 | 3.28 |
| K2O | 2.17 | 0.95 | 3.30 | 2.20 |
| P2O5 | 0.15 | 0.17 | 0.13 | 0.00 |
| LOI | 0.51 | 1.20 | 1.16 | 0.57 |
| Total | 99.21 | 100.09 | 100.20 | 100.00 |

**Table A-4.** Location of all samples studied from the Southern Brasilia and Ribeira Belts in this study. Coordinates are given for UTM southern hemisphere zone 23 with the WGS 84 ellipsoid.

| Tectonic Unit | Sample Location | Samples | Easting | Northing |
|---|---|---|---|---|
| Retrograded Eclogite | In Fazenda | 05b-13-13 | 541580 | 7569895 |
| Três Pontas–Varginha Nappe (Top) | Lixão | 05b-6-31b | 453417 | 7620799 |
| | Near Lixão | 05b-6-33 | 451837 | 7620153 |
| Três Pontas–Varginha Nappe (Middle) | Três Pontas Quarry | 04-6-11 | 450760 | 7631913 |
| | Três Pontas Quarry | 04-6-2 | 450760 | 7631913 |
| | Três Pontas Quarry | 05b-6-103 | 450760 | 7631913 |
| | Três Pontas Quarry | 05b-6-36 | 450760 | 7631913 |
| Três Pontas–Varginha Nappe (Bottom) | Four Level Quarry | 04-6-19 | 461883 | 7621214 |
| | Four Level Quarry | 05b-6-29 | 461883 | 7621214 |
| | Four Level Quarry | 05b-6-30 | 461883 | 7621214 |
| | Santo Antônio Quarry | 04-6-21 | 461599 | 7616241 |
| | Santo Antônio Quarry | 05b-6-108 | 461599 | 7616241 |
| | Santo Antônio Quarry | 05b-6-109 | 461599 | 7616241 |
| | Santo Antônio Quarry | 05b-6-110 | 461599 | 7616241 |
| Carvalhos Klippe | Carvalhos Waterfall | 05b-10-102 | 554895 | 7568729 |
| | Carvalhos Waterfall | 05b-10-65 | 554895 | 7568729 |
| | Railway Cut | 05b-10-74 | 562585 | 7563000 |
| | Waterfall | 05b-10-95 | 566843 | 7571961 |
| Carmo da Cachoeira Nappe | INCOPE Quarry | 05b-5-23 | 473686 | 7594399 |
| | INCOPE Quarry | 05b-5-22 | 473686 | 7594399 |
| | INCOPE Quarry | GR-05-3 | 473686 | 7594399 |
| | INCOPE Quarry | GR-05-4b | 473686 | 7594399 |
| | Abandoned Quarry | 05b-5-17 | 472873 | 7579213 |
| Andrelândia Nappe | Cristo Redemptor | 05b-8-56 | 572336 | 7596377 |
| Ribeira Belt | Shopping Rio Sul | 05b-RJ-114 | 687086 | 7460061 |
| Socorro–Guaxupé Nappe | Riverbed | 05-06-3 | 455322 | 7610069 |
| | Riverbed | 04-7-1 | 455322 | 7610069 |
| | Riverbed | 04-7-26 | 455322 | 7610069 |

*Appendix B: Supplementary Data for Chaper 3*

***Table B-1 – All monazite chemical analyses used in Chapter 3***

**Table B-1.** All monazite chemical analyses used in Chapter 3.

***Table B-2 – All monazite dates used in Chapter 3***

**Table B-2.** All (U-Th)-Pb chronologic data for the southern sector of the Southern Brasília Belt.

***Table B-3 – All p-values used in Chapter 3***

**Table B-3.** Summary of all t-test values for all ages.

**Table B-2.** All chemical data for monazite analyzed in chapter 3.

| | $UO_2$ | | $ThO_2$ | | | PbO | | $Y_2O_3$ | | | CaO | | $Ce_2O_3$ | | $P_2O_5$ | | $SiO_2$ | |
|---|---|---|---|---|---|---|---|---|---|---|---|---|---|---|---|---|---|---|
| Sample | wt. % | RSD (2σ%) | wt. % | RSD (2σ%) | k-raw | wt. % | RSD (2σ%) | wt. % | RSD (2σ%) | k-raw | wt. % | RSD (2σ%) | wt. % | RSD (2σ%) | wt. % | RSD (2σ%) | wt. % | RSD (2σ%) |
| Trebilcock-1 | 0.769 | 1.2 | 14.25 | 0.3 | 15.326 | 0.166 | 2.4 | 2.34 | 0.7 | 3.170 | 1.611 | 0.3 | 22.61 | 0.3 | 24.72 | 0.2 | 1.829 | 0.3 |
| Trebilcock-2 | 0.968 | 1.0 | 16.21 | 0.3 | 17.554 | 0.214 | 2.0 | 2.98 | 0.6 | 4.063 | 1.793 | 0.3 | 20.90 | 0.3 | 22.00 | 0.2 | 2.187 | 0.3 |
| Trebilcock-2 | 0.966 | 1.0 | 16.16 | 0.3 | 17.475 | 0.219 | 1.9 | 2.94 | 0.6 | 4.075 | 1.814 | 0.3 | 15.60 | 0.4 | 20.71 | 0.2 | 2.124 | 0.3 |
| Trebilcock-3 | 0.955 | 1.0 | 16.13 | 0.3 | 17.411 | 0.217 | 2.0 | 2.94 | 0.6 | 4.020 | 1.830 | 0.3 | 20.81 | 0.3 | 23.37 | 0.2 | 2.221 | 0.2 |
| Trebilcock-4 | 1.002 | 0.9 | 16.91 | 0.3 | 18.285 | 0.214 | 2.0 | 2.90 | 0.6 | 3.964 | 1.868 | 0.3 | 20.47 | 0.3 | 23.38 | 0.2 | 2.315 | 0.2 |
| Trebilcock-5 | 1.036 | 0.9 | 17.16 | 0.3 | 18.571 | 0.228 | 1.9 | 2.93 | 0.6 | 4.014 | 1.905 | 0.3 | 20.26 | 0.3 | 23.31 | 0.2 | 2.359 | 0.2 |
| 04-6-11 Mnz2-1 | 0.213 | 3.7 | 5.60 | 0.5 | 5.910 | 0.146 | 2.8 | 0.08 | 15.0 | 0.105 | 2.217 | 0.3 | 22.58 | 0.3 | 25.57 | 0.2 | 0.606 | 0.7 |
| 04-6-11 Mnz2-2 | 0.218 | 3.6 | 5.36 | 0.5 | 5.736 | 0.132 | 2.9 | 0.07 | 16.9 | 0.089 | 1.939 | 0.3 | 32.08 | 0.2 | 23.61 | 0.2 | 0.582 | 0.7 |
| 04-6-11 Mnz2-3 | 0.218 | 3.6 | 5.50 | 0.5 | 5.857 | 0.150 | 2.7 | 0.06 | 20.6 | 0.076 | 2.202 | 0.3 | 31.67 | 0.3 | 25.97 | 0.2 | 0.612 | 0.7 |
| 04-6-11 Mnz2-4 | 0.188 | 4.1 | 5.55 | 0.5 | 5.900 | 0.149 | 2.8 | 0.06 | 19.4 | 0.082 | 2.227 | 0.3 | 30.87 | 0.3 | 26.37 | 0.2 | 0.611 | 0.7 |
| 04-6-11 Mnz2-5 | 0.165 | 4.7 | 5.57 | 0.5 | 5.928 | 0.147 | 2.8 | 0.10 | 11.6 | 0.136 | 2.194 | 0.3 | 30.96 | 0.3 | 26.03 | 0.2 | 0.583 | 0.7 |
| 04-6-11 Mnz2-6 | 0.173 | 4.5 | 5.59 | 0.5 | 5.960 | 0.150 | 2.7 | 0.11 | 11.1 | 0.142 | 2.229 | 0.3 | 31.74 | 0.3 | 25.98 | 0.2 | 0.610 | 0.7 |
| 04-6-11 Mnz2-7 | 0.217 | 3.6 | 5.52 | 0.5 | 5.880 | 0.142 | 2.9 | 0.09 | 13.6 | 0.119 | 2.000 | 0.3 | 32.64 | 0.2 | 26.50 | 0.2 | 0.643 | 0.7 |
| 04-6-11 Mnz2-8 | 0.172 | 4.5 | 5.60 | 0.5 | 5.960 | 0.154 | 2.6 | 0.10 | 12.2 | 0.130 | 2.206 | 0.3 | 30.58 | 0.3 | 26.02 | 0.2 | 0.597 | 0.7 |
| 04-6-11 Mnz2-9 | 0.180 | 4.3 | 5.54 | 0.5 | 5.911 | 0.144 | 2.8 | 0.10 | 11.5 | 0.136 | 2.197 | 0.3 | 32.31 | 0.2 | 25.75 | 0.2 | 0.584 | 0.7 |
| 04-6-11 Mnz2-10 | 0.200 | 3.9 | 5.36 | 0.5 | 5.711 | 0.143 | 2.8 | 0.12 | 9.8 | 0.157 | 2.043 | 0.3 | 31.90 | 0.3 | 25.36 | 0.2 | 0.622 | 0.7 |
| 04-6-11 Mnz2-11 | 0.173 | 4.5 | 5.57 | 0.5 | 5.933 | 0.150 | 2.7 | 0.12 | 9.7 | 0.163 | 2.215 | 0.3 | 32.25 | 0.2 | 25.85 | 0.2 | 0.619 | 0.7 |
| 04-6-11 Mnz2-12 | 0.157 | 4.8 | 4.54 | 0.5 | 4.907 | 0.118 | 3.1 | 0.06 | 15.1 | 0.079 | 1.886 | 0.3 | 30.60 | 0.3 | 17.34 | 0.2 | 0.556 | 0.7 |
| 04-6-11 Mnz2-13 | 0.183 | 4.0 | 5.34 | 0.5 | 5.734 | 0.098 | 3.3 | 0.16 | 6.6 | 0.210 | 2.189 | 0.3 | 29.29 | 0.3 | 20.43 | 0.2 | 0.760 | 0.6 |
| 04-6-11 Mnz2-14 | 0.146 | 5.0 | 5.02 | 0.5 | 5.329 | 0.140 | 2.9 | 0.10 | 12.2 | 0.134 | 2.090 | 0.3 | 30.93 | 0.3 | 25.34 | 0.2 | 1.358 | 0.4 |
| 04-6-11 Mnz2-15 | 0.175 | 4.4 | 5.07 | 0.5 | 5.399 | 0.144 | 2.9 | 0.03 | 42.7 | 0.037 | 2.074 | 0.3 | 32.34 | 0.2 | 25.45 | 0.2 | 0.615 | 0.7 |
| 04-6-11 Mnz2-16 | 0.141 | 5.2 | 5.32 | 0.5 | 5.689 | 0.121 | 3.1 | 0.08 | 14.1 | 0.107 | 2.139 | 0.3 | 31.10 | 0.3 | 23.45 | 0.2 | 0.563 | 0.7 |
| 04-6-11 Mnz2-17 | 0.139 | 5.1 | 4.43 | 0.5 | 4.707 | 0.106 | 3.5 | 0.06 | 18.2 | 0.082 | 1.869 | 0.3 | 27.20 | 0.3 | 21.17 | 0.2 | 2.697 | 0.2 |
| 04-6-11 Mnz2-18 | 0.224 | 3.4 | 5.77 | 0.5 | 6.149 | 0.158 | 2.6 | 0.10 | 13.0 | 0.128 | 2.111 | 0.3 | 32.33 | 0.2 | 26.91 | 0.2 | 0.686 | 0.7 |
| 04-6-11 Mnz2-19 | 0.174 | 4.5 | 5.73 | 0.5 | 6.103 | 0.153 | 2.7 | 0.28 | 4.5 | 0.363 | 1.948 | 0.3 | 31.70 | 0.3 | 26.06 | 0.2 | 0.618 | 0.7 |
| 04-6-11 Mnz2-20 | 0.192 | 4.1 | 6.71 | 0.4 | 7.156 | 0.172 | 2.4 | 0.30 | 4.3 | 0.388 | 2.034 | 0.3 | 30.70 | 0.3 | 26.11 | 0.2 | 0.785 | 0.6 |
| 04-6-11 Mnz2-21 | 0.176 | 4.4 | 6.24 | 0.5 | 6.647 | 0.156 | 2.6 | 0.31 | 4.2 | 0.401 | 1.957 | 0.3 | 31.00 | 0.3 | 26.47 | 0.2 | 0.767 | 0.6 |
| 04-6-11 Mnz2-22 | 0.142 | 5.3 | 5.84 | 0.5 | 6.219 | 0.139 | 2.8 | 0.29 | 4.5 | 0.375 | 1.873 | 0.3 | 31.92 | 0.3 | 26.00 | 0.2 | 0.648 | 0.7 |
| 04-6-11 Mnz2-23 | 0.162 | 4.8 | 5.27 | 0.5 | 5.625 | 0.133 | 3.0 | 0.25 | 4.9 | 0.323 | 2.042 | 0.3 | 32.22 | 0.2 | 25.21 | 0.2 | 0.484 | 0.8 |
| 04-6-11 Mnz2-24 | 0.228 | 3.4 | 5.45 | 0.5 | 5.801 | 0.139 | 2.9 | 0.25 | 4.9 | 0.332 | 2.195 | 0.3 | 31.41 | 0.3 | 26.29 | 0.2 | 0.443 | 0.9 |
| 04-6-11 Mnz2-25 | 0.218 | 3.5 | 5.39 | 0.5 | 5.750 | 0.146 | 2.7 | 0.17 | 7.2 | 0.224 | 2.109 | 0.3 | 31.81 | 0.3 | 25.37 | 0.2 | 0.503 | 0.8 |
| 04-6-11 Mnz2-26 | 0.223 | 3.5 | 5.28 | 0.5 | 5.611 | 0.140 | 2.9 | 0.23 | 5.4 | 0.304 | 2.112 | 0.3 | 31.68 | 0.3 | 26.52 | 0.2 | 0.445 | 0.9 |
| 04-6-11 Mnz2-27 | 0.219 | 3.4 | 5.09 | 0.5 | 5.448 | 0.112 | 3.2 | 0.16 | 7.2 | 0.203 | 2.033 | 0.3 | 29.88 | 0.3 | 22.04 | 0.2 | 0.447 | 0.9 |
| 04-6-11 Mnz2-28 | 0.229 | 3.4 | 5.50 | 0.5 | 5.859 | 0.142 | 2.9 | 0.25 | 5.0 | 0.329 | 2.222 | 0.3 | 32.34 | 0.2 | 26.66 | 0.2 | 0.464 | 0.9 |

| | $UO_2$ | | $ThO_2$ | | | PbO | | $Y_2O_3$ | | | CaO | | $Ce_2O_3$ | | $P_2O_5$ | | $SiO_2$ | |
|---|---|---|---|---|---|---|---|---|---|---|---|---|---|---|---|---|---|---|
| Sample | wt. % | RSD (2σ%) | wt. % | RSD (2σ%) | k-raw | wt. % | RSD (2σ%) | wt. % | RSD (2σ%) | k-raw | wt. % | RSD (2σ%) | wt. % | RSD (2σ%) | wt. % | RSD (2σ%) | wt. % | RSD (2σ%) |
| 04-6-11 Mnz2-29 | 0.201 | 3.8 | 5.22 | 0.5 | 5.561 | 0.138 | 3.0 | 0.16 | 7.7 | 0.206 | 2.338 | 0.3 | 32.40 | 0.2 | 25.65 | 0.2 | 0.486 | 0.9 |
| 04-6-11 Mnz2-30 | 0.206 | 3.8 | 5.34 | 0.5 | 5.692 | 0.150 | 2.7 | 0.15 | 8.1 | 0.193 | 1.956 | 0.3 | 32.25 | 0.2 | 25.03 | 0.2 | 0.749 | 0.6 |
| 04-6-11 Mnz2-31 | 0.219 | 3.6 | 5.43 | 0.5 | 5.779 | 0.143 | 2.9 | 0.12 | 10.7 | 0.150 | 1.958 | 0.3 | 32.82 | 0.2 | 26.37 | 0.2 | 0.673 | 0.7 |
| 04-6-11 Mnz2-32 | 0.179 | 4.1 | 3.92 | 0.6 | 4.182 | 0.121 | 3.2 | 0.07 | 15.3 | 0.084 | 1.535 | 0.3 | 28.90 | 0.3 | 18.41 | 0.2 | 3.418 | 0.2 |
| 04-6-11 Mnz2-33 | 0.166 | 4.4 | 4.70 | 0.5 | 5.132 | 0.082 | 3.7 | 0.06 | 14.0 | 0.082 | 1.837 | 0.3 | 26.48 | 0.3 | 12.86 | 0.3 | 0.606 | 0.6 |
| 04-6-11 Mnz2-34 | 0.211 | 3.7 | 5.09 | 0.5 | 5.412 | 0.145 | 2.9 | 0.15 | 8.6 | 0.189 | 1.939 | 0.3 | 32.45 | 0.2 | 26.23 | 0.2 | 0.813 | 0.6 |
| 04-6-11 Mnz2-35 | 0.198 | 3.6 | 3.65 | 0.6 | 3.684 | 0.102 | 3.5 | 0.16 | 7.3 | 0.183 | 1.087 | 0.4 | 18.51 | 0.3 | 17.06 | 0.2 | 45.084 | 0.0 |
| treb | 1.048 | 0.9 | 17.35 | 0.3 | 18.787 | 0.229 | 1.9 | 2.96 | 0.6 | 4.064 | 1.957 | 0.3 | 19.94 | 0.3 | 22.92 | 0.2 | 2.365 | 0.2 |
| 04-6-11 Mnz1-2 | 0.005 | 96.1 | 0.02 | 32.6 | 0.024 | 0.000 | 100.0 | 0.04 | 21.1 | 0.049 | 0.219 | 1.2 | 0.05 | 30.6 | 0.43 | 3.7 | 18.601 | 0.1 |
| 04-6-11 Mnz1-3 | 0.052 | 13.0 | 0.00 | 100.0 | 0.000 | 0.000 | 100.0 | 0.00 | 100.0 | 0.000 | 0.007 | 33.2 | 0.11 | 16.0 | 1.01 | 2.3 | 35.329 | 0.0 |
| 04-6-11 Mnz1-4 | 0.175 | 4.2 | 5.44 | 0.5 | 5.810 | 0.138 | 2.7 | 0.27 | 4.6 | 0.345 | 2.201 | 0.3 | 30.65 | 0.3 | 23.31 | 0.2 | 1.395 | 0.3 |
| 04-6-11 Mnz1-5 | 0.231 | 3.4 | 5.51 | 0.5 | 5.873 | 0.150 | 2.7 | 0.19 | 6.5 | 0.249 | 2.248 | 0.3 | 32.60 | 0.2 | 26.46 | 0.2 | 0.498 | 0.8 |
| 04-6-11 Mnz1-6 | 0.216 | 3.6 | 4.42 | 0.5 | 4.689 | 0.150 | 2.8 | 0.19 | 6.3 | 0.248 | 1.968 | 0.3 | 30.18 | 0.3 | 24.18 | 0.2 | 1.910 | 0.3 |
| 04-6-11 Mnz1-7 | 0.198 | 3.9 | 5.64 | 0.5 | 6.002 | 0.143 | 2.8 | 0.21 | 6.0 | 0.270 | 2.262 | 0.3 | 32.74 | 0.2 | 26.35 | 0.2 | 1.057 | 0.4 |
| 04-6-11 Mnz1-8 | 0.000 | 100.0 | 4.65 | 0.5 | 4.861 | 0.072 | 4.3 | 0.17 | 6.4 | 0.220 | 2.974 | 0.2 | 19.96 | 0.3 | 21.06 | 0.2 | 6.815 | 0.1 |
| 04-6-11 Mnz1-9 | 0.156 | 4.3 | 3.88 | 0.6 | 3.999 | 0.085 | 3.8 | 0.29 | 4.5 | 0.365 | 1.359 | 0.4 | 17.40 | 0.4 | 18.03 | 0.2 | 13.945 | 0.1 |
| 04-6-11 Mnz1-10 | 0.063 | 5.4 | 0.86 | 1.6 | 0.850 | 0.041 | 8.1 | 0.10 | 11.1 | 0.117 | 1.359 | 0.4 | 1.66 | 1.4 | 4.37 | 0.6 | 26.589 | 0.1 |
| 04-6-11 Mnz1-11 | 0.036 | 9.8 | 2.69 | 0.7 | 2.723 | 0.016 | 9.9 | 0.10 | 9.4 | 0.120 | 2.241 | 0.3 | 6.44 | 0.6 | 12.84 | 0.3 | 15.325 | 0.1 |
| 04-6-11 Mnz1-12 | 0.138 | 3.9 | 4.82 | 0.5 | 5.026 | 0.039 | 4.5 | 0.18 | 6.0 | 0.236 | 2.063 | 0.3 | 13.49 | 0.4 | 17.08 | 0.2 | 6.232 | 0.1 |
| 04-6-11 Mnz1-13 | 0.178 | 4.0 | 5.87 | 0.5 | 6.223 | 0.126 | 3.0 | 0.07 | 17.8 | 0.094 | 2.234 | 0.3 | 30.57 | 0.3 | 26.18 | 0.2 | 2.996 | 0.2 |
| 04-6-11 Mnz1-14 | 0.039 | 16.1 | 1.59 | 1.0 | 1.592 | 0.052 | 6.2 | 0.00 | 100.0 | 0.000 | 0.806 | 0.5 | 15.28 | 0.4 | 5.51 | 0.4 | 54.120 | 0.0 |
| 04-6-11 Mnz1-15 | 0.222 | 3.4 | 4.51 | 0.5 | 4.823 | 0.122 | 3.2 | 0.04 | 25.9 | 0.053 | 2.049 | 0.3 | 30.58 | 0.3 | 20.61 | 0.2 | 1.808 | 0.3 |
| 04-6-11 Mnz1-16 | 0.189 | 3.9 | 5.67 | 0.5 | 6.052 | 0.131 | 2.8 | 0.05 | 25.7 | 0.060 | 2.251 | 0.3 | 29.48 | 0.3 | 23.32 | 0.2 | 1.102 | 0.4 |
| 04-6-11 Mnz1-17 | 0.183 | 4.3 | 5.91 | 0.5 | 6.243 | 0.157 | 2.6 | 0.28 | 4.4 | 0.374 | 2.069 | 0.3 | 24.05 | 0.3 | 25.77 | 0.2 | 0.633 | 0.7 |
| 04-6-11 Mnz1-18 | 0.166 | 4.7 | 5.11 | 0.5 | 5.435 | 0.145 | 2.8 | 0.28 | 4.5 | 0.359 | 2.012 | 0.3 | 30.54 | 0.3 | 25.56 | 0.2 | 0.621 | 0.7 |
| 04-6-11 Mnz1-19 | 0.155 | 4.6 | 3.46 | 0.6 | 3.584 | 0.119 | 2.6 | 0.32 | 3.3 | 0.413 | 1.867 | 0.3 | 12.98 | 0.4 | 15.31 | 0.2 | 7.936 | 0.1 |
| 04-6-11 Mnz1-20 | 0.189 | 4.1 | 5.92 | 0.5 | 6.301 | 0.149 | 2.8 | 0.32 | 4.1 | 0.413 | 2.644 | 0.2 | 30.88 | 0.3 | 26.22 | 0.2 | 0.640 | 0.7 |
| 04-6-11 Mnz1-21 | 0.196 | 4.1 | 6.00 | 0.5 | 6.327 | 0.171 | 2.4 | 0.29 | 4.3 | 0.385 | 2.838 | 0.2 | 21.07 | 0.3 | 25.46 | 0.2 | 0.606 | 0.7 |
| 04-6-11 Mnz1-22 | 0.179 | 4.5 | 5.69 | 0.5 | 5.976 | 0.165 | 2.5 | 0.29 | 4.1 | 0.396 | 2.962 | 0.2 | 17.56 | 0.3 | 24.82 | 0.2 | 0.565 | 0.7 |
| 04-6-11 Mnz1-23 | 0.283 | 2.6 | 5.97 | 0.5 | 6.311 | 0.189 | 1.9 | 0.29 | 4.4 | 0.384 | 2.394 | 0.3 | 24.43 | 0.3 | 25.74 | 0.2 | 1.172 | 0.4 |
| 04-6-11 Mnz1-24 | 0.023 | 19.7 | 5.28 | 0.5 | 5.543 | 0.071 | 4.1 | 0.24 | 5.6 | 0.321 | 2.104 | 0.3 | 22.93 | 0.3 | 25.32 | 0.2 | 2.653 | 0.2 |
| 04-6-11 Mnz1-25 | 0.166 | 4.4 | 5.51 | 0.5 | 5.853 | 0.132 | 3.1 | 0.23 | 5.7 | 0.304 | 2.210 | 0.3 | 32.29 | 0.2 | 27.77 | 0.2 | 0.666 | 0.7 |
| 04-6-11 Mnz1-26 | 0.039 | 13.6 | 4.84 | 0.5 | 5.104 | 0.071 | 4.1 | 0.18 | 6.8 | 0.232 | 2.276 | 0.3 | 23.25 | 0.3 | 22.11 | 0.2 | 3.385 | 0.2 |
| 04-6-11 Mnz1-27 | 0.215 | 3.6 | 5.11 | 0.5 | 5.442 | 0.147 | 2.8 | 0.26 | 4.7 | 0.340 | 2.092 | 0.3 | 32.55 | 0.2 | 25.73 | 0.2 | 0.708 | 0.6 |
| 04-6-11 Mnz1-28 | 0.042 | 16.0 | 0.00 | 100.0 | 0.000 | 0.000 | 100.0 | 0.00 | 100.0 | 0.000 | 0.012 | 18.5 | 0.19 | 10.0 | 1.05 | 2.2 | 34.981 | 0.0 |
| 04-6-11 Mnz1-29 | 0.022 | 30.1 | 0.03 | 38.9 | 0.025 | 0.000 | 100.0 | 0.00 | 100.0 | 0.000 | 0.007 | 33.5 | 0.12 | 14.8 | 0.98 | 2.4 | 34.832 | 0.0 |

| | $UO_2$ | | $ThO_2$ | | | PbO | | $Y_2O_3$ | | | CaO | | $Ce_2O_3$ | | $P_2O_5$ | | $SiO_2$ | |
|---|---|---|---|---|---|---|---|---|---|---|---|---|---|---|---|---|---|---|
| Sample | wt. % | RSD (2σ%) | wt. % | RSD (2σ%) | k-raw | wt. % | RSD (2σ%) | wt. % | RSD (2σ%) | k-raw | wt. % | RSD (2σ%) | wt. % | RSD (2σ%) | wt. % | RSD (2σ%) | wt. % | RSD (2σ%) |
| 04-6-11 Mnz1-30 | 0.050 | 13.6 | 0.00 | 100.0 | 0.000 | 0.000 | 100.0 | 0.00 | 100.0 | 0.000 | 0.007 | 35.4 | 0.07 | 24.0 | 1.03 | 2.2 | 34.705 | 0.0 |
| 04-6-11 Mnz1-31 | 0.066 | 10.7 | 1.12 | 1.3 | 1.112 | 0.031 | 11.0 | 0.01 | 263.1 | 0.006 | 0.358 | 0.9 | 6.46 | 0.6 | 6.51 | 0.5 | 30.642 | 0.1 |
| 04-6-11 Mnz1-32 | 0.235 | 3.3 | 5.51 | 0.5 | 5.856 | 0.140 | 2.9 | 0.25 | 5.1 | 0.322 | 2.177 | 0.3 | 30.60 | 0.3 | 26.62 | 0.2 | 0.439 | 0.9 |
| 04-6-11 Mnz1-33 | 0.245 | 3.2 | 5.50 | 0.5 | 5.842 | 0.150 | 2.7 | 0.26 | 4.9 | 0.338 | 2.433 | 0.3 | 29.26 | 0.3 | 26.51 | 0.2 | 0.427 | 1.0 |
| 04-6-11 Mnz1-34 | 0.194 | 4.0 | 5.31 | 0.5 | 5.655 | 0.140 | 2.9 | 0.25 | 5.1 | 0.321 | 2.116 | 0.3 | 32.26 | 0.2 | 26.45 | 0.2 | 0.484 | 0.9 |
| 04-6-11 Mnz1-35 | 0.151 | 4.9 | 5.97 | 0.5 | 6.337 | 0.153 | 2.8 | 0.33 | 4.3 | 0.430 | 2.104 | 0.3 | 32.62 | 0.2 | 29.06 | 0.2 | 0.766 | 0.6 |
| treb | 1.202 | 0.8 | 17.13 | 0.3 | 18.557 | 0.188 | 2.1 | 2.94 | 0.6 | 4.082 | 1.396 | 0.4 | 15.62 | 0.4 | 21.60 | 0.2 | 1.929 | 0.3 |
| treb | 0.950 | 1.0 | 16.11 | 0.3 | 17.413 | 0.212 | 2.0 | 2.95 | 0.6 | 4.028 | 1.805 | 0.3 | 20.61 | 0.3 | 22.77 | 0.2 | 2.216 | 0.2 |
| 04-6-11 Mnz1-38 | 0.069 | 10.5 | 4.28 | 0.5 | 4.613 | 0.076 | 4.6 | 0.13 | 7.7 | 0.171 | 2.517 | 0.2 | 29.75 | 0.3 | 17.52 | 0.2 | 0.493 | 0.8 |
| 04-6-11 Mnz1-39 | 0.171 | 4.6 | 5.31 | 0.5 | 5.615 | 0.138 | 2.9 | 0.30 | 4.1 | 0.400 | 2.942 | 0.2 | 24.92 | 0.3 | 25.54 | 0.2 | 0.514 | 0.8 |
| 04-6-11 Mnz1-40 | 0.221 | 3.6 | 5.50 | 0.5 | 5.800 | 0.149 | 2.8 | 0.12 | 10.0 | 0.164 | 2.299 | 0.3 | 22.87 | 0.3 | 26.00 | 0.2 | 0.469 | 0.9 |
| 04-6-11 Mnz1-41 | 0.196 | 3.9 | 5.27 | 0.5 | 5.616 | 0.136 | 2.9 | 0.25 | 4.9 | 0.322 | 2.029 | 0.3 | 31.86 | 0.3 | 25.10 | 0.2 | 0.550 | 0.8 |
| 04-6-11 Mnz1-42 | 0.171 | 4.5 | 5.84 | 0.5 | 6.210 | 0.161 | 2.6 | 0.30 | 4.4 | 0.391 | 2.060 | 0.3 | 32.15 | 0.3 | 26.98 | 0.2 | 0.738 | 0.6 |
| 04-6-11 Mnz1-43 | 0.166 | 4.6 | 5.19 | 0.5 | 5.518 | 0.133 | 3.1 | 0.29 | 4.6 | 0.376 | 2.917 | 0.2 | 31.85 | 0.3 | 26.89 | 0.2 | 0.576 | 0.8 |
| 04-6-11 Mnz1-44 | 0.183 | 4.0 | 5.08 | 0.5 | 5.470 | 0.108 | 3.2 | 0.20 | 5.2 | 0.264 | 2.794 | 0.2 | 27.77 | 0.3 | 18.38 | 0.2 | 0.586 | 0.7 |
| 04-6-11 Mnz1-45 | 0.167 | 4.5 | 5.64 | 0.5 | 5.999 | 0.140 | 2.9 | 0.30 | 4.4 | 0.385 | 2.702 | 0.2 | 31.50 | 0.3 | 26.49 | 0.2 | 0.699 | 0.6 |
| 04-6-11 Mnz1-46 | 0.192 | 4.0 | 5.41 | 0.5 | 5.757 | 0.129 | 3.1 | 0.27 | 4.8 | 0.349 | 2.208 | 0.3 | 32.58 | 0.2 | 27.04 | 0.2 | 0.498 | 0.9 |
| 04-6-11 Mnz1-47 | 0.235 | 3.4 | 5.56 | 0.5 | 5.918 | 0.154 | 2.7 | 0.25 | 5.2 | 0.327 | 2.179 | 0.3 | 32.67 | 0.2 | 27.37 | 0.2 | 0.476 | 0.9 |
| 04-6-11 Mnz1-48 | 0.238 | 3.2 | 5.62 | 0.5 | 5.970 | 0.142 | 2.8 | 0.20 | 6.7 | 0.256 | 2.219 | 0.3 | 31.55 | 0.3 | 27.42 | 0.2 | 0.459 | 1.0 |
| 04-6-11 Mnz1-49 | 0.227 | 3.5 | 5.66 | 0.5 | 5.993 | 0.158 | 2.6 | 0.20 | 6.0 | 0.271 | 2.347 | 0.3 | 25.69 | 0.3 | 25.72 | 0.2 | 0.463 | 0.9 |
| 04-6-11 Mnz1-50 | 0.260 | 3.0 | 5.64 | 0.5 | 6.001 | 0.170 | 2.3 | 0.20 | 6.2 | 0.265 | 2.298 | 0.3 | 29.56 | 0.3 | 25.46 | 0.2 | 0.466 | 0.9 |
| 04-6-11 Mnz1-51 | 0.206 | 3.8 | 5.52 | 0.5 | 5.872 | 0.143 | 2.9 | 0.28 | 4.6 | 0.370 | 2.109 | 0.3 | 31.65 | 0.3 | 26.69 | 0.2 | 0.486 | 0.9 |
| 04-6-11 Mnz1-52 | 0.173 | 4.4 | 4.25 | 0.6 | 4.571 | 0.119 | 3.2 | 0.01 | 86.6 | 0.015 | 1.892 | 0.3 | 31.11 | 0.3 | 19.70 | 0.2 | 0.507 | 0.8 |
| 04-6-11 Mnz1-53 | 0.172 | 4.5 | 5.24 | 0.5 | 5.577 | 0.137 | 3.0 | 0.28 | 4.6 | 0.360 | 1.943 | 0.3 | 32.19 | 0.2 | 25.96 | 0.2 | 0.574 | 0.7 |
| 04-6-11 Mnz1-54 | 0.189 | 4.2 | 5.62 | 0.5 | 5.935 | 0.163 | 2.5 | 0.31 | 4.0 | 0.417 | 3.246 | 0.2 | 22.05 | 0.3 | 24.95 | 0.2 | 0.583 | 0.7 |
| 04-6-11 Mnz1-55 | 0.189 | 4.2 | 5.76 | 0.5 | 6.086 | 0.160 | 2.6 | 0.31 | 4.0 | 0.421 | 3.294 | 0.2 | 21.84 | 0.3 | 24.67 | 0.2 | 0.595 | 0.7 |
| 04-6-11 Mnz1-56 | 0.130 | 5.9 | 5.43 | 0.5 | 5.767 | 0.140 | 3.0 | 0.35 | 4.0 | 0.460 | 2.283 | 0.3 | 32.79 | 0.2 | 27.51 | 0.2 | 1.015 | 0.5 |
| 04-6-11 Mnz1-57 | 0.173 | 4.4 | 4.97 | 0.5 | 5.303 | 0.130 | 3.0 | 0.25 | 4.8 | 0.329 | 1.936 | 0.3 | 31.72 | 0.3 | 24.16 | 0.2 | 0.727 | 0.6 |
| 04-6-11 Mnz1-58 | 0.159 | 4.9 | 5.33 | 0.5 | 5.612 | 0.134 | 3.1 | 0.28 | 4.5 | 0.373 | 1.977 | 0.3 | 22.24 | 0.3 | 25.99 | 0.2 | 0.545 | 0.8 |
| 04-6-11 Mnz1-59 | 0.166 | 4.7 | 4.79 | 0.5 | 5.089 | 0.126 | 3.2 | 0.31 | 4.2 | 0.398 | 2.321 | 0.3 | 30.44 | 0.3 | 25.55 | 0.2 | 0.547 | 0.8 |
| 04-6-11 Mnz1-60 | 0.175 | 4.5 | 5.52 | 0.5 | 5.861 | 0.141 | 2.9 | 0.32 | 4.1 | 0.414 | 1.949 | 0.3 | 29.67 | 0.3 | 25.87 | 0.2 | 0.593 | 0.7 |
| 04-6-11 Mnz1-61 | 0.159 | 4.9 | 5.39 | 0.5 | 5.685 | 0.139 | 2.9 | 0.28 | 4.5 | 0.373 | 1.955 | 0.3 | 23.61 | 0.3 | 25.69 | 0.2 | 0.541 | 0.8 |
| 04-6-11 Mnz1-62 | 0.161 | 4.8 | 5.31 | 0.5 | 5.642 | 0.141 | 2.9 | 0.27 | 4.7 | 0.356 | 1.953 | 0.3 | 30.59 | 0.3 | 25.93 | 0.2 | 0.522 | 0.8 |
| 04-6-11 Mnz1-63 | 0.228 | 3.5 | 5.48 | 0.5 | 5.781 | 0.144 | 2.9 | 0.28 | 4.5 | 0.368 | 2.168 | 0.3 | 22.95 | 0.3 | 25.67 | 0.2 | 0.454 | 0.9 |
| 04-6-11 Mnz1-64 | 0.242 | 3.3 | 5.56 | 0.5 | 5.927 | 0.160 | 2.6 | 0.29 | 4.5 | 0.373 | 2.189 | 0.3 | 32.30 | 0.2 | 26.20 | 0.2 | 0.480 | 0.9 |
| 04-6-11 Mnz1-65 | 0.214 | 3.7 | 5.59 | 0.5 | 5.894 | 0.146 | 2.8 | 0.20 | 6.1 | 0.272 | 2.305 | 0.3 | 21.33 | 0.3 | 25.78 | 0.2 | 0.448 | 0.9 |

| | $UO_2$ | | $ThO_2$ | | | PbO | | $Y_2O_3$ | | | CaO | | $Ce_2O_3$ | | $P_2O_5$ | | $SiO_2$ | |
|---|---|---|---|---|---|---|---|---|---|---|---|---|---|---|---|---|---|---|
| Sample | wt. % | RSD (2σ%) | wt. % | RSD (2σ%) | k-raw | wt. % | RSD (2σ%) | wt. % | RSD (2σ%) | k-raw | wt. % | RSD (2σ%) | wt. % | RSD (2σ%) | wt. % | RSD (2σ%) | wt. % | RSD (2σ%) |
| 04-6-11 Mnz1-66 | 0.226 | 3.4 | 5.06 | 0.5 | 5.457 | 0.104 | 3.6 | 0.16 | 7.4 | 0.202 | 2.080 | 0.3 | 30.85 | 0.3 | 19.40 | 0.2 | 0.386 | 1.0 |
| 04-6-11 Mnz1-67 | 0.095 | 7.8 | 5.60 | 0.5 | 6.002 | 0.109 | 3.5 | 0.23 | 5.1 | 0.299 | 2.071 | 0.3 | 31.37 | 0.3 | 22.27 | 0.2 | 0.790 | 0.5 |
| 04-6-11 Mnz1-68 | 0.151 | 5.0 | 5.55 | 0.5 | 5.918 | 0.135 | 2.9 | 0.10 | 12.9 | 0.125 | 2.130 | 0.3 | 31.61 | 0.3 | 25.06 | 0.2 | 0.726 | 0.6 |
| 04-6-11 Mnz1-69 | 0.209 | 3.8 | 5.87 | 0.5 | 6.193 | 0.148 | 2.8 | 0.16 | 7.8 | 0.209 | 2.320 | 0.3 | 22.05 | 0.3 | 25.52 | 0.2 | 0.554 | 0.8 |
| 04-6-11 Mnz1-70 | 0.231 | 3.4 | 5.78 | 0.5 | 6.154 | 0.158 | 2.6 | 0.19 | 6.7 | 0.247 | 2.359 | 0.3 | 30.57 | 0.3 | 25.83 | 0.2 | 0.476 | 0.9 |
| 04-6-11 Mnz1-71 | 0.233 | 3.4 | 6.06 | 0.5 | 6.402 | 0.158 | 2.6 | 0.21 | 6.0 | 0.277 | 2.399 | 0.3 | 22.24 | 0.3 | 25.55 | 0.2 | 0.481 | 0.9 |
| 04-6-11 Mnz1-72 | 0.232 | 3.5 | 5.73 | 0.5 | 6.037 | 0.146 | 2.8 | 0.19 | 6.5 | 0.254 | 2.410 | 0.3 | 21.00 | 0.3 | 25.29 | 0.2 | 0.453 | 0.9 |
| 04-6-11 Mnz1-73 | 0.212 | 3.7 | 5.42 | 0.5 | 5.771 | 0.142 | 2.9 | 0.24 | 5.3 | 0.316 | 2.287 | 0.3 | 30.72 | 0.3 | 25.84 | 0.2 | 0.445 | 0.9 |
| 04-6-11 Mnz1-74 | 0.219 | 3.6 | 5.39 | 0.5 | 5.728 | 0.148 | 2.8 | 0.26 | 4.9 | 0.338 | 2.214 | 0.3 | 30.70 | 0.3 | 26.02 | 0.2 | 0.451 | 0.9 |
| 04-6-11 Mnz1-75 | 0.240 | 3.3 | 5.59 | 0.5 | 5.950 | 0.155 | 2.6 | 0.25 | 5.1 | 0.332 | 2.195 | 0.3 | 30.64 | 0.3 | 26.09 | 0.2 | 0.466 | 0.9 |
| 04-6-11 Mnz1-76 | 0.161 | 4.8 | 5.20 | 0.5 | 5.527 | 0.140 | 2.9 | 0.30 | 4.3 | 0.389 | 1.974 | 0.3 | 31.02 | 0.3 | 25.90 | 0.2 | 0.547 | 0.8 |
| 04-6-11 Mnz1-77 | 0.169 | 4.7 | 5.35 | 0.5 | 5.638 | 0.141 | 2.9 | 0.33 | 3.8 | 0.442 | 2.326 | 0.3 | 22.43 | 0.3 | 25.30 | 0.2 | 0.538 | 0.8 |
| treb | 0.979 | 1.0 | 16.51 | 0.3 | 17.834 | 0.227 | 1.9 | 2.94 | 0.6 | 4.024 | 1.840 | 0.3 | 20.00 | 0.3 | 23.06 | 0.2 | 2.278 | 0.2 |
| treb | 1.007 | 0.9 | 16.78 | 0.3 | 18.148 | 0.234 | 1.9 | 2.91 | 0.6 | 3.990 | 1.874 | 0.3 | 19.96 | 0.3 | 23.09 | 0.2 | 2.315 | 0.2 |
| 04-6-11 Mnz1-80 | 0.163 | 4.8 | 5.08 | 0.5 | 5.343 | 0.135 | 3.0 | 0.31 | 4.1 | 0.412 | 2.525 | 0.3 | 20.97 | 0.3 | 25.08 | 0.2 | 0.517 | 0.8 |
| 04-6-11 Mnz1-81 | 0.234 | 3.4 | 5.40 | 0.5 | 5.758 | 0.141 | 2.9 | 0.25 | 5.1 | 0.325 | 2.202 | 0.3 | 31.64 | 0.3 | 25.66 | 0.2 | 0.452 | 0.9 |
| 04-6-11 Mnz1-82 | 0.228 | 3.4 | 5.50 | 0.5 | 5.856 | 0.143 | 2.8 | 0.24 | 5.3 | 0.313 | 2.242 | 0.3 | 31.12 | 0.3 | 25.88 | 0.2 | 0.457 | 0.9 |
| 04-6-11 Mnz1-83 | 0.226 | 3.5 | 5.48 | 0.5 | 5.841 | 0.144 | 2.8 | 0.21 | 6.2 | 0.269 | 2.271 | 0.3 | 31.36 | 0.3 | 25.90 | 0.2 | 0.457 | 0.9 |
| 04-6-11 Mnz1-84 | 0.231 | 3.4 | 5.91 | 0.5 | 6.299 | 0.151 | 2.7 | 0.19 | 6.8 | 0.244 | 2.384 | 0.3 | 31.04 | 0.3 | 26.05 | 0.2 | 0.499 | 0.8 |
| 04-6-11 Mnz1-85 | 0.167 | 4.7 | 5.25 | 0.5 | 5.580 | 0.132 | 3.1 | 0.33 | 4.0 | 0.426 | 2.234 | 0.3 | 30.54 | 0.3 | 25.77 | 0.2 | 0.571 | 0.8 |
| 04-6-11 Mnz1-86 | 0.216 | 3.6 | 5.61 | 0.5 | 5.953 | 0.156 | 2.6 | 0.21 | 6.1 | 0.274 | 2.218 | 0.3 | 27.23 | 0.3 | 25.77 | 0.2 | 0.480 | 0.9 |
| 04-6-11 Mnz1-87 | 0.151 | 5.1 | 5.13 | 0.5 | 5.461 | 0.136 | 3.0 | 0.28 | 4.6 | 0.363 | 1.947 | 0.3 | 32.17 | 0.3 | 25.48 | 0.2 | 0.724 | 0.6 |
| 04-6-11 Mnz1-88 | 0.170 | 4.6 | 5.39 | 0.5 | 5.673 | 0.157 | 2.6 | 0.30 | 4.2 | 0.406 | 3.262 | 0.2 | 19.82 | 0.3 | 24.86 | 0.2 | 0.527 | 0.8 |
| 04-6-11 Mnz1-89 | 0.040 | 16.6 | 0.03 | 33.4 | 0.029 | 0.000 | 100.0 | 0.01 | 247.8 | 0.006 | 0.009 | 25.6 | 0.13 | 14.4 | 0.91 | 2.6 | 35.598 | 0.0 |
| 04-6-11 Mnz1-90 | 0.145 | 5.3 | 5.04 | 0.5 | 5.345 | 0.134 | 3.0 | 0.26 | 5.0 | 0.336 | 2.266 | 0.3 | 28.81 | 0.3 | 23.84 | 0.2 | 2.908 | 0.2 |
| 04-6-11 Mnz1-91 | 0.198 | 3.9 | 5.75 | 0.5 | 6.123 | 0.147 | 2.8 | 0.36 | 3.7 | 0.465 | 2.342 | 0.3 | 30.83 | 0.3 | 25.66 | 0.2 | 0.681 | 0.7 |
| 04-6-11 Mnz1-92 | 0.217 | 3.7 | 5.50 | 0.5 | 5.799 | 0.146 | 2.8 | 0.26 | 4.9 | 0.341 | 2.182 | 0.3 | 22.74 | 0.3 | 25.66 | 0.2 | 0.470 | 0.9 |
| 04-6-11 Mnz1-93 | 0.199 | 3.9 | 5.70 | 0.5 | 6.080 | 0.143 | 2.9 | 0.34 | 3.8 | 0.447 | 2.512 | 0.3 | 31.35 | 0.3 | 25.27 | 0.2 | 0.637 | 0.7 |
| 04-6-11 Mnz1-94 | 0.194 | 4.1 | 5.62 | 0.5 | 5.946 | 0.146 | 2.8 | 0.34 | 3.8 | 0.449 | 2.999 | 0.2 | 23.38 | 0.3 | 25.10 | 0.2 | 0.595 | 0.7 |
| 04-6-11 Mnz1-95 | 0.160 | 4.4 | 4.16 | 0.6 | 4.432 | 0.081 | 4.6 | 0.28 | 4.9 | 0.362 | 2.051 | 0.3 | 21.01 | 0.3 | 17.69 | 0.2 | 0.489 | 0.9 |
| Trebilcock-4 | 0.996 | 1.0 | 16.69 | 0.3 | 18.050 | 0.222 | 1.9 | 2.93 | 0.6 | 4.015 | 1.882 | 0.3 | 20.15 | 0.3 | 23.05 | 0.2 | 2.314 | 0.2 |
| Trebilcock-5 | 1.012 | 0.9 | 16.74 | 0.3 | 18.095 | 0.233 | 1.9 | 2.92 | 0.6 | 4.001 | 1.865 | 0.3 | 20.23 | 0.3 | 23.14 | 0.2 | 2.320 | 0.2 |
| Trebilcock-6 | 0.961 | 1.0 | 16.27 | 0.3 | 17.577 | 0.218 | 2.0 | 2.96 | 0.6 | 4.044 | 1.829 | 0.3 | 20.56 | 0.3 | 23.17 | 0.2 | 2.253 | 0.2 |
| Trebilcock-7 | 1.016 | 0.9 | 16.79 | 0.3 | 18.170 | 0.221 | 1.9 | 2.91 | 0.6 | 3.988 | 1.884 | 0.3 | 20.29 | 0.3 | 22.93 | 0.2 | 2.338 | 0.2 |
| Trebilcock-8 | 1.064 | 0.9 | 17.40 | 0.3 | 18.845 | 0.239 | 1.8 | 2.94 | 0.6 | 4.035 | 1.963 | 0.3 | 19.95 | 0.3 | 22.88 | 0.2 | 2.416 | 0.2 |
| Trebilcock-9 | 1.069 | 0.9 | 17.45 | 0.3 | 18.959 | 0.223 | 1.9 | 3.00 | 0.6 | 4.105 | 1.926 | 0.3 | 20.14 | 0.3 | 21.55 | 0.2 | 2.371 | 0.2 |

| | $UO_2$ | | $ThO_2$ | | | PbO | | $Y_2O_3$ | | | CaO | | $Ce_2O_3$ | | $P_2O_5$ | | $SiO_2$ | |
|---|---|---|---|---|---|---|---|---|---|---|---|---|---|---|---|---|---|---|
| Sample | wt. % | RSD (2σ%) | wt. % | RSD (2σ%) | k-raw | wt. % | RSD (2σ%) | wt. % | RSD (2σ%) | k-raw | wt. % | RSD (2σ%) | wt. % | RSD (2σ%) | wt. % | RSD (2σ%) | wt. % | RSD (2σ%) |
| TU-1 117531 Spot-1 | 0.767 | 1.1 | 13.80 | 0.3 | 14.881 | 0.176 | 2.7 | 2.31 | 0.7 | 3.107 | 1.613 | 0.3 | 26.79 | 0.3 | 24.84 | 0.2 | 1.876 | 0.3 |
| TU-1 117531 Spot-2 | 0.746 | 1.1 | 13.68 | 0.3 | 14.746 | 0.185 | 2.6 | 2.31 | 0.7 | 3.101 | 1.605 | 0.3 | 26.97 | 0.3 | 24.95 | 0.2 | 1.855 | 0.3 |
| TU-1 117531 Spot-3 | 0.760 | 1.1 | 13.72 | 0.3 | 14.783 | 0.182 | 2.7 | 2.33 | 0.7 | 3.124 | 1.601 | 0.3 | 27.01 | 0.3 | 24.89 | 0.2 | 1.865 | 0.3 |
| TU-1 117531 Spot-4 | 0.753 | 1.1 | 13.69 | 0.3 | 14.758 | 0.184 | 2.6 | 2.33 | 0.7 | 3.133 | 1.601 | 0.3 | 26.97 | 0.3 | 24.87 | 0.2 | 1.864 | 0.3 |
| TU-1 117531 Spot-5 | 0.770 | 1.1 | 13.80 | 0.3 | 14.871 | 0.181 | 2.7 | 2.34 | 0.7 | 3.142 | 1.612 | 0.3 | 26.68 | 0.3 | 24.79 | 0.2 | 1.896 | 0.3 |
| TU-1 117531 Spot-6 | 0.767 | 1.1 | 13.69 | 0.3 | 14.763 | 0.182 | 2.6 | 2.25 | 0.7 | 3.022 | 1.598 | 0.3 | 26.77 | 0.3 | 24.72 | 0.2 | 1.855 | 0.3 |
| TU-1 117531 Spot-7 | 0.752 | 1.1 | 13.74 | 0.3 | 14.811 | 0.183 | 2.6 | 2.25 | 0.7 | 3.021 | 1.600 | 0.3 | 26.81 | 0.3 | 24.67 | 0.2 | 1.863 | 0.3 |
| TU-1 117531 Spot-8 | 0.780 | 1.0 | 13.88 | 0.3 | 14.970 | 0.191 | 2.5 | 2.28 | 0.7 | 3.058 | 1.611 | 0.3 | 26.75 | 0.3 | 24.82 | 0.2 | 1.909 | 0.3 |
| TU-1 117531 Spot-9 | 0.770 | 1.1 | 13.98 | 0.3 | 15.079 | 0.187 | 2.6 | 2.28 | 0.7 | 3.063 | 1.618 | 0.3 | 26.67 | 0.3 | 24.65 | 0.2 | 1.914 | 0.3 |
| TU-1 117531 Spot-10 | 0.769 | 1.1 | 13.88 | 0.3 | 14.964 | 0.184 | 2.6 | 2.28 | 0.7 | 3.057 | 1.609 | 0.3 | 26.71 | 0.3 | 24.73 | 0.2 | 1.915 | 0.3 |
| TU-1 117531 Spot-14 | 0.770 | 1.1 | 13.80 | 0.3 | 14.881 | 0.183 | 2.6 | 2.18 | 0.7 | 2.921 | 1.721 | 0.3 | 27.12 | 0.3 | 24.96 | 0.2 | 1.903 | 0.3 |
| TU-1 117531 Spot-15 | 0.749 | 1.1 | 13.74 | 0.3 | 14.813 | 0.184 | 2.6 | 2.23 | 0.7 | 2.991 | 1.719 | 0.3 | 27.00 | 0.3 | 24.98 | 0.2 | 1.901 | 0.3 |
| TU-1 117531 Spot-16 | 0.763 | 1.1 | 13.54 | 0.3 | 14.585 | 0.179 | 2.7 | 2.19 | 0.7 | 2.942 | 1.692 | 0.3 | 26.96 | 0.3 | 25.04 | 0.2 | 1.855 | 0.3 |
| TU-1 117531 Spot-17 | 0.753 | 1.1 | 13.58 | 0.3 | 14.635 | 0.188 | 2.6 | 2.20 | 0.7 | 2.944 | 1.697 | 0.3 | 27.00 | 0.3 | 24.86 | 0.2 | 1.858 | 0.3 |
| TU-1 117531 Spot-18 | 0.750 | 1.1 | 13.59 | 0.3 | 14.653 | 0.178 | 2.7 | 2.18 | 0.7 | 2.918 | 1.705 | 0.3 | 27.01 | 0.3 | 24.88 | 0.2 | 1.875 | 0.3 |
| 04-6-19-mnz5-spot1 | 0.306 | 2.3 | 5.64 | 0.5 | 6.030 | 0.167 | 2.8 | 0.04 | 26.0 | 0.051 | 1.344 | 0.4 | 33.19 | 0.3 | 25.83 | 0.2 | 0.317 | 1.2 |
| 04-6-19-mnz5-spot2 | 0.275 | 2.5 | 5.21 | 0.5 | 5.564 | 0.130 | 3.4 | 0.04 | 25.5 | 0.051 | 1.186 | 0.4 | 30.88 | 0.3 | 23.39 | 0.2 | 0.841 | 0.5 |
| 04-6-19-mnz5-spot3 | 0.416 | 1.7 | 4.51 | 0.5 | 4.761 | 0.137 | 3.3 | 0.07 | 14.8 | 0.090 | 1.017 | 0.5 | 30.28 | 0.3 | 23.96 | 0.2 | 4.834 | 0.1 |
| 04-6-19-mnz5-spot4 | 0.498 | 1.5 | 4.38 | 0.5 | 4.664 | 0.155 | 3.0 | 0.15 | 7.1 | 0.194 | 1.169 | 0.4 | 33.29 | 0.3 | 26.17 | 0.2 | 0.219 | 1.6 |
| 04-6-19-mnz5-spot5 | 0.523 | 1.4 | 4.07 | 0.6 | 4.332 | 0.147 | 3.1 | 0.17 | 6.3 | 0.218 | 1.097 | 0.4 | 33.45 | 0.3 | 26.35 | 0.2 | 0.224 | 1.6 |
| 04-6-19-mnz5-spot6 | 0.707 | 1.1 | 3.83 | 0.6 | 4.067 | 0.151 | 3.0 | 0.29 | 3.8 | 0.373 | 1.043 | 0.4 | 33.42 | 0.3 | 26.22 | 0.2 | 0.211 | 1.7 |
| 04-6-19-mnz5-spot7 | 0.686 | 1.1 | 3.82 | 0.6 | 4.056 | 0.174 | 2.6 | 0.30 | 3.6 | 0.392 | 1.046 | 0.4 | 33.33 | 0.3 | 26.17 | 0.2 | 0.199 | 1.8 |
| 04-6-19-mnz5-spot8 | 0.889 | 0.8 | 3.11 | 0.7 | 3.295 | 0.150 | 2.8 | 0.16 | 6.3 | 0.216 | 1.799 | 0.3 | 21.62 | 0.3 | 20.55 | 0.2 | 0.388 | 0.9 |
| 04-6-19-mnz5-spot9 | 0.453 | 1.5 | 3.40 | 0.6 | 3.680 | 0.109 | 3.6 | 0.08 | 8.2 | 0.099 | 1.274 | 0.4 | 25.13 | 0.3 | 14.08 | 0.2 | 0.525 | 0.6 |
| 04-6-19-mnz5-spot10 | 0.709 | 1.1 | 3.91 | 0.6 | 4.158 | 0.163 | 2.8 | 0.25 | 4.2 | 0.327 | 1.071 | 0.4 | 33.45 | 0.3 | 26.14 | 0.2 | 0.245 | 1.5 |
| 04-6-19-mnz5-spot11 | 0.938 | 0.9 | 3.57 | 0.6 | 3.792 | 0.176 | 2.6 | 0.22 | 4.7 | 0.289 | 0.960 | 0.5 | 33.44 | 0.3 | 26.02 | 0.2 | 0.234 | 1.6 |
| 04-6-19-mnz5-spot12 | 0.558 | 1.3 | 3.97 | 0.6 | 4.223 | 0.153 | 3.0 | 0.19 | 5.6 | 0.244 | 1.058 | 0.4 | 33.49 | 0.3 | 26.41 | 0.2 | 0.220 | 1.7 |
| 04-6-19-mnz5-spot13 | 0.524 | 1.4 | 4.58 | 0.5 | 4.870 | 0.160 | 2.9 | 0.19 | 5.6 | 0.247 | 1.191 | 0.4 | 32.85 | 0.3 | 26.44 | 0.2 | 0.211 | 1.7 |
| 04-6-19-mnz5-spot14 | 0.513 | 1.5 | 4.57 | 0.5 | 4.857 | 0.164 | 2.8 | 0.21 | 5.2 | 0.267 | 1.194 | 0.4 | 32.98 | 0.3 | 26.59 | 0.2 | 0.207 | 1.8 |
| 04-6-19-mnz5-spot15 | 0.527 | 1.4 | 4.37 | 0.5 | 4.653 | 0.156 | 2.9 | 0.19 | 5.4 | 0.253 | 1.153 | 0.4 | 33.15 | 0.3 | 26.54 | 0.2 | 0.220 | 1.7 |
| 04-6-19-mnz5-spot16 | 0.693 | 1.1 | 3.85 | 0.6 | 4.093 | 0.156 | 3.0 | 0.31 | 3.5 | 0.408 | 1.043 | 0.4 | 33.44 | 0.3 | 26.55 | 0.2 | 0.215 | 1.7 |
| 04-6-19-mnz5-spot17 | 0.839 | 0.9 | 3.92 | 0.6 | 4.167 | 0.168 | 2.8 | 0.20 | 5.3 | 0.257 | 1.030 | 0.4 | 33.42 | 0.3 | 26.28 | 0.2 | 0.235 | 1.6 |
| 04-6-19-mnz5-spot18 | 0.502 | 1.5 | 3.98 | 0.6 | 4.237 | 0.146 | 3.1 | 0.14 | 7.3 | 0.186 | 1.080 | 0.4 | 33.74 | 0.3 | 26.46 | 0.2 | 0.202 | 1.8 |
| 04-6-19-mnz5-spot19 | 0.997 | 0.8 | 3.87 | 0.6 | 4.119 | 0.185 | 2.5 | 0.21 | 5.0 | 0.275 | 1.019 | 0.4 | 33.35 | 0.3 | 26.48 | 0.2 | 0.221 | 1.7 |
| 04-6-19-mnz5-spot20 | 0.959 | 0.8 | 3.99 | 0.6 | 4.241 | 0.192 | 2.4 | 0.20 | 5.2 | 0.263 | 1.067 | 0.4 | 33.11 | 0.3 | 26.38 | 0.2 | 0.225 | 1.6 |

| | $UO_2$ | | $ThO_2$ | | | PbO | | $Y_2O_3$ | | | CaO | | $Ce_2O_3$ | | $P_2O_5$ | | $SiO_2$ | |
|---|---|---|---|---|---|---|---|---|---|---|---|---|---|---|---|---|---|---|
| Sample | wt. % | RSD (2σ%) | wt. % | RSD (2σ%) | k-raw | wt. % | RSD (2σ%) | wt. % | RSD (2σ%) | k-raw | wt. % | RSD (2σ%) | wt. % | RSD (2σ%) | wt. % | RSD (2σ%) | wt. % | RSD (2σ%) |
| 04-6-19-mnz5-spot21 | 1.043 | 0.8 | 4.17 | 0.6 | 4.445 | 0.196 | 2.4 | 0.21 | 5.0 | 0.272 | 1.062 | 0.4 | 33.08 | 0.3 | 26.28 | 0.2 | 0.171 | 2.1 |
| 04-6-19-mnz5-spot22 | 0.357 | 2.0 | 5.08 | 0.5 | 5.412 | 0.157 | 2.9 | 0.05 | 20.7 | 0.063 | 1.224 | 0.4 | 33.32 | 0.3 | 26.32 | 0.2 | 0.242 | 1.5 |
| 04-6-19-mnz5-spot23 | 0.342 | 2.1 | 6.04 | 0.4 | 6.456 | 0.177 | 2.6 | 0.05 | 18.8 | 0.070 | 1.411 | 0.4 | 33.17 | 0.3 | 26.28 | 0.2 | 0.299 | 1.2 |
| 04-6-19-mnz5-spot24 | 0.662 | 1.1 | 4.44 | 0.5 | 4.655 | 0.134 | 3.3 | 0.04 | 25.4 | 0.049 | 1.069 | 0.4 | 29.77 | 0.3 | 22.81 | 0.2 | 11.110 | 0.1 |
| 04-6-19-mnz5-spot25 | 0.451 | 1.6 | 5.60 | 0.5 | 5.940 | 0.164 | 2.8 | 0.04 | 24.8 | 0.052 | 1.315 | 0.4 | 31.13 | 0.3 | 24.60 | 0.2 | 4.820 | 0.1 |
| 04-6-19-mnz5-spot26 | 0.465 | 1.5 | 4.54 | 0.5 | 4.714 | 0.137 | 3.2 | 0.02 | 39.0 | 0.030 | 1.118 | 0.4 | 27.01 | 0.3 | 20.47 | 0.2 | 19.008 | 0.1 |
| 04-6-19-mnz5-spot27 | 0.691 | 1.1 | 3.91 | 0.6 | 4.153 | 0.151 | 3.0 | 0.32 | 3.4 | 0.418 | 1.050 | 0.4 | 33.38 | 0.3 | 26.42 | 0.2 | 0.181 | 1.9 |
| 04-6-19-mnz5-spot28 | 0.481 | 1.5 | 4.16 | 0.6 | 4.424 | 0.156 | 2.9 | 0.17 | 5.8 | 0.224 | 1.118 | 0.4 | 31.55 | 0.3 | 25.41 | 0.2 | 0.133 | 2.5 |
| 04-6-19-mnz5-spot29 | 0.398 | 1.8 | 4.78 | 0.5 | 5.088 | 0.159 | 2.9 | 0.12 | 8.4 | 0.155 | 1.228 | 0.4 | 31.32 | 0.3 | 25.19 | 0.2 | 0.214 | 1.6 |
| 04-6-19-mnz5-spot30 | 0.553 | 1.3 | 3.97 | 0.6 | 4.216 | 0.147 | 3.1 | 0.17 | 6.1 | 0.222 | 1.048 | 0.4 | 32.87 | 0.3 | 26.05 | 0.2 | 0.200 | 1.8 |
| TU-1 117531 Spot-18 | 0.750 | 1.1 | 13.44 | 0.3 | 14.472 | 0.178 | 2.7 | 2.10 | 0.7 | 2.822 | 1.692 | 0.3 | 27.03 | 0.3 | 25.33 | 0.2 | 1.853 | 0.3 |
| TU-1 117531 Spot-19 | 0.757 | 1.1 | 13.42 | 0.3 | 14.453 | 0.180 | 2.7 | 2.11 | 0.7 | 2.823 | 1.680 | 0.3 | 27.01 | 0.3 | 25.24 | 0.2 | 1.865 | 0.3 |
| TU-1 117531 Spot-20 | 0.746 | 1.1 | 13.42 | 0.3 | 14.456 | 0.184 | 2.6 | 2.11 | 0.7 | 2.824 | 1.682 | 0.3 | 27.09 | 0.3 | 25.21 | 0.2 | 1.853 | 0.3 |
| TU-1 117531 Spot-21 | 0.745 | 1.1 | 13.28 | 0.3 | 14.302 | 0.189 | 2.6 | 2.11 | 0.7 | 2.825 | 1.690 | 0.3 | 27.11 | 0.3 | 25.26 | 0.2 | 1.817 | 0.3 |
| TU-1 117531 Spot-22 | 0.757 | 1.1 | 13.61 | 0.3 | 14.664 | 0.182 | 2.7 | 2.14 | 0.7 | 2.874 | 1.707 | 0.3 | 27.03 | 0.3 | 25.29 | 0.2 | 1.881 | 0.3 |
| 04-6-19-mnz4-spot1 | 0.348 | 2.1 | 5.51 | 0.5 | 5.877 | 0.162 | 2.9 | 0.06 | 17.3 | 0.077 | 1.302 | 0.4 | 34.47 | 0.3 | 27.51 | 0.2 | 0.334 | 1.1 |
| 04-6-19-mnz4-spot2 | 0.366 | 2.0 | 5.07 | 0.5 | 5.401 | 0.165 | 2.8 | 0.06 | 16.9 | 0.080 | 1.229 | 0.4 | 34.69 | 0.3 | 27.58 | 0.2 | 0.182 | 1.9 |
| 04-6-19-mnz4-spot3 | 0.388 | 1.9 | 4.98 | 0.5 | 5.305 | 0.162 | 2.9 | 0.06 | 17.1 | 0.079 | 1.224 | 0.4 | 34.63 | 0.3 | 27.60 | 0.2 | 0.155 | 2.3 |
| 04-6-19-mnz4-spot4 | 0.388 | 1.9 | 3.50 | 0.6 | 3.712 | 0.126 | 3.6 | 0.14 | 7.5 | 0.182 | 0.901 | 0.5 | 35.06 | 0.3 | 27.61 | 0.2 | 0.226 | 1.6 |
| 04-6-19-mnz4-spot5 | 0.366 | 1.9 | 3.42 | 0.6 | 3.629 | 0.114 | 3.9 | 0.15 | 6.9 | 0.189 | 0.917 | 0.5 | 32.86 | 0.3 | 25.28 | 0.2 | 0.620 | 0.6 |
| 04-6-19-mnz4-spot6 | 0.403 | 1.8 | 3.56 | 0.6 | 3.781 | 0.127 | 3.6 | 0.13 | 8.1 | 0.168 | 0.979 | 0.5 | 35.17 | 0.3 | 27.78 | 0.2 | 0.227 | 1.6 |
| 04-6-19-mnz4-spot7 | 0.387 | 1.9 | 3.32 | 0.6 | 3.516 | 0.124 | 3.6 | 0.14 | 7.4 | 0.179 | 0.905 | 0.5 | 34.00 | 0.3 | 27.11 | 0.2 | 0.217 | 1.6 |
| 04-6-19-mnz4-spot8 | 0.386 | 1.9 | 3.54 | 0.6 | 3.751 | 0.125 | 3.6 | 0.14 | 7.5 | 0.184 | 0.929 | 0.5 | 35.28 | 0.3 | 27.89 | 0.2 | 0.229 | 1.6 |
| 04-6-19-mnz4-spot9 | 0.401 | 1.8 | 3.64 | 0.6 | 3.867 | 0.129 | 3.5 | 0.12 | 9.0 | 0.151 | 0.984 | 0.5 | 35.19 | 0.3 | 27.75 | 0.2 | 0.231 | 1.6 |
| 04-6-19-mnz4-spot10 | 0.380 | 1.9 | 3.60 | 0.6 | 3.818 | 0.121 | 3.7 | 0.12 | 8.4 | 0.161 | 0.928 | 0.5 | 35.23 | 0.3 | 27.63 | 0.2 | 0.236 | 1.6 |
| TU-1 117531 Spot-23 | 0.749 | 1.1 | 13.25 | 0.3 | 14.312 | 0.179 | 2.7 | 2.10 | 0.7 | 2.827 | 1.669 | 0.3 | 26.94 | 0.3 | 25.09 | 0.2 | 0.389 | 1.0 |
| TU-1 117531 Spot-24 | 0.761 | 1.1 | 13.30 | 0.3 | 14.366 | 0.176 | 2.7 | 2.09 | 0.7 | 2.818 | 1.682 | 0.3 | 27.03 | 0.3 | 25.01 | 0.2 | 0.388 | 1.0 |
| TU-1 117531 Spot-25 | 0.750 | 1.1 | 13.27 | 0.3 | 14.326 | 0.193 | 2.5 | 2.13 | 0.7 | 2.870 | 1.683 | 0.3 | 26.98 | 0.3 | 25.05 | 0.2 | 0.390 | 1.0 |
| TU-1 117531 Spot-26 | 0.767 | 1.1 | 13.29 | 0.3 | 14.355 | 0.175 | 2.7 | 2.08 | 0.7 | 2.806 | 1.677 | 0.3 | 27.06 | 0.3 | 25.16 | 0.2 | 0.396 | 1.0 |
| TU-1 117531 Spot-27 | 0.771 | 1.1 | 13.32 | 0.3 | 14.387 | 0.185 | 2.6 | 2.11 | 0.7 | 2.838 | 1.685 | 0.3 | 27.06 | 0.3 | 25.14 | 0.2 | 0.378 | 1.0 |
| 04-6-19-mnz8-spot1 | 0.572 | 1.3 | 3.76 | 0.6 | 3.989 | 0.143 | 3.2 | 0.09 | 11.5 | 0.117 | 1.036 | 0.4 | 33.73 | 0.3 | 27.01 | 0.2 | 0.239 | 1.5 |
| 04-6-19-mnz8-spot2 | 0.927 | 0.9 | 4.07 | 0.6 | 4.334 | 0.181 | 2.6 | 0.12 | 9.0 | 0.150 | 1.075 | 0.4 | 34.21 | 0.3 | 27.29 | 0.2 | 0.207 | 1.8 |
| 04-6-19-mnz8-spot3 | 0.947 | 0.9 | 4.35 | 0.5 | 4.629 | 0.190 | 2.5 | 0.11 | 9.8 | 0.138 | 1.128 | 0.4 | 33.57 | 0.3 | 27.07 | 0.2 | 0.242 | 1.5 |
| 04-6-19-mnz8-spot4 | 0.951 | 0.8 | 4.05 | 0.6 | 4.311 | 0.176 | 2.6 | 0.12 | 8.8 | 0.153 | 1.062 | 0.4 | 32.71 | 0.3 | 25.77 | 0.2 | 0.243 | 1.5 |
| 04-6-19-mnz8-spot5 | 0.909 | 0.9 | 3.57 | 0.6 | 3.790 | 0.165 | 2.8 | 0.54 | 2.1 | 0.704 | 1.048 | 0.4 | 32.41 | 0.3 | 25.91 | 0.2 | 0.231 | 1.6 |
| 04-6-19-mnz8-spot6 | 0.692 | 1.1 | 3.99 | 0.6 | 4.238 | 0.156 | 2.9 | 0.27 | 4.0 | 0.347 | 1.097 | 0.4 | 34.07 | 0.3 | 27.25 | 0.2 | 0.225 | 1.6 |

| | $UO_2$ | | $ThO_2$ | | | PbO | | $Y_2O_3$ | | | CaO | | $Ce_2O_3$ | | $P_2O_5$ | | $SiO_2$ | |
|---|---|---|---|---|---|---|---|---|---|---|---|---|---|---|---|---|---|---|
| Sample | wt. % | RSD (2σ%) | wt. % | RSD (2σ%) | k-raw | wt. % | RSD (2σ%) | wt. % | RSD (2σ%) | k-raw | wt. % | RSD (2σ%) | wt. % | RSD (2σ%) | wt. % | RSD (2σ%) | wt. % | RSD (2σ%) |
| TU-1 117531 Spot-27 | 0.759 | 1.1 | 13.26 | 0.3 | 14.316 | 0.177 | 2.7 | 2.10 | 0.7 | 2.822 | 1.676 | 0.3 | 26.95 | 0.3 | 25.10 | 0.2 | 0.628 | 0.6 |
| TU-1 117531 Spot-28 | 0.748 | 1.1 | 13.42 | 0.3 | 14.447 | 0.185 | 2.6 | 2.12 | 0.7 | 2.842 | 1.696 | 0.3 | 26.88 | 0.3 | 25.19 | 0.2 | 1.851 | 0.3 |
| TU-1 117531 Spot-29 | 0.743 | 1.1 | 13.33 | 0.3 | 14.357 | 0.181 | 2.7 | 2.14 | 0.7 | 2.865 | 1.679 | 0.3 | 27.07 | 0.3 | 25.18 | 0.2 | 1.842 | 0.3 |
| TU-1 117531 Spot-30 | 0.752 | 1.1 | 13.45 | 0.3 | 14.476 | 0.178 | 2.7 | 2.12 | 0.7 | 2.843 | 1.680 | 0.3 | 26.62 | 0.3 | 25.20 | 0.2 | 1.840 | 0.3 |
| TU-1 117531 Spot-31 | 0.736 | 1.1 | 14.56 | 0.3 | 15.720 | 0.180 | 2.6 | 2.33 | 0.7 | 3.133 | 1.637 | 0.3 | 27.13 | 0.3 | 25.15 | 0.2 | 1.895 | 0.3 |
| TU-1 117531 Spot-32 | 0.761 | 1.1 | 14.34 | 0.3 | 15.465 | 0.175 | 2.7 | 2.36 | 0.7 | 3.176 | 1.642 | 0.3 | 26.89 | 0.3 | 25.18 | 0.2 | 1.906 | 0.3 |
| TU-1 117531 Spot-33 | 0.735 | 1.1 | 14.25 | 0.3 | 15.367 | 0.184 | 2.6 | 2.33 | 0.7 | 3.136 | 1.629 | 0.3 | 26.68 | 0.3 | 25.12 | 0.2 | 1.913 | 0.3 |
| TU-1 117531 Spot-35 | 0.744 | 1.1 | 14.09 | 0.3 | 15.189 | 0.179 | 2.7 | 2.29 | 0.7 | 3.082 | 1.639 | 0.3 | 26.94 | 0.3 | 25.19 | 0.2 | 1.875 | 0.3 |
| TU-1 117531 Spot-36 | 0.757 | 1.1 | 14.08 | 0.3 | 15.172 | 0.180 | 2.7 | 2.31 | 0.7 | 3.099 | 1.650 | 0.3 | 26.77 | 0.3 | 25.42 | 0.2 | 1.906 | 0.3 |
| TU-1 117531 Spot-37 | 0.764 | 1.1 | 14.71 | 0.3 | 15.893 | 0.184 | 2.6 | 2.37 | 0.7 | 3.186 | 1.655 | 0.3 | 26.29 | 0.3 | 24.50 | 0.2 | 1.936 | 0.3 |
| TU-1 117531 Spot-37 | 0.750 | 1.1 | 14.68 | 0.3 | 15.861 | 0.173 | 2.8 | 2.24 | 0.7 | 3.012 | 1.657 | 0.3 | 26.50 | 0.3 | 24.78 | 0.2 | 1.918 | 0.3 |
| TU-1 117531 Spot-38 | 0.763 | 1.1 | 14.49 | 0.3 | 15.644 | 0.185 | 2.6 | 2.27 | 0.7 | 3.056 | 1.654 | 0.3 | 26.43 | 0.3 | 24.73 | 0.2 | 1.927 | 0.3 |
| TU-1 117531 Spot-39 | 0.760 | 1.1 | 14.36 | 0.3 | 15.499 | 0.187 | 2.6 | 2.28 | 0.7 | 3.061 | 1.637 | 0.3 | 26.35 | 0.3 | 24.65 | 0.2 | 1.913 | 0.3 |
| TU-1 117531 Spot-40 | 0.759 | 1.1 | 14.34 | 0.3 | 15.470 | 0.187 | 2.6 | 2.28 | 0.7 | 3.069 | 1.642 | 0.3 | 26.25 | 0.3 | 24.73 | 0.2 | 1.904 | 0.3 |
| TU-1 117531 Spot-40 | 0.761 | 1.1 | 14.45 | 0.3 | 15.621 | 0.182 | 2.7 | 2.14 | 0.7 | 2.881 | 1.628 | 0.3 | 26.39 | 0.3 | 24.21 | 0.2 | 1.850 | 0.3 |
| TU-1 117531 Spot-41 | 0.747 | 1.1 | 14.16 | 0.3 | 15.289 | 0.182 | 2.7 | 2.16 | 0.7 | 2.896 | 1.654 | 0.3 | 26.30 | 0.3 | 24.28 | 0.2 | 1.890 | 0.3 |
| TU-1 117531 Spot-42 | 0.744 | 1.1 | 14.06 | 0.3 | 15.171 | 0.187 | 2.6 | 2.19 | 0.7 | 2.942 | 1.621 | 0.3 | 26.28 | 0.3 | 24.42 | 0.2 | 1.872 | 0.3 |
| TU-1 117531 Spot-43 | 0.752 | 1.1 | 14.12 | 0.3 | 15.243 | 0.181 | 2.7 | 2.20 | 0.7 | 2.956 | 1.630 | 0.3 | 26.33 | 0.3 | 24.51 | 0.2 | 1.882 | 0.3 |
| 8153_Test1 | 0.402 | 1.9 | 7.77 | 0.4 | 8.308 | 0.157 | 2.9 | 0.49 | 2.3 | 0.641 | 0.607 | 0.6 | 31.24 | 0.2 | 25.86 | 0.2 | 1.283 | 0.3 |
| 8153_Test2 | 0.382 | 2.0 | 7.51 | 0.4 | 8.019 | 0.179 | 2.6 | 0.49 | 2.3 | 0.642 | 0.600 | 0.6 | 31.67 | 0.2 | 26.24 | 0.2 | 1.282 | 0.3 |
| 8153_Test3 | 0.005 | 63.1 | 0.00 | 100.0 | 0.000 | 0.003 | 64.5 | 0.00 | 100.0 | 0.000 | 0.002 | 50.9 | 0.02 | 47.4 | 0.00 | 100.0 | 0.024 | 4.6 |
| 8153_Test4 | 0.000 | 100.0 | 0.00 | 100.0 | 0.000 | 0.004 | 46.1 | 0.00 | 100.0 | 0.000 | 0.002 | 75.6 | 0.03 | 30.6 | 0.00 | 100.0 | 0.036 | 3.2 |
| 8153_Test5 | 0.000 | 100.0 | 0.00 | 115.7 | 0.005 | 0.000 | 100.0 | 0.00 | 100.0 | 0.000 | 0.000 | 100.0 | 0.03 | 23.9 | 0.00 | 322.7 | 0.032 | 4.0 |
| 8153_Test6 | 0.003 | 105.0 | 0.00 | 407.6 | 0.001 | 0.004 | 46.8 | 0.00 | 299.3 | 0.002 | 0.001 | 91.1 | 0.01 | 76.0 | 0.00 | 100.0 | 0.031 | 4.5 |
| 8153_Test7 | 0.000 | 100.0 | 0.00 | 100.0 | 0.000 | 0.001 | 209.8 | 0.00 | 100.0 | 0.000 | 0.001 | 84.5 | 0.02 | 48.5 | 0.00 | 100.0 | 0.030 | 4.8 |
| 05b-6-29_m1_1 | 0.327 | 2.3 | 5.77 | 0.5 | 6.143 | 0.172 | 2.7 | 0.03 | 30.3 | 0.043 | 1.334 | 0.4 | 31.29 | 0.2 | 26.89 | 0.2 | 0.229 | 1.2 |
| 05b-6-29_m1_2 | 0.313 | 2.4 | 5.59 | 0.5 | 5.947 | 0.174 | 2.6 | 0.09 | 11.8 | 0.112 | 1.294 | 0.4 | 32.16 | 0.2 | 27.46 | 0.2 | 0.215 | 1.3 |
| 05b-6-29_m1_3 | 0.323 | 2.3 | 4.56 | 0.5 | 4.828 | 0.145 | 3.1 | 0.48 | 2.3 | 0.632 | 1.076 | 0.4 | 31.52 | 0.2 | 27.13 | 0.2 | 0.224 | 1.3 |
| 05b-6-29_m1_4 | 0.320 | 2.4 | 4.34 | 0.6 | 4.596 | 0.146 | 3.1 | 0.51 | 2.1 | 0.671 | 1.088 | 0.4 | 31.64 | 0.2 | 27.17 | 0.2 | 0.283 | 1.0 |
| 05b-6-29_m1_5 | 0.337 | 2.3 | 4.70 | 0.5 | 4.984 | 0.152 | 3.0 | 0.51 | 2.2 | 0.660 | 1.168 | 0.4 | 31.70 | 0.2 | 27.38 | 0.2 | 0.227 | 1.3 |
| 05b-6-29_m1_6 | 0.378 | 2.0 | 4.60 | 0.5 | 4.878 | 0.150 | 2.9 | 0.48 | 2.2 | 0.632 | 1.386 | 0.4 | 30.42 | 0.2 | 25.87 | 0.2 | 0.249 | 1.1 |
| 05b-6-29_m1_7 | 0.374 | 2.0 | 4.37 | 0.6 | 4.631 | 0.153 | 3.0 | 0.49 | 2.2 | 0.645 | 1.241 | 0.4 | 31.29 | 0.2 | 26.99 | 0.2 | 0.214 | 1.3 |
| 05b-6-29_m1_8 | 0.368 | 2.1 | 4.43 | 0.6 | 4.692 | 0.149 | 3.0 | 0.50 | 2.2 | 0.658 | 1.252 | 0.4 | 31.52 | 0.2 | 26.95 | 0.2 | 0.236 | 1.2 |
| 05b-6-29_m1_9 | 0.395 | 1.9 | 4.46 | 0.6 | 4.732 | 0.154 | 2.9 | 0.52 | 2.1 | 0.674 | 1.252 | 0.4 | 31.14 | 0.2 | 26.73 | 0.2 | 0.224 | 1.3 |
| 05b-6-29_m1_10 | 0.382 | 2.0 | 4.43 | 0.6 | 4.693 | 0.145 | 3.1 | 0.50 | 2.2 | 0.655 | 1.247 | 0.4 | 31.32 | 0.2 | 26.66 | 0.2 | 0.226 | 1.3 |

| | $UO_2$ | | $ThO_2$ | | | PbO | | $Y_2O_3$ | | | CaO | | $Ce_2O_3$ | | $P_2O_5$ | | $SiO_2$ | |
|---|---|---|---|---|---|---|---|---|---|---|---|---|---|---|---|---|---|---|
| Sample | wt. % | RSD (2σ%) | wt. % | RSD (2σ%) | k-raw | wt. % | RSD (2σ%) | wt. % | RSD (2σ%) | k-raw | wt. % | RSD (2σ%) | wt. % | RSD (2σ%) | wt. % | RSD (2σ%) | wt. % | RSD (2σ%) |
| 05b-6-29_m1_11 | 0.369 | 2.1 | 4.41 | 0.6 | 4.673 | 0.142 | 3.2 | 0.49 | 2.2 | 0.636 | 1.228 | 0.4 | 31.34 | 0.2 | 26.63 | 0.2 | 0.211 | 1.3 |
| 05b-6-29_m1_12 | 0.345 | 2.2 | 4.34 | 0.6 | 4.607 | 0.142 | 3.1 | 0.47 | 2.3 | 0.617 | 1.203 | 0.4 | 31.02 | 0.2 | 26.11 | 0.2 | 0.267 | 1.1 |
| 05b-6-29_m1_13 | 0.325 | 2.3 | 5.18 | 0.5 | 5.512 | 0.159 | 2.8 | 0.15 | 6.9 | 0.192 | 1.306 | 0.4 | 31.06 | 0.2 | 26.28 | 0.2 | 0.217 | 1.3 |
| 05b-6-29_m1_14 | 0.327 | 2.3 | 5.56 | 0.5 | 5.919 | 0.163 | 2.8 | 0.02 | 52.3 | 0.024 | 1.306 | 0.4 | 31.01 | 0.2 | 26.23 | 0.2 | 0.235 | 1.2 |
| 05b-6-29_m1_15 | 0.324 | 2.3 | 5.63 | 0.5 | 6.002 | 0.172 | 2.7 | 0.04 | 23.1 | 0.056 | 1.306 | 0.4 | 31.55 | 0.2 | 26.63 | 0.2 | 0.196 | 1.4 |
| 05b-6-29_m1_16 | 0.328 | 2.3 | 5.48 | 0.5 | 5.845 | 0.169 | 2.7 | 0.02 | 51.2 | 0.025 | 1.281 | 0.4 | 30.96 | 0.2 | 25.74 | 0.2 | 0.217 | 1.3 |
| 05b-6-29_m1_17 | 0.326 | 2.3 | 5.75 | 0.5 | 6.120 | 0.178 | 2.6 | 0.02 | 52.2 | 0.025 | 1.320 | 0.4 | 31.57 | 0.2 | 26.85 | 0.2 | 0.198 | 1.4 |
| 05b-6-29_m1_18 | 0.321 | 2.4 | 5.67 | 0.5 | 6.046 | 0.167 | 2.8 | 0.04 | 26.4 | 0.049 | 1.316 | 0.4 | 31.68 | 0.2 | 26.60 | 0.2 | 0.201 | 1.4 |
| 05b-6-29_m1_19 | 0.266 | 2.8 | 5.41 | 0.5 | 5.762 | 0.163 | 2.8 | 0.02 | 56.0 | 0.023 | 1.255 | 0.4 | 31.57 | 0.2 | 26.37 | 0.2 | 0.182 | 1.5 |
| 05b-6-29_m1_20 | 0.245 | 3.0 | 5.62 | 0.5 | 5.990 | 0.167 | 2.7 | 0.00 | 762.3 | 0.002 | 1.255 | 0.4 | 31.89 | 0.2 | 26.42 | 0.2 | 0.219 | 1.3 |
| 05b-6-29_m1_21 | 0.304 | 2.5 | 5.60 | 0.5 | 5.969 | 0.163 | 2.8 | 0.00 | 100.0 | 0.000 | 1.290 | 0.4 | 31.54 | 0.2 | 26.52 | 0.2 | 0.212 | 1.3 |
| 05b-6-29_m1_22 | 0.316 | 2.4 | 5.64 | 0.5 | 6.015 | 0.162 | 2.8 | 0.00 | 100.0 | 0.000 | 1.308 | 0.4 | 30.94 | 0.2 | 25.95 | 0.2 | 0.228 | 1.2 |
| 05b-6-29_m1_23 | 0.271 | 2.8 | 6.22 | 0.4 | 6.647 | 0.181 | 2.5 | 0.00 | 1664.2 | 0.001 | 1.424 | 0.4 | 31.43 | 0.2 | 26.02 | 0.2 | 0.260 | 1.1 |
| 05b-6-29_m1_24 | 0.253 | 3.0 | 7.49 | 0.4 | 8.019 | 0.199 | 2.3 | 0.03 | 39.3 | 0.033 | 1.533 | 0.3 | 31.40 | 0.2 | 26.28 | 0.2 | 0.396 | 0.8 |
| 05b-6-29_m1_25 | 0.258 | 2.9 | 7.64 | 0.4 | 8.176 | 0.221 | 2.1 | 0.04 | 27.0 | 0.049 | 1.563 | 0.3 | 31.30 | 0.2 | 26.32 | 0.2 | 0.383 | 0.8 |
| 05b-6-29_m1_26 | 0.265 | 2.9 | 7.67 | 0.4 | 8.213 | 0.216 | 2.2 | 0.03 | 34.1 | 0.038 | 1.559 | 0.3 | 31.16 | 0.2 | 26.20 | 0.2 | 0.390 | 0.8 |
| 05b-6-29_m1_27 | 0.272 | 2.8 | 7.63 | 0.4 | 8.167 | 0.223 | 2.1 | 0.05 | 21.5 | 0.061 | 1.560 | 0.3 | 31.02 | 0.2 | 26.08 | 0.2 | 0.395 | 0.8 |
| 05b-6-29_m1_28 | 0.198 | 3.4 | 6.82 | 0.4 | 7.354 | 0.168 | 2.4 | 0.04 | 24.2 | 0.049 | 1.437 | 0.3 | 28.06 | 0.3 | 20.42 | 0.2 | 0.579 | 0.5 |
| 05b-6-29_m1_29 | 0.274 | 2.7 | 7.91 | 0.4 | 8.469 | 0.219 | 2.1 | 0.06 | 16.9 | 0.079 | 1.606 | 0.3 | 30.91 | 0.2 | 26.47 | 0.2 | 0.409 | 0.8 |
| 05b-6-29_m1_30 | 0.286 | 2.7 | 8.00 | 0.4 | 8.569 | 0.224 | 2.1 | 0.04 | 23.2 | 0.058 | 1.639 | 0.3 | 31.33 | 0.2 | 26.81 | 0.2 | 0.408 | 0.8 |
| 8153_8 | 0.384 | 2.0 | 7.25 | 0.4 | 7.752 | 0.179 | 2.6 | 0.49 | 2.2 | 0.645 | 0.594 | 0.6 | 31.41 | 0.2 | 25.21 | 0.2 | 1.239 | 0.3 |
| 8153_9 | 0.381 | 2.0 | 7.25 | 0.4 | 7.743 | 0.179 | 2.6 | 0.49 | 2.2 | 0.642 | 0.604 | 0.6 | 31.36 | 0.2 | 25.37 | 0.2 | 1.257 | 0.3 |
| 8153_10 | 0.395 | 1.9 | 7.22 | 0.4 | 7.715 | 0.184 | 2.5 | 0.49 | 2.2 | 0.645 | 0.595 | 0.6 | 31.50 | 0.2 | 25.36 | 0.2 | 1.245 | 0.3 |
| 8153_11 | 0.391 | 2.0 | 7.26 | 0.4 | 7.757 | 0.189 | 2.4 | 0.49 | 2.2 | 0.633 | 0.603 | 0.6 | 31.51 | 0.2 | 25.28 | 0.2 | 1.241 | 0.3 |
| 8153_12 | 0.404 | 1.9 | 7.26 | 0.4 | 7.757 | 0.179 | 2.6 | 0.48 | 2.2 | 0.631 | 0.596 | 0.6 | 31.36 | 0.2 | 25.36 | 0.2 | 1.234 | 0.3 |
| 8153_13 | 0.380 | 2.0 | 7.28 | 0.4 | 7.786 | 0.178 | 2.6 | 0.48 | 2.3 | 0.623 | 0.591 | 0.6 | 31.48 | 0.2 | 25.37 | 0.2 | 1.259 | 0.3 |
| 8153_14 | 0.395 | 2.0 | 7.20 | 0.4 | 7.699 | 0.179 | 2.5 | 0.50 | 2.2 | 0.648 | 0.591 | 0.6 | 31.48 | 0.2 | 25.31 | 0.2 | 1.243 | 0.3 |
| 8153_15 | 0.390 | 2.0 | 7.19 | 0.4 | 7.685 | 0.187 | 2.5 | 0.50 | 2.2 | 0.647 | 0.591 | 0.6 | 31.53 | 0.2 | 25.30 | 0.2 | 1.239 | 0.3 |
| 8153_16 | 0.394 | 1.9 | 7.21 | 0.4 | 7.712 | 0.182 | 2.5 | 0.47 | 2.3 | 0.619 | 0.593 | 0.6 | 31.45 | 0.2 | 25.31 | 0.2 | 1.243 | 0.3 |
| 8153_17 | 0.381 | 2.0 | 7.25 | 0.4 | 7.751 | 0.183 | 2.5 | 0.51 | 2.2 | 0.662 | 0.600 | 0.6 | 31.53 | 0.2 | 25.26 | 0.2 | 1.239 | 0.3 |
| 8153_18 | 0.384 | 2.0 | 7.34 | 0.4 | 7.844 | 0.189 | 2.4 | 0.50 | 2.2 | 0.658 | 0.601 | 0.6 | 31.66 | 0.2 | 25.52 | 0.2 | 1.244 | 0.3 |
| 05b-6-29_m4_rim1 | 0.481 | 1.6 | 5.29 | 0.5 | 5.627 | 0.164 | 2.8 | 0.09 | 10.8 | 0.120 | 1.272 | 0.4 | 32.21 | 0.2 | 27.61 | 0.2 | 0.271 | 1.1 |
| 05b-6-29_m4_rim2 | 0.365 | 2.1 | 6.74 | 0.4 | 7.189 | 0.202 | 2.3 | 0.05 | 20.8 | 0.062 | 1.456 | 0.3 | 31.49 | 0.2 | 27.27 | 0.2 | 0.331 | 0.9 |
| 05b-6-29_m4_rim3 | 0.341 | 2.2 | 6.99 | 0.4 | 7.464 | 0.194 | 2.4 | 0.05 | 19.8 | 0.066 | 1.484 | 0.3 | 31.56 | 0.2 | 27.44 | 0.2 | 0.340 | 0.9 |
| 05b-6-29_m4_rim4 | 0.344 | 2.2 | 6.79 | 0.4 | 7.245 | 0.187 | 2.5 | 0.06 | 15.8 | 0.082 | 1.439 | 0.4 | 31.74 | 0.2 | 27.54 | 0.2 | 0.325 | 0.9 |
| 05b-6-29_m4_rim5 | 0.412 | 1.9 | 6.49 | 0.4 | 6.924 | 0.197 | 2.3 | 0.08 | 12.7 | 0.103 | 1.430 | 0.4 | 31.88 | 0.2 | 27.48 | 0.2 | 0.303 | 1.0 |

| | $UO_2$ | | $ThO_2$ | | | PbO | | $Y_2O_3$ | | | CaO | | $Ce_2O_3$ | | $P_2O_5$ | | $SiO_2$ | |
|---|---|---|---|---|---|---|---|---|---|---|---|---|---|---|---|---|---|---|
| Sample | wt. % | RSD (2σ%) | wt. % | RSD (2σ%) | k-raw | wt. % | RSD (2σ%) | wt. % | RSD (2σ%) | k-raw | wt. % | RSD (2σ%) | wt. % | RSD (2σ%) | wt. % | RSD (2σ%) | wt. % | RSD (2σ%) |
| 05b-6-29_m4_rim6 | 0.382 | 2.0 | 6.61 | 0.4 | 7.044 | 0.203 | 2.3 | 0.06 | 17.0 | 0.077 | 1.434 | 0.4 | 31.93 | 0.2 | 27.60 | 0.2 | 0.311 | 0.9 |
| 05b-6-29_m4_rim7 | 0.465 | 1.7 | 6.33 | 0.4 | 6.746 | 0.194 | 2.4 | 0.07 | 14.2 | 0.092 | 1.417 | 0.4 | 32.20 | 0.2 | 27.61 | 0.2 | 0.291 | 1.0 |
| 05b-6-29_m4_rim8 | 0.484 | 1.6 | 6.27 | 0.4 | 6.687 | 0.186 | 2.5 | 0.06 | 15.9 | 0.082 | 1.403 | 0.4 | 32.09 | 0.2 | 27.72 | 0.2 | 0.289 | 1.0 |
| 05b-6-29_m4_rim9 | 0.483 | 1.6 | 5.51 | 0.5 | 5.866 | 0.182 | 2.5 | 0.07 | 13.5 | 0.097 | 1.290 | 0.4 | 32.33 | 0.2 | 27.74 | 0.2 | 0.243 | 1.2 |
| 05b-6-29_m4_rim10 | 0.489 | 1.6 | 5.77 | 0.5 | 6.139 | 0.178 | 2.6 | 0.07 | 15.2 | 0.086 | 1.321 | 0.4 | 32.08 | 0.2 | 27.65 | 0.2 | 0.254 | 1.1 |
| 05b-6-29_m4_rim11 | 0.501 | 1.5 | 6.07 | 0.5 | 6.466 | 0.189 | 2.4 | 0.05 | 18.9 | 0.068 | 1.402 | 0.4 | 32.09 | 0.2 | 27.68 | 0.2 | 0.269 | 1.1 |
| 05b-6-29_m4_rim12 | 0.494 | 1.6 | 6.46 | 0.4 | 6.884 | 0.208 | 2.2 | 0.06 | 16.9 | 0.077 | 1.598 | 0.3 | 31.75 | 0.2 | 27.56 | 0.2 | 0.295 | 1.0 |
| 05b-6-29_m4_rim13 | 0.419 | 1.8 | 6.40 | 0.4 | 6.819 | 0.191 | 2.4 | 0.08 | 13.0 | 0.100 | 1.494 | 0.3 | 31.81 | 0.2 | 27.49 | 0.2 | 0.293 | 1.0 |
| 05b-6-29_m4_rim14 | 0.416 | 1.8 | 6.49 | 0.4 | 6.921 | 0.199 | 2.3 | 0.07 | 14.3 | 0.091 | 1.429 | 0.4 | 31.63 | 0.2 | 27.53 | 0.2 | 0.309 | 0.9 |
| 05b-6-29_m4_rim15 | 0.410 | 1.9 | 4.69 | 0.5 | 4.969 | 0.158 | 2.9 | 0.56 | 2.0 | 0.730 | 1.131 | 0.4 | 31.54 | 0.2 | 27.91 | 0.2 | 0.228 | 1.2 |
| 05b-6-29_m4_rim16 | 0.436 | 1.8 | 4.57 | 0.5 | 4.838 | 0.161 | 2.8 | 0.57 | 1.9 | 0.746 | 1.119 | 0.4 | 31.27 | 0.2 | 27.76 | 0.2 | 0.227 | 1.2 |
| 05b-6-29_m4_rim17 | 0.435 | 1.8 | 4.77 | 0.5 | 5.048 | 0.165 | 2.8 | 0.56 | 2.0 | 0.732 | 1.155 | 0.4 | 31.36 | 0.2 | 27.87 | 0.2 | 0.227 | 1.2 |
| 05b-6-29_m4_rim18 | 0.436 | 1.8 | 4.69 | 0.5 | 4.964 | 0.162 | 2.8 | 0.55 | 2.0 | 0.726 | 1.142 | 0.4 | 31.23 | 0.2 | 27.81 | 0.2 | 0.230 | 1.2 |
| 05b-6-29_m4_rim19 | 0.356 | 2.1 | 4.36 | 0.6 | 4.609 | 0.145 | 3.1 | 0.53 | 2.1 | 0.689 | 1.048 | 0.4 | 31.77 | 0.2 | 27.95 | 0.2 | 0.212 | 1.3 |
| 05b-6-29_m4_rim20 | 0.384 | 2.0 | 3.88 | 0.6 | 4.099 | 0.148 | 3.0 | 0.55 | 2.0 | 0.719 | 1.114 | 0.4 | 31.94 | 0.2 | 27.79 | 0.2 | 0.195 | 1.4 |
| 05b-6-29_m4_rim21 | 0.392 | 1.9 | 3.82 | 0.6 | 4.037 | 0.137 | 3.3 | 0.55 | 2.0 | 0.711 | 1.140 | 0.4 | 31.59 | 0.2 | 27.81 | 0.2 | 0.189 | 1.5 |
| 05b-6-29_m4_rim22 | 0.385 | 2.0 | 3.81 | 0.6 | 4.026 | 0.139 | 3.2 | 0.55 | 2.0 | 0.723 | 1.134 | 0.4 | 31.84 | 0.2 | 27.93 | 0.2 | 0.180 | 1.5 |
| 05b-6-29_m4_rim23 | 0.369 | 2.0 | 3.81 | 0.6 | 4.028 | 0.134 | 3.3 | 0.54 | 2.0 | 0.703 | 1.102 | 0.4 | 32.01 | 0.2 | 27.94 | 0.2 | 0.188 | 1.5 |
| 05b-6-29_m4_rim24 | 0.371 | 2.0 | 3.86 | 0.6 | 4.084 | 0.137 | 3.2 | 0.55 | 2.0 | 0.713 | 1.126 | 0.4 | 32.03 | 0.2 | 27.93 | 0.2 | 0.186 | 1.5 |
| 05b-6-29_m4_rim25 | 0.388 | 1.9 | 4.02 | 0.6 | 4.252 | 0.139 | 3.2 | 0.52 | 2.1 | 0.674 | 1.119 | 0.4 | 31.93 | 0.2 | 27.78 | 0.2 | 0.205 | 1.4 |
| 8153_19 | 0.388 | 2.0 | 7.33 | 0.4 | 7.831 | 0.185 | 2.5 | 0.50 | 2.2 | 0.657 | 0.603 | 0.6 | 31.72 | 0.2 | 25.77 | 0.2 | 1.265 | 0.3 |
| 8153_20 | 0.379 | 2.0 | 7.26 | 0.4 | 7.762 | 0.181 | 2.5 | 0.47 | 2.3 | 0.618 | 0.604 | 0.6 | 31.38 | 0.2 | 25.27 | 0.2 | 1.247 | 0.3 |
| 8153_21 | 0.382 | 2.0 | 7.30 | 0.4 | 7.799 | 0.189 | 2.4 | 0.50 | 2.2 | 0.656 | 0.608 | 0.6 | 31.54 | 0.2 | 25.59 | 0.2 | 1.260 | 0.3 |
| 8153_22 | 0.385 | 2.0 | 7.29 | 0.4 | 7.788 | 0.180 | 2.6 | 0.50 | 2.2 | 0.658 | 0.595 | 0.6 | 31.70 | 0.2 | 25.62 | 0.2 | 1.260 | 0.3 |
| 8153_23 | 0.399 | 1.9 | 7.27 | 0.4 | 7.774 | 0.184 | 2.5 | 0.49 | 2.2 | 0.639 | 0.598 | 0.6 | 31.71 | 0.2 | 25.58 | 0.2 | 1.255 | 0.3 |
| 8153_24 | 0.384 | 2.0 | 7.28 | 0.4 | 7.782 | 0.178 | 2.6 | 0.50 | 2.2 | 0.648 | 0.600 | 0.6 | 31.51 | 0.2 | 25.66 | 0.2 | 1.246 | 0.3 |
| 8153_25 | 0.385 | 2.0 | 7.35 | 0.4 | 7.856 | 0.182 | 2.5 | 0.48 | 2.3 | 0.631 | 0.603 | 0.6 | 31.56 | 0.2 | 25.72 | 0.2 | 1.256 | 0.3 |
| 8153_26 | 0.398 | 1.9 | 7.36 | 0.4 | 7.860 | 0.185 | 2.5 | 0.49 | 2.2 | 0.645 | 0.610 | 0.6 | 31.64 | 0.2 | 26.00 | 0.2 | 1.270 | 0.3 |
| 8153_27 | 0.405 | 1.9 | 7.29 | 0.4 | 7.782 | 0.184 | 2.5 | 0.50 | 2.2 | 0.657 | 0.600 | 0.6 | 31.77 | 0.2 | 25.93 | 0.2 | 1.280 | 0.3 |
| 8153_28 | 0.403 | 1.9 | 7.35 | 0.4 | 7.847 | 0.187 | 2.5 | 0.49 | 2.2 | 0.644 | 0.609 | 0.6 | 31.50 | 0.2 | 25.88 | 0.2 | 1.277 | 0.3 |
| 8153_29 | 0.407 | 1.9 | 7.33 | 0.4 | 7.835 | 0.186 | 2.5 | 0.49 | 2.2 | 0.637 | 0.606 | 0.6 | 31.69 | 0.2 | 25.85 | 0.2 | 1.266 | 0.3 |
| 8153_30 | 0.383 | 2.0 | 7.29 | 0.4 | 7.791 | 0.185 | 2.5 | 0.49 | 2.2 | 0.644 | 0.608 | 0.6 | 31.47 | 0.2 | 25.69 | 0.2 | 1.267 | 0.3 |
| 05b-6-29_m4_core1 | 0.468 | 1.7 | 4.91 | 0.5 | 5.194 | 0.167 | 2.8 | 0.58 | 2.0 | 0.763 | 1.227 | 0.4 | 32.91 | 0.2 | 29.07 | 0.2 | 0.258 | 1.2 |
| 05b-6-29_m4_core2 | 0.430 | 1.8 | 4.83 | 0.5 | 5.116 | 0.157 | 2.9 | 0.56 | 2.0 | 0.731 | 1.189 | 0.4 | 31.24 | 0.2 | 27.80 | 0.2 | 0.255 | 1.1 |
| 05b-6-29_m4_core3 | 0.448 | 1.7 | 5.09 | 0.5 | 5.398 | 0.165 | 2.8 | 0.58 | 1.9 | 0.754 | 1.253 | 0.4 | 31.26 | 0.2 | 27.92 | 0.2 | 0.275 | 1.1 |
| 05b-6-29_m4_core4 | 0.441 | 1.7 | 5.20 | 0.5 | 5.514 | 0.172 | 2.7 | 0.54 | 2.0 | 0.711 | 1.260 | 0.4 | 31.05 | 0.2 | 27.84 | 0.2 | 0.271 | 1.1 |

| | $UO_2$ | | $ThO_2$ | | | PbO | | $Y_2O_3$ | | | CaO | | $Ce_2O_3$ | | $P_2O_5$ | | $SiO_2$ | |
|---|---|---|---|---|---|---|---|---|---|---|---|---|---|---|---|---|---|---|
| Sample | wt. % | RSD (2σ%) | wt. % | RSD (2σ%) | k-raw | wt. % | RSD (2σ%) | wt. % | RSD (2σ%) | k-raw | wt. % | RSD (2σ%) | wt. % | RSD (2σ%) | wt. % | RSD (2σ%) | wt. % | RSD (2σ%) |
| 05b-6-29_m4_core5 | 0.437 | 1.8 | 5.30 | 0.5 | 5.617 | 0.168 | 2.7 | 0.56 | 2.0 | 0.728 | 1.273 | 0.4 | 30.86 | 0.2 | 27.74 | 0.2 | 0.286 | 1.0 |
| 05b-6-29_m4_core6 | 0.473 | 1.6 | 5.15 | 0.5 | 5.454 | 0.172 | 2.7 | 0.60 | 1.9 | 0.785 | 1.256 | 0.4 | 30.96 | 0.2 | 27.89 | 0.2 | 0.267 | 1.1 |
| 05b-6-29_m4_core7 | 0.476 | 1.6 | 5.01 | 0.5 | 5.307 | 0.171 | 2.7 | 0.57 | 1.9 | 0.751 | 1.242 | 0.4 | 31.31 | 0.2 | 27.97 | 0.2 | 0.251 | 1.1 |
| 05b-6-29_m4_core8 | 0.472 | 1.6 | 4.94 | 0.5 | 5.231 | 0.169 | 2.7 | 0.59 | 1.9 | 0.767 | 1.215 | 0.4 | 31.05 | 0.2 | 28.00 | 0.2 | 0.244 | 1.2 |
| 05b-6-29_m4_core9 | 0.470 | 1.6 | 4.87 | 0.5 | 5.154 | 0.169 | 2.7 | 0.58 | 1.9 | 0.763 | 1.212 | 0.4 | 31.44 | 0.2 | 27.96 | 0.2 | 0.236 | 1.2 |
| 05b-6-29_m4_core10 | 0.440 | 1.7 | 4.96 | 0.5 | 5.255 | 0.165 | 2.7 | 0.56 | 2.0 | 0.733 | 1.211 | 0.4 | 31.51 | 0.2 | 27.99 | 0.2 | 0.259 | 1.1 |
| 05b-6-29_m4_core11 | 0.513 | 1.5 | 5.28 | 0.5 | 5.598 | 0.181 | 2.5 | 0.59 | 1.9 | 0.773 | 1.307 | 0.4 | 31.20 | 0.2 | 28.02 | 0.2 | 0.262 | 1.1 |
| 05b-6-29_m4_core12 | 0.481 | 1.6 | 5.17 | 0.5 | 5.473 | 0.173 | 2.6 | 0.61 | 1.8 | 0.799 | 1.266 | 0.4 | 30.95 | 0.2 | 27.90 | 0.2 | 0.249 | 1.1 |
| 05b-6-29_m4_core13 | 0.475 | 1.6 | 5.14 | 0.5 | 5.447 | 0.171 | 2.7 | 0.59 | 1.9 | 0.772 | 1.257 | 0.4 | 31.19 | 0.2 | 27.99 | 0.2 | 0.255 | 1.1 |
| 05b-6-29_m4_core14 | 0.379 | 2.0 | 3.90 | 0.6 | 4.125 | 0.126 | 3.5 | 0.55 | 2.0 | 0.718 | 1.082 | 0.4 | 31.92 | 0.2 | 28.05 | 0.2 | 0.203 | 1.4 |
| 05b-6-29_m4_core15 | 0.464 | 1.7 | 4.93 | 0.5 | 5.216 | 0.168 | 2.7 | 0.60 | 1.8 | 0.783 | 1.218 | 0.4 | 31.13 | 0.2 | 27.96 | 0.2 | 0.255 | 1.1 |
| 05b-6-29_m4_core16 | 0.474 | 1.6 | 5.14 | 0.5 | 5.450 | 0.165 | 2.8 | 0.61 | 1.8 | 0.800 | 1.269 | 0.4 | 30.87 | 0.2 | 27.88 | 0.2 | 0.250 | 1.1 |
| 05b-6-29_m4_core17 | 0.471 | 1.6 | 4.87 | 0.5 | 5.159 | 0.166 | 2.7 | 0.59 | 1.9 | 0.770 | 1.213 | 0.4 | 31.24 | 0.2 | 27.98 | 0.2 | 0.241 | 1.2 |
| 05b-6-29_m4_core18 | 0.472 | 1.6 | 5.20 | 0.5 | 5.511 | 0.174 | 2.6 | 0.62 | 1.8 | 0.818 | 1.251 | 0.4 | 30.88 | 0.2 | 27.86 | 0.2 | 0.268 | 1.1 |
| 05b-6-29_m4_core19 | 0.478 | 1.6 | 5.22 | 0.5 | 5.526 | 0.169 | 2.7 | 0.60 | 1.9 | 0.782 | 1.272 | 0.4 | 31.05 | 0.2 | 28.04 | 0.2 | 0.260 | 1.1 |
| 05b-6-29_m4_core20 | 0.478 | 1.6 | 5.23 | 0.5 | 5.536 | 0.177 | 2.6 | 0.60 | 1.9 | 0.786 | 1.265 | 0.4 | 30.93 | 0.2 | 27.97 | 0.2 | 0.265 | 1.1 |
| 05b-6-29_m4_core21 | 0.441 | 1.7 | 4.90 | 0.5 | 5.190 | 0.151 | 3.0 | 0.55 | 2.0 | 0.716 | 1.177 | 0.4 | 31.45 | 0.2 | 27.96 | 0.2 | 0.243 | 1.2 |
| 05b-6-29_m4_core22 | 0.432 | 1.8 | 4.83 | 0.5 | 5.113 | 0.164 | 2.8 | 0.57 | 1.9 | 0.744 | 1.175 | 0.4 | 31.38 | 0.2 | 27.91 | 0.2 | 0.245 | 1.2 |
| 05b-6-29_m4_core23 | 0.496 | 1.6 | 5.32 | 0.5 | 5.643 | 0.171 | 2.7 | 0.58 | 1.9 | 0.762 | 1.306 | 0.4 | 31.14 | 0.2 | 28.02 | 0.2 | 0.243 | 1.2 |
| 05b-6-29_m4_core24 | 0.522 | 1.5 | 5.49 | 0.5 | 5.827 | 0.187 | 2.5 | 0.58 | 1.9 | 0.760 | 1.380 | 0.4 | 30.87 | 0.2 | 27.89 | 0.2 | 0.255 | 1.1 |
| 05b-6-29_m4_core25 | 0.549 | 1.4 | 5.77 | 0.5 | 6.124 | 0.189 | 2.5 | 0.61 | 1.8 | 0.808 | 1.431 | 0.4 | 30.95 | 0.2 | 28.02 | 0.2 | 0.271 | 1.1 |
| 05b-6-29_m4_core26 | 0.495 | 1.6 | 5.41 | 0.5 | 5.734 | 0.178 | 2.6 | 0.58 | 1.9 | 0.767 | 1.310 | 0.4 | 30.98 | 0.2 | 27.95 | 0.2 | 0.286 | 1.0 |
| 05b-6-29_m4_core27 | 0.446 | 1.7 | 5.01 | 0.5 | 5.306 | 0.167 | 2.7 | 0.55 | 2.0 | 0.721 | 1.207 | 0.4 | 31.65 | 0.2 | 27.97 | 0.2 | 0.267 | 1.1 |
| 05b-6-29_m4_core28 | 0.416 | 1.8 | 4.81 | 0.5 | 5.093 | 0.164 | 2.8 | 0.55 | 2.0 | 0.724 | 1.178 | 0.4 | 31.60 | 0.2 | 28.03 | 0.2 | 0.277 | 1.0 |
| 05b-6-29_m4_core29 | 0.411 | 1.9 | 4.79 | 0.5 | 5.077 | 0.159 | 2.8 | 0.52 | 2.1 | 0.683 | 1.167 | 0.4 | 31.72 | 0.2 | 28.01 | 0.2 | 0.241 | 1.2 |
| 05b-6-29_m4_core30 | 0.473 | 1.6 | 5.12 | 0.5 | 5.426 | 0.171 | 2.7 | 0.60 | 1.9 | 0.782 | 1.251 | 0.4 | 31.11 | 0.2 | 27.89 | 0.2 | 0.253 | 1.1 |
| 8153_31 | 0.379 | 2.0 | 7.33 | 0.4 | 7.827 | 0.182 | 2.5 | 0.48 | 2.2 | 0.632 | 0.602 | 0.6 | 31.67 | 0.2 | 25.83 | 0.2 | 1.268 | 0.3 |
| 8153_32 | 0.393 | 2.0 | 7.28 | 0.4 | 7.782 | 0.187 | 2.4 | 0.52 | 2.1 | 0.673 | 0.607 | 0.6 | 31.59 | 0.2 | 25.74 | 0.2 | 1.255 | 0.3 |
| 8153_33 | 0.379 | 2.0 | 7.26 | 0.4 | 7.758 | 0.191 | 2.4 | 0.50 | 2.2 | 0.652 | 0.640 | 0.6 | 31.68 | 0.2 | 25.89 | 0.2 | 1.275 | 0.3 |
| 8153_34 | 0.399 | 1.9 | 7.26 | 0.4 | 7.758 | 0.189 | 2.4 | 0.49 | 2.2 | 0.637 | 0.598 | 0.6 | 31.50 | 0.2 | 25.75 | 0.2 | 1.268 | 0.3 |
| 8153_35 | 0.381 | 2.0 | 7.27 | 0.4 | 7.760 | 0.179 | 2.6 | 0.50 | 2.2 | 0.654 | 0.600 | 0.6 | 31.51 | 0.2 | 25.73 | 0.2 | 1.275 | 0.3 |
| 8153_36 | 0.395 | 2.0 | 7.26 | 0.4 | 7.755 | 0.189 | 2.4 | 0.49 | 2.2 | 0.640 | 0.715 | 0.6 | 31.50 | 0.2 | 25.61 | 0.2 | 1.262 | 0.3 |
| 8153_37 | 0.402 | 1.9 | 7.28 | 0.4 | 7.781 | 0.182 | 2.5 | 0.50 | 2.2 | 0.653 | 0.603 | 0.6 | 31.60 | 0.2 | 25.79 | 0.2 | 1.272 | 0.3 |
| 8153_38 | 0.391 | 2.0 | 7.30 | 0.4 | 7.803 | 0.184 | 2.5 | 0.49 | 2.2 | 0.634 | 0.590 | 0.6 | 31.54 | 0.2 | 25.69 | 0.2 | 1.270 | 0.3 |
| 8153_39 | 0.380 | 2.0 | 7.29 | 0.4 | 7.792 | 0.178 | 2.6 | 0.49 | 2.2 | 0.637 | 0.601 | 0.6 | 31.75 | 0.2 | 25.72 | 0.2 | 1.270 | 0.3 |
| 8153_40 | 0.399 | 1.9 | 7.32 | 0.4 | 7.822 | 0.188 | 2.5 | 0.49 | 2.2 | 0.640 | 0.584 | 0.6 | 31.52 | 0.2 | 25.70 | 0.2 | 1.270 | 0.3 |

| | $UO_2$ | | $ThO_2$ | | | PbO | | $Y_2O_3$ | | | CaO | | $Ce_2O_3$ | | $P_2O_5$ | | $SiO_2$ | |
|---|---|---|---|---|---|---|---|---|---|---|---|---|---|---|---|---|---|---|
| Sample | wt. % | RSD (2σ%) | wt. % | RSD (2σ%) | k-raw | wt. % | RSD (2σ%) | wt. % | RSD (2σ%) | k-raw | wt. % | RSD (2σ%) | wt. % | RSD (2σ%) | wt. % | RSD (2σ%) | wt. % | RSD (2σ%) |
| 05b-6-108_m1_1 | 0.132 | 5.4 | 6.19 | 0.5 | 6.587 | 0.162 | 2.8 | 0.05 | 18.9 | 0.070 | 2.071 | 0.3 | 31.61 | 0.2 | 27.87 | 0.2 | 0.233 | 1.2 |
| 05b-6-108_m1_2 | 0.127 | 5.6 | 6.48 | 0.4 | 6.897 | 0.170 | 2.7 | 0.05 | 20.2 | 0.065 | 2.142 | 0.3 | 31.14 | 0.2 | 27.80 | 0.2 | 0.239 | 1.2 |
| 05b-6-108_m1_3 | 0.130 | 5.5 | 6.59 | 0.4 | 7.013 | 0.181 | 2.5 | 0.05 | 18.5 | 0.071 | 2.183 | 0.3 | 31.20 | 0.2 | 27.75 | 0.2 | 0.246 | 1.2 |
| 05b-6-108_m1_4 | 0.140 | 5.1 | 6.71 | 0.4 | 7.147 | 0.174 | 2.6 | 0.05 | 18.9 | 0.069 | 2.210 | 0.3 | 31.39 | 0.2 | 27.76 | 0.2 | 0.240 | 1.2 |
| 05b-6-108_m1_5 | 0.157 | 4.6 | 6.79 | 0.4 | 7.234 | 0.187 | 2.5 | 0.07 | 14.5 | 0.091 | 2.250 | 0.3 | 31.21 | 0.2 | 27.74 | 0.2 | 0.245 | 1.2 |
| 05b-6-108_m1_6 | 0.151 | 4.8 | 6.56 | 0.4 | 6.988 | 0.174 | 2.6 | 0.04 | 24.9 | 0.053 | 2.189 | 0.3 | 30.92 | 0.2 | 27.59 | 0.2 | 0.240 | 1.2 |
| 05b-6-108_m1_7 | 0.126 | 5.7 | 6.61 | 0.4 | 7.041 | 0.163 | 2.8 | 0.05 | 18.5 | 0.071 | 2.199 | 0.3 | 31.58 | 0.2 | 27.64 | 0.2 | 0.240 | 1.2 |
| 05b-6-108_m1_8 | 0.136 | 5.3 | 6.58 | 0.4 | 7.014 | 0.172 | 2.7 | 0.04 | 22.3 | 0.059 | 2.232 | 0.3 | 31.56 | 0.2 | 27.88 | 0.2 | 0.246 | 1.2 |
| 05b-6-108_m1_9 | 0.142 | 5.1 | 7.19 | 0.4 | 7.666 | 0.182 | 2.5 | 0.06 | 17.1 | 0.077 | 2.059 | 0.3 | 31.13 | 0.2 | 27.69 | 0.2 | 0.287 | 1.0 |
| 05b-6-108_m1_10 | 0.146 | 4.9 | 6.83 | 0.4 | 7.276 | 0.184 | 2.5 | 0.06 | 16.7 | 0.079 | 1.873 | 0.3 | 31.37 | 0.2 | 27.82 | 0.2 | 0.263 | 1.1 |
| 05b-6-108_m1_11 | 0.127 | 5.7 | 6.60 | 0.4 | 7.029 | 0.179 | 2.5 | 0.05 | 22.1 | 0.059 | 1.781 | 0.3 | 31.85 | 0.2 | 27.80 | 0.2 | 0.277 | 1.1 |
| 05b-6-108_m1_12 | 0.137 | 5.2 | 7.13 | 0.4 | 7.601 | 0.188 | 2.4 | 0.04 | 24.8 | 0.053 | 1.978 | 0.3 | 31.01 | 0.2 | 27.78 | 0.2 | 0.282 | 1.0 |
| 05b-6-108_m1_13 | 0.150 | 4.8 | 7.04 | 0.4 | 7.503 | 0.174 | 2.6 | 0.07 | 14.7 | 0.089 | 2.237 | 0.3 | 31.45 | 0.2 | 27.77 | 0.2 | 0.277 | 1.1 |
| 05b-6-108_m1_14 | 0.145 | 4.9 | 6.84 | 0.4 | 7.286 | 0.181 | 2.5 | 0.04 | 26.7 | 0.049 | 2.270 | 0.3 | 31.09 | 0.2 | 27.70 | 0.2 | 0.246 | 1.2 |
| 05b-6-108_m1_15 | 0.138 | 5.2 | 6.81 | 0.4 | 7.253 | 0.179 | 2.5 | 0.07 | 15.0 | 0.088 | 2.291 | 0.3 | 30.71 | 0.2 | 27.66 | 0.2 | 0.246 | 1.2 |
| 05b-6-108_m1_16 | 0.138 | 5.2 | 6.74 | 0.4 | 7.180 | 0.177 | 2.6 | 0.05 | 20.5 | 0.064 | 2.281 | 0.3 | 31.12 | 0.2 | 27.83 | 0.2 | 0.250 | 1.2 |
| 05b-6-108_m1_17 | 0.144 | 5.0 | 6.76 | 0.4 | 7.209 | 0.184 | 2.5 | 0.05 | 19.9 | 0.066 | 2.239 | 0.3 | 31.27 | 0.2 | 27.72 | 0.2 | 0.246 | 1.2 |
| 05b-6-108_m1_18 | 0.132 | 5.4 | 6.51 | 0.4 | 6.935 | 0.177 | 2.6 | 0.04 | 25.1 | 0.052 | 2.257 | 0.3 | 31.15 | 0.2 | 27.78 | 0.2 | 0.237 | 1.2 |
| 05b-6-108_m1_19 | 0.150 | 4.8 | 6.71 | 0.4 | 7.151 | 0.175 | 2.6 | 0.06 | 17.1 | 0.077 | 2.255 | 0.3 | 31.01 | 0.2 | 27.80 | 0.2 | 0.242 | 1.2 |
| 05b-6-108_m1_20 | 0.144 | 5.0 | 6.72 | 0.4 | 7.162 | 0.177 | 2.6 | 0.06 | 16.9 | 0.078 | 2.270 | 0.3 | 31.12 | 0.2 | 27.77 | 0.2 | 0.245 | 1.2 |
| 05b-6-108_m1_21 | 0.144 | 5.0 | 6.73 | 0.4 | 7.168 | 0.170 | 2.7 | 0.05 | 18.4 | 0.071 | 2.276 | 0.3 | 31.39 | 0.2 | 27.89 | 0.2 | 0.242 | 1.2 |
| 05b-6-108_m1_22 | 0.143 | 5.0 | 6.74 | 0.4 | 7.177 | 0.176 | 2.6 | 0.04 | 23.4 | 0.056 | 2.283 | 0.3 | 31.05 | 0.2 | 27.80 | 0.2 | 0.246 | 1.2 |
| 05b-6-108_m1_23 | 0.126 | 5.7 | 6.53 | 0.4 | 6.957 | 0.170 | 2.7 | 0.04 | 23.0 | 0.057 | 2.245 | 0.3 | 31.49 | 0.2 | 27.84 | 0.2 | 0.234 | 1.2 |
| 05b-6-108_m1_24 | 0.147 | 4.9 | 6.54 | 0.4 | 6.966 | 0.173 | 2.6 | 0.05 | 19.6 | 0.067 | 2.229 | 0.3 | 31.46 | 0.2 | 27.72 | 0.2 | 0.238 | 1.2 |
| 05b-6-108_m1_25 | 0.126 | 5.7 | 6.80 | 0.4 | 7.248 | 0.173 | 2.6 | 0.07 | 15.1 | 0.087 | 2.255 | 0.3 | 31.20 | 0.2 | 27.79 | 0.2 | 0.243 | 1.2 |
| 05b-6-108_m1_26 | 0.156 | 4.6 | 6.81 | 0.4 | 7.251 | 0.182 | 2.5 | 0.08 | 13.2 | 0.099 | 2.268 | 0.3 | 31.17 | 0.2 | 27.81 | 0.2 | 0.247 | 1.2 |
| 05b-6-108_m1_27 | 0.147 | 4.9 | 6.74 | 0.4 | 7.182 | 0.179 | 2.6 | 0.05 | 18.6 | 0.071 | 2.260 | 0.3 | 31.29 | 0.2 | 27.63 | 0.2 | 0.259 | 1.1 |
| 05b-6-108_m1_28 | 0.144 | 4.9 | 6.76 | 0.4 | 7.203 | 0.183 | 2.5 | 0.07 | 14.5 | 0.091 | 2.277 | 0.3 | 31.55 | 0.2 | 27.77 | 0.2 | 0.273 | 1.1 |
| 05b-6-108_m1_29 | 0.134 | 5.3 | 6.34 | 0.4 | 6.753 | 0.168 | 2.7 | 0.06 | 17.4 | 0.075 | 2.231 | 0.3 | 31.59 | 0.2 | 27.74 | 0.2 | 0.220 | 1.3 |
| 05b-6-108_m1_30 | 0.133 | 5.4 | 6.54 | 0.4 | 6.968 | 0.176 | 2.6 | 0.05 | 19.7 | 0.067 | 2.193 | 0.3 | 30.89 | 0.2 | 27.74 | 0.2 | 0.234 | 1.2 |
| 05b-6-108_m1_31 | 0.141 | 5.1 | 6.52 | 0.4 | 6.945 | 0.163 | 2.8 | 0.07 | 13.8 | 0.095 | 2.193 | 0.3 | 31.44 | 0.2 | 27.71 | 0.2 | 0.235 | 1.2 |
| 05b-6-108_m1_32 | 0.125 | 5.7 | 6.32 | 0.4 | 6.732 | 0.169 | 2.7 | 0.06 | 17.9 | 0.073 | 2.112 | 0.3 | 31.68 | 0.2 | 27.61 | 0.2 | 0.237 | 1.2 |
| 05b-6-108_m1_33 | 0.148 | 4.8 | 6.68 | 0.4 | 7.121 | 0.163 | 2.8 | 0.04 | 22.2 | 0.059 | 2.263 | 0.3 | 31.46 | 0.2 | 27.77 | 0.2 | 0.239 | 1.2 |
| 05b-6-108_m1_34 | 0.142 | 5.1 | 6.68 | 0.4 | 7.124 | 0.180 | 2.5 | 0.06 | 16.7 | 0.079 | 2.269 | 0.3 | 31.49 | 0.2 | 27.67 | 0.2 | 0.241 | 1.2 |
| 05b-6-108_m1_35 | 0.133 | 5.4 | 6.21 | 0.5 | 6.612 | 0.166 | 2.7 | 0.05 | 20.1 | 0.065 | 2.094 | 0.3 | 31.71 | 0.2 | 27.67 | 0.2 | 0.232 | 1.2 |
| 05b-6-108_m1_36 | 0.134 | 5.3 | 6.65 | 0.4 | 7.086 | 0.178 | 2.6 | 0.04 | 27.1 | 0.048 | 2.205 | 0.3 | 31.51 | 0.2 | 27.78 | 0.2 | 0.247 | 1.2 |

| | $UO_2$ | | $ThO_2$ | | | PbO | | $Y_2O_3$ | | | CaO | | $Ce_2O_3$ | | $P_2O_5$ | | $SiO_2$ | |
|---|---|---|---|---|---|---|---|---|---|---|---|---|---|---|---|---|---|---|
| Sample | wt. % | RSD (2σ%) | wt. % | RSD (2σ%) | k-raw | wt. % | RSD (2σ%) | wt. % | RSD (2σ%) | k-raw | wt. % | RSD (2σ%) | wt. % | RSD (2σ%) | wt. % | RSD (2σ%) | wt. % | RSD (2σ%) |
| 05b-6-108_m1_37 | 0.120 | 5.9 | 6.28 | 0.4 | 6.692 | 0.171 | 2.7 | 0.02 | 56.8 | 0.023 | 2.280 | 0.3 | 31.64 | 0.2 | 27.78 | 0.2 | 0.217 | 1.3 |
| 05b-6-108_m1_38 | 0.145 | 4.9 | 6.27 | 0.4 | 6.675 | 0.166 | 2.8 | 0.03 | 31.7 | 0.041 | 2.325 | 0.3 | 31.73 | 0.2 | 27.80 | 0.2 | 0.212 | 1.3 |
| 05b-6-108_m1_39 | 0.117 | 6.1 | 6.21 | 0.5 | 6.607 | 0.164 | 2.8 | 0.04 | 24.0 | 0.055 | 2.293 | 0.3 | 31.90 | 0.2 | 27.80 | 0.2 | 0.211 | 1.3 |
| 05b-6-108_m1_40 | 0.131 | 5.4 | 6.26 | 0.5 | 6.659 | 0.163 | 2.8 | 0.04 | 22.7 | 0.058 | 2.335 | 0.3 | 31.53 | 0.2 | 27.74 | 0.2 | 0.215 | 1.3 |
| 8153_41 | 0.380 | 2.0 | 7.29 | 0.4 | 7.784 | 0.188 | 2.5 | 0.49 | 2.2 | 0.639 | 0.601 | 0.6 | 31.49 | 0.2 | 25.74 | 0.2 | 1.264 | 0.3 |
| 8153_42 | 0.392 | 2.0 | 7.34 | 0.4 | 7.834 | 0.184 | 2.5 | 0.51 | 2.1 | 0.672 | 0.593 | 0.6 | 31.60 | 0.2 | 25.97 | 0.2 | 1.280 | 0.3 |
| 8153_43 | 0.393 | 2.0 | 7.25 | 0.4 | 7.745 | 0.180 | 2.6 | 0.50 | 2.2 | 0.652 | 0.601 | 0.6 | 31.79 | 0.2 | 25.95 | 0.2 | 1.276 | 0.3 |
| 8153_44 | 0.380 | 2.0 | 7.29 | 0.4 | 7.787 | 0.181 | 2.5 | 0.49 | 2.2 | 0.644 | 0.598 | 0.6 | 31.49 | 0.2 | 25.82 | 0.2 | 1.268 | 0.3 |
| 8153_45 | 0.387 | 2.0 | 7.32 | 0.4 | 7.816 | 0.198 | 2.3 | 0.50 | 2.2 | 0.653 | 0.601 | 0.6 | 31.70 | 0.2 | 25.97 | 0.2 | 1.268 | 0.3 |
| 8153_46 | 0.380 | 2.0 | 7.31 | 0.4 | 7.806 | 0.179 | 2.6 | 0.52 | 2.1 | 0.676 | 0.603 | 0.6 | 31.58 | 0.2 | 26.02 | 0.2 | 1.270 | 0.3 |
| 8153_47 | 0.383 | 2.0 | 7.29 | 0.4 | 7.781 | 0.187 | 2.5 | 0.50 | 2.2 | 0.657 | 0.600 | 0.6 | 31.62 | 0.2 | 25.97 | 0.2 | 1.280 | 0.3 |
| 8153_48 | 0.376 | 2.0 | 7.33 | 0.4 | 7.829 | 0.190 | 2.4 | 0.50 | 2.2 | 0.652 | 0.598 | 0.6 | 31.56 | 0.2 | 26.09 | 0.2 | 1.279 | 0.3 |
| 8153_49 | 0.389 | 2.0 | 7.36 | 0.4 | 7.858 | 0.186 | 2.5 | 0.49 | 2.2 | 0.643 | 0.599 | 0.6 | 31.58 | 0.2 | 26.16 | 0.2 | 1.281 | 0.3 |
| 8153_50 | 0.392 | 2.0 | 7.29 | 0.4 | 7.779 | 0.179 | 2.6 | 0.48 | 2.3 | 0.622 | 0.602 | 0.6 | 31.59 | 0.2 | 26.08 | 0.2 | 1.286 | 0.3 |
| | | | | | | | | | | | | | | | | | | |
| TU_RenoMnt_pt1 | 0.814 | 0.8 | 16.14 | 0.2 | 17.403 | 0.240 | 1.8 | 2.36 | 0.7 | 2.893 | 1.615 | 0.3 | 22.02 | 0.2 | 23.10 | 0.2 | 2.332 | 0.2 |
| TU_RenoMnt_pt2 | 0.873 | 0.8 | 17.06 | 0.2 | 18.455 | 0.239 | 1.8 | 2.31 | 0.7 | 2.828 | 1.660 | 0.3 | 21.55 | 0.2 | 22.67 | 0.2 | 2.487 | 0.2 |
| TU_RenoMnt_pt3 | 0.855 | 0.8 | 16.31 | 0.2 | 17.602 | 0.237 | 1.8 | 2.36 | 0.7 | 2.889 | 1.616 | 0.3 | 21.89 | 0.2 | 22.80 | 0.2 | 2.367 | 0.2 |
| TU_RenoMnt_pt4 | 0.346 | 1.7 | 7.94 | 0.3 | 8.377 | 0.126 | 3.1 | 2.20 | 0.7 | 2.616 | 0.629 | 0.5 | 26.17 | 0.2 | 24.24 | 0.2 | 1.308 | 0.3 |
| TU_RenoMnt_pt5 | 0.348 | 1.7 | 7.78 | 0.3 | 8.209 | 0.126 | 3.1 | 2.19 | 0.7 | 2.602 | 0.606 | 0.5 | 26.25 | 0.2 | 24.53 | 0.2 | 1.300 | 0.3 |
| 8153_pt1 | 0.360 | 1.6 | 7.21 | 0.3 | 7.677 | 0.191 | 2.1 | 0.48 | 2.8 | 0.557 | 0.560 | 0.5 | 31.00 | 0.2 | 24.08 | 0.2 | 1.278 | 0.4 |
| 8153_pt2 | 0.384 | 1.5 | 7.65 | 0.3 | 8.153 | 0.194 | 2.1 | 0.47 | 2.9 | 0.543 | 0.579 | 0.5 | 30.95 | 0.2 | 24.35 | 0.2 | 1.372 | 0.3 |
| 8153_pt3 | 0.381 | 1.6 | 7.37 | 0.3 | 7.855 | 0.183 | 2.2 | 0.48 | 2.8 | 0.551 | 0.574 | 0.5 | 31.01 | 0.2 | 23.76 | 0.2 | 1.296 | 0.4 |
| 8153_pt4 | 0.384 | 1.6 | 7.52 | 0.3 | 8.011 | 0.192 | 2.1 | 0.48 | 2.8 | 0.560 | 0.568 | 0.5 | 31.04 | 0.2 | 24.32 | 0.2 | 1.353 | 0.3 |
| 8153_pt5 | 0.344 | 1.7 | 7.50 | 0.3 | 7.992 | 0.189 | 2.2 | 0.41 | 3.2 | 0.471 | 0.543 | 0.5 | 31.33 | 0.2 | 24.45 | 0.2 | 1.369 | 0.3 |
| 8153_pt6 | 0.200 | 2.9 | 6.52 | 0.4 | 6.933 | 0.166 | 2.4 | 0.30 | 4.3 | 0.349 | 0.594 | 0.5 | 31.63 | 0.2 | 25.12 | 0.2 | 1.114 | 0.4 |
| 8153_pt3 | 0.380 | 1.6 | 7.31 | 0.3 | 7.792 | 0.188 | 2.2 | 0.47 | 2.8 | 0.540 | 0.572 | 0.5 | 30.97 | 0.2 | 23.59 | 0.2 | 1.291 | 0.4 |
| 8153_pt3 | 0.358 | 1.7 | 7.50 | 0.3 | 7.985 | 0.181 | 2.3 | 0.48 | 2.7 | 0.560 | 0.587 | 0.5 | 31.27 | 0.2 | 24.60 | 0.2 | 1.310 | 0.3 |
| 8153_pt3 | 0.367 | 1.6 | 7.37 | 0.3 | 7.846 | 0.191 | 2.1 | 0.47 | 2.9 | 0.540 | 0.583 | 0.5 | 31.06 | 0.2 | 24.54 | 0.2 | 1.300 | 0.3 |
| 8153_pt3 | 0.391 | 1.5 | 7.34 | 0.3 | 7.814 | 0.190 | 2.2 | 0.49 | 2.7 | 0.566 | 0.575 | 0.5 | 31.19 | 0.2 | 24.88 | 0.2 | 1.299 | 0.4 |
| TU_RenoMnt_pt1 | 0.849 | 0.8 | 16.65 | 0.2 | 17.988 | 0.242 | 1.7 | 2.30 | 0.7 | 2.823 | 1.647 | 0.3 | 21.85 | 0.2 | 22.73 | 0.2 | 2.405 | 0.2 |
| 8153_1 | 0.371 | 1.6 | 7.34 | 0.3 | 7.810 | 0.190 | 2.2 | 0.51 | 2.6 | 0.589 | 0.580 | 0.5 | 31.14 | 0.2 | 24.57 | 0.2 | 1.297 | 0.4 |
| 8153_1 | 0.367 | 1.6 | 7.57 | 0.3 | 8.064 | 0.185 | 2.2 | 0.50 | 2.7 | 0.579 | 0.582 | 0.5 | 31.20 | 0.2 | 24.68 | 0.2 | 1.315 | 0.3 |
| 8153_2 | 0.363 | 1.6 | 7.42 | 0.3 | 7.902 | 0.182 | 2.2 | 0.51 | 2.6 | 0.589 | 0.585 | 0.5 | 31.14 | 0.2 | 24.46 | 0.2 | 1.309 | 0.3 |
| 8153_3 | 0.385 | 1.6 | 7.74 | 0.3 | 8.252 | 0.198 | 2.1 | 0.49 | 2.8 | 0.567 | 0.582 | 0.5 | 31.01 | 0.2 | 24.70 | 0.2 | 1.365 | 0.3 |
| 05b-6-31-Mnz1_pt2 | 0.116 | 4.7 | 4.69 | 0.4 | 4.982 | 0.136 | 2.9 | 0.03 | 49.2 | 0.030 | 1.704 | 0.2 | 31.85 | 0.2 | 25.41 | 0.2 | 0.169 | 2.1 |

| | $UO_2$ | | $ThO_2$ | | | PbO | | $Y_2O_3$ | | | CaO | | $Ce_2O_3$ | | $P_2O_5$ | | $SiO_2$ | |
|---|---|---|---|---|---|---|---|---|---|---|---|---|---|---|---|---|---|---|
| Sample | wt. % | RSD (2σ%) | wt. % | RSD (2σ%) | k-raw | wt. % | RSD (2σ%) | wt. % | RSD (2σ%) | k-raw | wt. % | RSD (2σ%) | wt. % | RSD (2σ%) | wt. % | RSD (2σ%) | wt. % | RSD (2σ%) |
| 05b-6-31-Mnz1_pt3 | 0.120 | 4.6 | 4.73 | 0.4 | 5.022 | 0.130 | 3.0 | 0.03 | 44.6 | 0.033 | 1.718 | 0.2 | 31.73 | 0.2 | 25.41 | 0.2 | 0.178 | 2.0 |
| 05b-6-31-Mnz1_pt4 | 0.129 | 4.2 | 4.68 | 0.4 | 4.971 | 0.127 | 3.0 | 0.03 | 47.1 | 0.031 | 1.720 | 0.2 | 31.79 | 0.2 | 25.39 | 0.2 | 0.184 | 1.9 |
| 05b-6-31-Mnz1_pt5 | 0.121 | 4.5 | 4.75 | 0.4 | 5.039 | 0.135 | 2.9 | 0.04 | 34.6 | 0.042 | 1.724 | 0.2 | 31.66 | 0.2 | 25.45 | 0.2 | 0.189 | 1.9 |
| 05b-6-31-Mnz1_pt6 | 0.129 | 4.2 | 5.12 | 0.4 | 5.442 | 0.142 | 2.7 | 0.03 | 45.4 | 0.032 | 1.763 | 0.2 | 31.46 | 0.2 | 25.48 | 0.2 | 0.200 | 1.8 |
| 05b-6-31-Mnz1_pt7 | 0.136 | 4.1 | 5.20 | 0.4 | 5.527 | 0.149 | 2.6 | 0.02 | 54.2 | 0.027 | 1.686 | 0.2 | 31.42 | 0.2 | 25.37 | 0.2 | 0.206 | 1.7 |
| 05b-6-31-Mnz1_pt8 | 0.131 | 4.2 | 5.22 | 0.4 | 5.534 | 0.151 | 2.6 | 0.03 | 38.8 | 0.039 | 1.654 | 0.2 | 31.37 | 0.2 | 26.31 | 0.2 | 0.790 | 0.5 |
| 05b-6-31-Mnz1_pt9 | 0.123 | 4.5 | 5.17 | 0.4 | 5.492 | 0.150 | 2.6 | 0.01 | 127.4 | 0.012 | 1.634 | 0.3 | 31.63 | 0.2 | 25.67 | 0.2 | 0.202 | 1.8 |
| 05b-6-31-Mnz1_pt10 | 0.135 | 4.1 | 5.04 | 0.4 | 5.358 | 0.139 | 2.8 | 0.01 | 107.6 | 0.014 | 1.608 | 0.3 | 31.54 | 0.2 | 25.36 | 0.2 | 0.195 | 1.8 |
| 05b-6-31-Mnz1_pt11 | 0.125 | 4.4 | 5.11 | 0.4 | 5.424 | 0.141 | 2.7 | 0.02 | 55.4 | 0.026 | 1.662 | 0.2 | 31.39 | 0.2 | 25.36 | 0.2 | 0.197 | 1.8 |
| 05b-6-31-Mnz1_pt12 | 0.130 | 4.2 | 5.10 | 0.4 | 5.416 | 0.140 | 2.8 | 0.02 | 69.1 | 0.021 | 1.699 | 0.2 | 31.34 | 0.2 | 25.68 | 0.2 | 0.197 | 1.8 |
| 05b-6-31-Mnz1_pt13 | 0.130 | 4.2 | 5.21 | 0.4 | 5.535 | 0.142 | 2.7 | 0.04 | 28.7 | 0.051 | 1.899 | 0.2 | 31.10 | 0.2 | 25.46 | 0.2 | 0.188 | 1.9 |
| 05b-6-31-Mnz1_pt14 | 0.148 | 3.7 | 5.08 | 0.4 | 5.401 | 0.143 | 2.7 | 0.06 | 19.5 | 0.075 | 1.876 | 0.2 | 31.02 | 0.2 | 25.23 | 0.2 | 0.185 | 1.9 |
| 8153_5 | 0.375 | 1.6 | 7.38 | 0.3 | 7.856 | 0.187 | 2.2 | 0.48 | 2.8 | 0.551 | 0.578 | 0.5 | 31.22 | 0.2 | 24.51 | 0.2 | 1.295 | 0.4 |
| 8153_6 | 0.372 | 1.6 | 7.38 | 0.3 | 7.861 | 0.188 | 2.2 | 0.50 | 2.7 | 0.582 | 0.577 | 0.5 | 31.10 | 0.2 | 24.61 | 0.2 | 1.307 | 0.3 |
| 8153_7 | 0.377 | 1.6 | 7.33 | 0.3 | 7.804 | 0.188 | 2.2 | 0.50 | 2.6 | 0.586 | 0.578 | 0.5 | 31.03 | 0.2 | 24.52 | 0.2 | 1.294 | 0.4 |
| 8153_8 | 0.366 | 1.6 | 7.35 | 0.3 | 7.827 | 0.191 | 2.1 | 0.47 | 2.9 | 0.548 | 0.581 | 0.5 | 31.19 | 0.2 | 24.71 | 0.2 | 1.309 | 0.3 |
| 8153_9 | 0.390 | 1.5 | 7.37 | 0.3 | 7.846 | 0.186 | 2.2 | 0.51 | 2.6 | 0.594 | 0.578 | 0.5 | 31.00 | 0.2 | 24.57 | 0.2 | 1.304 | 0.3 |
| 8153_10 | 0.372 | 1.6 | 7.38 | 0.3 | 7.851 | 0.197 | 2.1 | 0.49 | 2.7 | 0.573 | 0.586 | 0.5 | 31.12 | 0.2 | 24.91 | 0.2 | 1.332 | 0.3 |
| 8153_11 | 0.381 | 1.6 | 7.38 | 0.3 | 7.858 | 0.198 | 2.0 | 0.47 | 2.9 | 0.545 | 0.581 | 0.5 | 31.07 | 0.2 | 24.56 | 0.2 | 1.297 | 0.4 |
| 05b-6-31-Mnz1_pt15 | 0.248 | 2.3 | 5.08 | 0.4 | 5.371 | 0.164 | 2.4 | 0.91 | 1.5 | 1.069 | 1.531 | 0.3 | 29.95 | 0.2 | 25.51 | 0.2 | 0.279 | 1.3 |
| 05b-6-31-Mnz1_pt16 | 0.243 | 2.3 | 5.14 | 0.4 | 5.428 | 0.169 | 2.4 | 0.94 | 1.5 | 1.105 | 1.543 | 0.3 | 30.01 | 0.2 | 26.02 | 0.2 | 0.281 | 1.3 |
| 05b-6-31-Mnz1_pt17 | 0.420 | 1.4 | 4.24 | 0.5 | 4.481 | 0.150 | 2.6 | 0.58 | 2.3 | 0.678 | 1.350 | 0.3 | 30.82 | 0.2 | 25.33 | 0.2 | 0.208 | 1.7 |
| 05b-6-31-Mnz1_pt18 | 0.408 | 1.4 | 4.20 | 0.5 | 4.438 | 0.152 | 2.6 | 0.63 | 2.1 | 0.739 | 1.335 | 0.3 | 30.70 | 0.2 | 25.46 | 0.2 | 0.213 | 1.7 |
| 05b-6-31-Mnz1_pt19 | 0.380 | 1.5 | 4.10 | 0.5 | 4.325 | 0.145 | 2.7 | 0.64 | 2.1 | 0.749 | 1.273 | 0.3 | 30.94 | 0.2 | 25.64 | 0.2 | 0.208 | 1.7 |
| 05b-6-31-Mnz1_pt20 | 0.237 | 2.4 | 4.63 | 0.4 | 4.898 | 0.144 | 2.7 | 0.57 | 2.4 | 0.663 | 1.397 | 0.3 | 30.68 | 0.2 | 25.39 | 0.2 | 0.193 | 1.8 |
| 05b-6-31-Mnz1_pt21 | 0.265 | 2.1 | 4.45 | 0.5 | 4.697 | 0.143 | 2.7 | 0.83 | 1.7 | 0.973 | 1.323 | 0.3 | 30.40 | 0.2 | 25.23 | 0.2 | 0.221 | 1.6 |
| 05b-6-31-Mnz1_pt22 | 0.472 | 1.3 | 3.73 | 0.5 | 3.936 | 0.144 | 2.7 | 0.40 | 3.3 | 0.462 | 1.233 | 0.3 | 31.09 | 0.2 | 25.38 | 0.2 | 0.212 | 1.7 |
| 05b-6-31-Mnz1_pt23 | 0.506 | 1.2 | 4.18 | 0.5 | 4.417 | 0.156 | 2.5 | 0.38 | 3.5 | 0.447 | 1.346 | 0.3 | 31.08 | 0.2 | 25.35 | 0.2 | 0.246 | 1.5 |
| 05b-6-31-Mnz1_pt24 | 0.604 | 1.0 | 5.04 | 0.4 | 5.343 | 0.188 | 2.1 | 0.36 | 3.7 | 0.422 | 1.749 | 0.2 | 30.39 | 0.2 | 25.32 | 0.2 | 0.270 | 1.3 |
| 05b-6-31-Mnz1_pt25 | 0.479 | 1.2 | 3.77 | 0.5 | 3.980 | 0.146 | 2.7 | 0.36 | 3.7 | 0.413 | 1.271 | 0.3 | 31.33 | 0.2 | 25.35 | 0.2 | 0.222 | 1.6 |
| 05b-6-31-Mnz1_pt26 | 0.498 | 1.2 | 3.74 | 0.5 | 3.946 | 0.146 | 2.7 | 0.38 | 3.5 | 0.443 | 1.258 | 0.3 | 31.24 | 0.2 | 25.44 | 0.2 | 0.207 | 1.7 |
| 05b-6-31-Mnz1_pt27 | 0.449 | 1.3 | 3.81 | 0.5 | 4.025 | 0.140 | 2.8 | 0.37 | 3.6 | 0.429 | 1.197 | 0.3 | 31.33 | 0.2 | 25.46 | 0.2 | 0.215 | 1.7 |
| 05b-6-31-Mnz1_pt28 | 0.454 | 1.3 | 3.88 | 0.5 | 4.104 | 0.142 | 2.8 | 0.38 | 3.5 | 0.445 | 1.200 | 0.3 | 31.26 | 0.2 | 25.60 | 0.2 | 0.211 | 1.7 |
| 05b-6-31-Mnz1_pt29 | 0.445 | 1.3 | 3.85 | 0.5 | 4.074 | 0.138 | 2.8 | 0.39 | 3.4 | 0.453 | 1.186 | 0.3 | 31.26 | 0.2 | 25.22 | 0.2 | 0.212 | 1.7 |
| 05b-6-31-Mnz1_pt30 | 0.427 | 1.4 | 3.89 | 0.5 | 4.110 | 0.140 | 2.8 | 0.41 | 3.3 | 0.481 | 1.193 | 0.3 | 31.26 | 0.2 | 25.83 | 0.2 | 0.218 | 1.7 |
| 8153_12 | 0.389 | 1.5 | 7.29 | 0.3 | 7.761 | 0.189 | 2.2 | 0.46 | 2.9 | 0.532 | 0.573 | 0.5 | 31.16 | 0.2 | 24.43 | 0.2 | 1.304 | 0.3 |

| | $UO_2$ | | $ThO_2$ | | | PbO | | $Y_2O_3$ | | | CaO | | $Ce_2O_3$ | | $P_2O_5$ | | $SiO_2$ | |
|---|---|---|---|---|---|---|---|---|---|---|---|---|---|---|---|---|---|---|
| Sample | wt. % | RSD (2σ%) | wt. % | RSD (2σ%) | k-raw | wt. % | RSD (2σ%) | wt. % | RSD (2σ%) | k-raw | wt. % | RSD (2σ%) | wt. % | RSD (2σ%) | wt. % | RSD (2σ%) | wt. % | RSD (2σ%) |
| 8153_13 | 0.375 | 1.6 | 7.37 | 0.3 | 7.851 | 0.188 | 2.2 | 0.49 | 2.7 | 0.570 | 0.578 | 0.5 | 30.94 | 0.2 | 24.54 | 0.2 | 1.300 | 0.4 |
| 8153_14 | 0.373 | 1.6 | 7.32 | 0.3 | 7.795 | 0.196 | 2.1 | 0.49 | 2.8 | 0.564 | 0.580 | 0.5 | 31.15 | 0.2 | 24.34 | 0.2 | 1.296 | 0.4 |
| 8153_15 | 0.381 | 1.6 | 7.32 | 0.3 | 7.797 | 0.193 | 2.1 | 0.48 | 2.8 | 0.552 | 0.579 | 0.5 | 31.10 | 0.2 | 24.54 | 0.2 | 1.287 | 0.4 |
| TU_RenoMnt_pt6 | 0.917 | 0.8 | 17.17 | 0.2 | 18.583 | 0.247 | 1.7 | 2.32 | 0.7 | 2.850 | 1.676 | 0.3 | 21.50 | 0.2 | 22.30 | 0.2 | 2.482 | 0.2 |
| TU_RenoMnt_pt7 | 0.915 | 0.8 | 17.23 | 0.2 | 18.654 | 0.239 | 1.8 | 2.34 | 0.7 | 2.872 | 1.687 | 0.3 | 21.45 | 0.2 | 22.28 | 0.2 | 2.500 | 0.2 |
| TU_RenoMnt_pt8 | 0.913 | 0.8 | 17.43 | 0.2 | 18.880 | 0.243 | 1.7 | 2.31 | 0.7 | 2.834 | 1.686 | 0.3 | 21.45 | 0.2 | 22.33 | 0.2 | 2.524 | 0.2 |
| TU_RenoMnt_pt9 | 0.919 | 0.8 | 17.37 | 0.2 | 18.815 | 0.243 | 1.7 | 2.29 | 0.7 | 2.810 | 1.681 | 0.3 | 21.45 | 0.2 | 22.34 | 0.2 | 2.532 | 0.2 |
| TU_RenoMnt_pt10 | 0.895 | 0.8 | 17.27 | 0.2 | 18.689 | 0.240 | 1.7 | 2.30 | 0.7 | 2.827 | 1.672 | 0.3 | 21.48 | 0.2 | 22.51 | 0.2 | 2.518 | 0.2 |
| 05b-6-31-Mnz1_pt31 | 0.444 | 1.3 | 3.81 | 0.5 | 4.022 | 0.147 | 2.6 | 0.36 | 3.7 | 0.417 | 1.185 | 0.3 | 31.24 | 0.2 | 25.35 | 0.2 | 0.202 | 1.8 |
| 05b-6-31-Mnz1_pt32 | 0.450 | 1.3 | 3.85 | 0.5 | 4.068 | 0.143 | 2.7 | 0.39 | 3.5 | 0.448 | 1.190 | 0.3 | 31.23 | 0.2 | 25.34 | 0.2 | 0.209 | 1.7 |
| 05b-6-31-Mnz1_pt33 | 0.451 | 1.3 | 3.84 | 0.5 | 4.061 | 0.143 | 2.7 | 0.39 | 3.4 | 0.455 | 1.202 | 0.3 | 31.21 | 0.2 | 25.41 | 0.2 | 0.204 | 1.8 |
| 05b-6-31-Mnz1_pt34 | 0.499 | 1.2 | 4.07 | 0.5 | 4.308 | 0.152 | 2.6 | 0.39 | 3.4 | 0.453 | 1.353 | 0.3 | 31.03 | 0.2 | 25.44 | 0.2 | 0.246 | 1.5 |
| 05b-6-31-Mnz1_pt35 | 0.527 | 1.2 | 4.39 | 0.5 | 4.644 | 0.164 | 2.4 | 0.36 | 3.7 | 0.422 | 1.505 | 0.3 | 30.92 | 0.2 | 25.43 | 0.2 | 0.249 | 1.5 |
| 05b-6-31-Mnz1_pt36 | 0.549 | 1.1 | 4.66 | 0.4 | 4.932 | 0.166 | 2.4 | 0.38 | 3.5 | 0.448 | 1.613 | 0.3 | 30.60 | 0.2 | 25.34 | 0.2 | 0.259 | 1.4 |
| 05b-6-31-Mnz1_pt37 | 0.431 | 1.4 | 3.98 | 0.5 | 4.206 | 0.141 | 2.8 | 0.41 | 3.3 | 0.476 | 1.228 | 0.3 | 31.16 | 0.2 | 25.54 | 0.2 | 0.210 | 1.7 |
| 05b-6-31-Mnz1_pt38 | 0.485 | 1.2 | 3.78 | 0.5 | 3.990 | 0.147 | 2.7 | 0.39 | 3.4 | 0.458 | 1.235 | 0.3 | 31.22 | 0.2 | 25.54 | 0.2 | 0.208 | 1.7 |
| 05b-6-31-Mnz1_pt39 | 0.510 | 1.2 | 3.75 | 0.5 | 3.965 | 0.149 | 2.6 | 0.36 | 3.7 | 0.423 | 1.253 | 0.3 | 31.25 | 0.2 | 25.65 | 0.2 | 0.225 | 1.6 |
| 05b-6-31-Mnz1_pt40 | 0.635 | 1.0 | 5.16 | 0.4 | 5.476 | 0.191 | 2.1 | 0.39 | 3.4 | 0.455 | 1.773 | 0.2 | 30.20 | 0.2 | 25.38 | 0.2 | 0.291 | 1.3 |
| 05b-6-31-Mnz1_pt41 | 0.472 | 1.3 | 3.66 | 0.5 | 3.864 | 0.139 | 2.8 | 0.37 | 3.6 | 0.431 | 1.234 | 0.3 | 31.28 | 0.2 | 25.46 | 0.2 | 0.211 | 1.7 |
| 05b-6-31-Mnz1_pt42 | 0.535 | 1.1 | 4.43 | 0.5 | 4.688 | 0.168 | 2.4 | 0.37 | 3.6 | 0.431 | 1.715 | 0.2 | 30.75 | 0.2 | 25.16 | 0.2 | 0.235 | 1.5 |
| 05b-6-31-Mnz1_pt43 | 0.556 | 1.1 | 4.42 | 0.5 | 4.688 | 0.172 | 2.3 | 0.38 | 3.5 | 0.437 | 1.723 | 0.2 | 30.88 | 0.2 | 25.17 | 0.2 | 0.237 | 1.5 |
| TU_RenoMnt_pt11 | 0.880 | 0.8 | 16.89 | 0.2 | 18.267 | 0.230 | 1.8 | 2.28 | 0.7 | 2.795 | 1.640 | 0.3 | 21.79 | 0.2 | 22.47 | 0.2 | 2.462 | 0.2 |
| TU_RenoMnt_pt12 | 0.880 | 0.8 | 16.77 | 0.2 | 18.130 | 0.232 | 1.8 | 2.32 | 0.7 | 2.845 | 1.636 | 0.3 | 21.61 | 0.2 | 22.52 | 0.2 | 2.432 | 0.2 |
| TU_RenoMnt_pt13 | 0.853 | 0.8 | 16.25 | 0.2 | 17.548 | 0.237 | 1.8 | 2.35 | 0.7 | 2.872 | 1.613 | 0.3 | 22.00 | 0.2 | 22.68 | 0.2 | 2.341 | 0.2 |
| TU_RenoMnt_pt14 | 0.867 | 0.8 | 16.22 | 0.2 | 17.510 | 0.235 | 1.8 | 2.34 | 0.7 | 2.856 | 1.606 | 0.3 | 22.10 | 0.2 | 22.75 | 0.2 | 2.396 | 0.2 |
| TU_RenoMnt_pt15 | 0.869 | 0.8 | 16.47 | 0.2 | 17.779 | 0.242 | 1.7 | 2.34 | 0.7 | 2.863 | 1.628 | 0.3 | 22.00 | 0.2 | 22.79 | 0.2 | 2.490 | 0.2 |
| 8153_15 | 0.373 | 1.6 | 7.33 | 0.3 | 7.802 | 0.192 | 2.1 | 0.49 | 2.8 | 0.563 | 0.582 | 0.5 | 31.11 | 0.2 | 24.58 | 0.2 | 1.297 | 0.4 |
| 8153_16 | 0.381 | 1.6 | 7.35 | 0.3 | 7.830 | 0.187 | 2.2 | 0.50 | 2.7 | 0.577 | 0.575 | 0.5 | 31.18 | 0.2 | 24.68 | 0.2 | 1.309 | 0.4 |
| 8153_17 | 0.388 | 1.5 | 7.32 | 0.3 | 7.799 | 0.193 | 2.1 | 0.50 | 2.7 | 0.576 | 0.577 | 0.5 | 31.08 | 0.2 | 24.57 | 0.2 | 1.295 | 0.4 |
| 8153_18 | 0.388 | 1.5 | 7.36 | 0.3 | 7.836 | 0.186 | 2.2 | 0.49 | 2.8 | 0.567 | 0.580 | 0.5 | 31.16 | 0.2 | 24.77 | 0.2 | 1.305 | 0.4 |
| 05b-6-31-Mnz1_pt43 | 0.230 | 2.5 | 4.55 | 0.4 | 4.803 | 0.143 | 2.8 | 0.94 | 1.5 | 1.102 | 1.396 | 0.3 | 30.39 | 0.2 | 25.47 | 0.2 | 0.247 | 1.5 |
| 05b-6-31-Mnz1_pt44 | 0.238 | 2.4 | 4.65 | 0.4 | 4.906 | 0.146 | 2.7 | 0.96 | 1.5 | 1.117 | 1.401 | 0.3 | 30.24 | 0.2 | 25.50 | 0.2 | 0.250 | 1.4 |
| 05b-6-31-Mnz1_pt45 | 0.241 | 2.4 | 4.85 | 0.4 | 5.122 | 0.158 | 2.5 | 0.99 | 1.4 | 1.160 | 1.463 | 0.3 | 30.07 | 0.2 | 25.41 | 0.2 | 0.269 | 1.3 |
| 05b-6-31-Mnz1_pt46 | 0.467 | 1.3 | 3.65 | 0.5 | 3.855 | 0.139 | 2.8 | 0.37 | 3.7 | 0.423 | 1.208 | 0.3 | 31.29 | 0.2 | 25.43 | 0.2 | 0.218 | 1.7 |
| 05b-6-31-Mnz1_pt47 | 0.219 | 2.6 | 4.56 | 0.4 | 4.814 | 0.145 | 2.7 | 0.89 | 1.6 | 1.036 | 1.394 | 0.3 | 30.43 | 0.2 | 25.43 | 0.2 | 0.231 | 1.6 |
| 05b-6-31-Mnz1_pt48 | 0.231 | 2.5 | 4.62 | 0.4 | 4.872 | 0.147 | 2.7 | 0.94 | 1.5 | 1.094 | 1.401 | 0.3 | 30.38 | 0.2 | 25.53 | 0.2 | 0.244 | 1.5 |

| | $UO_2$ | | $ThO_2$ | | | PbO | | $Y_2O_3$ | | | CaO | | $Ce_2O_3$ | | $P_2O_5$ | | $SiO_2$ | |
|---|---|---|---|---|---|---|---|---|---|---|---|---|---|---|---|---|---|---|
| Sample | wt. % | RSD (2σ%) | wt. % | RSD (2σ%) | k-raw | wt. % | RSD (2σ%) | wt. % | RSD (2σ%) | k-raw | wt. % | RSD (2σ%) | wt. % | RSD (2σ%) | wt. % | RSD (2σ%) | wt. % | RSD (2σ%) |
| 05b-6-31-Mnz1_pt49 | 0.222 | 2.6 | 4.65 | 0.4 | 4.909 | 0.145 | 2.7 | 0.94 | 1.5 | 1.093 | 1.406 | 0.3 | 30.23 | 0.2 | 25.50 | 0.2 | 0.251 | 1.4 |
| 05b-6-31-Mnz1_pt50 | 0.220 | 2.6 | 4.65 | 0.4 | 4.909 | 0.156 | 2.5 | 0.94 | 1.5 | 1.101 | 1.403 | 0.3 | 30.22 | 0.2 | 25.49 | 0.2 | 0.247 | 1.5 |
| 05b-6-31-Mnz1_pt51 | 0.225 | 2.5 | 4.55 | 0.4 | 4.803 | 0.143 | 2.7 | 0.88 | 1.6 | 1.026 | 1.374 | 0.3 | 30.34 | 0.2 | 25.50 | 0.2 | 0.274 | 1.3 |
| 05b-6-31-Mnz1_pt52 | 0.216 | 2.6 | 4.54 | 0.4 | 4.786 | 0.150 | 2.6 | 0.87 | 1.6 | 1.018 | 1.382 | 0.3 | 30.37 | 0.2 | 25.64 | 0.2 | 0.262 | 1.4 |
| 05b-6-31-Mnz1_pt53 | 0.213 | 2.7 | 4.46 | 0.5 | 4.709 | 0.143 | 2.7 | 0.86 | 1.6 | 1.007 | 1.386 | 0.3 | 30.47 | 0.2 | 25.53 | 0.2 | 0.233 | 1.5 |
| 05b-6-31-Mnz1_pt54 | 0.217 | 2.6 | 4.56 | 0.4 | 4.809 | 0.152 | 2.6 | 0.91 | 1.6 | 1.064 | 1.398 | 0.3 | 30.35 | 0.2 | 25.48 | 0.2 | 0.245 | 1.5 |
| 05b-6-31-Mnz1_pt55 | 0.205 | 2.7 | 4.36 | 0.5 | 4.595 | 0.147 | 2.7 | 0.84 | 1.7 | 0.984 | 1.345 | 0.3 | 30.48 | 0.2 | 25.50 | 0.2 | 0.224 | 1.6 |
| 05b-6-31-Mnz1_pt56 | 0.227 | 2.5 | 4.52 | 0.4 | 4.772 | 0.149 | 2.6 | 0.88 | 1.6 | 1.032 | 1.378 | 0.3 | 30.30 | 0.2 | 25.26 | 0.2 | 0.267 | 1.3 |
| 05b-6-31-Mnz1_pt57 | 0.221 | 2.6 | 4.52 | 0.4 | 4.774 | 0.146 | 2.7 | 0.89 | 1.6 | 1.041 | 1.384 | 0.3 | 30.35 | 0.2 | 25.32 | 0.2 | 0.232 | 1.6 |
| 05b-6-31-Mnz1_pt58 | 0.238 | 2.4 | 4.59 | 0.4 | 4.843 | 0.148 | 2.7 | 0.92 | 1.5 | 1.076 | 1.402 | 0.3 | 30.46 | 0.2 | 25.45 | 0.2 | 0.243 | 1.5 |
| 05b-6-31-Mnz1_pt59 | 0.224 | 2.5 | 4.63 | 0.4 | 4.889 | 0.151 | 2.6 | 0.91 | 1.5 | 1.061 | 1.405 | 0.3 | 30.42 | 0.2 | 25.38 | 0.2 | 0.247 | 1.5 |
| 8153_19 | 0.380 | 1.6 | 7.39 | 0.3 | 7.874 | 0.191 | 2.1 | 0.51 | 2.7 | 0.588 | 0.585 | 0.5 | 31.06 | 0.2 | 24.55 | 0.2 | 1.311 | 0.4 |
| 8153_20 | 0.374 | 1.6 | 7.41 | 0.3 | 7.896 | 0.187 | 2.2 | 0.49 | 2.8 | 0.569 | 0.582 | 0.5 | 30.97 | 0.2 | 24.41 | 0.2 | 1.310 | 0.4 |
| 8153_21 | 0.377 | 1.6 | 7.32 | 0.3 | 7.799 | 0.188 | 2.2 | 0.48 | 2.9 | 0.553 | 0.579 | 0.5 | 31.10 | 0.2 | 24.40 | 0.2 | 1.317 | 0.3 |
| 8153_22 | 0.379 | 1.6 | 7.33 | 0.3 | 7.806 | 0.189 | 2.1 | 0.48 | 2.8 | 0.556 | 0.578 | 0.5 | 30.93 | 0.2 | 24.27 | 0.2 | 1.293 | 0.4 |
| 05b-6-31-Mnz1_pt60 | 0.149 | 3.7 | 4.85 | 0.4 | 5.142 | 0.145 | 2.7 | 0.06 | 21.4 | 0.069 | 1.751 | 0.2 | 31.37 | 0.2 | 25.42 | 0.2 | 0.176 | 2.0 |
| 05b-6-31-Mnz1_pt61 | 0.141 | 3.9 | 4.83 | 0.4 | 5.126 | 0.143 | 2.7 | 0.06 | 22.9 | 0.065 | 1.799 | 0.2 | 31.33 | 0.2 | 25.44 | 0.2 | 0.178 | 2.0 |
| 05b-6-31-Mnz1_pt62 | 0.168 | 3.3 | 4.92 | 0.4 | 5.216 | 0.144 | 2.7 | 0.12 | 11.3 | 0.134 | 1.713 | 0.2 | 31.07 | 0.2 | 25.73 | 0.2 | 0.173 | 2.1 |
| 05b-6-31-Mnz1_pt63 | 0.165 | 3.4 | 4.84 | 0.4 | 5.129 | 0.143 | 2.7 | 0.11 | 11.6 | 0.130 | 1.692 | 0.2 | 31.34 | 0.2 | 25.64 | 0.2 | 0.175 | 2.0 |
| 05b-6-31-Mnz1_pt64 | 0.224 | 2.5 | 4.51 | 0.4 | 4.756 | 0.147 | 2.7 | 0.89 | 1.6 | 1.041 | 1.391 | 0.3 | 30.46 | 0.2 | 25.42 | 0.2 | 0.234 | 1.5 |
| 05b-6-31-Mnz1_pt65 | 0.221 | 2.6 | 4.50 | 0.5 | 4.752 | 0.144 | 2.7 | 0.88 | 1.6 | 1.031 | 1.398 | 0.3 | 30.53 | 0.2 | 25.61 | 0.2 | 0.231 | 1.6 |
| TU_RenoMnt_pt12 | 0.901 | 0.8 | 16.48 | 0.2 | 17.808 | 0.240 | 1.7 | 2.35 | 0.7 | 2.877 | 1.624 | 0.3 | 21.82 | 0.2 | 22.35 | 0.2 | 2.370 | 0.2 |
| TU_RenoMnt_pt13 | 0.890 | 0.8 | 16.46 | 0.2 | 17.788 | 0.233 | 1.8 | 2.33 | 0.7 | 2.850 | 1.615 | 0.3 | 21.75 | 0.2 | 22.29 | 0.2 | 2.370 | 0.2 |
| TU_RenoMnt_pt14 | 0.878 | 0.8 | 16.42 | 0.2 | 17.747 | 0.236 | 1.8 | 2.31 | 0.7 | 2.829 | 1.618 | 0.3 | 21.91 | 0.2 | 22.48 | 0.2 | 2.371 | 0.2 |
| TU_RenoMnt_pt15 | 0.854 | 0.8 | 16.14 | 0.2 | 17.423 | 0.227 | 1.8 | 2.33 | 0.7 | 2.849 | 1.603 | 0.3 | 21.95 | 0.2 | 22.56 | 0.2 | 2.311 | 0.2 |
| 05b-6-31-Mnz2_pt1 | 0.095 | 5.9 | 6.02 | 0.4 | 6.398 | 0.164 | 2.4 | 0.15 | 8.6 | 0.179 | 1.477 | 0.3 | 30.35 | 0.2 | 25.88 | 0.2 | 0.252 | 1.5 |
| 05b-6-31-Mnz2_pt2 | 0.087 | 6.5 | 5.94 | 0.4 | 6.304 | 0.158 | 2.5 | 0.15 | 8.8 | 0.173 | 1.457 | 0.3 | 30.33 | 0.2 | 25.71 | 0.2 | 0.232 | 1.6 |
| 05b-6-31-Mnz2_pt3 | 0.097 | 5.8 | 6.01 | 0.4 | 6.389 | 0.165 | 2.4 | 0.15 | 8.8 | 0.175 | 1.479 | 0.3 | 30.36 | 0.2 | 25.82 | 0.2 | 0.248 | 1.5 |
| 05b-6-31-Mnz2_pt4 | 0.128 | 4.5 | 7.96 | 0.3 | 8.500 | 0.214 | 1.9 | 0.10 | 12.6 | 0.123 | 1.807 | 0.2 | 29.43 | 0.2 | 26.01 | 0.2 | 0.425 | 0.9 |
| 05b-6-31-Mnz2_pt5 | 0.124 | 4.6 | 7.99 | 0.3 | 8.526 | 0.219 | 1.9 | 0.12 | 10.9 | 0.141 | 1.794 | 0.2 | 29.63 | 0.2 | 25.78 | 0.2 | 0.371 | 1.0 |
| 05b-6-31-Mnz2_pt6 | 0.112 | 5.1 | 8.15 | 0.3 | 8.703 | 0.219 | 1.9 | 0.10 | 13.6 | 0.117 | 1.822 | 0.2 | 29.44 | 0.2 | 26.34 | 0.2 | 0.406 | 0.9 |
| 05b-6-31-Mnz2_pt7 | 0.104 | 5.4 | 6.38 | 0.4 | 6.773 | 0.176 | 2.3 | 0.22 | 6.2 | 0.253 | 1.577 | 0.3 | 30.13 | 0.2 | 26.17 | 0.2 | 0.281 | 1.3 |
| 05b-6-31-Mnz2_pt8 | 0.098 | 5.8 | 6.56 | 0.4 | 6.978 | 0.184 | 2.2 | 0.13 | 9.9 | 0.156 | 1.587 | 0.3 | 30.17 | 0.2 | 25.83 | 0.2 | 0.286 | 1.3 |
| 05b-6-31-Mnz2_pt9 | 0.099 | 5.7 | 6.75 | 0.4 | 7.186 | 0.181 | 2.2 | 0.14 | 9.2 | 0.167 | 1.630 | 0.3 | 29.99 | 0.2 | 25.65 | 0.2 | 0.288 | 1.3 |
| 05b-6-31-Mnz2_pt10 | 0.094 | 6.0 | 6.60 | 0.4 | 7.019 | 0.183 | 2.2 | 0.10 | 13.0 | 0.119 | 1.600 | 0.3 | 30.18 | 0.2 | 25.87 | 0.2 | 0.295 | 1.3 |
| 05b-6-31-Mnz2_pt11 | 0.149 | 3.8 | 5.51 | 0.4 | 5.825 | 0.160 | 2.5 | 0.83 | 1.7 | 0.971 | 1.484 | 0.3 | 29.75 | 0.2 | 25.57 | 0.2 | 0.247 | 1.5 |

| | $UO_2$ | | $ThO_2$ | | | PbO | | $Y_2O_3$ | | | CaO | | $Ce_2O_3$ | | $P_2O_5$ | | $SiO_2$ | |
|---|---|---|---|---|---|---|---|---|---|---|---|---|---|---|---|---|---|---|
| Sample | wt. % | RSD (2σ%) | wt. % | RSD (2σ%) | k-raw | wt. % | RSD (2σ%) | wt. % | RSD (2σ%) | k-raw | wt. % | RSD (2σ%) | wt. % | RSD (2σ%) | wt. % | RSD (2σ%) | wt. % | RSD (2σ%) |
| 05b-6-31-Mnz2_pt12 | 0.206 | 2.8 | 4.52 | 0.5 | 4.757 | 0.138 | 2.8 | 1.41 | 1.0 | 1.653 | 1.366 | 0.3 | 29.59 | 0.2 | 25.50 | 0.2 | 0.220 | 1.6 |
| 05b-6-31-Mnz2_pt13 | 0.212 | 2.7 | 4.44 | 0.5 | 4.674 | 0.144 | 2.7 | 1.44 | 1.0 | 1.691 | 1.359 | 0.3 | 29.73 | 0.2 | 25.42 | 0.2 | 0.210 | 1.7 |
| 05b-6-31-Mnz2_pt14 | 0.213 | 2.7 | 4.53 | 0.5 | 4.760 | 0.143 | 2.7 | 1.46 | 1.0 | 1.709 | 1.371 | 0.3 | 29.42 | 0.2 | 25.40 | 0.2 | 0.213 | 1.7 |
| 05b-6-31-Mnz2_pt15 | 0.227 | 2.5 | 4.42 | 0.5 | 4.657 | 0.145 | 2.7 | 1.29 | 1.1 | 1.505 | 1.365 | 0.3 | 29.60 | 0.2 | 25.04 | 0.2 | 0.216 | 1.6 |
| 05b-6-31-Mnz2_pt16 | 0.219 | 2.6 | 4.43 | 0.5 | 4.657 | 0.142 | 2.7 | 1.32 | 1.1 | 1.552 | 1.368 | 0.3 | 29.57 | 0.2 | 25.35 | 0.2 | 0.222 | 1.6 |
| 05b-6-31-Mnz2_pt17 | 0.213 | 2.7 | 4.42 | 0.5 | 4.649 | 0.146 | 2.7 | 1.44 | 1.0 | 1.695 | 1.353 | 0.3 | 29.61 | 0.2 | 25.40 | 0.2 | 0.214 | 1.7 |
| 05b-6-31-Mnz2_pt18 | 0.386 | 1.6 | 5.10 | 0.4 | 5.404 | 0.170 | 2.3 | 0.51 | 2.7 | 0.592 | 1.566 | 0.3 | 30.18 | 0.2 | 25.37 | 0.2 | 0.278 | 1.3 |
| 05b-6-31-Mnz2_pt19 | 0.363 | 1.6 | 4.64 | 0.4 | 4.905 | 0.159 | 2.4 | 0.50 | 2.7 | 0.587 | 1.523 | 0.3 | 30.56 | 0.2 | 25.40 | 0.2 | 0.251 | 1.4 |
| 05b-6-31-Mnz2_pt20 | 0.363 | 1.6 | 4.43 | 0.5 | 4.686 | 0.151 | 2.6 | 0.48 | 2.8 | 0.560 | 1.486 | 0.3 | 30.79 | 0.2 | 25.44 | 0.2 | 0.243 | 1.5 |
| 05b-6-31-Mnz2_pt21 | 0.363 | 1.6 | 4.35 | 0.5 | 4.605 | 0.146 | 2.7 | 0.45 | 3.0 | 0.529 | 1.441 | 0.3 | 30.92 | 0.2 | 25.50 | 0.2 | 0.249 | 1.5 |
| 05b-6-31-Mnz2_pt22 | 0.361 | 1.6 | 4.40 | 0.5 | 4.649 | 0.149 | 2.6 | 0.49 | 2.8 | 0.569 | 1.437 | 0.3 | 30.79 | 0.2 | 25.40 | 0.2 | 0.264 | 1.4 |
| 05b-6-31-Mnz2_pt23 | 0.313 | 1.9 | 5.19 | 0.4 | 5.501 | 0.162 | 2.4 | 0.55 | 2.5 | 0.643 | 1.448 | 0.3 | 29.97 | 0.2 | 25.15 | 0.2 | 0.296 | 1.2 |
| 05b-6-31-Mnz2_pt24 | 0.313 | 1.9 | 5.21 | 0.4 | 5.515 | 0.165 | 2.4 | 0.53 | 2.6 | 0.620 | 1.436 | 0.3 | 30.11 | 0.2 | 25.35 | 0.2 | 0.291 | 1.3 |
| 05b-6-31-Mnz2_pt25 | 0.318 | 1.9 | 5.24 | 0.4 | 5.544 | 0.162 | 2.4 | 0.56 | 2.4 | 0.656 | 1.439 | 0.3 | 30.06 | 0.2 | 25.32 | 0.2 | 0.286 | 1.3 |
| 05b-6-31-Mnz2_pt26 | 0.317 | 1.9 | 5.39 | 0.4 | 5.708 | 0.170 | 2.3 | 0.55 | 2.5 | 0.640 | 1.495 | 0.3 | 29.89 | 0.2 | 25.31 | 0.2 | 0.285 | 1.3 |
| 05b-6-31-Mnz2_pt27 | 0.359 | 1.7 | 5.38 | 0.4 | 5.700 | 0.174 | 2.3 | 0.54 | 2.5 | 0.628 | 1.505 | 0.3 | 29.91 | 0.2 | 25.23 | 0.2 | 0.294 | 1.2 |
| TU_RenoMnt_pt16 | 0.857 | 0.8 | 16.19 | 0.2 | 17.485 | 0.226 | 1.8 | 2.31 | 0.7 | 2.819 | 1.591 | 0.3 | 22.06 | 0.2 | 22.40 | 0.2 | 2.309 | 0.2 |
| TU_RenoMnt_pt17 | 0.866 | 0.8 | 16.17 | 0.2 | 17.468 | 0.230 | 1.8 | 2.32 | 0.7 | 2.836 | 1.597 | 0.3 | 22.13 | 0.2 | 22.30 | 0.2 | 2.305 | 0.2 |
| TU_RenoMnt_pt18 | 0.879 | 0.8 | 16.22 | 0.2 | 17.524 | 0.231 | 1.8 | 2.33 | 0.7 | 2.852 | 1.585 | 0.3 | 22.02 | 0.2 | 22.38 | 0.2 | 2.309 | 0.2 |
| TU_RenoMnt_pt19 | 0.845 | 0.8 | 15.95 | 0.2 | 17.218 | 0.219 | 1.9 | 2.32 | 0.7 | 2.830 | 1.605 | 0.3 | 22.24 | 0.2 | 22.52 | 0.2 | 2.234 | 0.2 |
| 8153_23 | 0.402 | 1.5 | 7.76 | 0.3 | 8.274 | 0.193 | 2.1 | 0.48 | 2.8 | 0.558 | 0.587 | 0.5 | 30.92 | 0.2 | 24.50 | 0.2 | 1.370 | 0.3 |
| 8153_24 | 0.393 | 1.5 | 7.69 | 0.3 | 8.199 | 0.193 | 2.1 | 0.48 | 2.8 | 0.555 | 0.578 | 0.5 | 31.16 | 0.2 | 24.51 | 0.2 | 1.351 | 0.3 |
| 8153_25 | 0.393 | 1.5 | 7.71 | 0.3 | 8.217 | 0.190 | 2.1 | 0.49 | 2.8 | 0.573 | 0.580 | 0.5 | 31.04 | 0.2 | 24.52 | 0.2 | 1.367 | 0.3 |
| 8153_26 | 0.394 | 1.5 | 7.62 | 0.3 | 8.124 | 0.191 | 2.1 | 0.48 | 2.8 | 0.563 | 0.576 | 0.5 | 31.01 | 0.2 | 24.61 | 0.2 | 1.350 | 0.3 |
| 8153_27 | 0.382 | 1.6 | 7.65 | 0.3 | 8.152 | 0.191 | 2.1 | 0.50 | 2.7 | 0.578 | 0.572 | 0.5 | 31.06 | 0.2 | 24.31 | 0.2 | 1.345 | 0.3 |
| 05b-6-31-Mnz2_pt28 | 0.382 | 1.6 | 5.14 | 0.4 | 5.444 | 0.171 | 2.3 | 0.50 | 2.7 | 0.582 | 1.560 | 0.3 | 30.21 | 0.2 | 25.32 | 0.2 | 0.272 | 1.3 |
| 05b-6-31-Mnz2_pt29 | 0.120 | 4.7 | 6.17 | 0.4 | 6.548 | 0.173 | 2.3 | 0.35 | 3.8 | 0.405 | 1.545 | 0.3 | 29.82 | 0.2 | 25.48 | 0.2 | 0.263 | 1.4 |
| 05b-6-31-Mnz2_pt30 | 0.143 | 4.0 | 7.06 | 0.3 | 7.525 | 0.192 | 2.1 | 0.23 | 5.7 | 0.273 | 1.704 | 0.2 | 29.70 | 0.2 | 25.49 | 0.2 | 0.310 | 1.2 |
| 05b-6-31-Mnz2_pt31 | 0.115 | 5.0 | 7.47 | 0.3 | 7.971 | 0.204 | 2.0 | 0.14 | 9.2 | 0.166 | 1.736 | 0.2 | 29.67 | 0.2 | 25.36 | 0.2 | 0.314 | 1.2 |
| 05b-6-31-Mnz2_pt32 | 0.098 | 5.7 | 5.85 | 0.4 | 6.218 | 0.156 | 2.5 | 0.14 | 8.9 | 0.169 | 1.447 | 0.3 | 30.15 | 0.2 | 25.56 | 0.2 | 0.232 | 1.5 |
| 05b-6-31-Mnz2_pt33 | 0.092 | 6.1 | 5.87 | 0.4 | 6.233 | 0.155 | 2.5 | 0.15 | 8.6 | 0.174 | 1.438 | 0.3 | 30.26 | 0.2 | 25.47 | 0.2 | 0.237 | 1.5 |
| 05b-6-31-Mnz2_pt34 | 0.097 | 5.8 | 5.99 | 0.4 | 6.364 | 0.160 | 2.4 | 0.15 | 8.7 | 0.173 | 1.466 | 0.3 | 30.04 | 0.2 | 25.46 | 0.2 | 0.246 | 1.5 |
| 05b-6-31-Mnz2_pt35 | 0.101 | 5.5 | 6.09 | 0.4 | 6.468 | 0.161 | 2.4 | 0.14 | 9.0 | 0.167 | 1.488 | 0.3 | 30.01 | 0.2 | 25.50 | 0.2 | 0.252 | 1.4 |
| 05b-6-31-Mnz2_pt36 | 0.108 | 5.2 | 6.08 | 0.4 | 6.467 | 0.157 | 2.5 | 0.15 | 8.7 | 0.172 | 1.498 | 0.3 | 29.98 | 0.2 | 25.44 | 0.2 | 0.245 | 1.5 |
| 05b-6-31-Mnz2_pt37 | 0.089 | 6.3 | 6.01 | 0.4 | 6.384 | 0.163 | 2.4 | 0.14 | 9.0 | 0.167 | 1.493 | 0.3 | 30.11 | 0.2 | 25.49 | 0.2 | 0.258 | 1.4 |
| 05b-6-31-Mnz2_pt38 | 0.098 | 5.7 | 5.98 | 0.4 | 6.349 | 0.164 | 2.4 | 0.16 | 8.0 | 0.187 | 1.473 | 0.3 | 30.14 | 0.2 | 25.49 | 0.2 | 0.247 | 1.5 |

| | $UO_2$ | | $ThO_2$ | | | PbO | | $Y_2O_3$ | | | CaO | | $Ce_2O_3$ | | $P_2O_5$ | | $SiO_2$ | |
|---|---|---|---|---|---|---|---|---|---|---|---|---|---|---|---|---|---|---|
| Sample | wt. % | RSD (2σ%) | wt. % | RSD (2σ%) | k-raw | wt. % | RSD (2σ%) | wt. % | RSD (2σ%) | k-raw | wt. % | RSD (2σ%) | wt. % | RSD (2σ%) | wt. % | RSD (2σ%) | wt. % | RSD (2σ%) |
| 05b-6-31-Mnz2_pt39 | 0.093 | 6.0 | 5.88 | 0.4 | 6.246 | 0.154 | 2.5 | 0.14 | 9.3 | 0.161 | 1.441 | 0.3 | 30.12 | 0.2 | 25.46 | 0.2 | 0.240 | 1.5 |
| 05b-6-31-Mnz2_pt40 | 0.096 | 5.8 | 5.84 | 0.4 | 6.207 | 0.149 | 2.6 | 0.14 | 9.4 | 0.158 | 1.439 | 0.3 | 30.09 | 0.2 | 25.34 | 0.2 | 0.242 | 1.5 |
| 05b-6-31-Mnz3_pt1 | 0.316 | 1.9 | 4.19 | 0.5 | 4.417 | 0.130 | 3.0 | 0.73 | 1.9 | 0.854 | 1.352 | 0.3 | 30.63 | 0.2 | 25.70 | 0.2 | 0.215 | 1.6 |
| 8153_28 | 0.403 | 1.5 | 7.74 | 0.3 | 8.248 | 0.194 | 2.1 | 0.50 | 2.7 | 0.576 | 0.586 | 0.5 | 30.90 | 0.2 | 24.48 | 0.2 | 1.362 | 0.3 |
| 8153_29 | 0.395 | 1.5 | 7.72 | 0.3 | 8.228 | 0.183 | 2.2 | 0.47 | 2.9 | 0.551 | 0.579 | 0.5 | 30.86 | 0.2 | 24.21 | 0.2 | 1.345 | 0.3 |
| 8153_30 | 0.390 | 1.6 | 7.67 | 0.3 | 8.183 | 0.184 | 2.2 | 0.48 | 2.8 | 0.558 | 0.582 | 0.5 | 30.90 | 0.2 | 24.18 | 0.2 | 1.341 | 0.3 |
| 8153_31 | 0.395 | 1.6 | 7.69 | 0.3 | 8.205 | 0.190 | 2.1 | 0.48 | 2.8 | 0.561 | 0.582 | 0.5 | 30.88 | 0.2 | 23.96 | 0.2 | 1.344 | 0.3 |
| 8153_32 | 0.371 | 1.6 | 7.25 | 0.3 | 7.715 | 0.175 | 2.3 | 0.49 | 2.7 | 0.570 | 0.561 | 0.5 | 31.08 | 0.2 | 24.56 | 0.2 | 1.257 | 0.4 |
| 8153_33 | 0.359 | 1.7 | 7.22 | 0.3 | 7.686 | 0.179 | 2.2 | 0.49 | 2.7 | 0.568 | 0.560 | 0.5 | 30.96 | 0.2 | 24.56 | 0.2 | 1.250 | 0.4 |
| TU_RenoMnt_pt20 | 0.693 | 1.0 | 16.34 | 0.2 | 17.672 | 0.224 | 1.8 | 2.14 | 0.7 | 2.622 | 1.663 | 0.3 | 22.06 | 0.2 | 22.43 | 0.2 | 2.044 | 0.2 |
| TU_RenoMnt_pt21 | 0.891 | 0.8 | 16.26 | 0.2 | 17.564 | 0.232 | 1.8 | 2.32 | 0.7 | 2.836 | 1.600 | 0.3 | 22.02 | 0.2 | 22.38 | 0.2 | 2.320 | 0.2 |
| TU_RenoMnt_pt22 | 0.885 | 0.8 | 17.23 | 0.2 | 18.667 | 0.237 | 1.7 | 2.27 | 0.7 | 2.789 | 1.661 | 0.3 | 21.55 | 0.2 | 22.16 | 0.2 | 2.357 | 0.2 |
| TU_RenoMnt_pt23 | 0.911 | 0.8 | 17.12 | 0.2 | 18.541 | 0.231 | 1.8 | 2.31 | 0.7 | 2.830 | 1.652 | 0.3 | 21.47 | 0.2 | 22.17 | 0.2 | 2.445 | 0.2 |
| TU_RenoMnt_pt24 | 0.897 | 0.8 | 16.78 | 0.2 | 18.148 | 0.232 | 1.8 | 2.35 | 0.7 | 2.875 | 1.634 | 0.3 | 21.57 | 0.2 | 22.35 | 0.2 | 2.411 | 0.2 |
| 05b-6-31-Mnz3_pt2 | 0.316 | 1.9 | 4.16 | 0.5 | 4.389 | 0.137 | 2.8 | 0.74 | 1.8 | 0.865 | 1.347 | 0.3 | 30.75 | 0.2 | 25.45 | 0.2 | 0.242 | 1.5 |
| 05b-6-31-Mnz3_pt3 | 0.313 | 1.9 | 4.18 | 0.5 | 4.408 | 0.141 | 2.7 | 0.77 | 1.8 | 0.902 | 1.354 | 0.3 | 30.80 | 0.2 | 25.67 | 0.2 | 0.228 | 1.6 |
| 05b-6-31-Mnz3_pt4 | 0.306 | 1.9 | 4.19 | 0.5 | 4.427 | 0.133 | 2.8 | 0.70 | 1.9 | 0.817 | 1.354 | 0.3 | 30.46 | 0.2 | 24.86 | 0.2 | 0.217 | 1.6 |
| 05b-6-31-Mnz3_pt5 | 0.308 | 1.9 | 4.22 | 0.5 | 4.450 | 0.139 | 2.8 | 0.74 | 1.9 | 0.860 | 1.325 | 0.3 | 30.83 | 0.2 | 25.53 | 0.2 | 0.215 | 1.7 |
| 05b-6-31-Mnz3_pt6 | 0.337 | 1.7 | 4.27 | 0.5 | 4.503 | 0.145 | 2.7 | 0.76 | 1.8 | 0.881 | 1.358 | 0.3 | 30.52 | 0.2 | 25.39 | 0.2 | 0.210 | 1.7 |
| 05b-6-31-Mnz3_pt7 | 0.312 | 1.9 | 4.16 | 0.5 | 4.391 | 0.147 | 2.6 | 0.70 | 2.0 | 0.816 | 1.387 | 0.3 | 30.61 | 0.2 | 25.54 | 0.2 | 0.215 | 1.7 |
| 05b-6-31-Mnz3_pt8 | 0.234 | 2.4 | 4.32 | 0.5 | 4.575 | 0.130 | 3.0 | 0.22 | 6.0 | 0.250 | 1.333 | 0.3 | 31.33 | 0.2 | 25.49 | 0.2 | 0.209 | 1.7 |
| 05b-6-31-Mnz3_pt9 | 0.217 | 2.6 | 4.48 | 0.5 | 4.741 | 0.132 | 2.9 | 0.21 | 6.6 | 0.239 | 1.383 | 0.3 | 31.16 | 0.2 | 26.34 | 0.2 | 0.308 | 1.2 |
| 05b-6-31-Mnz3_pt10 | 0.239 | 2.4 | 4.03 | 0.5 | 4.253 | 0.135 | 2.9 | 0.44 | 3.1 | 0.506 | 1.388 | 0.3 | 31.10 | 0.2 | 25.45 | 0.2 | 0.469 | 0.8 |
| 05b-6-31-Mnz3_pt11 | 0.272 | 2.1 | 3.80 | 0.5 | 4.007 | 0.127 | 3.0 | 0.66 | 2.1 | 0.767 | 1.399 | 0.3 | 31.20 | 0.2 | 25.29 | 0.2 | 0.201 | 1.8 |
| 05b-6-31-Mnz3_pt12 | 0.274 | 2.1 | 3.75 | 0.5 | 3.957 | 0.122 | 3.2 | 0.65 | 2.1 | 0.756 | 1.425 | 0.3 | 31.12 | 0.2 | 25.29 | 0.2 | 0.200 | 1.8 |
| 05b-6-31-Mnz3_pt13 | 0.264 | 2.2 | 3.82 | 0.5 | 4.026 | 0.125 | 3.1 | 0.65 | 2.1 | 0.759 | 1.434 | 0.3 | 31.07 | 0.2 | 25.35 | 0.2 | 0.196 | 1.8 |
| 05b-6-31-Mnz3_pt14 | 0.288 | 2.0 | 3.82 | 0.5 | 4.034 | 0.130 | 3.0 | 0.66 | 2.0 | 0.772 | 1.438 | 0.3 | 31.06 | 0.2 | 25.52 | 0.2 | 0.207 | 1.7 |
| 05b-6-31-Mnz3_pt15 | 0.277 | 2.1 | 3.83 | 0.5 | 4.042 | 0.129 | 3.0 | 0.66 | 2.1 | 0.770 | 1.444 | 0.3 | 30.98 | 0.2 | 25.46 | 0.2 | 0.203 | 1.7 |
| 05b-6-31-Mnz3_pt16 | 0.282 | 2.1 | 3.87 | 0.5 | 4.080 | 0.123 | 3.1 | 0.67 | 2.0 | 0.775 | 1.445 | 0.3 | 31.00 | 0.2 | 25.41 | 0.2 | 0.202 | 1.7 |
| 05b-6-31-Mnz3_pt17 | 0.256 | 2.3 | 3.88 | 0.5 | 4.090 | 0.127 | 3.0 | 0.66 | 2.1 | 0.769 | 1.449 | 0.3 | 31.05 | 0.2 | 25.52 | 0.2 | 0.211 | 1.7 |
| 05b-6-31-Mnz3_pt18 | 0.322 | 1.8 | 4.15 | 0.5 | 4.380 | 0.136 | 2.9 | 0.73 | 1.9 | 0.845 | 1.355 | 0.3 | 30.79 | 0.2 | 25.47 | 0.2 | 0.265 | 1.4 |
| 05b-6-31-Mnz3_pt19 | 0.307 | 1.9 | 4.23 | 0.5 | 4.459 | 0.137 | 2.8 | 0.76 | 1.9 | 0.882 | 1.368 | 0.3 | 30.76 | 0.2 | 26.33 | 0.2 | 0.235 | 1.6 |
| 05b-6-31-Mnz3_pt20 | 0.321 | 1.8 | 4.20 | 0.5 | 4.434 | 0.140 | 2.8 | 0.73 | 1.9 | 0.853 | 1.337 | 0.3 | 30.69 | 0.2 | 25.33 | 0.2 | 0.226 | 1.6 |
| 05b-6-31-Mnz3_pt21 | 0.327 | 1.8 | 4.22 | 0.5 | 4.455 | 0.137 | 2.8 | 0.74 | 1.8 | 0.864 | 1.373 | 0.3 | 30.63 | 0.2 | 25.36 | 0.2 | 0.223 | 1.6 |
| 05b-6-31-Mnz3_pt22 | 0.327 | 1.8 | 4.16 | 0.5 | 4.388 | 0.133 | 2.9 | 0.73 | 1.9 | 0.849 | 1.382 | 0.3 | 30.56 | 0.2 | 25.45 | 0.2 | 0.226 | 1.6 |
| 05b-6-31-Mnz3_pt23 | 0.326 | 1.8 | 4.26 | 0.5 | 4.491 | 0.150 | 2.6 | 0.73 | 1.9 | 0.848 | 1.434 | 0.3 | 30.69 | 0.2 | 25.81 | 0.2 | 0.246 | 1.5 |

| | $UO_2$ | | $ThO_2$ | | | PbO | | $Y_2O_3$ | | | CaO | | $Ce_2O_3$ | | $P_2O_5$ | | $SiO_2$ | |
|---|---|---|---|---|---|---|---|---|---|---|---|---|---|---|---|---|---|---|
| Sample | wt. % | RSD (2σ%) | wt. % | RSD (2σ%) | k-raw | wt. % | RSD (2σ%) | wt. % | RSD (2σ%) | k-raw | wt. % | RSD (2σ%) | wt. % | RSD (2σ%) | wt. % | RSD (2σ%) | wt. % | RSD (2σ%) |
| TU_RenoMnt_pt25 | 0.911 | 0.8 | 17.13 | 0.2 | 18.556 | 0.233 | 1.8 | 2.28 | 0.7 | 2.797 | 1.646 | 0.3 | 21.47 | 0.2 | 22.05 | 0.2 | 2.474 | 0.2 |
| TU_RenoMnt_pt26 | 0.934 | 0.8 | 17.62 | 0.2 | 19.105 | 0.251 | 1.7 | 2.27 | 0.7 | 2.781 | 1.676 | 0.3 | 21.39 | 0.2 | 21.98 | 0.2 | 2.547 | 0.2 |
| TU_RenoMnt_pt27 | 0.923 | 0.8 | 17.52 | 0.2 | 18.999 | 0.239 | 1.7 | 2.26 | 0.7 | 2.765 | 1.670 | 0.3 | 21.45 | 0.2 | 22.02 | 0.2 | 2.535 | 0.2 |
| TU_RenoMnt_pt28 | 0.913 | 0.8 | 17.44 | 0.2 | 18.903 | 0.244 | 1.7 | 2.23 | 0.7 | 2.738 | 1.665 | 0.3 | 21.47 | 0.2 | 22.13 | 0.2 | 2.534 | 0.2 |
| TU_RenoMnt_pt29 | 0.929 | 0.8 | 17.51 | 0.2 | 18.979 | 0.244 | 1.7 | 2.27 | 0.7 | 2.786 | 1.672 | 0.3 | 21.59 | 0.2 | 22.24 | 0.2 | 2.542 | 0.2 |
| TU_RenoMnt_pt30 | 0.906 | 0.8 | 17.59 | 0.2 | 19.057 | 0.242 | 1.7 | 2.31 | 0.7 | 2.833 | 1.675 | 0.3 | 21.63 | 0.2 | 22.37 | 0.2 | 2.549 | 0.2 |
| TU_RenoMnt_pt31 | 0.909 | 0.8 | 17.28 | 0.2 | 18.712 | 0.246 | 1.7 | 2.27 | 0.7 | 2.776 | 1.655 | 0.3 | 21.67 | 0.2 | 22.28 | 0.2 | 2.504 | 0.2 |
| 8153_34 | 0.358 | 1.7 | 7.23 | 0.3 | 7.698 | 0.180 | 2.2 | 0.48 | 2.8 | 0.554 | 0.569 | 0.5 | 31.14 | 0.2 | 24.66 | 0.2 | 1.267 | 0.4 |
| 8153_35 | 0.373 | 1.6 | 7.23 | 0.3 | 7.701 | 0.175 | 2.3 | 0.49 | 2.8 | 0.563 | 0.563 | 0.5 | 30.99 | 0.2 | 24.50 | 0.2 | 1.258 | 0.4 |
| 8153_36 | 0.385 | 1.6 | 7.35 | 0.3 | 7.838 | 0.186 | 2.2 | 0.51 | 2.6 | 0.587 | 0.573 | 0.5 | 31.10 | 0.2 | 23.99 | 0.2 | 1.288 | 0.4 |
| 8153_37 | 0.379 | 1.6 | 7.36 | 0.3 | 7.849 | 0.177 | 2.3 | 0.45 | 3.0 | 0.526 | 0.574 | 0.5 | 30.92 | 0.2 | 23.95 | 0.2 | 1.287 | 0.4 |
| 8153_38 | 0.374 | 1.6 | 7.34 | 0.3 | 7.824 | 0.186 | 2.2 | 0.47 | 2.9 | 0.544 | 0.573 | 0.5 | 31.03 | 0.2 | 23.91 | 0.2 | 1.296 | 0.4 |
| 8153_39 | 0.389 | 1.6 | 7.39 | 0.3 | 7.882 | 0.184 | 2.2 | 0.48 | 2.8 | 0.561 | 0.576 | 0.5 | 31.09 | 0.2 | 24.00 | 0.2 | 1.303 | 0.4 |
| 8153_40 | 0.380 | 1.6 | 7.38 | 0.3 | 7.869 | 0.187 | 2.2 | 0.51 | 2.6 | 0.589 | 0.574 | 0.5 | 31.19 | 0.2 | 24.09 | 0.2 | 1.289 | 0.4 |
| 8153_41 | 0.381 | 1.6 | 7.37 | 0.3 | 7.856 | 0.185 | 2.2 | 0.48 | 2.8 | 0.560 | 0.579 | 0.5 | 31.00 | 0.2 | 24.24 | 0.2 | 1.307 | 0.4 |
| 05b-6-31-Mnz4_pt1 | 0.172 | 3.3 | 5.93 | 0.4 | 6.316 | 0.165 | 2.4 | 0.08 | 16.2 | 0.090 | 1.535 | 0.3 | 31.09 | 0.2 | 25.08 | 0.2 | 0.249 | 1.4 |
| 05b-6-31-Mnz4_pt2 | 0.163 | 3.5 | 5.85 | 0.4 | 6.213 | 0.167 | 2.4 | 0.05 | 28.0 | 0.055 | 1.510 | 0.3 | 31.32 | 0.2 | 26.27 | 0.2 | 0.261 | 1.4 |
| 05b-6-31-Mnz4_pt3 | 0.157 | 3.6 | 5.66 | 0.4 | 6.016 | 0.153 | 2.5 | 0.05 | 25.5 | 0.057 | 1.456 | 0.3 | 31.32 | 0.2 | 24.99 | 0.2 | 0.248 | 1.4 |
| 05b-6-31-Mnz4_pt4 | 0.169 | 3.4 | 6.34 | 0.4 | 6.751 | 0.173 | 2.3 | 0.03 | 46.0 | 0.032 | 1.557 | 0.3 | 30.98 | 0.2 | 25.31 | 0.2 | 0.246 | 1.5 |
| 05b-6-31-Mnz4_pt5 | 0.174 | 3.3 | 6.16 | 0.4 | 6.559 | 0.166 | 2.4 | 0.04 | 32.8 | 0.045 | 1.537 | 0.3 | 31.08 | 0.2 | 25.10 | 0.2 | 0.236 | 1.5 |
| 05b-6-31-Mnz4_pt6 | 0.156 | 3.6 | 6.51 | 0.4 | 6.931 | 0.178 | 2.2 | 0.01 | 88.6 | 0.017 | 1.596 | 0.3 | 30.84 | 0.2 | 25.61 | 0.2 | 0.263 | 1.4 |
| 05b-6-31-Mnz4_pt7 | 0.156 | 3.6 | 6.11 | 0.4 | 6.506 | 0.163 | 2.4 | 0.03 | 40.7 | 0.036 | 1.506 | 0.3 | 31.19 | 0.2 | 25.35 | 0.2 | 0.251 | 1.4 |
| 05b-6-31-Mnz4_pt8 | 0.159 | 3.6 | 5.83 | 0.4 | 6.210 | 0.153 | 2.5 | 0.04 | 31.1 | 0.047 | 1.446 | 0.3 | 31.38 | 0.2 | 25.08 | 0.2 | 0.235 | 1.5 |
| 05b-6-31-Mnz4_pt9 | 0.109 | 4.8 | 4.73 | 0.4 | 4.974 | 0.131 | 2.8 | 0.05 | 27.8 | 0.052 | 1.630 | 0.3 | 24.42 | 0.2 | 21.03 | 0.2 | 8.174 | 0.1 |
| 05b-6-31-Mnz4_pt10 | 0.150 | 3.8 | 5.88 | 0.4 | 6.249 | 0.170 | 2.4 | 0.03 | 40.2 | 0.038 | 1.459 | 0.3 | 31.60 | 0.2 | 25.97 | 0.2 | 0.346 | 1.1 |
| 05b-6-31-Mnz4_pt11 | 0.151 | 3.8 | 5.89 | 0.4 | 6.264 | 0.163 | 2.4 | 0.02 | 75.7 | 0.019 | 1.467 | 0.3 | 31.34 | 0.2 | 25.17 | 0.2 | 0.242 | 1.5 |
| 05b-6-31-Mnz4_pt12 | 0.158 | 3.6 | 5.76 | 0.4 | 6.133 | 0.161 | 2.4 | 0.03 | 48.8 | 0.030 | 1.446 | 0.3 | 31.41 | 0.2 | 25.26 | 0.2 | 0.227 | 1.6 |
| 05b-6-31-Mnz4_pt13 | 0.152 | 3.8 | 5.75 | 0.4 | 6.122 | 0.162 | 2.4 | 0.02 | 55.0 | 0.027 | 1.445 | 0.3 | 31.42 | 0.2 | 25.22 | 0.2 | 0.229 | 1.6 |
| 05b-6-31-Mnz4_pt14 | 0.149 | 3.8 | 5.81 | 0.4 | 6.179 | 0.158 | 2.5 | 0.03 | 42.0 | 0.035 | 1.449 | 0.3 | 31.37 | 0.2 | 25.34 | 0.2 | 0.223 | 1.6 |
| 05b-6-31-Mnz4_pt15 | 0.153 | 3.7 | 5.90 | 0.4 | 6.278 | 0.161 | 2.5 | 0.04 | 30.2 | 0.049 | 1.468 | 0.3 | 31.37 | 0.2 | 25.31 | 0.2 | 0.235 | 1.5 |
| 05b-6-31-Mnz4_pt16 | 0.155 | 3.7 | 6.09 | 0.4 | 6.484 | 0.164 | 2.4 | 0.05 | 27.4 | 0.054 | 1.511 | 0.3 | 31.22 | 0.2 | 25.20 | 0.2 | 0.242 | 1.5 |
| 05b-6-31-Mnz4_pt17 | 0.159 | 3.6 | 5.95 | 0.4 | 6.335 | 0.162 | 2.4 | 0.03 | 38.0 | 0.039 | 1.500 | 0.3 | 31.22 | 0.2 | 25.18 | 0.2 | 0.233 | 1.5 |
| 05b-6-31-Mnz4_pt18 | 0.161 | 3.5 | 5.99 | 0.4 | 6.377 | 0.167 | 2.4 | 0.02 | 67.4 | 0.022 | 1.511 | 0.3 | 31.18 | 0.2 | 25.35 | 0.2 | 0.239 | 1.5 |
| 05b-6-31-Mnz4_pt19 | 0.160 | 3.5 | 5.98 | 0.4 | 6.369 | 0.160 | 2.5 | 0.04 | 28.0 | 0.052 | 1.489 | 0.3 | 31.23 | 0.2 | 25.25 | 0.2 | 0.238 | 1.5 |
| 05b-6-31-Mnz4_pt20 | 0.153 | 3.7 | 5.89 | 0.4 | 6.264 | 0.165 | 2.4 | 0.04 | 31.5 | 0.046 | 1.465 | 0.3 | 31.61 | 0.2 | 25.17 | 0.2 | 0.237 | 1.5 |
| 05b-6-31-Mnz4_pt21 | 0.144 | 3.9 | 5.88 | 0.4 | 6.261 | 0.158 | 2.5 | 0.02 | 50.6 | 0.029 | 1.468 | 0.3 | 31.34 | 0.2 | 25.18 | 0.2 | 0.254 | 1.4 |

| | $UO_2$ | | $ThO_2$ | | | PbO | | $Y_2O_3$ | | | CaO | | $Ce_2O_3$ | | $P_2O_5$ | | $SiO_2$ | |
|---|---|---|---|---|---|---|---|---|---|---|---|---|---|---|---|---|---|---|
| Sample | wt. % | RSD (2σ%) | wt. % | RSD (2σ%) | k-raw | wt. % | RSD (2σ%) | wt. % | RSD (2σ%) | k-raw | wt. % | RSD (2σ%) | wt. % | RSD (2σ%) | wt. % | RSD (2σ%) | wt. % | RSD (2σ%) |
| 05b-6-31-Mnz4_pt22 | 0.155 | 3.7 | 6.13 | 0.4 | 6.534 | 0.167 | 2.4 | 0.03 | 41.2 | 0.035 | 1.501 | 0.3 | 31.20 | 0.2 | 24.98 | 0.2 | 0.281 | 1.3 |
| 8153_41 | 0.382 | 1.6 | 7.39 | 0.3 | 7.876 | 0.192 | 2.1 | 0.46 | 2.9 | 0.538 | 0.579 | 0.5 | 31.07 | 0.2 | 24.18 | 0.2 | 1.314 | 0.3 |
| 8153_42 | 0.375 | 1.6 | 7.37 | 0.3 | 7.851 | 0.183 | 2.2 | 0.49 | 2.8 | 0.567 | 0.572 | 0.5 | 31.15 | 0.2 | 24.03 | 0.2 | 1.309 | 0.4 |
| 8153_43 | 0.380 | 1.6 | 7.32 | 0.3 | 7.801 | 0.185 | 2.2 | 0.48 | 2.8 | 0.556 | 0.578 | 0.5 | 31.05 | 0.2 | 23.96 | 0.2 | 1.285 | 0.4 |
| TU_RenoMnt_pt32 | 0.907 | 0.8 | 17.01 | 0.2 | 18.417 | 0.244 | 1.7 | 2.26 | 0.7 | 2.765 | 1.640 | 0.3 | 21.58 | 0.2 | 22.14 | 0.2 | 2.491 | 0.2 |
| | | | | | | | | | | | | | | | | | | |
| 8153_1 | 0.388 | 2.0 | 7.51 | 0.4 | 8.016 | 0.180 | 2.7 | 0.49 | 2.9 | 0.643 | 0.566 | 0.7 | 30.43 | 0.3 | 25.76 | 0.2 | 1.324 | 0.3 |
| 8153_3 | 0.393 | 2.0 | 7.40 | 0.4 | 7.895 | 0.185 | 2.6 | 0.51 | 2.8 | 0.666 | 0.560 | 0.7 | 30.58 | 0.3 | 25.86 | 0.2 | 1.312 | 0.3 |
| 8153_4 | 0.381 | 2.0 | 7.42 | 0.4 | 7.922 | 0.187 | 2.6 | 0.49 | 2.9 | 0.642 | 0.584 | 0.7 | 30.47 | 0.3 | 25.87 | 0.2 | 1.317 | 0.3 |
| 8153_5 | 0.387 | 2.0 | 7.73 | 0.4 | 8.250 | 0.193 | 2.5 | 0.51 | 2.8 | 0.662 | 0.574 | 0.7 | 30.52 | 0.3 | 26.05 | 0.2 | 1.374 | 0.3 |
| 8153_6 | 0.391 | 2.0 | 7.56 | 0.4 | 8.064 | 0.196 | 2.5 | 0.49 | 2.9 | 0.640 | 0.568 | 0.7 | 30.65 | 0.3 | 25.96 | 0.2 | 1.363 | 0.3 |
| 8153_7 | 0.380 | 2.0 | 7.67 | 0.4 | 8.186 | 0.184 | 2.6 | 0.47 | 3.0 | 0.619 | 0.573 | 0.7 | 30.59 | 0.3 | 26.00 | 0.2 | 1.371 | 0.3 |
| 8153_8 | 0.393 | 2.0 | 7.77 | 0.4 | 8.298 | 0.188 | 2.6 | 0.51 | 2.8 | 0.671 | 0.590 | 0.6 | 30.71 | 0.2 | 26.06 | 0.2 | 1.402 | 0.3 |
| 8153_9 | 0.398 | 1.9 | 7.67 | 0.4 | 8.188 | 0.191 | 2.5 | 0.50 | 2.8 | 0.655 | 0.582 | 0.7 | 30.35 | 0.3 | 26.03 | 0.2 | 1.377 | 0.3 |
| 8153_10 | 0.393 | 2.0 | 7.60 | 0.4 | 8.113 | 0.200 | 2.4 | 0.50 | 2.8 | 0.657 | 0.585 | 0.7 | 30.54 | 0.3 | 26.03 | 0.2 | 1.392 | 0.3 |
| TU_1 | 0.910 | 1.0 | 16.90 | 0.3 | 18.276 | 0.243 | 2.0 | 2.42 | 0.7 | 3.307 | 1.619 | 0.3 | 21.32 | 0.3 | 23.99 | 0.2 | 2.517 | 0.2 |
| TU_2 | 0.915 | 1.0 | 17.01 | 0.3 | 18.398 | 0.240 | 2.1 | 2.46 | 0.7 | 3.357 | 1.646 | 0.3 | 21.88 | 0.3 | 24.35 | 0.2 | 2.508 | 0.2 |
| TU_3 | 0.897 | 1.0 | 17.00 | 0.3 | 18.392 | 0.239 | 2.1 | 2.39 | 0.7 | 3.264 | 1.635 | 0.3 | 21.29 | 0.3 | 23.99 | 0.2 | 2.508 | 0.2 |
| TU_4 | 0.895 | 1.0 | 16.93 | 0.3 | 18.309 | 0.232 | 2.1 | 2.48 | 0.7 | 3.378 | 1.624 | 0.3 | 21.41 | 0.3 | 24.09 | 0.2 | 2.507 | 0.2 |
| 05b-6-103_m6_1 | 0.457 | 1.7 | 4.32 | 0.6 | 4.570 | 0.150 | 3.1 | 0.18 | 7.7 | 0.234 | 1.051 | 0.4 | 32.14 | 0.2 | 28.21 | 0.2 | 0.178 | 1.7 |
| 05b-6-103_m6_2 | 0.512 | 1.5 | 4.21 | 0.6 | 4.457 | 0.158 | 3.0 | 0.13 | 10.5 | 0.171 | 1.049 | 0.4 | 32.10 | 0.2 | 28.22 | 0.2 | 0.221 | 1.4 |
| 05b-6-103_m6_3 | 0.490 | 1.6 | 4.25 | 0.6 | 4.502 | 0.149 | 3.2 | 0.17 | 8.3 | 0.216 | 1.045 | 0.4 | 32.33 | 0.2 | 28.25 | 0.2 | 0.174 | 1.8 |
| 05b-6-103_m6_4 | 0.391 | 2.0 | 4.08 | 0.6 | 4.313 | 0.141 | 3.3 | 0.28 | 5.0 | 0.365 | 0.972 | 0.5 | 32.37 | 0.2 | 28.15 | 0.2 | 0.167 | 1.8 |
| 05b-6-103_m6_5 | 0.370 | 2.1 | 4.20 | 0.6 | 4.441 | 0.137 | 3.4 | 0.29 | 4.9 | 0.375 | 0.997 | 0.4 | 32.36 | 0.2 | 28.36 | 0.2 | 0.178 | 1.7 |
| 05b-6-103_m6_6 | 0.747 | 1.1 | 5.37 | 0.5 | 5.702 | 0.212 | 2.3 | 0.16 | 8.5 | 0.211 | 1.336 | 0.4 | 31.82 | 0.2 | 28.25 | 0.2 | 0.139 | 2.2 |
| 05b-6-103_m6_7 | 0.602 | 1.3 | 3.95 | 0.6 | 4.182 | 0.147 | 3.2 | 0.00 | 100.0 | 0.000 | 0.888 | 0.5 | 32.54 | 0.2 | 28.00 | 0.2 | 0.191 | 1.6 |
| 05b-6-103_m6_8 | 0.520 | 1.5 | 3.52 | 0.6 | 3.720 | 0.136 | 3.4 | 0.36 | 3.9 | 0.469 | 0.727 | 0.6 | 32.07 | 0.2 | 27.83 | 0.2 | 0.257 | 1.2 |
| 05b-6-103_m6_9 | 0.181 | 4.0 | 3.96 | 0.6 | 4.189 | 0.126 | 3.7 | 0.37 | 3.8 | 0.483 | 0.859 | 0.5 | 32.29 | 0.2 | 27.95 | 0.2 | 0.266 | 1.2 |
| 05b-6-103_m6_10 | 0.148 | 4.9 | 3.97 | 0.6 | 4.198 | 0.117 | 4.0 | 0.39 | 3.6 | 0.507 | 0.856 | 0.5 | 32.37 | 0.2 | 27.93 | 0.2 | 0.234 | 1.3 |
| 05b-6-103_m6_11 | 0.173 | 4.2 | 3.97 | 0.6 | 4.194 | 0.111 | 4.2 | 0.40 | 3.5 | 0.524 | 0.879 | 0.5 | 31.61 | 0.2 | 27.45 | 0.2 | 1.112 | 0.4 |
| 05b-6-103_m6_12 | 0.167 | 4.4 | 4.01 | 0.6 | 4.239 | 0.124 | 3.8 | 0.43 | 3.3 | 0.566 | 0.873 | 0.5 | 32.21 | 0.2 | 27.95 | 0.2 | 0.233 | 1.3 |
| 05b-6-103_m6_13 | 0.527 | 1.5 | 3.94 | 0.6 | 4.170 | 0.151 | 3.1 | 0.33 | 4.2 | 0.429 | 0.999 | 0.4 | 32.09 | 0.2 | 28.03 | 0.2 | 0.169 | 1.8 |
| 05b-6-103_m6_14 | 0.578 | 1.4 | 4.38 | 0.6 | 4.639 | 0.152 | 3.1 | 0.25 | 5.4 | 0.332 | 1.114 | 0.4 | 32.17 | 0.2 | 28.07 | 0.2 | 0.106 | 2.8 |
| 05b-6-103_m6_15 | 0.730 | 1.1 | 4.56 | 0.5 | 4.835 | 0.180 | 2.7 | 0.10 | 13.9 | 0.127 | 1.152 | 0.4 | 31.65 | 0.2 | 27.74 | 0.2 | 0.644 | 0.6 |
| 05b-6-103_m6_16 | 0.524 | 1.5 | 3.70 | 0.6 | 3.917 | 0.148 | 3.2 | 0.05 | 27.7 | 0.064 | 0.810 | 0.5 | 32.85 | 0.2 | 28.08 | 0.2 | 0.170 | 1.8 |
| 05b-6-103_m6_17 | 0.705 | 1.2 | 4.69 | 0.5 | 4.978 | 0.189 | 2.5 | 0.15 | 9.1 | 0.197 | 1.197 | 0.4 | 32.16 | 0.2 | 28.14 | 0.2 | 0.108 | 2.8 |

| | $UO_2$ | | $ThO_2$ | | | PbO | | $Y_2O_3$ | | | CaO | | $Ce_2O_3$ | | $P_2O_5$ | | $SiO_2$ | |
|---|---|---|---|---|---|---|---|---|---|---|---|---|---|---|---|---|---|---|
| Sample | wt. % | RSD (2σ%) | wt. % | RSD (2σ%) | k-raw | wt. % | RSD (2σ%) | wt. % | RSD (2σ%) | k-raw | wt. % | RSD (2σ%) | wt. % | RSD (2σ%) | wt. % | RSD (2σ%) | wt. % | RSD (2σ%) |
| 05b-6-103_m6_18 | 0.597 | 1.3 | 4.42 | 0.6 | 4.683 | 0.166 | 2.9 | 0.22 | 6.2 | 0.293 | 1.118 | 0.4 | 32.25 | 0.2 | 28.16 | 0.2 | 0.094 | 3.2 |
| 05b-6-103_m6_19 | 0.366 | 2.1 | 4.09 | 0.6 | 4.325 | 0.140 | 3.3 | 0.35 | 4.1 | 0.454 | 0.957 | 0.5 | 32.18 | 0.2 | 28.08 | 0.2 | 0.117 | 2.6 |
| 05b-6-103_m6_20 | 0.356 | 2.1 | 4.06 | 0.6 | 4.292 | 0.140 | 3.4 | 0.34 | 4.2 | 0.440 | 0.961 | 0.5 | 32.28 | 0.2 | 27.96 | 0.2 | 0.131 | 2.3 |
| 05b-6-103_m6_21 | 0.332 | 2.3 | 4.07 | 0.6 | 4.308 | 0.141 | 3.3 | 0.35 | 4.0 | 0.455 | 0.963 | 0.5 | 31.90 | 0.2 | 27.81 | 0.2 | 0.299 | 1.1 |
| 05b-6-103_m6_22 | 0.323 | 2.3 | 3.98 | 0.6 | 4.210 | 0.126 | 3.7 | 0.34 | 4.1 | 0.445 | 0.919 | 0.5 | 31.89 | 0.2 | 27.89 | 0.2 | 0.169 | 1.8 |
| 05b-6-103_m6_23 | 0.323 | 2.3 | 3.99 | 0.6 | 4.223 | 0.140 | 3.4 | 0.34 | 4.1 | 0.449 | 0.953 | 0.5 | 31.75 | 0.2 | 27.78 | 0.2 | 0.215 | 1.5 |
| 05b-6-103_m6_24 | 0.292 | 2.6 | 4.15 | 0.6 | 4.396 | 0.134 | 3.5 | 0.35 | 4.1 | 0.450 | 0.941 | 0.5 | 31.99 | 0.2 | 27.91 | 0.2 | 0.175 | 1.8 |
| 05b-6-103_m6_25 | 0.416 | 1.8 | 4.21 | 0.6 | 4.459 | 0.141 | 3.3 | 0.24 | 5.8 | 0.313 | 1.016 | 0.4 | 31.84 | 0.2 | 27.96 | 0.2 | 0.190 | 1.6 |
| 05b-6-103_m6_26 | 0.347 | 2.2 | 4.08 | 0.6 | 4.313 | 0.136 | 3.4 | 0.32 | 4.4 | 0.419 | 0.955 | 0.5 | 31.79 | 0.2 | 27.83 | 0.2 | 0.154 | 2.0 |
| 05b-6-103_m6_27 | 0.467 | 1.7 | 4.31 | 0.6 | 4.567 | 0.154 | 3.0 | 0.17 | 8.1 | 0.223 | 1.043 | 0.4 | 32.30 | 0.2 | 28.16 | 0.2 | 0.145 | 2.1 |
| 05b-6-103_m6_28 | 0.342 | 2.2 | 3.93 | 0.6 | 4.162 | 0.124 | 3.7 | 0.31 | 4.5 | 0.405 | 0.924 | 0.5 | 31.95 | 0.2 | 27.68 | 0.2 | 0.177 | 1.7 |
| 05b-6-103_m6_29 | 0.379 | 2.0 | 4.11 | 0.6 | 4.350 | 0.138 | 3.4 | 0.34 | 4.1 | 0.444 | 0.964 | 0.5 | 31.93 | 0.2 | 27.90 | 0.2 | 0.158 | 1.9 |
| 05b-6-103_m6_30 | 0.378 | 2.0 | 4.17 | 0.6 | 4.413 | 0.141 | 3.3 | 0.28 | 4.9 | 0.369 | 0.976 | 0.5 | 31.95 | 0.2 | 27.65 | 0.2 | 0.187 | 1.6 |
| 05b-6-103_m6_31 | 0.295 | 2.5 | 4.22 | 0.6 | 4.471 | 0.137 | 3.4 | 0.35 | 4.0 | 0.458 | 0.937 | 0.5 | 31.85 | 0.2 | 27.74 | 0.2 | 0.199 | 1.6 |
| 05b-6-103_m6_32 | 0.322 | 2.3 | 4.19 | 0.6 | 4.431 | 0.133 | 3.5 | 0.34 | 4.2 | 0.438 | 0.956 | 0.5 | 32.17 | 0.2 | 27.87 | 0.2 | 0.457 | 0.8 |
| 05b-6-103_m6_33 | 0.325 | 2.3 | 4.21 | 0.6 | 4.457 | 0.136 | 3.4 | 0.33 | 4.3 | 0.433 | 0.968 | 0.5 | 32.43 | 0.2 | 28.16 | 0.2 | 0.471 | 0.7 |
| 8153_11 | 0.404 | 1.9 | 7.58 | 0.4 | 8.099 | 0.179 | 2.7 | 0.52 | 2.7 | 0.679 | 0.577 | 0.7 | 30.54 | 0.3 | 25.73 | 0.2 | 1.343 | 0.3 |
| 8153_12 | 0.396 | 2.0 | 7.58 | 0.4 | 8.097 | 0.191 | 2.5 | 0.49 | 2.9 | 0.641 | 0.577 | 0.7 | 30.55 | 0.3 | 25.82 | 0.2 | 1.347 | 0.3 |
| 8153_13 | 0.381 | 2.0 | 7.63 | 0.4 | 8.143 | 0.186 | 2.6 | 0.51 | 2.8 | 0.668 | 0.577 | 0.7 | 30.53 | 0.3 | 25.80 | 0.2 | 1.361 | 0.3 |
| 8153_14 | 0.392 | 2.0 | 7.67 | 0.4 | 8.187 | 0.198 | 2.4 | 0.48 | 2.9 | 0.633 | 0.582 | 0.7 | 30.45 | 0.3 | 25.82 | 0.2 | 1.368 | 0.3 |
| 8153_15 | 0.406 | 1.9 | 7.57 | 0.4 | 8.082 | 0.185 | 2.6 | 0.51 | 2.8 | 0.665 | 0.587 | 0.6 | 30.63 | 0.3 | 25.97 | 0.2 | 1.373 | 0.3 |
| TU_5 | 0.930 | 1.0 | 17.35 | 0.3 | 18.798 | 0.247 | 2.0 | 2.39 | 0.7 | 3.268 | 1.659 | 0.3 | 21.10 | 0.3 | 23.61 | 0.2 | 2.577 | 0.2 |
| TU_6 | 0.921 | 1.0 | 16.99 | 0.3 | 18.394 | 0.239 | 2.1 | 2.38 | 0.7 | 3.246 | 1.646 | 0.3 | 21.27 | 0.3 | 23.64 | 0.2 | 2.483 | 0.2 |
| TU_7 | 0.885 | 1.0 | 16.76 | 0.3 | 18.130 | 0.239 | 2.1 | 2.40 | 0.7 | 3.271 | 1.622 | 0.3 | 21.42 | 0.3 | 23.78 | 0.2 | 2.441 | 0.2 |
| TU_8 | 0.874 | 1.0 | 16.18 | 0.3 | 17.474 | 0.230 | 2.2 | 2.45 | 0.7 | 3.333 | 1.591 | 0.3 | 21.58 | 0.3 | 24.09 | 0.2 | 2.382 | 0.2 |
| TU_9 | 0.887 | 1.0 | 16.31 | 0.3 | 17.619 | 0.227 | 2.2 | 2.47 | 0.7 | 3.359 | 1.599 | 0.3 | 21.66 | 0.3 | 24.15 | 0.2 | 2.393 | 0.2 |
| 05b-6-103_m6_34 | 0.710 | 1.2 | 4.45 | 0.6 | 4.717 | 0.183 | 2.6 | 0.16 | 8.6 | 0.209 | 0.970 | 0.5 | 31.46 | 0.2 | 27.78 | 0.2 | 0.215 | 1.5 |
| 05b-6-103_m6_35 | 0.850 | 1.0 | 4.29 | 0.6 | 4.546 | 0.182 | 2.6 | 0.08 | 16.2 | 0.110 | 1.110 | 0.4 | 31.68 | 0.2 | 27.89 | 0.2 | 0.115 | 2.6 |
| 05b-6-103_m6_36 | 0.711 | 1.2 | 4.40 | 0.6 | 4.662 | 0.179 | 2.7 | 0.15 | 9.0 | 0.200 | 0.961 | 0.5 | 31.46 | 0.2 | 27.62 | 0.2 | 0.218 | 1.4 |
| 05b-6-103_m6_37 | 0.728 | 1.1 | 4.42 | 0.6 | 4.684 | 0.180 | 2.7 | 0.19 | 7.4 | 0.244 | 0.930 | 0.5 | 31.10 | 0.2 | 27.53 | 0.2 | 0.259 | 1.2 |
| 05b-6-103_m6_38 | 0.644 | 1.3 | 4.27 | 0.6 | 4.528 | 0.181 | 2.6 | 0.15 | 9.1 | 0.197 | 0.860 | 0.5 | 31.49 | 0.2 | 27.45 | 0.2 | 0.257 | 1.2 |
| 05b-6-103_m6_39 | 0.655 | 1.2 | 4.51 | 0.6 | 4.777 | 0.181 | 2.7 | 0.15 | 8.9 | 0.202 | 0.902 | 0.5 | 31.33 | 0.2 | 27.52 | 0.2 | 0.281 | 1.1 |
| 05b-6-103_m6_40 | 0.694 | 1.2 | 4.87 | 0.5 | 5.165 | 0.194 | 2.5 | 0.16 | 8.6 | 0.208 | 0.944 | 0.5 | 31.17 | 0.2 | 27.56 | 0.2 | 0.304 | 1.1 |
| 05b-6-103_m6_41 | 0.582 | 1.4 | 4.07 | 0.6 | 4.312 | 0.155 | 3.1 | 0.15 | 9.5 | 0.189 | 0.818 | 0.5 | 31.76 | 0.2 | 27.61 | 0.2 | 0.253 | 1.3 |
| 05b-6-103_m6_42 | 0.633 | 1.3 | 4.28 | 0.6 | 4.540 | 0.159 | 3.0 | 0.16 | 8.6 | 0.210 | 0.887 | 0.5 | 31.40 | 0.2 | 27.59 | 0.2 | 0.263 | 1.2 |
| 05b-6-103_m6_43 | 0.631 | 1.3 | 4.16 | 0.6 | 4.409 | 0.166 | 2.8 | 0.16 | 8.4 | 0.212 | 0.852 | 0.5 | 31.56 | 0.2 | 27.19 | 0.2 | 0.244 | 1.3 |

| | $UO_2$ | | $ThO_2$ | | | PbO | | $Y_2O_3$ | | | CaO | | $Ce_2O_3$ | | $P_2O_5$ | | $SiO_2$ | |
|---|---|---|---|---|---|---|---|---|---|---|---|---|---|---|---|---|---|---|
| Sample | wt. % | RSD (2σ%) | wt. % | RSD (2σ%) | k-raw | wt. % | RSD (2σ%) | wt. % | RSD (2σ%) | k-raw | wt. % | RSD (2σ%) | wt. % | RSD (2σ%) | wt. % | RSD (2σ%) | wt. % | RSD (2σ%) |
| 05b-6-103_m6_44 | 0.559 | 1.4 | 4.13 | 0.6 | 4.376 | 0.154 | 3.1 | 0.20 | 7.1 | 0.254 | 0.862 | 0.5 | 31.71 | 0.2 | 27.72 | 0.2 | 0.210 | 1.5 |
| 05b-6-103_m6_45 | 0.626 | 1.3 | 4.08 | 0.6 | 4.319 | 0.165 | 2.9 | 0.25 | 5.6 | 0.323 | 0.862 | 0.5 | 31.42 | 0.2 | 27.53 | 0.2 | 0.232 | 1.4 |
| 05b-6-103_m6_46 | 0.800 | 1.0 | 4.88 | 0.5 | 5.182 | 0.203 | 2.4 | 0.05 | 29.9 | 0.060 | 1.234 | 0.4 | 32.35 | 0.2 | 28.20 | 0.2 | 0.109 | 2.7 |
| 05b-6-103_m6_47 | 0.587 | 1.4 | 4.14 | 0.6 | 4.385 | 0.164 | 2.9 | 0.18 | 7.8 | 0.233 | 0.887 | 0.5 | 31.87 | 0.2 | 27.88 | 0.2 | 0.200 | 1.6 |
| 05b-6-103_m6_48 | 0.623 | 1.3 | 4.19 | 0.6 | 4.443 | 0.171 | 2.8 | 0.17 | 7.9 | 0.226 | 0.857 | 0.5 | 31.52 | 0.2 | 27.60 | 0.2 | 0.230 | 1.4 |
| 05b-6-103_m6_49 | 0.655 | 1.2 | 4.45 | 0.6 | 4.715 | 0.173 | 2.8 | 0.16 | 8.8 | 0.206 | 0.919 | 0.5 | 31.42 | 0.2 | 27.72 | 0.2 | 0.237 | 1.3 |
| 05b-6-103_m6_50 | 0.677 | 1.2 | 4.60 | 0.5 | 4.884 | 0.189 | 2.5 | 0.15 | 9.1 | 0.198 | 1.041 | 0.4 | 31.60 | 0.2 | 27.76 | 0.2 | 0.179 | 1.7 |
| 05b-6-103_m6_51 | 0.593 | 1.3 | 3.86 | 0.6 | 4.087 | 0.163 | 2.9 | 0.14 | 9.7 | 0.184 | 0.815 | 0.5 | 31.90 | 0.2 | 27.69 | 0.2 | 0.227 | 1.4 |
| 05b-6-103_m6_52 | 0.665 | 1.2 | 4.42 | 0.6 | 4.687 | 0.168 | 2.9 | 0.18 | 7.8 | 0.230 | 0.893 | 0.5 | 31.18 | 0.2 | 27.59 | 0.2 | 0.270 | 1.2 |
| 05b-6-103_m6_53 | 0.597 | 1.3 | 3.77 | 0.6 | 3.990 | 0.161 | 2.9 | 0.19 | 7.2 | 0.250 | 0.804 | 0.5 | 31.82 | 0.2 | 27.71 | 0.2 | 0.205 | 1.5 |
| 05b-6-103_m6_54 | 0.680 | 1.2 | 4.02 | 0.6 | 4.261 | 0.167 | 2.8 | 0.19 | 7.4 | 0.243 | 0.845 | 0.5 | 31.41 | 0.2 | 27.51 | 0.2 | 0.254 | 1.3 |
| 05b-6-103_m6_55 | 0.654 | 1.2 | 3.98 | 0.6 | 4.214 | 0.153 | 3.1 | 0.19 | 7.3 | 0.244 | 0.848 | 0.5 | 31.44 | 0.2 | 27.62 | 0.2 | 0.220 | 1.4 |
| 05b-6-103_m6_56 | 0.682 | 1.2 | 4.71 | 0.5 | 4.998 | 0.192 | 2.5 | 0.15 | 9.1 | 0.197 | 0.938 | 0.5 | 31.22 | 0.2 | 27.49 | 0.2 | 0.286 | 1.1 |
| 05b-6-103_m6_57 | 0.697 | 1.2 | 4.94 | 0.5 | 5.241 | 0.188 | 2.6 | 0.13 | 10.6 | 0.169 | 0.955 | 0.5 | 31.21 | 0.2 | 27.44 | 0.2 | 0.307 | 1.1 |
| 05b-6-103_m6_58 | 0.684 | 1.2 | 4.64 | 0.5 | 4.926 | 0.176 | 2.7 | 0.13 | 10.3 | 0.175 | 0.913 | 0.5 | 31.43 | 0.2 | 27.48 | 0.2 | 0.276 | 1.2 |
| 05b-6-103_m6_59 | 0.666 | 1.2 | 4.83 | 0.5 | 5.130 | 0.183 | 2.6 | 0.15 | 9.2 | 0.195 | 0.945 | 0.5 | 31.24 | 0.2 | 27.39 | 0.2 | 0.299 | 1.1 |
| 05b-6-103_m6_60 | 0.657 | 1.2 | 4.96 | 0.5 | 5.260 | 0.188 | 2.6 | 0.15 | 9.1 | 0.198 | 0.969 | 0.5 | 31.37 | 0.2 | 27.55 | 0.2 | 0.305 | 1.1 |
| 05b-6-103_m6_61 | 0.681 | 1.2 | 4.77 | 0.5 | 5.057 | 0.184 | 2.6 | 0.14 | 9.5 | 0.188 | 0.942 | 0.5 | 31.31 | 0.2 | 27.40 | 0.2 | 0.294 | 1.1 |
| 05b-6-103_m6_62 | 0.657 | 1.2 | 4.66 | 0.5 | 4.942 | 0.183 | 2.6 | 0.16 | 8.7 | 0.204 | 0.931 | 0.5 | 31.34 | 0.2 | 27.26 | 0.2 | 0.784 | 0.5 |
| 05b-6-103_m6_63 | 0.575 | 1.4 | 3.85 | 0.6 | 4.076 | 0.149 | 3.1 | 0.16 | 8.4 | 0.212 | 0.861 | 0.5 | 31.85 | 0.2 | 27.34 | 0.2 | 0.325 | 1.0 |
| 05b-6-103_m6_64 | 0.359 | 2.1 | 2.84 | 0.7 | 3.002 | 0.103 | 4.5 | 0.25 | 5.5 | 0.330 | 0.619 | 0.6 | 32.69 | 0.2 | 27.79 | 0.2 | 0.128 | 2.4 |
| 05b-6-103_m6_65 | 0.431 | 1.8 | 3.04 | 0.7 | 3.208 | 0.119 | 3.9 | 0.19 | 7.3 | 0.248 | 0.669 | 0.6 | 32.59 | 0.2 | 27.67 | 0.2 | 0.190 | 1.6 |
| 05b-6-103_m6_66 | 0.709 | 1.2 | 4.39 | 0.6 | 4.651 | 0.174 | 2.8 | 0.19 | 7.3 | 0.245 | 0.907 | 0.5 | 31.17 | 0.2 | 27.50 | 0.2 | 0.253 | 1.3 |
| 05b-6-103_m6_67 | 0.670 | 1.2 | 4.25 | 0.6 | 4.497 | 0.177 | 2.7 | 0.17 | 8.3 | 0.216 | 0.868 | 0.5 | 31.39 | 0.2 | 27.62 | 0.2 | 0.224 | 1.4 |
| 05b-6-103_m6_68 | 0.558 | 1.4 | 3.47 | 0.6 | 3.668 | 0.136 | 3.4 | 0.15 | 9.0 | 0.198 | 0.762 | 0.5 | 31.97 | 0.2 | 27.55 | 0.2 | 0.178 | 1.7 |
| 8153_16 | 0.371 | 2.1 | 7.38 | 0.4 | 7.881 | 0.185 | 2.6 | 0.48 | 2.9 | 0.629 | 0.579 | 0.7 | 30.64 | 0.3 | 25.86 | 0.2 | 1.338 | 0.3 |
| 8153_17 | 0.389 | 2.0 | 7.32 | 0.4 | 7.811 | 0.181 | 2.7 | 0.52 | 2.7 | 0.682 | 0.578 | 0.7 | 30.45 | 0.3 | 25.73 | 0.2 | 1.341 | 0.3 |
| 8153_18 | 0.397 | 1.9 | 7.39 | 0.4 | 7.885 | 0.190 | 2.5 | 0.50 | 2.8 | 0.658 | 0.581 | 0.7 | 30.45 | 0.3 | 25.80 | 0.2 | 1.325 | 0.3 |
| 8153_19 | 0.377 | 2.1 | 7.31 | 0.4 | 7.805 | 0.187 | 2.6 | 0.48 | 2.9 | 0.623 | 0.576 | 0.7 | 30.69 | 0.3 | 25.80 | 0.2 | 1.340 | 0.3 |
| 8153_20 | 0.386 | 2.0 | 7.38 | 0.4 | 7.872 | 0.191 | 2.6 | 0.47 | 3.0 | 0.610 | 0.582 | 0.7 | 30.52 | 0.3 | 25.92 | 0.2 | 1.339 | 0.3 |
| TU_10 | 0.909 | 1.0 | 16.41 | 0.3 | 17.732 | 0.233 | 2.1 | 2.42 | 0.7 | 3.299 | 1.610 | 0.3 | 21.42 | 0.3 | 23.97 | 0.2 | 2.392 | 0.2 |
| TU_11 | 0.910 | 1.0 | 16.48 | 0.3 | 17.810 | 0.236 | 2.1 | 2.46 | 0.7 | 3.357 | 1.598 | 0.3 | 21.39 | 0.3 | 23.89 | 0.2 | 2.409 | 0.2 |
| TU_12 | 0.911 | 1.0 | 16.48 | 0.3 | 17.806 | 0.237 | 2.1 | 2.45 | 0.7 | 3.338 | 1.603 | 0.3 | 21.49 | 0.3 | 23.97 | 0.2 | 2.441 | 0.2 |
| TU_13 | 0.889 | 1.0 | 16.28 | 0.3 | 17.582 | 0.233 | 2.2 | 2.47 | 0.7 | 3.368 | 1.612 | 0.3 | 21.70 | 0.3 | 24.00 | 0.2 | 2.376 | 0.2 |
| TU_14 | 0.888 | 1.0 | 16.20 | 0.3 | 17.504 | 0.225 | 2.2 | 2.43 | 0.7 | 3.313 | 1.591 | 0.3 | 21.65 | 0.3 | 24.01 | 0.2 | 2.353 | 0.2 |
| 05b-6-103_m6_69 | 0.511 | 1.5 | 3.39 | 0.7 | 3.585 | 0.133 | 3.5 | 0.17 | 7.9 | 0.225 | 0.703 | 0.6 | 32.14 | 0.2 | 27.62 | 0.2 | 0.188 | 1.7 |

| | $UO_2$ | | $ThO_2$ | | | PbO | | $Y_2O_3$ | | | CaO | | $Ce_2O_3$ | | $P_2O_5$ | | $SiO_2$ | |
|---|---|---|---|---|---|---|---|---|---|---|---|---|---|---|---|---|---|---|
| Sample | wt. % | RSD (2σ%) | wt. % | RSD (2σ%) | k-raw | wt. % | RSD (2σ%) | wt. % | RSD (2σ%) | k-raw | wt. % | RSD (2σ%) | wt. % | RSD (2σ%) | wt. % | RSD (2σ%) | wt. % | RSD (2σ%) |
| 05b-6-103_m6_70 | 0.589 | 1.4 | 4.77 | 0.5 | 5.060 | 0.184 | 2.6 | 0.19 | 7.2 | 0.250 | 1.184 | 0.4 | 32.08 | 0.2 | 28.05 | 0.2 | 0.097 | 3.1 |
| 05b-6-103_m6_71 | 0.160 | 4.6 | 4.05 | 0.6 | 4.280 | 0.120 | 3.8 | 0.40 | 3.5 | 0.525 | 0.863 | 0.5 | 32.35 | 0.2 | 27.92 | 0.2 | 0.177 | 1.7 |
| 05b-6-103_m6_72 | 0.156 | 4.7 | 4.04 | 0.6 | 4.272 | 0.124 | 3.7 | 0.39 | 3.6 | 0.507 | 0.865 | 0.5 | 32.44 | 0.2 | 27.88 | 0.2 | 0.174 | 1.8 |
| 05b-6-103_m6_73 | 0.162 | 4.5 | 3.96 | 0.6 | 4.188 | 0.113 | 4.1 | 0.41 | 3.4 | 0.537 | 0.862 | 0.5 | 32.49 | 0.2 | 27.78 | 0.2 | 0.175 | 1.8 |
| 05b-6-103_m6_74 | 0.151 | 4.8 | 4.00 | 0.6 | 4.228 | 0.129 | 3.6 | 0.40 | 3.6 | 0.514 | 0.870 | 0.5 | 32.45 | 0.2 | 27.83 | 0.2 | 0.167 | 1.8 |
| 05b-6-103_m6_75 | 0.148 | 4.9 | 4.05 | 0.6 | 4.284 | 0.122 | 3.8 | 0.41 | 3.4 | 0.534 | 0.863 | 0.5 | 32.31 | 0.2 | 27.79 | 0.2 | 0.171 | 1.8 |
| 05b-6-103_m6_76 | 0.176 | 4.1 | 4.10 | 0.6 | 4.342 | 0.127 | 3.7 | 0.39 | 3.6 | 0.508 | 0.875 | 0.5 | 32.16 | 0.2 | 27.74 | 0.2 | 0.184 | 1.7 |
| 05b-6-103_m6_77 | 0.291 | 2.6 | 4.20 | 0.6 | 4.446 | 0.133 | 3.5 | 0.33 | 4.2 | 0.428 | 0.938 | 0.5 | 32.15 | 0.2 | 27.83 | 0.2 | 0.169 | 1.8 |
| 05b-6-103_m6_78 | 0.404 | 1.9 | 4.00 | 0.6 | 4.232 | 0.144 | 3.3 | 0.32 | 4.3 | 0.420 | 0.981 | 0.5 | 32.21 | 0.2 | 27.84 | 0.2 | 0.122 | 2.5 |
| 05b-6-103_m6_79 | 0.403 | 1.9 | 3.91 | 0.6 | 4.142 | 0.145 | 3.2 | 0.31 | 4.5 | 0.400 | 0.951 | 0.5 | 32.23 | 0.2 | 27.78 | 0.2 | 0.126 | 2.4 |
| 05b-6-103_m6_80 | 0.364 | 2.1 | 3.91 | 0.6 | 4.139 | 0.134 | 3.5 | 0.34 | 4.1 | 0.446 | 0.931 | 0.5 | 32.22 | 0.2 | 27.81 | 0.2 | 0.127 | 2.4 |
| 05b-6-103_m6_81 | 0.365 | 2.1 | 3.86 | 0.6 | 4.085 | 0.128 | 3.6 | 0.31 | 4.5 | 0.405 | 0.924 | 0.5 | 32.35 | 0.2 | 27.89 | 0.2 | 0.143 | 2.1 |
| 05b-6-103_m6_82 | 0.402 | 1.9 | 4.03 | 0.6 | 4.267 | 0.134 | 3.5 | 0.33 | 4.2 | 0.435 | 0.964 | 0.5 | 32.16 | 0.2 | 27.76 | 0.2 | 0.171 | 1.8 |
| 05b-6-103_m6_83 | 0.422 | 1.8 | 4.26 | 0.6 | 4.506 | 0.149 | 3.2 | 0.32 | 4.3 | 0.421 | 1.015 | 0.4 | 31.84 | 0.2 | 27.64 | 0.2 | 0.236 | 1.3 |
| 05b-6-103_m6_84 | 0.444 | 1.7 | 4.08 | 0.6 | 4.320 | 0.146 | 3.2 | 0.24 | 5.7 | 0.318 | 0.894 | 0.5 | 32.14 | 0.2 | 27.76 | 0.2 | 0.174 | 1.8 |
| 05b-6-103_m6_85 | 0.377 | 2.0 | 4.10 | 0.6 | 4.337 | 0.137 | 3.4 | 0.28 | 4.9 | 0.370 | 0.906 | 0.5 | 31.99 | 0.2 | 27.75 | 0.2 | 0.173 | 1.8 |
| 05b-6-103_m6_86 | 0.236 | 3.1 | 4.16 | 0.6 | 4.405 | 0.129 | 3.6 | 0.37 | 3.8 | 0.477 | 0.883 | 0.5 | 32.14 | 0.2 | 27.81 | 0.2 | 0.184 | 1.7 |
| 05b-6-103_m6_87 | 0.621 | 1.3 | 3.89 | 0.6 | 4.111 | 0.163 | 2.9 | 0.21 | 6.6 | 0.275 | 0.807 | 0.5 | 31.32 | 0.2 | 27.52 | 0.2 | 0.876 | 0.4 |
| 05b-6-103_m6_88 | 0.648 | 1.2 | 4.06 | 0.6 | 4.298 | 0.166 | 2.9 | 0.20 | 7.0 | 0.259 | 0.858 | 0.5 | 31.64 | 0.2 | 27.79 | 0.2 | 0.228 | 1.4 |
| 05b-6-103_m6_89 | 0.806 | 1.0 | 4.62 | 0.5 | 4.893 | 0.194 | 2.5 | 0.25 | 5.5 | 0.331 | 0.998 | 0.4 | 30.91 | 0.2 | 27.73 | 0.2 | 0.230 | 1.4 |
| 05b-6-103_m6_90 | 0.717 | 1.1 | 4.37 | 0.6 | 4.629 | 0.176 | 2.7 | 0.25 | 5.7 | 0.322 | 0.882 | 0.5 | 31.07 | 0.2 | 27.67 | 0.2 | 0.257 | 1.2 |
| 05b-6-103_m6_91 | 0.800 | 1.0 | 5.01 | 0.5 | 5.310 | 0.214 | 2.3 | 0.26 | 5.3 | 0.346 | 1.009 | 0.4 | 30.56 | 0.3 | 27.68 | 0.2 | 0.271 | 1.2 |
| 05b-6-103_m6_92 | 0.831 | 1.0 | 4.65 | 0.5 | 4.925 | 0.194 | 2.5 | 0.28 | 5.0 | 0.369 | 0.967 | 0.5 | 30.63 | 0.3 | 27.63 | 0.2 | 0.254 | 1.3 |
| 05b-6-103_m6_93 | 0.725 | 1.1 | 4.15 | 0.6 | 4.397 | 0.165 | 2.9 | 0.24 | 5.9 | 0.309 | 0.874 | 0.5 | 31.19 | 0.2 | 27.70 | 0.2 | 0.233 | 1.4 |
| 05b-6-103_m6_94 | 0.642 | 1.3 | 3.64 | 0.6 | 3.850 | 0.151 | 3.1 | 0.24 | 5.9 | 0.308 | 0.769 | 0.5 | 31.63 | 0.2 | 27.78 | 0.2 | 0.206 | 1.5 |
| 05b-6-103_m6_95 | 0.700 | 1.2 | 4.61 | 0.5 | 4.883 | 0.185 | 2.6 | 0.20 | 6.8 | 0.265 | 0.903 | 0.5 | 31.11 | 0.2 | 27.58 | 0.2 | 0.285 | 1.1 |
| 05b-6-103_m6_96 | 0.654 | 1.2 | 4.58 | 0.5 | 4.855 | 0.178 | 2.7 | 0.18 | 7.5 | 0.239 | 0.884 | 0.5 | 31.31 | 0.2 | 27.54 | 0.2 | 0.285 | 1.1 |
| 05b-6-103_m6_97 | 0.624 | 1.3 | 4.06 | 0.6 | 4.297 | 0.161 | 2.9 | 0.15 | 9.2 | 0.195 | 0.830 | 0.5 | 31.73 | 0.2 | 27.68 | 0.2 | 0.232 | 1.4 |
| 8153_21 | 0.382 | 2.0 | 7.38 | 0.4 | 7.877 | 0.184 | 2.6 | 0.50 | 2.8 | 0.649 | 0.582 | 0.7 | 30.67 | 0.3 | 25.90 | 0.2 | 1.351 | 0.3 |
| 8153_22 | 0.397 | 2.0 | 7.38 | 0.4 | 7.877 | 0.187 | 2.6 | 0.50 | 2.8 | 0.654 | 0.583 | 0.7 | 30.66 | 0.3 | 26.05 | 0.2 | 1.337 | 0.3 |
| 8153_23 | 0.379 | 2.0 | 7.37 | 0.4 | 7.867 | 0.188 | 2.6 | 0.48 | 3.0 | 0.622 | 0.582 | 0.7 | 30.58 | 0.3 | 25.91 | 0.2 | 1.353 | 0.3 |
| 8153_24 | 0.393 | 2.0 | 7.36 | 0.4 | 7.848 | 0.187 | 2.6 | 0.50 | 2.8 | 0.648 | 0.579 | 0.7 | 30.41 | 0.3 | 25.82 | 0.2 | 1.358 | 0.3 |
| 8153_25 | 0.398 | 2.0 | 7.38 | 0.4 | 7.876 | 0.196 | 2.5 | 0.51 | 2.8 | 0.665 | 0.576 | 0.7 | 30.80 | 0.2 | 25.93 | 0.2 | 1.373 | 0.3 |
| TU_15 | 0.899 | 1.0 | 16.12 | 0.3 | 17.411 | 0.226 | 2.2 | 2.44 | 0.7 | 3.318 | 1.586 | 0.3 | 21.63 | 0.3 | 24.00 | 0.2 | 2.364 | 0.2 |
| TU_16 | 0.903 | 1.0 | 16.32 | 0.3 | 17.630 | 0.233 | 2.1 | 2.47 | 0.7 | 3.365 | 1.621 | 0.3 | 21.69 | 0.3 | 24.13 | 0.2 | 2.387 | 0.2 |
| TU_17 | 0.912 | 1.0 | 16.48 | 0.3 | 17.809 | 0.250 | 2.0 | 2.46 | 0.7 | 3.355 | 1.620 | 0.3 | 21.61 | 0.3 | 24.12 | 0.2 | 2.460 | 0.2 |

| | $UO_2$ | | $ThO_2$ | | | PbO | | $Y_2O_3$ | | | CaO | | $Ce_2O_3$ | | $P_2O_5$ | | $SiO_2$ | |
|---|---|---|---|---|---|---|---|---|---|---|---|---|---|---|---|---|---|---|
| Sample | wt. % | RSD (2σ%) | wt. % | RSD (2σ%) | k-raw | wt. % | RSD (2σ%) | wt. % | RSD (2σ%) | k-raw | wt. % | RSD (2σ%) | wt. % | RSD (2σ%) | wt. % | RSD (2σ%) | wt. % | RSD (2σ%) |
| TU_18 | 0.917 | 1.0 | 16.57 | 0.3 | 17.918 | 0.234 | 2.1 | 2.46 | 0.7 | 3.352 | 1.614 | 0.3 | 21.57 | 0.3 | 23.96 | 0.2 | 2.429 | 0.2 |
| TU_19 | 0.898 | 1.0 | 16.55 | 0.3 | 17.892 | 0.231 | 2.1 | 2.43 | 0.7 | 3.309 | 1.618 | 0.3 | 21.49 | 0.3 | 23.96 | 0.2 | 2.425 | 0.2 |
| 05b-6-103_m5_1 | 0.465 | 1.7 | 6.04 | 0.5 | 6.426 | 0.193 | 2.5 | 0.12 | 11.8 | 0.151 | 1.426 | 0.4 | 31.48 | 0.2 | 27.97 | 0.2 | 0.333 | 1.0 |
| 05b-6-103_m5_2 | 0.456 | 1.7 | 5.86 | 0.5 | 6.235 | 0.195 | 2.5 | 0.14 | 9.6 | 0.186 | 1.386 | 0.4 | 31.58 | 0.2 | 27.90 | 0.2 | 0.179 | 1.7 |
| 05b-6-103_m5_3 | 0.517 | 1.5 | 5.75 | 0.5 | 6.109 | 0.181 | 2.7 | 0.14 | 9.6 | 0.186 | 1.365 | 0.4 | 31.49 | 0.2 | 27.93 | 0.2 | 0.159 | 1.9 |
| 05b-6-103_m5_4 | 0.507 | 1.6 | 5.65 | 0.5 | 6.010 | 0.194 | 2.5 | 0.16 | 8.3 | 0.215 | 1.354 | 0.4 | 31.50 | 0.2 | 27.85 | 0.2 | 0.161 | 1.9 |
| 05b-6-103_m5_5 | 0.472 | 1.7 | 5.24 | 0.5 | 5.560 | 0.179 | 2.7 | 0.21 | 6.4 | 0.280 | 1.257 | 0.4 | 31.88 | 0.2 | 27.99 | 0.2 | 0.142 | 2.1 |
| 05b-6-103_m5_6 | 0.406 | 1.9 | 4.64 | 0.5 | 4.917 | 0.145 | 3.2 | 0.30 | 4.6 | 0.393 | 1.105 | 0.4 | 32.10 | 0.2 | 28.00 | 0.2 | 0.141 | 2.1 |
| 05b-6-103_m5_7 | 0.458 | 1.7 | 5.07 | 0.5 | 5.382 | 0.165 | 2.9 | 0.25 | 5.4 | 0.332 | 1.231 | 0.4 | 31.88 | 0.2 | 27.95 | 0.2 | 0.140 | 2.2 |
| 05b-6-103_m5_8 | 0.474 | 1.7 | 5.71 | 0.5 | 6.076 | 0.178 | 2.7 | 0.16 | 8.6 | 0.208 | 1.360 | 0.4 | 31.82 | 0.2 | 27.94 | 0.2 | 0.161 | 1.9 |
| 05b-6-103_m5_9 | 0.465 | 1.7 | 6.02 | 0.5 | 6.405 | 0.193 | 2.5 | 0.14 | 9.5 | 0.186 | 1.414 | 0.4 | 31.56 | 0.2 | 28.01 | 0.2 | 0.233 | 1.3 |
| 05b-6-103_m5_10 | 0.419 | 1.8 | 5.14 | 0.5 | 5.422 | 0.167 | 2.8 | 0.18 | 7.4 | 0.237 | 1.226 | 0.4 | 29.64 | 0.3 | 26.23 | 0.2 | 3.895 | 0.2 |
| 05b-6-103_m5_11 | 0.719 | 1.1 | 5.49 | 0.5 | 5.838 | 0.199 | 2.4 | 0.08 | 16.6 | 0.107 | 1.345 | 0.4 | 32.09 | 0.2 | 28.05 | 0.2 | 0.115 | 2.6 |
| 05b-6-103_m5_12 | 0.518 | 1.5 | 4.96 | 0.5 | 5.268 | 0.169 | 2.8 | 0.20 | 7.0 | 0.256 | 1.195 | 0.4 | 31.96 | 0.2 | 28.07 | 0.2 | 0.112 | 2.7 |
| 05b-6-103_m5_13 | 0.166 | 4.4 | 3.97 | 0.6 | 4.196 | 0.117 | 3.9 | 0.42 | 3.4 | 0.544 | 0.874 | 0.5 | 32.48 | 0.2 | 27.95 | 0.2 | 0.179 | 1.7 |
| 05b-6-103_m5_14 | 0.178 | 4.1 | 3.96 | 0.6 | 4.192 | 0.120 | 3.9 | 0.40 | 3.5 | 0.520 | 0.869 | 0.5 | 32.67 | 0.2 | 28.00 | 0.2 | 0.174 | 1.8 |
| 05b-6-103_m5_15 | 0.171 | 4.3 | 3.98 | 0.6 | 4.214 | 0.113 | 4.1 | 0.43 | 3.3 | 0.556 | 0.874 | 0.5 | 32.36 | 0.2 | 27.77 | 0.2 | 0.192 | 1.6 |
| 05b-6-103_m5_16 | 0.236 | 3.1 | 4.26 | 0.6 | 4.508 | 0.127 | 3.7 | 0.37 | 3.8 | 0.477 | 0.954 | 0.5 | 32.13 | 0.2 | 27.76 | 0.2 | 0.871 | 0.5 |
| 05b-6-103_m5_17 | 0.762 | 1.1 | 4.57 | 0.5 | 4.837 | 0.188 | 2.6 | 0.44 | 3.2 | 0.576 | 0.941 | 0.5 | 31.09 | 0.2 | 27.71 | 0.2 | 0.248 | 1.3 |
| 05b-6-103_m5_18 | 0.863 | 1.0 | 4.39 | 0.6 | 4.659 | 0.185 | 2.6 | 0.10 | 13.7 | 0.130 | 1.085 | 0.4 | 32.52 | 0.2 | 28.02 | 0.2 | 0.074 | 4.0 |
| 05b-6-103_m5_19 | 0.843 | 1.0 | 4.38 | 0.6 | 4.652 | 0.190 | 2.5 | 0.05 | 25.9 | 0.069 | 1.094 | 0.4 | 32.28 | 0.2 | 28.17 | 0.2 | 0.071 | 4.1 |
| 05b-6-103_m5_20 | 0.895 | 0.9 | 4.32 | 0.6 | 4.582 | 0.189 | 2.5 | 0.10 | 13.1 | 0.137 | 1.075 | 0.4 | 32.18 | 0.2 | 28.04 | 0.2 | 0.080 | 3.7 |
| 05b-6-103_m5_21 | 0.830 | 1.0 | 4.53 | 0.5 | 4.806 | 0.196 | 2.5 | 0.30 | 4.6 | 0.394 | 1.049 | 0.4 | 31.81 | 0.2 | 27.86 | 0.2 | 0.173 | 1.8 |
| 05b-6-103_m5_22 | 0.786 | 1.1 | 4.80 | 0.5 | 5.091 | 0.192 | 2.5 | 0.31 | 4.5 | 0.400 | 1.043 | 0.4 | 31.49 | 0.2 | 27.76 | 0.2 | 0.218 | 1.4 |
| 05b-6-103_m5_23 | 0.534 | 1.5 | 4.15 | 0.6 | 4.380 | 0.155 | 3.0 | 0.30 | 4.5 | 0.392 | 0.978 | 0.5 | 29.84 | 0.3 | 26.28 | 0.2 | 2.938 | 0.2 |
| 05b-6-103_m5_24 | 0.586 | 1.4 | 4.56 | 0.5 | 4.830 | 0.172 | 2.8 | 0.45 | 3.2 | 0.584 | 0.901 | 0.5 | 30.62 | 0.3 | 27.21 | 0.2 | 0.291 | 1.1 |
| 05b-6-103_m5_25 | 0.619 | 1.3 | 5.47 | 0.5 | 5.810 | 0.200 | 2.4 | 0.40 | 3.5 | 0.526 | 1.012 | 0.4 | 30.88 | 0.3 | 27.57 | 0.2 | 0.346 | 1.0 |
| 05b-6-103_m5_26 | 0.627 | 1.3 | 5.12 | 0.5 | 5.429 | 0.187 | 2.6 | 0.35 | 4.0 | 0.462 | 1.053 | 0.4 | 31.35 | 0.2 | 27.72 | 0.2 | 0.256 | 1.2 |
| 05b-6-103_m5_27 | 0.598 | 1.3 | 5.24 | 0.5 | 5.557 | 0.193 | 2.5 | 0.42 | 3.4 | 0.548 | 0.979 | 0.5 | 31.12 | 0.2 | 27.57 | 0.2 | 0.334 | 1.0 |
| 05b-6-103_m5_28 | 0.583 | 1.4 | 5.12 | 0.5 | 5.435 | 0.186 | 2.6 | 0.41 | 3.4 | 0.540 | 0.976 | 0.5 | 31.10 | 0.2 | 27.52 | 0.2 | 0.324 | 1.0 |
| 05b-6-103_m5_29 | 0.631 | 1.3 | 5.47 | 0.5 | 5.802 | 0.202 | 2.4 | 0.40 | 3.5 | 0.523 | 1.022 | 0.4 | 30.72 | 0.3 | 27.46 | 0.2 | 0.359 | 0.9 |
| 05b-6-103_m5_30 | 0.687 | 1.2 | 5.30 | 0.5 | 5.621 | 0.198 | 2.4 | 0.42 | 3.4 | 0.550 | 0.997 | 0.4 | 30.98 | 0.2 | 27.62 | 0.2 | 0.351 | 0.9 |
| 05b-6-103_m5_31 | 0.680 | 1.2 | 4.64 | 0.5 | 4.913 | 0.175 | 2.7 | 0.44 | 3.2 | 0.578 | 0.925 | 0.5 | 31.26 | 0.2 | 27.73 | 0.2 | 0.272 | 1.2 |
| 05b-6-103_m5_32 | 0.632 | 1.3 | 4.19 | 0.6 | 4.432 | 0.169 | 2.8 | 0.46 | 3.1 | 0.594 | 0.877 | 0.5 | 31.57 | 0.2 | 27.80 | 0.2 | 0.223 | 1.4 |
| 05b-6-103_m5_33 | 0.618 | 1.3 | 4.50 | 0.6 | 4.769 | 0.176 | 2.7 | 0.48 | 3.0 | 0.623 | 0.909 | 0.5 | 31.32 | 0.2 | 27.81 | 0.2 | 0.247 | 1.3 |
| 05b-6-103_m5_34 | 0.565 | 1.4 | 4.00 | 0.6 | 4.229 | 0.160 | 3.0 | 0.44 | 3.2 | 0.580 | 0.858 | 0.5 | 31.13 | 0.2 | 27.76 | 0.2 | 0.294 | 1.1 |

| | $UO_2$ | | $ThO_2$ | | | PbO | | $Y_2O_3$ | | | CaO | | $Ce_2O_3$ | | $P_2O_5$ | | $SiO_2$ | |
|---|---|---|---|---|---|---|---|---|---|---|---|---|---|---|---|---|---|---|
| Sample | wt. % | RSD (2σ%) | wt. % | RSD (2σ%) | k-raw | wt. % | RSD (2σ%) | wt. % | RSD (2σ%) | k-raw | wt. % | RSD (2σ%) | wt. % | RSD (2σ%) | wt. % | RSD (2σ%) | wt. % | RSD (2σ%) |
| 05b-6-103_m5_35 | 0.609 | 1.3 | 3.67 | 0.6 | 3.883 | 0.157 | 3.0 | 0.45 | 3.1 | 0.589 | 0.792 | 0.5 | 31.79 | 0.2 | 27.75 | 0.2 | 0.217 | 1.4 |
| 05b-6-103_m5_36 | 0.650 | 1.2 | 4.65 | 0.5 | 4.924 | 0.182 | 2.6 | 0.42 | 3.3 | 0.554 | 0.925 | 0.5 | 30.98 | 0.2 | 27.56 | 0.2 | 0.290 | 1.1 |
| 05b-6-103_m5_37 | 0.625 | 1.3 | 3.83 | 0.6 | 4.049 | 0.153 | 3.1 | 0.44 | 3.2 | 0.574 | 0.812 | 0.5 | 31.61 | 0.2 | 27.69 | 0.2 | 0.215 | 1.5 |
| 05b-6-103_m5_38 | 0.603 | 1.3 | 3.92 | 0.6 | 4.136 | 0.162 | 2.9 | 0.43 | 3.3 | 0.559 | 0.806 | 0.5 | 31.42 | 0.2 | 27.72 | 0.2 | 0.832 | 0.5 |
| 05b-6-103_m5_39 | 0.514 | 1.5 | 2.98 | 0.7 | 3.142 | 0.130 | 3.6 | 0.43 | 3.3 | 0.563 | 0.648 | 0.6 | 32.30 | 0.2 | 27.95 | 0.2 | 0.181 | 1.7 |
| 05b-6-103_m5_40 | 0.538 | 1.5 | 3.28 | 0.7 | 3.465 | 0.135 | 3.5 | 0.45 | 3.2 | 0.586 | 0.701 | 0.6 | 32.10 | 0.2 | 27.84 | 0.2 | 0.187 | 1.7 |
| 05b-6-103_m5_41 | 0.617 | 1.3 | 4.35 | 0.6 | 4.609 | 0.177 | 2.7 | 0.46 | 3.1 | 0.595 | 0.902 | 0.5 | 31.28 | 0.2 | 27.65 | 0.2 | 0.258 | 1.2 |
| 05b-6-103_m5_42 | 0.794 | 1.1 | 6.66 | 0.4 | 7.101 | 0.235 | 2.1 | 0.03 | 43.5 | 0.041 | 1.606 | 0.3 | 31.45 | 0.2 | 28.17 | 0.2 | 0.137 | 2.2 |
| 05b-6-103_m5_43 | 0.748 | 1.1 | 5.44 | 0.5 | 5.783 | 0.203 | 2.4 | 0.07 | 20.7 | 0.085 | 1.239 | 0.4 | 32.25 | 0.2 | 28.14 | 0.2 | 0.148 | 2.1 |
| 05b-6-103_m5_44 | 0.669 | 1.2 | 4.63 | 0.5 | 4.913 | 0.179 | 2.7 | 0.05 | 24.9 | 0.071 | 1.054 | 0.4 | 32.81 | 0.2 | 28.14 | 0.2 | 0.152 | 2.0 |
| 05b-6-103_m5_45 | 0.670 | 1.2 | 4.66 | 0.5 | 4.948 | 0.175 | 2.7 | 0.04 | 32.2 | 0.055 | 1.045 | 0.4 | 32.59 | 0.2 | 28.08 | 0.2 | 0.152 | 2.0 |
| 05b-6-103_m5_46 | 0.637 | 1.3 | 4.73 | 0.5 | 5.025 | 0.180 | 2.7 | 0.04 | 32.5 | 0.054 | 1.028 | 0.4 | 32.59 | 0.2 | 28.10 | 0.2 | 0.190 | 1.6 |
| 05b-6-103_m5_47 | 0.649 | 1.2 | 4.95 | 0.5 | 5.260 | 0.177 | 2.7 | 0.03 | 40.0 | 0.044 | 1.035 | 0.4 | 32.25 | 0.2 | 27.94 | 0.2 | 0.248 | 1.3 |
| 05b-6-103_m5_48 | 0.697 | 1.2 | 5.25 | 0.5 | 5.578 | 0.201 | 2.4 | 0.05 | 25.9 | 0.068 | 1.103 | 0.4 | 32.24 | 0.2 | 27.92 | 0.2 | 0.270 | 1.2 |
| 05b-6-103_m5_49 | 0.650 | 1.2 | 4.82 | 0.5 | 5.117 | 0.172 | 2.8 | 0.05 | 28.8 | 0.061 | 1.051 | 0.4 | 32.40 | 0.2 | 27.84 | 0.2 | 0.280 | 1.1 |
| 05b-6-103_m5_50 | 0.545 | 1.5 | 5.35 | 0.5 | 5.690 | 0.188 | 2.6 | 0.09 | 15.3 | 0.115 | 1.211 | 0.4 | 32.27 | 0.2 | 27.98 | 0.2 | 0.228 | 1.4 |
| 05b-6-103_m5_51 | 0.551 | 1.4 | 5.29 | 0.5 | 5.620 | 0.189 | 2.5 | 0.10 | 13.0 | 0.136 | 1.185 | 0.4 | 32.23 | 0.2 | 28.02 | 0.2 | 0.256 | 1.2 |
| 05b-6-103_m5_52 | 0.584 | 1.4 | 5.16 | 0.5 | 5.484 | 0.184 | 2.6 | 0.12 | 11.7 | 0.151 | 1.151 | 0.4 | 32.30 | 0.2 | 28.05 | 0.2 | 0.239 | 1.3 |
| 05b-6-103_m5_53 | 0.577 | 1.4 | 4.98 | 0.5 | 5.284 | 0.178 | 2.7 | 0.08 | 16.3 | 0.109 | 1.081 | 0.4 | 31.66 | 0.2 | 27.73 | 0.2 | 0.376 | 0.9 |
| 05b-6-103_m5_54 | 0.451 | 1.7 | 5.87 | 0.5 | 6.241 | 0.185 | 2.6 | 0.14 | 9.4 | 0.189 | 1.293 | 0.4 | 31.78 | 0.2 | 28.08 | 0.2 | 0.224 | 1.4 |
| 05b-6-103_m5_55 | 0.456 | 1.7 | 6.01 | 0.5 | 6.386 | 0.184 | 2.6 | 0.15 | 9.4 | 0.193 | 1.335 | 0.4 | 31.56 | 0.2 | 28.23 | 0.2 | 0.229 | 1.4 |
| 05b-6-103_m5_56 | 0.462 | 1.7 | 5.72 | 0.5 | 6.086 | 0.180 | 2.7 | 0.12 | 11.0 | 0.162 | 1.226 | 0.4 | 31.93 | 0.2 | 28.03 | 0.2 | 0.227 | 1.4 |
| 05b-6-103_m5_57 | 0.668 | 1.2 | 5.66 | 0.5 | 6.026 | 0.207 | 2.3 | 0.07 | 20.3 | 0.087 | 1.308 | 0.4 | 31.72 | 0.2 | 27.95 | 0.2 | 0.184 | 1.7 |
| 05b-6-103_m5_58 | 0.672 | 1.2 | 5.80 | 0.5 | 6.166 | 0.205 | 2.4 | 0.09 | 14.5 | 0.122 | 1.408 | 0.4 | 32.01 | 0.2 | 28.32 | 0.2 | 0.141 | 2.2 |
| 8153_26 | 0.390 | 2.0 | 7.38 | 0.4 | 7.875 | 0.195 | 2.5 | 0.49 | 2.9 | 0.636 | 0.587 | 0.6 | 30.63 | 0.3 | 25.95 | 0.2 | 1.340 | 0.3 |
| 8153_27 | 0.387 | 2.0 | 7.38 | 0.4 | 7.877 | 0.193 | 2.5 | 0.51 | 2.8 | 0.665 | 0.581 | 0.7 | 30.54 | 0.3 | 25.92 | 0.2 | 1.335 | 0.3 |
| 8153_28 | 0.391 | 2.0 | 7.38 | 0.4 | 7.872 | 0.181 | 2.7 | 0.47 | 3.0 | 0.610 | 0.580 | 0.7 | 30.78 | 0.3 | 25.94 | 0.2 | 1.344 | 0.3 |
| 8153_29 | 0.383 | 2.0 | 7.38 | 0.4 | 7.872 | 0.195 | 2.5 | 0.49 | 2.8 | 0.644 | 0.592 | 0.6 | 30.64 | 0.3 | 25.89 | 0.2 | 1.338 | 0.3 |
| 8153_30 | 0.389 | 2.0 | 7.40 | 0.4 | 7.900 | 0.184 | 2.6 | 0.49 | 2.8 | 0.646 | 0.574 | 0.7 | 30.56 | 0.3 | 25.83 | 0.2 | 1.327 | 0.3 |
| 8153_31 | 0.396 | 2.0 | 7.35 | 0.4 | 7.849 | 0.193 | 2.5 | 0.52 | 2.7 | 0.675 | 0.579 | 0.7 | 30.59 | 0.3 | 25.79 | 0.2 | 1.320 | 0.3 |
| TU_20 | 0.927 | 1.0 | 17.16 | 0.3 | 18.581 | 0.242 | 2.1 | 2.44 | 0.7 | 3.333 | 1.637 | 0.3 | 21.13 | 0.3 | 23.76 | 0.2 | 2.526 | 0.2 |
| TU_21 | 0.933 | 1.0 | 17.20 | 0.3 | 18.621 | 0.236 | 2.1 | 2.42 | 0.7 | 3.298 | 1.654 | 0.3 | 21.09 | 0.3 | 23.69 | 0.2 | 2.541 | 0.2 |
| TU_22 | 0.944 | 1.0 | 17.27 | 0.3 | 18.697 | 0.244 | 2.1 | 2.44 | 0.7 | 3.334 | 1.660 | 0.3 | 21.17 | 0.3 | 23.76 | 0.2 | 2.529 | 0.2 |
| TU_23 | 0.907 | 1.0 | 16.63 | 0.3 | 17.982 | 0.236 | 2.1 | 2.46 | 0.7 | 3.358 | 1.607 | 0.3 | 21.33 | 0.3 | 23.75 | 0.2 | 2.429 | 0.2 |
| TU_24 | 0.884 | 1.0 | 16.48 | 0.3 | 17.813 | 0.241 | 2.1 | 2.46 | 0.7 | 3.347 | 1.643 | 0.3 | 21.47 | 0.3 | 23.99 | 0.2 | 2.373 | 0.2 |
| 8153_32 | 0.393 | 2.0 | 7.27 | 0.4 | 7.759 | 0.182 | 2.7 | 0.48 | 2.9 | 0.624 | 0.575 | 0.7 | 30.52 | 0.3 | 25.66 | 0.2 | 1.316 | 0.3 |

| | $UO_2$ | | $ThO_2$ | | | PbO | | $Y_2O_3$ | | | CaO | | $Ce_2O_3$ | | $P_2O_5$ | | $SiO_2$ | |
|---|---|---|---|---|---|---|---|---|---|---|---|---|---|---|---|---|---|---|
| Sample | wt. % | RSD (2σ%) | wt. % | RSD (2σ%) | k-raw | wt. % | RSD (2σ%) | wt. % | RSD (2σ%) | k-raw | wt. % | RSD (2σ%) | wt. % | RSD (2σ%) | wt. % | RSD (2σ%) | wt. % | RSD (2σ%) |
| 8153_33 | 0.384 | 2.0 | 7.34 | 0.4 | 7.837 | 0.173 | 2.8 | 0.48 | 2.9 | 0.627 | 0.580 | 0.7 | 30.54 | 0.3 | 25.68 | 0.2 | 1.312 | 0.3 |
| 8153_34 | 0.398 | 2.0 | 7.33 | 0.4 | 7.823 | 0.185 | 2.6 | 0.49 | 2.9 | 0.637 | 0.582 | 0.7 | 30.74 | 0.3 | 25.88 | 0.2 | 1.311 | 0.3 |
| 8153_35 | 0.394 | 2.0 | 7.35 | 0.4 | 7.842 | 0.182 | 2.7 | 0.50 | 2.8 | 0.648 | 0.584 | 0.7 | 30.81 | 0.2 | 25.77 | 0.2 | 1.306 | 0.3 |
| 8153_36 | 0.390 | 2.0 | 7.34 | 0.4 | 7.836 | 0.178 | 2.7 | 0.48 | 2.9 | 0.629 | 0.578 | 0.7 | 30.54 | 0.3 | 25.72 | 0.2 | 1.307 | 0.3 |
| TU_25 | 0.936 | 1.0 | 17.17 | 0.3 | 18.585 | 0.243 | 2.1 | 2.44 | 0.7 | 3.329 | 1.651 | 0.3 | 21.13 | 0.3 | 23.78 | 0.2 | 2.525 | 0.2 |
| TU_26 | 0.926 | 1.0 | 17.44 | 0.3 | 18.897 | 0.241 | 2.1 | 2.38 | 0.7 | 3.251 | 1.649 | 0.3 | 21.02 | 0.3 | 23.62 | 0.2 | 2.571 | 0.2 |
| TU_27 | 0.867 | 1.0 | 16.69 | 0.3 | 18.047 | 0.237 | 2.1 | 2.42 | 0.7 | 3.304 | 1.665 | 0.3 | 21.31 | 0.3 | 24.06 | 0.2 | 2.366 | 0.2 |
| TU_28 | 0.927 | 1.0 | 17.03 | 0.3 | 18.434 | 0.236 | 2.1 | 2.36 | 0.7 | 3.224 | 1.658 | 0.3 | 21.19 | 0.3 | 23.78 | 0.2 | 2.500 | 0.2 |
| TU_29 | 0.936 | 1.0 | 17.07 | 0.3 | 18.480 | 0.244 | 2.0 | 2.38 | 0.7 | 3.251 | 1.645 | 0.3 | 21.16 | 0.3 | 23.65 | 0.2 | 2.506 | 0.2 |
| 8153_37 | 0.375 | 2.1 | 7.33 | 0.4 | 7.831 | 0.190 | 2.5 | 0.48 | 2.9 | 0.623 | 0.573 | 0.7 | 30.64 | 0.3 | 25.55 | 0.2 | 1.314 | 0.3 |
| 8153_38 | 0.386 | 2.0 | 7.44 | 0.4 | 7.946 | 0.190 | 2.5 | 0.50 | 2.8 | 0.659 | 0.579 | 0.7 | 30.74 | 0.3 | 25.83 | 0.2 | 1.313 | 0.3 |
| 8153_39 | 0.376 | 2.1 | 7.36 | 0.4 | 7.856 | 0.180 | 2.7 | 0.52 | 2.7 | 0.681 | 0.584 | 0.7 | 30.63 | 0.3 | 25.76 | 0.2 | 1.302 | 0.3 |
| 8153_40 | 0.391 | 2.0 | 7.37 | 0.4 | 7.866 | 0.184 | 2.6 | 0.52 | 2.7 | 0.674 | 0.581 | 0.7 | 30.52 | 0.3 | 25.92 | 0.2 | 1.310 | 0.3 |
| 8153_41 | 0.399 | 2.0 | 7.42 | 0.4 | 7.910 | 0.183 | 2.7 | 0.52 | 2.8 | 0.675 | 0.582 | 0.7 | 30.67 | 0.3 | 26.14 | 0.2 | 1.319 | 0.3 |
| TU_30 | 0.875 | 1.0 | 15.75 | 0.3 | 16.976 | 0.218 | 2.3 | 2.50 | 0.7 | 3.398 | 1.626 | 0.3 | 21.88 | 0.3 | 24.50 | 0.2 | 2.264 | 0.2 |
| TU_31 | 0.855 | 1.0 | 16.00 | 0.3 | 17.258 | 0.231 | 2.2 | 2.49 | 0.7 | 3.389 | 1.636 | 0.3 | 21.78 | 0.3 | 24.58 | 0.2 | 2.285 | 0.2 |
| TU_32 | 0.862 | 1.0 | 16.21 | 0.3 | 17.491 | 0.226 | 2.2 | 2.49 | 0.7 | 3.396 | 1.618 | 0.3 | 21.67 | 0.3 | 24.53 | 0.2 | 2.319 | 0.2 |
| TU_33 | 0.874 | 1.0 | 16.45 | 0.3 | 17.755 | 0.232 | 2.2 | 2.49 | 0.7 | 3.388 | 1.618 | 0.3 | 21.90 | 0.3 | 24.69 | 0.2 | 2.420 | 0.2 |
| TU_34 | 0.895 | 1.0 | 16.48 | 0.3 | 17.791 | 0.232 | 2.2 | 2.47 | 0.7 | 3.373 | 1.596 | 0.3 | 21.65 | 0.3 | 24.47 | 0.2 | 2.430 | 0.2 |
| | | | | | | | | | | | | | | | | | | |
| 8153-1 | 0.397 | 1.9 | 7.58 | 0.4 | 8.082 | 0.192 | 2.5 | 0.51 | 2.3 | 0.662 | 0.574 | 0.6 | 30.87 | 0.3 | 26.90 | 0.2 | 1.381 | 0.3 |
| 8153-2 | 0.404 | 1.9 | 7.33 | 0.4 | 7.819 | 0.185 | 2.6 | 0.52 | 2.3 | 0.679 | 0.576 | 0.6 | 31.03 | 0.2 | 26.20 | 0.2 | 1.308 | 0.3 |
| 8153-3 | 0.396 | 1.9 | 7.31 | 0.4 | 7.796 | 0.181 | 2.6 | 0.54 | 2.2 | 0.702 | 0.580 | 0.6 | 30.72 | 0.3 | 26.10 | 0.2 | 1.310 | 0.3 |
| 8153-4 | 0.395 | 1.9 | 7.30 | 0.4 | 7.787 | 0.191 | 2.5 | 0.52 | 2.3 | 0.676 | 0.574 | 0.6 | 31.04 | 0.2 | 26.22 | 0.2 | 1.315 | 0.3 |
| 8153-5 | 0.397 | 1.9 | 7.28 | 0.4 | 7.771 | 0.179 | 2.7 | 0.52 | 2.2 | 0.683 | 0.580 | 0.6 | 30.72 | 0.3 | 25.88 | 0.2 | 1.305 | 0.3 |
| 8153-6 | 0.421 | 1.8 | 7.56 | 0.4 | 8.064 | 0.180 | 2.6 | 0.49 | 2.4 | 0.639 | 0.574 | 0.6 | 30.96 | 0.3 | 26.88 | 0.2 | 1.360 | 0.3 |
| 8153-7 | 0.386 | 2.0 | 7.14 | 0.4 | 7.602 | 0.180 | 2.6 | 0.47 | 2.5 | 0.614 | 0.560 | 0.7 | 30.99 | 0.3 | 26.78 | 0.2 | 1.263 | 0.3 |
| 8153-8 | 0.337 | 2.2 | 7.36 | 0.4 | 7.857 | 0.183 | 2.6 | 0.42 | 2.8 | 0.546 | 0.533 | 0.7 | 31.06 | 0.2 | 25.81 | 0.2 | 1.331 | 0.3 |
| 05-6-36_m2_pt1 | 0.441 | 1.6 | 3.46 | 0.6 | 3.664 | 0.120 | 3.6 | 0.17 | 6.3 | 0.216 | 0.739 | 0.5 | 34.30 | 0.2 | 28.88 | 0.2 | 0.138 | 2.1 |
| 05-6-36_m2_pt2 | 0.329 | 2.1 | 3.78 | 0.6 | 4.000 | 0.119 | 3.6 | 0.18 | 6.0 | 0.227 | 0.747 | 0.5 | 33.78 | 0.2 | 28.68 | 0.2 | 0.175 | 1.7 |
| 05-6-36_m2_pt3 | 0.350 | 2.0 | 4.02 | 0.5 | 4.251 | 0.137 | 3.1 | 0.17 | 6.0 | 0.227 | 0.781 | 0.5 | 33.53 | 0.2 | 28.64 | 0.2 | 0.185 | 1.6 |
| 05-6-36_m2_pt4 | 0.366 | 1.9 | 4.37 | 0.5 | 4.633 | 0.146 | 3.0 | 0.18 | 5.7 | 0.241 | 0.845 | 0.5 | 33.34 | 0.2 | 28.68 | 0.2 | 0.202 | 1.5 |
| 05-6-36_m2_pt5 | 0.384 | 1.9 | 4.43 | 0.5 | 4.690 | 0.152 | 2.9 | 0.16 | 6.5 | 0.209 | 0.856 | 0.5 | 33.09 | 0.2 | 28.61 | 0.2 | 0.207 | 1.4 |
| 05-6-36_m2_pt6 | 0.395 | 1.8 | 4.65 | 0.5 | 4.930 | 0.160 | 2.7 | 0.17 | 6.2 | 0.221 | 0.884 | 0.4 | 32.98 | 0.2 | 28.56 | 0.2 | 0.219 | 1.4 |
| 05-6-36_m2_pt7 | 0.395 | 1.8 | 4.58 | 0.5 | 4.858 | 0.155 | 2.8 | 0.18 | 5.7 | 0.239 | 0.867 | 0.5 | 33.03 | 0.2 | 28.61 | 0.2 | 0.220 | 1.4 |
| 05-6-36_m2_pt8 | 0.389 | 1.8 | 4.59 | 0.5 | 4.864 | 0.155 | 2.8 | 0.18 | 5.8 | 0.236 | 0.871 | 0.5 | 33.02 | 0.2 | 28.56 | 0.2 | 0.221 | 1.4 |

| | $UO_2$ | | $ThO_2$ | | | PbO | | $Y_2O_3$ | | | CaO | | $Ce_2O_3$ | | $P_2O_5$ | | $SiO_2$ | |
|---|---|---|---|---|---|---|---|---|---|---|---|---|---|---|---|---|---|---|
| Sample | wt. % | RSD (2σ%) | wt. % | RSD (2σ%) | k-raw | wt. % | RSD (2σ%) | wt. % | RSD (2σ%) | k-raw | wt. % | RSD (2σ%) | wt. % | RSD (2σ%) | wt. % | RSD (2σ%) | wt. % | RSD (2σ%) |
| 05-6-36_m2_pt9 | 0.443 | 1.6 | 4.83 | 0.5 | 5.123 | 0.160 | 2.7 | 0.19 | 5.5 | 0.251 | 0.910 | 0.4 | 32.76 | 0.2 | 28.69 | 0.2 | 0.232 | 1.3 |
| 05-6-36_m2_pt10 | 0.481 | 1.5 | 5.00 | 0.5 | 5.306 | 0.171 | 2.6 | 0.21 | 5.0 | 0.274 | 0.966 | 0.4 | 32.54 | 0.2 | 28.65 | 0.2 | 0.232 | 1.3 |
| 05-6-36_m2_pt11 | 0.465 | 1.6 | 4.99 | 0.5 | 5.288 | 0.176 | 2.5 | 0.22 | 4.7 | 0.289 | 0.957 | 0.4 | 32.28 | 0.2 | 28.41 | 0.2 | 0.250 | 1.2 |
| 05-6-36_m2_pt12 | 0.435 | 1.7 | 4.78 | 0.5 | 5.066 | 0.161 | 2.7 | 0.18 | 6.0 | 0.229 | 0.914 | 0.4 | 32.00 | 0.2 | 28.47 | 0.2 | 0.227 | 1.3 |
| 05-6-36_m2_pt13 | 0.405 | 1.8 | 4.40 | 0.5 | 4.662 | 0.151 | 2.9 | 0.18 | 5.8 | 0.235 | 0.864 | 0.5 | 33.01 | 0.2 | 28.55 | 0.2 | 0.204 | 1.5 |
| 05-6-36_m2_pt14 | 0.326 | 2.1 | 3.36 | 0.6 | 3.547 | 0.107 | 4.0 | 0.18 | 5.9 | 0.229 | 0.659 | 0.5 | 34.01 | 0.2 | 28.63 | 0.2 | 0.151 | 1.9 |
| 05-6-36_m2_pt15 | 0.373 | 1.9 | 3.59 | 0.6 | 3.794 | 0.124 | 3.4 | 0.14 | 7.7 | 0.178 | 0.725 | 0.5 | 33.79 | 0.2 | 28.91 | 0.2 | 0.158 | 1.9 |
| 05-6-36_m2_pt16 | 0.379 | 1.9 | 4.43 | 0.5 | 4.691 | 0.152 | 2.8 | 0.16 | 6.7 | 0.203 | 0.834 | 0.5 | 32.85 | 0.2 | 28.53 | 0.2 | 0.208 | 1.4 |
| 05-6-36_m2_pt17 | 0.379 | 1.9 | 4.37 | 0.5 | 4.629 | 0.145 | 3.0 | 0.16 | 6.6 | 0.204 | 0.827 | 0.5 | 33.26 | 0.2 | 28.71 | 0.2 | 0.205 | 1.4 |
| 05-6-36_m2_pt18 | 0.323 | 2.2 | 4.00 | 0.5 | 4.234 | 0.128 | 3.4 | 0.19 | 5.5 | 0.248 | 0.762 | 0.5 | 33.65 | 0.2 | 28.73 | 0.2 | 0.187 | 1.6 |
| 05-6-36_m2_pt19 | 0.321 | 2.2 | 3.78 | 0.6 | 3.999 | 0.128 | 3.3 | 0.15 | 6.9 | 0.195 | 0.730 | 0.5 | 33.85 | 0.2 | 28.77 | 0.2 | 0.178 | 1.7 |
| 05-6-36_m2_pt20 | 0.290 | 2.4 | 3.47 | 0.6 | 3.674 | 0.112 | 3.8 | 0.16 | 6.5 | 0.207 | 0.670 | 0.5 | 34.08 | 0.2 | 28.68 | 0.2 | 0.161 | 1.8 |
| 05-6-36_m2_pt21 | 0.287 | 2.4 | 3.36 | 0.6 | 3.550 | 0.113 | 3.7 | 0.14 | 7.2 | 0.187 | 0.654 | 0.5 | 34.09 | 0.2 | 28.78 | 0.2 | 0.158 | 1.9 |
| 05-6-36_m2_pt22 | 0.691 | 1.1 | 3.82 | 0.6 | 4.042 | 0.156 | 2.8 | 0.08 | 13.3 | 0.100 | 0.893 | 0.4 | 33.40 | 0.2 | 28.80 | 0.2 | 0.126 | 2.3 |
| 8153-9 | 0.329 | 2.2 | 7.17 | 0.4 | 7.647 | 0.188 | 2.4 | 0.44 | 2.5 | 0.568 | 0.523 | 0.6 | 31.57 | 0.2 | 26.16 | 0.2 | 1.313 | 0.3 |
| 8153-10 | 0.348 | 2.0 | 7.49 | 0.4 | 7.997 | 0.186 | 2.4 | 0.42 | 2.6 | 0.546 | 0.531 | 0.6 | 31.33 | 0.2 | 26.14 | 0.2 | 1.367 | 0.3 |
| 8153-11 | 0.343 | 2.1 | 7.55 | 0.4 | 8.062 | 0.183 | 2.4 | 0.44 | 2.5 | 0.576 | 0.534 | 0.6 | 31.12 | 0.2 | 26.08 | 0.2 | 1.366 | 0.3 |
| 8153-12 | 0.343 | 2.1 | 7.38 | 0.4 | 7.880 | 0.181 | 2.5 | 0.43 | 2.5 | 0.555 | 0.527 | 0.6 | 31.46 | 0.2 | 26.25 | 0.2 | 1.331 | 0.3 |
| 8153-13 | 0.373 | 1.9 | 7.46 | 0.4 | 7.964 | 0.183 | 2.4 | 0.43 | 2.5 | 0.567 | 0.527 | 0.6 | 31.34 | 0.2 | 26.32 | 0.2 | 1.366 | 0.3 |
| 8153-14 | 0.358 | 2.0 | 7.39 | 0.4 | 7.886 | 0.186 | 2.4 | 0.43 | 2.5 | 0.558 | 0.533 | 0.6 | 31.39 | 0.2 | 26.27 | 0.2 | 1.360 | 0.3 |
| 8153-15 | 0.351 | 2.0 | 7.58 | 0.4 | 8.087 | 0.184 | 2.4 | 0.42 | 2.6 | 0.547 | 0.542 | 0.6 | 31.37 | 0.2 | 26.34 | 0.2 | 1.368 | 0.3 |
| 05-6-36_m2_pt23 | 0.365 | 1.9 | 4.24 | 0.5 | 4.488 | 0.135 | 3.2 | 0.18 | 5.8 | 0.235 | 0.817 | 0.5 | 33.23 | 0.2 | 28.80 | 0.2 | 0.200 | 1.5 |
| 05-6-36_m2_pt24 | 0.368 | 1.9 | 4.37 | 0.5 | 4.627 | 0.143 | 3.0 | 0.15 | 7.2 | 0.190 | 0.827 | 0.5 | 33.35 | 0.2 | 28.78 | 0.2 | 0.205 | 1.5 |
| 05-6-36_m2_pt25 | 0.385 | 1.9 | 4.40 | 0.5 | 4.661 | 0.146 | 3.0 | 0.18 | 6.0 | 0.228 | 0.841 | 0.5 | 33.11 | 0.2 | 28.76 | 0.2 | 0.207 | 1.4 |
| 05-6-36_m2_pt26 | 0.421 | 1.7 | 4.70 | 0.5 | 4.982 | 0.164 | 2.7 | 0.20 | 5.3 | 0.259 | 0.908 | 0.4 | 32.80 | 0.2 | 28.72 | 0.2 | 0.233 | 1.3 |
| 05-6-36_m2_pt27 | 0.426 | 1.7 | 4.91 | 0.5 | 5.202 | 0.161 | 2.7 | 0.18 | 5.9 | 0.233 | 0.923 | 0.4 | 32.53 | 0.2 | 28.67 | 0.2 | 0.234 | 1.3 |
| 05-6-36_m2_pt28 | 0.431 | 1.7 | 4.70 | 0.5 | 4.977 | 0.150 | 2.9 | 0.19 | 5.5 | 0.249 | 0.884 | 0.4 | 32.80 | 0.2 | 28.62 | 0.2 | 0.238 | 1.3 |
| 05-6-36_m2_pt29 | 0.424 | 1.7 | 4.63 | 0.5 | 4.912 | 0.154 | 2.9 | 0.17 | 6.0 | 0.228 | 0.893 | 0.4 | 32.76 | 0.2 | 28.52 | 0.2 | 0.215 | 1.4 |
| 05-6-36_m2_pt30 | 0.407 | 1.8 | 4.32 | 0.5 | 4.579 | 0.144 | 3.0 | 0.17 | 6.0 | 0.228 | 0.830 | 0.5 | 33.01 | 0.2 | 28.64 | 0.2 | 0.212 | 1.4 |
| 05-6-36_m2_pt31 | 0.364 | 1.9 | 4.12 | 0.5 | 4.356 | 0.142 | 3.0 | 0.17 | 6.1 | 0.223 | 0.800 | 0.5 | 33.25 | 0.2 | 28.64 | 0.2 | 0.200 | 1.5 |
| 05-6-36_m2_pt32 | 0.333 | 2.1 | 3.88 | 0.6 | 4.103 | 0.123 | 3.5 | 0.16 | 6.7 | 0.201 | 0.747 | 0.5 | 33.52 | 0.2 | 28.63 | 0.2 | 0.247 | 1.2 |
| 05-6-36_m2_pt33 | 0.565 | 1.3 | 3.65 | 0.6 | 3.865 | 0.138 | 3.1 | 0.19 | 5.6 | 0.244 | 0.888 | 0.4 | 33.46 | 0.2 | 28.89 | 0.2 | 0.146 | 2.0 |
| 05-6-36_m2_pt34 | 0.640 | 1.2 | 3.59 | 0.6 | 3.796 | 0.142 | 3.1 | 0.17 | 6.2 | 0.218 | 0.962 | 0.4 | 33.04 | 0.2 | 28.94 | 0.2 | 0.081 | 3.5 |
| 05-6-36_m2_pt35 | 0.504 | 1.4 | 3.20 | 0.6 | 3.378 | 0.125 | 3.4 | 0.18 | 5.9 | 0.231 | 0.769 | 0.5 | 33.81 | 0.2 | 28.85 | 0.2 | 0.111 | 2.6 |
| 8153-16 | 0.341 | 2.1 | 7.56 | 0.4 | 8.074 | 0.176 | 2.5 | 0.42 | 2.6 | 0.545 | 0.533 | 0.6 | 31.07 | 0.2 | 26.19 | 0.2 | 1.362 | 0.3 |
| 8153-17 | 0.332 | 2.1 | 7.30 | 0.4 | 7.786 | 0.176 | 2.5 | 0.45 | 2.4 | 0.593 | 0.530 | 0.6 | 31.29 | 0.2 | 26.29 | 0.2 | 1.306 | 0.3 |

| | $UO_2$ | | $ThO_2$ | | | PbO | | $Y_2O_3$ | | | CaO | | $Ce_2O_3$ | | $P_2O_5$ | | $SiO_2$ | |
|---|---|---|---|---|---|---|---|---|---|---|---|---|---|---|---|---|---|---|
| Sample | wt. % | RSD (2σ%) | wt. % | RSD (2σ%) | k-raw | wt. % | RSD (2σ%) | wt. % | RSD (2σ%) | k-raw | wt. % | RSD (2σ%) | wt. % | RSD (2σ%) | wt. % | RSD (2σ%) | wt. % | RSD (2σ%) |
| 8153-18 | 0.346 | 2.1 | 7.41 | 0.4 | 7.909 | 0.180 | 2.5 | 0.43 | 2.5 | 0.555 | 0.536 | 0.6 | 31.41 | 0.2 | 26.20 | 0.2 | 1.335 | 0.3 |
| 8153-19 | 0.332 | 2.1 | 7.22 | 0.4 | 7.702 | 0.174 | 2.5 | 0.43 | 2.5 | 0.565 | 0.517 | 0.7 | 31.30 | 0.2 | 26.00 | 0.2 | 1.286 | 0.3 |
| 8153-20 | 0.342 | 2.1 | 7.38 | 0.4 | 7.880 | 0.180 | 2.5 | 0.42 | 2.5 | 0.554 | 0.529 | 0.6 | 31.13 | 0.2 | 25.62 | 0.2 | 1.315 | 0.3 |
| 8153-21 | 0.328 | 2.2 | 7.12 | 0.4 | 7.591 | 0.181 | 2.5 | 0.43 | 2.5 | 0.560 | 0.521 | 0.6 | 31.51 | 0.2 | 26.39 | 0.2 | 1.300 | 0.3 |
| 05-6-36_m2_pt36 | 0.306 | 2.3 | 3.63 | 0.6 | 3.835 | 0.122 | 3.5 | 0.15 | 6.8 | 0.199 | 0.705 | 0.5 | 33.75 | 0.2 | 28.66 | 0.2 | 0.275 | 1.1 |
| 05-6-36_m2_pt37 | 0.347 | 2.0 | 4.15 | 0.5 | 4.397 | 0.137 | 3.1 | 0.16 | 6.6 | 0.206 | 0.790 | 0.5 | 33.26 | 0.2 | 28.62 | 0.2 | 0.211 | 1.4 |
| 05-6-36_m2_pt38 | 0.310 | 2.3 | 3.73 | 0.6 | 3.947 | 0.119 | 3.6 | 0.15 | 7.0 | 0.194 | 0.716 | 0.5 | 33.74 | 0.2 | 28.69 | 0.2 | 0.201 | 1.5 |
| 05-6-36_m2_pt39 | 0.312 | 2.2 | 4.01 | 0.5 | 4.248 | 0.128 | 3.4 | 0.15 | 7.0 | 0.193 | 0.762 | 0.5 | 33.45 | 0.2 | 28.65 | 0.2 | 0.210 | 1.4 |
| 05-6-36_m2_pt40 | 0.318 | 2.2 | 4.15 | 0.5 | 4.391 | 0.130 | 3.3 | 0.17 | 6.3 | 0.216 | 0.768 | 0.5 | 33.57 | 0.2 | 28.73 | 0.2 | 0.224 | 1.3 |
| 05-6-36_m2_pt41 | 0.290 | 2.4 | 3.61 | 0.6 | 3.816 | 0.122 | 3.5 | 0.14 | 7.3 | 0.185 | 0.694 | 0.5 | 33.75 | 0.2 | 28.70 | 0.2 | 0.210 | 1.4 |
| 05-6-36_m2_pt42 | 0.301 | 2.3 | 3.77 | 0.6 | 3.985 | 0.123 | 3.5 | 0.16 | 6.6 | 0.206 | 0.717 | 0.5 | 33.83 | 0.2 | 28.67 | 0.2 | 0.206 | 1.5 |
| 05-6-36_m2_pt43 | 0.328 | 2.2 | 4.34 | 0.5 | 4.595 | 0.138 | 3.1 | 0.16 | 6.4 | 0.212 | 0.802 | 0.5 | 33.24 | 0.2 | 28.70 | 0.2 | 0.233 | 1.3 |
| 05-6-36_m2_pt44 | 0.335 | 2.1 | 4.11 | 0.5 | 4.352 | 0.126 | 3.4 | 0.14 | 7.3 | 0.185 | 0.770 | 0.5 | 33.66 | 0.2 | 28.78 | 0.2 | 0.226 | 1.3 |
| 05-6-36_m2_pt45 | 0.326 | 2.2 | 4.26 | 0.5 | 4.508 | 0.135 | 3.2 | 0.16 | 6.6 | 0.205 | 0.793 | 0.5 | 33.42 | 0.2 | 28.72 | 0.2 | 0.236 | 1.3 |
| 05-6-36_m2_pt46 | 0.323 | 2.2 | 4.35 | 0.5 | 4.607 | 0.140 | 3.1 | 0.15 | 7.1 | 0.193 | 0.809 | 0.5 | 33.38 | 0.2 | 28.71 | 0.2 | 0.242 | 1.3 |
| 05-6-36_m2_pt47 | 0.555 | 1.3 | 3.93 | 0.6 | 4.159 | 0.155 | 2.8 | 0.16 | 6.6 | 0.209 | 0.875 | 0.5 | 33.41 | 0.2 | 29.03 | 0.2 | 0.160 | 1.8 |
| 05-6-36_m2_pt48 | 0.379 | 1.9 | 3.85 | 0.6 | 4.072 | 0.133 | 3.3 | 0.17 | 6.0 | 0.224 | 0.773 | 0.5 | 33.38 | 0.2 | 28.68 | 0.2 | 0.205 | 1.5 |
| 05-6-36_m2_pt49 | 0.364 | 2.0 | 3.90 | 0.6 | 4.124 | 0.139 | 3.1 | 0.18 | 5.9 | 0.231 | 0.773 | 0.5 | 33.64 | 0.2 | 28.80 | 0.2 | 0.206 | 1.5 |
| 8153-22 | 0.379 | 1.9 | 7.16 | 0.4 | 7.632 | 0.181 | 2.4 | 0.51 | 2.2 | 0.663 | 0.560 | 0.6 | 31.05 | 0.2 | 26.78 | 0.2 | 1.273 | 0.3 |
| 8153-23 | 0.399 | 1.8 | 7.19 | 0.4 | 7.665 | 0.175 | 2.5 | 0.48 | 2.3 | 0.624 | 0.556 | 0.6 | 31.20 | 0.2 | 26.74 | 0.2 | 1.276 | 0.3 |
| 8153-24 | 0.380 | 1.9 | 7.21 | 0.4 | 7.687 | 0.182 | 2.4 | 0.51 | 2.2 | 0.661 | 0.551 | 0.6 | 30.99 | 0.2 | 26.63 | 0.2 | 1.263 | 0.3 |
| 8153-25 | 0.390 | 1.9 | 7.19 | 0.4 | 7.654 | 0.183 | 2.4 | 0.50 | 2.2 | 0.650 | 0.549 | 0.6 | 30.95 | 0.2 | 26.90 | 0.2 | 1.277 | 0.3 |
| 8153-26 | 0.393 | 1.8 | 7.19 | 0.4 | 7.663 | 0.189 | 2.4 | 0.48 | 2.3 | 0.624 | 0.557 | 0.6 | 31.16 | 0.2 | 26.85 | 0.2 | 1.290 | 0.3 |
| 8153-27 | 0.399 | 1.8 | 7.17 | 0.4 | 7.641 | 0.179 | 2.5 | 0.50 | 2.2 | 0.649 | 0.557 | 0.6 | 31.12 | 0.2 | 26.92 | 0.2 | 1.272 | 0.3 |
| 05-6-36_m7_pt1 | 0.681 | 1.1 | 4.19 | 0.5 | 4.439 | 0.166 | 2.6 | 0.29 | 3.7 | 0.377 | 1.024 | 0.4 | 32.86 | 0.2 | 28.87 | 0.2 | 0.082 | 3.4 |
| 05-6-36_m7_pt2 | 0.730 | 1.0 | 4.25 | 0.5 | 4.501 | 0.169 | 2.6 | 0.28 | 3.8 | 0.371 | 1.034 | 0.4 | 32.82 | 0.2 | 28.91 | 0.2 | 0.087 | 3.3 |
| 05-6-36_m7_pt3 | 0.345 | 2.0 | 3.31 | 0.6 | 3.496 | 0.109 | 3.9 | 0.16 | 6.5 | 0.209 | 0.672 | 0.5 | 33.58 | 0.2 | 28.73 | 0.2 | 0.150 | 2.0 |
| 05-6-36_m7_pt4 | 0.512 | 1.4 | 4.93 | 0.5 | 5.228 | 0.174 | 2.5 | 0.19 | 5.5 | 0.249 | 0.963 | 0.4 | 32.22 | 0.2 | 28.59 | 0.2 | 0.224 | 1.3 |
| 05-6-36_m7_pt5 | 0.467 | 1.6 | 4.60 | 0.5 | 4.875 | 0.157 | 2.8 | 0.17 | 6.0 | 0.225 | 0.912 | 0.4 | 32.44 | 0.2 | 28.48 | 0.2 | 0.223 | 1.3 |
| 05-6-36_m7_pt6 | 0.429 | 1.7 | 4.58 | 0.5 | 4.849 | 0.158 | 2.8 | 0.16 | 6.7 | 0.203 | 0.896 | 0.4 | 32.50 | 0.2 | 28.59 | 0.2 | 0.228 | 1.3 |
| 05-6-36_m7_pt7 | 0.421 | 1.7 | 4.59 | 0.5 | 4.862 | 0.156 | 2.8 | 0.14 | 7.2 | 0.188 | 0.900 | 0.4 | 32.71 | 0.2 | 28.59 | 0.2 | 0.243 | 1.3 |
| 05-6-36_m7_pt8 | 0.423 | 1.7 | 4.77 | 0.5 | 5.060 | 0.162 | 2.7 | 0.20 | 5.3 | 0.255 | 0.948 | 0.4 | 32.40 | 0.2 | 28.19 | 0.2 | 0.269 | 1.1 |
| 05-6-36_m7_pt9 | 0.335 | 2.1 | 4.32 | 0.5 | 4.580 | 0.142 | 3.1 | 0.14 | 7.3 | 0.186 | 0.820 | 0.5 | 33.09 | 0.2 | 28.56 | 0.2 | 0.230 | 1.3 |
| 05-6-36_m7_pt10 | 0.431 | 1.7 | 4.80 | 0.5 | 5.092 | 0.163 | 2.7 | 0.14 | 7.2 | 0.189 | 0.919 | 0.4 | 32.58 | 0.2 | 28.38 | 0.2 | 0.249 | 1.2 |
| 05-6-36_m7_pt11 | 0.464 | 1.6 | 4.73 | 0.5 | 5.008 | 0.159 | 2.8 | 0.18 | 5.9 | 0.238 | 0.912 | 0.4 | 32.41 | 0.2 | 28.94 | 0.2 | 0.291 | 1.1 |
| 05-6-36_m7_pt12 | 0.513 | 1.4 | 4.89 | 0.5 | 5.179 | 0.161 | 2.7 | 0.20 | 5.4 | 0.256 | 0.949 | 0.4 | 32.17 | 0.2 | 28.51 | 0.2 | 0.254 | 1.2 |

| | $UO_2$ | | $ThO_2$ | | | PbO | | $Y_2O_3$ | | | CaO | | $Ce_2O_3$ | | $P_2O_5$ | | $SiO_2$ | |
|---|---|---|---|---|---|---|---|---|---|---|---|---|---|---|---|---|---|---|
| Sample | wt. % | RSD (2σ%) | wt. % | RSD (2σ%) | k-raw | wt. % | RSD (2σ%) | wt. % | RSD (2σ%) | k-raw | wt. % | RSD (2σ%) | wt. % | RSD (2σ%) | wt. % | RSD (2σ%) | wt. % | RSD (2σ%) |
| 05-6-36_m7_pt13 | 0.457 | 1.6 | 4.20 | 0.5 | 4.448 | 0.143 | 3.0 | 0.20 | 5.4 | 0.255 | 0.844 | 0.5 | 32.98 | 0.2 | 28.68 | 0.2 | 0.197 | 1.5 |
| 05-6-36_m7_pt14 | 0.458 | 1.6 | 3.88 | 0.6 | 4.100 | 0.142 | 3.1 | 0.23 | 4.7 | 0.295 | 0.807 | 0.5 | 32.65 | 0.2 | 28.52 | 0.2 | 0.258 | 1.2 |
| 05-6-36_m7_pt15 | 0.480 | 1.5 | 4.48 | 0.5 | 4.750 | 0.161 | 2.7 | 0.22 | 4.8 | 0.286 | 0.860 | 0.5 | 32.57 | 0.2 | 28.55 | 0.2 | 0.232 | 1.3 |
| 05-6-36_m7_pt16 | 0.495 | 1.5 | 4.95 | 0.5 | 5.244 | 0.165 | 2.7 | 0.20 | 5.2 | 0.264 | 0.922 | 0.4 | 32.38 | 0.2 | 28.59 | 0.2 | 0.265 | 1.2 |
| 05-6-36_m7_pt17 | 0.424 | 1.7 | 5.17 | 0.5 | 5.490 | 0.162 | 2.7 | 0.14 | 7.4 | 0.184 | 0.949 | 0.4 | 32.43 | 0.2 | 28.50 | 0.2 | 0.287 | 1.1 |
| 05-6-36_m7_pt18 | 0.479 | 1.5 | 4.60 | 0.5 | 4.870 | 0.172 | 2.5 | 0.21 | 5.0 | 0.277 | 0.868 | 0.5 | 32.66 | 0.2 | 28.68 | 0.2 | 0.235 | 1.3 |
| 05-6-36_m7_pt19 | 0.501 | 1.5 | 4.26 | 0.5 | 4.504 | 0.153 | 2.9 | 0.24 | 4.5 | 0.308 | 0.825 | 0.5 | 32.61 | 0.2 | 28.81 | 0.2 | 0.228 | 1.3 |
| 05-6-36_m7_pt20 | 0.505 | 1.4 | 4.26 | 0.5 | 4.500 | 0.158 | 2.8 | 0.26 | 4.2 | 0.337 | 0.833 | 0.5 | 32.37 | 0.2 | 28.99 | 0.2 | 0.227 | 1.3 |
| 8153-28 | 0.376 | 1.9 | 7.20 | 0.4 | 7.668 | 0.180 | 2.5 | 0.51 | 2.2 | 0.663 | 0.545 | 0.6 | 31.23 | 0.2 | 26.84 | 0.2 | 1.277 | 0.3 |
| 8153-29 | 0.391 | 1.9 | 7.21 | 0.4 | 7.677 | 0.180 | 2.5 | 0.49 | 2.2 | 0.645 | 0.560 | 0.6 | 31.04 | 0.2 | 26.92 | 0.2 | 1.292 | 0.3 |
| 8153-30 | 0.394 | 1.8 | 7.19 | 0.4 | 7.660 | 0.180 | 2.5 | 0.49 | 2.2 | 0.645 | 0.555 | 0.6 | 31.01 | 0.2 | 26.97 | 0.2 | 1.296 | 0.3 |
| 8153-31 | 0.391 | 1.8 | 7.19 | 0.4 | 7.661 | 0.183 | 2.4 | 0.51 | 2.2 | 0.661 | 0.551 | 0.6 | 31.05 | 0.2 | 27.00 | 0.2 | 1.284 | 0.3 |
| 8153-32 | 0.383 | 1.9 | 7.14 | 0.4 | 7.599 | 0.182 | 2.4 | 0.50 | 2.2 | 0.653 | 0.553 | 0.6 | 30.94 | 0.2 | 27.00 | 0.2 | 1.282 | 0.3 |
| 8153-33 | 0.394 | 1.8 | 7.20 | 0.4 | 7.663 | 0.172 | 2.6 | 0.50 | 2.2 | 0.660 | 0.558 | 0.6 | 31.11 | 0.2 | 27.04 | 0.2 | 1.289 | 0.3 |
| 05-6-36_m7_pt21 | 0.709 | 1.1 | 4.24 | 0.5 | 4.482 | 0.170 | 2.6 | 0.44 | 2.5 | 0.571 | 1.069 | 0.4 | 32.63 | 0.2 | 28.94 | 0.2 | 0.066 | 4.2 |
| 05-6-36_m7_pt22 | 0.711 | 1.1 | 4.16 | 0.5 | 4.407 | 0.168 | 2.6 | 0.42 | 2.6 | 0.543 | 1.060 | 0.4 | 32.49 | 0.2 | 28.84 | 0.2 | 0.059 | 4.7 |
| 05-6-36_m7_pt23 | 0.672 | 1.1 | 4.22 | 0.5 | 4.469 | 0.168 | 2.6 | 0.44 | 2.5 | 0.569 | 1.069 | 0.4 | 32.67 | 0.2 | 29.00 | 0.2 | 0.059 | 4.7 |
| 05-6-36_m7_pt24 | 0.616 | 1.2 | 4.27 | 0.5 | 4.523 | 0.166 | 2.6 | 0.46 | 2.4 | 0.595 | 1.067 | 0.4 | 32.40 | 0.2 | 28.79 | 0.2 | 0.054 | 5.1 |
| 05-6-36_m7_pt25 | 0.655 | 1.1 | 4.25 | 0.5 | 4.501 | 0.168 | 2.6 | 0.46 | 2.4 | 0.600 | 1.057 | 0.4 | 32.61 | 0.2 | 28.80 | 0.2 | 0.051 | 5.5 |
| 05-6-36_m7_pt26 | 0.641 | 1.2 | 4.28 | 0.5 | 4.526 | 0.172 | 2.6 | 0.51 | 2.2 | 0.666 | 1.075 | 0.4 | 32.50 | 0.2 | 28.83 | 0.2 | 0.050 | 5.5 |
| 05-6-36_m7_pt27 | 0.639 | 1.2 | 4.26 | 0.5 | 4.513 | 0.159 | 2.8 | 0.50 | 2.2 | 0.649 | 1.072 | 0.4 | 32.48 | 0.2 | 28.75 | 0.2 | 0.050 | 5.5 |
| 05-6-36_m7_pt28 | 0.679 | 1.1 | 4.29 | 0.5 | 4.543 | 0.171 | 2.6 | 0.47 | 2.3 | 0.616 | 1.077 | 0.4 | 32.43 | 0.2 | 28.76 | 0.2 | 0.047 | 5.9 |
| 05-6-36_m7_pt29 | 0.595 | 1.2 | 3.71 | 0.6 | 3.916 | 0.155 | 2.8 | 0.88 | 1.3 | 1.143 | 0.815 | 0.5 | 32.18 | 0.2 | 28.59 | 0.2 | 0.151 | 1.9 |
| 05-6-36_m7_pt30 | 0.542 | 1.4 | 3.77 | 0.6 | 3.984 | 0.151 | 2.9 | 0.51 | 2.2 | 0.664 | 0.790 | 0.5 | 32.41 | 0.2 | 28.50 | 0.2 | 0.179 | 1.6 |
| 05-6-36_m7_pt31 | 0.519 | 1.4 | 3.68 | 0.6 | 3.888 | 0.139 | 3.1 | 0.37 | 3.0 | 0.480 | 0.756 | 0.5 | 32.76 | 0.2 | 28.56 | 0.2 | 0.167 | 1.8 |
| 05-6-36_m7_pt32 | 0.377 | 1.9 | 3.69 | 0.6 | 3.900 | 0.128 | 3.3 | 0.17 | 6.0 | 0.227 | 0.710 | 0.5 | 33.27 | 0.2 | 28.61 | 0.2 | 0.165 | 1.8 |
| 05-6-36_m7_pt33 | 0.443 | 1.6 | 4.57 | 0.5 | 4.841 | 0.151 | 2.9 | 0.19 | 5.6 | 0.245 | 0.889 | 0.4 | 32.91 | 0.2 | 28.69 | 0.2 | 0.196 | 1.5 |
| 05-6-36_m7_pt34 | 0.510 | 1.4 | 4.39 | 0.5 | 4.651 | 0.155 | 2.8 | 0.20 | 5.4 | 0.256 | 0.931 | 0.4 | 32.91 | 0.2 | 28.78 | 0.2 | 0.151 | 1.9 |
| 05-6-36_m7_pt35 | 0.716 | 1.1 | 4.31 | 0.5 | 4.567 | 0.171 | 2.6 | 0.30 | 3.6 | 0.391 | 1.068 | 0.4 | 32.72 | 0.2 | 28.91 | 0.2 | 0.065 | 4.3 |
| 05-6-36_m7_pt36 | 0.704 | 1.1 | 4.23 | 0.5 | 4.481 | 0.171 | 2.6 | 0.32 | 3.3 | 0.418 | 1.061 | 0.4 | 32.34 | 0.2 | 28.68 | 0.2 | 0.083 | 3.4 |
| 05-6-36_m7_pt37 | 0.706 | 1.1 | 4.25 | 0.5 | 4.494 | 0.167 | 2.6 | 0.44 | 2.5 | 0.579 | 1.072 | 0.4 | 32.54 | 0.2 | 28.76 | 0.2 | 0.059 | 4.7 |
| 05-6-36_m7_pt38 | 0.600 | 1.2 | 4.32 | 0.5 | 4.573 | 0.163 | 2.7 | 0.47 | 2.3 | 0.615 | 1.083 | 0.4 | 32.39 | 0.2 | 29.05 | 0.2 | 0.057 | 4.9 |
| 05-6-36_m7_pt39 | 0.571 | 1.3 | 4.27 | 0.5 | 4.519 | 0.170 | 2.6 | 0.46 | 2.4 | 0.600 | 1.067 | 0.4 | 32.33 | 0.2 | 28.84 | 0.2 | 0.060 | 4.6 |
| 05-6-36_m7_pt40 | 0.624 | 1.2 | 4.24 | 0.5 | 4.488 | 0.159 | 2.8 | 0.49 | 2.3 | 0.636 | 1.052 | 0.4 | 32.52 | 0.2 | 28.94 | 0.2 | 0.063 | 4.5 |
| 8153-34 | 0.400 | 1.8 | 7.25 | 0.4 | 7.732 | 0.187 | 2.4 | 0.49 | 2.2 | 0.643 | 0.574 | 0.6 | 31.02 | 0.2 | 26.26 | 0.2 | 1.315 | 0.3 |
| 8153-35 | 0.383 | 1.9 | 7.28 | 0.4 | 7.769 | 0.183 | 2.4 | 0.51 | 2.2 | 0.662 | 0.573 | 0.6 | 31.14 | 0.2 | 26.23 | 0.2 | 1.312 | 0.3 |

| | $UO_2$ | | $ThO_2$ | | | PbO | | $Y_2O_3$ | | | CaO | | $Ce_2O_3$ | | $P_2O_5$ | | $SiO_2$ | |
|---|---|---|---|---|---|---|---|---|---|---|---|---|---|---|---|---|---|---|
| Sample | wt. % | RSD (2σ%) | wt. % | RSD (2σ%) | k-raw | wt. % | RSD (2σ%) | wt. % | RSD (2σ%) | k-raw | wt. % | RSD (2σ%) | wt. % | RSD (2σ%) | wt. % | RSD (2σ%) | wt. % | RSD (2σ%) |
| 8153-36 | 0.395 | 1.8 | 7.25 | 0.4 | 7.736 | 0.187 | 2.4 | 0.51 | 2.2 | 0.665 | 0.575 | 0.6 | 31.13 | 0.2 | 26.30 | 0.2 | 1.322 | 0.3 |
| 8153-37 | 0.388 | 1.9 | 7.29 | 0.4 | 7.778 | 0.185 | 2.4 | 0.50 | 2.2 | 0.649 | 0.575 | 0.6 | 30.88 | 0.2 | 26.09 | 0.2 | 1.306 | 0.3 |
| 8153-38 | 0.400 | 1.8 | 7.28 | 0.4 | 7.766 | 0.192 | 2.3 | 0.51 | 2.2 | 0.664 | 0.581 | 0.6 | 30.84 | 0.2 | 26.02 | 0.2 | 1.296 | 0.3 |
| 8153-39 | 0.397 | 1.8 | 7.28 | 0.4 | 7.773 | 0.182 | 2.5 | 0.52 | 2.1 | 0.674 | 0.573 | 0.6 | 30.94 | 0.2 | 25.99 | 0.2 | 1.299 | 0.3 |
| 05-6-36_m7_pt41 | 0.376 | 1.9 | 4.32 | 0.5 | 4.572 | 0.150 | 2.9 | 0.13 | 7.7 | 0.175 | 0.837 | 0.5 | 33.12 | 0.2 | 28.68 | 0.2 | 0.181 | 1.6 |
| 05-6-36_m7_pt42 | 0.381 | 1.9 | 4.26 | 0.5 | 4.516 | 0.143 | 3.0 | 0.12 | 8.4 | 0.161 | 0.838 | 0.5 | 33.33 | 0.2 | 28.81 | 0.2 | 0.177 | 1.7 |
| 05-6-36_m7_pt43 | 0.398 | 1.8 | 4.21 | 0.5 | 4.455 | 0.145 | 3.0 | 0.12 | 9.0 | 0.150 | 0.833 | 0.5 | 33.18 | 0.2 | 28.73 | 0.2 | 0.179 | 1.6 |
| 05-6-36_m7_pt44 | 0.399 | 1.8 | 4.22 | 0.5 | 4.469 | 0.139 | 3.1 | 0.13 | 7.9 | 0.172 | 0.837 | 0.5 | 33.09 | 0.2 | 28.56 | 0.2 | 0.179 | 1.7 |
| 05-6-36_m7_pt45 | 0.374 | 1.9 | 3.95 | 0.5 | 4.177 | 0.133 | 3.3 | 0.13 | 8.1 | 0.167 | 0.757 | 0.5 | 33.33 | 0.2 | 28.51 | 0.2 | 0.188 | 1.6 |
| 05-6-36_m7_pt46 | 0.490 | 1.5 | 4.02 | 0.5 | 4.256 | 0.151 | 2.9 | 0.23 | 4.6 | 0.299 | 0.819 | 0.5 | 32.68 | 0.2 | 28.17 | 0.2 | 0.208 | 1.4 |
| 05-6-36_m7_pt47 | 0.540 | 1.4 | 4.42 | 0.5 | 4.677 | 0.166 | 2.6 | 0.25 | 4.2 | 0.329 | 0.885 | 0.4 | 32.48 | 0.2 | 28.49 | 0.2 | 0.194 | 1.5 |
| 05-6-36_m7_pt48 | 0.536 | 1.4 | 4.49 | 0.5 | 4.757 | 0.164 | 2.7 | 0.25 | 4.2 | 0.331 | 0.888 | 0.4 | 32.53 | 0.2 | 28.52 | 0.2 | 0.212 | 1.4 |
| 05-6-36_m7_pt49 | 0.532 | 1.4 | 4.20 | 0.5 | 4.443 | 0.154 | 2.8 | 0.26 | 4.1 | 0.337 | 0.854 | 0.5 | 32.64 | 0.2 | 28.51 | 0.2 | 0.188 | 1.6 |
| 05-6-36_m7_pt50 | 0.492 | 1.5 | 4.37 | 0.5 | 4.626 | 0.154 | 2.8 | 0.23 | 4.5 | 0.302 | 0.867 | 0.5 | 32.49 | 0.2 | 28.51 | 0.2 | 0.212 | 1.4 |
| 05-6-36_m7_pt51 | 0.504 | 1.4 | 4.23 | 0.5 | 4.479 | 0.151 | 2.9 | 0.22 | 4.8 | 0.286 | 0.849 | 0.5 | 32.76 | 0.2 | 28.59 | 0.2 | 0.184 | 1.6 |
| 05-6-36_m7_pt52 | 0.503 | 1.5 | 4.55 | 0.5 | 4.818 | 0.156 | 2.8 | 0.20 | 5.2 | 0.265 | 0.881 | 0.4 | 32.54 | 0.2 | 28.58 | 0.2 | 0.212 | 1.4 |
| 05-6-36_m7_pt53 | 0.435 | 1.7 | 4.46 | 0.5 | 4.721 | 0.160 | 2.7 | 0.17 | 6.1 | 0.225 | 0.861 | 0.5 | 32.64 | 0.2 | 28.70 | 0.2 | 0.284 | 1.1 |
| 05-6-36_m7_pt54 | 0.539 | 1.4 | 4.19 | 0.5 | 4.433 | 0.152 | 2.9 | 0.28 | 3.8 | 0.362 | 0.857 | 0.5 | 32.59 | 0.2 | 28.57 | 0.2 | 0.201 | 1.5 |
| 05-6-36_m7_pt55 | 0.511 | 1.4 | 4.89 | 0.5 | 5.182 | 0.171 | 2.6 | 0.21 | 4.9 | 0.280 | 0.935 | 0.4 | 32.32 | 0.2 | 28.40 | 0.2 | 0.262 | 1.2 |
| 05-6-36_m7_pt56 | 0.503 | 1.5 | 4.84 | 0.5 | 5.129 | 0.165 | 2.6 | 0.20 | 5.3 | 0.259 | 0.930 | 0.4 | 32.21 | 0.2 | 28.43 | 0.2 | 0.240 | 1.3 |
| 05-6-36_m7_pt57 | 0.447 | 1.6 | 4.64 | 0.5 | 4.922 | 0.148 | 3.0 | 0.18 | 5.8 | 0.233 | 0.895 | 0.4 | 32.55 | 0.2 | 28.47 | 0.2 | 0.220 | 1.4 |
| 05-6-36_m7_pt58 | 0.441 | 1.6 | 4.92 | 0.5 | 5.217 | 0.158 | 2.8 | 0.18 | 5.9 | 0.231 | 0.916 | 0.4 | 32.36 | 0.2 | 28.38 | 0.2 | 0.258 | 1.2 |
| 05-6-36_m7_pt59 | 0.403 | 1.8 | 4.88 | 0.5 | 5.178 | 0.170 | 2.6 | 0.15 | 7.0 | 0.192 | 0.922 | 0.4 | 32.48 | 0.2 | 28.41 | 0.2 | 0.237 | 1.3 |
| 05-6-36_m7_pt60 | 0.447 | 1.6 | 5.04 | 0.5 | 5.351 | 0.177 | 2.5 | 0.18 | 5.9 | 0.229 | 0.932 | 0.4 | 32.32 | 0.2 | 28.35 | 0.2 | 0.258 | 1.2 |
| 05-6-36_m7_pt61 | 0.419 | 1.7 | 4.86 | 0.5 | 5.156 | 0.167 | 2.6 | 0.14 | 7.1 | 0.188 | 0.915 | 0.4 | 32.39 | 0.2 | 28.11 | 0.2 | 0.266 | 1.1 |
| 05-6-36_m7_pt62 | 0.441 | 1.6 | 4.77 | 0.5 | 5.060 | 0.169 | 2.6 | 0.18 | 5.8 | 0.234 | 0.916 | 0.4 | 32.28 | 0.2 | 28.36 | 0.2 | 0.234 | 1.3 |
| 05-6-36_m7_pt63 | 0.407 | 1.8 | 4.04 | 0.5 | 4.272 | 0.140 | 3.1 | 0.18 | 5.8 | 0.235 | 0.787 | 0.5 | 32.85 | 0.2 | 28.35 | 0.2 | 0.192 | 1.5 |
| 05-6-36_m7_pt64 | 0.619 | 1.2 | 4.80 | 0.5 | 5.085 | 0.175 | 2.5 | 0.48 | 2.3 | 0.630 | 0.933 | 0.4 | 31.65 | 0.2 | 28.24 | 0.2 | 0.262 | 1.2 |
| 05-6-36_m7_pt65 | 0.434 | 1.7 | 3.80 | 0.6 | 4.024 | 0.138 | 3.2 | 0.19 | 5.5 | 0.247 | 0.780 | 0.5 | 33.03 | 0.2 | 28.53 | 0.2 | 0.184 | 1.6 |
| 05-6-36_m7_pt66 | 0.438 | 1.6 | 4.17 | 0.5 | 4.416 | 0.144 | 3.0 | 0.16 | 6.5 | 0.209 | 0.841 | 0.5 | 32.77 | 0.2 | 28.49 | 0.2 | 0.193 | 1.5 |
| 05-6-36_m7_pt67 | 0.410 | 1.7 | 4.34 | 0.5 | 4.599 | 0.146 | 3.0 | 0.17 | 6.2 | 0.218 | 0.829 | 0.5 | 32.76 | 0.2 | 28.43 | 0.2 | 0.208 | 1.4 |
| 05-6-36_m7_pt68 | 0.457 | 1.6 | 4.39 | 0.5 | 4.647 | 0.152 | 2.9 | 0.20 | 5.3 | 0.258 | 0.837 | 0.5 | 32.74 | 0.2 | 28.56 | 0.2 | 0.213 | 1.4 |
| 05-6-36_m7_pt69 | 0.462 | 1.6 | 4.04 | 0.5 | 4.274 | 0.152 | 2.9 | 0.23 | 4.6 | 0.297 | 0.789 | 0.5 | 32.98 | 0.2 | 28.47 | 0.2 | 0.199 | 1.5 |
| 05-6-36_m7_pt70 | 0.438 | 1.6 | 4.30 | 0.5 | 4.556 | 0.145 | 3.0 | 0.20 | 5.3 | 0.258 | 0.821 | 0.5 | 32.92 | 0.2 | 28.53 | 0.2 | 0.201 | 1.5 |
| 8153-40 | 0.374 | 1.9 | 7.30 | 0.4 | 7.791 | 0.189 | 2.4 | 0.50 | 2.2 | 0.652 | 0.577 | 0.6 | 30.89 | 0.2 | 25.91 | 0.2 | 1.304 | 0.3 |
| 8153-41 | 0.385 | 1.9 | 7.32 | 0.4 | 7.810 | 0.191 | 2.3 | 0.51 | 2.1 | 0.669 | 0.571 | 0.6 | 30.81 | 0.2 | 25.94 | 0.2 | 1.315 | 0.3 |

| | $UO_2$ | | $ThO_2$ | | | PbO | | $Y_2O_3$ | | | CaO | | $Ce_2O_3$ | | $P_2O_5$ | | $SiO_2$ | |
|---|---|---|---|---|---|---|---|---|---|---|---|---|---|---|---|---|---|---|
| Sample | wt. % | RSD (2σ%) | wt. % | RSD (2σ%) | k-raw | wt. % | RSD (2σ%) | wt. % | RSD (2σ%) | k-raw | wt. % | RSD (2σ%) | wt. % | RSD (2σ%) | wt. % | RSD (2σ%) | wt. % | RSD (2σ%) |
| 8153-42 | 0.395 | 1.8 | 7.23 | 0.4 | 7.715 | 0.190 | 2.4 | 0.49 | 2.2 | 0.642 | 0.571 | 0.6 | 30.88 | 0.2 | 25.93 | 0.2 | 1.303 | 0.3 |
| 8153-43 | 0.387 | 1.9 | 7.26 | 0.4 | 7.752 | 0.190 | 2.4 | 0.50 | 2.2 | 0.656 | 0.571 | 0.6 | 31.15 | 0.2 | 25.80 | 0.2 | 1.309 | 0.3 |
| 8153-44 | 0.390 | 1.8 | 7.26 | 0.4 | 7.753 | 0.188 | 2.4 | 0.52 | 2.1 | 0.684 | 0.581 | 0.6 | 30.99 | 0.2 | 25.72 | 0.2 | 1.318 | 0.3 |
| 8153-45 | 0.388 | 1.8 | 7.28 | 0.4 | 7.769 | 0.186 | 2.4 | 0.53 | 2.1 | 0.686 | 0.575 | 0.6 | 30.95 | 0.2 | 25.65 | 0.2 | 1.309 | 0.3 |
| 05-6-36_m7_pt71 | 0.621 | 1.2 | 4.23 | 0.5 | 4.463 | 0.172 | 2.6 | 0.85 | 1.4 | 1.116 | 0.862 | 0.5 | 30.84 | 0.2 | 28.39 | 0.2 | 0.205 | 1.4 |
| 05-6-36_m7_pt72 | 0.609 | 1.2 | 3.92 | 0.6 | 4.132 | 0.172 | 2.6 | 1.23 | 1.0 | 1.616 | 0.798 | 0.5 | 31.47 | 0.2 | 28.50 | 0.2 | 0.196 | 1.5 |
| 05-6-36_m7_pt73 | 0.690 | 1.1 | 4.14 | 0.5 | 4.355 | 0.180 | 2.5 | 1.49 | 0.9 | 1.961 | 0.870 | 0.5 | 30.56 | 0.2 | 28.47 | 0.2 | 0.199 | 1.5 |
| 05-6-36_m7_pt74 | 0.654 | 1.2 | 3.85 | 0.6 | 4.054 | 0.167 | 2.6 | 1.52 | 0.8 | 1.997 | 0.834 | 0.5 | 31.20 | 0.2 | 28.59 | 0.2 | 0.182 | 1.6 |
| 05-6-36_m7_pt75 | 0.658 | 1.1 | 3.81 | 0.6 | 4.014 | 0.165 | 2.7 | 1.42 | 0.9 | 1.863 | 0.819 | 0.5 | 31.31 | 0.2 | 28.58 | 0.2 | 0.177 | 1.7 |
| 05-6-36_m7_pt76 | 0.617 | 1.2 | 3.63 | 0.6 | 3.823 | 0.161 | 2.7 | 1.41 | 0.9 | 1.840 | 0.792 | 0.5 | 31.46 | 0.2 | 28.62 | 0.2 | 0.165 | 1.8 |
| 05-6-36_m7_pt77 | 0.612 | 1.2 | 3.75 | 0.6 | 3.952 | 0.164 | 2.7 | 1.35 | 0.9 | 1.768 | 0.807 | 0.5 | 31.40 | 0.2 | 28.58 | 0.2 | 0.180 | 1.6 |
| 05-6-36_m7_pt78 | 0.571 | 1.3 | 3.47 | 0.6 | 3.658 | 0.152 | 2.9 | 1.29 | 1.0 | 1.684 | 0.757 | 0.5 | 31.74 | 0.2 | 28.64 | 0.2 | 0.164 | 1.8 |
| 05-6-36_m7_pt79 | 0.671 | 1.1 | 4.03 | 0.5 | 4.251 | 0.178 | 2.5 | 1.37 | 0.9 | 1.794 | 0.852 | 0.5 | 31.16 | 0.2 | 28.58 | 0.2 | 0.187 | 1.6 |
| 05-6-36_m7_pt80 | 0.650 | 1.2 | 4.00 | 0.5 | 4.212 | 0.172 | 2.6 | 1.29 | 1.0 | 1.689 | 0.844 | 0.5 | 31.31 | 0.2 | 28.50 | 0.2 | 0.197 | 1.5 |
| 05-6-36_m7_pt81 | 0.646 | 1.2 | 3.87 | 0.6 | 4.083 | 0.170 | 2.6 | 1.16 | 1.1 | 1.523 | 0.833 | 0.5 | 31.56 | 0.2 | 28.53 | 0.2 | 0.185 | 1.6 |
| 05-6-36_m7_pt82 | 0.658 | 1.1 | 4.07 | 0.5 | 4.294 | 0.173 | 2.6 | 1.24 | 1.0 | 1.626 | 0.855 | 0.5 | 31.31 | 0.2 | 28.55 | 0.2 | 0.193 | 1.5 |
| 05-6-36_m7_pt83 | 0.538 | 1.4 | 3.61 | 0.6 | 3.804 | 0.135 | 3.2 | 0.80 | 1.5 | 1.041 | 0.827 | 0.5 | 32.35 | 0.2 | 28.62 | 0.2 | 0.095 | 3.0 |
| 05-6-36_m7_pt84 | 0.550 | 1.3 | 3.74 | 0.6 | 3.950 | 0.153 | 2.9 | 0.82 | 1.4 | 1.068 | 0.764 | 0.5 | 31.93 | 0.2 | 28.50 | 0.2 | 0.173 | 1.7 |
| 05-6-36_m7_pt85 | 0.661 | 1.1 | 4.07 | 0.5 | 4.300 | 0.166 | 2.6 | 0.97 | 1.2 | 1.270 | 0.855 | 0.5 | 31.73 | 0.2 | 28.50 | 0.2 | 0.185 | 1.6 |
| 05-6-36_m7_pt86 | 0.646 | 1.2 | 3.96 | 0.5 | 4.178 | 0.161 | 2.7 | 0.96 | 1.2 | 1.252 | 0.844 | 0.5 | 31.73 | 0.2 | 28.60 | 0.2 | 0.183 | 1.6 |
| 05-6-36_m7_pt87 | 0.650 | 1.2 | 3.88 | 0.6 | 4.088 | 0.168 | 2.6 | 1.00 | 1.2 | 1.303 | 0.825 | 0.5 | 31.72 | 0.2 | 28.54 | 0.2 | 0.177 | 1.7 |
| 05-6-36_m7_pt88 | 0.662 | 1.1 | 4.18 | 0.5 | 4.413 | 0.183 | 2.4 | 1.09 | 1.1 | 1.423 | 0.862 | 0.5 | 31.28 | 0.2 | 28.58 | 0.2 | 0.218 | 1.4 |
| 05-6-36_m7_pt89 | 0.691 | 1.1 | 4.15 | 0.5 | 4.374 | 0.171 | 2.6 | 1.18 | 1.0 | 1.546 | 0.888 | 0.4 | 31.40 | 0.2 | 28.56 | 0.2 | 0.198 | 1.5 |
| 05-6-36_m7_pt90 | 0.665 | 1.1 | 4.62 | 0.5 | 4.873 | 0.197 | 2.3 | 1.26 | 1.0 | 1.652 | 0.937 | 0.4 | 30.91 | 0.2 | 28.26 | 0.2 | 0.256 | 1.2 |
| 05-6-36_m7_pt91 | 0.638 | 1.2 | 4.10 | 0.5 | 4.324 | 0.174 | 2.5 | 1.24 | 1.0 | 1.630 | 0.845 | 0.5 | 31.28 | 0.2 | 28.44 | 0.2 | 0.213 | 1.4 |
| 05-6-36_m7_pt92 | 0.671 | 1.1 | 4.36 | 0.5 | 4.605 | 0.175 | 2.5 | 1.24 | 1.0 | 1.627 | 0.889 | 0.4 | 30.99 | 0.2 | 28.35 | 0.2 | 0.218 | 1.4 |
| 05-6-36_m7_pt93 | 0.648 | 1.2 | 4.28 | 0.5 | 4.517 | 0.173 | 2.6 | 1.03 | 1.2 | 1.355 | 0.867 | 0.5 | 31.44 | 0.2 | 28.40 | 0.2 | 0.211 | 1.4 |
| 05-6-36_m7_pt94 | 0.615 | 1.2 | 4.03 | 0.5 | 4.250 | 0.162 | 2.7 | 0.95 | 1.2 | 1.246 | 0.814 | 0.5 | 32.00 | 0.2 | 28.44 | 0.2 | 0.199 | 1.5 |
| 05-6-36_m7_pt95 | 0.512 | 1.4 | 3.13 | 0.6 | 3.298 | 0.136 | 3.2 | 1.17 | 1.1 | 1.524 | 0.647 | 0.6 | 32.13 | 0.2 | 28.56 | 0.2 | 0.157 | 1.9 |
| 05-6-36_m7_pt96 | 0.676 | 1.1 | 4.22 | 0.5 | 4.445 | 0.174 | 2.6 | 1.39 | 0.9 | 1.829 | 0.872 | 0.5 | 30.98 | 0.2 | 28.43 | 0.2 | 0.200 | 1.5 |
| 05-6-36_m7_pt97 | 0.631 | 1.2 | 4.14 | 0.5 | 4.365 | 0.171 | 2.6 | 1.18 | 1.0 | 1.546 | 0.832 | 0.5 | 31.41 | 0.2 | 28.50 | 0.2 | 0.213 | 1.4 |
| 05-6-36_m7_pt98 | 0.609 | 1.2 | 3.79 | 0.6 | 3.997 | 0.161 | 2.7 | 1.22 | 1.0 | 1.599 | 0.786 | 0.5 | 31.44 | 0.2 | 28.50 | 0.2 | 0.197 | 1.5 |
| 05-6-36_m7_pt99 | 0.568 | 1.3 | 3.54 | 0.6 | 3.728 | 0.151 | 2.9 | 0.94 | 1.3 | 1.223 | 0.746 | 0.5 | 32.10 | 0.2 | 28.48 | 0.2 | 0.165 | 1.8 |
| 05-6-36_m7_pt100 | 0.589 | 1.3 | 3.80 | 0.6 | 4.007 | 0.159 | 2.8 | 0.87 | 1.4 | 1.130 | 0.783 | 0.5 | 32.00 | 0.2 | 28.49 | 0.2 | 0.188 | 1.6 |
| 05-6-36_m7_pt101 | 0.594 | 1.3 | 3.72 | 0.6 | 3.913 | 0.165 | 2.7 | 1.43 | 0.9 | 1.877 | 0.775 | 0.5 | 31.25 | 0.2 | 28.42 | 0.2 | 0.175 | 1.7 |
| 05-6-36_m7_pt102 | 0.568 | 1.3 | 3.61 | 0.6 | 3.800 | 0.150 | 2.9 | 1.40 | 0.9 | 1.833 | 0.756 | 0.5 | 31.62 | 0.2 | 28.66 | 0.2 | 0.180 | 1.6 |

| | $UO_2$ | | $ThO_2$ | | | PbO | | $Y_2O_3$ | | | CaO | | $Ce_2O_3$ | | $P_2O_5$ | | $SiO_2$ | |
|---|---|---|---|---|---|---|---|---|---|---|---|---|---|---|---|---|---|---|
| Sample | wt. % | RSD (2σ%) | wt. % | RSD (2σ%) | k-raw | wt. % | RSD (2σ%) | wt. % | RSD (2σ%) | k-raw | wt. % | RSD (2σ%) | wt. % | RSD (2σ%) | wt. % | RSD (2σ%) | wt. % | RSD (2σ%) |
| 05-6-36_m7_pt103 | 0.620 | 1.2 | 4.06 | 0.5 | 4.280 | 0.165 | 2.7 | 1.45 | 0.9 | 1.900 | 0.835 | 0.5 | 31.14 | 0.2 | 28.51 | 0.2 | 0.194 | 1.5 |
| 05-6-36_m7_pt104 | 0.646 | 1.2 | 4.24 | 0.5 | 4.469 | 0.175 | 2.5 | 1.49 | 0.9 | 1.960 | 0.870 | 0.5 | 30.91 | 0.2 | 28.46 | 0.2 | 0.205 | 1.4 |
| 05-6-36_m7_pt105 | 0.651 | 1.2 | 4.21 | 0.5 | 4.435 | 0.171 | 2.6 | 1.50 | 0.9 | 1.973 | 0.865 | 0.5 | 30.64 | 0.2 | 28.45 | 0.2 | 0.206 | 1.4 |
| 05-6-36_m7_pt106 | 0.614 | 1.2 | 3.92 | 0.6 | 4.126 | 0.172 | 2.6 | 1.54 | 0.8 | 2.020 | 0.817 | 0.5 | 31.08 | 0.2 | 28.57 | 0.2 | 0.194 | 1.5 |
| 8153-46 | 0.389 | 1.9 | 7.28 | 0.4 | 7.775 | 0.196 | 2.3 | 0.50 | 2.2 | 0.651 | 0.581 | 0.6 | 30.93 | 0.2 | 25.66 | 0.2 | 1.314 | 0.3 |
| 8153-47 | 0.395 | 1.8 | 7.27 | 0.4 | 7.758 | 0.189 | 2.4 | 0.53 | 2.1 | 0.692 | 0.576 | 0.6 | 30.80 | 0.2 | 25.56 | 0.2 | 1.313 | 0.3 |
| 8153-48 | 0.400 | 1.8 | 7.25 | 0.4 | 7.739 | 0.194 | 2.3 | 0.53 | 2.1 | 0.692 | 0.575 | 0.6 | 30.99 | 0.2 | 25.83 | 0.2 | 1.317 | 0.3 |
| 8153-49 | 0.388 | 1.9 | 7.26 | 0.4 | 7.745 | 0.193 | 2.3 | 0.51 | 2.2 | 0.665 | 0.567 | 0.6 | 31.04 | 0.2 | 25.86 | 0.2 | 1.314 | 0.3 |
| 8153-50 | 0.373 | 1.9 | 7.22 | 0.4 | 7.701 | 0.185 | 2.4 | 0.50 | 2.2 | 0.652 | 0.578 | 0.6 | 30.93 | 0.2 | 26.01 | 0.2 | 1.325 | 0.3 |
| 8153-51 | 0.388 | 1.9 | 7.26 | 0.4 | 7.747 | 0.183 | 2.5 | 0.55 | 2.0 | 0.719 | 0.573 | 0.6 | 31.18 | 0.2 | 26.15 | 0.2 | 1.317 | 0.3 |
| 8153-52 | 0.383 | 1.9 | 7.30 | 0.4 | 7.782 | 0.188 | 2.4 | 0.51 | 2.2 | 0.665 | 0.578 | 0.6 | 31.47 | 0.2 | 26.37 | 0.2 | 1.323 | 0.3 |
| 05-6-36_m3_pt1 | 0.441 | 1.6 | 4.25 | 0.5 | 4.495 | 0.157 | 2.8 | 0.40 | 2.7 | 0.523 | 0.856 | 0.5 | 32.25 | 0.2 | 28.32 | 0.2 | 0.197 | 1.5 |
| 05-6-36_m3_pt2 | 0.444 | 1.6 | 4.30 | 0.5 | 4.551 | 0.160 | 2.7 | 0.42 | 2.6 | 0.549 | 0.852 | 0.5 | 32.26 | 0.2 | 28.32 | 0.2 | 0.228 | 1.3 |
| 05-6-36_m3_pt3 | 0.411 | 1.7 | 4.02 | 0.5 | 4.253 | 0.139 | 3.1 | 0.37 | 3.0 | 0.476 | 0.792 | 0.5 | 32.58 | 0.2 | 28.35 | 0.2 | 0.195 | 1.5 |
| 05-6-36_m3_pt4 | 0.405 | 1.8 | 3.99 | 0.5 | 4.223 | 0.142 | 3.0 | 0.35 | 3.1 | 0.457 | 0.779 | 0.5 | 32.60 | 0.2 | 28.33 | 0.2 | 0.201 | 1.5 |
| 05-6-36_m3_pt5 | 0.407 | 1.8 | 4.19 | 0.5 | 4.429 | 0.153 | 2.9 | 0.35 | 3.1 | 0.455 | 0.824 | 0.5 | 32.28 | 0.2 | 28.34 | 0.2 | 0.195 | 1.5 |
| 05-6-36_m3_pt6 | 0.392 | 1.8 | 4.17 | 0.5 | 4.416 | 0.146 | 3.0 | 0.35 | 3.1 | 0.456 | 0.819 | 0.5 | 32.39 | 0.2 | 28.29 | 0.2 | 0.199 | 1.5 |
| 05-6-36_m3_pt7 | 0.355 | 2.0 | 3.43 | 0.6 | 3.625 | 0.116 | 3.7 | 0.35 | 3.1 | 0.456 | 0.677 | 0.5 | 32.89 | 0.2 | 28.38 | 0.2 | 0.170 | 1.7 |
| 05-6-36_m3_pt8 | 0.342 | 2.1 | 3.57 | 0.6 | 3.772 | 0.130 | 3.3 | 0.34 | 3.2 | 0.438 | 0.726 | 0.5 | 32.60 | 0.2 | 28.29 | 0.2 | 0.165 | 1.8 |
| 05-6-36_m3_pt9 | 0.364 | 1.9 | 3.86 | 0.6 | 4.086 | 0.130 | 3.3 | 0.31 | 3.5 | 0.405 | 0.760 | 0.5 | 32.44 | 0.2 | 28.21 | 0.2 | 0.178 | 1.7 |
| 05-6-36_m3_pt10 | 0.313 | 2.2 | 3.34 | 0.6 | 3.531 | 0.116 | 3.7 | 0.28 | 3.8 | 0.369 | 0.681 | 0.5 | 32.93 | 0.2 | 28.13 | 0.2 | 0.167 | 1.8 |
| 05-6-36_m3_pt11 | 0.327 | 2.0 | 3.18 | 0.6 | 3.323 | 0.117 | 3.5 | 0.34 | 3.1 | 0.430 | 0.701 | 0.5 | 24.17 | 0.3 | 21.62 | 0.2 | 7.082 | 0.1 |
| 05-6-36_m3_pt12 | 0.333 | 2.0 | 3.18 | 0.6 | 3.335 | 0.121 | 3.5 | 0.31 | 3.4 | 0.393 | 0.677 | 0.5 | 27.54 | 0.3 | 24.37 | 0.2 | 4.410 | 0.1 |
| 05-6-36_m3_pt13 | 0.373 | 1.9 | 3.21 | 0.6 | 3.392 | 0.127 | 3.4 | 0.37 | 2.9 | 0.482 | 0.670 | 0.5 | 32.90 | 0.2 | 28.29 | 0.2 | 0.191 | 1.5 |
| 05-6-36_m3_pt14 | 0.354 | 2.0 | 3.30 | 0.6 | 3.465 | 0.118 | 3.6 | 0.37 | 2.9 | 0.472 | 0.741 | 0.5 | 29.60 | 0.2 | 25.82 | 0.2 | 3.008 | 0.2 |
| 05-6-36_m3_pt15 | 0.466 | 1.6 | 4.46 | 0.5 | 4.716 | 0.158 | 2.8 | 0.41 | 2.6 | 0.541 | 0.898 | 0.4 | 32.10 | 0.2 | 28.23 | 0.2 | 0.218 | 1.4 |
| 05-6-36_m3_pt16 | 0.563 | 1.3 | 4.09 | 0.5 | 4.328 | 0.165 | 2.7 | 0.45 | 2.5 | 0.582 | 0.989 | 0.4 | 31.50 | 0.2 | 27.99 | 0.2 | 0.550 | 0.6 |
| 05-6-36_m3_pt17 | 0.302 | 2.1 | 2.17 | 0.8 | 2.242 | 0.092 | 4.3 | 0.28 | 3.5 | 0.352 | 0.842 | 0.5 | 19.57 | 0.3 | 17.46 | 0.2 | 12.507 | 0.1 |
| 05-6-36_m3_pt18 | 0.421 | 1.7 | 4.05 | 0.5 | 4.285 | 0.147 | 3.0 | 0.38 | 2.9 | 0.492 | 0.898 | 0.4 | 32.03 | 0.2 | 28.22 | 0.2 | 0.401 | 0.8 |
| 05-6-36_m3_pt19 | 0.418 | 1.7 | 4.43 | 0.5 | 4.686 | 0.156 | 2.8 | 0.35 | 3.1 | 0.455 | 0.888 | 0.4 | 32.33 | 0.2 | 28.25 | 0.2 | 0.206 | 1.4 |
| 05-6-36_m3_pt20 | 0.318 | 2.2 | 3.52 | 0.6 | 3.716 | 0.122 | 3.5 | 0.32 | 3.3 | 0.419 | 0.729 | 0.5 | 33.10 | 0.2 | 28.44 | 0.2 | 0.171 | 1.7 |
| 05-6-36_m3_pt21 | 0.358 | 2.0 | 3.76 | 0.6 | 3.979 | 0.132 | 3.3 | 0.34 | 3.2 | 0.441 | 0.755 | 0.5 | 32.67 | 0.2 | 28.27 | 0.2 | 0.180 | 1.6 |
| 05-6-36_m3_pt22 | 0.397 | 1.8 | 4.08 | 0.5 | 4.311 | 0.148 | 2.9 | 0.37 | 3.0 | 0.477 | 0.805 | 0.5 | 32.47 | 0.2 | 28.29 | 0.2 | 0.198 | 1.5 |
| 05-6-36_m3_pt23 | 0.441 | 1.6 | 4.27 | 0.5 | 4.518 | 0.147 | 3.0 | 0.39 | 2.8 | 0.508 | 0.879 | 0.4 | 32.19 | 0.2 | 28.16 | 0.2 | 0.209 | 1.4 |
| 05-6-36_m3_pt24 | 0.403 | 1.8 | 4.12 | 0.5 | 4.359 | 0.143 | 3.0 | 0.36 | 3.0 | 0.475 | 0.816 | 0.5 | 32.31 | 0.2 | 28.11 | 0.2 | 0.204 | 1.5 |
| 05-6-36_m3_pt25 | 0.460 | 1.6 | 4.54 | 0.5 | 4.808 | 0.156 | 2.8 | 0.44 | 2.5 | 0.574 | 0.882 | 0.4 | 32.02 | 0.2 | 28.16 | 0.2 | 0.219 | 1.4 |

| | $UO_2$ | | $ThO_2$ | | | PbO | | $Y_2O_3$ | | | CaO | | $Ce_2O_3$ | | $P_2O_5$ | | $SiO_2$ | |
|---|---|---|---|---|---|---|---|---|---|---|---|---|---|---|---|---|---|---|
| Sample | wt. % | RSD (2σ%) | wt. % | RSD (2σ%) | k-raw | wt. % | RSD (2σ%) | wt. % | RSD (2σ%) | k-raw | wt. % | RSD (2σ%) | wt. % | RSD (2σ%) | wt. % | RSD (2σ%) | wt. % | RSD (2σ%) |
| 05-6-36_m3_pt26 | 0.442 | 1.6 | 4.31 | 0.5 | 4.558 | 0.150 | 2.9 | 0.41 | 2.7 | 0.537 | 0.854 | 0.5 | 32.13 | 0.2 | 28.18 | 0.2 | 0.202 | 1.5 |
| 05-6-36_m3_pt27 | 0.372 | 1.9 | 3.76 | 0.6 | 3.972 | 0.137 | 3.1 | 0.35 | 3.1 | 0.452 | 0.739 | 0.5 | 32.18 | 0.2 | 28.03 | 0.2 | 0.178 | 1.7 |
| 05-6-36_m3_pt28 | 0.290 | 2.4 | 3.28 | 0.6 | 3.465 | 0.111 | 3.8 | 0.30 | 3.6 | 0.385 | 0.651 | 0.6 | 33.05 | 0.2 | 28.21 | 0.2 | 0.162 | 1.8 |
| 8153-53 | 0.420 | 1.7 | 7.56 | 0.4 | 8.063 | 0.192 | 2.3 | 0.51 | 2.2 | 0.670 | 0.570 | 0.6 | 30.95 | 0.2 | 26.81 | 0.2 | 1.393 | 0.3 |
| 8153-54 | 0.414 | 1.8 | 7.55 | 0.4 | 8.042 | 0.191 | 2.4 | 0.50 | 2.2 | 0.660 | 0.576 | 0.6 | 30.77 | 0.2 | 26.83 | 0.2 | 1.371 | 0.3 |
| 8153-55 | 0.414 | 1.8 | 7.59 | 0.4 | 8.090 | 0.195 | 2.3 | 0.51 | 2.2 | 0.663 | 0.576 | 0.6 | 30.99 | 0.2 | 26.88 | 0.2 | 1.366 | 0.3 |
| 8153-56 | 0.418 | 1.7 | 7.59 | 0.4 | 8.093 | 0.199 | 2.3 | 0.51 | 2.2 | 0.664 | 0.577 | 0.6 | 30.79 | 0.2 | 26.88 | 0.2 | 1.372 | 0.3 |
| 8153-57 | 0.407 | 1.8 | 7.40 | 0.4 | 7.889 | 0.179 | 2.5 | 0.49 | 2.3 | 0.643 | 0.561 | 0.6 | 30.79 | 0.2 | 26.81 | 0.2 | 1.337 | 0.3 |
| 8153-58 | 0.401 | 1.8 | 7.53 | 0.4 | 8.031 | 0.188 | 2.4 | 0.51 | 2.2 | 0.670 | 0.564 | 0.6 | 30.84 | 0.2 | 26.72 | 0.2 | 1.349 | 0.3 |
| 8153-59 | 0.413 | 1.8 | 7.52 | 0.4 | 8.017 | 0.198 | 2.3 | 0.52 | 2.2 | 0.675 | 0.579 | 0.6 | 31.14 | 0.2 | 26.83 | 0.2 | 1.346 | 0.3 |
| 05-6-36_m3_pt29 | 0.601 | 1.2 | 3.98 | 0.5 | 4.202 | 0.162 | 2.7 | 0.71 | 1.6 | 0.921 | 0.830 | 0.5 | 31.59 | 0.2 | 28.14 | 0.2 | 0.209 | 1.4 |
| 05-6-36_m3_pt30 | 0.675 | 1.1 | 4.23 | 0.5 | 4.469 | 0.180 | 2.5 | 0.85 | 1.4 | 1.110 | 0.864 | 0.5 | 31.08 | 0.2 | 28.01 | 0.2 | 0.220 | 1.4 |
| 05-6-36_m3_pt31 | 0.636 | 1.2 | 3.48 | 0.6 | 3.668 | 0.151 | 2.9 | 0.95 | 1.3 | 1.245 | 0.755 | 0.5 | 31.77 | 0.2 | 28.19 | 0.2 | 0.175 | 1.7 |
| 05-6-36_m3_pt32 | 0.603 | 1.2 | 3.18 | 0.6 | 3.353 | 0.140 | 3.1 | 0.90 | 1.3 | 1.172 | 0.693 | 0.5 | 31.72 | 0.2 | 28.28 | 0.2 | 0.159 | 1.8 |
| 05-6-36_m3_pt33 | 0.646 | 1.2 | 3.28 | 0.6 | 3.462 | 0.143 | 3.1 | 0.93 | 1.3 | 1.209 | 0.740 | 0.5 | 31.91 | 0.2 | 28.26 | 0.2 | 0.155 | 1.9 |
| 05-6-36_m3_pt34 | 0.630 | 1.2 | 3.51 | 0.6 | 3.706 | 0.159 | 2.7 | 0.78 | 1.5 | 1.019 | 0.767 | 0.5 | 31.90 | 0.2 | 28.17 | 0.2 | 0.176 | 1.7 |
| 05-6-36_m3_pt35 | 0.580 | 1.3 | 3.43 | 0.6 | 3.620 | 0.145 | 3.0 | 0.70 | 1.7 | 0.914 | 0.729 | 0.5 | 32.08 | 0.2 | 28.21 | 0.2 | 0.169 | 1.7 |
| 05-6-36_m3_pt36 | 0.587 | 1.3 | 3.47 | 0.6 | 3.664 | 0.157 | 2.8 | 0.74 | 1.6 | 0.969 | 0.762 | 0.5 | 32.09 | 0.2 | 28.23 | 0.2 | 0.171 | 1.7 |
| 05-6-36_m3_pt37 | 0.590 | 1.3 | 3.62 | 0.6 | 3.818 | 0.153 | 2.9 | 0.77 | 1.5 | 1.000 | 0.781 | 0.5 | 31.78 | 0.2 | 28.33 | 0.2 | 0.181 | 1.6 |
| 05-6-36_m3_pt38 | 0.699 | 1.1 | 4.31 | 0.5 | 4.560 | 0.178 | 2.5 | 0.75 | 1.6 | 0.976 | 0.905 | 0.4 | 31.42 | 0.2 | 28.25 | 0.2 | 0.216 | 1.4 |
| 05-6-36_m3_pt39 | 0.621 | 1.2 | 4.28 | 0.5 | 4.523 | 0.172 | 2.6 | 0.60 | 1.9 | 0.779 | 0.891 | 0.4 | 31.69 | 0.2 | 28.24 | 0.2 | 0.207 | 1.4 |
| 05-6-36_m3_pt40 | 0.558 | 1.3 | 3.88 | 0.6 | 4.097 | 0.155 | 2.8 | 0.65 | 1.8 | 0.854 | 0.796 | 0.5 | 31.58 | 0.2 | 28.05 | 0.2 | 0.203 | 1.5 |
| 05-6-36_m3_pt41 | 0.579 | 1.3 | 3.87 | 0.6 | 4.091 | 0.161 | 2.7 | 0.63 | 1.8 | 0.828 | 0.802 | 0.5 | 31.59 | 0.2 | 28.12 | 0.2 | 0.226 | 1.3 |
| 05-6-36_m3_pt42 | 0.600 | 1.2 | 4.07 | 0.5 | 4.306 | 0.165 | 2.7 | 0.68 | 1.7 | 0.884 | 0.841 | 0.5 | 31.58 | 0.2 | 28.11 | 0.2 | 0.217 | 1.4 |
| 05-6-36_m3_pt43 | 0.563 | 1.3 | 3.65 | 0.6 | 3.855 | 0.155 | 2.8 | 0.66 | 1.8 | 0.859 | 0.768 | 0.5 | 31.91 | 0.2 | 28.16 | 0.2 | 0.196 | 1.5 |
| 05-6-36_m3_pt44 | 0.695 | 1.1 | 4.32 | 0.5 | 4.562 | 0.195 | 2.3 | 0.84 | 1.4 | 1.096 | 0.889 | 0.4 | 31.31 | 0.2 | 28.18 | 0.2 | 0.230 | 1.3 |
| 05-6-36_m3_pt45 | 0.714 | 1.1 | 4.26 | 0.5 | 4.505 | 0.182 | 2.4 | 0.88 | 1.4 | 1.155 | 0.899 | 0.4 | 31.26 | 0.2 | 28.23 | 0.2 | 0.212 | 1.4 |
| 05-6-36_m3_pt46 | 0.688 | 1.1 | 4.43 | 0.5 | 4.687 | 0.186 | 2.4 | 0.86 | 1.4 | 1.133 | 0.897 | 0.4 | 30.87 | 0.2 | 27.99 | 0.2 | 0.243 | 1.2 |
| 05-6-36_m3_pt47 | 0.710 | 1.1 | 4.49 | 0.5 | 4.751 | 0.191 | 2.3 | 0.88 | 1.4 | 1.147 | 0.925 | 0.4 | 31.10 | 0.2 | 28.04 | 0.2 | 0.230 | 1.3 |
| 05-6-36_m3_pt48 | 0.673 | 1.1 | 4.52 | 0.5 | 4.778 | 0.175 | 2.5 | 0.74 | 1.6 | 0.968 | 0.928 | 0.4 | 31.03 | 0.2 | 27.97 | 0.2 | 0.229 | 1.3 |
| 05-6-36_m3_pt49 | 0.636 | 1.2 | 4.50 | 0.5 | 4.762 | 0.172 | 2.6 | 0.69 | 1.7 | 0.900 | 0.907 | 0.4 | 31.41 | 0.2 | 28.01 | 0.2 | 0.225 | 1.3 |
| 05-6-36_m3_pt50 | 0.609 | 1.2 | 4.07 | 0.5 | 4.297 | 0.158 | 2.8 | 0.69 | 1.7 | 0.900 | 0.832 | 0.5 | 31.78 | 0.2 | 28.04 | 0.2 | 0.211 | 1.4 |
| 05-6-36_m3_pt51 | 0.646 | 1.2 | 4.29 | 0.5 | 4.534 | 0.174 | 2.5 | 0.67 | 1.7 | 0.873 | 0.878 | 0.5 | 31.33 | 0.2 | 27.94 | 0.2 | 0.223 | 1.3 |
| 05-6-36_m3_pt52 | 0.577 | 1.3 | 4.08 | 0.5 | 4.313 | 0.160 | 2.8 | 0.69 | 1.7 | 0.898 | 0.823 | 0.5 | 31.67 | 0.2 | 27.92 | 0.2 | 0.226 | 1.3 |
| 05-6-36_m3_pt53 | 0.558 | 1.3 | 4.10 | 0.5 | 4.330 | 0.158 | 2.8 | 0.58 | 2.0 | 0.756 | 0.824 | 0.5 | 31.77 | 0.2 | 28.08 | 0.2 | 0.211 | 1.4 |
| 05-6-36_m3_pt54 | 0.600 | 1.2 | 4.52 | 0.5 | 4.777 | 0.177 | 2.5 | 0.61 | 1.9 | 0.804 | 0.918 | 0.4 | 31.44 | 0.2 | 28.23 | 0.2 | 0.281 | 1.1 |

| | $UO_2$ | | $ThO_2$ | | | PbO | | $Y_2O_3$ | | | CaO | | $Ce_2O_3$ | | $P_2O_5$ | | $SiO_2$ | |
|---|---|---|---|---|---|---|---|---|---|---|---|---|---|---|---|---|---|---|
| Sample | wt. % | RSD (2σ%) | wt. % | RSD (2σ%) | k-raw | wt. % | RSD (2σ%) | wt. % | RSD (2σ%) | k-raw | wt. % | RSD (2σ%) | wt. % | RSD (2σ%) | wt. % | RSD (2σ%) | wt. % | RSD (2σ%) |
| 05-6-36_m3_pt55 | 0.599 | 1.2 | 4.50 | 0.5 | 4.760 | 0.174 | 2.5 | 0.57 | 2.0 | 0.748 | 0.899 | 0.4 | 31.68 | 0.2 | 28.06 | 0.2 | 0.232 | 1.3 |
| 05-6-36_m3_pt56 | 0.543 | 1.4 | 4.24 | 0.5 | 4.487 | 0.152 | 2.9 | 0.52 | 2.2 | 0.685 | 0.870 | 0.5 | 31.98 | 0.2 | 28.20 | 0.2 | 0.213 | 1.4 |
| 05-6-36_m3_pt57 | 0.517 | 1.4 | 4.37 | 0.5 | 4.625 | 0.166 | 2.7 | 0.52 | 2.1 | 0.683 | 0.843 | 0.5 | 31.82 | 0.2 | 28.07 | 0.2 | 0.236 | 1.3 |
| 05-6-36_m3_pt58 | 0.553 | 1.3 | 4.67 | 0.5 | 4.942 | 0.172 | 2.6 | 0.51 | 2.2 | 0.669 | 0.924 | 0.4 | 31.55 | 0.2 | 28.19 | 0.2 | 0.229 | 1.3 |
| 05-6-36_m3_pt59 | 0.562 | 1.3 | 4.69 | 0.5 | 4.961 | 0.173 | 2.5 | 0.52 | 2.2 | 0.681 | 0.933 | 0.4 | 31.59 | 0.2 | 28.17 | 0.2 | 0.227 | 1.3 |
| 05-6-36_m3_pt60 | 0.503 | 1.5 | 4.48 | 0.5 | 4.742 | 0.164 | 2.7 | 0.47 | 2.4 | 0.615 | 0.899 | 0.4 | 31.94 | 0.2 | 28.19 | 0.2 | 0.217 | 1.4 |
| 05-6-36_m3_pt61 | 0.368 | 1.9 | 3.63 | 0.6 | 3.835 | 0.124 | 3.5 | 0.35 | 3.1 | 0.455 | 0.731 | 0.5 | 32.67 | 0.2 | 28.29 | 0.2 | 0.168 | 1.8 |
| 8153-60 | 0.422 | 1.7 | 7.48 | 0.4 | 7.976 | 0.193 | 2.3 | 0.48 | 2.4 | 0.625 | 0.560 | 0.6 | 30.85 | 0.2 | 26.82 | 0.2 | 1.346 | 0.3 |
| 8153-61 | 0.402 | 1.8 | 7.54 | 0.4 | 8.038 | 0.186 | 2.4 | 0.51 | 2.2 | 0.665 | 0.571 | 0.6 | 30.85 | 0.2 | 26.79 | 0.2 | 1.358 | 0.3 |
| 8153-62 | 0.410 | 1.8 | 7.51 | 0.4 | 8.008 | 0.185 | 2.4 | 0.50 | 2.3 | 0.653 | 0.572 | 0.6 | 30.83 | 0.2 | 26.73 | 0.2 | 1.362 | 0.3 |
| 8153-63 | 0.382 | 1.9 | 7.35 | 0.4 | 7.835 | 0.182 | 2.5 | 0.49 | 2.3 | 0.645 | 0.558 | 0.6 | 30.91 | 0.2 | 26.86 | 0.2 | 1.326 | 0.3 |
| 8153-64 | 0.388 | 1.9 | 7.42 | 0.4 | 7.906 | 0.185 | 2.4 | 0.51 | 2.2 | 0.670 | 0.560 | 0.6 | 30.87 | 0.2 | 27.21 | 0.2 | 1.341 | 0.3 |
| 8153-65 | 0.390 | 1.8 | 7.55 | 0.4 | 8.037 | 0.190 | 2.4 | 0.50 | 2.3 | 0.653 | 0.564 | 0.6 | 30.88 | 0.2 | 27.28 | 0.2 | 1.353 | 0.3 |
| 05-6-36_m5_pt1 | 0.484 | 1.5 | 4.35 | 0.5 | 4.629 | 0.145 | 3.0 | 0.17 | 5.9 | 0.219 | 1.079 | 0.4 | 32.20 | 0.2 | 26.20 | 0.2 | 0.170 | 1.7 |
| 05-6-36_m5_pt2 | 0.425 | 1.7 | 4.74 | 0.5 | 5.026 | 0.147 | 3.0 | 0.06 | 16.0 | 0.085 | 1.145 | 0.4 | 32.30 | 0.2 | 28.63 | 0.2 | 0.100 | 2.9 |
| 05-6-36_m5_pt3 | 0.404 | 1.8 | 4.65 | 0.5 | 4.925 | 0.153 | 2.9 | 0.07 | 15.0 | 0.091 | 1.121 | 0.4 | 32.28 | 0.2 | 28.56 | 0.2 | 0.095 | 3.0 |
| 05-6-36_m5_pt4 | 0.419 | 1.7 | 4.36 | 0.5 | 4.617 | 0.149 | 2.9 | 0.08 | 13.1 | 0.104 | 1.063 | 0.4 | 32.52 | 0.2 | 28.57 | 0.2 | 0.095 | 3.0 |
| 05-6-36_m5_pt5 | 0.405 | 1.8 | 4.46 | 0.5 | 4.729 | 0.148 | 2.9 | 0.11 | 9.8 | 0.138 | 1.078 | 0.4 | 32.17 | 0.2 | 28.50 | 0.2 | 0.102 | 2.8 |
| 05-6-36_m5_pt6 | 0.393 | 1.8 | 4.52 | 0.5 | 4.787 | 0.151 | 2.9 | 0.08 | 12.9 | 0.104 | 1.094 | 0.4 | 31.98 | 0.2 | 28.10 | 0.2 | 0.120 | 2.4 |
| 05-6-36_m5_pt7 | 0.402 | 1.8 | 4.45 | 0.5 | 4.712 | 0.152 | 2.9 | 0.07 | 15.7 | 0.086 | 1.083 | 0.4 | 32.46 | 0.2 | 28.46 | 0.2 | 0.097 | 2.9 |
| 05-6-36_m5_pt8 | 0.436 | 1.7 | 4.08 | 0.5 | 4.315 | 0.148 | 2.9 | 0.32 | 3.4 | 0.421 | 0.877 | 0.4 | 32.41 | 0.2 | 28.26 | 0.2 | 0.170 | 1.7 |
| 05-6-36_m5_pt9 | 0.411 | 1.7 | 4.09 | 0.5 | 4.325 | 0.151 | 2.9 | 0.38 | 2.9 | 0.497 | 0.802 | 0.5 | 32.10 | 0.2 | 28.31 | 0.2 | 0.197 | 1.5 |
| 05-6-36_m5_pt10 | 0.418 | 1.7 | 3.40 | 0.6 | 3.591 | 0.128 | 3.4 | 0.30 | 3.6 | 0.393 | 0.854 | 0.5 | 32.25 | 0.2 | 28.50 | 0.2 | 0.071 | 4.0 |
| 05-6-36_m5_pt11 | 0.412 | 1.7 | 3.46 | 0.6 | 3.653 | 0.128 | 3.4 | 0.29 | 3.7 | 0.380 | 0.887 | 0.4 | 32.59 | 0.2 | 28.61 | 0.2 | 0.065 | 4.3 |
| 05-6-36_m5_pt12 | 0.424 | 1.7 | 3.55 | 0.6 | 3.751 | 0.133 | 3.2 | 0.31 | 3.5 | 0.401 | 0.902 | 0.4 | 32.40 | 0.2 | 28.45 | 0.2 | 0.081 | 3.5 |
| 05-6-36_m5_pt13 | 0.412 | 1.7 | 3.57 | 0.6 | 3.770 | 0.127 | 3.4 | 0.32 | 3.4 | 0.415 | 0.905 | 0.4 | 32.30 | 0.2 | 28.52 | 0.2 | 0.084 | 3.4 |
| 05-6-36_m5_pt14 | 0.443 | 1.6 | 3.63 | 0.6 | 3.834 | 0.117 | 3.7 | 0.32 | 3.3 | 0.422 | 0.921 | 0.4 | 32.31 | 0.2 | 28.48 | 0.2 | 0.091 | 3.1 |
| 05-6-36_m5_pt15 | 0.440 | 1.6 | 3.64 | 0.6 | 3.842 | 0.129 | 3.3 | 0.33 | 3.3 | 0.427 | 0.922 | 0.4 | 32.23 | 0.2 | 28.50 | 0.2 | 0.077 | 3.7 |
| 05-6-36_m5_pt16 | 0.331 | 2.1 | 3.18 | 0.6 | 3.350 | 0.107 | 4.0 | 0.53 | 2.1 | 0.695 | 0.779 | 0.5 | 32.74 | 0.2 | 28.80 | 0.2 | 0.084 | 3.4 |
| 05-6-36_m5_pt17 | 0.424 | 1.7 | 4.59 | 0.5 | 4.856 | 0.162 | 2.7 | 0.40 | 2.7 | 0.528 | 1.087 | 0.4 | 31.85 | 0.2 | 28.61 | 0.2 | 0.090 | 3.1 |
| 05-6-36_m5_pt18 | 0.236 | 2.9 | 4.01 | 0.5 | 4.237 | 0.121 | 3.5 | 0.44 | 2.5 | 0.572 | 0.881 | 0.4 | 32.68 | 0.2 | 28.52 | 0.2 | 0.145 | 2.0 |
| 05-6-36_m5_pt19 | 0.388 | 1.8 | 3.43 | 0.6 | 3.619 | 0.128 | 3.4 | 0.44 | 2.5 | 0.572 | 0.678 | 0.5 | 32.54 | 0.2 | 28.29 | 0.2 | 0.176 | 1.7 |
| 05-6-36_m5_pt20 | 0.540 | 1.4 | 4.30 | 0.5 | 4.546 | 0.161 | 2.7 | 0.58 | 2.0 | 0.759 | 0.852 | 0.5 | 31.73 | 0.2 | 28.24 | 0.2 | 0.222 | 1.4 |
| 05-6-36_m5_pt21 | 0.464 | 1.6 | 3.87 | 0.6 | 4.090 | 0.140 | 3.1 | 0.52 | 2.2 | 0.682 | 0.774 | 0.5 | 32.16 | 0.2 | 28.41 | 0.2 | 0.213 | 1.4 |
| 05-6-36_m5_pt22 | 0.611 | 1.2 | 4.64 | 0.5 | 4.910 | 0.174 | 2.5 | 0.64 | 1.8 | 0.836 | 0.939 | 0.4 | 31.44 | 0.2 | 28.28 | 0.2 | 0.230 | 1.3 |
| 05-6-36_m5_pt23 | 0.449 | 1.6 | 2.67 | 0.7 | 2.810 | 0.113 | 3.8 | 0.53 | 2.1 | 0.688 | 0.578 | 0.6 | 33.14 | 0.2 | 28.52 | 0.2 | 0.122 | 2.4 |

| | $UO_2$ | | $ThO_2$ | | | PbO | | $Y_2O_3$ | | | CaO | | $Ce_2O_3$ | | $P_2O_5$ | | $SiO_2$ | |
|---|---|---|---|---|---|---|---|---|---|---|---|---|---|---|---|---|---|---|
| Sample | wt. % | RSD (2σ%) | wt. % | RSD (2σ%) | k-raw | wt. % | RSD (2σ%) | wt. % | RSD (2σ%) | k-raw | wt. % | RSD (2σ%) | wt. % | RSD (2σ%) | wt. % | RSD (2σ%) | wt. % | RSD (2σ%) |
| 05-6-36_m5_pt24 | 0.453 | 1.6 | 2.50 | 0.7 | 2.634 | 0.109 | 3.9 | 0.50 | 2.2 | 0.652 | 0.555 | 0.6 | 33.19 | 0.2 | 27.97 | 0.2 | 0.124 | 2.3 |
| 05-6-36_m5_pt25 | 0.532 | 1.4 | 3.89 | 0.6 | 4.113 | 0.155 | 2.8 | 0.64 | 1.8 | 0.829 | 0.800 | 0.5 | 32.12 | 0.2 | 28.40 | 0.2 | 0.187 | 1.6 |
| 05-6-36_m5_pt26 | 0.524 | 1.4 | 3.75 | 0.6 | 3.962 | 0.143 | 3.0 | 0.74 | 1.6 | 0.970 | 0.784 | 0.5 | 31.95 | 0.2 | 28.38 | 0.2 | 0.181 | 1.6 |
| 05-6-36_m5_pt27 | 0.585 | 1.3 | 3.93 | 0.6 | 4.146 | 0.163 | 2.7 | 0.92 | 1.3 | 1.206 | 0.830 | 0.5 | 31.44 | 0.2 | 28.40 | 0.2 | 0.189 | 1.6 |
| 05-6-36_m5_pt28 | 0.621 | 1.2 | 4.07 | 0.5 | 4.300 | 0.177 | 2.5 | 0.93 | 1.3 | 1.218 | 0.848 | 0.5 | 31.75 | 0.2 | 28.45 | 0.2 | 0.211 | 1.4 |
| 05-6-36_m5_pt29 | 0.611 | 1.2 | 4.44 | 0.5 | 4.696 | 0.167 | 2.6 | 0.76 | 1.5 | 0.998 | 0.950 | 0.4 | 31.82 | 0.2 | 28.42 | 0.2 | 0.199 | 1.5 |
| 05-6-36_m5_pt30 | 0.589 | 1.3 | 4.24 | 0.5 | 4.478 | 0.169 | 2.6 | 0.79 | 1.5 | 1.039 | 0.845 | 0.5 | 31.31 | 0.2 | 27.96 | 0.2 | 0.261 | 1.2 |
| 05-6-36_m5_pt31 | 0.624 | 1.2 | 4.29 | 0.5 | 4.534 | 0.174 | 2.5 | 0.73 | 1.6 | 0.956 | 0.878 | 0.5 | 31.46 | 0.2 | 28.19 | 0.2 | 0.226 | 1.3 |
| 05-6-36_m5_pt32 | 0.587 | 1.3 | 4.04 | 0.5 | 4.265 | 0.167 | 2.6 | 0.70 | 1.7 | 0.917 | 0.838 | 0.5 | 31.72 | 0.2 | 28.37 | 0.2 | 0.208 | 1.4 |
| 8153-66 | 0.396 | 1.8 | 7.43 | 0.4 | 7.923 | 0.186 | 2.4 | 0.49 | 2.3 | 0.645 | 0.556 | 0.6 | 31.09 | 0.2 | 26.86 | 0.2 | 1.346 | 0.3 |
| 8153-67 | 0.402 | 1.8 | 7.47 | 0.4 | 7.957 | 0.191 | 2.4 | 0.51 | 2.2 | 0.673 | 0.563 | 0.6 | 30.89 | 0.2 | 26.80 | 0.2 | 1.351 | 0.3 |
| 8153-68 | 0.423 | 1.7 | 7.58 | 0.4 | 8.086 | 0.189 | 2.4 | 0.49 | 2.3 | 0.646 | 0.575 | 0.6 | 30.86 | 0.2 | 26.75 | 0.2 | 1.377 | 0.3 |
| 8153-69 | 0.404 | 1.8 | 7.49 | 0.4 | 7.980 | 0.185 | 2.4 | 0.48 | 2.3 | 0.630 | 0.565 | 0.6 | 30.79 | 0.2 | 26.80 | 0.2 | 1.394 | 0.3 |
| 8153-70 | 0.405 | 1.8 | 7.48 | 0.4 | 7.970 | 0.185 | 2.4 | 0.48 | 2.3 | 0.632 | 0.564 | 0.6 | 31.17 | 0.2 | 26.86 | 0.2 | 1.366 | 0.3 |
| 8153-71 | 0.403 | 1.8 | 7.49 | 0.4 | 7.988 | 0.184 | 2.5 | 0.52 | 2.2 | 0.679 | 0.565 | 0.6 | 30.97 | 0.2 | 26.86 | 0.2 | 1.366 | 0.3 |
| 05-6-36_m5_pt33 | 0.464 | 1.6 | 4.80 | 0.5 | 5.082 | 0.168 | 2.6 | 0.41 | 2.7 | 0.532 | 0.899 | 0.4 | 31.79 | 0.2 | 28.02 | 0.2 | 0.291 | 1.1 |
| 05-6-36_m5_pt34 | 0.516 | 1.4 | 5.18 | 0.5 | 5.494 | 0.178 | 2.5 | 0.34 | 3.2 | 0.442 | 1.082 | 0.4 | 32.12 | 0.2 | 28.38 | 0.2 | 0.195 | 1.5 |
| 05-6-36_m5_pt35 | 0.544 | 1.4 | 4.93 | 0.5 | 5.227 | 0.169 | 2.6 | 0.20 | 5.2 | 0.267 | 1.070 | 0.4 | 32.61 | 0.2 | 28.64 | 0.2 | 0.143 | 2.0 |
| 05-6-36_m5_pt36 | 0.545 | 1.3 | 4.98 | 0.5 | 5.288 | 0.173 | 2.5 | 0.05 | 22.5 | 0.060 | 1.097 | 0.4 | 32.83 | 0.2 | 28.60 | 0.2 | 0.136 | 2.1 |
| 05-6-36_m5_pt37 | 0.475 | 1.5 | 4.11 | 0.5 | 4.354 | 0.143 | 3.0 | 0.09 | 12.0 | 0.113 | 0.875 | 0.5 | 33.15 | 0.2 | 28.60 | 0.2 | 0.140 | 2.1 |
| 05-6-36_m5_pt38 | 0.451 | 1.6 | 3.91 | 0.6 | 4.127 | 0.141 | 3.1 | 0.49 | 2.3 | 0.635 | 0.762 | 0.5 | 32.31 | 0.2 | 28.34 | 0.2 | 0.205 | 1.5 |
| 05-6-36_m5_pt39 | 0.667 | 1.1 | 7.82 | 0.4 | 8.348 | 0.258 | 1.8 | 0.23 | 4.6 | 0.305 | 1.752 | 0.3 | 30.57 | 0.2 | 28.50 | 0.2 | 0.134 | 2.1 |
| 05-6-36_m5_pt40 | 0.436 | 1.7 | 3.94 | 0.6 | 4.167 | 0.151 | 2.9 | 0.50 | 2.2 | 0.656 | 0.797 | 0.5 | 32.31 | 0.2 | 28.46 | 0.2 | 0.181 | 1.6 |
| 05-6-36_m5_pt41 | 0.714 | 1.1 | 5.88 | 0.4 | 6.245 | 0.216 | 2.1 | 0.59 | 1.9 | 0.773 | 1.161 | 0.4 | 30.61 | 0.2 | 28.15 | 0.2 | 0.280 | 1.1 |
| 05-6-36_m5_pt42 | 0.288 | 2.4 | 3.34 | 0.6 | 3.525 | 0.110 | 3.9 | 0.63 | 1.8 | 0.820 | 0.807 | 0.5 | 32.53 | 0.2 | 28.59 | 0.2 | 0.085 | 3.3 |
| 05-6-36_m5_pt43 | 0.284 | 2.4 | 3.33 | 0.6 | 3.513 | 0.111 | 3.8 | 0.65 | 1.8 | 0.846 | 0.812 | 0.5 | 32.53 | 0.2 | 28.63 | 0.2 | 0.076 | 3.7 |
| 05-6-36_m5_pt44 | 0.297 | 2.3 | 3.36 | 0.6 | 3.541 | 0.116 | 3.7 | 0.63 | 1.8 | 0.815 | 0.816 | 0.5 | 32.44 | 0.2 | 28.48 | 0.2 | 0.077 | 3.7 |
| 05-6-36_m5_pt45 | 0.333 | 2.1 | 3.25 | 0.6 | 3.426 | 0.107 | 4.0 | 0.58 | 2.0 | 0.752 | 0.792 | 0.5 | 32.60 | 0.2 | 28.67 | 0.2 | 0.070 | 4.0 |
| 05-6-36_m5_pt46 | 0.339 | 2.1 | 3.19 | 0.6 | 3.362 | 0.115 | 3.7 | 0.56 | 2.0 | 0.731 | 0.782 | 0.5 | 32.81 | 0.2 | 28.67 | 0.2 | 0.075 | 3.8 |
| 05-6-36_m5_pt47 | 0.348 | 2.0 | 3.24 | 0.6 | 3.420 | 0.118 | 3.6 | 0.55 | 2.1 | 0.711 | 0.785 | 0.5 | 32.62 | 0.2 | 28.72 | 0.2 | 0.079 | 3.6 |
| 05-6-36_m5_pt48 | 0.331 | 2.1 | 3.23 | 0.6 | 3.408 | 0.112 | 3.8 | 0.59 | 1.9 | 0.766 | 0.788 | 0.5 | 32.71 | 0.2 | 28.68 | 0.2 | 0.071 | 4.0 |
| 05-6-36_m5_pt49 | 0.336 | 2.1 | 3.21 | 0.6 | 3.385 | 0.117 | 3.7 | 0.58 | 1.9 | 0.761 | 0.792 | 0.5 | 32.61 | 0.2 | 28.60 | 0.2 | 0.071 | 4.0 |
| 05-6-36_m5_pt50 | 0.341 | 2.1 | 3.26 | 0.6 | 3.438 | 0.117 | 3.6 | 0.57 | 2.0 | 0.741 | 0.787 | 0.5 | 32.71 | 0.2 | 28.62 | 0.2 | 0.070 | 4.0 |
| 05-6-36_m5_pt51 | 0.318 | 2.2 | 3.26 | 0.6 | 3.435 | 0.113 | 3.8 | 0.57 | 2.0 | 0.744 | 0.788 | 0.5 | 32.70 | 0.2 | 28.65 | 0.2 | 0.073 | 3.9 |
| 05-6-36_m5_pt52 | 0.337 | 2.1 | 3.17 | 0.6 | 3.347 | 0.114 | 3.7 | 0.58 | 2.0 | 0.748 | 0.782 | 0.5 | 32.57 | 0.2 | 28.55 | 0.2 | 0.071 | 4.0 |
| 05-6-36_m5_pt53 | 0.358 | 2.0 | 3.24 | 0.6 | 3.413 | 0.121 | 3.5 | 0.52 | 2.2 | 0.681 | 0.785 | 0.5 | 32.67 | 0.2 | 28.59 | 0.2 | 0.074 | 3.8 |

| | $UO_2$ | | $ThO_2$ | | | PbO | | $Y_2O_3$ | | | CaO | | $Ce_2O_3$ | | $P_2O_5$ | | $SiO_2$ | |
|---|---|---|---|---|---|---|---|---|---|---|---|---|---|---|---|---|---|---|
| Sample | wt. % | RSD (2σ%) | wt. % | RSD (2σ%) | k-raw | wt. % | RSD (2σ%) | wt. % | RSD (2σ%) | k-raw | wt. % | RSD (2σ%) | wt. % | RSD (2σ%) | wt. % | RSD (2σ%) | wt. % | RSD (2σ%) |
| 05-6-36_m5_pt54 | 0.367 | 1.9 | 3.30 | 0.6 | 3.483 | 0.120 | 3.6 | 0.51 | 2.2 | 0.668 | 0.824 | 0.5 | 32.63 | 0.2 | 28.71 | 0.2 | 0.070 | 4.0 |
| 05-6-36_m5_pt55 | 0.376 | 1.9 | 3.83 | 0.6 | 4.046 | 0.133 | 3.2 | 0.48 | 2.4 | 0.621 | 0.919 | 0.4 | 32.72 | 0.2 | 28.68 | 0.2 | 0.086 | 3.3 |
| 05-6-36_m5_pt56 | 0.253 | 2.7 | 3.56 | 0.6 | 3.752 | 0.121 | 3.5 | 0.50 | 2.3 | 0.645 | 0.801 | 0.5 | 32.73 | 0.2 | 28.61 | 0.2 | 0.131 | 2.2 |
| 05-6-36_m5_pt57 | 0.305 | 2.3 | 3.23 | 0.6 | 3.403 | 0.110 | 3.9 | 0.53 | 2.1 | 0.686 | 0.759 | 0.5 | 32.72 | 0.2 | 28.58 | 0.2 | 0.099 | 2.9 |
| 05-6-36_m5_pt58 | 0.336 | 2.1 | 3.18 | 0.6 | 3.355 | 0.117 | 3.6 | 0.56 | 2.0 | 0.727 | 0.789 | 0.5 | 32.52 | 0.2 | 28.58 | 0.2 | 0.072 | 3.9 |
| 05-6-36_m5_pt59 | 0.377 | 1.9 | 3.54 | 0.6 | 3.741 | 0.123 | 3.5 | 0.42 | 2.6 | 0.552 | 0.862 | 0.5 | 32.43 | 0.2 | 28.53 | 0.2 | 0.079 | 3.6 |
| 8153-72 | 0.430 | 1.7 | 7.75 | 0.4 | 8.264 | 0.199 | 2.3 | 0.52 | 2.2 | 0.688 | 0.600 | 0.6 | 30.86 | 0.2 | 26.88 | 0.2 | 1.412 | 0.3 |
| 8153-73 | 0.410 | 1.8 | 7.49 | 0.4 | 7.977 | 0.194 | 2.3 | 0.51 | 2.2 | 0.673 | 0.564 | 0.6 | 30.88 | 0.2 | 27.05 | 0.2 | 1.367 | 0.3 |
| 8153-74 | 0.415 | 1.8 | 7.58 | 0.4 | 8.076 | 0.193 | 2.3 | 0.50 | 2.3 | 0.656 | 0.568 | 0.6 | 30.86 | 0.2 | 26.80 | 0.2 | 1.378 | 0.3 |
| 8153-75 | 0.413 | 1.8 | 7.45 | 0.4 | 7.937 | 0.189 | 2.4 | 0.50 | 2.3 | 0.651 | 0.561 | 0.6 | 30.91 | 0.2 | 26.79 | 0.2 | 1.347 | 0.3 |
| 8153-76 | 0.420 | 1.7 | 7.56 | 0.4 | 8.056 | 0.194 | 2.3 | 0.51 | 2.2 | 0.664 | 0.567 | 0.6 | 30.82 | 0.2 | 26.82 | 0.2 | 1.357 | 0.3 |
| 8153-77 | 0.409 | 1.8 | 7.53 | 0.4 | 8.028 | 0.188 | 2.4 | 0.50 | 2.3 | 0.652 | 0.559 | 0.6 | 30.59 | 0.2 | 26.71 | 0.2 | 1.384 | 0.3 |
| 8153-78 | 0.399 | 1.8 | 7.58 | 0.4 | 8.078 | 0.185 | 2.4 | 0.50 | 2.2 | 0.659 | 0.568 | 0.6 | 30.98 | 0.2 | 26.73 | 0.2 | 1.387 | 0.3 |
| 05-6-36_m5_pt60 | 0.466 | 1.6 | 3.98 | 0.5 | 4.209 | 0.142 | 3.0 | 0.30 | 3.6 | 0.397 | 0.994 | 0.4 | 32.16 | 0.2 | 28.64 | 0.2 | 0.078 | 3.7 |
| 05-6-36_m5_pt61 | 0.449 | 1.6 | 3.86 | 0.6 | 4.078 | 0.142 | 3.1 | 0.33 | 3.3 | 0.435 | 0.978 | 0.4 | 32.34 | 0.2 | 28.65 | 0.2 | 0.069 | 4.1 |
| 05-6-36_m5_pt62 | 0.428 | 1.7 | 3.55 | 0.6 | 3.747 | 0.132 | 3.3 | 0.30 | 3.6 | 0.397 | 0.900 | 0.4 | 32.59 | 0.2 | 28.61 | 0.2 | 0.066 | 4.3 |
| 05-6-36_m5_pt63 | 0.419 | 1.7 | 3.68 | 0.6 | 3.887 | 0.127 | 3.4 | 0.33 | 3.3 | 0.432 | 0.930 | 0.4 | 32.45 | 0.2 | 28.64 | 0.2 | 0.059 | 4.8 |
| 05-6-36_m5_pt64 | 0.437 | 1.6 | 3.74 | 0.6 | 3.954 | 0.134 | 3.2 | 0.34 | 3.2 | 0.449 | 0.945 | 0.4 | 32.46 | 0.2 | 28.58 | 0.2 | 0.060 | 4.7 |
| 05-6-36_m5_pt65 | 0.436 | 1.6 | 3.67 | 0.6 | 3.881 | 0.144 | 3.0 | 0.38 | 2.9 | 0.491 | 0.940 | 0.4 | 32.37 | 0.2 | 28.66 | 0.2 | 0.058 | 4.9 |
| 05-6-36_m5_pt66 | 0.435 | 1.6 | 3.70 | 0.6 | 3.903 | 0.134 | 3.3 | 0.37 | 3.0 | 0.485 | 0.936 | 0.4 | 32.37 | 0.2 | 28.68 | 0.2 | 0.063 | 4.4 |
| 05-6-36_m5_pt67 | 0.422 | 1.7 | 3.62 | 0.6 | 3.821 | 0.134 | 3.2 | 0.36 | 3.1 | 0.463 | 0.923 | 0.4 | 32.45 | 0.2 | 28.65 | 0.2 | 0.062 | 4.5 |
| 05-6-36_m5_pt68 | 0.424 | 1.7 | 3.68 | 0.6 | 3.885 | 0.125 | 3.5 | 0.36 | 3.1 | 0.463 | 0.932 | 0.4 | 32.38 | 0.2 | 28.68 | 0.2 | 0.059 | 4.8 |
| 05-6-36_m5_pt69 | 0.425 | 1.7 | 3.72 | 0.6 | 3.929 | 0.132 | 3.3 | 0.37 | 3.0 | 0.483 | 0.926 | 0.4 | 32.43 | 0.2 | 28.68 | 0.2 | 0.067 | 4.2 |
| 05-6-36_m5_pt70 | 0.413 | 1.7 | 3.63 | 0.6 | 3.838 | 0.136 | 3.2 | 0.35 | 3.1 | 0.461 | 0.922 | 0.4 | 32.38 | 0.2 | 28.62 | 0.2 | 0.065 | 4.3 |
| 05-6-36_m5_pt71 | 0.420 | 1.7 | 3.54 | 0.6 | 3.740 | 0.120 | 3.6 | 0.30 | 3.7 | 0.385 | 0.891 | 0.4 | 32.38 | 0.2 | 28.64 | 0.2 | 0.061 | 4.6 |
| 05-6-36_m5_pt72 | 0.431 | 1.7 | 3.46 | 0.6 | 3.657 | 0.129 | 3.4 | 0.30 | 3.6 | 0.395 | 0.880 | 0.4 | 32.40 | 0.2 | 28.68 | 0.2 | 0.060 | 4.7 |
| 05-6-36_m5_pt73 | 0.423 | 1.7 | 3.44 | 0.6 | 3.631 | 0.127 | 3.4 | 0.29 | 3.7 | 0.379 | 0.877 | 0.5 | 32.34 | 0.2 | 28.65 | 0.2 | 0.062 | 4.5 |
| 05-6-36_m5_pt74 | 0.414 | 1.7 | 4.36 | 0.5 | 4.610 | 0.146 | 3.0 | 0.11 | 9.6 | 0.143 | 1.068 | 0.4 | 32.46 | 0.2 | 28.58 | 0.2 | 0.401 | 0.8 |
| 05-6-36_m5_pt75 | 0.378 | 1.9 | 4.43 | 0.5 | 4.692 | 0.136 | 3.2 | 0.09 | 11.7 | 0.117 | 1.068 | 0.4 | 32.68 | 0.2 | 28.71 | 0.2 | 0.116 | 2.5 |
| 05-6-36_m5_pt76 | 0.426 | 1.7 | 4.24 | 0.5 | 4.484 | 0.146 | 3.0 | 0.10 | 10.3 | 0.133 | 1.034 | 0.4 | 32.56 | 0.2 | 28.71 | 0.2 | 0.099 | 2.9 |
| 05-6-36_m5_pt77 | 0.411 | 1.7 | 4.36 | 0.5 | 4.622 | 0.144 | 3.0 | 0.09 | 11.2 | 0.122 | 1.061 | 0.4 | 32.51 | 0.2 | 28.71 | 0.2 | 0.091 | 3.1 |
| 05-6-36_m5_pt78 | 0.401 | 1.8 | 4.45 | 0.5 | 4.717 | 0.144 | 3.0 | 0.08 | 13.7 | 0.100 | 1.069 | 0.4 | 32.56 | 0.2 | 28.65 | 0.2 | 0.094 | 3.0 |
| 05-6-36_m5_pt79 | 0.397 | 1.8 | 4.33 | 0.5 | 4.583 | 0.157 | 2.8 | 0.10 | 10.5 | 0.130 | 1.048 | 0.4 | 32.55 | 0.2 | 28.69 | 0.2 | 0.096 | 3.0 |
| 05-6-36_m5_pt80 | 0.418 | 1.7 | 3.92 | 0.6 | 4.141 | 0.135 | 3.2 | 0.24 | 4.6 | 0.308 | 0.979 | 0.4 | 32.09 | 0.2 | 28.70 | 0.2 | 0.061 | 4.7 |
| 05-6-36_m5_pt81 | 0.471 | 1.5 | 3.92 | 0.6 | 4.144 | 0.142 | 3.1 | 0.31 | 3.5 | 0.408 | 0.994 | 0.4 | 32.17 | 0.2 | 28.57 | 0.2 | 0.070 | 4.0 |
| 05-6-36_m5_pt82 | 0.469 | 1.5 | 3.81 | 0.6 | 4.026 | 0.135 | 3.2 | 0.29 | 3.8 | 0.379 | 0.969 | 0.4 | 32.12 | 0.2 | 28.64 | 0.2 | 0.070 | 4.1 |

| | $UO_2$ | | $ThO_2$ | | | PbO | | $Y_2O_3$ | | | CaO | | $Ce_2O_3$ | | $P_2O_5$ | | $SiO_2$ | |
|---|---|---|---|---|---|---|---|---|---|---|---|---|---|---|---|---|---|---|
| Sample | wt. % | RSD (2σ%) | wt. % | RSD (2σ%) | k-raw | wt. % | RSD (2σ%) | wt. % | RSD (2σ%) | k-raw | wt. % | RSD (2σ%) | wt. % | RSD (2σ%) | wt. % | RSD (2σ%) | wt. % | RSD (2σ%) |
| 05-6-36_m5_pt83 | 0.427 | 1.7 | 3.83 | 0.6 | 4.043 | 0.136 | 3.2 | 0.28 | 3.8 | 0.369 | 0.944 | 0.4 | 32.16 | 0.2 | 28.73 | 0.2 | 0.082 | 3.5 |
| 05-6-36_m5_pt84 | 0.456 | 1.6 | 4.61 | 0.5 | 4.885 | 0.152 | 2.9 | 0.13 | 7.9 | 0.176 | 1.121 | 0.4 | 32.06 | 0.2 | 28.59 | 0.2 | 0.099 | 2.9 |
| 05-6-36_m5_pt85 | 0.409 | 1.8 | 4.51 | 0.5 | 4.772 | 0.150 | 2.9 | 0.09 | 11.7 | 0.117 | 1.098 | 0.4 | 32.12 | 0.2 | 28.70 | 0.2 | 0.104 | 2.8 |
| 8153-79 | 0.389 | 1.9 | 7.27 | 0.4 | 7.749 | 0.188 | 2.4 | 0.50 | 2.2 | 0.660 | 0.575 | 0.6 | 31.13 | 0.2 | 26.42 | 0.2 | 1.321 | 0.3 |
| 8153-80 | 0.391 | 1.8 | 7.19 | 0.4 | 7.670 | 0.182 | 2.5 | 0.52 | 2.2 | 0.679 | 0.574 | 0.6 | 31.10 | 0.2 | 26.20 | 0.2 | 1.311 | 0.3 |
| 8153-81 | 0.404 | 1.8 | 7.19 | 0.4 | 7.661 | 0.186 | 2.4 | 0.51 | 2.2 | 0.665 | 0.574 | 0.6 | 30.87 | 0.2 | 26.27 | 0.2 | 1.303 | 0.3 |
| 8153-82 | 0.403 | 1.8 | 7.21 | 0.4 | 7.685 | 0.182 | 2.5 | 0.50 | 2.3 | 0.648 | 0.566 | 0.6 | 30.97 | 0.2 | 26.24 | 0.2 | 1.306 | 0.3 |
| 8153-83 | 0.392 | 1.8 | 7.15 | 0.4 | 7.623 | 0.187 | 2.4 | 0.51 | 2.2 | 0.665 | 0.580 | 0.6 | 30.91 | 0.2 | 26.20 | 0.2 | 1.313 | 0.3 |
| 8153-84 | 0.390 | 1.8 | 7.25 | 0.4 | 7.730 | 0.190 | 2.4 | 0.51 | 2.2 | 0.667 | 0.570 | 0.6 | 30.95 | 0.2 | 26.13 | 0.2 | 1.305 | 0.3 |
| 8153-85 | 0.388 | 1.9 | 7.21 | 0.4 | 7.693 | 0.189 | 2.4 | 0.51 | 2.2 | 0.670 | 0.571 | 0.6 | 30.89 | 0.2 | 26.02 | 0.2 | 1.322 | 0.3 |
| 8153-86 | 0.390 | 1.9 | 7.18 | 0.4 | 7.660 | 0.186 | 2.4 | 0.52 | 2.2 | 0.680 | 0.566 | 0.6 | 31.02 | 0.2 | 25.82 | 0.2 | 1.312 | 0.3 |
| 8153-87 | 0.387 | 1.9 | 7.21 | 0.4 | 7.691 | 0.184 | 2.4 | 0.53 | 2.1 | 0.687 | 0.570 | 0.6 | 31.01 | 0.2 | 25.67 | 0.2 | 1.325 | 0.3 |
| 8153-88 | 0.388 | 1.9 | 7.19 | 0.4 | 7.679 | 0.191 | 2.4 | 0.51 | 2.2 | 0.671 | 0.572 | 0.6 | 30.95 | 0.2 | 25.62 | 0.2 | 1.329 | 0.3 |
| 8153-89 | 0.878 | 0.9 | 15.69 | 0.3 | 16.920 | 0.238 | 1.9 | 2.37 | 0.6 | 3.219 | 1.534 | 0.3 | 22.01 | 0.3 | 24.67 | 0.2 | 2.219 | 0.2 |
| 8153-90 | 0.906 | 0.9 | 15.91 | 0.3 | 17.162 | 0.235 | 2.0 | 2.35 | 0.6 | 3.202 | 1.526 | 0.3 | 21.60 | 0.3 | 24.46 | 0.2 | 2.255 | 0.2 |
| 8153-91 | 0.901 | 0.9 | 16.75 | 0.2 | 18.089 | 0.237 | 2.0 | 2.48 | 0.6 | 3.383 | 1.632 | 0.3 | 22.22 | 0.3 | 24.69 | 0.2 | 2.498 | 0.2 |
| 8153-92 | 0.880 | 0.9 | 16.24 | 0.2 | 17.523 | 0.238 | 1.9 | 2.48 | 0.6 | 3.377 | 1.591 | 0.3 | 22.23 | 0.3 | 24.59 | 0.2 | 2.405 | 0.2 |
| 8153-93 | 0.846 | 1.0 | 15.80 | 0.3 | 17.042 | 0.234 | 2.0 | 2.49 | 0.6 | 3.382 | 1.586 | 0.3 | 22.07 | 0.3 | 24.39 | 0.2 | 2.345 | 0.2 |
| 8153-94 | 0.861 | 0.9 | 15.78 | 0.3 | 17.021 | 0.225 | 2.1 | 2.49 | 0.6 | 3.386 | 1.594 | 0.3 | 21.87 | 0.3 | 24.33 | 0.2 | 2.293 | 0.2 |
| 8153-95 | 0.873 | 0.9 | 15.96 | 0.3 | 17.206 | 0.236 | 2.0 | 2.50 | 0.6 | 3.403 | 1.593 | 0.3 | 22.13 | 0.3 | 24.64 | 0.2 | 2.371 | 0.2 |
| 8153-96 | 0.908 | 0.9 | 16.54 | 0.2 | 17.866 | 0.240 | 1.9 | 2.46 | 0.6 | 3.347 | 1.605 | 0.3 | 21.71 | 0.3 | 24.48 | 0.2 | 2.484 | 0.2 |
| 8153-97 | 0.914 | 0.9 | 16.84 | 0.2 | 18.182 | 0.239 | 2.0 | 2.50 | 0.6 | 3.403 | 1.627 | 0.3 | 21.90 | 0.3 | 24.85 | 0.2 | 2.520 | 0.2 |
| test1 | 0.408 | 1.9 | 7.41 | 0.4 | 7.909 | 0.192 | 2.4 | 0.52 | 2.3 | 0.676 | 0.583 | 0.7 | 31.31 | 0.3 | 25.95 | 0.2 | 1.278 | 0.3 |
| test2 | 0.412 | 1.9 | 7.42 | 0.4 | 7.922 | 0.187 | 2.5 | 0.50 | 2.4 | 0.657 | 0.577 | 0.7 | 31.37 | 0.3 | 25.87 | 0.2 | 1.269 | 0.3 |
| test3 | 0.401 | 2.0 | 7.45 | 0.4 | 7.955 | 0.185 | 2.5 | 0.51 | 2.4 | 0.662 | 0.579 | 0.7 | 31.21 | 0.3 | 25.99 | 0.2 | 1.276 | 0.3 |
| test4 | 0.410 | 1.9 | 7.46 | 0.4 | 7.971 | 0.188 | 2.5 | 0.50 | 2.4 | 0.652 | 0.588 | 0.6 | 31.34 | 0.2 | 25.95 | 0.2 | 1.265 | 0.3 |
| test5 | 0.414 | 1.9 | 7.44 | 0.4 | 7.952 | 0.181 | 2.6 | 0.52 | 2.3 | 0.683 | 0.579 | 0.7 | 31.25 | 0.3 | 25.86 | 0.2 | 1.257 | 0.3 |
| test6 | 0.396 | 2.0 | 7.41 | 0.4 | 7.912 | 0.184 | 2.5 | 0.51 | 2.4 | 0.664 | 0.583 | 0.7 | 31.19 | 0.3 | 25.83 | 0.2 | 1.257 | 0.3 |
| test7 | 0.421 | 1.9 | 7.41 | 0.4 | 7.913 | 0.180 | 2.6 | 0.52 | 2.3 | 0.686 | 0.576 | 0.7 | 31.37 | 0.3 | 26.09 | 0.2 | 1.260 | 0.3 |
| test8 | 0.411 | 1.9 | 7.45 | 0.4 | 7.960 | 0.195 | 2.4 | 0.51 | 2.4 | 0.663 | 0.585 | 0.7 | 31.46 | 0.2 | 26.03 | 0.2 | 1.265 | 0.3 |
| test9 | 0.404 | 2.0 | 7.39 | 0.4 | 7.886 | 0.188 | 2.5 | 0.54 | 2.2 | 0.701 | 0.593 | 0.6 | 31.45 | 0.3 | 26.26 | 0.2 | 1.276 | 0.3 |
| test10 | 0.397 | 2.0 | 7.38 | 0.4 | 7.883 | 0.173 | 2.7 | 0.52 | 2.3 | 0.683 | 0.580 | 0.7 | 31.39 | 0.2 | 26.15 | 0.2 | 1.296 | 0.3 |
| test11 | 0.397 | 2.0 | 7.42 | 0.4 | 7.925 | 0.187 | 2.5 | 0.50 | 2.4 | 0.655 | 0.587 | 0.7 | 31.15 | 0.3 | 26.07 | 0.2 | 1.290 | 0.3 |
| test12 | 0.408 | 1.9 | 7.42 | 0.4 | 7.926 | 0.185 | 2.5 | 0.52 | 2.3 | 0.676 | 0.585 | 0.7 | 31.38 | 0.3 | 25.96 | 0.2 | 1.274 | 0.3 |
| 05-10-65_m3_p1 | 0.974 | 0.9 | 5.46 | 0.5 | 5.804 | 0.211 | 2.3 | 0.26 | 4.3 | 0.345 | 1.214 | 0.4 | 28.69 | 0.3 | 26.91 | 0.2 | 0.110 | 2.7 |

| | $UO_2$ | | $ThO_2$ | | | PbO | | $Y_2O_3$ | | | CaO | | $Ce_2O_3$ | | $P_2O_5$ | | $SiO_2$ | |
|---|---|---|---|---|---|---|---|---|---|---|---|---|---|---|---|---|---|---|
| Sample | wt. % | RSD (2σ%) | wt. % | RSD (2σ%) | k-raw | wt. % | RSD (2σ%) | wt. % | RSD (2σ%) | k-raw | wt. % | RSD (2σ%) | wt. % | RSD (2σ%) | wt. % | RSD (2σ%) | wt. % | RSD (2σ%) |
| 05-10-65_m3_p2 | 0.831 | 1.0 | 5.28 | 0.5 | 5.601 | 0.202 | 2.4 | 0.31 | 3.7 | 0.412 | 1.219 | 0.4 | 29.29 | 0.3 | 27.48 | 0.2 | 0.063 | 4.7 |
| 05-10-65_m3_p3 | 0.831 | 1.0 | 5.32 | 0.5 | 5.642 | 0.202 | 2.3 | 0.33 | 3.5 | 0.438 | 1.220 | 0.4 | 29.20 | 0.3 | 27.68 | 0.2 | 0.061 | 4.8 |
| 05-10-65_m3_p4 | 0.742 | 1.1 | 4.89 | 0.5 | 5.185 | 0.184 | 2.5 | 0.40 | 3.0 | 0.519 | 1.117 | 0.4 | 29.92 | 0.3 | 27.67 | 0.2 | 0.060 | 4.9 |
| 05-10-65_m3_p5 | 0.758 | 1.1 | 4.98 | 0.5 | 5.279 | 0.187 | 2.5 | 0.38 | 3.1 | 0.496 | 1.135 | 0.4 | 29.92 | 0.3 | 27.67 | 0.2 | 0.050 | 5.9 |
| 05-10-65_m3_p6 | 0.762 | 1.1 | 4.90 | 0.5 | 5.194 | 0.189 | 2.5 | 0.39 | 3.0 | 0.508 | 1.135 | 0.4 | 30.00 | 0.3 | 27.72 | 0.2 | 0.046 | 6.4 |
| 05-10-65_m3_p7 | 0.760 | 1.1 | 5.09 | 0.5 | 5.395 | 0.190 | 2.5 | 0.42 | 2.8 | 0.555 | 1.175 | 0.4 | 29.69 | 0.3 | 27.77 | 0.2 | 0.047 | 6.2 |
| 05-10-65_m3_p8 | 0.812 | 1.1 | 5.02 | 0.5 | 5.314 | 0.196 | 2.4 | 0.43 | 2.7 | 0.567 | 1.181 | 0.4 | 29.50 | 0.3 | 27.65 | 0.2 | 0.057 | 5.1 |
| 05-10-65_m3_p9 | 0.759 | 1.1 | 5.04 | 0.5 | 5.335 | 0.194 | 2.4 | 0.44 | 2.7 | 0.582 | 1.169 | 0.4 | 29.65 | 0.3 | 27.69 | 0.2 | 0.050 | 5.8 |
| 05-10-65_m3_p10 | 0.715 | 1.2 | 4.73 | 0.5 | 5.003 | 0.187 | 2.5 | 0.51 | 2.3 | 0.673 | 1.074 | 0.4 | 30.15 | 0.3 | 27.74 | 0.2 | 0.047 | 6.3 |
| 05-10-65_m3_p11 | 0.756 | 1.1 | 4.76 | 0.5 | 5.044 | 0.179 | 2.6 | 0.54 | 2.2 | 0.707 | 1.096 | 0.4 | 29.84 | 0.3 | 27.69 | 0.2 | 0.085 | 3.5 |
| 05-10-65_m3_p12 | 0.760 | 1.1 | 4.78 | 0.5 | 5.057 | 0.175 | 2.7 | 0.56 | 2.2 | 0.730 | 1.096 | 0.4 | 29.99 | 0.3 | 27.68 | 0.2 | 0.045 | 6.5 |
| 05-10-65_m3_p13 | 0.791 | 1.1 | 4.85 | 0.5 | 5.131 | 0.178 | 2.6 | 0.54 | 2.2 | 0.706 | 1.102 | 0.4 | 29.58 | 0.3 | 27.58 | 0.2 | 0.050 | 5.9 |
| 05-10-65_m3_p14 | 0.760 | 1.1 | 5.29 | 0.5 | 5.609 | 0.190 | 2.4 | 0.40 | 2.9 | 0.525 | 1.234 | 0.4 | 29.17 | 0.3 | 27.07 | 0.2 | 0.145 | 2.1 |
| 05-10-65_m3_p15 | 0.737 | 1.1 | 5.19 | 0.5 | 5.506 | 0.187 | 2.5 | 0.36 | 3.2 | 0.470 | 1.216 | 0.4 | 29.30 | 0.3 | 26.85 | 0.2 | 0.157 | 1.9 |
| 05-10-65_m3_p16 | 0.724 | 1.2 | 4.90 | 0.5 | 5.192 | 0.180 | 2.6 | 0.49 | 2.4 | 0.641 | 1.102 | 0.4 | 30.22 | 0.3 | 27.69 | 0.2 | 0.041 | 7.1 |
| 05-10-65_m3_p17 | 0.715 | 1.2 | 4.81 | 0.5 | 5.092 | 0.181 | 2.6 | 0.53 | 2.3 | 0.698 | 1.074 | 0.4 | 30.32 | 0.3 | 27.65 | 0.2 | 0.041 | 7.1 |
| 05-10-65_m3_p18 | 0.704 | 1.2 | 4.53 | 0.6 | 4.799 | 0.171 | 2.7 | 0.54 | 2.2 | 0.703 | 1.016 | 0.4 | 30.46 | 0.3 | 27.67 | 0.2 | 0.041 | 7.2 |
| 05-10-65_m3_p19 | 0.673 | 1.2 | 4.51 | 0.6 | 4.779 | 0.175 | 2.6 | 0.42 | 2.8 | 0.550 | 1.005 | 0.5 | 30.62 | 0.3 | 27.73 | 0.2 | 0.048 | 6.1 |
| 05-10-65_m3_p20 | 0.678 | 1.2 | 4.60 | 0.5 | 4.868 | 0.172 | 2.7 | 0.47 | 2.5 | 0.618 | 1.024 | 0.4 | 30.44 | 0.3 | 27.72 | 0.2 | 0.037 | 8.0 |
| 05-10-65_m3_p21 | 0.682 | 1.2 | 4.74 | 0.5 | 5.017 | 0.168 | 2.8 | 0.43 | 2.7 | 0.568 | 1.050 | 0.4 | 30.40 | 0.3 | 27.74 | 0.2 | 0.057 | 5.2 |
| 05-10-65_m3_p22 | 0.694 | 1.2 | 4.79 | 0.5 | 5.071 | 0.177 | 2.7 | 0.44 | 2.7 | 0.576 | 1.084 | 0.4 | 30.10 | 0.3 | 27.63 | 0.2 | 0.039 | 7.6 |
| 05-10-65_m3_p23 | 0.672 | 1.2 | 4.65 | 0.5 | 4.927 | 0.174 | 2.7 | 0.41 | 2.8 | 0.542 | 1.036 | 0.4 | 30.45 | 0.3 | 27.75 | 0.2 | 0.043 | 6.8 |
| 05-10-65_m3_p24 | 0.504 | 1.6 | 4.25 | 0.6 | 4.502 | 0.150 | 3.0 | 0.26 | 4.3 | 0.343 | 0.782 | 0.5 | 32.25 | 0.2 | 27.63 | 0.2 | 0.195 | 1.6 |
| 05-10-65_m3_p25 | 0.431 | 1.9 | 4.37 | 0.6 | 4.637 | 0.147 | 3.1 | 0.25 | 4.7 | 0.321 | 0.787 | 0.5 | 32.15 | 0.2 | 27.58 | 0.2 | 0.202 | 1.6 |
| 05-10-65_m3_p26 | 0.553 | 1.5 | 4.25 | 0.6 | 4.499 | 0.154 | 3.0 | 0.38 | 3.1 | 0.500 | 0.902 | 0.5 | 31.30 | 0.3 | 27.64 | 0.2 | 0.091 | 3.3 |
| 05-10-65_m3_p27 | 0.728 | 1.2 | 5.05 | 0.5 | 5.349 | 0.188 | 2.5 | 0.44 | 2.7 | 0.579 | 1.176 | 0.4 | 29.82 | 0.3 | 27.59 | 0.2 | 0.058 | 5.1 |
| 05-10-65_m3_p28 | 0.764 | 1.1 | 5.18 | 0.5 | 5.487 | 0.188 | 2.5 | 0.46 | 2.6 | 0.606 | 1.202 | 0.4 | 29.67 | 0.3 | 27.66 | 0.2 | 0.044 | 6.7 |
| 05-10-65_m3_p29 | 0.744 | 1.1 | 5.23 | 0.5 | 5.541 | 0.190 | 2.5 | 0.41 | 2.9 | 0.536 | 1.222 | 0.4 | 29.70 | 0.3 | 27.65 | 0.2 | 0.049 | 5.9 |
| 05-10-65_m3_p30 | 0.872 | 1.0 | 5.20 | 0.5 | 5.511 | 0.204 | 2.3 | 0.29 | 3.9 | 0.381 | 1.171 | 0.4 | 29.50 | 0.3 | 27.54 | 0.2 | 0.091 | 3.3 |
| 05-10-65_m3_p31 | 0.913 | 1.0 | 5.53 | 0.5 | 5.869 | 0.199 | 2.4 | 0.25 | 4.5 | 0.333 | 1.203 | 0.4 | 28.94 | 0.3 | 27.41 | 0.2 | 0.126 | 2.4 |
| 8153-13 | 0.405 | 2.0 | 7.34 | 0.4 | 7.842 | 0.188 | 2.5 | 0.47 | 2.5 | 0.613 | 0.580 | 0.7 | 30.86 | 0.3 | 25.49 | 0.2 | 1.261 | 0.3 |
| 8153-14 | 0.409 | 2.0 | 7.32 | 0.4 | 7.820 | 0.186 | 2.5 | 0.49 | 2.4 | 0.644 | 0.584 | 0.7 | 31.02 | 0.3 | 25.70 | 0.2 | 1.266 | 0.3 |
| 8153-15 | 0.416 | 1.9 | 7.31 | 0.4 | 7.809 | 0.182 | 2.6 | 0.52 | 2.3 | 0.678 | 0.589 | 0.7 | 31.21 | 0.3 | 25.80 | 0.2 | 1.264 | 0.3 |
| 8153-16 | 0.419 | 1.9 | 7.35 | 0.4 | 7.851 | 0.187 | 2.5 | 0.51 | 2.3 | 0.666 | 0.574 | 0.7 | 31.15 | 0.3 | 25.82 | 0.2 | 1.278 | 0.3 |
| 8153-17 | 0.409 | 2.0 | 7.35 | 0.4 | 7.847 | 0.196 | 2.4 | 0.50 | 2.4 | 0.659 | 0.580 | 0.7 | 31.19 | 0.3 | 25.95 | 0.2 | 1.283 | 0.3 |
| 8153-18 | 0.407 | 2.0 | 7.32 | 0.4 | 7.820 | 0.192 | 2.5 | 0.51 | 2.4 | 0.661 | 0.576 | 0.7 | 31.07 | 0.3 | 25.78 | 0.2 | 1.280 | 0.3 |

| | $UO_2$ | | $ThO_2$ | | | PbO | | $Y_2O_3$ | | | CaO | | $Ce_2O_3$ | | $P_2O_5$ | | $SiO_2$ | |
|---|---|---|---|---|---|---|---|---|---|---|---|---|---|---|---|---|---|---|
| Sample | wt. % | RSD (2σ%) | wt. % | RSD (2σ%) | k-raw | wt. % | RSD (2σ%) | wt. % | RSD (2σ%) | k-raw | wt. % | RSD (2σ%) | wt. % | RSD (2σ%) | wt. % | RSD (2σ%) | wt. % | RSD (2σ%) |
| 8153-19 | 0.406 | 2.0 | 7.30 | 0.4 | 7.790 | 0.183 | 2.6 | 0.50 | 2.4 | 0.658 | 0.574 | 0.7 | 30.99 | 0.3 | 25.89 | 0.2 | 1.278 | 0.3 |
| 8153-20 | 0.424 | 1.9 | 7.22 | 0.4 | 7.704 | 0.176 | 2.7 | 0.51 | 2.3 | 0.671 | 0.579 | 0.7 | 30.71 | 0.3 | 25.56 | 0.2 | 1.278 | 0.3 |
| 8153-21 | 0.414 | 1.9 | 7.32 | 0.4 | 7.814 | 0.187 | 2.5 | 0.51 | 2.3 | 0.667 | 0.577 | 0.7 | 30.98 | 0.3 | 25.61 | 0.2 | 1.277 | 0.3 |
| 8153-22 | 0.414 | 1.9 | 7.23 | 0.4 | 7.721 | 0.181 | 2.6 | 0.51 | 2.3 | 0.664 | 0.568 | 0.7 | 30.77 | 0.3 | 25.50 | 0.2 | 1.277 | 0.3 |
| 05-10-65_m3_p32 | 0.401 | 2.0 | 4.11 | 0.6 | 4.357 | 0.134 | 3.4 | 0.27 | 4.3 | 0.350 | 0.741 | 0.6 | 32.15 | 0.2 | 27.61 | 0.2 | 0.201 | 1.6 |
| 05-10-65_m3_p33 | 0.407 | 1.9 | 4.18 | 0.6 | 4.425 | 0.137 | 3.3 | 0.25 | 4.6 | 0.328 | 0.747 | 0.6 | 32.30 | 0.2 | 27.57 | 0.2 | 0.206 | 1.6 |
| 05-10-65_m3_p34 | 0.442 | 1.8 | 4.31 | 0.6 | 4.572 | 0.151 | 3.0 | 0.24 | 4.8 | 0.310 | 0.789 | 0.5 | 32.01 | 0.2 | 27.60 | 0.2 | 0.213 | 1.5 |
| 05-10-65_m3_p35 | 0.402 | 2.0 | 3.83 | 0.6 | 4.056 | 0.128 | 3.5 | 0.24 | 4.6 | 0.317 | 0.707 | 0.6 | 32.14 | 0.2 | 27.27 | 0.2 | 0.175 | 1.8 |
| 05-10-65_m3_p36 | 0.382 | 2.1 | 3.95 | 0.6 | 4.186 | 0.133 | 3.4 | 0.27 | 4.3 | 0.350 | 0.715 | 0.6 | 32.42 | 0.2 | 27.50 | 0.2 | 0.195 | 1.6 |
| 05-10-65_m3_p37 | 0.425 | 1.9 | 4.06 | 0.6 | 4.306 | 0.142 | 3.2 | 0.24 | 4.8 | 0.311 | 0.753 | 0.5 | 32.27 | 0.2 | 27.48 | 0.2 | 0.186 | 1.7 |
| 05-10-65_m3_p38 | 0.422 | 1.9 | 3.77 | 0.6 | 3.992 | 0.133 | 3.4 | 0.26 | 4.5 | 0.332 | 0.710 | 0.6 | 32.39 | 0.2 | 27.46 | 0.2 | 0.181 | 1.7 |
| 05-10-65_m3_p39 | 0.440 | 1.8 | 4.00 | 0.6 | 4.234 | 0.138 | 3.3 | 0.26 | 4.3 | 0.343 | 0.748 | 0.6 | 32.23 | 0.2 | 27.51 | 0.2 | 0.176 | 1.8 |
| 05-10-65_m3_p40 | 0.458 | 1.7 | 4.03 | 0.6 | 4.267 | 0.141 | 3.2 | 0.25 | 4.7 | 0.319 | 0.740 | 0.6 | 32.08 | 0.2 | 27.42 | 0.2 | 0.196 | 1.6 |
| 05-10-65_m3_p41 | 0.444 | 1.8 | 4.23 | 0.6 | 4.480 | 0.151 | 3.1 | 0.25 | 4.5 | 0.326 | 0.758 | 0.5 | 32.08 | 0.2 | 27.39 | 0.2 | 0.199 | 1.6 |
| 05-10-65_m3_p42 | 0.446 | 1.8 | 4.34 | 0.6 | 4.600 | 0.140 | 3.3 | 0.23 | 5.0 | 0.294 | 0.781 | 0.5 | 32.14 | 0.2 | 27.40 | 0.2 | 0.204 | 1.6 |
| 05-10-65_m3_p43 | 0.463 | 1.7 | 4.33 | 0.6 | 4.590 | 0.152 | 3.0 | 0.26 | 4.5 | 0.334 | 0.811 | 0.5 | 31.72 | 0.3 | 27.37 | 0.2 | 0.187 | 1.7 |
| 05-10-65_m3_p44 | 0.843 | 1.0 | 4.58 | 0.6 | 4.854 | 0.187 | 2.5 | 0.26 | 4.3 | 0.346 | 1.020 | 0.4 | 30.00 | 0.3 | 27.39 | 0.2 | 0.078 | 3.8 |
| 05-10-65_m3_p45 | 0.807 | 1.1 | 4.57 | 0.6 | 4.838 | 0.184 | 2.6 | 0.23 | 4.9 | 0.304 | 1.036 | 0.4 | 30.13 | 0.3 | 27.64 | 0.2 | 0.064 | 4.7 |
| 05-10-65_m3_p46 | 0.882 | 1.0 | 5.02 | 0.5 | 5.320 | 0.202 | 2.4 | 0.25 | 4.6 | 0.323 | 1.106 | 0.4 | 29.46 | 0.3 | 27.27 | 0.2 | 0.091 | 3.3 |
| 05-10-65_m3_p47 | 1.010 | 0.9 | 5.66 | 0.5 | 6.011 | 0.229 | 2.1 | 0.26 | 4.3 | 0.343 | 1.241 | 0.4 | 28.43 | 0.3 | 27.07 | 0.2 | 0.116 | 2.6 |
| 05-10-65_m3_p48 | 0.354 | 2.2 | 3.45 | 0.7 | 3.647 | 0.122 | 3.7 | 0.27 | 4.3 | 0.345 | 0.654 | 0.6 | 32.54 | 0.2 | 27.50 | 0.2 | 0.157 | 2.0 |
| 05-10-65_m3_p49 | 0.402 | 2.0 | 3.83 | 0.6 | 4.060 | 0.130 | 3.5 | 0.25 | 4.6 | 0.322 | 0.713 | 0.6 | 32.27 | 0.2 | 27.35 | 0.2 | 0.187 | 1.7 |
| 05-10-65_m3_p50 | 0.438 | 1.8 | 4.28 | 0.6 | 4.535 | 0.137 | 3.3 | 0.24 | 4.8 | 0.310 | 0.759 | 0.5 | 32.02 | 0.2 | 27.37 | 0.2 | 0.221 | 1.4 |
| 05-10-65_m3_p51 | 0.407 | 1.9 | 3.74 | 0.6 | 3.964 | 0.126 | 3.6 | 0.24 | 4.7 | 0.314 | 0.683 | 0.6 | 32.60 | 0.2 | 27.35 | 0.2 | 0.192 | 1.6 |
| 05-10-65_m3_p52 | 0.396 | 2.0 | 3.68 | 0.6 | 3.892 | 0.130 | 3.5 | 0.23 | 5.0 | 0.296 | 0.682 | 0.6 | 32.51 | 0.2 | 27.39 | 0.2 | 0.193 | 1.6 |
| 05-10-65_m3_p53 | 0.537 | 1.5 | 4.33 | 0.6 | 4.588 | 0.157 | 2.9 | 0.22 | 5.2 | 0.286 | 0.773 | 0.5 | 32.07 | 0.2 | 27.39 | 0.2 | 0.225 | 1.4 |
| 05-10-65_m3_p54 | 0.677 | 1.2 | 5.58 | 0.5 | 5.937 | 0.196 | 2.4 | 0.19 | 6.0 | 0.247 | 0.966 | 0.5 | 31.07 | 0.3 | 27.15 | 0.2 | 0.339 | 1.0 |
| 05-10-65_m3_p55 | 0.578 | 1.4 | 4.89 | 0.5 | 5.195 | 0.157 | 3.0 | 0.19 | 5.9 | 0.249 | 0.875 | 0.5 | 31.74 | 0.3 | 27.27 | 0.2 | 0.236 | 1.4 |
| 05-10-65_m3_p56 | 0.484 | 1.7 | 3.78 | 0.6 | 4.000 | 0.133 | 3.5 | 0.22 | 5.2 | 0.283 | 0.712 | 0.6 | 32.60 | 0.2 | 27.49 | 0.2 | 0.180 | 1.7 |
| 05-10-65_m3_p57 | 0.441 | 1.8 | 3.96 | 0.6 | 4.189 | 0.142 | 3.2 | 0.24 | 4.8 | 0.311 | 0.758 | 0.5 | 32.34 | 0.2 | 27.56 | 0.2 | 0.164 | 1.9 |
| 05-10-65_m3_p58 | 0.510 | 1.6 | 5.00 | 0.5 | 5.313 | 0.171 | 2.7 | 0.26 | 4.5 | 0.336 | 0.896 | 0.5 | 31.66 | 0.3 | 27.45 | 0.2 | 0.249 | 1.3 |
| 05-10-65_m3_p59 | 0.480 | 1.7 | 4.29 | 0.6 | 4.543 | 0.156 | 2.9 | 0.28 | 4.2 | 0.360 | 0.813 | 0.5 | 31.90 | 0.3 | 27.43 | 0.2 | 0.176 | 1.8 |
| 05-10-65_m3_p60 | 0.401 | 2.0 | 3.97 | 0.6 | 4.206 | 0.131 | 3.5 | 0.27 | 4.3 | 0.349 | 0.732 | 0.6 | 32.54 | 0.2 | 27.58 | 0.2 | 0.180 | 1.7 |
| 05-10-65_m3_p61 | 0.410 | 1.9 | 3.62 | 0.6 | 3.832 | 0.124 | 3.7 | 0.24 | 4.8 | 0.312 | 0.682 | 0.6 | 32.83 | 0.2 | 27.66 | 0.2 | 0.160 | 2.0 |
| 05-10-65_m3_p62 | 0.387 | 2.0 | 3.92 | 0.6 | 4.156 | 0.127 | 3.6 | 0.26 | 4.4 | 0.340 | 0.729 | 0.6 | 32.58 | 0.2 | 27.60 | 0.2 | 0.177 | 1.8 |
| 8153-23 | 0.417 | 1.9 | 7.60 | 0.4 | 8.114 | 0.197 | 2.4 | 0.50 | 2.4 | 0.655 | 0.582 | 0.7 | 31.08 | 0.3 | 26.03 | 0.2 | 1.330 | 0.3 |

| | $UO_2$ | | $ThO_2$ | | | PbO | | $Y_2O_3$ | | | CaO | | $Ce_2O_3$ | | $P_2O_5$ | | $SiO_2$ | |
|---|---|---|---|---|---|---|---|---|---|---|---|---|---|---|---|---|---|---|
| Sample | wt. % | RSD (2σ%) | wt. % | RSD (2σ%) | k-raw | wt. % | RSD (2σ%) | wt. % | RSD (2σ%) | k-raw | wt. % | RSD (2σ%) | wt. % | RSD (2σ%) | wt. % | RSD (2σ%) | wt. % | RSD (2σ%) |
| 8153-24 | 0.406 | 2.0 | 7.34 | 0.4 | 7.835 | 0.190 | 2.5 | 0.50 | 2.4 | 0.648 | 0.564 | 0.7 | 31.23 | 0.3 | 25.94 | 0.2 | 1.286 | 0.3 |
| 8153-25 | 0.421 | 1.9 | 7.30 | 0.4 | 7.791 | 0.193 | 2.5 | 0.49 | 2.4 | 0.646 | 0.568 | 0.7 | 31.30 | 0.3 | 26.12 | 0.2 | 1.282 | 0.3 |
| 8153-26 | 0.411 | 2.0 | 7.52 | 0.4 | 8.025 | 0.192 | 2.5 | 0.50 | 2.4 | 0.656 | 0.580 | 0.7 | 30.79 | 0.3 | 25.82 | 0.2 | 1.313 | 0.3 |
| 8153-27 | 0.406 | 2.0 | 7.52 | 0.4 | 8.030 | 0.181 | 2.6 | 0.50 | 2.4 | 0.649 | 0.580 | 0.7 | 31.12 | 0.3 | 26.17 | 0.2 | 1.304 | 0.3 |
| 8153-28 | 0.420 | 1.9 | 7.47 | 0.4 | 7.974 | 0.189 | 2.5 | 0.50 | 2.4 | 0.649 | 0.576 | 0.7 | 30.95 | 0.3 | 25.91 | 0.2 | 1.304 | 0.3 |
| 8153-29 | 0.398 | 2.1 | 7.46 | 0.4 | 7.962 | 0.183 | 2.6 | 0.51 | 2.4 | 0.663 | 0.577 | 0.7 | 31.21 | 0.3 | 26.06 | 0.2 | 1.302 | 0.3 |
| 8153-30 | 0.425 | 1.9 | 7.49 | 0.4 | 8.003 | 0.184 | 2.6 | 0.50 | 2.4 | 0.647 | 0.578 | 0.7 | 31.09 | 0.3 | 25.92 | 0.2 | 1.302 | 0.3 |
| 8153-31 | 0.431 | 1.9 | 7.71 | 0.4 | 8.232 | 0.192 | 2.5 | 0.51 | 2.4 | 0.663 | 0.589 | 0.7 | 30.88 | 0.3 | 25.89 | 0.2 | 1.330 | 0.3 |
| 8153-32 | 0.433 | 1.9 | 7.61 | 0.4 | 8.128 | 0.192 | 2.5 | 0.52 | 2.3 | 0.679 | 0.594 | 0.7 | 31.18 | 0.3 | 26.02 | 0.2 | 1.342 | 0.3 |
| 8153-33 | 0.427 | 1.9 | 7.66 | 0.4 | 8.177 | 0.191 | 2.5 | 0.51 | 2.4 | 0.665 | 0.585 | 0.7 | 30.92 | 0.3 | 25.99 | 0.2 | 1.329 | 0.3 |
| 8153-34 | 0.417 | 2.0 | 7.56 | 0.4 | 8.075 | 0.193 | 2.5 | 0.49 | 2.5 | 0.638 | 0.585 | 0.7 | 31.43 | 0.3 | 25.96 | 0.2 | 1.310 | 0.3 |
| 8153-35 | 0.412 | 2.0 | 7.51 | 0.4 | 8.018 | 0.200 | 2.4 | 0.50 | 2.4 | 0.660 | 0.582 | 0.7 | 31.00 | 0.3 | 26.04 | 0.2 | 1.309 | 0.3 |
| 8153-36 | 0.420 | 2.0 | 7.45 | 0.4 | 7.955 | 0.190 | 2.5 | 0.52 | 2.3 | 0.676 | 0.578 | 0.7 | 31.04 | 0.3 | 26.07 | 0.2 | 1.310 | 0.3 |
| 8153-37 | 0.409 | 2.0 | 7.47 | 0.4 | 7.975 | 0.181 | 2.6 | 0.51 | 2.4 | 0.665 | 0.575 | 0.7 | 30.99 | 0.3 | 25.97 | 0.2 | 1.317 | 0.3 |
| 8153-38 | 0.423 | 1.9 | 7.41 | 0.4 | 7.905 | 0.197 | 2.4 | 0.49 | 2.5 | 0.638 | 0.570 | 0.7 | 31.19 | 0.3 | 26.11 | 0.2 | 1.305 | 0.3 |
| 05-10-65_m3_p63 | 0.448 | 1.8 | 4.44 | 0.6 | 4.701 | 0.149 | 3.1 | 0.27 | 4.3 | 0.351 | 0.818 | 0.5 | 32.29 | 0.3 | 27.79 | 0.2 | 0.208 | 1.5 |
| 05-10-65_m3_p64 | 0.435 | 1.9 | 4.43 | 0.6 | 4.695 | 0.152 | 3.1 | 0.29 | 4.1 | 0.373 | 0.817 | 0.5 | 32.36 | 0.3 | 27.77 | 0.2 | 0.210 | 1.5 |
| 05-10-65_m3_p65 | 0.455 | 1.8 | 4.36 | 0.6 | 4.620 | 0.157 | 3.0 | 0.30 | 3.9 | 0.389 | 0.839 | 0.5 | 31.86 | 0.3 | 27.66 | 0.2 | 0.191 | 1.7 |
| 05-10-65_m3_p66 | 0.409 | 2.0 | 4.11 | 0.6 | 4.353 | 0.138 | 3.4 | 0.27 | 4.2 | 0.357 | 0.793 | 0.5 | 32.50 | 0.3 | 27.74 | 0.2 | 0.184 | 1.7 |
| 05-10-65_m3_p67 | 0.403 | 2.0 | 3.77 | 0.6 | 3.986 | 0.133 | 3.4 | 0.32 | 3.7 | 0.411 | 0.730 | 0.6 | 32.49 | 0.3 | 27.65 | 0.2 | 0.172 | 1.8 |
| 05-10-65_m3_p68 | 0.361 | 2.2 | 3.75 | 0.6 | 3.968 | 0.128 | 3.6 | 0.32 | 3.6 | 0.421 | 0.721 | 0.6 | 32.71 | 0.2 | 27.80 | 0.2 | 0.169 | 1.9 |
| 05-10-65_m3_p69 | 0.381 | 2.1 | 3.98 | 0.6 | 4.213 | 0.128 | 3.6 | 0.29 | 4.1 | 0.371 | 0.762 | 0.5 | 32.64 | 0.2 | 27.83 | 0.2 | 0.181 | 1.8 |
| 05-10-65_m3_p70 | 0.393 | 2.0 | 3.90 | 0.6 | 4.126 | 0.130 | 3.5 | 0.28 | 4.1 | 0.364 | 0.750 | 0.6 | 32.69 | 0.2 | 27.81 | 0.2 | 0.165 | 1.9 |
| 05-10-65_m3_p71 | 0.401 | 2.0 | 3.73 | 0.6 | 3.945 | 0.138 | 3.3 | 0.27 | 4.3 | 0.346 | 0.729 | 0.6 | 32.90 | 0.2 | 27.87 | 0.2 | 0.161 | 1.9 |
| 05-10-65_m3_p72 | 0.389 | 2.1 | 3.68 | 0.6 | 3.900 | 0.127 | 3.6 | 0.26 | 4.4 | 0.338 | 0.695 | 0.6 | 32.91 | 0.2 | 27.82 | 0.2 | 0.167 | 1.9 |
| 05-10-65_m3_p73 | 0.428 | 1.9 | 3.96 | 0.6 | 4.196 | 0.133 | 3.5 | 0.25 | 4.6 | 0.327 | 0.742 | 0.6 | 32.60 | 0.2 | 27.78 | 0.2 | 0.180 | 1.8 |
| 05-10-65_m3_p74 | 0.570 | 1.5 | 4.50 | 0.6 | 4.765 | 0.169 | 2.8 | 0.25 | 4.6 | 0.328 | 0.892 | 0.5 | 31.74 | 0.3 | 27.70 | 0.2 | 0.176 | 1.8 |
| 05-10-65_m3_p75 | 0.475 | 1.7 | 4.25 | 0.6 | 4.509 | 0.146 | 3.2 | 0.27 | 4.3 | 0.353 | 0.798 | 0.5 | 32.32 | 0.3 | 27.57 | 0.2 | 0.201 | 1.6 |
| 05-10-65_m3_p76 | 0.614 | 1.4 | 5.18 | 0.5 | 5.502 | 0.179 | 2.7 | 0.25 | 4.5 | 0.332 | 1.008 | 0.5 | 31.11 | 0.3 | 27.59 | 0.2 | 0.206 | 1.6 |
| 05-10-65_m3_p77 | 0.487 | 1.7 | 4.71 | 0.5 | 5.002 | 0.170 | 2.8 | 0.24 | 4.8 | 0.313 | 0.854 | 0.5 | 32.24 | 0.3 | 27.62 | 0.2 | 0.228 | 1.4 |
| 05-10-65_m3_p78 | 1.194 | 0.8 | 7.58 | 0.4 | 8.079 | 0.287 | 1.8 | 0.22 | 5.2 | 0.293 | 1.613 | 0.3 | 27.02 | 0.3 | 27.38 | 0.2 | 0.173 | 1.8 |
| 05-10-65_m3_p79 | 1.176 | 0.8 | 7.42 | 0.4 | 7.906 | 0.281 | 1.8 | 0.22 | 5.0 | 0.299 | 1.567 | 0.3 | 27.13 | 0.3 | 27.25 | 0.2 | 0.182 | 1.7 |
| 05-10-65_m3_p80 | 1.223 | 0.8 | 7.94 | 0.4 | 8.474 | 0.297 | 1.7 | 0.22 | 5.1 | 0.296 | 1.688 | 0.3 | 26.48 | 0.3 | 27.33 | 0.2 | 0.179 | 1.7 |
| 05-10-65_m2_pt1 | 0.174 | 4.4 | 3.21 | 0.7 | 3.403 | 0.097 | 4.7 | 0.10 | 11.3 | 0.127 | 0.826 | 0.5 | 35.38 | 0.2 | 28.16 | 0.2 | 0.103 | 3.0 |
| 05-10-65_m2_pt2 | 0.081 | 9.3 | 3.15 | 0.7 | 3.338 | 0.090 | 5.0 | 0.01 | 130.8 | 0.011 | 0.740 | 0.6 | 35.15 | 0.2 | 28.08 | 0.2 | 0.053 | 5.7 |
| 05-10-65_m2_pt3 | 0.149 | 5.1 | 3.28 | 0.7 | 3.477 | 0.093 | 4.8 | 0.05 | 24.8 | 0.058 | 0.856 | 0.5 | 35.43 | 0.2 | 28.22 | 0.2 | 0.073 | 4.2 |

| | $UO_2$ | | $ThO_2$ | | | PbO | | $Y_2O_3$ | | | CaO | | $Ce_2O_3$ | | $P_2O_5$ | | $SiO_2$ | |
|---|---|---|---|---|---|---|---|---|---|---|---|---|---|---|---|---|---|---|
| Sample | wt. % | RSD (2σ%) | wt. % | RSD (2σ%) | k-raw | wt. % | RSD (2σ%) | wt. % | RSD (2σ%) | k-raw | wt. % | RSD (2σ%) | wt. % | RSD (2σ%) | wt. % | RSD (2σ%) | wt. % | RSD (2σ%) |
| 05-10-65_m2_pt4 | 0.113 | 6.6 | 3.20 | 0.7 | 3.385 | 0.079 | 5.6 | 0.07 | 16.1 | 0.089 | 0.903 | 0.5 | 34.96 | 0.2 | 27.83 | 0.2 | 0.113 | 2.8 |
| 05-10-65_m2_pt5 | 0.145 | 5.2 | 2.88 | 0.7 | 3.052 | 0.071 | 6.3 | 0.09 | 12.5 | 0.115 | 0.672 | 0.6 | 35.36 | 0.2 | 28.21 | 0.2 | 0.104 | 3.0 |
| 05-10-65_m2_pt6 | 0.076 | 9.8 | 3.54 | 0.7 | 3.747 | 0.081 | 5.5 | 0.01 | 159.2 | 0.009 | 0.833 | 0.5 | 35.05 | 0.2 | 28.27 | 0.2 | 0.054 | 5.6 |
| 05-10-65_m2_pt7 | 0.066 | 11.3 | 2.70 | 0.8 | 2.854 | 0.073 | 6.0 | 0.00 | 100.0 | 0.000 | 0.415 | 0.8 | 36.04 | 0.2 | 28.37 | 0.2 | 0.037 | 8.2 |
| 05-10-65_m2_pt8 | 0.171 | 4.5 | 2.77 | 0.8 | 2.932 | 0.080 | 5.6 | 0.09 | 12.9 | 0.113 | 0.598 | 0.6 | 35.69 | 0.2 | 28.28 | 0.2 | 0.076 | 4.0 |
| 05-10-65_m2_pt9 | 0.069 | 10.7 | 2.56 | 0.8 | 2.713 | 0.069 | 6.4 | 0.00 | 100.0 | 0.000 | 0.472 | 0.8 | 36.08 | 0.2 | 28.05 | 0.2 | 0.046 | 6.6 |
| 05-10-65_m2_pt10 | 0.069 | 10.7 | 2.50 | 0.8 | 2.648 | 0.067 | 6.6 | 0.00 | 100.0 | 0.000 | 0.491 | 0.7 | 36.29 | 0.2 | 27.94 | 0.2 | 0.038 | 8.1 |
| 05-10-65_m2_pt11 | 0.101 | 7.4 | 2.53 | 0.8 | 2.680 | 0.062 | 7.1 | 0.04 | 25.3 | 0.057 | 0.490 | 0.8 | 36.15 | 0.2 | 28.20 | 0.2 | 0.080 | 3.8 |
| 05-10-65_m2_pt12 | 0.056 | 13.2 | 2.44 | 0.8 | 2.579 | 0.061 | 7.3 | 0.00 | 100.0 | 0.000 | 0.404 | 0.9 | 36.50 | 0.2 | 28.21 | 0.2 | 0.037 | 8.3 |
| 05-10-65_m2_pt13 | 0.070 | 10.6 | 2.47 | 0.8 | 2.615 | 0.063 | 6.9 | 0.00 | 100.0 | 0.000 | 0.508 | 0.7 | 35.99 | 0.2 | 28.15 | 0.2 | 0.041 | 7.4 |
| 05-10-65_m2_pt14 | 0.078 | 9.4 | 2.34 | 0.8 | 2.471 | 0.058 | 7.5 | 0.00 | 100.0 | 0.000 | 0.537 | 0.7 | 35.65 | 0.2 | 27.94 | 0.2 | 0.045 | 6.8 |
| 05-10-65_m2_pt15 | 0.053 | 13.9 | 2.00 | 0.9 | 2.115 | 0.059 | 7.4 | 0.00 | 100.0 | 0.000 | 0.557 | 0.7 | 36.63 | 0.2 | 28.06 | 0.2 | 0.052 | 5.8 |
| 05-10-65_m2_pt16 | 0.087 | 8.5 | 2.10 | 0.9 | 2.224 | 0.057 | 7.6 | 0.04 | 30.2 | 0.047 | 0.738 | 0.6 | 36.42 | 0.2 | 27.70 | 0.2 | 0.068 | 4.4 |
| 05-10-65_m2_pt17 | 0.074 | 10.0 | 2.08 | 0.9 | 2.204 | 0.062 | 7.0 | 0.02 | 50.6 | 0.028 | 0.539 | 0.7 | 36.59 | 0.2 | 28.03 | 0.2 | 0.047 | 6.5 |
| 8153-39 | 0.407 | 2.0 | 7.49 | 0.4 | 7.995 | 0.183 | 2.6 | 0.49 | 2.4 | 0.646 | 0.576 | 0.7 | 30.97 | 0.3 | 26.04 | 0.2 | 1.314 | 0.3 |
| 8153-40 | 0.402 | 2.0 | 7.46 | 0.4 | 7.964 | 0.194 | 2.5 | 0.51 | 2.3 | 0.669 | 0.575 | 0.7 | 30.69 | 0.3 | 25.83 | 0.2 | 1.314 | 0.3 |
| 8153-41 | 0.424 | 1.9 | 7.63 | 0.4 | 8.151 | 0.188 | 2.5 | 0.51 | 2.4 | 0.663 | 0.582 | 0.7 | 30.84 | 0.3 | 25.90 | 0.2 | 1.320 | 0.3 |
| 8153-42 | 0.403 | 2.0 | 7.47 | 0.4 | 7.981 | 0.198 | 2.4 | 0.48 | 2.5 | 0.623 | 0.575 | 0.7 | 31.03 | 0.3 | 25.91 | 0.2 | 1.324 | 0.3 |
| 8153-43 | 0.419 | 2.0 | 7.50 | 0.4 | 8.006 | 0.187 | 2.6 | 0.51 | 2.3 | 0.668 | 0.585 | 0.7 | 31.08 | 0.3 | 25.92 | 0.2 | 1.328 | 0.3 |
| 8153-44 | 0.418 | 2.0 | 7.50 | 0.4 | 8.008 | 0.191 | 2.5 | 0.50 | 2.4 | 0.657 | 0.581 | 0.7 | 31.21 | 0.3 | 25.84 | 0.2 | 1.316 | 0.3 |
| 8153-45 | 0.418 | 2.0 | 7.60 | 0.4 | 8.116 | 0.200 | 2.4 | 0.51 | 2.3 | 0.673 | 0.579 | 0.7 | 30.59 | 0.3 | 25.78 | 0.2 | 1.314 | 0.3 |
| 8153-46 | 0.414 | 2.0 | 7.53 | 0.4 | 8.041 | 0.187 | 2.6 | 0.49 | 2.4 | 0.646 | 0.579 | 0.7 | 31.06 | 0.3 | 25.87 | 0.2 | 1.293 | 0.3 |
| 8153-47 | 0.436 | 1.9 | 7.62 | 0.4 | 8.137 | 0.187 | 2.6 | 0.49 | 2.5 | 0.637 | 0.593 | 0.7 | 30.87 | 0.3 | 25.83 | 0.2 | 1.322 | 0.3 |
| 8153-48 | 0.421 | 1.9 | 7.46 | 0.4 | 7.967 | 0.191 | 2.5 | 0.51 | 2.4 | 0.661 | 0.581 | 0.7 | 30.91 | 0.3 | 25.96 | 0.2 | 1.286 | 0.3 |
| 05-10-102_m1_pt1 | 0.185 | 4.0 | 1.12 | 1.4 | 1.183 | 0.038 | 11.1 | 0.43 | 2.8 | 0.547 | 0.460 | 0.8 | 36.98 | 0.2 | 28.32 | 0.2 | 0.024 | 12.1 |
| 05-10-102_m1_pt2 | 0.208 | 3.6 | 1.17 | 1.4 | 1.230 | 0.043 | 10.0 | 0.40 | 2.9 | 0.513 | 0.350 | 0.9 | 37.02 | 0.2 | 28.36 | 0.2 | 0.030 | 9.9 |
| 05-10-102_m1_pt3 | 0.075 | 9.6 | 1.24 | 1.3 | 1.309 | 0.033 | 12.7 | 0.11 | 10.6 | 0.135 | 0.282 | 1.1 | 37.34 | 0.2 | 28.36 | 0.2 | 0.031 | 9.4 |
| 05-10-102_m1_pt4 | 0.041 | 17.4 | 1.34 | 1.2 | 1.414 | 0.044 | 9.6 | 0.03 | 42.3 | 0.033 | 0.233 | 1.3 | 37.16 | 0.2 | 28.22 | 0.2 | 0.028 | 10.6 |
| 05-10-102_m1_pt5 | 0.062 | 11.6 | 2.11 | 0.9 | 2.229 | 0.058 | 7.4 | 0.06 | 17.5 | 0.081 | 0.357 | 0.9 | 36.87 | 0.2 | 28.21 | 0.2 | 0.031 | 9.8 |
| 05-10-102_m1_pt6 | 0.285 | 2.7 | 1.19 | 1.3 | 1.260 | 0.054 | 8.0 | 0.48 | 2.5 | 0.613 | 0.354 | 0.9 | 36.50 | 0.2 | 28.07 | 0.2 | 0.049 | 6.0 |
| 05-10-102_m1_pt7 | 0.293 | 2.6 | 1.20 | 1.3 | 1.268 | 0.060 | 7.2 | 0.49 | 2.5 | 0.624 | 0.352 | 0.9 | 36.48 | 0.2 | 28.33 | 0.2 | 0.027 | 11.0 |
| 05-10-102_m1_pt8 | 0.051 | 14.2 | 1.53 | 1.1 | 1.616 | 0.043 | 9.9 | 0.20 | 5.6 | 0.261 | 0.386 | 0.9 | 37.80 | 0.2 | 28.40 | 0.2 | 0.036 | 8.3 |
| 05-10-102_m1_pt9 | 0.051 | 14.0 | 1.35 | 1.2 | 1.425 | 0.037 | 11.6 | 0.02 | 50.1 | 0.028 | 0.207 | 1.4 | 37.53 | 0.2 | 28.28 | 0.2 | 0.030 | 9.9 |
| 05-10-102_m1_pt10 | 0.024 | 29.3 | 1.08 | 1.5 | 1.137 | 0.028 | 15.2 | 0.02 | 62.4 | 0.023 | 0.215 | 1.4 | 37.66 | 0.2 | 28.40 | 0.2 | 0.027 | 11.2 |
| 05-10-102_m1_pt11 | 0.032 | 22.2 | 1.25 | 1.3 | 1.320 | 0.041 | 10.4 | 0.02 | 59.1 | 0.024 | 0.222 | 1.4 | 37.45 | 0.2 | 28.31 | 0.2 | 0.036 | 8.3 |
| 05-10-102_m1_pt12 | 0.137 | 5.3 | 1.17 | 1.4 | 1.232 | 0.039 | 10.9 | 0.30 | 3.9 | 0.382 | 0.305 | 1.1 | 36.73 | 0.2 | 28.36 | 0.2 | 0.039 | 7.6 |

| | $UO_2$ | | $ThO_2$ | | | PbO | | $Y_2O_3$ | | | CaO | | $Ce_2O_3$ | | $P_2O_5$ | | $SiO_2$ | |
|---|---|---|---|---|---|---|---|---|---|---|---|---|---|---|---|---|---|---|
| Sample | wt. % | RSD (2σ%) | wt. % | RSD (2σ%) | k-raw | wt. % | RSD (2σ%) | wt. % | RSD (2σ%) | k-raw | wt. % | RSD (2σ%) | wt. % | RSD (2σ%) | wt. % | RSD (2σ%) | wt. % | RSD (2σ%) |
| 05-10-102_m1_pt13 | 0.246 | 3.0 | 1.15 | 1.4 | 1.209 | 0.050 | 8.6 | 0.48 | 2.5 | 0.615 | 0.379 | 0.9 | 36.19 | 0.2 | 28.30 | 0.2 | 0.034 | 8.5 |
| 05-10-102_m1_pt14 | 0.247 | 3.0 | 1.18 | 1.4 | 1.244 | 0.052 | 8.2 | 0.39 | 3.0 | 0.501 | 0.418 | 0.8 | 36.81 | 0.2 | 28.31 | 0.2 | 0.033 | 9.0 |
| 05-10-102_m1_pt15 | 0.296 | 2.6 | 1.17 | 1.4 | 1.235 | 0.058 | 7.4 | 0.48 | 2.5 | 0.613 | 0.409 | 0.8 | 36.19 | 0.2 | 28.29 | 0.2 | 0.042 | 6.9 |
| 05-10-102_m1_pt16 | 0.242 | 3.1 | 1.17 | 1.4 | 1.238 | 0.060 | 7.1 | 0.40 | 3.0 | 0.511 | 0.373 | 0.9 | 36.52 | 0.2 | 28.28 | 0.2 | 0.036 | 8.1 |
| 05-10-102_m1_pt17 | 0.139 | 5.3 | 1.16 | 1.4 | 1.220 | 0.044 | 9.6 | 0.35 | 3.3 | 0.449 | 0.338 | 1.0 | 37.17 | 0.2 | 28.42 | 0.2 | 0.040 | 7.3 |
| 05-10-102_m1_pt18 | 0.049 | 14.7 | 1.18 | 1.4 | 1.243 | 0.034 | 12.4 | 0.09 | 11.9 | 0.120 | 0.232 | 1.3 | 37.81 | 0.2 | 28.52 | 0.2 | 0.035 | 8.6 |
| 05-10-102_m1_pt19 | 0.025 | 28.7 | 1.04 | 1.5 | 1.094 | 0.029 | 14.7 | 0.03 | 32.4 | 0.043 | 0.215 | 1.4 | 37.79 | 0.2 | 28.46 | 0.2 | 0.031 | 9.7 |
| 05-10-102_m1_pt20 | 0.234 | 3.2 | 1.18 | 1.4 | 1.243 | 0.050 | 8.5 | 0.40 | 3.0 | 0.508 | 0.332 | 1.0 | 36.93 | 0.2 | 28.44 | 0.2 | 0.030 | 10.0 |
| 8153-49 | 0.405 | 2.0 | 7.46 | 0.4 | 7.965 | 0.187 | 2.5 | 0.51 | 2.3 | 0.666 | 0.573 | 0.7 | 30.74 | 0.3 | 25.92 | 0.2 | 1.316 | 0.3 |
| 8153-50 | 0.402 | 2.0 | 7.61 | 0.4 | 8.125 | 0.191 | 2.5 | 0.53 | 2.3 | 0.688 | 0.584 | 0.7 | 31.44 | 0.3 | 26.23 | 0.2 | 1.335 | 0.3 |
| 8153-51 | 0.399 | 2.0 | 7.41 | 0.4 | 7.906 | 0.180 | 2.6 | 0.48 | 2.5 | 0.623 | 0.564 | 0.7 | 31.23 | 0.3 | 26.18 | 0.2 | 1.296 | 0.3 |
| 8153-52 | 0.413 | 1.9 | 7.41 | 0.4 | 7.904 | 0.193 | 2.4 | 0.51 | 2.3 | 0.667 | 0.572 | 0.7 | 31.12 | 0.3 | 26.29 | 0.2 | 1.307 | 0.3 |
| 8153-53 | 0.415 | 1.9 | 7.65 | 0.4 | 8.169 | 0.190 | 2.5 | 0.52 | 2.3 | 0.684 | 0.583 | 0.7 | 31.22 | 0.3 | 26.42 | 0.2 | 1.349 | 0.3 |
| 8153-54 | 0.405 | 2.0 | 7.72 | 0.4 | 8.241 | 0.197 | 2.4 | 0.52 | 2.3 | 0.686 | 0.591 | 0.7 | 31.46 | 0.3 | 26.70 | 0.2 | 1.386 | 0.3 |
| 8153-55 | 0.442 | 1.8 | 7.64 | 0.4 | 8.164 | 0.195 | 2.4 | 0.51 | 2.3 | 0.666 | 0.588 | 0.7 | 31.32 | 0.3 | 25.94 | 0.2 | 1.352 | 0.3 |
| 8153-56 | 0.418 | 1.9 | 7.40 | 0.4 | 7.900 | 0.196 | 2.4 | 0.50 | 2.4 | 0.649 | 0.571 | 0.7 | 31.03 | 0.3 | 25.88 | 0.2 | 1.324 | 0.3 |
| 8153-57 | 0.406 | 2.0 | 7.50 | 0.4 | 8.003 | 0.185 | 2.6 | 0.50 | 2.4 | 0.654 | 0.564 | 0.7 | 30.97 | 0.3 | 26.08 | 0.2 | 1.316 | 0.3 |
| 8153-58 | 0.412 | 2.0 | 7.52 | 0.4 | 8.032 | 0.182 | 2.6 | 0.47 | 2.5 | 0.619 | 0.572 | 0.7 | 31.15 | 0.3 | 26.12 | 0.2 | 1.333 | 0.3 |
| 05-10-102_m2_pt1 | 0.274 | 2.8 | 3.33 | 0.7 | 3.501 | 0.116 | 3.9 | 1.79 | 0.8 | 2.344 | 0.666 | 0.6 | 31.17 | 0.3 | 27.78 | 0.2 | 0.145 | 2.1 |
| 05-10-102_m2_pt2 | 0.390 | 2.0 | 3.73 | 0.6 | 3.924 | 0.139 | 3.3 | 1.81 | 0.8 | 2.369 | 0.746 | 0.5 | 31.08 | 0.3 | 27.81 | 0.2 | 0.170 | 1.8 |
| 05-10-102_m2_pt3 | 0.453 | 1.8 | 3.60 | 0.6 | 3.783 | 0.145 | 3.2 | 1.77 | 0.8 | 2.327 | 0.744 | 0.5 | 30.66 | 0.3 | 27.83 | 0.2 | 0.162 | 1.9 |
| 05-10-102_m2_pt4 | 1.548 | 0.6 | 5.89 | 0.5 | 6.229 | 0.281 | 1.8 | 1.66 | 0.8 | 2.213 | 1.508 | 0.4 | 25.96 | 0.3 | 27.48 | 0.2 | 0.086 | 3.4 |
| 05-10-102_m2_pt5 | 0.596 | 1.4 | 3.96 | 0.6 | 4.163 | 0.160 | 2.9 | 1.96 | 0.7 | 2.583 | 0.855 | 0.5 | 30.27 | 0.3 | 27.82 | 0.2 | 0.150 | 2.0 |
| 05-10-102_m2_pt6 | 0.454 | 1.8 | 3.53 | 0.6 | 3.709 | 0.134 | 3.4 | 1.85 | 0.8 | 2.428 | 0.752 | 0.5 | 30.55 | 0.3 | 27.88 | 0.2 | 0.143 | 2.1 |
| 05-10-102_m2_pt7 | 0.649 | 1.3 | 3.47 | 0.7 | 3.648 | 0.159 | 2.9 | 2.03 | 0.7 | 2.665 | 0.819 | 0.5 | 30.24 | 0.3 | 27.90 | 0.2 | 0.110 | 2.7 |
| 05-10-102_m2_pt8 | 0.394 | 2.0 | 3.27 | 0.7 | 3.435 | 0.126 | 3.6 | 1.77 | 0.8 | 2.315 | 0.699 | 0.6 | 31.73 | 0.3 | 28.02 | 0.2 | 0.132 | 2.3 |
| 05-10-102_m2_pt9 | 0.396 | 2.0 | 3.55 | 0.6 | 3.737 | 0.123 | 3.7 | 1.78 | 0.8 | 2.325 | 0.743 | 0.6 | 31.73 | 0.3 | 27.94 | 0.2 | 0.137 | 2.2 |
| 05-10-102_m2_pt10 | 0.364 | 2.1 | 3.36 | 0.7 | 3.534 | 0.128 | 3.5 | 1.76 | 0.8 | 2.301 | 0.708 | 0.6 | 31.78 | 0.2 | 27.89 | 0.2 | 0.139 | 2.2 |
| 05-10-102_m2_pt11 | 0.367 | 2.1 | 3.68 | 0.6 | 3.864 | 0.133 | 3.4 | 1.85 | 0.8 | 2.425 | 0.751 | 0.5 | 30.61 | 0.3 | 27.92 | 0.2 | 0.143 | 2.1 |
| 05-10-102_m2_pt12 | 0.366 | 2.1 | 3.77 | 0.6 | 3.959 | 0.138 | 3.3 | 1.89 | 0.8 | 2.483 | 0.757 | 0.5 | 30.42 | 0.3 | 27.89 | 0.2 | 0.156 | 2.0 |
| 05-10-102_m2_pt13 | 0.405 | 2.0 | 3.55 | 0.6 | 3.729 | 0.141 | 3.2 | 1.80 | 0.8 | 2.366 | 0.735 | 0.6 | 30.76 | 0.3 | 27.93 | 0.2 | 0.156 | 2.0 |
| 05-10-102_m2_pt14 | 0.418 | 1.9 | 3.65 | 0.6 | 3.834 | 0.135 | 3.4 | 1.91 | 0.8 | 2.504 | 0.749 | 0.6 | 30.83 | 0.3 | 27.77 | 0.2 | 0.153 | 2.0 |
| 05-10-102_m2_pt15 | 0.472 | 1.7 | 3.66 | 0.6 | 3.857 | 0.137 | 3.4 | 1.73 | 0.8 | 2.265 | 0.780 | 0.5 | 31.31 | 0.3 | 27.92 | 0.2 | 0.142 | 2.2 |
| 05-10-102_m2_pt16 | 1.040 | 0.9 | 6.65 | 0.4 | 7.052 | 0.255 | 1.9 | 1.16 | 1.1 | 1.540 | 1.662 | 0.3 | 27.20 | 0.3 | 27.65 | 0.2 | 0.065 | 4.4 |
| 05-10-102_m2_pt17 | 1.063 | 0.9 | 6.57 | 0.4 | 6.966 | 0.253 | 1.9 | 1.35 | 1.0 | 1.797 | 1.658 | 0.3 | 27.16 | 0.3 | 27.66 | 0.2 | 0.075 | 3.8 |
| 05-10-102_m2_pt18 | 1.129 | 0.8 | 7.46 | 0.4 | 7.924 | 0.280 | 1.8 | 1.23 | 1.1 | 1.646 | 1.826 | 0.3 | 26.37 | 0.3 | 27.54 | 0.2 | 0.123 | 2.4 |

| | $UO_2$ | | $ThO_2$ | | | PbO | | $Y_2O_3$ | | | CaO | | $Ce_2O_3$ | | $P_2O_5$ | | $SiO_2$ | |
|---|---|---|---|---|---|---|---|---|---|---|---|---|---|---|---|---|---|---|
| Sample | wt. % | RSD (2σ%) | wt. % | RSD (2σ%) | k-raw | wt. % | RSD (2σ%) | wt. % | RSD (2σ%) | k-raw | wt. % | RSD (2σ%) | wt. % | RSD (2σ%) | wt. % | RSD (2σ%) | wt. % | RSD (2σ%) |
| 05-10-102_m2_pt19 | 0.957 | 0.9 | 6.01 | 0.5 | 6.373 | 0.232 | 2.1 | 1.15 | 1.1 | 1.528 | 1.530 | 0.3 | 28.65 | 0.3 | 27.80 | 0.2 | 0.066 | 4.4 |
| 05-10-102_m2_pt20 | 0.819 | 1.1 | 5.80 | 0.5 | 6.147 | 0.213 | 2.3 | 1.10 | 1.2 | 1.458 | 1.443 | 0.4 | 29.10 | 0.3 | 27.81 | 0.2 | 0.052 | 5.6 |
| 05-10-102_m2_pt21 | 0.833 | 1.0 | 6.12 | 0.5 | 6.487 | 0.223 | 2.2 | 1.11 | 1.2 | 1.469 | 1.510 | 0.3 | 28.28 | 0.3 | 27.71 | 0.2 | 0.045 | 6.4 |
| 05-10-102_m2_pt22 | 0.812 | 1.1 | 5.50 | 0.5 | 5.821 | 0.202 | 2.4 | 1.10 | 1.2 | 1.455 | 1.357 | 0.4 | 29.06 | 0.3 | 27.80 | 0.2 | 0.050 | 5.8 |
| 05-10-102_m2_pt23 | 0.807 | 1.1 | 5.58 | 0.5 | 5.905 | 0.201 | 2.4 | 1.09 | 1.2 | 1.435 | 1.374 | 0.4 | 29.23 | 0.3 | 27.97 | 0.2 | 0.048 | 6.1 |
| 05-10-102_m2_pt24 | 0.853 | 1.0 | 6.18 | 0.5 | 6.553 | 0.232 | 2.1 | 1.12 | 1.2 | 1.489 | 1.536 | 0.3 | 28.45 | 0.3 | 27.85 | 0.2 | 0.056 | 5.2 |
| 05-10-102_m2_pt25 | 0.840 | 1.0 | 6.14 | 0.5 | 6.510 | 0.225 | 2.1 | 1.10 | 1.2 | 1.452 | 1.541 | 0.3 | 28.75 | 0.3 | 27.84 | 0.2 | 0.060 | 4.9 |
| 05-10-102_m2_pt26 | 0.855 | 1.0 | 6.10 | 0.5 | 6.463 | 0.219 | 2.2 | 1.11 | 1.2 | 1.476 | 1.508 | 0.4 | 28.67 | 0.3 | 27.79 | 0.2 | 0.048 | 6.0 |
| 05-10-102_m2_pt27 | 0.875 | 1.0 | 6.10 | 0.5 | 6.461 | 0.229 | 2.1 | 1.12 | 1.2 | 1.486 | 1.514 | 0.4 | 28.79 | 0.3 | 27.87 | 0.2 | 0.055 | 5.3 |
| 05-10-102_m2_pt28 | 1.084 | 0.8 | 6.67 | 0.4 | 7.059 | 0.262 | 1.9 | 1.45 | 0.9 | 1.935 | 1.717 | 0.3 | 26.69 | 0.3 | 27.69 | 0.2 | 0.058 | 4.9 |
| 05-10-102_m2_pt29 | 1.176 | 0.8 | 7.82 | 0.4 | 8.304 | 0.295 | 1.7 | 1.41 | 1.0 | 1.886 | 1.964 | 0.3 | 26.01 | 0.3 | 27.68 | 0.2 | 0.066 | 4.4 |
| 05-10-102_m2_pt30 | 0.882 | 1.0 | 6.41 | 0.5 | 6.801 | 0.234 | 2.1 | 1.14 | 1.1 | 1.516 | 1.580 | 0.3 | 28.20 | 0.3 | 27.71 | 0.2 | 0.048 | 6.0 |
| 05-10-102_m2_pt31 | 1.101 | 0.8 | 6.77 | 0.4 | 7.175 | 0.256 | 1.9 | 1.39 | 1.0 | 1.855 | 1.715 | 0.3 | 26.01 | 0.3 | 27.58 | 0.2 | 0.063 | 4.5 |
| 05-10-102_m2_pt32 | 1.003 | 0.9 | 6.86 | 0.4 | 7.275 | 0.253 | 1.9 | 1.26 | 1.0 | 1.683 | 1.699 | 0.3 | 27.19 | 0.3 | 27.70 | 0.2 | 0.063 | 4.6 |
| 05-10-102_m2_pt33 | 1.317 | 0.7 | 7.98 | 0.4 | 8.469 | 0.309 | 1.6 | 1.58 | 0.9 | 2.133 | 2.013 | 0.3 | 24.59 | 0.3 | 27.41 | 0.2 | 0.140 | 2.1 |
| 05-10-102_m2_pt34 | 0.988 | 0.9 | 6.46 | 0.5 | 6.844 | 0.239 | 2.0 | 1.33 | 1.0 | 1.769 | 1.634 | 0.3 | 27.47 | 0.3 | 27.86 | 0.2 | 0.054 | 5.3 |
| 8153-59 | 0.359 | 2.2 | 7.70 | 0.4 | 8.228 | 0.193 | 2.5 | 0.44 | 2.7 | 0.575 | 0.550 | 0.7 | 31.84 | 0.2 | 26.51 | 0.2 | 1.381 | 0.3 |
| 8153-60 | 0.349 | 2.3 | 7.58 | 0.4 | 8.092 | 0.185 | 2.6 | 0.42 | 2.8 | 0.551 | 0.555 | 0.7 | 32.21 | 0.2 | 26.44 | 0.2 | 1.362 | 0.3 |
| 8153-61 | 0.348 | 2.3 | 7.49 | 0.4 | 8.001 | 0.183 | 2.6 | 0.43 | 2.7 | 0.564 | 0.544 | 0.7 | 32.09 | 0.2 | 26.30 | 0.2 | 1.320 | 0.3 |
| 8153-62 | 0.357 | 2.2 | 7.55 | 0.4 | 8.071 | 0.189 | 2.5 | 0.44 | 2.7 | 0.569 | 0.553 | 0.7 | 32.14 | 0.2 | 26.29 | 0.2 | 1.350 | 0.3 |
| 8153-63 | 0.347 | 2.3 | 7.63 | 0.4 | 8.152 | 0.182 | 2.6 | 0.42 | 2.9 | 0.544 | 0.548 | 0.7 | 31.90 | 0.2 | 26.27 | 0.2 | 1.359 | 0.3 |
| 8153-64 | 0.363 | 2.2 | 7.44 | 0.4 | 7.951 | 0.178 | 2.7 | 0.44 | 2.7 | 0.573 | 0.539 | 0.7 | 32.18 | 0.2 | 26.28 | 0.2 | 1.316 | 0.3 |
| 8153-65 | 0.352 | 2.3 | 7.56 | 0.4 | 8.073 | 0.196 | 2.4 | 0.44 | 2.7 | 0.577 | 0.543 | 0.7 | 31.95 | 0.2 | 26.09 | 0.2 | 1.348 | 0.3 |
| 8153-66 | 0.343 | 2.3 | 7.34 | 0.4 | 7.842 | 0.182 | 2.6 | 0.43 | 2.7 | 0.564 | 0.533 | 0.7 | 32.01 | 0.2 | 26.16 | 0.2 | 1.311 | 0.3 |
| 8153-67 | 0.343 | 2.3 | 7.26 | 0.4 | 7.758 | 0.177 | 2.7 | 0.43 | 2.7 | 0.563 | 0.523 | 0.7 | 32.13 | 0.2 | 26.13 | 0.2 | 1.295 | 0.3 |
| 8153-68 | 0.345 | 2.3 | 7.37 | 0.4 | 7.872 | 0.181 | 2.6 | 0.44 | 2.7 | 0.578 | 0.536 | 0.7 | 32.09 | 0.2 | 26.00 | 0.2 | 1.306 | 0.3 |
| 8153-69 | 0.354 | 2.3 | 7.27 | 0.4 | 7.760 | 0.178 | 2.7 | 0.44 | 2.7 | 0.575 | 0.531 | 0.7 | 32.21 | 0.2 | 26.24 | 0.2 | 1.307 | 0.3 |
| 8153-70 | 0.373 | 2.2 | 7.57 | 0.4 | 8.088 | 0.186 | 2.6 | 0.43 | 2.7 | 0.564 | 0.540 | 0.7 | 31.90 | 0.2 | 26.24 | 0.2 | 1.380 | 0.3 |
| 05-10-102_m3_p1 | 1.580 | 0.6 | 8.75 | 0.4 | 9.308 | 0.352 | 1.5 | 1.49 | 0.9 | 2.020 | 2.227 | 0.3 | 23.25 | 0.3 | 27.19 | 0.2 | 0.086 | 3.4 |
| 05-10-102_m3_p2 | 1.630 | 0.6 | 9.14 | 0.4 | 9.737 | 0.368 | 1.4 | 1.29 | 1.0 | 1.743 | 2.291 | 0.3 | 22.98 | 0.3 | 27.25 | 0.2 | 0.062 | 4.7 |
| 05-10-102_m3_p3 | 1.848 | 0.6 | 10.02 | 0.4 | 10.650 | 0.404 | 1.3 | 2.22 | 0.7 | 3.039 | 2.567 | 0.3 | 20.99 | 0.3 | 27.26 | 0.2 | 0.054 | 5.3 |
| 05-10-102_m3_p4 | 1.660 | 0.6 | 9.08 | 0.4 | 9.646 | 0.368 | 1.4 | 1.84 | 0.8 | 2.494 | 2.381 | 0.3 | 22.62 | 0.3 | 27.28 | 0.2 | 0.072 | 4.0 |
| 05-10-102_m3_p5 | 1.882 | 0.5 | 9.39 | 0.4 | 9.970 | 0.387 | 1.4 | 2.19 | 0.7 | 2.997 | 2.418 | 0.3 | 21.54 | 0.3 | 27.30 | 0.2 | 0.058 | 4.9 |
| 05-10-102_m3_p6 | 1.661 | 0.6 | 8.49 | 0.4 | 8.999 | 0.362 | 1.4 | 2.35 | 0.6 | 3.193 | 2.168 | 0.3 | 22.70 | 0.3 | 27.33 | 0.2 | 0.052 | 5.5 |
| 05-10-102_m3_p7 | 2.008 | 0.5 | 10.01 | 0.4 | 10.632 | 0.425 | 1.3 | 2.44 | 0.6 | 3.350 | 2.604 | 0.3 | 20.30 | 0.3 | 27.15 | 0.2 | 0.070 | 4.1 |
| 05-10-102_m3_p8 | 1.944 | 0.5 | 9.38 | 0.4 | 9.959 | 0.404 | 1.3 | 2.24 | 0.7 | 3.064 | 2.456 | 0.3 | 20.82 | 0.3 | 27.12 | 0.2 | 0.075 | 3.8 |

| | $UO_2$ | | $ThO_2$ | | | PbO | | $Y_2O_3$ | | | CaO | | $Ce_2O_3$ | | $P_2O_5$ | | $SiO_2$ | |
|---|---|---|---|---|---|---|---|---|---|---|---|---|---|---|---|---|---|---|
| Sample | wt. % | RSD (2σ%) | wt. % | RSD (2σ%) | k-raw | wt. % | RSD (2σ%) | wt. % | RSD (2σ%) | k-raw | wt. % | RSD (2σ%) | wt. % | RSD (2σ%) | wt. % | RSD (2σ%) | wt. % | RSD (2σ%) |
| 05-10-102_m3_p9 | 1.842 | 0.6 | 8.52 | 0.4 | 9.040 | 0.374 | 1.4 | 2.08 | 0.7 | 2.826 | 2.297 | 0.3 | 22.31 | 0.3 | 27.21 | 0.2 | 0.076 | 3.8 |
| 05-10-102_m3_p10 | 1.953 | 0.5 | 8.79 | 0.4 | 9.322 | 0.398 | 1.3 | 2.25 | 0.7 | 3.069 | 2.355 | 0.3 | 21.41 | 0.3 | 27.15 | 0.2 | 0.068 | 4.2 |
| 05-10-102_m3_p11 | 1.673 | 0.6 | 8.79 | 0.4 | 9.336 | 0.368 | 1.4 | 1.83 | 0.8 | 2.486 | 2.327 | 0.3 | 22.83 | 0.3 | 27.24 | 0.2 | 0.082 | 3.5 |
| 05-10-102_m3_p12 | 1.550 | 0.6 | 8.66 | 0.4 | 9.202 | 0.341 | 1.5 | 1.76 | 0.8 | 2.389 | 2.243 | 0.3 | 22.92 | 0.3 | 27.08 | 0.2 | 0.172 | 1.7 |
| 05-10-102_m3_p13 | 1.703 | 0.6 | 9.34 | 0.4 | 9.945 | 0.380 | 1.4 | 1.49 | 0.9 | 2.027 | 2.417 | 0.3 | 22.22 | 0.3 | 27.10 | 0.2 | 0.091 | 3.2 |
| 05-10-102_m3_p14 | 1.831 | 0.6 | 10.55 | 0.3 | 11.280 | 0.412 | 1.3 | 0.95 | 1.3 | 1.291 | 2.642 | 0.3 | 21.52 | 0.3 | 26.82 | 0.2 | 0.258 | 1.2 |
| 05-10-102_m3_p15 | 1.254 | 0.8 | 8.21 | 0.4 | 8.686 | 0.327 | 1.6 | 2.40 | 0.6 | 3.250 | 2.042 | 0.3 | 23.26 | 0.3 | 27.35 | 0.2 | 0.059 | 4.8 |
| 05-10-102_m4_p1 | 0.250 | 3.1 | 4.35 | 0.6 | 4.602 | 0.131 | 3.5 | 0.35 | 3.3 | 0.462 | 1.007 | 0.5 | 32.91 | 0.2 | 28.22 | 0.2 | 0.120 | 2.5 |
| 05-10-102_m4_p2 | 0.246 | 3.1 | 4.46 | 0.6 | 4.720 | 0.125 | 3.6 | 0.35 | 3.4 | 0.450 | 1.022 | 0.4 | 32.94 | 0.2 | 28.22 | 0.2 | 0.128 | 2.4 |
| 05-10-102_m4_p3 | 0.386 | 2.1 | 5.75 | 0.5 | 6.107 | 0.167 | 2.8 | 0.46 | 2.6 | 0.596 | 1.282 | 0.4 | 32.22 | 0.2 | 27.85 | 0.2 | 0.304 | 1.1 |
| 05-10-102_m4_p4 | 0.620 | 1.3 | 5.07 | 0.5 | 5.384 | 0.180 | 2.6 | 0.43 | 2.7 | 0.561 | 1.197 | 0.4 | 32.19 | 0.2 | 28.13 | 0.2 | 0.101 | 3.0 |
| 05-10-102_m4_p5 | 0.253 | 3.0 | 3.47 | 0.7 | 3.650 | 0.106 | 4.2 | 0.75 | 1.6 | 0.968 | 0.920 | 0.5 | 31.10 | 0.3 | 26.53 | 0.2 | 1.998 | 0.3 |
| 05-10-102_m4_p6 | 0.306 | 2.5 | 3.67 | 0.6 | 3.880 | 0.117 | 3.9 | 0.51 | 2.3 | 0.663 | 0.811 | 0.5 | 32.21 | 0.2 | 27.64 | 0.2 | 0.719 | 0.5 |
| 05-10-102_m4_p7 | 0.278 | 2.8 | 3.56 | 0.6 | 3.764 | 0.109 | 4.1 | 0.41 | 2.9 | 0.532 | 0.787 | 0.5 | 33.09 | 0.2 | 28.01 | 0.2 | 0.218 | 1.5 |
| 05-10-102_m4_p8 | 0.260 | 3.0 | 3.92 | 0.6 | 4.144 | 0.118 | 3.8 | 0.35 | 3.3 | 0.455 | 0.877 | 0.5 | 33.19 | 0.2 | 28.08 | 0.2 | 0.200 | 1.6 |
| 05-10-102_m4_p9 | 0.213 | 3.6 | 3.71 | 0.6 | 3.916 | 0.104 | 4.3 | 0.60 | 2.0 | 0.786 | 0.837 | 0.5 | 33.00 | 0.2 | 28.11 | 0.2 | 0.129 | 2.4 |
| 05-10-102_m4_p10 | 0.225 | 3.4 | 3.59 | 0.6 | 3.781 | 0.116 | 3.9 | 1.37 | 1.0 | 1.794 | 0.794 | 0.5 | 31.61 | 0.3 | 28.15 | 0.2 | 0.146 | 2.1 |
| 05-10-102_m4_p11 | 0.267 | 2.9 | 3.48 | 0.7 | 3.661 | 0.107 | 4.2 | 1.36 | 1.0 | 1.770 | 0.794 | 0.5 | 31.11 | 0.3 | 27.58 | 0.2 | 1.070 | 0.4 |
| 05-10-102_m4_p12 | 0.466 | 1.7 | 4.52 | 0.6 | 4.774 | 0.150 | 3.1 | 1.00 | 1.3 | 1.313 | 1.025 | 0.4 | 31.26 | 0.3 | 27.99 | 0.2 | 0.258 | 1.3 |
| 05-10-102_m4_p13 | 0.715 | 1.2 | 7.52 | 0.4 | 8.005 | 0.251 | 1.9 | 0.69 | 1.8 | 0.913 | 1.711 | 0.3 | 28.59 | 0.3 | 28.07 | 0.2 | 0.071 | 4.2 |
| 05-10-102_m4_p14 | 0.668 | 1.3 | 7.27 | 0.4 | 7.736 | 0.240 | 2.0 | 0.52 | 2.3 | 0.683 | 1.685 | 0.3 | 28.58 | 0.3 | 27.95 | 0.2 | 0.134 | 2.3 |
| 05-10-102_m4_p15 | 0.304 | 2.6 | 4.02 | 0.6 | 4.250 | 0.123 | 3.7 | 0.42 | 2.8 | 0.550 | 0.884 | 0.5 | 33.11 | 0.2 | 28.03 | 0.2 | 0.253 | 1.3 |
| 05-10-102_m4_p16 | 0.294 | 2.6 | 3.57 | 0.6 | 3.773 | 0.105 | 4.3 | 0.40 | 2.9 | 0.522 | 0.798 | 0.5 | 33.72 | 0.2 | 28.05 | 0.2 | 0.235 | 1.4 |
| 8153-71 | 0.351 | 2.3 | 7.20 | 0.4 | 7.681 | 0.179 | 2.7 | 0.44 | 2.7 | 0.579 | 0.525 | 0.7 | 32.19 | 0.2 | 26.27 | 0.2 | 1.308 | 0.3 |
| 8153-72 | 0.366 | 2.2 | 7.47 | 0.4 | 7.973 | 0.192 | 2.5 | 0.42 | 2.8 | 0.549 | 0.542 | 0.7 | 31.98 | 0.2 | 26.29 | 0.2 | 1.364 | 0.3 |
| 8153-73 | 0.361 | 2.2 | 7.45 | 0.4 | 7.953 | 0.187 | 2.5 | 0.44 | 2.7 | 0.570 | 0.536 | 0.7 | 32.05 | 0.2 | 26.33 | 0.2 | 1.355 | 0.3 |
| 8153-74 | 0.341 | 2.3 | 7.31 | 0.4 | 7.800 | 0.183 | 2.6 | 0.41 | 2.9 | 0.540 | 0.530 | 0.7 | 31.99 | 0.2 | 26.31 | 0.2 | 1.317 | 0.3 |
| 8153-75 | 0.363 | 2.2 | 7.57 | 0.4 | 8.093 | 0.184 | 2.6 | 0.43 | 2.8 | 0.557 | 0.550 | 0.7 | 31.99 | 0.3 | 26.23 | 0.2 | 1.381 | 0.3 |
| 8153-76 | 0.361 | 2.2 | 7.62 | 0.4 | 8.140 | 0.199 | 2.4 | 0.43 | 2.8 | 0.559 | 0.548 | 0.7 | 32.20 | 0.2 | 26.44 | 0.2 | 1.375 | 0.3 |
| 8153-77 | 0.362 | 2.2 | 7.75 | 0.4 | 8.281 | 0.191 | 2.5 | 0.42 | 2.8 | 0.551 | 0.564 | 0.7 | 31.96 | 0.3 | 26.33 | 0.2 | 1.407 | 0.3 |
| 8153-78 | 0.380 | 2.1 | 7.52 | 0.4 | 8.033 | 0.186 | 2.6 | 0.44 | 2.7 | 0.571 | 0.550 | 0.7 | 32.12 | 0.2 | 26.36 | 0.2 | 1.372 | 0.3 |
| 8153-79 | 0.373 | 2.2 | 7.56 | 0.4 | 8.079 | 0.188 | 2.5 | 0.44 | 2.7 | 0.572 | 0.539 | 0.7 | 32.01 | 0.2 | 26.44 | 0.2 | 1.375 | 0.3 |
| 8153-80 | 0.375 | 2.2 | 7.61 | 0.4 | 8.126 | 0.190 | 2.5 | 0.44 | 2.7 | 0.581 | 0.552 | 0.7 | 32.02 | 0.3 | 26.74 | 0.2 | 1.397 | 0.3 |
| 8153-81 | 0.368 | 2.2 | 7.69 | 0.4 | 8.217 | 0.190 | 2.5 | 0.43 | 2.8 | 0.562 | 0.544 | 0.7 | 32.24 | 0.2 | 26.63 | 0.2 | 1.383 | 0.3 |
| 8153-82 | 0.357 | 2.2 | 7.70 | 0.4 | 8.218 | 0.195 | 2.5 | 0.43 | 2.8 | 0.568 | 0.550 | 0.7 | 31.87 | 0.3 | 26.58 | 0.2 | 1.374 | 0.3 |
| 05-10-102_m4_p17 | 0.618 | 1.4 | 5.62 | 0.5 | 5.957 | 0.196 | 2.4 | 0.50 | 2.4 | 0.661 | 1.289 | 0.4 | 29.93 | 0.3 | 28.01 | 0.2 | 0.182 | 1.7 |

| | $UO_2$ | | $ThO_2$ | | | PbO | | $Y_2O_3$ | | | CaO | | $Ce_2O_3$ | | $P_2O_5$ | | $SiO_2$ | |
|---|---|---|---|---|---|---|---|---|---|---|---|---|---|---|---|---|---|---|
| Sample | wt. % | RSD (2σ%) | wt. % | RSD (2σ%) | k-raw | wt. % | RSD (2σ%) | wt. % | RSD (2σ%) | k-raw | wt. % | RSD (2σ%) | wt. % | RSD (2σ%) | wt. % | RSD (2σ%) | wt. % | RSD (2σ%) |
| 05-10-102_m4_p18 | 0.490 | 1.7 | 4.58 | 0.6 | 4.853 | 0.157 | 3.0 | 0.47 | 2.6 | 0.611 | 1.033 | 0.4 | 31.80 | 0.3 | 28.16 | 0.2 | 0.081 | 3.7 |
| 05-10-102_m4_p19 | 0.670 | 1.3 | 8.19 | 0.4 | 8.733 | 0.265 | 1.9 | 0.54 | 2.2 | 0.714 | 1.821 | 0.3 | 28.76 | 0.3 | 28.03 | 0.2 | 0.167 | 1.9 |
| 05-10-102_m4_p20 | 0.422 | 1.9 | 5.93 | 0.5 | 6.300 | 0.179 | 2.6 | 0.35 | 3.3 | 0.454 | 1.414 | 0.4 | 30.50 | 0.3 | 27.73 | 0.2 | 0.575 | 0.6 |
| 05-10-102_m4_p21 | 0.536 | 1.5 | 4.93 | 0.5 | 5.223 | 0.169 | 2.8 | 0.46 | 2.6 | 0.609 | 1.129 | 0.4 | 31.25 | 0.3 | 28.24 | 0.2 | 0.038 | 7.7 |
| 05-10-102_m4_p22 | 0.551 | 1.5 | 6.21 | 0.5 | 6.602 | 0.205 | 2.3 | 0.52 | 2.3 | 0.678 | 1.378 | 0.4 | 31.02 | 0.3 | 27.95 | 0.2 | 0.273 | 1.2 |
| 05-10-102_m4_p23 | 0.774 | 1.1 | 8.56 | 0.4 | 9.128 | 0.279 | 1.8 | 0.54 | 2.2 | 0.719 | 1.938 | 0.3 | 27.16 | 0.3 | 27.95 | 0.2 | 0.071 | 4.1 |
| 05-10-102_m4_p24 | 0.876 | 1.0 | 6.15 | 0.5 | 6.520 | 0.224 | 2.1 | 0.57 | 2.1 | 0.750 | 1.443 | 0.4 | 28.30 | 0.3 | 27.97 | 0.2 | 0.054 | 5.3 |
| 05-10-102_m4_p25 | 0.738 | 1.2 | 6.28 | 0.5 | 6.672 | 0.218 | 2.2 | 0.52 | 2.3 | 0.685 | 1.411 | 0.4 | 29.17 | 0.3 | 27.85 | 0.2 | 0.148 | 2.1 |
| 05-10-102_m4_p26 | 0.476 | 1.7 | 4.95 | 0.5 | 5.249 | 0.163 | 2.8 | 0.47 | 2.5 | 0.620 | 1.076 | 0.4 | 31.67 | 0.3 | 27.82 | 0.2 | 0.353 | 1.0 |
| 05-10-102_m5_p1 | 0.172 | 4.4 | 4.16 | 0.6 | 4.400 | 0.123 | 3.7 | 0.43 | 2.7 | 0.565 | 0.948 | 0.5 | 31.79 | 0.3 | 28.10 | 0.2 | 0.145 | 2.1 |
| 05-10-102_m5_p2 | 0.164 | 4.6 | 4.15 | 0.6 | 4.384 | 0.120 | 3.8 | 0.42 | 2.8 | 0.542 | 0.932 | 0.5 | 31.74 | 0.3 | 27.94 | 0.2 | 0.162 | 1.9 |
| 05-10-102_m5_p3 | 0.172 | 4.4 | 4.11 | 0.6 | 4.342 | 0.121 | 3.8 | 0.39 | 3.0 | 0.510 | 0.934 | 0.5 | 31.83 | 0.3 | 27.98 | 0.2 | 0.151 | 2.0 |
| 05-10-102_m5_p4 | 0.150 | 5.0 | 4.07 | 0.6 | 4.300 | 0.120 | 3.8 | 0.38 | 3.1 | 0.493 | 0.918 | 0.5 | 31.76 | 0.3 | 27.94 | 0.2 | 0.144 | 2.1 |
| 05-10-102_m5_p5 | 0.149 | 5.0 | 4.04 | 0.6 | 4.270 | 0.116 | 3.9 | 0.34 | 3.4 | 0.444 | 0.919 | 0.5 | 31.73 | 0.3 | 27.79 | 0.2 | 0.127 | 2.4 |
| 05-10-102_m5_p6 | 0.555 | 1.5 | 5.90 | 0.5 | 6.276 | 0.187 | 2.5 | 0.35 | 3.3 | 0.460 | 1.368 | 0.4 | 31.03 | 0.3 | 27.84 | 0.2 | 0.172 | 1.8 |
| 05-10-102_m5_p7 | 0.647 | 1.3 | 5.49 | 0.5 | 5.833 | 0.189 | 2.5 | 0.37 | 3.1 | 0.490 | 1.315 | 0.4 | 31.47 | 0.3 | 27.77 | 0.2 | 0.162 | 1.9 |
| 05-10-102_m5_p8 | 0.621 | 1.3 | 5.51 | 0.5 | 5.851 | 0.189 | 2.5 | 0.36 | 3.2 | 0.475 | 1.306 | 0.4 | 31.36 | 0.3 | 27.64 | 0.2 | 0.162 | 1.9 |
| 05-10-102_m5_p9 | 0.163 | 4.6 | 4.58 | 0.6 | 4.845 | 0.125 | 3.6 | 0.35 | 3.2 | 0.461 | 0.990 | 0.5 | 31.53 | 0.3 | 27.56 | 0.2 | 0.248 | 1.3 |
| 05-10-102_m5_p10 | 0.175 | 4.3 | 4.42 | 0.6 | 4.682 | 0.125 | 3.6 | 0.39 | 3.0 | 0.503 | 0.919 | 0.5 | 31.57 | 0.3 | 27.66 | 0.2 | 0.228 | 1.4 |
| 05-10-102_m5_p11 | 0.188 | 4.0 | 4.35 | 0.6 | 4.601 | 0.122 | 3.7 | 0.39 | 3.0 | 0.503 | 0.933 | 0.5 | 32.15 | 0.2 | 27.83 | 0.2 | 0.208 | 1.5 |
| 05-10-102_m5_p12 | 0.656 | 1.3 | 6.06 | 0.5 | 6.445 | 0.199 | 2.4 | 0.39 | 2.9 | 0.515 | 1.432 | 0.4 | 31.10 | 0.3 | 27.79 | 0.2 | 0.181 | 1.7 |
| 05-10-102_m5_p13 | 0.630 | 1.3 | 6.28 | 0.5 | 6.685 | 0.209 | 2.3 | 0.39 | 2.9 | 0.519 | 1.460 | 0.4 | 30.57 | 0.3 | 27.76 | 0.2 | 0.202 | 1.5 |
| 05-10-102_m5_p14 | 0.420 | 1.9 | 7.15 | 0.4 | 7.614 | 0.209 | 2.3 | 0.45 | 2.6 | 0.586 | 1.505 | 0.4 | 30.99 | 0.3 | 27.80 | 0.2 | 0.332 | 1.0 |
| 05-10-102_m5_p15 | 0.334 | 2.4 | 6.66 | 0.4 | 7.086 | 0.187 | 2.5 | 0.44 | 2.7 | 0.575 | 1.291 | 0.4 | 30.93 | 0.3 | 27.56 | 0.2 | 0.429 | 0.8 |
| 05-10-102_m5_p16 | 0.500 | 1.6 | 6.02 | 0.5 | 6.392 | 0.190 | 2.5 | 0.40 | 2.9 | 0.519 | 1.325 | 0.4 | 30.95 | 0.3 | 27.82 | 0.2 | 0.252 | 1.3 |
| 05-10-102_m5_p17 | 0.534 | 1.5 | 5.92 | 0.5 | 6.287 | 0.194 | 2.4 | 0.37 | 3.1 | 0.488 | 1.383 | 0.4 | 31.05 | 0.3 | 27.96 | 0.2 | 0.179 | 1.7 |
| 05-10-102_m5_p18 | 0.296 | 2.6 | 5.19 | 0.5 | 5.499 | 0.154 | 3.0 | 0.34 | 3.4 | 0.439 | 1.187 | 0.4 | 31.01 | 0.3 | 27.77 | 0.2 | 0.411 | 0.8 |
| 05-10-102_m5_p19 | 0.175 | 4.3 | 3.96 | 0.6 | 4.191 | 0.118 | 3.8 | 0.40 | 2.9 | 0.525 | 0.921 | 0.5 | 32.46 | 0.2 | 28.03 | 0.2 | 0.173 | 1.8 |
| 8153-83 | 0.360 | 2.2 | 7.68 | 0.4 | 8.208 | 0.194 | 2.5 | 0.43 | 2.8 | 0.556 | 0.547 | 0.7 | 31.82 | 0.3 | 26.24 | 0.2 | 1.379 | 0.3 |
| 8153-84 | 0.359 | 2.2 | 7.48 | 0.4 | 7.991 | 0.189 | 2.5 | 0.46 | 2.6 | 0.596 | 0.544 | 0.7 | 31.95 | 0.3 | 26.40 | 0.2 | 1.353 | 0.3 |
| 8153-85 | 0.334 | 2.4 | 7.32 | 0.4 | 7.811 | 0.185 | 2.6 | 0.43 | 2.7 | 0.566 | 0.536 | 0.7 | 31.91 | 0.3 | 26.37 | 0.2 | 1.314 | 0.3 |
| 8153-86 | 0.342 | 2.4 | 7.46 | 0.4 | 7.966 | 0.179 | 2.6 | 0.44 | 2.7 | 0.573 | 0.541 | 0.7 | 31.94 | 0.3 | 26.38 | 0.2 | 1.323 | 0.3 |
| 8153-87 | 0.330 | 2.4 | 7.31 | 0.4 | 7.805 | 0.180 | 2.6 | 0.42 | 2.8 | 0.554 | 0.530 | 0.7 | 32.07 | 0.3 | 26.30 | 0.2 | 1.297 | 0.3 |
| 8153-88 | 0.355 | 2.3 | 7.53 | 0.4 | 8.044 | 0.184 | 2.6 | 0.42 | 2.8 | 0.553 | 0.540 | 0.7 | 31.69 | 0.3 | 26.19 | 0.2 | 1.356 | 0.3 |
| 8153-89 | 0.335 | 2.4 | 7.53 | 0.4 | 8.047 | 0.183 | 2.6 | 0.45 | 2.6 | 0.587 | 0.545 | 0.7 | 31.73 | 0.3 | 26.10 | 0.2 | 1.344 | 0.3 |
| 8153-90 | 0.353 | 2.3 | 7.57 | 0.4 | 8.091 | 0.186 | 2.5 | 0.41 | 2.9 | 0.539 | 0.547 | 0.7 | 31.96 | 0.3 | 26.23 | 0.2 | 1.351 | 0.3 |

| | $UO_2$ | | $ThO_2$ | | | PbO | | $Y_2O_3$ | | | CaO | | $Ce_2O_3$ | | $P_2O_5$ | | $SiO_2$ | |
|---|---|---|---|---|---|---|---|---|---|---|---|---|---|---|---|---|---|---|
| Sample | wt. % | RSD (2σ%) | wt. % | RSD (2σ%) | k-raw | wt. % | RSD (2σ%) | wt. % | RSD (2σ%) | k-raw | wt. % | RSD (2σ%) | wt. % | RSD (2σ%) | wt. % | RSD (2σ%) | wt. % | RSD (2σ%) |
| 8153-91 | 0.353 | 2.3 | 7.54 | 0.4 | 8.063 | 0.189 | 2.5 | 0.42 | 2.8 | 0.543 | 0.538 | 0.7 | 32.07 | 0.3 | 26.13 | 0.2 | 1.341 | 0.3 |
| 8153-92 | 0.364 | 2.2 | 7.45 | 0.4 | 7.955 | 0.179 | 2.7 | 0.44 | 2.7 | 0.572 | 0.534 | 0.7 | 32.30 | 0.2 | 26.23 | 0.2 | 1.335 | 0.3 |
| 8153-93 | 0.349 | 2.3 | 7.41 | 0.4 | 7.910 | 0.185 | 2.6 | 0.43 | 2.8 | 0.557 | 0.537 | 0.7 | 32.08 | 0.3 | 26.24 | 0.2 | 1.338 | 0.3 |
| 8153-94 | 0.346 | 2.3 | 7.27 | 0.4 | 7.761 | 0.181 | 2.6 | 0.43 | 2.8 | 0.556 | 0.531 | 0.7 | 32.36 | 0.2 | 26.37 | 0.2 | 1.332 | 0.3 |
| 05-10-102_m5_p20 | 0.170 | 4.5 | 4.25 | 0.6 | 4.494 | 0.123 | 3.7 | 0.41 | 2.9 | 0.532 | 0.991 | 0.5 | 32.13 | 0.3 | 27.89 | 0.2 | 0.160 | 1.9 |
| 05-10-102_m5_p21 | 0.575 | 1.4 | 7.90 | 0.4 | 8.435 | 0.246 | 2.0 | 0.43 | 2.7 | 0.565 | 1.786 | 0.3 | 30.23 | 0.3 | 27.89 | 0.2 | 0.209 | 1.5 |
| 05-10-102_m5_p22 | 0.559 | 1.5 | 6.85 | 0.4 | 7.304 | 0.221 | 2.2 | 0.40 | 2.9 | 0.526 | 1.548 | 0.3 | 30.97 | 0.3 | 27.71 | 0.2 | 0.223 | 1.4 |
| 05-10-102_m5_p23 | 0.404 | 2.0 | 6.98 | 0.4 | 7.434 | 0.211 | 2.3 | 0.46 | 2.6 | 0.603 | 1.454 | 0.4 | 30.38 | 0.3 | 27.46 | 0.2 | 0.346 | 1.0 |
| 05-10-102_m5_p24 | 0.568 | 1.5 | 7.53 | 0.4 | 8.034 | 0.228 | 2.1 | 0.43 | 2.7 | 0.573 | 1.704 | 0.3 | 30.30 | 0.3 | 27.74 | 0.2 | 0.207 | 1.5 |
| 05-10-102_m5_p25 | 0.550 | 1.5 | 7.27 | 0.4 | 7.740 | 0.228 | 2.1 | 0.42 | 2.8 | 0.557 | 1.663 | 0.3 | 30.37 | 0.3 | 27.95 | 0.2 | 0.352 | 1.0 |
| 05-10-102_m5_p26 | 0.563 | 1.5 | 7.52 | 0.4 | 8.018 | 0.236 | 2.1 | 0.44 | 2.7 | 0.582 | 1.684 | 0.3 | 29.68 | 0.3 | 27.68 | 0.2 | 0.232 | 1.4 |
| 05-10-102_m5_p27 | 0.616 | 1.4 | 6.38 | 0.5 | 6.789 | 0.207 | 2.3 | 0.40 | 2.9 | 0.533 | 1.473 | 0.4 | 30.62 | 0.3 | 27.67 | 0.2 | 0.215 | 1.5 |
| 05-10-102_m5_p28 | 0.613 | 1.4 | 6.14 | 0.5 | 6.533 | 0.207 | 2.3 | 0.39 | 3.0 | 0.509 | 1.440 | 0.4 | 31.06 | 0.3 | 27.77 | 0.2 | 0.191 | 1.6 |
| 05-10-102_m5_p29 | 0.178 | 4.2 | 4.11 | 0.6 | 4.355 | 0.115 | 3.9 | 0.37 | 3.1 | 0.476 | 0.911 | 0.5 | 31.61 | 0.3 | 26.96 | 0.2 | 0.279 | 1.2 |
| 05-10-102_m5_p30 | 0.161 | 4.7 | 4.46 | 0.6 | 4.724 | 0.121 | 3.8 | 0.40 | 2.9 | 0.522 | 0.988 | 0.5 | 31.50 | 0.3 | 27.82 | 0.2 | 0.182 | 1.7 |
| 05-10-102_m5_p31 | 0.544 | 1.5 | 5.89 | 0.5 | 6.256 | 0.185 | 2.6 | 0.40 | 2.9 | 0.521 | 1.338 | 0.4 | 30.92 | 0.3 | 27.84 | 0.2 | 0.180 | 1.7 |
| 05-10-102_m5_p32 | 0.444 | 1.8 | 6.47 | 0.5 | 6.891 | 0.186 | 2.5 | 0.40 | 2.9 | 0.528 | 1.424 | 0.4 | 30.51 | 0.3 | 26.73 | 0.2 | 0.284 | 1.1 |
| 05-10-102_m5_p33 | 0.510 | 1.6 | 9.51 | 0.4 | 10.177 | 0.283 | 1.8 | 0.52 | 2.3 | 0.687 | 1.973 | 0.3 | 28.45 | 0.3 | 27.51 | 0.2 | 0.420 | 0.8 |
| 05-10-102_m5_p34 | 0.461 | 1.8 | 8.44 | 0.4 | 9.019 | 0.238 | 2.0 | 0.47 | 2.5 | 0.616 | 1.793 | 0.3 | 28.75 | 0.3 | 27.02 | 0.2 | 0.354 | 0.9 |
| 05-10-102_m5_p35 | 0.223 | 3.5 | 5.91 | 0.5 | 6.284 | 0.164 | 2.8 | 0.31 | 3.7 | 0.403 | 1.138 | 0.4 | 31.24 | 0.3 | 27.49 | 0.2 | 0.369 | 0.9 |
| 05-10-102_m5_p36 | 0.257 | 3.0 | 5.42 | 0.5 | 5.751 | 0.150 | 3.1 | 0.40 | 2.9 | 0.519 | 1.129 | 0.4 | 31.71 | 0.3 | 27.67 | 0.2 | 0.309 | 1.1 |
| 05-10-102_m5_p37 | 0.560 | 1.5 | 8.01 | 0.4 | 8.545 | 0.246 | 2.0 | 0.43 | 2.7 | 0.567 | 1.799 | 0.3 | 30.08 | 0.3 | 27.96 | 0.2 | 0.211 | 1.5 |
| 05-10-102_m6_p1 | 0.642 | 1.3 | 3.39 | 0.7 | 3.557 | 0.162 | 2.9 | 2.52 | 0.6 | 3.319 | 0.882 | 0.5 | 29.52 | 0.3 | 28.11 | 0.2 | 0.085 | 3.5 |
| 05-10-102_m6_p2 | 0.346 | 2.3 | 4.26 | 0.6 | 4.486 | 0.149 | 3.1 | 1.56 | 0.9 | 2.045 | 0.919 | 0.5 | 30.81 | 0.3 | 28.11 | 0.2 | 0.082 | 3.7 |
| 05-10-102_m6_p3 | 0.512 | 1.6 | 3.96 | 0.6 | 4.175 | 0.142 | 3.3 | 1.03 | 1.3 | 1.350 | 0.840 | 0.5 | 31.37 | 0.3 | 27.78 | 0.2 | 0.151 | 2.1 |
| 05-10-102_m6_p4 | 0.551 | 1.5 | 4.07 | 0.6 | 4.281 | 0.164 | 2.8 | 1.98 | 0.7 | 2.601 | 0.956 | 0.5 | 30.23 | 0.3 | 28.12 | 0.2 | 0.080 | 3.7 |
| 05-10-102_m6_p5 | 0.556 | 1.5 | 4.03 | 0.6 | 4.242 | 0.156 | 3.0 | 1.96 | 0.8 | 2.577 | 0.955 | 0.5 | 30.21 | 0.3 | 28.14 | 0.2 | 0.055 | 5.3 |
| 05-10-102_m6_p6 | 0.397 | 2.0 | 4.10 | 0.6 | 4.344 | 0.134 | 3.4 | 0.36 | 3.3 | 0.464 | 0.793 | 0.5 | 32.54 | 0.2 | 27.92 | 0.2 | 0.186 | 1.7 |
| 05-10-102_m6_p7 | 0.380 | 2.1 | 3.59 | 0.6 | 3.794 | 0.124 | 3.7 | 0.34 | 3.5 | 0.439 | 0.730 | 0.6 | 32.97 | 0.2 | 28.20 | 0.2 | 0.154 | 2.0 |
| 05-10-102_m6_p8 | 0.363 | 2.2 | 3.40 | 0.7 | 3.598 | 0.114 | 4.0 | 0.42 | 2.8 | 0.548 | 0.699 | 0.6 | 32.98 | 0.2 | 28.06 | 0.2 | 0.135 | 2.3 |
| 05-10-102_m6_p9 | 0.452 | 1.8 | 3.52 | 0.7 | 3.708 | 0.133 | 3.4 | 1.18 | 1.1 | 1.547 | 0.789 | 0.5 | 31.72 | 0.3 | 28.14 | 0.2 | 0.097 | 3.1 |
| 05-10-102_m6_p10 | 0.487 | 1.7 | 3.71 | 0.6 | 3.901 | 0.135 | 3.4 | 1.57 | 0.9 | 2.057 | 0.850 | 0.5 | 30.79 | 0.3 | 28.11 | 0.2 | 0.088 | 3.4 |
| 05-10-102_m6_p11 | 0.395 | 2.0 | 3.98 | 0.6 | 4.207 | 0.133 | 3.5 | 0.54 | 2.3 | 0.699 | 0.768 | 0.5 | 31.91 | 0.3 | 27.83 | 0.2 | 0.156 | 2.0 |
| 05-10-102_m6_p12 | 0.381 | 2.1 | 3.86 | 0.6 | 4.061 | 0.137 | 3.4 | 1.49 | 0.9 | 1.953 | 0.764 | 0.5 | 31.41 | 0.3 | 28.17 | 0.2 | 0.125 | 2.4 |
| 05-10-102_m6_p13 | 0.370 | 2.1 | 3.56 | 0.7 | 3.752 | 0.127 | 3.6 | 0.86 | 1.5 | 1.119 | 0.718 | 0.6 | 32.30 | 0.2 | 28.05 | 0.2 | 0.132 | 2.4 |
| 05-10-102_m6_p14 | 0.241 | 3.2 | 3.19 | 0.7 | 3.366 | 0.096 | 4.7 | 0.34 | 3.5 | 0.437 | 0.624 | 0.6 | 33.10 | 0.2 | 28.06 | 0.2 | 0.129 | 2.4 |

| | $UO_2$ | | $ThO_2$ | | | PbO | | $Y_2O_3$ | | | CaO | | $Ce_2O_3$ | | $P_2O_5$ | | $SiO_2$ | |
|---|---|---|---|---|---|---|---|---|---|---|---|---|---|---|---|---|---|---|
| Sample | wt. % | RSD (2σ%) | wt. % | RSD (2σ%) | k-raw | wt. % | RSD (2σ%) | wt. % | RSD (2σ%) | k-raw | wt. % | RSD (2σ%) | wt. % | RSD (2σ%) | wt. % | RSD (2σ%) | wt. % | RSD (2σ%) |
| 05-10-102_m6_p15 | 0.377 | 2.1 | 3.41 | 0.7 | 3.608 | 0.122 | 3.7 | 0.40 | 2.9 | 0.526 | 0.683 | 0.6 | 33.04 | 0.2 | 28.12 | 0.2 | 0.155 | 2.0 |
| 05-10-102_m6_p16 | 0.735 | 1.2 | 3.28 | 0.7 | 3.436 | 0.154 | 3.0 | 2.70 | 0.6 | 3.568 | 0.908 | 0.5 | 29.58 | 0.3 | 27.97 | 0.2 | 0.137 | 2.2 |
| 05-10-102_m6_p17 | 0.520 | 1.6 | 3.78 | 0.6 | 3.973 | 0.155 | 3.0 | 1.98 | 0.7 | 2.601 | 0.939 | 0.5 | 29.74 | 0.3 | 27.71 | 0.2 | 0.149 | 2.1 |
| 05-10-102_m6_p18 | 0.509 | 1.6 | 3.90 | 0.6 | 4.104 | 0.158 | 3.0 | 1.97 | 0.8 | 2.589 | 0.910 | 0.5 | 30.33 | 0.3 | 28.16 | 0.2 | 0.057 | 5.2 |
| 05-10-102_m6_p19 | 0.439 | 1.8 | 3.96 | 0.6 | 4.159 | 0.143 | 3.3 | 1.88 | 0.8 | 2.470 | 0.894 | 0.5 | 30.37 | 0.3 | 28.06 | 0.2 | 0.210 | 1.5 |
| 05-10-102_m6_p20 | 0.359 | 2.2 | 3.29 | 0.7 | 3.469 | 0.110 | 4.1 | 0.42 | 2.8 | 0.544 | 0.716 | 0.6 | 32.27 | 0.2 | 27.51 | 0.2 | 1.024 | 0.4 |
| 05-10-102_m6_p21 | 0.366 | 2.2 | 3.46 | 0.7 | 3.642 | 0.126 | 3.6 | 1.57 | 0.9 | 2.051 | 0.687 | 0.6 | 31.23 | 0.3 | 27.36 | 0.2 | 0.129 | 2.3 |
| 8153-95 | 0.339 | 2.4 | 7.52 | 0.4 | 8.034 | 0.192 | 2.5 | 0.43 | 2.8 | 0.559 | 0.539 | 0.7 | 31.87 | 0.3 | 26.07 | 0.2 | 1.366 | 0.3 |
| 8153-96 | 0.346 | 2.3 | 7.39 | 0.4 | 7.890 | 0.183 | 2.6 | 0.43 | 2.8 | 0.560 | 0.535 | 0.7 | 32.03 | 0.3 | 26.32 | 0.2 | 1.335 | 0.3 |
| 8153-97 | 0.336 | 2.4 | 7.35 | 0.4 | 7.850 | 0.180 | 2.7 | 0.43 | 2.8 | 0.562 | 0.528 | 0.7 | 31.95 | 0.3 | 26.36 | 0.2 | 1.345 | 0.3 |
| 8153-98 | 0.346 | 2.3 | 7.33 | 0.4 | 7.826 | 0.179 | 2.7 | 0.45 | 2.7 | 0.583 | 0.544 | 0.7 | 32.06 | 0.3 | 26.36 | 0.2 | 1.339 | 0.3 |
| 8153-99 | 0.368 | 2.2 | 7.61 | 0.4 | 8.130 | 0.198 | 2.4 | 0.45 | 2.7 | 0.589 | 0.544 | 0.7 | 31.75 | 0.3 | 26.28 | 0.2 | 1.383 | 0.3 |
| 8153-100 | 0.365 | 2.2 | 7.62 | 0.4 | 8.138 | 0.192 | 2.5 | 0.43 | 2.8 | 0.561 | 0.548 | 0.7 | 31.69 | 0.3 | 26.30 | 0.2 | 1.398 | 0.3 |
| 8153-101 | 0.372 | 2.2 | 7.49 | 0.4 | 7.995 | 0.191 | 2.5 | 0.43 | 2.8 | 0.563 | 0.540 | 0.7 | 32.01 | 0.3 | 26.34 | 0.2 | 1.362 | 0.3 |
| 8153-102 | 0.357 | 2.3 | 7.52 | 0.4 | 8.030 | 0.189 | 2.5 | 0.45 | 2.7 | 0.584 | 0.545 | 0.7 | 31.69 | 0.3 | 26.33 | 0.2 | 1.357 | 0.3 |
| 8153-103 | 0.354 | 2.3 | 7.67 | 0.4 | 8.194 | 0.187 | 2.6 | 0.43 | 2.8 | 0.557 | 0.553 | 0.7 | 31.52 | 0.3 | 26.32 | 0.2 | 1.382 | 0.3 |
| 8153-104 | 0.361 | 2.2 | 7.73 | 0.4 | 8.257 | 0.188 | 2.5 | 0.44 | 2.7 | 0.573 | 0.557 | 0.7 | 31.72 | 0.3 | 26.20 | 0.2 | 1.384 | 0.3 |
| 05-10-102_m6_p22 | 0.501 | 1.6 | 4.53 | 0.6 | 4.794 | 0.150 | 3.1 | 0.47 | 2.6 | 0.610 | 0.858 | 0.5 | 32.07 | 0.3 | 27.80 | 0.2 | 0.222 | 1.5 |
| 05-10-102_m6_p23 | 0.497 | 1.6 | 4.41 | 0.6 | 4.674 | 0.148 | 3.1 | 0.51 | 2.4 | 0.665 | 0.843 | 0.5 | 31.98 | 0.3 | 27.89 | 0.2 | 0.209 | 1.5 |
| 05-10-102_m6_p24 | 0.490 | 1.7 | 4.53 | 0.6 | 4.801 | 0.165 | 2.8 | 0.52 | 2.3 | 0.679 | 0.867 | 0.5 | 32.11 | 0.3 | 27.92 | 0.2 | 0.223 | 1.4 |
| 05-10-102_m6_p25 | 0.521 | 1.6 | 4.65 | 0.5 | 4.930 | 0.169 | 2.8 | 0.59 | 2.1 | 0.774 | 0.893 | 0.5 | 31.66 | 0.3 | 27.60 | 0.2 | 0.241 | 1.3 |
| 05-10-102_m6_p26 | 0.496 | 1.6 | 4.33 | 0.6 | 4.586 | 0.143 | 3.3 | 0.49 | 2.5 | 0.641 | 0.832 | 0.5 | 31.90 | 0.3 | 27.81 | 0.2 | 0.207 | 1.5 |
| 05-10-102_m6_p27 | 0.511 | 1.6 | 4.30 | 0.6 | 4.545 | 0.149 | 3.1 | 0.48 | 2.5 | 0.627 | 0.825 | 0.5 | 31.55 | 0.3 | 27.85 | 0.2 | 0.208 | 1.5 |
| 05-10-102_m6_p28 | 0.517 | 1.6 | 4.53 | 0.6 | 4.796 | 0.153 | 3.1 | 0.54 | 2.3 | 0.701 | 0.865 | 0.5 | 31.98 | 0.3 | 28.01 | 0.2 | 0.222 | 1.5 |
| 05-10-102_m6_p29 | 0.514 | 1.6 | 4.61 | 0.6 | 4.876 | 0.161 | 2.9 | 0.62 | 2.0 | 0.805 | 0.881 | 0.5 | 31.84 | 0.3 | 27.95 | 0.2 | 0.229 | 1.4 |
| 05-10-102_m6_p30 | 0.515 | 1.6 | 4.58 | 0.6 | 4.842 | 0.160 | 2.9 | 0.71 | 1.8 | 0.922 | 0.876 | 0.5 | 31.60 | 0.3 | 27.92 | 0.2 | 0.226 | 1.4 |
| 05-10-102_m6_p31 | 0.495 | 1.7 | 4.23 | 0.6 | 4.475 | 0.139 | 3.3 | 0.83 | 1.5 | 1.088 | 0.817 | 0.5 | 31.59 | 0.3 | 27.93 | 0.2 | 0.207 | 1.5 |
| 05-10-102_m6_p32 | 0.546 | 1.5 | 4.02 | 0.6 | 4.245 | 0.151 | 3.1 | 1.07 | 1.2 | 1.404 | 0.839 | 0.5 | 31.60 | 0.3 | 28.04 | 0.2 | 0.169 | 1.9 |
| 05-10-102_m6_p33 | 0.551 | 1.5 | 4.30 | 0.6 | 4.545 | 0.156 | 3.0 | 0.72 | 1.7 | 0.939 | 0.869 | 0.5 | 31.86 | 0.3 | 27.98 | 0.2 | 0.187 | 1.7 |
| 05-10-102_m6_p34 | 0.523 | 1.6 | 4.73 | 0.5 | 5.021 | 0.162 | 2.9 | 0.47 | 2.5 | 0.607 | 0.905 | 0.5 | 31.51 | 0.3 | 26.97 | 0.2 | 0.263 | 1.2 |
| 05-10-102_m6_p35 | 0.484 | 1.7 | 4.57 | 0.6 | 4.841 | 0.153 | 3.1 | 0.41 | 2.9 | 0.538 | 0.877 | 0.5 | 32.30 | 0.3 | 28.00 | 0.2 | 0.219 | 1.5 |
| 05-10-102_m6_p36 | 0.483 | 1.7 | 4.53 | 0.6 | 4.801 | 0.164 | 2.8 | 0.41 | 2.9 | 0.537 | 0.883 | 0.5 | 31.95 | 0.3 | 28.00 | 0.2 | 0.219 | 1.5 |
| 05-10-102_m6_p37 | 0.463 | 1.7 | 3.84 | 0.6 | 4.060 | 0.131 | 3.5 | 0.42 | 2.9 | 0.547 | 0.757 | 0.5 | 32.01 | 0.3 | 27.91 | 0.2 | 0.173 | 1.8 |
| 05-10-102_m6_p38 | 0.475 | 1.7 | 4.46 | 0.6 | 4.728 | 0.147 | 3.2 | 0.44 | 2.7 | 0.571 | 0.839 | 0.5 | 31.76 | 0.3 | 27.85 | 0.2 | 0.218 | 1.5 |
| 05-10-102_m6_p39 | 0.479 | 1.7 | 4.34 | 0.6 | 4.589 | 0.156 | 3.0 | 0.42 | 2.8 | 0.547 | 0.819 | 0.5 | 31.57 | 0.3 | 27.77 | 0.2 | 0.209 | 1.5 |
| 05-10-102_m6_p40 | 0.484 | 1.7 | 4.44 | 0.6 | 4.699 | 0.151 | 3.1 | 0.43 | 2.8 | 0.561 | 0.837 | 0.5 | 31.62 | 0.3 | 27.83 | 0.2 | 0.216 | 1.5 |

| | $UO_2$ | | $ThO_2$ | | | PbO | | $Y_2O_3$ | | | CaO | | $Ce_2O_3$ | | $P_2O_5$ | | $SiO_2$ | |
|---|---|---|---|---|---|---|---|---|---|---|---|---|---|---|---|---|---|---|
| Sample | wt. % | RSD (2σ%) | wt. % | RSD (2σ%) | k-raw | wt. % | RSD (2σ%) | wt. % | RSD (2σ%) | k-raw | wt. % | RSD (2σ%) | wt. % | RSD (2σ%) | wt. % | RSD (2σ%) | wt. % | RSD (2σ%) |
| 05-10-102_m6_p41 | 0.465 | 1.7 | 4.34 | 0.6 | 4.596 | 0.164 | 2.8 | 0.46 | 2.6 | 0.600 | 0.831 | 0.5 | 31.47 | 0.3 | 27.77 | 0.2 | 0.213 | 1.5 |
| 05-10-102_m6_p42 | 0.488 | 1.7 | 4.59 | 0.6 | 4.862 | 0.163 | 2.9 | 0.50 | 2.4 | 0.656 | 0.868 | 0.5 | 31.35 | 0.3 | 27.81 | 0.2 | 0.230 | 1.4 |
| 05-10-102_m6_p43 | 0.414 | 1.9 | 4.30 | 0.6 | 4.555 | 0.141 | 3.3 | 0.34 | 3.4 | 0.449 | 0.809 | 0.5 | 31.56 | 0.3 | 27.77 | 0.2 | 0.195 | 1.6 |
| 05-10-102_m6_p44 | 0.417 | 1.9 | 4.23 | 0.6 | 4.481 | 0.148 | 3.1 | 0.37 | 3.2 | 0.477 | 0.812 | 0.5 | 32.10 | 0.3 | 27.96 | 0.2 | 0.194 | 1.6 |
| 05-10-102_m6_p45 | 0.431 | 1.9 | 4.28 | 0.6 | 4.535 | 0.136 | 3.4 | 0.38 | 3.1 | 0.499 | 0.808 | 0.5 | 31.82 | 0.3 | 27.96 | 0.2 | 0.208 | 1.5 |
| 05-10-102_m6_p46 | 0.442 | 1.8 | 4.31 | 0.6 | 4.561 | 0.150 | 3.1 | 0.40 | 3.0 | 0.517 | 0.828 | 0.5 | 31.80 | 0.3 | 28.05 | 0.2 | 0.197 | 1.6 |
| 05-10-102_m6_p47 | 0.497 | 1.6 | 4.55 | 0.6 | 4.814 | 0.149 | 3.1 | 0.41 | 2.9 | 0.533 | 0.869 | 0.5 | 31.82 | 0.3 | 27.95 | 0.2 | 0.209 | 1.5 |
| 05-10-102_m6_p48 | 0.501 | 1.6 | 4.61 | 0.6 | 4.889 | 0.155 | 3.0 | 0.42 | 2.8 | 0.554 | 0.887 | 0.5 | 31.96 | 0.3 | 27.92 | 0.2 | 0.216 | 1.5 |
| 05-10-102_m6_p49 | 0.400 | 2.0 | 3.63 | 0.6 | 3.833 | 0.131 | 3.5 | 0.36 | 3.3 | 0.468 | 0.737 | 0.6 | 32.75 | 0.2 | 28.07 | 0.2 | 0.163 | 1.9 |
| 05-10-102_m6_p50 | 0.501 | 1.6 | 4.07 | 0.6 | 4.306 | 0.152 | 3.1 | 0.52 | 2.3 | 0.681 | 0.814 | 0.5 | 32.02 | 0.3 | 27.95 | 0.2 | 0.172 | 1.8 |
| 05-10-102_m6_p51 | 0.457 | 1.8 | 3.90 | 0.6 | 4.124 | 0.144 | 3.2 | 0.51 | 2.4 | 0.671 | 0.769 | 0.5 | 31.80 | 0.3 | 27.89 | 0.2 | 0.170 | 1.8 |
| 05-10-102_m6_p52 | 0.449 | 1.8 | 4.03 | 0.6 | 4.262 | 0.133 | 3.5 | 0.48 | 2.5 | 0.631 | 0.804 | 0.5 | 32.35 | 0.3 | 27.92 | 0.2 | 0.185 | 1.7 |
| 05-10-102_m6_p53 | 0.492 | 1.7 | 4.12 | 0.6 | 4.356 | 0.153 | 3.1 | 0.49 | 2.5 | 0.634 | 0.827 | 0.5 | 32.28 | 0.3 | 28.04 | 0.2 | 0.175 | 1.8 |
| 05-10-102_m6_p54 | 0.542 | 1.5 | 4.37 | 0.6 | 4.627 | 0.153 | 3.1 | 0.60 | 2.1 | 0.779 | 0.878 | 0.5 | 31.80 | 0.3 | 27.95 | 0.2 | 0.191 | 1.7 |
| 05-10-102_m6_p55 | 0.541 | 1.5 | 4.37 | 0.6 | 4.621 | 0.150 | 3.1 | 0.59 | 2.1 | 0.777 | 0.882 | 0.5 | 31.67 | 0.3 | 27.87 | 0.2 | 0.192 | 1.7 |
| 05-10-102_m6_p56 | 0.519 | 1.6 | 4.28 | 0.6 | 4.532 | 0.153 | 3.1 | 0.45 | 2.7 | 0.581 | 0.849 | 0.5 | 31.92 | 0.3 | 27.95 | 0.2 | 0.175 | 1.8 |
| 05-10-102_m6_p57 | 0.432 | 1.9 | 3.89 | 0.6 | 4.118 | 0.141 | 3.3 | 0.41 | 2.9 | 0.538 | 0.770 | 0.5 | 31.97 | 0.3 | 27.85 | 0.2 | 0.165 | 1.9 |
| 05-10-102_m6_p58 | 0.439 | 1.8 | 3.66 | 0.6 | 3.873 | 0.122 | 3.7 | 0.41 | 2.9 | 0.528 | 0.750 | 0.6 | 33.09 | 0.2 | 28.01 | 0.2 | 0.153 | 2.1 |
| 05-10-102_m6_p59 | 0.425 | 1.9 | 3.58 | 0.6 | 3.784 | 0.139 | 3.3 | 0.40 | 3.0 | 0.522 | 0.720 | 0.6 | 32.07 | 0.3 | 28.06 | 0.2 | 0.156 | 2.0 |
| 05-10-102_m6_p60 | 0.479 | 1.7 | 4.00 | 0.6 | 4.237 | 0.146 | 3.2 | 0.39 | 3.0 | 0.511 | 0.797 | 0.5 | 32.77 | 0.2 | 27.93 | 0.2 | 0.169 | 1.9 |
| 05-10-102_m6_p61 | 0.432 | 1.9 | 3.97 | 0.6 | 4.196 | 0.134 | 3.5 | 0.43 | 2.8 | 0.554 | 0.654 | 0.6 | 32.37 | 0.3 | 27.99 | 0.2 | 0.122 | 2.5 |
| 8153-105 | 0.351 | 2.3 | 7.68 | 0.4 | 8.201 | 0.184 | 2.6 | 0.44 | 2.7 | 0.574 | 0.570 | 0.7 | 31.75 | 0.3 | 26.34 | 0.2 | 1.385 | 0.3 |
| 8153-106 | 0.349 | 2.3 | 7.71 | 0.4 | 8.235 | 0.190 | 2.5 | 0.44 | 2.7 | 0.579 | 0.558 | 0.7 | 31.66 | 0.3 | 26.23 | 0.2 | 1.387 | 0.3 |
| 8153-107 | 0.383 | 2.1 | 7.77 | 0.4 | 8.305 | 0.198 | 2.4 | 0.43 | 2.8 | 0.562 | 0.555 | 0.7 | 32.28 | 0.3 | 26.52 | 0.2 | 1.406 | 0.3 |
| 8153-108 | 0.345 | 2.3 | 7.58 | 0.4 | 8.096 | 0.196 | 2.4 | 0.44 | 2.7 | 0.569 | 0.544 | 0.7 | 31.84 | 0.3 | 26.18 | 0.2 | 1.366 | 0.3 |
| 8153-109 | 0.352 | 2.3 | 7.42 | 0.4 | 7.923 | 0.186 | 2.6 | 0.43 | 2.8 | 0.562 | 0.535 | 0.7 | 32.06 | 0.3 | 26.28 | 0.2 | 1.359 | 0.3 |
| 05-10-102_m6_p62 | 0.002 | 249.6 | 0.04 | 23.1 | 0.042 | 0.013 | 26.7 | 0.00 | 100.0 | 0.000 | 0.021 | 10.9 | 0.00 | 100.0 | 0.12 | 7.3 | 0.012 | 16.3 |
| 05-10-102_m6_p63 | 0.160 | 4.3 | 0.02 | 53.3 | 0.019 | 0.094 | 4.6 | 11.22 | 0.2 | 15.465 | 0.025 | 9.6 | 0.00 | 100.0 | 8.80 | 0.3 | 12.694 | 0.1 |
| 05-10-102_m6_p64 | 0.595 | 1.4 | 4.23 | 0.6 | 4.444 | 0.182 | 2.6 | 2.06 | 0.7 | 2.714 | 0.883 | 0.5 | 30.08 | 0.3 | 28.08 | 0.2 | 0.183 | 1.7 |
| 05-10-102_m6_p65 | 0.601 | 1.4 | 4.38 | 0.6 | 4.619 | 0.169 | 2.8 | 1.51 | 0.9 | 1.980 | 0.903 | 0.5 | 30.58 | 0.3 | 27.93 | 0.2 | 0.183 | 1.7 |
| 05-10-102_m6_p66 | 0.390 | 2.0 | 3.51 | 0.6 | 3.686 | 0.136 | 3.3 | 1.88 | 0.8 | 2.460 | 0.664 | 0.6 | 30.95 | 0.3 | 27.96 | 0.2 | 0.119 | 2.5 |
| 05-10-102_m6_p67 | 0.475 | 1.7 | 3.46 | 0.7 | 3.642 | 0.138 | 3.3 | 1.30 | 1.0 | 1.697 | 0.708 | 0.6 | 30.85 | 0.3 | 27.84 | 0.2 | 0.178 | 1.7 |
| 05-10-102_m6_p68 | 0.593 | 1.4 | 4.07 | 0.6 | 4.294 | 0.150 | 3.0 | 1.39 | 1.0 | 1.819 | 0.879 | 0.5 | 30.69 | 0.3 | 27.18 | 0.2 | 0.317 | 1.0 |
| 05-10-102_m6_p69 | 0.567 | 1.4 | 4.53 | 0.6 | 4.782 | 0.169 | 2.8 | 1.25 | 1.1 | 1.634 | 0.891 | 0.5 | 31.07 | 0.3 | 27.84 | 0.2 | 0.232 | 1.4 |
| 05-10-102_m6_p70 | 0.530 | 1.5 | 4.33 | 0.6 | 4.576 | 0.167 | 2.8 | 1.05 | 1.2 | 1.376 | 0.847 | 0.5 | 31.20 | 0.3 | 27.84 | 0.2 | 0.221 | 1.4 |
| 05-10-102_m6_p71 | 0.542 | 1.5 | 4.55 | 0.5 | 4.802 | 0.162 | 2.9 | 1.24 | 1.1 | 1.621 | 0.872 | 0.5 | 30.39 | 0.3 | 27.69 | 0.2 | 0.248 | 1.3 |

| | $UO_2$ | | $ThO_2$ | | | PbO | | $Y_2O_3$ | | | CaO | | $Ce_2O_3$ | | $P_2O_5$ | | $SiO_2$ | |
|---|---|---|---|---|---|---|---|---|---|---|---|---|---|---|---|---|---|---|
| Sample | wt. % | RSD (2σ%) | wt. % | RSD (2σ%) | k-raw | wt. % | RSD (2σ%) | wt. % | RSD (2σ%) | k-raw | wt. % | RSD (2σ%) | wt. % | RSD (2σ%) | wt. % | RSD (2σ%) | wt. % | RSD (2σ%) |
| 05-10-102_m6_p72 | 0.532 | 1.5 | 4.44 | 0.6 | 4.690 | 0.162 | 2.9 | 1.19 | 1.1 | 1.563 | 0.901 | 0.5 | 30.59 | 0.3 | 27.69 | 0.2 | 0.315 | 1.0 |
| 05-10-102_m6_p73 | 0.541 | 1.5 | 4.54 | 0.5 | 4.797 | 0.165 | 2.8 | 1.28 | 1.0 | 1.683 | 0.884 | 0.5 | 30.93 | 0.3 | 27.82 | 0.2 | 0.235 | 1.3 |
| 05-10-102_m6_p74 | 0.576 | 1.4 | 4.33 | 0.6 | 4.567 | 0.167 | 2.8 | 1.37 | 1.0 | 1.799 | 0.880 | 0.5 | 30.80 | 0.3 | 27.95 | 0.2 | 0.197 | 1.6 |
| 05-10-102_m6_p75 | 0.574 | 1.4 | 4.15 | 0.6 | 4.383 | 0.159 | 2.9 | 1.36 | 1.0 | 1.778 | 0.861 | 0.5 | 31.12 | 0.3 | 27.77 | 0.2 | 0.194 | 1.6 |
| 05-10-102_m6_p76 | 0.556 | 1.5 | 3.99 | 0.6 | 4.205 | 0.151 | 3.0 | 1.20 | 1.1 | 1.574 | 0.838 | 0.5 | 31.42 | 0.3 | 28.00 | 0.2 | 0.171 | 1.8 |
| 05-10-102_m6_p77 | 0.533 | 1.5 | 4.27 | 0.6 | 4.512 | 0.157 | 2.9 | 0.81 | 1.5 | 1.058 | 0.859 | 0.5 | 31.84 | 0.2 | 27.93 | 0.2 | 0.189 | 1.6 |
| 05-10-102_m6_p78 | 0.504 | 1.6 | 3.79 | 0.6 | 3.994 | 0.154 | 3.0 | 1.06 | 1.2 | 1.392 | 0.773 | 0.5 | 28.63 | 0.3 | 26.45 | 0.2 | 0.382 | 0.9 |
| 05-10-102_m6_p79 | 0.550 | 1.5 | 4.04 | 0.6 | 4.262 | 0.149 | 3.1 | 1.28 | 1.0 | 1.676 | 0.842 | 0.5 | 30.81 | 0.3 | 27.92 | 0.2 | 0.171 | 1.8 |
| 05-10-102_m6_p80 | 0.580 | 1.4 | 4.11 | 0.6 | 4.331 | 0.159 | 2.9 | 1.37 | 1.0 | 1.802 | 0.857 | 0.5 | 30.85 | 0.3 | 27.86 | 0.2 | 0.187 | 1.7 |
| 05-10-102_m6_p81 | 0.343 | 2.2 | 2.58 | 0.8 | 2.620 | 0.155 | 3.0 | 9.25 | 0.3 | 12.744 | 0.559 | 0.7 | 20.05 | 0.3 | 24.99 | 0.2 | 0.175 | 1.7 |
| 05-10-102_m6_p82 | 0.569 | 1.4 | 4.18 | 0.6 | 4.408 | 0.165 | 2.8 | 1.26 | 1.1 | 1.650 | 0.863 | 0.5 | 31.07 | 0.3 | 27.77 | 0.2 | 0.181 | 1.7 |
| 8153-117 | 0.403 | 2.0 | 7.46 | 0.4 | 7.968 | 0.188 | 2.5 | 0.52 | 2.3 | 0.674 | 0.589 | 0.7 | 31.43 | 0.3 | 25.82 | 0.2 | 1.316 | 0.3 |
| 8153-118 | 0.393 | 2.0 | 7.37 | 0.4 | 7.873 | 0.194 | 2.4 | 0.51 | 2.3 | 0.663 | 0.587 | 0.7 | 31.38 | 0.3 | 25.86 | 0.2 | 1.323 | 0.3 |
| 8153-119 | 0.414 | 1.9 | 7.37 | 0.4 | 7.869 | 0.181 | 2.6 | 0.50 | 2.3 | 0.658 | 0.584 | 0.7 | 31.10 | 0.3 | 25.83 | 0.2 | 1.305 | 0.3 |
| 8153-120 | 0.385 | 2.1 | 7.42 | 0.4 | 7.920 | 0.176 | 2.7 | 0.49 | 2.4 | 0.639 | 0.592 | 0.6 | 31.56 | 0.2 | 26.03 | 0.2 | 1.327 | 0.3 |
| 8153-121 | 0.411 | 2.0 | 7.40 | 0.4 | 7.898 | 0.182 | 2.6 | 0.51 | 2.3 | 0.666 | 0.587 | 0.7 | 31.50 | 0.3 | 26.08 | 0.2 | 1.329 | 0.3 |
| 8153-122 | 0.405 | 2.0 | 7.45 | 0.4 | 7.952 | 0.180 | 2.6 | 0.52 | 2.3 | 0.675 | 0.598 | 0.6 | 31.66 | 0.2 | 26.12 | 0.2 | 1.325 | 0.3 |
| 8153-123 | 0.402 | 2.0 | 7.41 | 0.4 | 7.910 | 0.186 | 2.6 | 0.51 | 2.3 | 0.666 | 0.588 | 0.7 | 31.52 | 0.2 | 26.11 | 0.2 | 1.325 | 0.3 |
| 8153-124 | 0.390 | 2.1 | 7.38 | 0.4 | 7.880 | 0.186 | 2.6 | 0.51 | 2.3 | 0.662 | 0.584 | 0.7 | 31.47 | 0.3 | 26.04 | 0.2 | 1.324 | 0.3 |
| 8153-125 | 0.415 | 1.9 | 7.42 | 0.4 | 7.928 | 0.191 | 2.5 | 0.49 | 2.5 | 0.636 | 0.581 | 0.7 | 31.72 | 0.2 | 26.18 | 0.2 | 1.333 | 0.3 |
| 8153-126 | 0.406 | 2.0 | 7.39 | 0.4 | 7.893 | 0.193 | 2.5 | 0.52 | 2.3 | 0.680 | 0.586 | 0.7 | 31.76 | 0.2 | 26.28 | 0.2 | 1.325 | 0.3 |
| 8153-127 | 0.403 | 2.0 | 7.41 | 0.4 | 7.908 | 0.200 | 2.4 | 0.52 | 2.3 | 0.684 | 0.589 | 0.7 | 31.48 | 0.3 | 26.12 | 0.2 | 1.325 | 0.3 |
| 8153-128 | 0.399 | 2.0 | 7.43 | 0.4 | 7.928 | 0.193 | 2.4 | 0.52 | 2.3 | 0.679 | 0.584 | 0.7 | 31.32 | 0.3 | 26.16 | 0.2 | 1.324 | 0.3 |
| 8153-129 | 0.406 | 2.0 | 7.44 | 0.4 | 7.945 | 0.189 | 2.5 | 0.52 | 2.3 | 0.680 | 0.583 | 0.7 | 31.03 | 0.3 | 26.14 | 0.2 | 1.319 | 0.3 |
| 8153-130 | 0.399 | 2.0 | 7.46 | 0.4 | 7.960 | 0.190 | 2.5 | 0.50 | 2.4 | 0.652 | 0.597 | 0.6 | 31.43 | 0.3 | 26.15 | 0.2 | 1.324 | 0.3 |
| 8153-131 | 0.409 | 2.0 | 7.42 | 0.4 | 7.921 | 0.194 | 2.4 | 0.50 | 2.4 | 0.659 | 0.587 | 0.7 | 31.54 | 0.3 | 26.02 | 0.2 | 1.334 | 0.3 |
| 8153-132 | 0.405 | 2.0 | 7.44 | 0.4 | 7.948 | 0.183 | 2.6 | 0.49 | 2.4 | 0.635 | 0.585 | 0.7 | 31.43 | 0.3 | 25.94 | 0.2 | 1.313 | 0.3 |
| | | | | | | | | | | | | | | | | | | |
| test1 | 0.400 | 2.0 | 4.71 | 0.5 | 4.992 | 0.205 | 2.6 | 0.50 | 2.2 | 0.655 | 0.589 | 0.6 | 30.72 | 0.2 | 25.67 | 0.2 | 1.429 | 0.3 |
| test2 | 0.401 | 2.0 | 4.63 | 0.5 | 4.907 | 0.191 | 2.8 | 0.49 | 2.3 | 0.629 | 0.569 | 0.7 | 31.03 | 0.2 | 25.28 | 0.2 | 1.382 | 0.3 |
| test3 | 0.410 | 1.9 | 4.68 | 0.5 | 4.969 | 0.193 | 2.7 | 0.50 | 2.2 | 0.645 | 0.567 | 0.7 | 30.89 | 0.2 | 25.07 | 0.2 | 1.358 | 0.3 |
| test4 | 0.334 | 2.3 | 4.76 | 0.5 | 5.051 | 0.212 | 2.5 | 0.43 | 2.5 | 0.561 | 0.534 | 0.7 | 31.42 | 0.2 | 25.37 | 0.2 | 1.386 | 0.3 |
| test5 | 0.348 | 2.3 | 7.68 | 0.4 | 8.202 | 0.210 | 2.6 | 0.44 | 2.6 | 0.569 | 0.545 | 0.7 | 31.95 | 0.2 | 26.43 | 0.2 | 1.424 | 0.3 |
| test6 | 0.348 | 2.3 | 7.63 | 0.4 | 8.148 | 0.195 | 2.7 | 0.42 | 2.8 | 0.546 | 0.545 | 0.7 | 31.80 | 0.2 | 26.46 | 0.2 | 1.423 | 0.3 |
| test7 | 0.341 | 2.3 | 7.60 | 0.4 | 8.117 | 0.174 | 2.7 | 0.42 | 2.8 | 0.543 | 0.544 | 0.7 | 31.74 | 0.2 | 26.00 | 0.2 | 1.414 | 0.3 |
| 8153-01 | 0.337 | 2.3 | 7.62 | 0.4 | 8.151 | 0.186 | 2.6 | 0.42 | 2.6 | 0.552 | 0.558 | 0.7 | 31.60 | 0.2 | 25.53 | 0.2 | 1.387 | 0.3 |

| | $UO_2$ | | $ThO_2$ | | | PbO | | $Y_2O_3$ | | | CaO | | $Ce_2O_3$ | | $P_2O_5$ | | $SiO_2$ | |
|---|---|---|---|---|---|---|---|---|---|---|---|---|---|---|---|---|---|---|
| Sample | wt. % | RSD (2σ%) | wt. % | RSD (2σ%) | k-raw | wt. % | RSD (2σ%) | wt. % | RSD (2σ%) | k-raw | wt. % | RSD (2σ%) | wt. % | RSD (2σ%) | wt. % | RSD (2σ%) | wt. % | RSD (2σ%) |
| 8153-2 | 0.351 | 2.2 | 7.57 | 0.4 | 8.100 | 0.183 | 2.6 | 0.42 | 2.7 | 0.545 | 0.546 | 0.7 | 31.52 | 0.2 | 25.31 | 0.2 | 1.371 | 0.3 |
| 8153-3 | 0.352 | 2.2 | 7.60 | 0.4 | 8.131 | 0.184 | 2.6 | 0.41 | 2.7 | 0.539 | 0.541 | 0.7 | 31.57 | 0.2 | 25.37 | 0.2 | 1.372 | 0.3 |
| 8153-4 | 0.322 | 2.4 | 7.29 | 0.4 | 7.793 | 0.180 | 2.7 | 0.39 | 2.9 | 0.511 | 0.520 | 0.7 | 31.91 | 0.2 | 25.39 | 0.2 | 1.326 | 0.3 |
| 8153-5 | 0.350 | 2.3 | 7.38 | 0.4 | 7.892 | 0.181 | 2.6 | 0.43 | 2.6 | 0.564 | 0.537 | 0.7 | 32.19 | 0.2 | 25.55 | 0.2 | 1.334 | 0.3 |
| GR-05-4b_m2_1 | 0.870 | 1.0 | 3.08 | 0.7 | 3.243 | 0.138 | 3.4 | 1.16 | 1.1 | 1.523 | 0.796 | 0.5 | 30.10 | 0.3 | 27.47 | 0.2 | 0.233 | 1.3 |
| GR-05-4b_m2_2 | 0.818 | 1.0 | 3.01 | 0.7 | 3.162 | 0.144 | 3.3 | 1.30 | 1.0 | 1.699 | 0.771 | 0.5 | 29.98 | 0.3 | 27.46 | 0.2 | 0.252 | 1.2 |
| GR-05-4b_m2_3 | 0.847 | 1.0 | 3.37 | 0.7 | 3.545 | 0.167 | 2.9 | 1.08 | 1.2 | 1.420 | 0.837 | 0.5 | 30.21 | 0.3 | 27.55 | 0.2 | 0.232 | 1.3 |
| GR-05-4b_m2_4 | 1.031 | 0.9 | 3.98 | 0.6 | 4.194 | 0.184 | 2.6 | 1.16 | 1.1 | 1.531 | 0.981 | 0.5 | 28.62 | 0.3 | 27.38 | 0.2 | 0.246 | 1.3 |
| GR-05-4b_m2_5 | 1.140 | 0.8 | 3.68 | 0.6 | 3.875 | 0.190 | 2.5 | 1.30 | 1.0 | 1.702 | 0.979 | 0.5 | 29.82 | 0.3 | 27.53 | 0.2 | 0.233 | 1.3 |
| GR-05-4b_m2_6 | 0.900 | 1.0 | 3.27 | 0.7 | 3.444 | 0.159 | 3.0 | 1.15 | 1.1 | 1.501 | 0.834 | 0.5 | 30.05 | 0.3 | 27.47 | 0.2 | 0.221 | 1.4 |
| GR-05-4b_m2_7 | 0.910 | 0.9 | 3.35 | 0.7 | 3.535 | 0.162 | 2.9 | 1.10 | 1.1 | 1.437 | 0.862 | 0.5 | 30.18 | 0.3 | 27.48 | 0.2 | 0.212 | 1.5 |
| GR-05-4b_m2_8 | 0.910 | 0.9 | 3.39 | 0.6 | 3.579 | 0.156 | 3.0 | 1.05 | 1.2 | 1.378 | 0.863 | 0.5 | 30.41 | 0.3 | 27.43 | 0.2 | 0.209 | 1.5 |
| GR-05-4b_m2_9 | 0.925 | 0.9 | 2.86 | 0.7 | 3.011 | 0.154 | 3.1 | 1.11 | 1.1 | 1.447 | 0.809 | 0.5 | 30.96 | 0.2 | 27.55 | 0.2 | 0.186 | 1.6 |
| GR-05-4b_m2_10 | 0.943 | 0.9 | 2.90 | 0.7 | 3.058 | 0.149 | 3.1 | 1.15 | 1.1 | 1.498 | 0.809 | 0.5 | 30.92 | 0.2 | 27.57 | 0.2 | 0.183 | 1.7 |
| GR-05-4b_m2_11 | 0.846 | 1.0 | 3.62 | 0.6 | 3.822 | 0.152 | 3.1 | 1.02 | 1.2 | 1.330 | 0.908 | 0.5 | 29.73 | 0.3 | 26.57 | 0.2 | 0.371 | 0.9 |
| GR-05-4b_m2_12 | 0.895 | 1.0 | 3.51 | 0.6 | 3.701 | 0.162 | 2.9 | 1.06 | 1.2 | 1.385 | 0.862 | 0.5 | 30.25 | 0.3 | 26.78 | 0.2 | 0.242 | 1.3 |
| GR-05-4b_m2_13 | 0.788 | 1.1 | 3.10 | 0.7 | 3.271 | 0.150 | 3.2 | 1.04 | 1.2 | 1.352 | 0.773 | 0.5 | 30.77 | 0.2 | 27.33 | 0.2 | 0.193 | 1.6 |
| GR-05-4b_m2_14 | 0.774 | 1.1 | 3.23 | 0.7 | 3.401 | 0.148 | 3.2 | 1.06 | 1.2 | 1.382 | 0.798 | 0.5 | 30.79 | 0.2 | 27.40 | 0.2 | 0.212 | 1.5 |
| GR-05-4b_m2_15 | 0.841 | 1.0 | 3.08 | 0.7 | 3.240 | 0.152 | 3.1 | 1.20 | 1.1 | 1.565 | 0.785 | 0.5 | 30.22 | 0.3 | 27.29 | 0.2 | 0.220 | 1.4 |
| 8153-6 | 0.422 | 1.9 | 7.88 | 0.4 | 8.424 | 0.193 | 2.5 | 0.50 | 2.3 | 0.655 | 0.614 | 0.6 | 30.98 | 0.2 | 25.78 | 0.2 | 1.419 | 0.3 |
| 8153-7 | 0.403 | 2.0 | 7.60 | 0.4 | 8.113 | 0.193 | 2.5 | 0.48 | 2.4 | 0.630 | 0.587 | 0.6 | 31.26 | 0.2 | 26.00 | 0.2 | 1.400 | 0.3 |
| 8153-8 | 0.412 | 1.9 | 7.68 | 0.4 | 8.207 | 0.197 | 2.5 | 0.52 | 2.2 | 0.674 | 0.596 | 0.6 | 30.98 | 0.2 | 25.83 | 0.2 | 1.404 | 0.3 |
| 8153-9 | 0.391 | 2.0 | 7.46 | 0.4 | 7.966 | 0.191 | 2.5 | 0.49 | 2.3 | 0.640 | 0.574 | 0.7 | 31.17 | 0.2 | 25.87 | 0.2 | 1.386 | 0.3 |
| 8153-10 | 0.401 | 2.0 | 7.54 | 0.4 | 8.054 | 0.198 | 2.5 | 0.49 | 2.3 | 0.644 | 0.593 | 0.6 | 31.41 | 0.2 | 25.96 | 0.2 | 1.391 | 0.3 |
| 8153-11 | 0.395 | 2.0 | 7.60 | 0.4 | 8.114 | 0.198 | 2.4 | 0.51 | 2.2 | 0.672 | 0.590 | 0.6 | 31.60 | 0.2 | 26.06 | 0.2 | 1.408 | 0.3 |
| GR-05-4b_m2_16 | 0.989 | 0.9 | 3.63 | 0.6 | 3.829 | 0.175 | 2.7 | 1.08 | 1.2 | 1.408 | 0.862 | 0.5 | 30.33 | 0.2 | 27.08 | 0.2 | 0.223 | 1.4 |
| GR-05-4b_m2_17 | 1.398 | 0.7 | 3.94 | 0.6 | 4.156 | 0.217 | 2.3 | 1.38 | 0.9 | 1.816 | 1.135 | 0.4 | 29.19 | 0.3 | 27.05 | 0.2 | 0.225 | 1.4 |
| GR-05-4b_m2_18 | 1.135 | 0.8 | 3.89 | 0.6 | 4.107 | 0.204 | 2.4 | 1.20 | 1.1 | 1.575 | 1.029 | 0.4 | 29.66 | 0.3 | 27.09 | 0.2 | 0.227 | 1.4 |
| GR-05-4b_m2_19 | 1.108 | 0.8 | 3.73 | 0.6 | 3.940 | 0.186 | 2.6 | 1.13 | 1.1 | 1.484 | 0.967 | 0.5 | 29.98 | 0.3 | 27.16 | 0.2 | 0.231 | 1.3 |
| GR-05-4b_m2_20 | 1.274 | 0.7 | 4.23 | 0.6 | 4.477 | 0.208 | 2.4 | 1.19 | 1.1 | 1.568 | 1.106 | 0.4 | 29.53 | 0.3 | 27.01 | 0.2 | 0.258 | 1.2 |
| GR-05-4b_m2_21 | 0.885 | 1.0 | 3.07 | 0.7 | 3.235 | 0.156 | 3.0 | 1.05 | 1.2 | 1.366 | 0.801 | 0.5 | 30.58 | 0.2 | 27.00 | 0.2 | 0.199 | 1.5 |
| GR-05-4b_m2_22 | 0.912 | 1.0 | 3.11 | 0.7 | 3.282 | 0.165 | 2.9 | 1.06 | 1.2 | 1.388 | 0.822 | 0.5 | 30.88 | 0.2 | 27.04 | 0.2 | 0.209 | 1.5 |
| GR-05-4b_m2_23 | 0.773 | 1.1 | 3.07 | 0.7 | 3.236 | 0.148 | 3.2 | 1.00 | 1.2 | 1.304 | 0.784 | 0.5 | 30.74 | 0.2 | 27.03 | 0.2 | 0.191 | 1.6 |
| GR-05-4b_m2_24 | 1.341 | 0.7 | 4.50 | 0.5 | 4.756 | 0.227 | 2.2 | 1.19 | 1.1 | 1.572 | 1.156 | 0.4 | 28.92 | 0.3 | 26.99 | 0.2 | 0.280 | 1.1 |
| GR-05-4b_m2_25 | 1.419 | 0.7 | 4.50 | 0.5 | 4.757 | 0.245 | 2.0 | 1.23 | 1.0 | 1.627 | 1.206 | 0.4 | 28.92 | 0.3 | 26.96 | 0.2 | 0.264 | 1.2 |
| GR-05-4b_m2_26 | 1.265 | 0.7 | 3.98 | 0.6 | 4.200 | 0.209 | 2.3 | 1.35 | 1.0 | 1.780 | 1.057 | 0.4 | 29.37 | 0.3 | 27.01 | 0.2 | 0.245 | 1.3 |

| | $UO_2$ | | $ThO_2$ | | | PbO | | $Y_2O_3$ | | | CaO | | $Ce_2O_3$ | | $P_2O_5$ | | $SiO_2$ | |
|---|---|---|---|---|---|---|---|---|---|---|---|---|---|---|---|---|---|---|
| Sample | wt. % | RSD (2σ%) | wt. % | RSD (2σ%) | k-raw | wt. % | RSD (2σ%) | wt. % | RSD (2σ%) | k-raw | wt. % | RSD (2σ%) | wt. % | RSD (2σ%) | wt. % | RSD (2σ%) | wt. % | RSD (2σ%) |
| GR-05-4b_m2_27 | 1.130 | 0.8 | 3.84 | 0.6 | 4.058 | 0.196 | 2.5 | 1.20 | 1.1 | 1.574 | 1.023 | 0.4 | 29.72 | 0.3 | 27.03 | 0.2 | 0.221 | 1.4 |
| GR-05-4b_m2_28 | 0.837 | 1.0 | 2.92 | 0.7 | 3.062 | 0.154 | 3.0 | 1.07 | 1.2 | 1.405 | 0.733 | 0.5 | 26.52 | 0.3 | 26.69 | 0.2 | 0.172 | 1.8 |
| GR-05-4b_m2_29 | 0.776 | 1.1 | 2.78 | 0.7 | 2.928 | 0.137 | 3.4 | 1.00 | 1.2 | 1.300 | 0.714 | 0.6 | 30.88 | 0.2 | 26.23 | 0.2 | 0.180 | 1.7 |
| GR-05-4b_m2_30 | 0.835 | 1.0 | 2.80 | 0.7 | 2.954 | 0.146 | 3.2 | 1.02 | 1.2 | 1.334 | 0.736 | 0.5 | 31.06 | 0.2 | 26.83 | 0.2 | 0.173 | 1.8 |
| GR-05-4b_m2_31 | 0.764 | 1.1 | 3.29 | 0.7 | 3.467 | 0.148 | 3.2 | 0.97 | 1.3 | 1.272 | 0.820 | 0.5 | 30.63 | 0.2 | 26.72 | 0.2 | 0.209 | 1.5 |
| GR-05-4b_m2_32 | 0.785 | 1.1 | 2.94 | 0.7 | 3.100 | 0.148 | 3.2 | 1.00 | 1.2 | 1.305 | 0.725 | 0.6 | 30.76 | 0.2 | 26.71 | 0.2 | 0.198 | 1.5 |
| GR-05-4b_m2_33 | 1.081 | 0.8 | 3.70 | 0.6 | 3.906 | 0.186 | 2.6 | 1.09 | 1.2 | 1.430 | 0.943 | 0.5 | 29.98 | 0.3 | 26.75 | 0.2 | 0.252 | 1.2 |
| GR-05-4b_m2_34 | 1.412 | 0.7 | 4.64 | 0.5 | 4.910 | 0.246 | 2.0 | 1.21 | 1.1 | 1.588 | 1.189 | 0.4 | 28.93 | 0.3 | 26.67 | 0.2 | 0.274 | 1.1 |
| GR-05-4b_m2_35 | 0.761 | 1.1 | 3.03 | 0.7 | 3.193 | 0.144 | 3.2 | 1.05 | 1.2 | 1.375 | 0.770 | 0.5 | 30.85 | 0.2 | 26.94 | 0.2 | 0.183 | 1.7 |
| 8153-12 | 0.422 | 1.9 | 7.51 | 0.4 | 8.021 | 0.190 | 2.5 | 0.49 | 2.4 | 0.634 | 0.597 | 0.6 | 30.94 | 0.2 | 25.73 | 0.2 | 1.381 | 0.3 |
| 8153-13 | 0.405 | 2.0 | 7.52 | 0.4 | 8.031 | 0.183 | 2.7 | 0.48 | 2.4 | 0.625 | 0.593 | 0.6 | 30.91 | 0.2 | 25.46 | 0.2 | 1.388 | 0.3 |
| 8153-14 | 0.399 | 2.0 | 7.52 | 0.4 | 8.043 | 0.186 | 2.6 | 0.50 | 2.3 | 0.656 | 0.582 | 0.6 | 30.84 | 0.2 | 25.16 | 0.2 | 1.379 | 0.3 |
| 8153-15 | 0.407 | 2.0 | 7.39 | 0.4 | 7.892 | 0.192 | 2.5 | 0.49 | 2.3 | 0.640 | 0.568 | 0.7 | 30.95 | 0.2 | 25.36 | 0.2 | 1.372 | 0.3 |
| 8153-16 | 0.409 | 2.0 | 7.44 | 0.4 | 7.950 | 0.198 | 2.5 | 0.49 | 2.3 | 0.639 | 0.569 | 0.7 | 31.06 | 0.2 | 25.41 | 0.2 | 1.368 | 0.3 |
| GR-05-4b_m2_36 | 1.017 | 0.9 | 3.80 | 0.6 | 4.015 | 0.174 | 2.8 | 1.00 | 1.2 | 1.312 | 0.911 | 0.5 | 30.27 | 0.3 | 26.55 | 0.2 | 0.255 | 1.2 |
| GR-05-4b_m2_37 | 1.011 | 0.9 | 3.41 | 0.6 | 3.597 | 0.172 | 2.8 | 1.05 | 1.2 | 1.373 | 0.916 | 0.5 | 30.27 | 0.3 | 26.68 | 0.2 | 0.223 | 1.4 |
| GR-05-4b_m2_38 | 0.879 | 1.0 | 3.16 | 0.7 | 3.337 | 0.157 | 3.0 | 1.04 | 1.2 | 1.352 | 0.780 | 0.5 | 30.22 | 0.2 | 26.56 | 0.2 | 0.211 | 1.4 |
| GR-05-4b_m2_39 | 0.919 | 0.9 | 3.73 | 0.6 | 3.944 | 0.170 | 2.8 | 1.03 | 1.2 | 1.345 | 0.904 | 0.5 | 30.09 | 0.3 | 26.52 | 0.2 | 0.233 | 1.3 |
| GR-05-4b_m2_40 | 1.156 | 0.8 | 4.28 | 0.6 | 4.524 | 0.204 | 2.4 | 1.08 | 1.2 | 1.418 | 1.055 | 0.4 | 29.52 | 0.3 | 26.56 | 0.2 | 0.276 | 1.1 |
| GR-05-4b_m2_41 | 1.077 | 0.8 | 3.56 | 0.6 | 3.758 | 0.181 | 2.7 | 1.12 | 1.1 | 1.466 | 0.946 | 0.5 | 29.86 | 0.3 | 26.69 | 0.2 | 0.211 | 1.5 |
| GR-05-4b_m2_42 | 0.910 | 1.0 | 3.61 | 0.6 | 3.817 | 0.170 | 2.8 | 1.06 | 1.2 | 1.389 | 0.908 | 0.5 | 30.09 | 0.3 | 26.57 | 0.2 | 0.215 | 1.4 |
| GR-05-4b_m2_43 | 1.279 | 0.7 | 3.88 | 0.6 | 4.099 | 0.215 | 2.3 | 1.25 | 1.0 | 1.635 | 1.079 | 0.4 | 29.44 | 0.3 | 26.68 | 0.2 | 0.229 | 1.4 |
| GR-05-4b_m2_44 | 0.976 | 0.9 | 3.52 | 0.6 | 3.719 | 0.176 | 2.7 | 1.04 | 1.2 | 1.355 | 0.921 | 0.5 | 30.42 | 0.2 | 26.69 | 0.2 | 0.228 | 1.4 |
| GR-05-4b_m2_45 | 1.238 | 0.7 | 4.01 | 0.6 | 4.234 | 0.206 | 2.4 | 1.30 | 1.0 | 1.706 | 1.057 | 0.4 | 29.45 | 0.3 | 26.74 | 0.2 | 0.242 | 1.3 |
| 8153-17 | 0.399 | 2.0 | 7.52 | 0.4 | 8.033 | 0.194 | 2.5 | 0.52 | 2.2 | 0.677 | 0.585 | 0.6 | 31.09 | 0.2 | 25.45 | 0.2 | 1.384 | 0.3 |
| 8153-18 | 0.406 | 2.0 | 7.44 | 0.4 | 7.949 | 0.198 | 2.5 | 0.51 | 2.2 | 0.667 | 0.579 | 0.7 | 31.01 | 0.2 | 25.41 | 0.2 | 1.383 | 0.3 |
| 8153-19 | 0.405 | 2.0 | 7.51 | 0.4 | 8.031 | 0.201 | 2.4 | 0.47 | 2.4 | 0.614 | 0.588 | 0.6 | 31.07 | 0.2 | 25.24 | 0.2 | 1.387 | 0.3 |
| 8153-20 | 0.406 | 2.0 | 7.42 | 0.4 | 7.926 | 0.193 | 2.5 | 0.49 | 2.4 | 0.634 | 0.578 | 0.7 | 30.94 | 0.2 | 25.63 | 0.2 | 1.386 | 0.3 |
| 8153-21 | 0.400 | 2.0 | 7.37 | 0.4 | 7.872 | 0.194 | 2.5 | 0.51 | 2.3 | 0.665 | 0.583 | 0.7 | 31.41 | 0.2 | 26.01 | 0.2 | 1.378 | 0.3 |
| 05-5-22_m6_1 | 0.954 | 0.9 | 3.44 | 0.6 | 3.619 | 0.176 | 2.7 | 2.15 | 0.7 | 2.836 | 0.901 | 0.5 | 29.26 | 0.3 | 27.14 | 0.2 | 0.235 | 1.3 |
| 05-5-22_m6_2 | 0.912 | 0.9 | 4.15 | 0.6 | 4.378 | 0.180 | 2.7 | 1.47 | 0.9 | 1.940 | 0.968 | 0.5 | 28.89 | 0.3 | 26.89 | 0.2 | 0.285 | 1.1 |
| 05-5-22_m6_3 | 0.838 | 1.0 | 3.30 | 0.7 | 3.471 | 0.163 | 2.9 | 1.90 | 0.7 | 2.491 | 0.833 | 0.5 | 29.18 | 0.3 | 27.00 | 0.2 | 0.228 | 1.3 |
| 05-5-22_m6_4 | 1.016 | 0.9 | 5.00 | 0.5 | 5.287 | 0.207 | 2.4 | 1.45 | 0.9 | 1.918 | 1.152 | 0.4 | 28.27 | 0.3 | 26.89 | 0.2 | 0.335 | 1.0 |
| 05-5-22_m6_5 | 0.864 | 1.0 | 3.42 | 0.6 | 3.591 | 0.169 | 2.8 | 2.05 | 0.7 | 2.701 | 0.860 | 0.5 | 29.41 | 0.3 | 27.08 | 0.2 | 0.226 | 1.4 |
| 05-5-22_m6_6 | 0.840 | 1.0 | 3.30 | 0.7 | 3.468 | 0.170 | 2.8 | 2.07 | 0.7 | 2.720 | 0.824 | 0.5 | 29.45 | 0.3 | 27.10 | 0.2 | 0.224 | 1.4 |
| 05-5-22_m6_7 | 0.837 | 1.0 | 3.38 | 0.6 | 3.554 | 0.175 | 2.7 | 1.76 | 0.8 | 2.306 | 0.841 | 0.5 | 29.69 | 0.3 | 27.08 | 0.2 | 0.218 | 1.4 |

| | $UO_2$ | | $ThO_2$ | | | PbO | | $Y_2O_3$ | | | CaO | | $Ce_2O_3$ | | $P_2O_5$ | | $SiO_2$ | |
|---|---|---|---|---|---|---|---|---|---|---|---|---|---|---|---|---|---|---|
| Sample | wt. % | RSD (2σ%) | wt. % | RSD (2σ%) | k-raw | wt. % | RSD (2σ%) | wt. % | RSD (2σ%) | k-raw | wt. % | RSD (2σ%) | wt. % | RSD (2σ%) | wt. % | RSD (2σ%) | wt. % | RSD (2σ%) |
| 05-5-22_m6_8 | 1.113 | 0.8 | 4.37 | 0.6 | 4.609 | 0.208 | 2.3 | 1.93 | 0.7 | 2.556 | 1.071 | 0.4 | 28.45 | 0.3 | 26.97 | 0.2 | 0.277 | 1.1 |
| 05-5-22_m6_9 | 0.798 | 1.1 | 3.53 | 0.6 | 3.711 | 0.173 | 2.7 | 2.24 | 0.6 | 2.956 | 0.892 | 0.5 | 29.33 | 0.3 | 27.05 | 0.2 | 0.189 | 1.6 |
| 05-5-22_m4_1 | 0.931 | 0.9 | 3.69 | 0.6 | 3.866 | 0.188 | 2.6 | 2.57 | 0.6 | 3.394 | 0.936 | 0.5 | 28.92 | 0.3 | 27.54 | 0.2 | 0.269 | 1.2 |
| 05-5-22_m4_2 | 0.924 | 0.9 | 3.38 | 0.6 | 3.537 | 0.174 | 2.7 | 2.52 | 0.6 | 3.331 | 0.896 | 0.5 | 28.70 | 0.3 | 27.31 | 0.2 | 0.443 | 0.7 |
| 05-5-22_m4_3 | 0.745 | 1.1 | 3.29 | 0.7 | 3.450 | 0.162 | 2.9 | 2.13 | 0.7 | 2.804 | 0.847 | 0.5 | 29.72 | 0.3 | 27.44 | 0.2 | 0.173 | 1.7 |
| 05-5-22_m4_4 | 0.799 | 1.1 | 3.62 | 0.6 | 3.797 | 0.166 | 2.9 | 2.38 | 0.6 | 3.138 | 0.888 | 0.5 | 29.24 | 0.3 | 27.54 | 0.2 | 0.208 | 1.5 |
| 05-5-22_m4_5 | 1.033 | 0.9 | 3.44 | 0.6 | 3.611 | 0.186 | 2.6 | 2.19 | 0.7 | 2.891 | 0.901 | 0.5 | 29.09 | 0.3 | 27.46 | 0.2 | 0.209 | 1.5 |
| 05-5-22_m4_6 | 0.717 | 1.2 | 3.18 | 0.7 | 3.336 | 0.149 | 3.2 | 2.12 | 0.7 | 2.782 | 0.838 | 0.5 | 29.69 | 0.3 | 27.37 | 0.2 | 0.309 | 1.0 |
| 05-5-22_m4_7 | 0.861 | 1.0 | 3.41 | 0.6 | 3.572 | 0.170 | 2.8 | 2.41 | 0.6 | 3.176 | 0.860 | 0.5 | 29.28 | 0.3 | 27.53 | 0.2 | 0.198 | 1.5 |
| 05-5-22_m4_8 | 0.827 | 1.0 | 3.33 | 0.7 | 3.495 | 0.176 | 2.7 | 2.47 | 0.6 | 3.258 | 0.852 | 0.5 | 29.40 | 0.3 | 27.68 | 0.2 | 0.188 | 1.6 |
| 05-5-22_m4_9 | 0.877 | 1.0 | 3.57 | 0.6 | 3.742 | 0.168 | 2.9 | 2.49 | 0.6 | 3.291 | 0.934 | 0.5 | 28.76 | 0.3 | 27.53 | 0.2 | 0.201 | 1.5 |
| 05-5-22_m4_10 | 0.785 | 1.1 | 3.57 | 0.6 | 3.750 | 0.176 | 2.7 | 2.32 | 0.6 | 3.055 | 0.905 | 0.5 | 29.24 | 0.3 | 27.47 | 0.2 | 0.269 | 1.2 |
| 8153-22 | 0.396 | 2.0 | 7.40 | 0.4 | 7.902 | 0.181 | 2.7 | 0.49 | 2.3 | 0.645 | 0.570 | 0.7 | 31.08 | 0.2 | 25.78 | 0.2 | 1.367 | 0.3 |
| 8153-23 | 0.403 | 2.0 | 7.49 | 0.4 | 8.001 | 0.188 | 2.6 | 0.49 | 2.3 | 0.647 | 0.590 | 0.6 | 30.94 | 0.2 | 25.69 | 0.2 | 1.395 | 0.3 |
| 8153-24 | 0.414 | 1.9 | 7.46 | 0.4 | 7.972 | 0.182 | 2.7 | 0.50 | 2.3 | 0.648 | 0.576 | 0.7 | 30.83 | 0.2 | 25.35 | 0.2 | 1.387 | 0.3 |
| 8153-25 | 0.389 | 2.0 | 7.35 | 0.4 | 7.849 | 0.186 | 2.6 | 0.47 | 2.4 | 0.609 | 0.571 | 0.7 | 30.94 | 0.2 | 25.38 | 0.2 | 1.364 | 0.3 |
| 8153-26 | 0.413 | 1.9 | 7.56 | 0.4 | 8.082 | 0.194 | 2.5 | 0.50 | 2.3 | 0.648 | 0.584 | 0.6 | 31.00 | 0.2 | 25.42 | 0.2 | 1.411 | 0.3 |
| 05-5-22_m7_1 | 0.931 | 0.9 | 3.18 | 0.7 | 3.348 | 0.167 | 2.8 | 1.75 | 0.8 | 2.289 | 0.839 | 0.5 | 28.92 | 0.3 | 25.12 | 0.2 | 0.206 | 1.5 |
| 05-5-22_m7_2 | 0.788 | 1.1 | 3.05 | 0.7 | 3.221 | 0.153 | 3.1 | 1.70 | 0.8 | 2.219 | 0.788 | 0.5 | 29.92 | 0.3 | 25.20 | 0.2 | 0.174 | 1.7 |
| 05-5-22_m7_3 | 0.780 | 1.1 | 3.30 | 0.7 | 3.474 | 0.167 | 2.8 | 2.00 | 0.7 | 2.621 | 0.834 | 0.5 | 29.80 | 0.3 | 26.58 | 0.2 | 0.191 | 1.6 |
| 05-5-22_m7_4 | 0.780 | 1.1 | 3.12 | 0.7 | 3.275 | 0.160 | 3.0 | 1.95 | 0.7 | 2.562 | 0.794 | 0.5 | 29.98 | 0.3 | 26.74 | 0.2 | 0.173 | 1.7 |
| 05-5-22_m7_5 | 0.947 | 0.9 | 3.59 | 0.6 | 3.785 | 0.169 | 2.8 | 1.35 | 1.0 | 1.767 | 0.910 | 0.5 | 29.49 | 0.3 | 26.61 | 0.2 | 0.240 | 1.3 |
| 05-5-22_m7_6 | 1.290 | 0.7 | 3.57 | 0.6 | 3.757 | 0.215 | 2.3 | 2.09 | 0.7 | 2.756 | 1.022 | 0.4 | 28.20 | 0.3 | 26.72 | 0.2 | 0.211 | 1.4 |
| 05-5-22_m7_7 | 0.827 | 1.0 | 3.40 | 0.6 | 3.572 | 0.169 | 2.8 | 1.99 | 0.7 | 2.614 | 0.868 | 0.5 | 29.70 | 0.3 | 26.72 | 0.2 | 0.203 | 1.5 |
| 05-5-22_m7_8 | 0.816 | 1.0 | 3.19 | 0.7 | 3.364 | 0.161 | 2.9 | 1.28 | 1.0 | 1.678 | 0.788 | 0.5 | 29.90 | 0.3 | 26.57 | 0.2 | 0.214 | 1.4 |
| 05-5-22_m7_9 | 0.741 | 1.1 | 3.35 | 0.7 | 3.527 | 0.152 | 3.1 | 2.06 | 0.7 | 2.706 | 0.841 | 0.5 | 29.79 | 0.3 | 26.65 | 0.2 | 0.187 | 1.6 |
| 05-5-22_m7_10 | 0.869 | 1.0 | 3.27 | 0.7 | 3.436 | 0.169 | 2.8 | 1.88 | 0.7 | 2.481 | 0.893 | 0.5 | 28.16 | 0.3 | 26.44 | 0.2 | 0.191 | 1.6 |
| 05-5-22_m3_1 | 1.012 | 0.9 | 3.82 | 0.6 | 4.016 | 0.192 | 2.5 | 2.17 | 0.7 | 2.865 | 0.940 | 0.5 | 29.23 | 0.3 | 27.00 | 0.2 | 0.222 | 1.4 |
| 05-5-22_m3_2 | 1.084 | 0.8 | 3.95 | 0.6 | 4.152 | 0.205 | 2.4 | 2.40 | 0.6 | 3.175 | 0.998 | 0.4 | 28.70 | 0.3 | 26.94 | 0.2 | 0.234 | 1.3 |
| 05-5-22_m3_3 | 0.998 | 0.9 | 3.95 | 0.6 | 4.157 | 0.202 | 2.4 | 2.13 | 0.7 | 2.809 | 0.966 | 0.5 | 28.97 | 0.3 | 26.86 | 0.2 | 0.312 | 1.0 |
| 05-5-22_m3_4 | 1.098 | 0.8 | 4.22 | 0.6 | 4.443 | 0.213 | 2.3 | 2.24 | 0.6 | 2.953 | 1.091 | 0.4 | 27.90 | 0.3 | 26.25 | 0.2 | 0.720 | 0.5 |
| 05-5-22_m3_5 | 1.138 | 0.8 | 4.04 | 0.6 | 4.247 | 0.198 | 2.4 | 2.29 | 0.6 | 3.018 | 1.043 | 0.4 | 28.46 | 0.3 | 26.70 | 0.2 | 0.462 | 0.7 |
| 05-5-22_m3_6 | 0.892 | 1.0 | 2.75 | 0.7 | 2.885 | 0.157 | 3.0 | 2.25 | 0.6 | 2.948 | 0.834 | 0.5 | 29.66 | 0.3 | 26.85 | 0.2 | 0.168 | 1.8 |
| 05-5-22_m3_7 | 1.028 | 0.9 | 3.78 | 0.6 | 3.974 | 0.206 | 2.3 | 2.22 | 0.7 | 2.928 | 0.938 | 0.5 | 28.90 | 0.3 | 26.83 | 0.2 | 0.228 | 1.3 |
| 05-5-22_m3_8 | 1.089 | 0.8 | 3.91 | 0.6 | 4.114 | 0.204 | 2.4 | 2.34 | 0.6 | 3.090 | 0.980 | 0.5 | 28.78 | 0.3 | 26.89 | 0.2 | 0.236 | 1.3 |
| 05-5-22_m3_9 | 0.984 | 0.9 | 3.70 | 0.6 | 3.888 | 0.188 | 2.6 | 2.19 | 0.7 | 2.885 | 0.939 | 0.5 | 29.22 | 0.3 | 26.78 | 0.2 | 0.244 | 1.3 |

| | $UO_2$ | | $ThO_2$ | | | PbO | | $Y_2O_3$ | | | CaO | | $Ce_2O_3$ | | $P_2O_5$ | | $SiO_2$ | |
|---|---|---|---|---|---|---|---|---|---|---|---|---|---|---|---|---|---|---|
| Sample | wt. % | RSD (2σ%) | wt. % | RSD (2σ%) | k-raw | wt. % | RSD (2σ%) | wt. % | RSD (2σ%) | k-raw | wt. % | RSD (2σ%) | wt. % | RSD (2σ%) | wt. % | RSD (2σ%) | wt. % | RSD (2σ%) |
| 05-5-22_m3_10 | 0.980 | 0.9 | 4.02 | 0.6 | 4.225 | 0.196 | 2.5 | 2.17 | 0.7 | 2.869 | 0.988 | 0.5 | 28.89 | 0.3 | 26.91 | 0.2 | 0.245 | 1.3 |
| 05-5-22_m3_11 | 0.929 | 0.9 | 5.33 | 0.5 | 5.640 | 0.217 | 2.2 | 1.14 | 1.1 | 1.508 | 1.162 | 0.4 | 27.98 | 0.3 | 26.46 | 0.2 | 0.346 | 0.9 |
| 05-5-22_m3_12 | 0.806 | 1.1 | 2.91 | 0.7 | 3.054 | 0.156 | 3.0 | 1.98 | 0.7 | 2.594 | 0.763 | 0.5 | 29.71 | 0.3 | 26.93 | 0.2 | 0.169 | 1.8 |
| 05-5-22_m3_13 | 1.007 | 0.9 | 3.07 | 0.7 | 3.223 | 0.176 | 2.7 | 2.15 | 0.7 | 2.833 | 0.848 | 0.5 | 29.17 | 0.3 | 26.85 | 0.2 | 0.186 | 1.6 |
| 05-5-22_m3_14 | 0.853 | 1.0 | 3.24 | 0.7 | 3.400 | 0.163 | 2.9 | 2.12 | 0.7 | 2.785 | 0.825 | 0.5 | 29.36 | 0.3 | 26.87 | 0.2 | 0.206 | 1.5 |
| 05-5-22_m3_15 | 0.824 | 1.0 | 3.21 | 0.7 | 3.371 | 0.157 | 3.0 | 2.06 | 0.7 | 2.702 | 0.822 | 0.5 | 29.72 | 0.3 | 26.85 | 0.2 | 0.190 | 1.6 |
| 05-5-22_m3_16 | 1.057 | 0.8 | 4.09 | 0.6 | 4.301 | 0.209 | 2.3 | 2.27 | 0.6 | 2.994 | 1.028 | 0.4 | 28.81 | 0.3 | 26.73 | 0.2 | 0.246 | 1.3 |
| 05-5-22_m3_17 | 1.070 | 0.8 | 4.20 | 0.6 | 4.419 | 0.203 | 2.4 | 2.27 | 0.6 | 3.000 | 1.089 | 0.4 | 28.57 | 0.3 | 26.73 | 0.2 | 0.274 | 1.1 |
| 05-5-22_m3_18 | 0.928 | 0.9 | 3.93 | 0.6 | 4.136 | 0.191 | 2.5 | 2.04 | 0.7 | 2.693 | 0.978 | 0.5 | 29.23 | 0.3 | 26.80 | 0.2 | 0.256 | 1.2 |
| 05-5-22_m3_19 | 0.798 | 1.1 | 2.88 | 0.7 | 3.022 | 0.152 | 3.1 | 1.99 | 0.7 | 2.616 | 0.752 | 0.5 | 29.82 | 0.3 | 26.98 | 0.2 | 0.173 | 1.7 |
| 05-5-22_m3_20 | 1.077 | 0.8 | 3.18 | 0.7 | 3.336 | 0.185 | 2.6 | 2.02 | 0.7 | 2.659 | 0.875 | 0.5 | 28.81 | 0.3 | 26.88 | 0.2 | 0.211 | 1.4 |
| 8153-27 | 0.375 | 2.1 | 7.11 | 0.4 | 7.582 | 0.185 | 2.6 | 0.49 | 2.3 | 0.642 | 0.557 | 0.7 | 31.15 | 0.2 | 25.97 | 0.2 | 1.316 | 0.3 |
| 8153-28 | 0.375 | 2.1 | 7.12 | 0.4 | 7.598 | 0.181 | 2.7 | 0.48 | 2.3 | 0.627 | 0.561 | 0.7 | 31.24 | 0.2 | 25.97 | 0.2 | 1.305 | 0.3 |
| 8153-29 | 0.361 | 2.2 | 7.09 | 0.4 | 7.560 | 0.183 | 2.6 | 0.49 | 2.3 | 0.644 | 0.564 | 0.7 | 31.29 | 0.2 | 26.00 | 0.2 | 1.316 | 0.3 |
| 8153-30 | 0.382 | 2.1 | 7.13 | 0.4 | 7.605 | 0.179 | 2.7 | 0.50 | 2.3 | 0.646 | 0.559 | 0.7 | 31.21 | 0.2 | 26.02 | 0.2 | 1.314 | 0.3 |
| 8153-31 | 0.394 | 2.0 | 7.13 | 0.4 | 7.607 | 0.179 | 2.7 | 0.50 | 2.3 | 0.653 | 0.572 | 0.7 | 31.29 | 0.2 | 26.10 | 0.2 | 1.319 | 0.3 |
| 8153-32 | 0.374 | 2.1 | 7.14 | 0.4 | 7.615 | 0.178 | 2.7 | 0.50 | 2.3 | 0.652 | 0.569 | 0.7 | 31.38 | 0.2 | 26.26 | 0.2 | 1.321 | 0.3 |
| 8153-33 | 0.363 | 2.2 | 7.12 | 0.4 | 7.592 | 0.188 | 2.6 | 0.50 | 2.3 | 0.655 | 0.569 | 0.7 | 31.30 | 0.2 | 26.27 | 0.2 | 1.325 | 0.3 |
| 8153-34 | 0.374 | 2.1 | 7.15 | 0.4 | 7.623 | 0.189 | 2.6 | 0.52 | 2.2 | 0.675 | 0.565 | 0.7 | 31.27 | 0.2 | 26.18 | 0.2 | 1.323 | 0.3 |
| 8153-35 | 0.367 | 2.2 | 7.10 | 0.4 | 7.575 | 0.179 | 2.7 | 0.49 | 2.3 | 0.643 | 0.566 | 0.7 | 31.23 | 0.2 | 26.13 | 0.2 | 1.320 | 0.3 |
| 8153-36 | 0.378 | 2.1 | 7.07 | 0.4 | 7.538 | 0.191 | 2.5 | 0.48 | 2.3 | 0.631 | 0.558 | 0.7 | 31.13 | 0.2 | 25.92 | 0.2 | 1.298 | 0.3 |
| 8153-37 | 0.382 | 2.1 | 7.13 | 0.4 | 7.608 | 0.191 | 2.5 | 0.50 | 2.3 | 0.650 | 0.555 | 0.7 | 31.27 | 0.2 | 25.95 | 0.2 | 1.306 | 0.3 |
| 8153-38 | 0.374 | 2.1 | 7.14 | 0.4 | 7.619 | 0.184 | 2.6 | 0.48 | 2.4 | 0.624 | 0.562 | 0.7 | 31.36 | 0.2 | 25.87 | 0.2 | 1.315 | 0.3 |
| 8153-39 | 0.379 | 2.1 | 7.09 | 0.4 | 7.566 | 0.182 | 2.7 | 0.48 | 2.3 | 0.630 | 0.560 | 0.7 | 31.39 | 0.2 | 26.00 | 0.2 | 1.321 | 0.3 |
| 8153-40 | 0.368 | 2.2 | 7.13 | 0.4 | 7.601 | 0.177 | 2.7 | 0.49 | 2.3 | 0.645 | 0.573 | 0.7 | 31.43 | 0.2 | 26.15 | 0.2 | 1.326 | 0.3 |
| 8153-41 | 0.375 | 2.1 | 7.07 | 0.4 | 7.536 | 0.185 | 2.6 | 0.48 | 2.3 | 0.632 | 0.579 | 0.7 | 31.46 | 0.2 | 26.14 | 0.2 | 1.324 | 0.3 |
| 8153-42 | 0.387 | 2.0 | 7.12 | 0.4 | 7.589 | 0.182 | 2.7 | 0.49 | 2.3 | 0.637 | 0.715 | 0.6 | 31.31 | 0.2 | 26.24 | 0.2 | 1.322 | 0.3 |
| 8153-43 | 0.373 | 2.1 | 7.10 | 0.4 | 7.575 | 0.183 | 2.6 | 0.50 | 2.3 | 0.657 | 0.595 | 0.6 | 31.39 | 0.2 | 26.26 | 0.2 | 1.338 | 0.3 |
| 8153-44 | 0.375 | 2.1 | 7.15 | 0.4 | 7.621 | 0.190 | 2.6 | 0.49 | 2.3 | 0.644 | 0.565 | 0.7 | 31.27 | 0.2 | 26.28 | 0.2 | 1.320 | 0.3 |
| 8153-45 | 0.382 | 2.1 | 7.10 | 0.4 | 7.576 | 0.180 | 2.7 | 0.49 | 2.3 | 0.637 | 0.566 | 0.7 | 31.27 | 0.2 | 26.18 | 0.2 | 1.317 | 0.3 |
| 8153-46 | 0.375 | 2.1 | 7.09 | 0.4 | 7.559 | 0.183 | 2.6 | 0.50 | 2.3 | 0.646 | 0.568 | 0.7 | 31.34 | 0.2 | 26.10 | 0.2 | 1.316 | 0.3 |
| 8153-47 | 0.374 | 2.1 | 7.23 | 0.4 | 7.715 | 0.183 | 2.6 | 0.51 | 2.2 | 0.662 | 0.581 | 0.6 | 31.41 | 0.2 | 26.09 | 0.2 | 1.321 | 0.3 |
| 8153-48 | 0.377 | 2.1 | 7.21 | 0.4 | 7.691 | 0.182 | 2.6 | 0.49 | 2.3 | 0.639 | 0.568 | 0.7 | 31.31 | 0.2 | 25.90 | 0.2 | 1.314 | 0.3 |
| 8153-49 | 0.387 | 2.0 | 7.16 | 0.4 | 7.646 | 0.239 | 2.1 | 0.46 | 2.4 | 0.603 | 0.570 | 0.7 | 31.27 | 0.2 | 25.88 | 0.2 | 1.310 | 0.3 |
| 8153-50 | 0.380 | 2.1 | 7.16 | 0.4 | 7.643 | 0.177 | 2.7 | 0.50 | 2.3 | 0.656 | 0.573 | 0.7 | 31.17 | 0.2 | 25.84 | 0.2 | 1.313 | 0.3 |
| 8153-51 | 0.383 | 2.1 | 7.22 | 0.4 | 7.708 | 0.183 | 2.6 | 0.51 | 2.2 | 0.662 | 0.576 | 0.7 | 31.12 | 0.2 | 25.81 | 0.2 | 1.316 | 0.3 |

| Sample | $UO_2$ wt. % | RSD (2σ%) | $ThO_2$ wt. % | RSD (2σ%) | k-raw | PbO wt. % | RSD (2σ%) | $Y_2O_3$ wt. % | RSD (2σ%) | k-raw | CaO wt. % | RSD (2σ%) | $Ce_2O_3$ wt. % | RSD (2σ%) | $P_2O_5$ wt. % | RSD (2σ%) | $SiO_2$ wt. % | RSD (2σ%) |
|---|---|---|---|---|---|---|---|---|---|---|---|---|---|---|---|---|---|---|
| TU-1 117531 Spot-1 | 0.725 | 1.1 | 13.81 | 0.3 | 14.830 | 0.182 | 7.7 | 2.50 | 0.6 | 3.389 | 1.610 | 0.3 | 22.92 | 0.3 | 24.80 | 0.2 | 1.854 | 0.3 |
| TU-1 117531 Spot-2 | 0.731 | 1.1 | 13.66 | 0.3 | 14.668 | 0.182 | 2.7 | 2.48 | 0.6 | 3.360 | 1.605 | 0.3 | 23.05 | 0.3 | 24.87 | 0.2 | 1.826 | 0.3 |
| TU-1 117531 Spot-3 | 0.727 | 1.1 | 13.91 | 0.3 | 14.940 | 0.193 | 2.6 | 2.52 | 0.6 | 3.410 | 1.612 | 0.3 | 23.21 | 0.3 | 24.84 | 0.2 | 1.864 | 0.3 |
| TU-1 117531 Spot-4 | 0.727 | 1.1 | 13.85 | 0.3 | 14.874 | 0.187 | 2.6 | 2.54 | 0.6 | 3.437 | 1.605 | 0.3 | 23.10 | 0.3 | 24.76 | 0.2 | 1.873 | 0.3 |
| TU-1 117531 Spot-5 | 0.738 | 1.1 | 13.72 | 0.3 | 14.733 | 0.187 | 2.7 | 2.53 | 0.6 | 3.429 | 1.598 | 0.3 | 23.13 | 0.3 | 24.93 | 0.2 | 1.830 | 0.3 |
| TU-1 117531 Spot-6 | 0.715 | 1.1 | 13.49 | 0.3 | 14.490 | 0.184 | 2.7 | 2.42 | 0.6 | 3.272 | 1.598 | 0.3 | 23.38 | 0.3 | 24.78 | 0.2 | 1.794 | 0.3 |
| 05B-6-23-mnz6-1 | 0.779 | 1.0 | 3.33 | 0.6 | 3.517 | 0.163 | 2.9 | 0.83 | 1.4 | 1.078 | 0.879 | 0.5 | 30.38 | 0.3 | 26.77 | 0.2 | 0.210 | 1.8 |
| 05B-6-23-mnz6-2 | 0.574 | 1.3 | 3.54 | 0.6 | 3.737 | 0.147 | 3.2 | 0.76 | 1.5 | 0.992 | 0.870 | 0.5 | 30.45 | 0.3 | 26.82 | 0.2 | 0.390 | 1.0 |
| 05B-6-23-mnz6-3 | 0.637 | 1.2 | 3.04 | 0.7 | 3.200 | 0.134 | 3.5 | 0.81 | 1.5 | 1.055 | 0.830 | 0.5 | 30.28 | 0.3 | 26.51 | 0.2 | 1.032 | 0.4 |
| 05B-6-23-mnz6-4 | 0.624 | 1.2 | 2.19 | 0.9 | 2.279 | 0.113 | 4.0 | 1.45 | 0.9 | 1.853 | 0.981 | 0.5 | 27.21 | 0.3 | 25.07 | 0.2 | 6.582 | 0.1 |
| 05B-6-23-mnz6-5 | 0.733 | 1.1 | 2.72 | 0.7 | 2.868 | 0.134 | 3.5 | 0.40 | 2.7 | 0.521 | 0.728 | 0.6 | 31.47 | 0.3 | 26.90 | 0.2 | 0.653 | 0.7 |
| 05B-6-23-mnz6-6 | 0.703 | 1.1 | 3.34 | 0.7 | 3.522 | 0.147 | 3.2 | 0.81 | 1.5 | 1.052 | 0.856 | 0.5 | 30.50 | 0.3 | 26.84 | 0.2 | 0.171 | 2.2 |
| 05B-6-23-mnz6-7 | 0.867 | 0.9 | 3.97 | 0.6 | 4.196 | 0.186 | 2.6 | 0.87 | 1.4 | 1.138 | 1.000 | 0.4 | 30.08 | 0.3 | 26.98 | 0.2 | 0.196 | 1.9 |
| 05B-6-23-mnz6-8 | 0.858 | 0.9 | 2.71 | 0.7 | 2.848 | 0.155 | 3.0 | 1.41 | 0.9 | 1.845 | 0.748 | 0.5 | 29.36 | 0.3 | 26.81 | 0.2 | 0.184 | 2.0 |
| 05B-6-23-mnz5-1 | 0.905 | 0.9 | 3.93 | 0.6 | 4.156 | 0.180 | 2.7 | 0.33 | 3.3 | 0.430 | 0.969 | 0.5 | 30.54 | 0.3 | 27.38 | 0.2 | 0.256 | 1.5 |
| 05B-6-23-mnz5-2 | 0.890 | 0.9 | 3.95 | 0.6 | 4.178 | 0.177 | 2.7 | 0.33 | 3.3 | 0.432 | 0.973 | 0.5 | 30.49 | 0.3 | 27.43 | 0.2 | 0.248 | 1.6 |
| 05B-6-23-mnz5-3 | 0.927 | 0.9 | 4.48 | 0.5 | 4.750 | 0.198 | 2.5 | 0.23 | 4.6 | 0.302 | 1.055 | 0.4 | 30.07 | 0.3 | 27.26 | 0.2 | 0.333 | 1.2 |
| 05B-6-23-mnz5-4 | 0.998 | 0.8 | 4.90 | 0.5 | 5.199 | 0.211 | 2.3 | 0.21 | 5.0 | 0.276 | 1.122 | 0.4 | 29.93 | 0.3 | 27.19 | 0.2 | 0.318 | 1.2 |
| 05B-6-23-mnz5-5 | 0.748 | 1.1 | 3.02 | 0.7 | 3.189 | 0.140 | 3.4 | 0.22 | 4.9 | 0.284 | 0.758 | 0.5 | 31.20 | 0.3 | 27.44 | 0.2 | 0.232 | 1.7 |
| 05B-6-23-mnz5-6 | 0.757 | 1.1 | 2.96 | 0.7 | 3.125 | 0.140 | 3.4 | 0.24 | 4.5 | 0.305 | 0.762 | 0.5 | 31.35 | 0.3 | 27.52 | 0.2 | 0.234 | 1.7 |
| 05B-6-23-mnz5-7 | 0.907 | 0.9 | 3.44 | 0.6 | 3.637 | 0.176 | 2.7 | 0.20 | 5.3 | 0.258 | 0.874 | 0.5 | 30.96 | 0.3 | 27.57 | 0.2 | 0.217 | 1.8 |
| 05B-6-23-mnz5-8 | 0.718 | 1.1 | 3.02 | 0.7 | 3.183 | 0.143 | 3.3 | 0.35 | 3.1 | 0.453 | 0.771 | 0.5 | 31.36 | 0.3 | 27.52 | 0.2 | 0.231 | 1.7 |
| 05B-6-23-mnz5-9 | 0.758 | 1.0 | 3.05 | 0.7 | 3.220 | 0.152 | 3.1 | 0.46 | 2.4 | 0.603 | 0.785 | 0.5 | 30.84 | 0.3 | 27.44 | 0.2 | 0.222 | 1.7 |
| 05B-6-23-mnz5-10 | 0.835 | 1.0 | 3.11 | 0.7 | 3.279 | 0.142 | 3.3 | 0.26 | 4.0 | 0.340 | 0.765 | 0.5 | 29.99 | 0.3 | 26.71 | 0.2 | 1.876 | 0.3 |
| 05B-6-23-mnz5-11 | 0.731 | 1.1 | 2.82 | 0.7 | 2.973 | 0.135 | 3.4 | 0.27 | 3.9 | 0.348 | 0.721 | 0.6 | 31.49 | 0.3 | 27.59 | 0.2 | 0.226 | 1.7 |
| 05B-6-23-mnz1-1 | 0.750 | 1.1 | 2.83 | 0.7 | 2.987 | 0.138 | 3.4 | 0.47 | 2.3 | 0.614 | 0.747 | 0.5 | 31.30 | 0.3 | 27.21 | 0.2 | 0.219 | 1.7 |
| 05B-6-23-mnz1-2 | 0.746 | 1.1 | 3.19 | 0.7 | 3.374 | 0.147 | 3.2 | 0.42 | 2.6 | 0.545 | 0.788 | 0.5 | 31.18 | 0.3 | 27.25 | 0.2 | 0.224 | 1.7 |
| 05B-6-23-mnz1-3 | 0.876 | 0.9 | 2.81 | 0.7 | 2.944 | 0.143 | 3.2 | 0.90 | 1.3 | 1.165 | 0.718 | 0.6 | 27.44 | 0.3 | 24.97 | 0.2 | 3.709 | 0.2 |
| 05B-6-23-mnz1-4 | 0.791 | 1.0 | 3.45 | 0.6 | 3.644 | 0.157 | 3.0 | 0.71 | 1.6 | 0.927 | 0.854 | 0.5 | 30.72 | 0.3 | 27.15 | 0.2 | 0.211 | 1.8 |
| 05B-6-23-mnz1-5 | 0.771 | 1.0 | 3.16 | 0.7 | 3.340 | 0.147 | 3.2 | 0.60 | 1.9 | 0.776 | 0.795 | 0.5 | 30.80 | 0.3 | 27.11 | 0.2 | 0.176 | 2.1 |
| 05B-6-23-mnz1-6 | 0.802 | 1.0 | 3.63 | 0.6 | 3.835 | 0.165 | 2.9 | 0.69 | 1.7 | 0.897 | 0.884 | 0.5 | 30.06 | 0.3 | 27.02 | 0.2 | 0.202 | 1.8 |
| 05B-6-23-mnz1-7 | 0.910 | 0.9 | 3.31 | 0.6 | 3.500 | 0.170 | 2.8 | 0.46 | 2.4 | 0.596 | 0.844 | 0.5 | 30.48 | 0.3 | 27.09 | 0.2 | 0.235 | 1.6 |
| 05B-6-23-mnz2-1 | 0.797 | 1.0 | 3.97 | 0.6 | 4.184 | 0.174 | 2.8 | 0.95 | 1.3 | 1.248 | 0.959 | 0.5 | 29.91 | 0.3 | 27.74 | 0.2 | 0.220 | 1.8 |
| 05B-6-23-mnz2-2 | 0.756 | 1.0 | 3.19 | 0.7 | 3.359 | 0.150 | 3.1 | 0.90 | 1.3 | 1.179 | 0.836 | 0.5 | 30.30 | 0.3 | 27.67 | 0.2 | 0.228 | 1.7 |
| 05B-6-23-mnz2-3 | 0.847 | 1.0 | 3.18 | 0.7 | 3.339 | 0.162 | 2.9 | 1.29 | 1.0 | 1.685 | 0.807 | 0.5 | 29.45 | 0.3 | 27.58 | 0.2 | 0.219 | 1.8 |

| | $UO_2$ | | $ThO_2$ | | | PbO | | $Y_2O_3$ | | | CaO | | $Ce_2O_3$ | | $P_2O_5$ | | $SiO_2$ | |
|---|---|---|---|---|---|---|---|---|---|---|---|---|---|---|---|---|---|---|
| Sample | wt. % | RSD (2σ%) | wt. % | RSD (2σ%) | k-raw | wt. % | RSD (2σ%) | wt. % | RSD (2σ%) | k-raw | wt. % | RSD (2σ%) | wt. % | RSD (2σ%) | wt. % | RSD (2σ%) | wt. % | RSD (2σ%) |
| 05B-6-23-mnz2-4 | 0.816 | 1.0 | 3.07 | 0.7 | 3.236 | 0.149 | 3.2 | 0.41 | 2.7 | 0.539 | 0.780 | 0.5 | 31.24 | 0.3 | 27.69 | 0.2 | 0.231 | 1.7 |
| 05B-6-23-mnz2-5 | 0.640 | 1.2 | 3.46 | 0.6 | 3.652 | 0.143 | 3.3 | 0.79 | 1.5 | 1.038 | 0.852 | 0.5 | 30.57 | 0.3 | 27.62 | 0.2 | 0.218 | 1.7 |
| 05B-6-23-mnz2-6 | 0.812 | 1.0 | 3.32 | 0.7 | 3.495 | 0.169 | 2.8 | 1.04 | 1.2 | 1.363 | 0.847 | 0.5 | 29.89 | 0.3 | 27.54 | 0.2 | 0.106 | 3.5 |
| 05B-6-23-mnz3-1 | 0.816 | 1.0 | 2.87 | 0.7 | 3.016 | 0.153 | 3.1 | 1.11 | 1.1 | 1.459 | 0.751 | 0.5 | 29.64 | 0.3 | 27.62 | 0.2 | 0.225 | 1.7 |
| 05B-6-23-mnz3-2 | 0.595 | 1.3 | 3.69 | 0.6 | 3.895 | 0.142 | 3.3 | 0.72 | 1.6 | 0.935 | 0.861 | 0.5 | 30.70 | 0.3 | 27.65 | 0.2 | 0.236 | 1.7 |
| 05B-6-23-mnz3-3 | 0.769 | 1.0 | 3.63 | 0.6 | 3.822 | 0.165 | 2.9 | 0.89 | 1.4 | 1.161 | 0.930 | 0.5 | 30.15 | 0.3 | 27.66 | 0.2 | 0.225 | 1.7 |
| 05B-6-23-mnz3-4 | 0.773 | 1.0 | 3.65 | 0.6 | 3.845 | 0.162 | 2.9 | 0.90 | 1.3 | 1.183 | 0.921 | 0.5 | 30.35 | 0.3 | 27.69 | 0.2 | 0.222 | 1.8 |
| 05B-6-23-mnz3-5 | 0.972 | 0.8 | 3.62 | 0.6 | 3.811 | 0.184 | 2.6 | 1.03 | 1.2 | 1.346 | 0.931 | 0.5 | 29.84 | 0.3 | 27.72 | 0.2 | 0.226 | 1.7 |
| 05B-6-23-mnz3-6 | 0.725 | 1.1 | 3.41 | 0.6 | 3.589 | 0.163 | 2.9 | 0.89 | 1.3 | 1.168 | 0.869 | 0.5 | 30.41 | 0.3 | 27.74 | 0.2 | 0.219 | 1.8 |
| 05B-6-23-mnz4-1 | 0.817 | 1.0 | 2.94 | 0.7 | 3.099 | 0.150 | 3.1 | 0.67 | 1.7 | 0.877 | 1.060 | 0.4 | 28.04 | 0.3 | 25.24 | 0.2 | 0.541 | 0.8 |
| 05B-6-23-mnz4-2 | 0.829 | 1.0 | 2.73 | 0.7 | 2.880 | 0.160 | 2.9 | 0.71 | 1.6 | 0.925 | 0.899 | 0.5 | 30.97 | 0.3 | 27.35 | 0.2 | 0.231 | 1.7 |
| 05B-6-23-mnz4-3 | 0.853 | 0.9 | 2.81 | 0.7 | 2.963 | 0.150 | 3.2 | 0.75 | 1.6 | 0.980 | 0.930 | 0.5 | 30.76 | 0.3 | 27.37 | 0.2 | 0.263 | 1.5 |
| TU-1 117531 Spot-7 | 0.722 | 1.1 | 13.59 | 0.3 | 14.616 | 0.189 | 2.6 | 2.49 | 0.6 | 3.386 | 1.583 | 0.3 | 22.81 | 0.3 | 24.91 | 0.2 | 0.571 | 0.7 |
| TU-1 117531 Spot-8 | 0.738 | 1.1 | 13.82 | 0.3 | 14.838 | 0.192 | 2.6 | 2.49 | 0.6 | 3.375 | 1.594 | 0.3 | 23.07 | 0.3 | 24.99 | 0.2 | 1.862 | 0.3 |
| TU-1 117531 Spot-9 | 0.724 | 1.1 | 13.65 | 0.3 | 14.653 | 0.188 | 2.7 | 2.50 | 0.6 | 3.380 | 1.593 | 0.3 | 23.19 | 0.3 | 25.02 | 0.2 | 1.853 | 0.3 |
| TU-1 117531 Spot-10 | 0.742 | 1.1 | 13.78 | 0.3 | 14.789 | 0.189 | 2.6 | 2.47 | 0.6 | 3.348 | 1.587 | 0.3 | 23.07 | 0.3 | 24.99 | 0.2 | 1.872 | 0.3 |

**Table B-1.** All (U-Th)-Pb chronologic data for the southern sector of the Southern Brasília Belt.

| Sample | Zone | Date | Error (2σ) |
|---|---|---|---|
| 05B-6-23-mnz6-1 | Core | 640 | 18 |
| 05B-6-23-mnz6-2 | Core | 627 | 20 |
| 05B-6-23-mnz6-7 | Core | 632 | 16 |
| 05B-6-23-mnz6-8 | Core | 639 | 19 |
| 05B-6-23-mnz5-3 | Core | 616 | 15 |
| 05B-6-23-mnz5-7 | Core | 641 | 17 |
| 05B-6-23-mnz5-8 | Core | 621 | 20 |
| 05B-6-23-mnz5-9 | Core | 638 | 19 |
| 05B-6-23-mnz1-3 | Core | 581 | 18 |
| 05B-6-23-mnz1-7 | Core | 632 | 17 |
| 05B-6-23-mnz2-3 | Core | 623 | 18 |
| 05B-6-23-mnz2-6 | Core | 647 | 18 |
| 05B-6-23-mnz3-1 | Core | 632 | 19 |
| 05B-6-23-mnz3-2 | Core | 605 | 19 |
| 05B-6-23-mnz3-3 | Core | 623 | 17 |
| 05B-6-23-mnz3-5 | Core | 624 | 16 |
| 05B-6-23-mnz3-6 | Core | 653 | 18 |
| 05B-6-23-mnz4-2 | Core | 679 | 19 |
| | | | |
| 05B-6-23-mnz6-3 | Rim | 606 | 20 |
| 05B-6-23-mnz6-4 | Rim | 603 | 24 |
| 05B-6-23-mnz6-5 | Rim | 608 | 20 |
| 05B-6-23-mnz6-6 | Rim | 602 | 19 |
| 05B-6-23-mnz5-1 | Rim | 612 | 16 |
| 05B-6-23-mnz5-2 | Rim | 602 | 16 |
| 05B-6-23-mnz5-4 | Rim | 606 | 14 |
| 05B-6-23-mnz5-5 | Rim | 598 | 19 |
| 05B-6-23-mnz5-6 | Rim | 602 | 20 |
| 05B-6-23-mnz5-10 | Rim | 568 | 18 |
| 05B-6-23-mnz5-11 | Rim | 604 | 20 |
| 05B-6-23-mnz1-1 | Rim | 607 | 20 |
| 05B-6-23-mnz1-2 | Rim | 609 | 19 |
| 05B-6-23-mnz1-4 | Rim | 604 | 18 |
| 05B-6-23-mnz1-5 | Rim | 600 | 19 |
| 05B-6-23-mnz1-6 | Rim | 611 | 17 |
| 05B-6-23-mnz2-1 | Rim | 613 | 16 |
| 05B-6-23-mnz2-2 | Rim | 608 | 19 |
| 05B-6-23-mnz2-4 | Rim | 607 | 18 |
| 05B-6-23-mnz2-5 | Rim | 595 | 19 |
| 05B-6-23-mnz3-4 | Rim | 608 | 17 |
| 05B-6-23-mnz4-1 | Rim | 618 | 18 |
| 05B-6-23-mnz4-3 | Rim | 617 | 19 |
| | | | |
| 05b-6-31-Mnz1_pt8 | Unsure | 620 | 16 |
| 05b-6-31-Mnz1_pt9 | Unsure | 624 | 16 |
| 05b-6-31-Mnz1_pt36 | Core | 591 | 14 |
| 05b-6-31-Mnz1_pt37 | Core | 599 | 16 |
| 05b-6-31-Mnz1_pt40 | Core | 607 | 12 |
| 05b-6-31-Mnz1_pt28 | Core | 607 | 16 |

| Sample | Zone | Date | Error (2σ) |
|---|---|---|---|
| 05b-6-31-Mnz1_pt30 | Core | 609 | 16 |
| 05b-6-31-Mnz1_pt27 | Core | 609 | 16 |
| 05b-6-31-Mnz1_pt33 | Core | 610 | 16 |
| 05b-6-31-Mnz1_pt35 | Core | 610 | 14 |
| 05b-6-31-Mnz1_pt43 | Core | 612 | 17 |
| 05b-6-31-Mnz1_pt34 | Core | 613 | 15 |
| 05b-6-31-Mnz1_pt23 | Core | 613 | 15 |
| 05b-6-31-Mnz1_pt49 | Core | 613 | 16 |
| 05b-6-31-Mnz1_pt41 | Core | 614 | 17 |
| 05b-6-31-Mnz1_pt44 | Core | 614 | 16 |
| 05b-6-31-Mnz1_pt32 | Core | 616 | 16 |
| 05b-6-31-Mnz1_pt24 | Core | 617 | 13 |
| 05b-6-31-Mnz1_pt26 | Core | 625 | 16 |
| 05b-6-31-Mnz1_pt38 | Core | 626 | 16 |
| 05b-6-31-Mnz1_pt22 | Core | 626 | 16 |
| 05b-6-31-Mnz1_pt25 | Core | 630 | 16 |
| 05b-6-31-Mnz1_pt31 | Core | 640 | 16 |
| 05b-6-31-Mnz1_pt15 | Mantle | 636 | 15 |
| 05b-6-31-Mnz1_pt16 | Mantle | 649 | 15 |
| 05b-6-31-Mnz1_pt17 | Mantle | 611 | 16 |
| 05b-6-31-Mnz1_pt20 | Mantle | 611 | 16 |
| 05b-6-31-Mnz1_pt21 | Mantle | 612 | 17 |
| 05b-6-31-Mnz1_pt19 | Mantle | 622 | 16 |
| 05b-6-31-Mnz1_pt18 | Mantle | 628 | 16 |
| 05b-6-31-Mnz1_pt51 | Mantle | 617 | 17 |
| 05b-6-31-Mnz1_pt46 | Mantle | 620 | 17 |
| 05b-6-31-Mnz1_pt48 | Mantle | 624 | 16 |
| 05b-6-31-Mnz1_pt47 | Mantle | 626 | 17 |
| 05b-6-31-Mnz1_pt58 | Mantle | 628 | 16 |
| 05b-6-31-Mnz1_pt57 | Mantle | 631 | 17 |
| 05b-6-31-Mnz1_pt39 | Mantle | 632 | 16 |
| 05b-6-31-Mnz1_pt53 | Mantle | 632 | 17 |
| 05b-6-31-Mnz1_pt43 | Mantle | 633 | 14 |
| 05b-6-31-Mnz1_pt45 | Mantle | 637 | 16 |
| 05b-6-31-Mnz1_pt64 | Mantle | 638 | 17 |
| 05b-6-31-Mnz1_pt59 | Mantle | 640 | 16 |
| 05b-6-31-Mnz1_pt56 | Mantle | 646 | 17 |
| 05b-6-31-Mnz1_pt52 | Mantle | 651 | 17 |
| 05b-6-31-Mnz1_pt54 | Mantle | 655 | 17 |
| 05b-6-31-Mnz1_pt50 | Mantle | 660 | 16 |
| 05b-6-31-Mnz1_pt55 | Mantle | 664 | 17 |
| 05b-6-31-Mnz1_pt4 | Rim | 578 | 17 |
| 05b-6-31-Mnz1_pt13 | Rim | 584 | 16 |
| 05b-6-31-Mnz1_pt12 | Rim | 587 | 16 |
| 05b-6-31-Mnz1_pt10 | Rim | 589 | 16 |
| 05b-6-31-Mnz1_pt3 | Rim | 590 | 17 |
| 05b-6-31-Mnz1_pt11 | Rim | 592 | 16 |
| 05b-6-31-Mnz1_pt6 | Rim | 594 | 16 |
| 05b-6-31-Mnz1_pt29 | Rim | 594 | 16 |
| 05b-6-31-Mnz1_pt14 | Rim | 595 | 16 |
| 05b-6-31-Mnz1_pt5 | Rim | 606 | 17 |
| 05b-6-31-Mnz1_pt7 | Rim | 608 | 16 |
| 05b-6-31-Mnz1_pt62 | Rim | 610 | 16 |

| Sample | Zone | Date | Error (2σ) |
|---|---|---|---|
| 05b-6-31-Mnz1_pt63 | Rim | 610 | 16 |
| 05b-6-31-Mnz1_pt2 | Rim | 624 | 17 |
| 05b-6-31-Mnz1_pt61 | Rim | 627 | 17 |
| 05b-6-31-Mnz1_pt60 | Rim | 629 | 17 |
| 05b-6-31-Mnz1_pt65 | Rim | 629 | 17 |
| | | | |
| 05b-6-103_m5_1 | Rim | 601 | 15 |
| 05b-6-103_m5_10 | Rim | 603 | 17 |
| 05b-6-103_m5_11 | Rim | 598 | 14 |
| 05b-6-103_m5_12 | Rim | 596 | 16 |
| 05b-6-103_m5_13 | Rim | 608 | 24 |
| 05b-6-103_m5_14 | Rim | 616 | 24 |
| 05b-6-103_m5_15 | Rim | 580 | 24 |
| 05b-6-103_m5_16 | Rim | 592 | 21 |
| 05b-6-103_m5_17 | Rim | 623 | 15 |
| 05b-6-103_m5_18 | Rim | 603 | 15 |
| 05b-6-103_m5_19 | Rim | 627 | 15 |
| 05b-6-103_m5_2 | Rim | 624 | 15 |
| 05b-6-103_m5_20 | Rim | 612 | 15 |
| 05b-6-103_m5_22 | Rim | 611 | 15 |
| 05b-6-103_m5_3 | Rim | 573 | 15 |
| 05b-6-103_m5_31 | Rim | 596 | 16 |
| 05b-6-103_m5_37 | Rim | 609 | 18 |
| 05b-6-103_m5_4 | Rim | 625 | 15 |
| 05b-6-103_m5_42 | Rim | 598 | 12 |
| 05b-6-103_m5_43 | Rim | 606 | 14 |
| 05b-6-103_m5_44 | Rim | 617 | 16 |
| 05b-6-103_m5_45 | Rim | 600 | 16 |
| 05b-6-103_m5_46 | Rim | 622 | 16 |
| 05b-6-103_m5_47 | Rim | 591 | 15 |
| 05b-6-103_m5_49 | Rim | 585 | 16 |
| 05b-6-103_m5_5 | Rim | 620 | 16 |
| 05b-6-103_m5_50 | Rim | 622 | 15 |
| 05b-6-103_m5_52 | Rim | 613 | 15 |
| 05b-6-103_m5_53 | Rim | 611 | 16 |
| 05b-6-103_m5_54 | Rim | 594 | 15 |
| 05b-6-103_m5_55 | Rim | 580 | 15 |
| 05b-6-103_m5_56 | Rim | 586 | 15 |
| 05b-6-103_m5_57 | Rim | 621 | 14 |
| 05b-6-103_m5_58 | Rim | 603 | 14 |
| 05b-6-103_m5_6 | Rim | 572 | 18 |
| 05b-6-103_m5_7 | Rim | 593 | 17 |
| 05b-6-103_m5_8 | Rim | 577 | 15 |
| 05b-6-103_m5_9 | Rim | 603 | 15 |
| 05b-6-103_m6_14 | Rim | 568 | 17 |
| 05b-6-103_m6_22 | Rim | 584 | 21 |
| 05b-6-103_m6_25 | Rim | 592 | 19 |
| 05b-6-103_m6_26 | Rim | 611 | 20 |
| 05b-6-103_m6_28 | Rim | 576 | 21 |
| 05b-6-103_m6_29 | Rim | 605 | 20 |
| 05b-6-103_m6_3 | Rim | 598 | 18 |
| 05b-6-103_m6_30 | Rim | 612 | 20 |
| 05b-6-103_m6_32 | Rim | 595 | 20 |

| Sample | Zone | Date | Error (2σ) |
|---|---|---|---|
| 05b-6-103_m6_33 | Rim | 605 | 20 |
| 05b-6-103_m6_35 | Rim | 604 | 15 |
| 05b-6-103_m6_41 | Rim | 613 | 18 |
| 05b-6-103_m6_42 | Rim | 589 | 17 |
| 05b-6-103_m6_44 | Rim | 606 | 18 |
| 05b-6-103_m6_49 | Rim | 616 | 16 |
| 05b-6-103_m6_5 | Rim | 594 | 20 |
| 05b-6-103_m6_52 | Rim | 596 | 17 |
| 05b-6-103_m6_55 | Rim | 605 | 18 |
| 05b-6-103_m6_58 | Rim | 600 | 16 |
| 05b-6-103_m6_59 | Rim | 613 | 16 |
| 05b-6-103_m6_63 | Rim | 610 | 18 |
| 05b-6-103_m6_64 | Rim | 597 | 26 |
| 05b-6-103_m6_66 | Rim | 608 | 16 |
| 05b-6-103_m6_68 | Rim | 605 | 20 |
| 05b-6-103_m6_69 | Rim | 616 | 21 |
| 05b-6-103_m6_7 | Rim | 584 | 18 |
| 05b-6-103_m6_73 | Rim | 591 | 24 |
| 05b-6-103_m6_77 | Rim | 606 | 21 |
| 05b-6-103_m6_8 | Rim | 609 | 20 |
| 05b-6-103_m6_81 | Rim | 593 | 21 |
| 05b-6-103_m6_82 | Rim | 587 | 20 |
| 05b-6-103_m6_85 | Rim | 602 | 20 |
| 05b-6-103_m6_86 | Rim | 613 | 22 |
| 05b-6-103_m6_93 | Rim | 592 | 17 |
| | | | |
| 05b-6-103_m5_21 | Core | 633 | 15 |
| 05b-6-103_m5_23 | Core | 616 | 18 |
| 05b-6-103_m5_24 | Core | 621 | 17 |
| 05b-6-103_m5_25 | Core | 627 | 15 |
| 05b-6-103_m5_26 | Core | 611 | 15 |
| 05b-6-103_m5_27 | Core | 628 | 15 |
| 05b-6-103_m5_28 | Core | 620 | 16 |
| 05b-6-103_m5_29 | Core | 629 | 15 |
| 05b-6-103_m5_30 | Core | 616 | 15 |
| 05b-6-103_m5_32 | Core | 632 | 17 |
| 05b-6-103_m5_33 | Core | 631 | 17 |
| 05b-6-103_m5_34 | Core | 639 | 18 |
| 05b-6-103_m5_35 | Core | 645 | 19 |
| 05b-6-103_m5_36 | Core | 630 | 16 |
| 05b-6-103_m5_38 | Core | 643 | 18 |
| 05b-6-103_m5_39 | Core | 649 | 23 |
| 05b-6-103_m5_40 | Core | 624 | 21 |
| 05b-6-103_m5_41 | Core | 650 | 17 |
| 05b-6-103_m5_48 | Core | 629 | 14 |
| 05b-6-103_m5_51 | Core | 628 | 15 |
| 05b-6-103_m6_1 | Core | 609 | 18 |
| 05b-6-103_m6_10 | Core | 613 | 24 |
| 05b-6-103_m6_11 | Core | 570 | 24 |
| 05b-6-103_m6_12 | Core | 637 | 23 |
| 05b-6-103_m6_13 | Core | 626 | 19 |
| 05b-6-103_m6_15 | Core | 610 | 16 |
| 05b-6-103_m6_16 | Core | 642 | 20 |

| Sample | Zone | Date | Error (2σ) |
|---|---|---|---|
| 05b-6-103_m6_17 | Core | 635 | 15 |
| 05b-6-103_m6_18 | Core | 608 | 17 |
| 05b-6-103_m6_19 | Core | 618 | 20 |
| 05b-6-103_m6_2 | Core | 633 | 18 |
| 05b-6-103_m6_20 | Core | 626 | 20 |
| 05b-6-103_m6_21 | Core | 642 | 20 |
| 05b-6-103_m6_23 | Core | 647 | 21 |
| 05b-6-103_m6_24 | Core | 616 | 21 |
| 05b-6-103_m6_27 | Core | 622 | 18 |
| 05b-6-103_m6_31 | Core | 618 | 21 |
| 05b-6-103_m6_34 | Core | 633 | 16 |
| 05b-6-103_m6_36 | Core | 626 | 16 |
| 05b-6-103_m6_37 | Core | 619 | 16 |
| 05b-6-103_m6_38 | Core | 666 | 17 |
| 05b-6-103_m6_39 | Core | 638 | 16 |
| 05b-6-103_m6_4 | Core | 617 | 20 |
| 05b-6-103_m6_40 | Core | 637 | 15 |
| 05b-6-103_m6_43 | Core | 627 | 17 |
| 05b-6-103_m6_45 | Core | 630 | 17 |
| 05b-6-103_m6_46 | Core | 636 | 14 |
| 05b-6-103_m6_47 | Core | 634 | 18 |
| 05b-6-103_m6_48 | Core | 643 | 17 |
| 05b-6-103_m6_50 | Core | 649 | 16 |
| 05b-6-103_m6_51 | Core | 659 | 18 |
| 05b-6-103_m6_53 | Core | 662 | 18 |
| 05b-6-103_m6_54 | Core | 627 | 17 |
| 05b-6-103_m6_56 | Core | 648 | 16 |
| 05b-6-103_m6_57 | Core | 612 | 15 |
| 05b-6-103_m6_6 | Core | 638 | 14 |
| 05b-6-103_m6_60 | Core | 622 | 15 |
| 05b-6-103_m6_61 | Core | 617 | 15 |
| 05b-6-103_m6_62 | Core | 627 | 16 |
| 05b-6-103_m6_65 | Core | 626 | 24 |
| 05b-6-103_m6_67 | Core | 644 | 17 |
| 05b-6-103_m6_70 | Core | 644 | 16 |
| 05b-6-103_m6_71 | Core | 617 | 23 |
| 05b-6-103_m6_72 | Core | 636 | 23 |
| 05b-6-103_m6_74 | Core | 673 | 24 |
| 05b-6-103_m6_75 | Core | 631 | 23 |
| 05b-6-103_m6_76 | Core | 635 | 23 |
| 05b-6-103_m6_78 | Core | 632 | 20 |
| 05b-6-103_m6_79 | Core | 648 | 20 |
| 05b-6-103_m6_80 | Core | 616 | 21 |
| 05b-6-103_m6_83 | Core | 619 | 19 |
| 05b-6-103_m6_84 | Core | 621 | 19 |
| 05b-6-103_m6_87 | Core | 643 | 18 |
| 05b-6-103_m6_88 | Core | 628 | 17 |
| 05b-6-103_m6_9 | Core | 647 | 23 |
| 05b-6-103_m6_90 | Core | 615 | 16 |
| 05b-6-103_m6_91 | Core | 658 | 14 |
| 05b-6-103_m6_92 | Core | 616 | 15 |
| 05b-6-103_m6_94 | Core | 614 | 19 |
| 05b-6-103_m6_95 | Core | 629 | 16 |

| Sample | Zone | Date | Error (2σ) |
|---|---|---|---|
| 05b-6-103_m6_96 | Core | 621 | 16 |
| 05b-6-103_m6_97 | Core | 621 | 18 |
| | | | |
| 05-6-36_m3_pt23 | Core | 604 | 17 |
| 05-6-36_m3_pt24 | Core | 615 | 18 |
| 05-6-36_m3_pt25 | Core | 596 | 16 |
| 05-6-36_m3_pt26 | Core | 609 | 17 |
| 05-6-36_m3_pt29 | Core | 632 | 17 |
| 05-6-36_m3_pt30 | Core | 647 | 15 |
| 05-6-36_m3_pt31 | Core | 627 | 18 |
| 05-6-36_m3_pt32 | Core | 627 | 19 |
| 05-6-36_m3_pt33 | Core | 610 | 18 |
| 05-6-36_m3_pt34 | Core | 662 | 17 |
| 05-6-36_m3_pt35 | Core | 630 | 18 |
| 05-6-36_m3_pt36 | Core | 679 | 18 |
| 05-6-36_m3_pt37 | Core | 637 | 18 |
| 05-6-36_m3_pt38 | Core | 626 | 15 |
| 05-6-36_m3_pt39 | Core | 636 | 16 |
| 05-6-36_m3_pt40 | Core | 631 | 17 |
| 05-6-36_m3_pt41 | Core | 650 | 17 |
| 05-6-36_m3_pt42 | Core | 640 | 16 |
| 05-6-36_m3_pt43 | Core | 659 | 18 |
| 05-6-36_m3_pt44 | Core | 687 | 15 |
| 05-6-36_m3_pt45 | Core | 639 | 15 |
| 05-6-36_m3_pt46 | Core | 635 | 15 |
| 05-6-36_m3_pt47 | Core | 649 | 15 |
| 05-6-36_m3_pt48 | Core | 605 | 15 |
| 05-6-36_m3_pt49 | Core | 608 | 15 |
| 05-6-36_m3_pt50 | Core | 596 | 16 |
| 05-6-36_m3_pt51 | Core | 631 | 16 |
| 05-6-36_m3_pt52 | Core | 622 | 17 |
| 05-6-36_m3_pt53 | Core | 623 | 17 |
| 05-6-36_m3_pt54 | Core | 638 | 15 |
| 05-6-36_m3_pt55 | Core | 629 | 16 |
| 05-6-36_m3_pt56 | Core | 593 | 17 |
| 05-6-36_m3_pt57 | Core | 639 | 16 |
| 05-6-36_m3_pt58 | Core | 619 | 16 |
| 05-6-36_m3_pt59 | Core | 620 | 15 |
| 05-6-36_m3_pt60 | Core | 624 | 16 |
| 05-6-36_m3_pt61 | Core | 598 | 20 |
| 05-6-36_m3_pt1 | Core | 647 | 17 |
| 05-6-36_m3_pt10 | Core | 621 | 22 |
| 05-6-36_m3_pt11 | Core | 635 | 22 |
| 05-6-36_m3_pt12 | Core | 660 | 22 |
| 05-6-36_m3_pt13 | Core | 667 | 22 |
| 05-6-36_m3_pt16 | Core | 647 | 17 |
| 05-6-36_m3_pt17 | Core | 676 | 28 |
| 05-6-36_m3_pt18 | Core | 633 | 18 |
| 05-6-36_m3_pt19 | Core | 631 | 17 |
| 05-6-36_m3_pt2 | Core | 649 | 17 |
| 05-6-36_m3_pt20 | Core | 629 | 22 |
| 05-6-36_m3_pt21 | Core | 624 | 20 |
| 05-6-36_m3_pt22 | Core | 645 | 18 |

| Sample | Zone | Date | Error (2σ) |
|---|---|---|---|
| 05-6-36_m3_pt27 | Core | 654 | 20 |
| 05-6-36_m3_pt28 | Core | 614 | 23 |
| 05-6-36_m3_pt3 | Core | 605 | 18 |
| 05-6-36_m3_pt4 | Core | 626 | 19 |
| 05-6-36_m3_pt5 | Core | 647 | 18 |
| 05-6-36_m3_pt6 | Core | 625 | 18 |
| 05-6-36_m3_pt7 | Core | 590 | 21 |
| 05-6-36_m3_pt8 | Core | 648 | 21 |
| 05-6-36_m3_pt9 | Core | 602 | 20 |
| 05-6-36_m3_pt14 | Core | 620 | 22 |
| 05-6-36_m3_pt15 | Core | 619 | 17 |
| 05-6-36_m5_pt10 | Core | 627 | 20 |
| 05-6-36_m5_pt11 | Core | 622 | 20 |
| 05-6-36_m5_pt17 | Core | 637 | 17 |
| 05-6-36_m5_pt19 | Core | 634 | 21 |
| 05-6-36_m5_pt23 | Core | 634 | 23 |
| 05-6-36_m5_pt24 | Core | 636 | 24 |
| 05-6-36_m5_pt25 | Core | 638 | 18 |
| 05-6-36_m5_pt27 | Core | 647 | 17 |
| 05-6-36_m5_pt28 | Core | 670 | 16 |
| 05-6-36_m5_pt29 | Core | 602 | 16 |
| 05-6-36_m5_pt30 | Core | 636 | 16 |
| 05-6-36_m5_pt31 | Core | 639 | 16 |
| 05-6-36_m5_pt32 | Core | 653 | 17 |
| 05-6-36_m5_pt33 | Core | 625 | 16 |
| 05-6-36_m5_pt40 | Core | 654 | 18 |
| 05-6-36_m5_pt44 | Core | 624 | 22 |
| 05-6-36_m5_pt46 | Core | 620 | 23 |
| 05-6-36_m5_pt47 | Core | 627 | 22 |
| 05-6-36_m5_pt49 | Core | 631 | 23 |
| 05-6-36_m5_pt50 | Core | 621 | 22 |
| 05-6-36_m5_pt51 | Core | 610 | 23 |
| 05-6-36_m5_pt52 | Core | 622 | 23 |
| 05-6-36_m5_pt53 | Core | 638 | 22 |
| 05-6-36_m5_pt54 | Core | 618 | 22 |
| 05-6-36_m5_pt55 | Core | 614 | 19 |
| 05-6-36_m5_pt56 | Core | 643 | 22 |
| 05-6-36_m5_pt57 | Core | 604 | 23 |
| 05-6-36_m5_pt58 | Core | 634 | 23 |
| 05-6-36_m5_pt70 | Core | 638 | 20 |
| 05-6-36_m5_pt72 | Core | 617 | 20 |
| 05-6-36_m5_pt73 | Core | 619 | 20 |
| 05-6-36_m5_pt79 | Core | 658 | 17 |
| 05-6-36_m5_pt8 | Core | 629 | 18 |
| 05-6-36_m5_pt9 | Core | 647 | 18 |
| 05-6-36_m7_pt92 | Core | 615 | 15 |
| 05-6-36_m7_pt85 | Core | 617 | 16 |
| 05-6-36_m7_pt105 | Core | 618 | 16 |
| 05-6-36_m7_pt103 | Core | 620 | 16 |
| 05-6-36_m7_pt94 | Core | 620 | 16 |
| 05-6-36_m7_pt96 | Core | 620 | 16 |
| 05-6-36_m7_pt93 | Core | 624 | 16 |
| 05-6-36_m7_pt102 | Core | 628 | 18 |

| Sample | Zone | Date | Error (2σ) |
|---|---|---|---|
| 05-6-36_m7_pt104 | Core | 633 | 16 |
| 05-6-36_m7_pt75 | Core | 633 | 17 |
| 05-6-36_m7_pt99 | Core | 635 | 18 |
| 05-6-36_m7_pt74 | Core | 636 | 17 |
| 05-6-36_m7_pt97 | Core | 636 | 16 |
| 05-6-36_m7_pt84 | Core | 637 | 18 |
| 05-6-36_m7_pt71 | Core | 638 | 16 |
| 05-6-36_m7_pt82 | Core | 638 | 16 |
| 05-6-36_m7_pt100 | Core | 641 | 17 |
| 05-6-36_m7_pt98 | Core | 641 | 17 |
| 05-6-36_m7_pt80 | Core | 646 | 16 |
| 05-6-36_m7_pt87 | Core | 646 | 16 |
| 05-6-36_m7_pt91 | Core | 646 | 16 |
| 05-6-36_m7_pt73 | Core | 648 | 16 |
| 05-6-36_m7_pt95 | Core | 648 | 20 |
| 05-6-36_m7_pt78 | Core | 650 | 18 |
| 05-6-36_m7_pt76 | Core | 652 | 17 |
| 05-6-36_m7_pt81 | Core | 653 | 16 |
| 05-6-36_m7_pt77 | Core | 655 | 17 |
| 05-6-36_m7_pt79 | Core | 656 | 16 |
| 05-6-36_m7_pt106 | Core | 663 | 17 |
| 05-6-36_m7_pt101 | Core | 665 | 17 |
| 05-6-36_m7_pt72 | Core | 667 | 17 |
| 05-6-36_m7_pt90 | Core | 668 | 15 |
| 05-6-36_m7_pt88 | Core | 684 | 16 |
| 05-6-36_m7_pt62 | Core | 640 | 16 |
| 05-6-36_m7_pt53 | Core | 641 | 17 |
| 05-6-36_m7_pt69 | Core | 641 | 18 |
| | | | |
| 05-6-36_m2_pt1 | Rim | 574 | 20 |
| 05-6-36_m2_pt10 | Rim | 610 | 15 |
| 05-6-36_m2_pt11 | Rim | 635 | 15 |
| 05-6-36_m2_pt12 | Rim | 610 | 16 |
| 05-6-36_m2_pt13 | Rim | 620 | 17 |
| 05-6-36_m2_pt14 | Rim | 568 | 22 |
| 05-6-36_m2_pt15 | Rim | 608 | 20 |
| 05-6-36_m2_pt16 | Rim | 630 | 17 |
| 05-6-36_m2_pt17 | Rim | 606 | 18 |
| 05-6-36_m2_pt18 | Rim | 601 | 20 |
| 05-6-36_m2_pt19 | Rim | 621 | 20 |
| 05-6-36_m2_pt2 | Rim | 574 | 20 |
| 05-6-36_m2_pt20 | Rim | 597 | 22 |
| 05-6-36_m2_pt21 | Rim | 620 | 22 |
| 05-6-36_m2_pt22 | Rim | 601 | 16 |
| 05-6-36_m2_pt23 | Rim | 586 | 18 |
| 05-6-36_m2_pt24 | Rim | 606 | 18 |
| 05-6-36_m2_pt25 | Rim | 605 | 17 |
| 05-6-36_m2_pt26 | Rim | 634 | 16 |
| 05-6-36_m2_pt27 | Rim | 602 | 16 |
| 05-6-36_m2_pt28 | Rim | 577 | 16 |
| 05-6-36_m2_pt29 | Rim | 602 | 17 |
| 05-6-36_m2_pt3 | Rim | 621 | 19 |
| 05-6-36_m2_pt30 | Rim | 600 | 18 |

| Sample | Zone | Date | Error (2σ) |
|---|---|---|---|
| 05-6-36_m2_pt31 | Rim | 627 | 18 |
| 05-6-36_m2_pt32 | Rim | 584 | 20 |
| 05-6-36_m2_pt33 | Rim | 587 | 18 |
| 05-6-36_m2_pt34 | Rim | 584 | 17 |
| 05-6-36_m2_pt35 | Rim | 605 | 20 |
| 05-6-36_m2_pt36 | Rim | 622 | 21 |
| 05-6-36_m2_pt37 | Rim | 611 | 19 |
| 05-6-36_m2_pt38 | Rim | 591 | 21 |
| 05-6-36_m2_pt39 | Rim | 599 | 20 |
| 05-6-36_m2_pt4 | Rim | 618 | 18 |
| 05-6-36_m2_pt40 | Rim | 590 | 19 |
| 05-6-36_m2_pt41 | Rim | 630 | 21 |
| 05-6-36_m2_pt42 | Rim | 608 | 21 |
| 05-6-36_m2_pt43 | Rim | 602 | 18 |
| 05-6-36_m2_pt44 | Rim | 570 | 19 |
| 05-6-36_m2_pt45 | Rim | 596 | 19 |
| 05-6-36_m2_pt46 | Rim | 612 | 18 |
| 05-6-36_m2_pt47 | Rim | 633 | 17 |
| 05-6-36_m2_pt48 | Rim | 615 | 19 |
| 05-6-36_m2_pt49 | Rim | 643 | 19 |
| 05-6-36_m2_pt5 | Rim | 631 | 17 |
| 05-6-36_m2_pt6 | Rim | 632 | 17 |
| 05-6-36_m2_pt7 | Rim | 623 | 17 |
| 05-6-36_m2_pt8 | Rim | 621 | 17 |
| 05-6-36_m2_pt9 | Rim | 597 | 16 |
| 05-6-36_m5_pt1 | Rim | 573 | 16 |
| 05-6-36_m5_pt12 | Rim | 630 | 20 |
| 05-6-36_m5_pt13 | Rim | 605 | 20 |
| 05-6-36_m5_pt14 | Rim | 539 | 19 |
| 05-6-36_m5_pt15 | Rim | 595 | 19 |
| 05-6-36_m5_pt16 | Rim | 582 | 23 |
| 05-6-36_m5_pt18 | Rim | 593 | 21 |
| 05-6-36_m5_pt2 | Rim | 566 | 16 |
| 05-6-36_m5_pt20 | Rim | 616 | 16 |
| 05-6-36_m5_pt21 | Rim | 608 | 18 |
| 05-6-36_m5_pt22 | Rim | 611 | 15 |
| 05-6-36_m5_pt26 | Rim | 606 | 18 |
| 05-6-36_m5_pt3 | Rim | 603 | 17 |
| 05-6-36_m5_pt34 | Rim | 609 | 15 |
| 05-6-36_m5_pt35 | Rim | 591 | 15 |
| 05-6-36_m5_pt36 | Rim | 602 | 15 |
| 05-6-36_m5_pt37 | Rim | 596 | 18 |
| 05-6-36_m5_pt38 | Rim | 612 | 18 |
| 05-6-36_m5_pt39 | Rim | 608 | 11 |
| 05-6-36_m5_pt4 | Rim | 611 | 17 |
| 05-6-36_m5_pt41 | Rim | 614 | 12 |
| 05-6-36_m5_pt42 | Rim | 594 | 23 |
| 05-6-36_m5_pt43 | Rim | 607 | 23 |
| 05-6-36_m5_pt45 | Rim | 571 | 23 |
| 05-6-36_m5_pt48 | Rim | 598 | 23 |
| 05-6-36_m5_pt5 | Rim | 602 | 17 |
| 05-6-36_m5_pt59 | Rim | 603 | 21 |
| 05-6-36_m5_pt6 | Rim | 615 | 17 |

| Sample | Zone | Date | Error (2σ) |
|---|---|---|---|
| 05-6-36_m5_pt60 | Rim | 606 | 18 |
| 05-6-36_m5_pt61 | Rim | 622 | 18 |
| 05-6-36_m5_pt62 | Rim | 623 | 20 |
| 05-6-36_m5_pt63 | Rim | 591 | 19 |
| 05-6-36_m5_pt64 | Rim | 605 | 19 |
| 05-6-36_m5_pt65 | Rim | 660 | 19 |
| 05-6-36_m5_pt66 | Rim | 608 | 19 |
| 05-6-36_m5_pt67 | Rim | 625 | 20 |
| 05-6-36_m5_pt68 | Rim | 576 | 19 |
| 05-6-36_m5_pt69 | Rim | 604 | 19 |
| 05-6-36_m5_pt7 | Rim | 620 | 17 |
| 05-6-36_m5_pt71 | Rim | 569 | 20 |
| 05-6-36_m5_pt74 | Rim | 603 | 17 |
| 05-6-36_m5_pt75 | Rim | 567 | 18 |
| 05-6-36_m5_pt76 | Rim | 611 | 18 |
| 05-6-36_m5_pt77 | Rim | 595 | 17 |
| 05-6-36_m5_pt78 | Rim | 587 | 17 |
| 05-6-36_m5_pt80 | Rim | 601 | 19 |
| 05-6-36_m5_pt81 | Rim | 607 | 18 |
| 05-6-36_m5_pt82 | Rim | 591 | 19 |
| 05-6-36_m5_pt83 | Rim | 609 | 19 |
| 05-6-36_m5_pt84 | Rim | 585 | 16 |
| 05-6-36_m5_pt85 | Rim | 603 | 17 |
| 05-6-36_m7_pt57 | Rim | 570 | 16 |
| 05-6-36_m7_pt12 | Rim | 578 | 15 |
| 05-6-36_m7_pt3 | Rim | 580 | 22 |
| 05-6-36_m7_pt17 | Rim | 582 | 15 |
| 05-6-36_m7_pt13 | Rim | 589 | 17 |
| 05-6-36_m7_pt40 | Rim | 589 | 16 |
| 05-6-36_m7_pt16 | Rim | 591 | 15 |
| 05-6-36_m7_pt70 | Rim | 592 | 17 |
| 05-6-36_m7_pt52 | Rim | 593 | 16 |
| 05-6-36_m7_pt44 | Rim | 594 | 18 |
| 05-6-36_m7_pt2 | Rim | 597 | 15 |
| 05-6-36_m7_pt54 | Rim | 599 | 17 |
| 05-6-36_m7_pt11 | Rim | 600 | 16 |
| 05-6-36_m7_pt56 | Rim | 600 | 15 |
| 05-6-36_m7_pt64 | Rim | 600 | 15 |
| 05-6-36_m7_pt5 | Rim | 602 | 16 |
| 05-6-36_m7_pt51 | Rim | 602 | 17 |
| 05-6-36_m7_pt45 | Rim | 604 | 19 |
| 05-6-36_m7_pt66 | Rim | 604 | 18 |
| 05-6-36_m7_pt1 | Rim | 605 | 15 |
| 05-6-36_m7_pt58 | Rim | 605 | 16 |
| 05-6-36_m7_pt67 | Rim | 605 | 17 |
| 05-6-36_m7_pt49 | Rim | 607 | 17 |
| 05-6-36_m7_pt50 | Rim | 607 | 17 |
| 05-6-36_m7_pt68 | Rim | 608 | 17 |
| 05-6-36_m7_pt19 | Rim | 609 | 17 |
| 05-6-36_m7_pt63 | Rim | 611 | 18 |
| 05-6-36_m7_pt42 | Rim | 612 | 18 |
| 05-6-36_m7_pt55 | Rim | 614 | 15 |
| 05-6-36_m7_pt48 | Rim | 615 | 16 |

| Sample | Zone | Date | Error (2σ) |
|---|---|---|---|
| 05-6-36_m7_pt9 | Rim | 615 | 18 |
| 05-6-36_m7_pt7 | Rim | 617 | 17 |
| 05-6-36_m7_pt14 | Rim | 618 | 19 |
| 05-6-36_m7_pt8 | Rim | 618 | 16 |
| 05-6-36_m7_pt10 | Rim | 619 | 16 |
| 05-6-36_m7_pt43 | Rim | 619 | 18 |
| 05-6-36_m7_pt65 | Rim | 619 | 19 |
| 05-6-36_m7_pt4 | Rim | 620 | 15 |
| 05-6-36_m7_pt6 | Rim | 621 | 17 |
| 05-6-36_m7_pt15 | Rim | 624 | 16 |
| 05-6-36_m7_pt47 | Rim | 628 | 16 |
| 05-6-36_m7_pt20 | Rim | 629 | 17 |
| 05-6-36_m7_pt46 | Rim | 630 | 17 |
| 05-6-36_m7_pt61 | Rim | 632 | 16 |
| 05-6-36_m7_pt41 | Rim | 636 | 18 |
| 05-6-36_m7_pt60 | Rim | 639 | 15 |
| 05-6-36_m7_pt18 | Rim | 659 | 16 |
| 05-6-36_m7_pt27 | Rim | 566 | 16 |
| 05-6-36_m7_pt33 | Rim | 588 | 17 |
| 05-6-36_m7_pt37 | Rim | 596 | 15 |
| 05-6-36_m7_pt34 | Rim | 600 | 16 |
| 05-6-36_m7_pt35 | Rim | 602 | 15 |
| 05-6-36_m7_pt31 | Rim | 603 | 18 |
| 05-6-36_m7_pt21 | Rim | 604 | 15 |
| 05-6-36_m7_pt22 | Rim | 604 | 15 |
| 05-6-36_m7_pt38 | Rim | 608 | 16 |
| 05-6-36_m7_pt25 | Rim | 610 | 15 |
| 05-6-36_m7_pt32 | Rim | 611 | 20 |
| 05-6-36_m7_pt36 | Rim | 611 | 15 |
| 05-6-36_m7_pt23 | Rim | 612 | 15 |
| 05-6-36_m7_pt28 | Rim | 615 | 15 |
| 05-6-36_m7_pt24 | Rim | 618 | 16 |
| 05-6-36_m7_pt26 | Rim | 627 | 16 |
| 05-6-36_m7_pt29 | Rim | 632 | 17 |
| 05-6-36_m7_pt30 | Rim | 636 | 18 |
| 05-6-36_m7_pt39 | Rim | 646 | 16 |
| 05-6-36_m7_pt83 | Rim | 581 | 18 |
| 05-6-36_m7_pt86 | Rim | 611 | 16 |
| 05-6-36_m7_pt89 | Rim | 614 | 16 |
| | | | |
| 04-6-11_m3_pt23 | Rim | 556 | 17 |
| 04-6-11_m3_pt47 | Rim | 564 | 16 |
| 04-6-11_m1_pt8 | Rim | 564 | 17 |
| 04-6-11_m1_pt4 | Rim | 565 | 17 |
| 04-6-11_m3_pt29 | Rim | 566 | 17 |
| 04-6-11_m3_pt18 | Rim | 568 | 20 |
| 04-6-11_m1_pt7 | Rim | 573 | 17 |
| 04-6-11_m3_pt25 | Rim | 573 | 17 |
| 04-6-11_m3_pt39 | Rim | 574 | 17 |
| 04-6-11_m1_pt1 | Rim | 574 | 17 |
| 04-6-11_m3_pt31 | Rim | 574 | 16 |
| 04-6-11_m3_pt41 | Rim | 575 | 16 |
| 04-6-11_m3_pt28 | Rim | 576 | 16 |

| Sample | Zone | Date | Error (2σ) |
|---|---|---|---|
| 04-6-11_m3_pt51 | Rim | 577 | 16 |
| 04-6-11_m3_pt37 | Rim | 578 | 17 |
| 04-6-11_m3_pt12 | Rim | 580 | 19 |
| 04-6-11_m3_pt38 | Rim | 583 | 16 |
| 04-6-11_m3_pt6 | Rim | 583 | 16 |
| 04-6-11_m3_pt3 | Rim | 584 | 16 |
| 04-6-11_m3_pt2 | Rim | 585 | 16 |
| 04-6-11_m1_pt15 | Rim | 585 | 17 |
| 04-6-11_m3_pt46 | Rim | 587 | 16 |
| 04-6-11_m3_pt26 | Rim | 587 | 16 |
| 04-6-11_m3_pt35 | Rim | 587 | 20 |
| 04-6-11_m3_pt24 | Rim | 587 | 17 |
| 04-6-11_m1_pt21 | Rim | 588 | 17 |
| 04-6-11_m1_pt16 | Rim | 588 | 18 |
| 04-6-11_m3_pt1 | Rim | 591 | 16 |
| 04-6-11_m1_pt3 | Rim | 594 | 17 |
| 04-6-11_m3_pt34 | Rim | 594 | 19 |
| 04-6-11_m1_pt6 | Rim | 597 | 16 |
| 04-6-11_m1_pt9 | Rim | 598 | 17 |
| 04-6-11_m3_pt49 | Rim | 598 | 16 |
| 04-6-11_m3_pt8 | Rim | 600 | 17 |
| 04-6-11_m3_pt36 | Rim | 603 | 19 |
| 04-6-11_m3_pt7 | Rim | 608 | 17 |
| | | | |
| 04-6-11_m1_pt13 | Core | 592 | 16 |
| 04-6-11_m3_pt52 | Core | 596 | 16 |
| 04-6-11_m3_pt32 | Core | 598 | 16 |
| 04-6-11_m3_pt19 | Core | 598 | 16 |
| 04-6-11_m3_pt9 | Core | 599 | 16 |
| 04-6-11_m3_pt44 | Core | 600 | 16 |
| 04-6-11_m3_pt42 | Core | 601 | 16 |
| 04-6-11_m1_pt14 | Core | 602 | 17 |
| 04-6-11_m3_pt45 | Core | 603 | 16 |
| 04-6-11_m3_pt21 | Core | 604 | 17 |
| 04-6-11_m3_pt50 | Core | 607 | 16 |
| 04-6-11_m3_pt4 | Core | 609 | 16 |
| 04-6-11_m3_pt20 | Core | 609 | 16 |
| 04-6-11_m3_pt22 | Core | 609 | 17 |
| 04-6-11_m3_pt10 | Core | 610 | 15 |
| 04-6-11_m3_pt33 | Core | 611 | 18 |
| 04-6-11_m3_pt48 | Core | 612 | 16 |
| 04-6-11_m1_pt17 | Core | 614 | 17 |
| 04-6-11_m1_pt5 | Core | 614 | 16 |
| 04-6-11_m1_pt18 | Core | 615 | 16 |
| 04-6-11_m1_pt22 | Core | 617 | 17 |
| 04-6-11_m3_pt30 | Core | 618 | 16 |
| 04-6-11_m3_pt13 | Core | 618 | 18 |
| 04-6-11_m3_pt5 | Core | 618 | 15 |
| 04-6-11_m1_pt20 | Core | 621 | 17 |
| 04-6-11_m3_pt11 | Core | 623 | 16 |
| 04-6-11_m1_pt12 | Core | 623 | 17 |
| 04-6-11_m3_pt15 | Core | 624 | 20 |
| 04-6-11_m3_pt16 | Core | 624 | 20 |

| Sample | Zone | Date | Error (2σ) |
|---|---|---|---|
| 04-6-11_m1_pt19 | Core | 625 | 16 |
| 04-6-11_m1_pt2 | Core | 634 | 17 |
| | | | |
| 05-10-65_m2_pt1 | Rim | 602 | 28 |
| 05-10-65_m2_pt10 | Rim | 579 | 37 |
| 05-10-65_m2_pt11 | Rim | 514 | 36 |
| 05-10-65_m2_pt12 | Rim | 547 | 39 |
| 05-10-65_m2_pt13 | Rim | 554 | 38 |
| 05-10-65_m2_pt14 | Rim | 530 | 39 |
| 05-10-65_m2_pt15 | Rim | 637 | 46 |
| 05-10-65_m2_pt16 | Rim | 564 | 42 |
| 05-10-65_m2_pt17 | Rim | 626 | 43 |
| 05-10-65_m2_pt3 | Rim | 582 | 27 |
| 05-10-65_m2_pt4 | Rim | 526 | 29 |
| 05-10-65_m2_pt5 | Rim | 496 | 31 |
| 05-10-65_m2_pt6 | Rim | 507 | 28 |
| 05-10-65_m2_pt7 | Rim | 598 | 35 |
| 05-10-65_m2_pt8 | Rim | 563 | 31 |
| 05-10-65_m2_pt9 | Rim | 582 | 37 |
| | | | |
| 05-10-65_m3_p1 | Core | 572 | 12 |
| 05-10-65_m3_p10 | Core | 618 | 15 |
| 05-10-65_m3_p11 | Core | 578 | 15 |
| 05-10-65_m3_p12 | Core | 563 | 15 |
| 05-10-65_m3_p13 | Core | 559 | 14 |
| 05-10-65_m3_p14 | Core | 574 | 13 |
| 05-10-65_m3_p15 | Core | 575 | 14 |
| 05-10-65_m3_p16 | Core | 581 | 15 |
| 05-10-65_m3_p17 | Core | 591 | 15 |
| 05-10-65_m3_p18 | Core | 584 | 15 |
| 05-10-65_m3_p19 | Core | 610 | 16 |
| 05-10-65_m3_p2 | Core | 591 | 13 |
| 05-10-65_m3_p20 | Core | 589 | 15 |
| 05-10-65_m3_p21 | Core | 564 | 15 |
| 05-10-65_m3_p22 | Core | 605 | 15 |
| 05-10-65_m3_p23 | Core | 595 | 15 |
| 05-10-65_m3_p24 | Core | 598 | 17 |
| 05-10-65_m3_p25 | Core | 595 | 18 |
| 05-10-65_m3_p26 | Core | 591 | 17 |
| 05-10-65_m3_p27 | Core | 591 | 14 |
| 05-10-65_m3_p28 | Core | 573 | 14 |
| 05-10-65_m3_p29 | Core | 579 | 14 |
| 05-10-65_m3_p3 | Core | 590 | 13 |
| 05-10-65_m3_p30 | Core | 594 | 13 |
| 05-10-65_m3_p31 | Core | 549 | 13 |
| 05-10-65_m3_p32 | Core | 580 | 19 |
| 05-10-65_m3_p33 | Core | 585 | 19 |
| 05-10-65_m3_p34 | Core | 620 | 18 |
| 05-10-65_m3_p35 | Core | 583 | 20 |
| 05-10-65_m3_p36 | Core | 597 | 20 |
| 05-10-65_m3_p37 | Core | 612 | 19 |
| 05-10-65_m3_p38 | Core | 606 | 20 |
| 05-10-65_m3_p39 | Core | 598 | 19 |

| Sample | Zone | Date | Error (2σ) |
|---|---|---|---|
| 05-10-65_m3_p4 | Core | 589 | 14 |
| 05-10-65_m3_p40 | Core | 600 | 19 |
| 05-10-65_m3_p41 | Core | 622 | 18 |
| 05-10-65_m3_p42 | Core | 568 | 18 |
| 05-10-65_m3_p43 | Core | 611 | 18 |
| 05-10-65_m3_p44 | Core | 596 | 14 |
| 05-10-65_m3_p45 | Core | 600 | 15 |
| 05-10-65_m3_p46 | Core | 601 | 14 |
| 05-10-65_m3_p47 | Core | 599 | 12 |
| 05-10-65_m3_p48 | Core | 621 | 22 |
| 05-10-65_m3_p49 | Core | 594 | 20 |
| 05-10-65_m3_p5 | Core | 588 | 14 |
| 05-10-65_m3_p50 | Core | 564 | 18 |
| 05-10-65_m3_p51 | Core | 582 | 20 |
| 05-10-65_m3_p52 | Core | 615 | 21 |
| 05-10-65_m3_p53 | Core | 606 | 17 |
| 05-10-65_m3_p54 | Core | 590 | 14 |
| 05-10-65_m3_p55 | Core | 545 | 16 |
| 05-10-65_m3_p56 | Core | 579 | 19 |
| 05-10-65_m3_p57 | Core | 618 | 19 |
| 05-10-65_m3_p58 | Core | 598 | 16 |
| 05-10-65_m3_p59 | Core | 626 | 18 |
| 05-10-65_m3_p6 | Core | 600 | 14 |
| 05-10-65_m3_p60 | Core | 581 | 20 |
| 05-10-65_m3_p61 | Core | 586 | 21 |
| 05-10-65_m3_p62 | Core | 573 | 20 |
| 05-10-65_m3_p63 | Core | 593 | 18 |
| 05-10-65_m3_p64 | Core | 610 | 18 |
| 05-10-65_m3_p65 | Core | 632 | 18 |
| 05-10-65_m3_p66 | Core | 593 | 19 |
| 05-10-65_m3_p67 | Core | 612 | 20 |
| 05-10-65_m3_p68 | Core | 609 | 21 |
| 05-10-65_m3_p69 | Core | 575 | 20 |
| 05-10-65_m3_p7 | Core | 587 | 14 |
| 05-10-65_m3_p70 | Core | 590 | 20 |
| 05-10-65_m3_p71 | Core | 643 | 21 |
| 05-10-65_m3_p72 | Core | 602 | 21 |
| 05-10-65_m3_p73 | Core | 580 | 20 |
| 05-10-65_m3_p74 | Core | 622 | 17 |
| 05-10-65_m3_p75 | Core | 592 | 18 |
| 05-10-65_m3_p76 | Core | 605 | 15 |
| 05-10-65_m3_p77 | Core | 632 | 17 |
| 05-10-65_m3_p78 | Core | 588 | 10 |
| 05-10-65_m3_p79 | Core | 585 | 10 |
| 05-10-65_m3_p8 | Core | 597 | 14 |
| 05-10-65_m3_p80 | Core | 585 | 10 |
| 05-10-65_m3_p9 | Core | 605 | 14 |
| | | | |
| 05-10-102_m1_pt3 | Core | 526 | 66 |
| 05-10-102_m1_pt5 | Core | 593 | 43 |
| 05-10-102_m1_pt6 | Core | 580 | 46 |
| 05-10-102_m1_pt8 | Core | 595 | 58 |
| 05-10-102_m1_pt9 | Core | 571 | 65 |

| Sample | Zone | Date | Error (2σ) |
|---|---|---|---|
| 05-10-102_m1_pt1 | Core | 504 | 56 |
| 05-10-102_m1_pt10 | Core | 564 | 85 |
| 05-10-102_m1_pt12 | Core | 556 | 61 |
| 05-10-102_m1_pt13 | Core | 583 | 50 |
| 05-10-102_m1_pt14 | Core | 604 | 49 |
| 05-10-102_m1_pt15 | Core | 621 | 45 |
| 05-10-102_m1_pt17 | Core | 634 | 60 |
| 05-10-102_m1_pt18 | Core | 597 | 73 |
| 05-10-102_m1_pt19 | Core | 608 | 88 |
| 05-10-102_m1_pt2 | Core | 529 | 53 |
| 05-10-102_m1_pt20 | Core | 594 | 50 |
| 05-10-102_m1_pt7 | Core | 636 | 45 |
| 05-10-102_m2_pt1 | Core | 616 | 24 |
| 05-10-102_m2_pt10 | Core | 635 | 23 |
| 05-10-102_m2_pt11 | Core | 614 | 21 |
| 05-10-102_m2_pt12 | Core | 627 | 21 |
| 05-10-102_m2_pt13 | Core | 656 | 21 |
| 05-10-102_m2_pt14 | Core | 607 | 21 |
| 05-10-102_m2_pt15 | Core | 598 | 20 |
| 05-10-102_m2_pt2 | Core | 629 | 21 |
| 05-10-102_m2_pt3 | Core | 645 | 20 |
| 05-10-102_m2_pt4 | Core | 592 | 10 |
| 05-10-102_m2_pt5 | Core | 616 | 18 |
| 05-10-102_m2_pt6 | Core | 602 | 21 |
| 05-10-102_m2_pt7 | Core | 644 | 18 |
| 05-10-102_m2_pt8 | Core | 626 | 23 |
| 05-10-102_m2_pt9 | Core | 574 | 21 |
| 05-10-102_m6_p1 | Core | 661 | 19 |
| 05-10-102_m6_p10 | Core | 580 | 20 |
| 05-10-102_m6_p11 | Core | 589 | 20 |
| 05-10-102_m6_p12 | Core | 612 | 21 |
| 05-10-102_m6_p13 | Core | 616 | 22 |
| 05-10-102_m6_p14 | Core | 567 | 26 |
| 05-10-102_m6_p15 | Core | 614 | 22 |
| 05-10-102_m6_p16 | Core | 604 | 18 |
| 05-10-102_m6_p17 | Core | 641 | 19 |
| 05-10-102_m6_p18 | Core | 641 | 19 |
| 05-10-102_m6_p19 | Core | 600 | 20 |
| 05-10-102_m6_p2 | Core | 633 | 19 |
| 05-10-102_m6_p20 | Core | 581 | 23 |
| 05-10-102_m6_p21 | Core | 616 | 22 |
| 05-10-102_m6_p3 | Core | 580 | 19 |
| 05-10-102_m6_p4 | Core | 634 | 18 |
| 05-10-102_m6_p5 | Core | 604 | 18 |
| 05-10-102_m6_p6 | Core | 581 | 19 |
| 05-10-102_m6_p7 | Core | 601 | 22 |
| 05-10-102_m6_p8 | Core | 581 | 23 |
| 05-10-102_m6_p9 | Core | 612 | 21 |
| 05-10-102_m6_p22 | Core | 568 | 17 |
| 05-10-102_m6_p23 | Core | 571 | 18 |
| 05-10-102_m6_p24 | Core | 629 | 17 |
| 05-10-102_m6_p25 | Core | 621 | 17 |
| 05-10-102_m6_p26 | Core | 559 | 18 |

| Sample | Zone | Date | Error (2σ) |
|---|---|---|---|
| 05-10-102_m6_p27 | Core | 584 | 18 |
| 05-10-102_m6_p28 | Core | 575 | 17 |
| 05-10-102_m6_p29 | Core | 599 | 17 |
| 05-10-102_m6_p30 | Core | 597 | 17 |
| 05-10-102_m6_p31 | Core | 552 | 18 |
| 05-10-102_m6_p32 | Core | 599 | 18 |
| 05-10-102_m6_p33 | Core | 596 | 17 |
| 05-10-102_m6_p34 | Core | 589 | 16 |
| 05-10-102_m6_p35 | Core | 583 | 17 |
| 05-10-102_m6_p36 | Core | 627 | 17 |
| 05-10-102_m6_p37 | Core | 573 | 20 |
| 05-10-102_m6_p38 | Core | 569 | 18 |
| 05-10-102_m6_p39 | Core | 620 | 18 |
| 05-10-102_m6_p40 | Core | 587 | 18 |
| 05-10-102_m6_p41 | Core | 654 | 18 |
| 05-10-102_m6_p42 | Core | 617 | 17 |
| 05-10-102_m6_p43 | Core | 605 | 19 |
| 05-10-102_m6_p44 | Core | 623 | 19 |
| 05-10-102_m6_p45 | Core | 560 | 19 |
| 05-10-102_m6_p46 | Core | 609 | 18 |
| 05-10-102_m6_p47 | Core | 567 | 17 |
| 05-10-102_m6_p48 | Core | 580 | 17 |
| 05-10-102_m6_p49 | Core | 621 | 21 |
| 05-10-102_m6_p50 | Core | 620 | 18 |
| 05-10-102_m6_p51 | Core | 623 | 19 |
| 05-10-102_m6_p52 | Core | 563 | 19 |
| 05-10-102_m6_p53 | Core | 621 | 18 |
| 05-10-102_m6_p54 | Core | 579 | 17 |
| 05-10-102_m6_p55 | Core | 572 | 17 |
| 05-10-102_m6_p56 | Core | 597 | 18 |
| 05-10-102_m6_p57 | Core | 622 | 20 |
| 05-10-102_m6_p58 | Core | 561 | 21 |
| 05-10-102_m6_p59 | Core | 653 | 21 |
| 05-10-102_m6_p60 | Core | 612 | 19 |
| 05-10-102_m6_p61 | Core | 579 | 20 |
| 05-10-102_m6_p64 | Core | 669 | 17 |
| 05-10-102_m6_p65 | Core | 612 | 17 |
| 05-10-102_m6_p66 | Core | 644 | 22 |
| 05-10-102_m6_p67 | Core | 628 | 21 |
| 05-10-102_m6_p68 | Core | 572 | 17 |
| 05-10-102_m6_p69 | Core | 610 | 17 |
| 05-10-102_m6_p70 | Core | 637 | 17 |
| 05-10-102_m6_p71 | Core | 592 | 17 |
| 05-10-102_m6_p72 | Core | 604 | 17 |
| 05-10-102_m6_p73 | Core | 598 | 17 |
| 05-10-102_m6_p74 | Core | 616 | 17 |
| 05-10-102_m6_p75 | Core | 607 | 17 |
| 05-10-102_m6_p76 | Core | 600 | 18 |
| 05-10-102_m6_p77 | Core | 607 | 17 |
| 05-10-102_m6_p78 | Core | 653 | 19 |
| 05-10-102_m6_p79 | Core | 587 | 18 |
| 05-10-102_m6_p80 | Core | 609 | 17 |
| 05-10-102_m6_p82 | Core | 627 | 17 |

| Sample | Zone | Date | Error (2σ) |
|---|---|---|---|
| 05-10-102_m2_pt16 | Rim | 589 | 11 |
| 05-10-102_m2_pt17 | Rim | 584 | 11 |
| 05-10-102_m2_pt18 | Rim | 584 | 10 |
| 05-10-102_m2_pt19 | Rim | 589 | 12 |
| 05-10-102_m2_pt20 | Rim | 582 | 13 |
| 05-10-102_m2_pt21 | Rim | 585 | 12 |
| 05-10-102_m2_pt22 | Rim | 573 | 13 |
| 05-10-102_m2_pt23 | Rim | 567 | 13 |
| 05-10-102_m2_pt24 | Rim | 600 | 12 |
| 05-10-102_m2_pt25 | Rim | 588 | 12 |
| 05-10-102_m2_pt26 | Rim | 573 | 12 |
| 05-10-102_m2_pt27 | Rim | 594 | 12 |
| 05-10-102_m2_pt28 | Rim | 594 | 11 |
| 05-10-102_m2_pt29 | Rim | 587 | 10 |
| 05-10-102_m2_pt30 | Rim | 586 | 12 |
| 05-10-102_m2_pt31 | Rim | 573 | 11 |
| 05-10-102_m2_pt32 | Rim | 579 | 11 |
| 05-10-102_m2_pt33 | Rim | 583 | 9 |
| 05-10-102_m2_pt34 | Rim | 573 | 11 |
| 05-10-102_m3_p1 | Rim | 588 | 8 |
| 05-10-102_m3_p10 | Rim | 605 | 8 |
| 05-10-102_m3_p11 | Rim | 599 | 8 |
| 05-10-102_m3_p12 | Rim | 576 | 8 |
| 05-10-102_m3_p13 | Rim | 592 | 8 |
| 05-10-102_m3_p14 | Rim | 583 | 7 |
| 05-10-102_m3_p15 | Rim | 611 | 9 |
| 05-10-102_m3_p2 | Rim | 592 | 8 |
| 05-10-102_m3_p3 | Rim | 583 | 7 |
| 05-10-102_m3_p4 | Rim | 589 | 8 |
| 05-10-102_m3_p5 | Rim | 576 | 8 |
| 05-10-102_m3_p6 | Rim | 599 | 8 |
| 05-10-102_m3_p7 | Rim | 592 | 7 |
| 05-10-102_m3_p8 | Rim | 594 | 7 |
| 05-10-102_m3_p9 | Rim | 595 | 8 |
| 05-10-102_m4_p1 | Rim | 593 | 20 |
| 05-10-102_m4_p10 | Rim | 610 | 24 |
| 05-10-102_m4_p11 | Rim | 558 | 24 |
| 05-10-102_m4_p12 | Rim | 574 | 18 |
| 05-10-102_m4_p2 | Rim | 559 | 20 |
| 05-10-102_m4_p5 | Rim | 570 | 24 |
| 05-10-102_m4_p9 | Rim | 548 | 24 |
| 05-10-102_m4_p13 | Rim | 596 | 11 |
| 05-10-102_m4_p14 | Rim | 595 | 12 |
| 05-10-102_m4_p15 | Rim | 574 | 21 |
| 05-10-102_m4_p16 | Rim | 540 | 23 |
| 05-10-102_m4_p17 | Rim | 601 | 14 |
| 05-10-102_m4_p18 | Rim | 592 | 17 |
| 05-10-102_m4_p19 | Rim | 599 | 11 |
| 05-10-102_m4_p20 | Rim | 575 | 15 |
| 05-10-102_m4_p21 | Rim | 593 | 16 |
| 05-10-102_m4_p22 | Rim | 599 | 14 |
| 05-10-102_m4_p23 | Rim | 588 | 10 |

| Sample | Zone | Date | Error (2σ) |
|---|---|---|---|
| 05-10-102_m4_p24 | Rim | 583 | 12 |
| 05-10-102_m4_p25 | Rim | 588 | 13 |
| 05-10-102_m4_p26 | Rim | 566 | 16 |
| 05-10-102_m4_p3 | Rim | 557 | 15 |
| 05-10-102_m4_p4 | Rim | 592 | 15 |
| 05-10-102_m4_p6 | Rim | 581 | 22 |
| 05-10-102_m4_p7 | Rim | 568 | 23 |
| 05-10-102_m4_p8 | Rim | 582 | 22 |
| 05-10-102_m5_p1 | Rim | 610 | 22 |
| 05-10-102_m5_p10 | Rim | 587 | 21 |
| 05-10-102_m5_p11 | Rim | 577 | 21 |
| 05-10-102_m5_p12 | Rim | 570 | 13 |
| 05-10-102_m5_p13 | Rim | 590 | 13 |
| 05-10-102_m5_p14 | Rim | 578 | 13 |
| 05-10-102_m5_p15 | Rim | 568 | 14 |
| 05-10-102_m5_p16 | Rim | 582 | 14 |
| 05-10-102_m5_p17 | Rim | 595 | 14 |
| 05-10-102_m5_p18 | Rim | 587 | 17 |
| 05-10-102_m5_p19 | Rim | 611 | 23 |
| 05-10-102_m5_p2 | Rim | 601 | 22 |
| 05-10-102_m5_p20 | Rim | 598 | 22 |
| 05-10-102_m5_p21 | Rim | 591 | 11 |
| 05-10-102_m5_p22 | Rim | 598 | 13 |
| 05-10-102_m5_p23 | Rim | 596 | 13 |
| 05-10-102_m5_p24 | Rim | 572 | 12 |
| 05-10-102_m5_p25 | Rim | 590 | 12 |
| 05-10-102_m5_p26 | Rim | 591 | 12 |
| 05-10-102_m5_p27 | Rim | 578 | 13 |
| 05-10-102_m5_p28 | Rim | 596 | 13 |
| 05-10-102_m5_p29 | Rim | 575 | 22 |
| 05-10-102_m5_p3 | Rim | 608 | 22 |
| 05-10-102_m5_p30 | Rim | 567 | 21 |
| 05-10-102_m5_p31 | Rim | 566 | 14 |
| 05-10-102_m5_p32 | Rim | 552 | 14 |
| 05-10-102_m5_p33 | Rim | 595 | 10 |
| 05-10-102_m5_p34 | Rim | 562 | 11 |
| 05-10-102_m5_p35 | Rim | 581 | 16 |
| 05-10-102_m5_p36 | Rim | 562 | 17 |
| 05-10-102_m5_p37 | Rim | 589 | 11 |
| 05-10-102_m5_p4 | Rim | 615 | 23 |
| 05-10-102_m5_p5 | Rim | 602 | 23 |
| 05-10-102_m5_p6 | Rim | 568 | 14 |
| 05-10-102_m5_p7 | Rim | 583 | 14 |
| 05-10-102_m5_p8 | Rim | 588 | 14 |
| 05-10-102_m5_p9 | Rim | 574 | 21 |
| | | | |
| 04-6-19-mnz4-spot2 | Core | 622 | 17 |
| 04-6-19-mnz4-spot3 | Core | 612 | 17 |
| 04-6-19-mnz4-spot4 | Core | 619 | 21 |
| 04-6-19-mnz4-spot6 | Core | 614 | 21 |
| 04-6-19-mnz4-spot7 | Core | 634 | 22 |
| 04-6-19-mnz4-spot8 | Core | 611 | 22 |
| 04-6-19-mnz5-spot10 | Core | 613 | 17 |

| Sample | Zone | Date | Error (2σ) |
|---|---|---|---|
| 04-6-19-mnz5-spot11 | Core | 623 | 15 |
| 04-6-19-mnz5-spot12 | Core | 616 | 18 |
| 04-6-19-mnz5-spot18 | Core | 610 | 18 |
| 04-6-19-mnz5-spot19 | Core | 606 | 15 |
| 04-6-19-mnz5-spot20 | Core | 632 | 15 |
| 04-6-19-mnz5-spot21 | Core | 615 | 14 |
| 04-6-19-mnz5-spot22 | Core | 594 | 17 |
| 04-6-19-mnz5-spot23 | Core | 585 | 15 |
| 04-6-19-mnz5-spot28 | Core | 641 | 18 |
| 04-6-19-mnz5-spot7 | Core | 672 | 17 |
| | | | |
| 04-6-19-mnz4-spot1 | Rim | 571 | 16 |
| 04-6-19-mnz4-spot10 | Rim | 588 | 21 |
| 04-6-19-mnz4-spot5 | Rim | 583 | 22 |
| 04-6-19-mnz4-spot9 | Rim | 612 | 21 |
| 04-6-19-mnz5-spot1 | Rim | 593 | 16 |
| 04-6-19-mnz5-spot13 | Rim | 599 | 17 |
| 04-6-19-mnz5-spot14 | Rim | 610 | 17 |
| 04-6-19-mnz5-spot15 | Rim | 602 | 17 |
| 04-6-19-mnz5-spot16 | Rim | 595 | 17 |
| 04-6-19-mnz5-spot17 | Rim | 593 | 16 |
| 04-6-19-mnz5-spot2 | Rim | 504 | 17 |
| 04-6-19-mnz5-spot24 | Rim | 479 | 16 |
| 04-6-19-mnz5-spot25 | Rim | 547 | 15 |
| 04-6-19-mnz5-spot26 | Rim | 532 | 16 |
| 04-6-19-mnz5-spot27 | Rim | 575 | 17 |
| 04-6-19-mnz5-spot29 | Rim | 614 | 17 |
| 04-6-19-mnz5-spot3 | Rim | 551 | 18 |
| 04-6-19-mnz5-spot30 | Rim | 597 | 18 |
| 04-6-19-mnz5-spot4 | Rim | 606 | 17 |
| 04-6-19-mnz5-spot5 | Rim | 596 | 18 |
| 04-6-19-mnz5-spot6 | Rim | 578 | 17 |
| 04-6-19-mnz5-spot8 | Rim | 582 | 16 |
| 04-6-19-mnz5-spot9 | Rim | 524 | 19 |
| 04-6-19-mnz8-spot1 | Rim | 596 | 18 |
| 04-6-19-mnz8-spot2 | Rim | 598 | 15 |
| 04-6-19-mnz8-spot3 | Rim | 599 | 14 |
| 04-6-19-mnz8-spot4 | Rim | 579 | 15 |
| 04-6-19-mnz8-spot5 | Rim | 588 | 16 |
| 04-6-19-mnz8-spot6 | Rim | 585 | 17 |
| | | | |
| GR-05-4b_m2_8 | Single Zone | 563 | 17 |
| GR-05-4b_m2_36 | Single Zone | 564 | 15 |
| GR-05-4b_m2_20 | Single Zone | 572 | 13 |
| GR-05-4b_m2_10 | Single Zone | 573 | 18 |
| GR-05-4b_m2_4 | Single Zone | 578 | 15 |
| GR-05-4b_m2_12 | Single Zone | 580 | 17 |
| GR-05-4b_m2_2 | Single Zone | 580 | 19 |
| GR-05-4b_m2_39 | Single Zone | 583 | 16 |
| GR-05-4b_m2_19 | Single Zone | 584 | 15 |
| GR-05-4b_m2_40 | Single Zone | 586 | 14 |
| GR-05-4b_m2_17 | Single Zone | 586 | 13 |
| GR-05-4b_m2_6 | Single Zone | 587 | 17 |

| Sample | Zone | Date | Error (2σ) |
|---|---|---|---|
| GR-05-4b_m2_41 | Single Zone | 588 | 15 |
| GR-05-4b_m2_7 | Single Zone | 590 | 17 |
| GR-05-4b_m2_16 | Single Zone | 590 | 15 |
| GR-05-4b_m2_24 | Single Zone | 590 | 12 |
| GR-05-4b_m2_45 | Single Zone | 590 | 14 |
| GR-05-4b_m2_31 | Single Zone | 591 | 18 |
| GR-05-4b_m2_5 | Single Zone | 591 | 15 |
| GR-05-4b_m2_37 | Single Zone | 591 | 16 |
| GR-05-4b_m2_14 | Single Zone | 592 | 18 |
| GR-05-4b_m2_29 | Single Zone | 593 | 20 |
| GR-05-4b_m2_26 | Single Zone | 594 | 13 |
| GR-05-4b_m2_33 | Single Zone | 594 | 15 |
| GR-05-4b_m2_42 | Single Zone | 597 | 16 |
| GR-05-4b_m2_38 | Single Zone | 598 | 17 |
| GR-05-4b_m2_35 | Single Zone | 599 | 19 |
| GR-05-4b_m2_27 | Single Zone | 600 | 14 |
| GR-05-4b_m2_15 | Single Zone | 600 | 18 |
| GR-05-4b_m2_21 | Single Zone | 601 | 18 |
| GR-05-4b_m2_9 | Single Zone | 602 | 18 |
| GR-05-4b_m2_44 | Single Zone | 604 | 16 |
| GR-05-4b_m2_13 | Single Zone | 606 | 19 |
| GR-05-4b_m2_23 | Single Zone | 608 | 19 |
| GR-05-4b_m2_34 | Single Zone | 613 | 12 |
| GR-05-4b_m2_43 | Single Zone | 614 | 13 |
| GR-05-4b_m2_30 | Single Zone | 615 | 19 |
| GR-05-4b_m2_32 | Single Zone | 616 | 19 |
| GR-05-4b_m2_18 | Single Zone | 618 | 14 |
| GR-05-4b_m2_25 | Single Zone | 620 | 12 |
| GR-05-4b_m2_22 | Single Zone | 624 | 17 |
| GR-05-4b_m2_28 | Single Zone | 624 | 18 |
| | | | |
| 05-5-22_m6_4 | Single Zone | 573 | 13 |
| 05-5-22_m6_2 | Single Zone | 577 | 15 |
| 05-5-22_m3_5 | Single Zone | 579 | 14 |
| 05-5-22_m7_5 | Single Zone | 581 | 16 |
| 05-5-22_m4_9 | Single Zone | 585 | 17 |
| 05-5-22_m6_8 | Single Zone | 593 | 14 |
| 05-5-22_m7_9 | Single Zone | 594 | 18 |
| 05-5-22_m3_17 | Single Zone | 597 | 14 |
| 05-5-22_m3_15 | Single Zone | 598 | 18 |
| 05-5-22_m4_4 | Single Zone | 599 | 17 |
| 05-5-22_m3_11 | Single Zone | 601 | 13 |
| 05-5-22_m6_1 | Single Zone | 605 | 16 |
| 05-5-22_m4_6 | Single Zone | 606 | 19 |
| 05-5-22_m7_1 | Single Zone | 609 | 17 |
| 05-5-22_m3_14 | Single Zone | 609 | 18 |
| 05-5-22_m6_3 | Single Zone | 611 | 17 |
| 05-5-22_m6_5 | Single Zone | 612 | 17 |
| 05-5-22_m4_2 | Single Zone | 612 | 17 |
| 05-5-22_m3_1 | Single Zone | 612 | 15 |
| 05-5-22_m4_7 | Single Zone | 614 | 17 |
| 05-5-22_m7_2 | Single Zone | 616 | 19 |
| 05-5-22_m4_5 | Single Zone | 616 | 16 |

| Sample | Zone | Date | Error (2σ) |
|---|---|---|---|
| 05-5-22_m3_8 | Single Zone | 619 | 14 |
| 05-5-22_m3_10 | Single Zone | 620 | 15 |
| 05-5-22_m3_9 | Single Zone | 620 | 15 |
| 05-5-22_m3_2 | Single Zone | 620 | 15 |
| 05-5-22_m3_4 | Single Zone | 621 | 14 |
| 05-5-22_m3_6 | Single Zone | 621 | 18 |
| 05-5-22_m3_18 | Single Zone | 622 | 15 |
| 05-5-22_m3_13 | Single Zone | 625 | 17 |
| 05-5-22_m3_20 | Single Zone | 625 | 16 |
| 05-5-22_m7_7 | Single Zone | 628 | 17 |
| 05-5-22_m7_10 | Single Zone | 628 | 17 |
| 05-5-22_m7_6 | Single Zone | 628 | 14 |
| 05-5-22_m7_8 | Single Zone | 629 | 18 |
| 05-5-22_m4_1 | Single Zone | 630 | 16 |
| 05-5-22_m3_16 | Single Zone | 630 | 14 |
| 05-5-22_m6_6 | Single Zone | 634 | 17 |
| 05-5-22_m6_9 | Single Zone | 634 | 17 |
| 05-5-22_m3_12 | Single Zone | 636 | 19 |
| 05-5-22_m7_4 | Single Zone | 637 | 19 |
| 05-5-22_m3_3 | Single Zone | 637 | 15 |
| 05-5-22_m4_3 | Single Zone | 637 | 19 |
| 05-5-22_m7_3 | Single Zone | 646 | 18 |
| 05-5-22_m4_10 | Single Zone | 647 | 17 |
| 05-5-22_m6_7 | Single Zone | 652 | 17 |
| 05-5-22_m4_8 | Single Zone | 653 | 18 |
| 05-5-22_m3_7 | Single Zone | 654 | 15 |
| | | | |
| 05b-6-108_m1_9 | Single Zone | 562 | 14 |
| 05b-6-108_m1_25 | Single Zone | 567 | 15 |
| 05b-6-108_m1_4 | Single Zone | 573 | 15 |
| 05b-6-108_m1_19 | Single Zone | 574 | 15 |
| 05b-6-108_m1_8 | Single Zone | 578 | 15 |
| 05b-6-108_m1_22 | Single Zone | 580 | 15 |
| 05b-6-108_m1_1 | Single Zone | 580 | 16 |
| 05b-6-108_m1_40 | Single Zone | 580 | 16 |
| 05b-6-108_m1_23 | Single Zone | 580 | 15 |
| 05b-6-108_m1_16 | Single Zone | 582 | 15 |
| 05b-6-108_m1_24 | Single Zone | 582 | 15 |
| 05b-6-108_m1_20 | Single Zone | 582 | 15 |
| 05b-6-108_m1_6 | Single Zone | 583 | 15 |
| 05b-6-108_m1_38 | Single Zone | 583 | 16 |
| 05b-6-108_m1_15 | Single Zone | 584 | 15 |
| 05b-6-108_m1_2 | Single Zone | 585 | 15 |
| 05b-6-108_m1_29 | Single Zone | 586 | 15 |
| 05b-6-108_m1_14 | Single Zone | 586 | 15 |
| 05b-6-108_m1_12 | Single Zone | 587 | 14 |
| 05b-6-108_m1_26 | Single Zone | 587 | 14 |
| 05b-6-108_m1_27 | Single Zone | 588 | 15 |
| 05b-6-108_m1_39 | Single Zone | 590 | 16 |
| 05b-6-108_m1_35 | Single Zone | 591 | 16 |
| 05b-6-108_m1_32 | Single Zone | 594 | 16 |
| 05b-6-108_m1_34 | Single Zone | 594 | 15 |
| 05b-6-108_m1_36 | Single Zone | 596 | 15 |

| Sample | Zone | Date | Error (2σ) |
|---|---|---|---|
| 05b-6-108_m1_10 | Single Zone | 596 | 14 |
| 05b-6-108_m1_30 | Single Zone | 596 | 15 |
| 05b-6-108_m1_28 | Single Zone | 597 | 15 |
| 05b-6-108_m1_18 | Single Zone | 603 | 15 |
| 05b-6-108_m1_17 | Single Zone | 603 | 15 |
| 05b-6-108_m1_11 | Single Zone | 603 | 15 |
| 05b-6-108_m1_5 | Single Zone | 606 | 15 |
| 05b-6-108_m1_37 | Single Zone | 606 | 16 |
| 05b-6-108_m1_3 | Single Zone | 609 | 15 |
| | | | |
| 05b-6-29_m1_24 | Single Zone | 567 | 13 |
| 05b-6-29_m4_core14 | Single Zone | 570 | 20 |
| 05b-6-29_m1_22 | Single Zone | 572 | 16 |
| 05b-6-29_m4_core16 | Single Zone | 574 | 16 |
| 05b-6-29_m4_core23 | Single Zone | 575 | 15 |
| 05b-6-29_m4_core5 | Single Zone | 583 | 16 |
| 05b-6-29_m1_14 | Single Zone | 583 | 16 |
| 05b-6-29_m1_21 | Single Zone | 583 | 16 |
| 05b-6-29_m4_core19 | Single Zone | 584 | 15 |
| 05b-6-29_m4_core25 | Single Zone | 585 | 14 |
| 05b-6-29_m1_18 | Single Zone | 587 | 16 |
| 05b-6-29_m4_core3 | Single Zone | 588 | 16 |
| 05b-6-29_m4_core2 | Single Zone | 589 | 17 |
| 05b-6-29_m1_29 | Single Zone | 589 | 12 |
| 05b-6-29_m1_30 | Single Zone | 591 | 12 |
| 05b-6-29_m1_11 | Single Zone | 592 | 18 |
| 05b-6-29_m4_core26 | Single Zone | 593 | 15 |
| 05b-6-29_m1_1 | Single Zone | 595 | 15 |
| 05b-6-29_m1_26 | Single Zone | 598 | 13 |
| 05b-6-29_m4_core13 | Single Zone | 598 | 16 |
| 05b-6-29_m1_13 | Single Zone | 599 | 17 |
| 05b-6-29_m4_core30 | Single Zone | 599 | 16 |
| 05b-6-29_m4_core6 | Single Zone | 600 | 16 |
| 05b-6-29_m1_10 | Single Zone | 601 | 18 |
| 05b-6-29_m1_23 | Single Zone | 601 | 15 |
| 05b-6-29_m4_core10 | Single Zone | 603 | 16 |
| 05b-6-29_m4_core12 | Single Zone | 603 | 15 |
| 05b-6-29_m4_core18 | Single Zone | 603 | 15 |
| 05b-6-29_m1_6 | Single Zone | 604 | 17 |
| 05b-6-29_m4_core27 | Single Zone | 604 | 16 |
| 05b-6-29_m1_3 | Single Zone | 605 | 18 |
| 05b-6-29_m4_core1 | Single Zone | 605 | 17 |
| 05b-6-29_m4_core4 | Single Zone | 605 | 16 |
| 05b-6-29_m1_12 | Single Zone | 606 | 19 |
| 05b-6-29_m1_15 | Single Zone | 606 | 16 |
| 05b-6-29_m4_core17 | Single Zone | 606 | 16 |
| 05b-6-29_m4_core29 | Single Zone | 606 | 17 |
| 05b-6-29_m4_core8 | Single Zone | 607 | 16 |
| 05b-6-29_m4_core24 | Single Zone | 607 | 14 |
| 05b-6-29_m4_core20 | Single Zone | 609 | 15 |
| 05b-6-29_m1_16 | Single Zone | 609 | 16 |
| 05b-6-29_m4_core7 | Single Zone | 609 | 16 |
| 05b-6-29_m4_core15 | Single Zone | 609 | 16 |

| Sample | Zone | Date | Error (2σ) |
|---|---|---|---|
| 05b-6-29_m4_core11 | Single Zone | 610 | 15 |
| 05b-6-29_m1_5 | Single Zone | 610 | 18 |
| 05b-6-29_m1_19 | Single Zone | 612 | 17 |
| 05b-6-29_m4_core22 | Single Zone | 612 | 16 |
| 05b-6-29_m4_core9 | Single Zone | 617 | 16 |
| 05b-6-29_m1_20 | Single Zone | 617 | 16 |
| 05b-6-29_m1_25 | Single Zone | 617 | 13 |
| 05b-6-29_m1_27 | Single Zone | 618 | 13 |
| 05b-6-29_m1_17 | Single Zone | 619 | 16 |
| 05b-6-29_m1_8 | Single Zone | 620 | 18 |
| 05b-6-29_m1_2 | Single Zone | 621 | 16 |
| 05b-6-29_m4_core28 | Single Zone | 621 | 17 |
| 05b-6-29_m1_9 | Single Zone | 626 | 18 |
| 05b-6-29_m1_4 | Single Zone | 630 | 19 |
| 05b-6-29_m1_7 | Single Zone | 638 | 18 |

**Table B-3.** All monazite p-values used in Chapter 3.

| | | | | 05-10-65 | 04-6-11 | 04-6-19 | 04-6-11 | 05-10-102 | 05-6-108 | 05-10-65 | GR-05-4B | 05-6-31 | 05b-6-29 | 05-6-103 | 05b-5-23 |
|---|---|---|---|---|---|---|---|---|---|---|---|---|---|---|---|
| | | age | | 561 | 562 | 579 | 582 | 587 | 588 | 592 | 595 | 595 | 601 | 602 | 605 |
| | | 1σ | | 42 | 28 | 33 | 12 | 15 | 11 | 19 | 15 | 17 | 15 | 14 | 10 |
| | age | 1σ | n | 16 | 98 | 29 | 36 | 97 | 35 | 80 | 42 | 13 | 58 | 72 | 23 |
| 05-10-65 | 561 | 42 | 16 | **0.500** | **0.474** | **0.072** | **0.031** | **0.014** | **0.011** | 0.005 | 0.003 | 0.003 | 0.001 | 0.001 | 0.000 |
| 04-6-11 | 562 | 28 | 98 | **0.474** | **0.500** | 0.006 | 0.000 | 0.000 | 0.000 | 0.000 | 0.000 | 0.000 | 0.000 | 0.000 | 0.000 |
| 04-6-19 | 579 | 33 | 29 | **0.072** | 0.006 | **0.500** | **0.313** | **0.124** | **0.090** | **0.029** | 0.010 | **0.021** | 0.001 | 0.000 | 0.000 |
| 04-6-11 | 582 | 12 | 36 | **0.031** | 0.000 | **0.313** | **0.500** | **0.049** | **0.024** | 0.001 | 0.000 | **0.010** | 0.000 | 0.000 | 0.000 |
| 05-10-102 | 587 | 15 | 97 | **0.014** | 0.000 | **0.124** | **0.049** | **0.500** | **0.290** | **0.022** | 0.001 | **0.047** | 0.000 | 0.000 | 0.000 |
| 05-6-108 | 588 | 11 | 35 | **0.011** | 0.000 | **0.090** | **0.024** | **0.290** | **0.500** | **0.084** | 0.009 | **0.078** | 0.000 | 0.000 | 0.000 |
| 05-10-65 | 592 | 19 | 80 | 0.005 | 0.000 | **0.029** | 0.001 | **0.022** | **0.084** | **0.500** | **0.143** | **0.248** | 0.001 | 0.000 | 0.000 |
| GR-05-4B | 595 | 15 | 42 | 0.003 | 0.000 | 0.010 | 0.000 | 0.001 | 0.009 | **0.143** | **0.500** | **0.486** | **0.031** | 0.006 | 0.001 |
| 05-6-31 | 595 | 17 | 13 | 0.003 | 0.000 | **0.021** | **0.010** | **0.047** | **0.078** | **0.248** | **0.486** | **0.500** | **0.141** | **0.085** | **0.036** |
| 05b-6-29 | 601 | 15 | 58 | 0.001 | 0.000 | 0.001 | 0.000 | 0.000 | 0.000 | 0.001 | **0.031** | **0.141** | **0.500** | **0.283** | **0.075** |
| 05-6-103 | 602 | 14 | 72 | 0.001 | 0.000 | 0.000 | 0.000 | 0.000 | 0.000 | 0.000 | 0.006 | **0.085** | **0.283** | **0.500** | **0.156** |
| 05b-5-23 | 605 | 10 | 23 | 0.000 | 0.000 | 0.000 | 0.000 | 0.000 | 0.000 | 0.000 | 0.001 | **0.036** | **0.075** | **0.156** | **0.500** |
| 05-10-102 | 606 | 29 | 111 | 0.000 | 0.000 | 0.000 | 0.000 | 0.000 | 0.000 | 0.000 | 0.003 | **0.038** | **0.093** | **0.172** | **0.453** |
| 05-6-36 | 607 | 19 | 169 | 0.000 | 0.000 | 0.000 | 0.000 | 0.000 | 0.000 | 0.000 | 0.000 | **0.017** | 0.009 | **0.022** | **0.246** |
| 04-6-11 | 611 | 10 | 31 | 0.000 | 0.000 | 0.000 | 0.000 | 0.000 | 0.000 | 0.000 | 0.000 | 0.003 | 0.000 | 0.000 | **0.019** |
| 05b-5-22 | 617 | 20 | 48 | 0.000 | 0.000 | 0.000 | 0.000 | 0.000 | 0.000 | 0.000 | 0.000 | 0.000 | 0.000 | 0.000 | 0.001 |
| 04-6-19 | 619 | 19 | 17 | 0.000 | 0.000 | 0.000 | 0.000 | 0.000 | 0.000 | 0.000 | 0.000 | 0.001 | 0.001 | 0.002 | 0.007 |
| 05-6-31 | 624 | 11 | 21 | 0.000 | 0.000 | 0.000 | 0.000 | 0.000 | 0.000 | 0.000 | 0.000 | 0.000 | 0.000 | 0.000 | 0.000 |
| 05-6-103 | 630 | 15 | 82 | 0.000 | 0.000 | 0.000 | 0.000 | 0.000 | 0.000 | 0.000 | 0.000 | 0.000 | 0.000 | 0.000 | 0.000 |
| 05b-5-23 | 631 | 20 | 18 | 0.000 | 0.000 | 0.000 | 0.000 | 0.000 | 0.000 | 0.000 | 0.000 | 0.000 | 0.000 | 0.000 | 0.000 |
| 05-6-31 | 634 | 15 | 24 | 0.000 | 0.000 | 0.000 | 0.000 | 0.000 | 0.000 | 0.000 | 0.000 | 0.000 | 0.000 | 0.000 | 0.000 |
| 05-6-36 | 635 | 19 | 131 | 0.000 | 0.000 | 0.000 | 0.000 | 0.000 | 0.000 | 0.000 | 0.000 | 0.000 | 0.000 | 0.000 | 0.000 |
| 04-7-1 | 622 | 14 | 7 | 0.000 | 0.000 | 0.000 | 0.000 | 0.000 | 0.000 | 0.001 | 0.001 | 0.001 | 0.004 | 0.005 | **0.010** |
| 05-6-31b | 647 | 6 | 7 | 0.000 | 0.000 | 0.000 | 0.000 | 0.000 | 0.000 | 0.000 | 0.000 | 0.000 | 0.000 | 0.000 | 0.000 |
| 04-6-11 | 648 | 6 | 6 | 0.000 | 0.000 | 0.000 | 0.000 | 0.000 | 0.000 | 0.000 | 0.000 | 0.000 | 0.000 | 0.000 | 0.000 |
| 05-13-13 | 678 | 15 | 4 | 0.000 | 0.000 | 0.000 | 0.001 | 0.001 | 0.001 | 0.001 | 0.001 | 0.000 | 0.001 | 0.001 | 0.001 |

| | 05-10-102 | 05-6-36 | 04-6-11 | 05b-5-22 | 04-6-19 | 05-6-31 | 05-6-103 | 05b-5-23 | 05-6-31 | 05-6-36 | 04-7-1 | 05-6-31b | 04-6-11 | 05-13-13 |
|---|---|---|---|---|---|---|---|---|---|---|---|---|---|---|
| | 606 | 607 | 611 | 617 | 619 | 624 | 630 | 631 | 634 | 635 | 622 | 647 | 648 | 678 |
| | 29 | 19 | 10 | 20 | 19 | 11 | 15 | 20 | 15 | 19 | 14 | 6 | 6 | 15 |
| | 111 | 169 | 31 | 48 | 17 | 21 | 82 | 18 | 24 | 131 | 7 | 7 | 6 | 4 |
| 05-10-65 | 0.000 | 0.000 | 0.000 | 0.000 | 0.000 | 0.000 | 0.000 | 0.000 | 0.000 | 0.000 | 0.000 | 0.000 | 0.000 | 0.000 |
| 04-6-11 | 0.000 | 0.000 | 0.000 | 0.000 | 0.000 | 0.000 | 0.000 | 0.000 | 0.000 | 0.000 | 0.000 | 0.000 | 0.000 | 0.000 |
| 04-6-19 | 0.000 | 0.000 | 0.000 | 0.000 | 0.000 | 0.000 | 0.000 | 0.000 | 0.000 | 0.000 | 0.000 | 0.000 | 0.000 | 0.000 |
| 04-6-11 | 0.000 | 0.000 | 0.000 | 0.000 | 0.000 | 0.000 | 0.000 | 0.000 | 0.000 | 0.000 | 0.000 | 0.000 | 0.000 | 0.001 |
| 05-10-102 | 0.000 | 0.000 | 0.000 | 0.000 | 0.000 | 0.000 | 0.000 | 0.000 | 0.000 | 0.000 | 0.000 | 0.000 | 0.000 | 0.001 |
| 05-6-108 | 0.000 | 0.000 | 0.000 | 0.000 | 0.000 | 0.000 | 0.000 | 0.000 | 0.000 | 0.000 | 0.000 | 0.000 | 0.000 | 0.001 |
| 05-10-65 | 0.000 | 0.000 | 0.000 | 0.000 | 0.000 | 0.000 | 0.000 | 0.000 | 0.000 | 0.000 | 0.001 | 0.000 | 0.000 | 0.001 |
| GR-05-4B | 0.003 | 0.000 | 0.000 | 0.000 | 0.000 | 0.000 | 0.000 | 0.000 | 0.000 | 0.000 | 0.001 | 0.000 | 0.000 | 0.001 |
| 05-6-31 | **0.038** | **0.017** | 0.003 | 0.000 | 0.001 | 0.000 | 0.000 | 0.000 | 0.000 | 0.000 | 0.001 | 0.000 | 0.000 | 0.000 |
| 05b-6-29 | **0.093** | 0.009 | 0.000 | 0.000 | 0.001 | 0.000 | 0.000 | 0.000 | 0.000 | 0.000 | 0.004 | 0.000 | 0.000 | 0.001 |
| 05-6-103 | **0.172** | **0.022** | 0.000 | 0.000 | 0.002 | 0.000 | 0.000 | 0.000 | 0.000 | 0.000 | 0.005 | 0.000 | 0.000 | 0.001 |
| 05b-5-23 | **0.453** | **0.246** | **0.019** | 0.001 | 0.007 | 0.000 | 0.000 | 0.000 | 0.000 | 0.000 | **0.010** | 0.000 | 0.000 | 0.001 |
| 05-10-102 | **0.500** | **0.338** | **0.053** | 0.003 | **0.012** | 0.000 | 0.000 | 0.000 | 0.000 | 0.000 | **0.011** | 0.000 | 0.000 | 0.001 |
| 05-6-36 | **0.338** | **0.500** | **0.040** | 0.002 | **0.013** | 0.000 | 0.000 | 0.000 | 0.000 | 0.000 | **0.016** | 0.000 | 0.000 | 0.001 |
| 04-6-11 | **0.053** | **0.040** | **0.500** | **0.052** | **0.073** | 0.000 | 0.000 | 0.000 | 0.000 | 0.000 | **0.045** | 0.000 | 0.000 | 0.001 |
| 05b-5-22 | 0.003 | 0.002 | **0.052** | **0.500** | **0.365** | **0.025** | 0.000 | 0.008 | 0.000 | 0.000 | **0.198** | 0.000 | 0.000 | 0.001 |
| 04-6-19 | **0.012** | **0.013** | **0.073** | **0.365** | **0.500** | **0.149** | **0.014** | **0.037** | 0.006 | 0.002 | **0.317** | 0.000 | 0.000 | 0.000 |
| 05-6-31 | 0.000 | 0.000 | 0.000 | **0.025** | **0.149** | **0.500** | **0.018** | **0.106** | 0.008 | 0.000 | **0.361** | 0.000 | 0.000 | 0.003 |
| 05-6-103 | 0.000 | 0.000 | 0.000 | 0.000 | **0.014** | **0.018** | **0.500** | **0.457** | **0.176** | **0.025** | **0.087** | 0.000 | 0.000 | 0.004 |
| 05b-5-23 | 0.000 | 0.000 | 0.000 | 0.008 | **0.037** | **0.106** | **0.457** | **0.500** | **0.317** | **0.213** | **0.113** | 0.003 | 0.002 | 0.001 |
| 05-6-31 | 0.000 | 0.000 | 0.000 | 0.000 | 0.006 | 0.008 | **0.176** | **0.317** | **0.500** | **0.347** | **0.042** | 0.001 | 0.001 | 0.002 |
| 05-6-36 | 0.000 | 0.000 | 0.000 | 0.000 | 0.002 | 0.000 | **0.025** | **0.213** | **0.347** | **0.500** | **0.025** | 0.000 | 0.001 | 0.005 |
| 04-7-1 | **0.011** | **0.016** | **0.045** | **0.198** | **0.317** | **0.361** | **0.087** | **0.113** | **0.042** | **0.025** | **0.500** | 0.002 | 0.001 | 0.000 |
| 05-6-31b | 0.000 | 0.000 | 0.000 | 0.000 | 0.000 | 0.000 | 0.000 | 0.003 | 0.001 | 0.000 | 0.002 | **0.500** | **0.381** | **0.013** |
| 04-6-11 | 0.000 | 0.000 | 0.000 | 0.000 | 0.000 | 0.000 | 0.000 | 0.002 | 0.001 | 0.001 | 0.001 | **0.381** | **0.500** | **0.015** |
| 05-13-13 | 0.001 | 0.001 | 0.001 | 0.001 | 0.000 | 0.003 | 0.004 | 0.001 | 0.002 | 0.005 | 0.000 | **0.013** | **0.015** | **0.500** |

*Appendix C – Protocol for monazite dating used at the University of Maryland*

EPMA (U-Th)-Pb Monazite Dating Technique
Procedure Outline

## Grain Mapping

1. Coat samples with a standard carbon coat, and load samples into EPMA.
2. Set the accelerating voltage to 15 kV and the cup current to 250 nA.
3. Conduct peak searches for U, Th, Pb and Y on appropriate standards (*e.g.*, UO2 for U, Thorite for Th, Galena or PbCO3 for Pb, and YPO4 for Y) for the x-rays on the spectrometers listed in Table C-1 (also in the 'Monazite X-Ray Map Settings' Google Spreadsheet).

**Table C-1.**

| Channel | Element | X-Ray | Crystal | Peak |
|---|---|---|---|---|
| 2 | U | Mβ | PETH | 119.072 |
| 3 | Th | Mα | PETJ | 132.431 |
| 4 | Pb | Mα | PETJ | 169.321 |
| 5 | Y | Lα | TAP | 69.926 |

4. Locate the unknown monazite grain, and make note of its dimensions.
5. Move the crosshairs to the center of the grain, and read and store the point.
6. Adjust the pixel size to be somewhere between 0.5 and 1 μm, depending on the desired resolution. This should be 0.5 μm if you wish to calculate a monazite age map.
7. Adjust the map dimensions so that the total map area is slightly larger than the monazite grain.
8. Set the collection time to *ca.* 200 ms. This should be longer (400-500 ms) if you are expecting low counts, or you wish to calculate a monazite age map.
9. Press apply, and begin map collection.

## Chemical Dating

1. Coat samples with a standard carbon coat.
2. Load stage containing the **Hanchar Epoxy Mount**, **Reno Mount**, and **samples** into EPMA.

***Standardization***

3. Open the Google Spreadsheet 'Monazite EPMA Settings.'
4. In the spreadsheet, copy the previous standardization and paste it 2 rows below the last line of text. Update the date, and username. You will be editing the information in this part of the spreadsheet as you go.

5. Set the accelerating voltage to 15 kV, the cup current to 200 nA, and the beam diameter to your desired width (typically 3-5 μm).
6. Open the quantitative analysis window (Analysis -> Quantitative Analysis).
7. Click Sample and choose the Group and Sample name of your choice.
8. In the Measurement menu, check that the correction method is "Oxide" for Material and "ZAF" for Correction Method.
9. Open the Element Condition window (from the Measurement Menu). Under the "WDS" section, click "Elements." Choose U, Th, Pb, Y, Ca, Ce, P and Si. Press OK.
10. Click "Meas. order." U (PETH) should be the only element on Ch 2. Channel 3 should have Th (PETJ) first, and Ca (PETJ) second. Channel 4 should have Pb (PETJ) first and Ce (PETJ) second. Channel 5 should have Y (TAP) first, P (TAP) second and Si (TAP) last. Press OK.
11. Click "Element Condition" next, and leave this window in the background. We will come back to this window later.
12. In the "JEOL EPMA Menu," click 'Analysis' and choose 'Standard Analysis.'

*The steps 13- 45 will be completed for each of the elements on the appropriate standard in Table C-2 (these are the same standards/elements in the 'Monazite EPMA Settings' Google Spreadsheet). Note: Hanchar Epoxy Mount is different from Hanchar Mount!*

**Table C-2.**

| Element | X-ray | Ch | xtal | Count Time (peak/bkgd) | Standard | Mount |
|---|---|---|---|---|---|---|
| Pb | Mα | 4 | PETJ | 240/120 | PbCO3 | Hanchar Epoxy |
| Y | Lα | 5 | TAP | 30/15 | YPO4 | UMD REE |
| P | Kα | 5 | TAP | 10/5 | YPO4 | UMD REE |
| U | Mβ | 2 | PETH | 80/40 | UO2 | Hanchar Epoxy |
| Th | Mα | 3 | PETJ | 80/40 | ThSiO4-jx1 | Hanchar Epoxy |
| Si | Kα | 5 | TAP | 100/50 | ThSiO4-jx1 | Hanchar Epoxy |
| Ca | Kα | 3 | PETJ | 60/30 | Grt-12442 | UMD Mineral |
| Ce | Lα | 4 | PETJ | 10/5 | CePO4 | UMD REE |

13. In the "Standard Analysis" menu, choose "Sample," and open the standard you wish to set up.
14. Move the stage to the appropriate standard in the appropriate Mount.
15. With the BSE image as your guide, zoom in so that the BSE image shows only the grain.
16. In the "JEOL EPMA Menu," click 'Monitor' and choose 'Peak Search.'
17. Click 'Element.'
18. In the box labeled 'Element,' type the element symbol.
19. Click the appropriate x-ray button for 'X-Ray.'
20. Click the appropriate channel number button for 'Channel.'
21. Click the appropriate crystal button for 'Crystal.'
22. Click the "2" button for 'Pksk no.'
23. Click 'Search.'

24. Record the peak value in the Google Spreadsheet.
25. In the "JEOL EPMA Menu," click 'Monitor' and choose 'SCA Scan.'
26. In the pulldown menu next to 'Signal:', choose "CH-X" (Where X represents the appropriate channel number for this element)
27. Press the "Base L" button.
28. In the window that opens, press the "SCA" button.
29. In the window that opens, set the settings to those used in the last monazite microprobe dating session (these data are in the Google Spreadsheet).
30. In the "SCA Scan" window, press "Start."
31. Adjust the High V and Gain settings until the ENTIRE (extremely important for Pb, U, Th and Y!) peak is greater than the Base (V) value and the ENTIRE (extremely important for Pb, U, Th and Y!) peak fits within the Window (V). The minimum value for Base (V) should be 0.5, but ideally 0.7. The peak height (count) should be maximized if possible. It is highly unlikely that these values will change drastically since the last analytical session. If they are very different, please contact Piccoli or Reno – something may be wrong.
32. Input this data into the Google Spreadsheet.
33. Go to the "Element Condition" window that you opened in step 11.
34. Click the "Elem- _" button that corresponds to the element that was just analyzed to open the "WDS Element Data Table" for that element.
35. Find the column that is appropriate for the channel, crystal and X-ray being analyzed for the element in question. Click the column header to select that column.
36. Press the "Read" button to read the peak value and SCA settings.
37. CHECK that ALL of the settings in this column EXACTLY match the settings for this element in the Google Spreadsheet (including background positions, mes. time, etc.). Also ensure that "Peak Seak" is set to 0, and that "Diff/Int" is set to "Diff." Press OK.
38. In the "Standard Analysis" window, choose "Measurement," and "Stage Condition."
39. Choose "Pos. Input."
40. Move the stage to a point on the standard that is suitable for analysis, and press "Read" and then "Store."
41. Set "Accumulation" to 4.
42. Press the "confirm" button, and choose 4 points for standardization.
43. Press Close in the Stage Condition Input window.
44. Press Close in the Stage Condition window.
45. Repeat steps 13 – 45 for each element.

46. In the "WDS Element Window," CHECK that ALL of the settings for ALL of the elements EXACTLY match the settings in the Google Spreadsheet.
47. Repeat step 46.
48. Consider repeating step 47.
49. In the "WDS Element Condition" window, click OK.
50. In the "Element Condition" window, click Close.
51. In the main SCA Scan window, click Exit.

52. In the "Standard Analysis" window, click "Measurement," and choose "EOS Condition."
53. Press "Read." Make sure that the "Probe Scan" button is turned OFF, and that the accelerating voltage is 15 kV and the current is 2.00e-07A.
54. In the "Standard Analysis" window, click "Measurement," and choose "Preset Measurement."
55. Make sure the appropriate 6 standards are checked, and press the yellow "Acquire" button. Standardization takes between 1-2 hours.

***Reference Monazite Testing***

56. In the "Standard Analysis" window, click "Measurement," and choose "EOS Condition."
57. Press "Read." Make sure that the "Probe Scan" button is turned OFF, and that the accelerating voltage is 15 kV and the current is 2.00e-07A.
58. Move the stage to a grain of GSC-8153 (*ca.* 501 Ma) or Trebilcock (*ca.* 280 Ma) in the Reno Mount.
59. In the "Quantitative Analysis" window, choose "Measurement" and "Stage Condition."
60. Choose "Pos. Input."
61. Move the stage to a point on the reference monazite that is appropriate for analysis, and make sure that the crosshairs are in focus. Please avoid any SIMS pits.
62. In the Stage Condition Input window, press "Read" and then "Store," or just press the "STOR" button on the joystick. The accumulation should be set to "1".
63. Put a comment in the comment section that indicates which reference monazite you are analyzing. Please, DO NOT USE SPACES – this causes problems with data processing later on.
64. Press "Apply" and then press the down arrow.
65. Input 2 or 3 more points.
66. Close the Stage condition window.
67. In the "Quantitative Analysis" window, choose "Measurement" and then "Preset Measurement."
68. Press "Acquire" to run the analyses. Each point takes *ca.* 9 minutes.
69. Run the output through the fly.c program to calculate a date for each of these 3 or 4 points. If the dates are within an acceptable range of the accepted date, proceed to unknown measurement. If dates are too old, or too young, go back to step 13, and figure it out.

***Unknown Data Acquisition***

70. Move the stage to the unknown monazite grains.
71. Set up points by following steps 59-64 for each point.
    a. Three points should be run on EACH of GSC-8153 and Trebilcock after every 12-15 unknown analyses.
72. Close the Stage condition window.

73. In the “Quantitative Analysis” window, choose “Measurement” and then “Preset Measurement.”
74. Press “Acquire” to run the analyses. Each point takes *ca.* 9 minutes.
75. Export the data from the probe for date and error calculation en masse using the lead.c program.

```
#include <stdio.h>
#include <math.h>

main(int argc, char *argv[])
{
     FILE *fp;
     if(argc !=4) {
     printf("correct usage: ./a.out input_file
age_output_file mathematica_output_file\n\n./a.out is the
command to run this program ('a.out' should be replaced
with the correct filename)\ninput_file is the full
filename for the file that contains the raw
data\nage_output_file is the name of a file that this
program will create containing the
dates\nmathematica_output_file is the name of a file that
this program will create containing code formatted for
input into mathematica\n\n");
     return 2;
     }
     if((fp = fopen(argv[1], "r")) == NULL) {
     printf("%s can't be opened.\n", argv[1]);
     return 1;
     }
     fclose(fp);



/* Definition of Constants */
long double Avnumb, Thlambda, U238lambda, U235lambda;
long double Uwt, Th232wt, U238wt, U235wt, Pb208wt,
Pb207wt, Pb206wt, Thfact, Ufact, Pbfact, Yfact;
int i;
Thlambda = 4.9475e-11;
U238lambda = 1.55125e-10;
U235lambda =9.8485e-10;
Avnumb = 6.022E23;
Th232wt = 232.03806;
Uwt = 238.0289;
U238wt = 238.0507847;
U235wt = 235.0439242;
Pb208wt = 207.976627;
Pb206wt = 205.97444;
Pb207wt = 206.975872;
Thfact = 0.878809;
Ufact = 0.881498;
Pbfact = 0.928318;
Yfact = 0.787440;

/* Definition of Input Variables */
```

```
float ThO2, UO2, PbO, Y2O3, CtsTh, CtsU, CtsPb, CtsY, EY,
Et, krawTh, krawY, Date, ETh, EU, EPb, EThRel, EPbRel,
EURel, EYRel, PbThStd, PbYStd, PbPbStd, ThThStd, YYStd,
EPbPbStdRel, EPbThStdRel, EThThStdRel, EPbYStdRel,
EYYStdRel, UThStd, UUStd, EUUStdRel, EUThStdRel;
char comment[30];

/*Definition of Working Variables */
long double Th, U, Pb, Y, U238, U235, DTh, DU235, DU238,
NTh, NU235, NU238, Pb206, Pb207, Pb208, expint, expout,
Udiv, TotPb, DiffPb, DiffPer;
int m, lines, p, r;

/*counts the number of lines in the input file*/

lines=1;
m=0;
char* data = (char*)data;
fp = fopen(argv[1], "r");

while ((m = getc(fp)) != EOF) {
     if (m == '\n')
          lines++;
}
printf("%i points.\n", lines);
fseek(fp, 0L, SEEK_SET);

/*opens the output files for writing*/

FILE *fp2;
if((fp2 = fopen(argv[2], "w")) == NULL){
     printf("%s can't be opened.\n", argv[2]);
return 2;
}
fprintf(fp2,
"Comment\tDate\tError\tDate\tError\tTh\tU\tPb\tPb208\tPb2
06\tPb207\tCalc Pb\tDiff Pb\tDiff Pb Percent\n");

FILE *fp3;
fp3 = fopen(argv[3], "w");

int count=0;

/*main calculations*/
for(i=lines; i>0; i--){

     count++;
     fscanf(fp, "%s%f%f%f%f%f%f%f", comment, &UO2,
&ThO2, &PbO, &EURel, &EThRel, &EPbRel, &krawTh, &krawY);
     printf("\n********************\n\n%s %f %f %f %f %f
%f\n", comment, UO2, ThO2, PbO, EU, ETh, EPb);

     /*fscanf(fp,
"%s%f%f%f%f%f%f%f%f%f%f%f%f%f%f%f%f%f%f%f%f%f%f%f%f%f%f",
```

```
comment, &ThO2, &UO2, &PbO, &Y2O3, &CtsTh, &CtsU, &CtsPb,
&CtsY, &EThRel, &EPbRel, &EURel, &EYRel, &PbThStd,
&PbYStd, &PbPbStd, &ThThStd, &YYStd, &EPbPbStdRel,
&EPbThStdRel, &EThThStdRel, &EPbYStdRel, &EYYStdRel,
&UThStd, &UUStd, &EUUStdRel, &EUThStdRel);
     printf("\n********************\n\n%s %f %f %f\n",
comment, ThO2, UO2, PbO);*/
     /*printf("\n********************\n\ncomment:%s\nThO2
: %f\nUO2: %f\nPbO: %f\nY2O3: %f\nCtsTh: %f\nCtsU:
%f\nCtsPb: %f\nCtsY: %f\nEThRel: %f\nEPbRel: %f\nEURel:
%f\nEYRel: %f\nPbThStd: %f\nPbYStd: %f\nPbPbStd:
%f\nThThStd: %f\nYYStd: %f\nEPbPbStdRel: %f\nEPbThStdRel:
%f\nEThThStdRel: %f\nEPbYStdRel: %f\nEYYStdRel:
%f\nUThStd: %f\nUUStd: %f\nEUUStdRel: %f\nEUThStdRel:
%f\n", comment, ThO2, UO2,
PbO,Y2O3,CtsTh,CtsU,CtsPb,CtsY,EThRel,EPbRel,EURel,EYRel,
PbThStd,PbYStd,PbPbStd,ThThStd,YYStd,EPbPbStdRel,EPbThStd
Rel,EThThStdRel,EPbYStdRel,EYYStdRel,UThStd,UUStd,EUUStdR
el,EUThStdRel);*/
     Th = ThO2 * Thfact;
     U = UO2 * Ufact;
     Pb = PbO * Pbfact;
     Y = Y2O3 * Yfact;
     Udiv = 137.88/138.88;
     fprintf(fp2, "%s\t", comment);
     fprintf(fp3, "%i,%s,{%i,", count, comment, count);

     /*Calculation of Absolute Uncertainties from
Relative Input Values*/

     long double EPbCorr, EUCorr, EPbPbStd, EPbThStd,
EThThStd, EPbYStd, EYYStd, EUUStd, EUThStd;

     ETh = Th * EThRel/100;
     EPb = Pb * EPbRel/100;
     EU = U * EURel/100;
     EY = Y * EYRel/100;

     /*printf("Eth = %f\nEPb = %f\tEPbRel = %f\tPb =
%Lf\nEU = %f\tEURel = %f\tU = %Lf\n", ETh, EPb, EPbRel,
Pb, EU, EURel, U);*/
     /*EPbPbStd = PbPbStd * EPbPbStdRel/100;
     EPbThStd = PbThStd * EPbThStdRel/100;
     EThThStd = ThThStd * EThThStdRel/100;
     EPbYStd = PbYStd * EPbYStdRel/100;
     EYYStd = YYStd * EYYStdRel/100;
     EUUStd = UUStd * EUUStdRel/100;
     EPbYStd = PbYStd * EPbYStdRel/100;
     EUThStd = UThStd * EUThStdRel/100;*/
/*   printf("EY = %f\n", EY);*/

     /*printf("Y = %Lf\nEY = %f\nEPbPbStd = %Lf\nEPbThStd
= %Lf\nEThThStd = %Lf\nEYYStd = %Lf\nEPbYStd = %Lf\n", Y,
EY, EPbPbStd, EPbThStd, EThThStd, EYYStd, EPbYStd);*/
```

```
     /*Corrected Pb*/

     long double PbCorr;
     PbCorr = Pb - 0.002136 * krawY - 0.0003542 * krawTh;
     Pb = PbCorr;
     fprintf(fp3, "%6.2Lf,", Pb*10000);

     /*Corrected Pb error*/
/*
     printf("ETh = %f\n", ETh);
     printf("EPb = %Lf\n", ((CtsPb *
EPbRel/100)/CtsPb)*Pb);

     printf("EPbcts = %f\n", EPb);
     EPbCorr = sqrt(pow(EPb,2) +
pow((1+((PbThStd*CtsTh)/(pow((PbPbStd),2)*ThThStd))+(PbYS
td*CtsY)/((pow(PbPbStd,2))*YYStd)),2)*pow(EPbPbStd,2) +
pow(((-CtsTh)/(PbPbStd*ThThStd)),2)*pow(EPbThStd,2) +
pow(((PbThStd*CtsTh)/(PbPbStd*pow(ThThStd,2))),2)*pow(ETh
ThStd,2) + pow(((-
PbThStd)/(PbPbStd*ThThStd)),2)*pow(ETh,2) + pow(((-
CtsY)/(PbPbStd*YYStd)),2)*pow(EPbYStd,2) +
pow(((PbYStd*Y)/(PbPbStd*pow(YYStd,2))),2)*pow(EYYStd,2)
+ pow(((-PbYStd)/(PbPbStd*YYStd)),2)*pow(EY,2));
     printf("EPbcts = %Lf\n", EPbCorr);

     EPb = (EPbCorr/CtsPb)*Pb;
     printf("EPb = %f\n", EPb);
*/
     /*Corrected U*/

     long double UCorr;
     UCorr = U - 0.006648 * krawTh;
     U = UCorr;
     fprintf(fp3, "%6.2Lf,", U*10000);
     fprintf(fp3, "%6.2Lf,", Th*10000);
     fprintf(fp3, "%6.2f,", EPb*10000);
     fprintf(fp3, "%6.2f,", ETh*10000);
     fprintf(fp3, "%6.2f,", EU*10000);

     /*Corrected U error*/
/*
     EUCorr = sqrt(pow(EU,2) +
pow((1+(UThStd*Th)/(pow(UUStd,2)*ThThStd)),2)*pow(EUUStd,
2) + pow(((-Th)/(UUStd*ThThStd)),2)*pow(EUThStd,2) +
pow(((UThStd*Th)/(UUStd*pow(ThThStd,2))),2)*pow(EThThStd,
2) + pow(((-UThStd)/(UUStd*ThThStd)),2)*pow(ETh,2));

     printf("EU = %f\t\tEUCorr = %Lf\n", EU, EUCorr);
     EU = (EUCorr/CtsU)*U;
     printf("EUCorr = %Lf\tCtsU = %f\tU = %Lf\tEU =
%f\n", EUCorr, CtsU, U, EU);
*/
     /*Date Calculation*/
```

```
     long double PbDiff, PbTest, PbCalc, Date2, DateDiff,
Date3;

     r=0;
     PbCalc = 0.0000;
     Date2 = 2.5E9;
     DateDiff = Date2;
     PbDiff = PbCalc - Pb;

     while (fabs(PbDiff) > 0.00005) {

          PbCalc = ((Th/Th232wt)*(exp(Thlambda*Date2)-
1)*Pb208wt) + ((U/Uwt)*Udiv*(exp(U238lambda*Date2)-
1)*Pb206wt) + ((U/Uwt)*(1-Udiv)*(exp(U235lambda*Date2)-
1)*Pb207wt);
          PbTest = PbCalc - Pb;
          /*printf("%d Date2 %Lf PbTest %Lf\n", r, Date2,
PbTest);*/
          if (PbTest > 0.00001) {
                    Date3 = Date2;
                    Date2 = Date2 - (0.5 * DateDiff);
                    DateDiff = fabs(Date3 - Date2);
          }
          else
               if (PbTest < -0.00001) {
                    Date3 = Date2;
                    Date2 = Date2 + (0.5 * DateDiff);
                    DateDiff = fabs(Date3 - Date2);
          }
          PbDiff = PbCalc-Pb;
          r++;
          if(r>50) {
               printf("\nITERATION ERROR r = %d\tDate too
high/low?\t----------ERROR----------ERROR----------\n",
r);
               PbDiff = 0.00000;
          }
          /*printf("%i ",r);*/
     }
     printf("\nCalculated Date:%10.0Lf\n", Date2);
     fprintf(fp2, "%10.0Lf\t", Date2);
     fprintf(fp3, "%4.1Lf,", Date2/1000000);
     /*printf("EPb = %f\nETh = %f\nEU = %f\n", EPb, ETh,
EU);*/

     /*error calculation*/

     long double a, b, c, d, j, k, z, DateError, SRTop,
PbPart, ThPart, UPart;

     /*EPb = EPbCorr;*/
     /*EU = EUCorr;*/
     a = Pb208wt/Th232wt;
     b = (Pb206wt*137.88)/(Uwt*138.88);
```

```
     c = (Pb207wt/Uwt)*(1-(137.88/138.88));
     d = exp(Thlambda*Date2);
     j = exp(U238lambda*Date2);
     k = exp(U235lambda*Date2);
     z = (a * d * Th * Thlambda) + (c * k * U235lambda *
U) + (b * j * U238lambda * U);
     PbPart = pow(EPb,2);
     ThPart = pow((a*d-a),2)*pow(ETh,2);
     UPart = pow(((b*j-b)+(c*k-c)),2)*pow(EU,2);
     SRTop = PbPart - ThPart - UPart;
     /*printf("PbPart = %0.10Lf\nThPart = %0.10Lf\nUPart
= %0.10Lf\nSRTop = %0.10Lf\n", PbPart, ThPart, UPart,
SRTop);*/

     DateError = sqrt(SRTop/pow(z,2));

     /*printf("Error = %Lf\na = %Lf\nb = %Lf\nc = %Lf\nd
= %Lf\nj = %Lf\nk = %Lf\nz = %0.15Lf\nEPb = %f\nETh =
%f\nEU = %f\n", DateError, a, b, c, d, j, k, z, EPb, ETh,
EU);*/
     printf("Error = %10.0Lf\n\n", DateError);
     fprintf(fp2,
"%10.0Lf\t%4.0Lf\t%4.0Lf\t%0.5Lf\t%0.5Lf\t%0.5Lf\t",
DateError, Date2/1000000, DateError/1000000, Th, U, Pb);
     fprintf(fp3, "%4.1Lf}\n", DateError/1000000);

     /*Pb contribution from Th*/
     NTh = (Th/Th232wt)*Avnumb;
     expint = (Thlambda * Date2);
     expout = exp(expint) - 1;
     DTh = NTh * expout;
     Pb208 = DTh * Pb208wt/Avnumb;
     printf("Pb208 = %0.5Lf\n", Pb208);
     fprintf(fp2, "%Lf\t", Pb208);

     /*Pb contribution from U238*/
     U238 = U * Udiv;
     NU238 = (U238/U238wt)*Avnumb;
     DU238 = NU238 * (exp(U238lambda * Date2) - 1);
     Pb206 = DU238 * Pb206wt/Avnumb;
     printf("Pb206 = %0.5Lf\n", Pb206);
     fprintf(fp2, "%Lf\t", Pb206);

     /*Pb contribution from U235*/
     U235 = U * (1 - (137.88/138.88));
     NU235 = (U235/U235wt)*Avnumb;
     DU235 = NU235 * (exp(U235lambda * Date2) - 1);
     Pb207 = DU235 * Pb207wt/Avnumb;
     printf("Pb207 = %0.5Lf\n", Pb207);
     fprintf(fp2, "%Lf\t", Pb207);

     TotPb = Pb206 + Pb207 + Pb208;
     DiffPb = fabs(Pb - TotPb);
     DiffPer = DiffPb/Pb;
```

```
     printf("Total Lead = %0.5Lf\nDifference between
measured & calculated lead = %0.5Lf (%0.1Lf%%)\n", TotPb,
(TotPb - PbCalc), (TotPb - PbCalc)/PbCalc *100 );
     fprintf(fp2, "%Lf\t", TotPb);
     fprintf(fp2, "%Lf\t", DiffPb);
     fprintf(fp2, "%Lf\n", DiffPer);

     //fprintf(fp3, "\n");
     //fprintf(fp3,
"%6.0Lf,%6.0Lf,%6.0Lf,%6.0Lf,%6.0Lf,%6.0Lf,%f,%f}\n",
Pb*10000, Th*10000, U*10000, EPb*Pb*10000, ETh*Th*10000,
EU*U*10000, Date2, DateError);
}

fclose(fp);
fclose(fp2);
}
```

# References


Alkmim, F. F., Marshak, S., Pedrosa-Soares, A. C., Peres, G. G., Cruz, S. C. P. & Whittington, A., 2006. Kinematic evolution of the Araçuaí-West Congo orogen in Brazil and Africa: Nutcracker tectonics during the Neoproterozoic assembly of Gondwana. *Precambrian Research*, **149**(1-2), 43-64.

Appold, M. S. & Garven, G., 1999. The hydrology of ore formation in the Southeast Missouri district: Numerical models of topography-driven fluid flow during the Ouachita Orogeny. *Economic Geology and the Bulletin of the Society of Economic Geologists*, **94**(6), 913-935.

Ayers, J. C., Miller, C., Gorisch, B. & Millman, J., 1999. Textural development of monazite during high-grade metamorphism: Hydrothermal growth kinetics, with implications for U,Th-Pb geochronology. *American Mineralogist*, **84**(11-12), 1766-1780.

Baldwin, J. A. & Brown, M., 2008. Age and duration of ultrahigh-temperature metamorphism in the Anapolis-Itaucu Complex, Southern Brasilia Belt, central Brazil - constraints from U-Pb geochronology, mineral rare earth element chemistry and trace-element thermometry. *Journal of Metamorphic Geology*, **26**(2), 213-233.

Baldwin, J. A., Brown, M. & Schmitz, M. D., 2007. First application of titanium-in-zircon thermometry to ultrahigh-temperature metamorphism. *Geology*, **35**(4), 295-298.

Baldwin, J. A., Powell, R., Brown, M., Moraes, R. & Fuck, R. A., 2005. Modelling of mineral equilibria in ultrahigh-temperature metamorphic rocks from the Anapolis-Itaucu Complex, central Brazil. *Journal of Metamorphic Geology*, **23**(7), 511-531.

Baldwin, J. A., Powell, R., Williams, M. L. & Goncalves, P., 2007. Formation of eclogite, and reaction during exhumation to mid-crustal levels, Snowbird tectonic zone, western Canadian Shield. *Journal of Metamorphic Geology*, **25**(9), 953-974.

Bea, F. & Montero, P., 1999. Behavior of accessory phases and redistribution of Zr, REE, Y, Th, and U during metamorphism and partial melting of metapelites in the lower crust: an example from the Kinzigite Formation of Ivrea-Verbano, NW Italy. *Geochimica et Cosmochimica Acta*, **63**(7-8), 1133-1153

Bingen, B., Austrheim, H. & Whitehouse, M. J., 2001. Ilmenite as a source for zirconium during high-grade metamorphism? Textural evidence from the Caledonides of western Norway and implications for zircon geochronology. *Journal of Petrology*, **42**(2), 355-375.

Bingen, B. & van Breemen, O., 1998. U-Pb monazite ages in amphibolite- to granulite-facies orthogneiss reflect hydrous mineral breakdown reactions: Sveconorwegian Province of SW Norway. *Contributions to Mineralogy and Petrology*, **132**(4), 336-353.

Braun, I., Montel, J. M. & Nicollet, C., 1998. Electron microprobe dating of monazites from high-grade gneisses and pegmatites of the Kerala Khondalite Belt, southern India. *Chemical Geology*, **146**(1-2), 65-85.

Brown, M., 2002. Prograde and Retrograde Processes in Migmatites Revisited. *Geology*, **20**, 25-40.

Brown, M., 2007. Crustal melting and melt extraction, ascent and emplacement in orogens: mechanisms and consequences. *Journal of the Geological Society, London*, **164**, 709-730.

Brown, M. & Korhonen, F. J., 2009. Some remarks on melting and extreme metamorphism of crustal rocks. In: *Physics and Chemistry of the Earth's Interior* (eds Gupta, A. K. & Dasgupta, S.), pp. 67-88, Springer.

Buick, I. S., Hermann, J., Williams, I. S., Gibson, R. L. & Rubatto, D., 2006. Age and petrogenesis of garnet–cordierite–orthoamphibole gneisses from the Central Zone of the Limpopo Belt, South Africa. *Lithos*, **88**, 150-172.

Campos Neto, M. D., 2000. Orogenic systems from Southwestern Gondwana: An approach to Brasiliano–Pan African Cycle and orogenic collage in Southeastern Brazil. In: *Tectonic Evolution of South America* (eds Cordani, U. G., Milani, E. J., Thomaz Filho, A. & Campos, D. A.), pp. 335-365, Rio de Janeiro.

Campos Neto, M. D. C., Basei, M. A. S., Vlach, S. R. F., Caby, R., Szabo, G. A. J. & Vasconcelos, P., 2004. Migração de Orógenos e Superposição de Orogêneses: Um Esboço da Colagem Brasiliana no Sul do Cráton do São Francisco, SE - Brasil. *Revista do Instituto de Geociências - USP*, **4**(1), 13-40.

Campos Neto, M. D. C. & Caby, R., 1999. Neoproterozoic high-pressure metamorphism and tectonic constraint from the nappe system south of the Sao Francisco Craton, southeast Brazil. *Precambrian Research*, **97**(1-2), 3-26.

Campos Neto, M. D. C. & Caby, R., 2000. Terrane accretion and upward extrusion of high-pressure granulites in the Neoproterozoic nappes of southeast Brazil: Petrologic and structural constraints. *Tectonics*, **19**(4), 669-687.

Cherniak, D. J., Watson, E. B., Grove, M. & Harrison, T. M., 2004. Pb diffusion in monazite: A combined RBS/SIMS study. *Geochimica Et Cosmochimica Acta*, **68**(4), 829-840.

Cherniak, D. J., Watson, E. B., Harrison, T. M. & Grove, M., 2000. Pb diffusion in monazite: a progress report on a combined RBS/SIMS study. *EOS, Transactions, American Geophysical Union*, **41**(S25).

Cocherie, A. & Albarede, F., 2001. An improved U-Th-Pb age calculation for electron microprobe dating of monazite. *Geochimica Et Cosmochimica Acta*, **65**(24), 4509-4522.

Cocherie, A., Mezeme, E. B., Legendre, O., Fanning, C. M., Faure, M. & Rossi, P., 2005. Electron-microprobe dating as a tool for determining the closure of Th-U-Pb systems in migmatitic monazites. *Lithos*, **87**, 276-288.

Coggon, R. & Holland, T. J. B., 2002. Mixing properties of phengitic micas and revised garnet-phengite thermobarometers. *Journal of Metamorphic Geology*, **20**(7), 683-696.

Copeland, P., Parrish, R. R. & Harrison, T. M., 1988. Identification of Inherited Radiogenic Pb in Monazite and Its Implications for U-Pb Systematics. *Nature*, **333**(6175), 760-763.

Corfu, F., 1988. Differential Response of U-Pb Systems in Coexisting Accessory Minerals, Winnipeg River Subprovince, Canadian Shield - Implications for Archean Crustal Growth and Stabilization. *Contributions to Mineralogy and Petrology*, **98**(3), 312-325.

Corrie, S. L. & Kohn, M. J., 2008. Trace-element distributions in silicates during prograde metamorphic reactions: implications for monazite formation. *Journal of Metamorphic Geology*, **26**(4), 451-464.

Crowley, J. L. & Ghent, E. D., 1999. An electron microprobe study of the U-Th-Pb systematics of metamorphosed monazite: the role of Ph diffusion versus overgrowth and recrystallization. *Chemical Geology*, **157**(3-4), 285-302.

Dahl, P. S., 1997. A crystal-chemical basis for Pb retention and fission-track annealing systematics in U-bearing minerals, with implications for geochronology. *Earth and Planetary Science Letters*, **150**(3-4), 277-290.

Dahl, P. S., Terry, M. P., Jercinovic, M. J., Williams, M. L., Hamilton, M. A., Foland, K. A., Clement, S. M. & Friberg, L. M., 2005. Electron probe (Ultrachron) microchronometry of metamorphic monazite: Unraveling the timing of polyphase thermotectonism in the easternmost Wyoming Craton (Black Hills, South Dakota). *American Mineralogist*, **90**(11-12), 1712-1728.

Devore, J. L., 2008. *Probability and statistics for engineering and the sciences*.

Thomson/Brooks/Cole, Belmont, CA.

DeWolf, C. P., Belshaw, N. & Onions, R. K., 1993. A metamorphic history from micron-scale Pb-207/Pb-206 chronometry of Archean Monazite. *Earth and Planetary Science Letters*, **120**(3-4), 207-220.

Diener, J. F. A., White, R. W. & Powell, R., 2008. Granulite facies metamorphism and subsolidus fluid-absent reworking, Strangways Range, Arunta Block, central Australia. *Journal of Metamorphic Geology*, **26**(6), 603-622.

Ferreira, C. F., Naldrett, A. J. & Gorton, M. P., 1998. REE and pyroxene compositional variation across the Niquelandia layered intrusion, Brazil: Petrological and metallogenetic implications, pp. B1-B22.

Ferreira, C. F., Nilson, A. A. & Naldrett, A. J., 1992. The Niquelandia Mafic–Ultramafic Complex, Goias, Brazil - A contribution to the opheiolite X stratiform controversy based on new geological and structural data. *Precambrian Research*, **59**(1-2), 125-143.

Ferriss, E. D., Essene, E. J. & Becker, U., 2008. Computational study of the effect of pressure on the Ti-in-zircon geothermometer. *European Journal of Mineralogy*, **20**, 745-755.

Ferry, J. M. & Watson, E. B., 2007. New thermodynamic models and revised calibrations for the Ti-in-zircon and Zr-in-rutile thermometers. *Contributions to Mineralogy and Petrology*, **154**(4), 429-437.

Foster, G., Gibson, H. D., Parrish, R., Horstwood, M., Fraser, J. & Tindle, A., 2002. Textural, chemical and isotopic insights into the nature and behaviour of metamorphic monazite. *Chemical Geology*, **191**, 183-207.

Foster, G., Kinny, P., Vance, D., Prince, C. & Harris, N., 2000. The significance of monazite U-Th-Pb age data in metamorphic assemblages; a combined study of monazite and garnet chronometry. *Earth and Planetary Science Letters*, **181**(3), 327-340.

Foster, G., Parrish, R. R., Horstwood, M. S. A., Chenery, S., Pyle, J. & Gibson, H. D., 2004. The generation of prograde P-T-t points and paths; a textural, compositional, and chronological study of metamorphic monazite. *Earth and Planetary Science Letters*, **228**(1-2), 125-142.

Fuck, R. A., Pimentel, M. M. & Silva, L. J. H. D., 1994. Compartimentação tectônica da porção oriental da Província Tocantins. In: *38o Congresso Brasileiro de Geologia*, pp. 215-216, Balneário Camboriú, SBG.

Garcia, M. D. & Campos Neto, M. D., 2003. Contrasting metamorphic conditions in the Neoproterozoic collision-related Nappes south of Sao Francisco Craton, SE Brazil. *Journal of South American Earth Sciences*, **15**(8), 853-870.

Garven, G., 1995. Continental-Scale Groundwater-Flow and Geologic Processes. *Annual Review of Earth and Planetary Sciences*, **23**, 89-117.

Ge, S. M. & Garven, G., 1992. Hydromechanical Modeling of Tectonically Driven Groundwater-Flow with Application to the Arkoma Foreland Basin. *Journal of Geophysical Research-Solid Earth*, **97**(B6), 9119-9144.

Glodny, J., Austrheim, H. & Kuehn, A., 2008. Diffusion versus recrystallization processes in Rb–Sr geochronology: Isotopic relics in eclogite facies rocks, Western Gneiss Region, Norway *Geochimica et Cosmochimica Acta*, **72**(2), 506-525.

Goncalves, P., Williams, M. L. & Jercinovic, M. J., 2005. Electron-microprobe age mapping of monazite. *American Mineralogist*, **90**(4), 578-585.

Harley, S. L. & Kelly, N. M., 2007. The impact of zircon-garnet REE distribution data on the interpretation of zircon U-Pb ages in complex high-grade terrains: An example from the Rauer Islands, East Antarctica. *Chemical Geology*, **241**(1-2), 62-87.

Harrison, T. M., 1981. Diffusion of Ar-40 in hornblende. *Contributions to Mineralogy and Petrology*, **78**(3), 324-331.

Harrison, T. M., Duncan, I. & McDougall, I., 1985. Diffusion of Ar-40 in biotite - temperature, pressure and compositional effects. *Geochimica Et Cosmochimica Acta*, **49**(11), 2461-2468.

Harrison, T. M. & McDougall, I., 1980. Diffusion of radiogenic and excess Ar-40 in hornblende revealed by Ar-40-Ar-39 age spectrum analysis. *Geochimica Et Cosmochimica Acta*, **44**(12), 2005-2020.

Harrison, T. M., Mckeegan, K. D. & Lefort, P., 1995. Detection of Inherited Monazite in the Manaslu Leukogranite by Pb-208/Th-232 Ion Microprobe Dating - Crystallization Age and Tectonic Implications. *Earth and Planetary Science Letters*, **133**(3-4), 271-282.

Heilbron, M. & Machado, N., 2003. Timing of terrane accretion in the Neoproterozoic–Eopaleozoic Ribeira orogen (se Brazil). *Precambrian Research*, **125**, 87-112.

Heilbron, M., Mohriak, W., Valeriano, C., Milani, E. J., Almeida, J. & Tupinambá, M., 2000. From collision to extension: The roots of the southeastern continental margin of Brazil. In: *Atlantic Rifts and Continental Margins* (eds Talwani, M. & Mohriak, W. U.) *Geophysical Monograph*, pp. 1-32, American Geophysical Union.

Heilbron, M., Valeriano, C., Tassinari, J., Almeida, M., Tupinambá, O., Siga, J. R. & Trouw, R. A. J., 2008. Correlation of Neoproterozoic terranes between the

Ribeira Belt, SE Brazil and its African counterpart: comparative tectonic evolution and open questions. *Geological Society, London, Special Publications*, **294**, 211-237.

Hermann, J. & Rubatto, D., 2003. Relating zircon and monazite domains to garnet growth zones: age and duration of granulite facies metamorphism in the Val Malenco lower crust. *Journal of Metamorphic Geology*, **21**(9), 833-852.

Hokada, T. & Harley, S. L., 2004. Zircon growth in UHT leucosome: constraints from zircon–garnet rare earth elements (REE) relations in Napier Complex, East Antarctica. *Journal of Mineralogical and Petrological Sciences*, **99**, 180-190.

Holland, T. & Powell, R., 2003. Activity-composition relations for phases in petrological calculations: an asymmetric multicomponent formulation. *Contributions to Mineralogy and Petrology*, **145**(4), 492-501.

Holland, T. J. B. & Powell, R., 1998. An internally consistent thermodynamic data set for phases of petrological interest. *Journal of Metamorphic Geology*, **16**(3), 309-343.

Hoskin, P. W. O. & Schaltegger, U., 2003. The composition of zircon and igneous and metamorphic petrogenesis. In: *Zircon* (eds Hanchar, J. M. & Hoskin, P. W. O.) *Reviews in Mineralogy*, Mineralogical Society of America, Washington.

Jercinovic, M. J. & Williams, M. L., 2005. Analytical perils (and progress) in electron microprobe trace element analysis applied to geochronology: Background acquisition, interferences, and beam irradiation effects. *American Mineralogist*, **90**, 526-546.

Jercinovic, M. J., Williams, M. L. & Lane, E. D., 2008. In-situ trace element analysis of monazite and other fine-grained accessory minerals by EPMA. *Chemical Geology*, **254**(3-4), 197-215.

Junges, S. L., Pimentel, M. M. & de Moraes, R., 2002. Nd isotopic study of the Neoproterozoic Mara Rosa Arc, central Brazil: implications for the evolution of the Brasilia Belt. *Precambrian Research*, **117**(1-2), 101-118.

Kelly, N. M. & Harley, S. L., 2005. An integrated microtextural and chemical approach to zircon geochronology: refining the Archaean history of the Napier Complex, east Antarctica. *Contributions to Mineralogy and Petrology*, **149**(1), 57-84.

Kelsey, D. E., Clark, C. & Hand, M., 2008. Thermobarometric modelling of zircon and monazite growth in melt-bearing systems: examples using model metapelitic and metapsammitic granulites. *Journal of Metamorphic Geology*, **26**, 199-212.

Kelsey, D. E., Powell, R., Wilson, C. J. L. & Steele, D. A., 2003. (Th+U)-Pb monazite ages from Al-Mg-rich metapelites, Rauer Group, east Antarctica. *Contributions to Mineralogy and Petrology*, **146**(3), 326-340.

Kingsbury, J. A., Miller, C. F., Wooden, J. L. & Harrison, T. M., 1993. Monazite paragenesis and U-Pb systematics in the rocks of the eastern Mojave Desert, California, USA – Implications for thermochronometry. *Chemical Geology*, **110**, 147-167.

Kretz, R., 1983. Symbols for Rock-Forming Minerals. *American Mineralogist*, **68**(1-2), 277-279.

Kuhn, A., Stuwe, K. & Trouw, R. A. J., 2004. Metamorphic evolution of the Ribeira belt: Evidence from outcrops in the Rio de Janeiro area, Brazil. *Journal of Petrology*, **45**(11), 2303-2323.

Ludwig, K. R., 1994. Isoplot, a plotting and regression program for radiogenic-isotope data (ed Survey, U. S. G.), pp. 45.

Machado, N., Valladares, C., Heilbron, M. & Valeriano, C., 1996. U-Pb geochronology of the central Ribeira belt (Brazil) and implications for the evolution of the Brazilian orogeny. *Precambrian Research*, **79**(3-4), 347-361.

Martin, A. J., Gehrels, G. E. & DeCelles, P. G., 2007. The tectonic significance of (U,Th)/Pb ages of monazite inclusions in garnet from the Himalaya of central Nepal. *Chemical Geology*, **244**, 1-24.

Martins, L., Vlach, S. & Janasi, V., 2009. Reaction microtextures of monazite: Correlation between chemical and age domains in the Nazar´e Paulista migmatite, SE Brazil. *Chemical Geology*, **in press**.

McDougall, I. & Harrison, T. M., 1999. *Geochronology and Thermochronology by the 40Ar/39Ar Method*. Oxford University Press.

McDonough, W. F. & Sun, S. S., 1995. The Composition of the Earth. *Chemical Geology*, **120**(3-4), 223-253.

Möller, A., O'Brien, P. J., Kennedy, A. & Kroner, A., 2002. Polyphase zircon in ultrahigh-temperature granulites (Rogaland, SW Norway): constraints for Pb diffusion in zircon. *Journal of Metamorphic Geology*, **20**(8), 727-740.

Montel, J. M., Foret, S., Veschambre, M., Nicollet, C. & Provost, A., 1996. Electron microprobe dating of monazite. *Chemical Geology*, **131**(1-4), 37-53.

Montel, J. M., Kornprobst, J. & Vielzeuf, D., 2000. Preservation of old U-Th-Pb ages in shielded monazite: example from the Beni Bousera Hercynian kinzigites (Morocco). *Journal of Metamorphic Geology*, **18**(3), 335-342.

Moraes, R., Brown, M., Fuck, R. A., Camargo, M. A. & Lima, T. M., 2002. Characterization and P-T evolution of melt-bearing ultrahigh-temperature granulites: An example from the Anapolis-Itaucu Complex of the Brasilia Fold Belt, Brazil. *Journal of Petrology*, **43**(9), 1673-1705.

Moraes, R., Brown, M., Fuck, R. A., Camargo, M. A. & Lima, T. M., 2002. Characterization and P-T evolution of melt-bearing ultrahigh-temperature granulites: an example from the Anápolis-Itauçu Complex of the Brasília Fold Belt, Brazil. *Journal of Petrology*, **43**, 1673-1705.

Moraes, R. & Fuck, R. A., 2000. Ultra-high-temperature metamorphism in central Brazil: The Barro Alto complex. *Journal of Metamorphic Geology*, **18**(4), 345-358.

Nakamura, E. & Kushiro, I., 1998. Trace element diffusion in jadeite and diopside melts at high pressures and its geochemical implication. *Geochimica et Cosmochimica Acta*, **62**(18), 3151-3160.

Nakamura, E., Makishima, A., Moriguti, T., Kobayashi, K., Sakaguchi, C., Yokoyama, T., Tanaka, R., Kuritani, T. & Takei, H., 2003. Comprehensive geochemical analyses of small amounts (< 100mg) of extraterrestrial samples for the analytical competition related to the sample return mission MUSES-C. *Inst. Space Astronaut. Sci. Rep. SP.*, **16**, 49-101.

Paciullo, F. V. P., 1997. A sequência deposicional Andrelândia*, Universidade Federal do Rio de Janeiro, Rio de Janeiro.*

Parrish, R. R., 1990. U-Pb Dating of Monazite and Its Application to Geological Problems. *Canadian Journal of Earth Sciences*, **27**(11), 1431-1450.

Pimentel, M. M., Jost, H. & Fuck, R. A., 2004. O embasamento da Faixa Brasília e o Arco Magmático de Goías. In: *Geologia do Continente Sul Americano: Evolução da obra de Fernando Flávio Marques de Almeida* (eds Mantesso Neto, V., Bartorelli, A., Carneiro, C. R. & Brito Neves, B. B.), pp. 355-368, Editora Beca, São Paulo.

Powell, R. & Downes, J., 1990. Garnet porphyroblast-bearing leucosomes in metapelites: mechanisms and an example from Broken Hill, Australia. In: *High Temperature Metamorphism and Crustal Anatexis* (eds Ashworth, J. R. & Brown, M.), pp. 105-123, Unwin-Hyman, London.

Powell, R., Hergt, J. & Woodhead, J., 2002. Improving isochron calculations with robust statistics and the bootstrap. *Chemical Geology*, **185**(3-4), 191-204.

Powell, R., Holland, T. & Worley, B., 1998. Calculating phase diagrams involving solid solutions via non-linear equations, with examples using THERMOCALC. *Journal of Metamorphic Geology*, **16**(4), 577-588.

Pyle, J. M. & Spear, F. S., 2003. Four generations of accessory-phase growth in low-pressure migmatites from SW New Hampshire. *American Mineralogist*, **88**(2-3), 338-351.

Pyle, J. M., Spear, F. S., Wark, D. A., Daniel, C. G. & Storm, L. C., 2005. Contributions to precision and accuracy of monazite microprobe ages. *American Mineralogist*, **90**(4), 547-577.

Ribeiro, A., Trouw, R. A. J., Andreis, R. R., Paciullo, F. V. P. & Valença, J. G., 1995. Evolução das Bacias Proterozóicas e o Termo-Tectonismo Brasiliano na Margem Sul do Cráton do São Francisco. *Revista Brasíleira de Geosciências*, **24**(4), 235-248.

Roberts, M. P. & Finger, F., 1997. Do U-Pb zircon ages from granulites reflect peak metamorphic conditions? *Geology*, **25**(4), 319-322.

Rubatto, D., 2002. Zircon trace element geochemistry: partitioning with garnet and the link between U-Pb ages and metamorphism. *Chemical Geology*, **184**(1-2), 123-138.

Rubatto, D. & Hermann, J., 2003. Zircon formation during fluid circulation in eclogites (Monviso, Western Alps): Implications for Zr and Hf budget in subduction zones. *Geochimica Et Cosmochimica Acta*, **67**(12), 2173-2187.

Rubatto, D. & Hermann, J., 2007. Experimental zircon/melt and zircon/garnet trace element partitioning and implications for the geochronology of crustal rocks. *Chemical Geology*, **241**(1-2), 38-61.

Rubatto, D., Hermann, J. & Buick, I. S., 2006. Temperature and bulk composition control on the growth of monazite and zircon during low-pressure anatexis (Mount Stafford, central Australia). *Journal of Petrology*, **47**(10), 1973-1996.

Rubatto, D., Williams, I. S. & Buick, I. S., 2001. Zircon and monazite response to prograde metamorphism in the Reynolds Range, central Australia. *Contributions to Mineralogy and Petrology*, **140**(4), 458-468.

Schaltegger, U., Fanning, C. M., Gunther, D., Maurin, J. C., Schulmann, K. & Gebauer, D., 1999. Growth, annealing and recrystallization of zircon and preservation of monazite in high-grade metamorphism: conventional and in-situ U-Pb isotope, cathodoluminescence and microchemical evidence. *Contributions to Mineralogy and Petrology*, **134**(2-3), 186-201.

Scherrer, N. C., Engi, M., Gnos, E., Jakob, V. & Liechti, A., 2000. Monazite analysis; from sample preparation to microprobe age dating and REE quantification. *Schweizerische Mineralogische Und Petrographische Mitteilungen*, **80**(1), 93-105.

Schmitt, R. D., Trouw, R. A. J., Medeiros, S. R. & Dantas, E. L., 2008. Age and

geotectonic setting of Late Neoproterozoic juvenile mafic gneisses and associated paragneisses from the Ribeira belt (SE Brazil) based on geochemistry and Sm-Nd data - Implications on Gondwana assembly. *Gondwana Research*, **13**(4), 502-515.

Schmitt, R. D., Trouw, R. A. J., Van Schmus, W. R. & Pimentel, M. M., 2004. Late amalgamation in the central part of West Gondwana: new geochronological. data and the characterization of a Cambrian collisional orogeny in the Ribeira Belt (SE Brazil). *Precambrian Research*, **133**(1-2), 29-61.

Schmitz, M. D. & Bowring, S. A., 2003. Constraints on the thermal evolution of continental lithosphere from U-Pb accessory mineral thermochronometry of lower crustal xenoliths, southern Africa. *Contributions to Mineralogy and Petrology*, **144**(5), 592-618.

Seydoux-Guillaume, A. M., Paquette, J. L., Wiedenbeck, M., Montel, J. M. & Heinrich, W., 2002. Experimental resetting of the U-Th-Pb systems in monazite. *Chemical Geology*, **191**, 165-181.

Simpson, R. L., Parrish, R. R., Searle, M. P. & Waters, D. J., 2000. Two episodes of monazite crystallization during metamorphism and crustal melting in the Everest region of the Nepalese Himalaya. *Geology*, **28**(5), 403-406.

Smith, H. A. & Giletti, B. J., 1997. Lead diffusion in monazite. *Geochimica Et Cosmochimica Acta*, **61**(5), 1047-1055.

Spear, F. S. & Parrish, R. R., 1996. Petrology and cooling rates of the Valhalla complex, British Columbia, Canada. *Journal of Petrology*, **37**(4), 733-765.

Suzuki, K., Adachi, M. & Tanaka, T., 1991. Middle Precambrian provenance of Jurassic sandstone in the Mino Terrane, Central Japan – Th-U-Total Pb evidence from an electron-microprobe monazite study. *Sedimentary Geology*, **75**(1-2), 141-147.

Tabachnick, B. G. & Fidell, L. S., 1996. *Using multivariate statistics*. Pearson/Allyn & Bacon, Boston, MA.

Terry, M. P., Robinson, P., Hamilton, M. A. & Jercinovic, M. J., 2000. Monazite geochronology of UHP and HP metamorphism, deformation, and exhumation, Nordoyane, Western Gneiss Region, Norway. *American Mineralogist*, **85**(11-12), 1651-1664.

Tomascak, P. B., Krogstad, E. J. & Walker, R. J., 1996. U-Pb monazite geochronology of granitic rocks from Maine: Implications for late paleozoic tectonics in the northern Appalachians. *Journal of Geology*, **104**(2), 185-195.

Trouw, R. A. J., Moraes, R., Reno, B. L. & Brown, M., 2006. The High-Pressure Granulites of the Andrelândia Nappe Complex, Brazil Field Trip Guide. In:

*Granuiltes & Granulites 2006*, Brasília, Brazil.

Trouw, R. A. J. & Pankhurst, R. J., 1992. Idades radiométricas ao sul do Cráton do São Francisco baseada em análise metamórfica. In: *Congresso Brasileiro de Geologia 27*, pp. 327, SBG, São Paulo.

Trouw, R. A. J., Ribeiro, A. & Paciullo, F. V. P., 1983. Geologia estrutural dos Grupos São João del Rei, Carranca e Andrelândia, sul de Minas Gerais. *Anais da Academia brasileira de Ciêincias*, **55**, 71-85.

Trouw, R. A. J., Ribeiro, A., Paciullo, F. V. P. & Heilbron, M., 2000. Interference between the Neoproterozoic Brasília and Ribeira Belts, with special emphasis on high pressure granulites. 31st International Geological Congress. Field Trip Guide., pp. 45, Rio de Janeiro.

Tukey, J. W., 1977. *Exploratory Data Analysis*. Addison-Wesley, Reading, MA.

Usui, T., Kobayashi, K. & Nakamura, E., 2002. U-Pb isotope systematics of micro-zircon inclusions - Implications for the age and origin of eclogite xenolith from the Colorado Plateau. *Proceedings of the Japan Academy Series B-Physical and Biological Sciences*, **78**, 51-56.

Valeriano, C., Pimentel, M. M., Heilbron, M., Almeida, J. & Trouw, R. A. J., 2008. Tectonic evolution of the Brasília Belt, Central Brazil, and early assembly of Gondwana. In: *West Gondwana: Pre-Cenozoic correlations across the South Atlantic Region* (eds Pankhurst, R. J., Trouw, R. A. J., Brito Neves, B. B. & de Wit, M. J.), pp. 197-210, Geological Society of London.

Vlach, S. R. F. & Gualda, G. A. R., 2000. Microprobe monazite dating and the ages of some granitic and metamorphic rocks from southeastern Brazil. *Revista Brasileira de Geociências*, **30**(1), 214-218.

Watson, E. B., Wark, D. A. & Thomas, J. B., 2006. Crystallization thermometers for zircon and rutile. *Contributions to Mineralogy and Petrology*, **151**(4), 413-433.

White, R. W. & Powell, R., 2002. Melt loss and the preservation of granulite facies mineral assemblages. *Journal of Metamorphic Geology*, **20**(7), 621-632.

White, R. W., Powell, R. & Clarke, G. L., 2003. Prograde metamorphic assemblage evolution during partial melting of metasedimentary rocks at low pressures: Migmatites from Mt Stafford, central Australia. *Journal of Petrology*, **44**(11), 1937-1960.

White, R. W., Powell, R. & Halpin, J. A., 2004. Spatially-focussed melt formation in aluminous metapelites from Broken Hill, Australia. *Journal of Metamorphic Geology*, **22**, 825-845.

White, R. W., Powell, R. & Holland, T., 2001. Calculation of partial melting equilibria in the system Na2O-CaO-K2O-FeO-MgO-Al2O3-SiO2-H2O (NCKFMASH). *Journal of Metamorphic Geology*, **19**(2), 139-153.

White, R. W., Powell, R. & Holland, T. J. B., 2007. Progress relating to calculation of partial melting equilibria for metapelites. *Journal of Metamorphic Geology*, **25**(5), 511-527.

White, R. W., Powell, R., Holland, T. J. B. & Worley, B. A., 2000. The effect of TiO2 and Fe2O3 on metapelitic assemblages at greenschist and amphibolite facies conditions: mineral equilibria calculations in the system K2O-FeO-MgO-Al2O3-SiO2-H2O-TiO2-Fe2O3. *Journal of Metamorphic Geology*, **18**(5), 497-511.

Whitehouse, M. J. & Platt, J. P., 2003. Dating high-grade metamorphism - constraints from rare-earth elements in zircon and garnet. *Contributions to Mineralogy and Petrology*, **145**(1), 61-74.

Williams, I. S., Compston, W. & Chappell, B. W., 1983. Zircon and monazite U-Pb systems and the histories of I-Type magmas, Berridale Batholith, Australia. *Journal of Petrology*, **24**(1), 76-97.

Williams, M. L. & Jercinovic, M. J., 2002. Microprobe monazite geochronology: putting absolute time into microstructural analysis. *Journal of Structural Geology*, **24**(6-7), 1013-1028.

Williams, M. L., Jercinovic, M. J., Goncalves, P. & Mahan, K., 2006. Format and philosophy for collecting, compiling, and reporting microprobe monazite ages. *Chemical Geology*, **225**(1-2), 1-15.

Williams, M. L., Jercinovic, M. J. & Hetherington, C. J., 2007. Microprobe monazite geochronology: Understanding geologic processes by integrating composition and chronology. *Annual Review of Earth and Planetary Sciences*, **35**, 137-175.

Williams, M. L., Jercinovic, M. J. & Terry, M. P., 1999. Age mapping and dating of monazite on the electron microprobe: Deconvoluting multistage tectonic histories. *Geology*, **27**(11), 1023-1026.

Yokoyama, T., Makishima, A. & Nakamura, E., 1999. Evaluation of the coprecipitation of incompatible trace elements with fluoride during silicate rock dissolution by acid digestion. *Chemical Geology*, **157**(3-4), 175-187.

Yoshikawa, M. & Nakamura, E., 1993. Precise isotope determination of trace amounts of Sr in magnesium-rich samples. *Japanese Journal of Mineralogy, Petrology and Economic Geology*, **88**, 548-561.

Zhu, X. K. & O'Nions, R. K., 1999. Zonation of monazite in metamorphic rocks and its implications for high temperature thermochronology: a case study from the Lewisian terrain. *Earth and Planetary Science Letters*, **171**(2), 209-220.